OFFICE OF ENVIRONMENTAL HEALTH HAZARD ASSESSMENT

Proposition 65

Evidence on the Carcinogenicity of Perfluorooctane Sulfonic Acid (PFOS) and Its Salts and Transformation and Degradation Precursors

September 2021

Reproductive and Cancer Hazard Assessment Branch
Office of Environmental Health Hazard Assessment
California Environmental Protection Agency

CONTRIBUTORS

The Office of Environmental Health Hazard Assessment's (OEHHA) Reproductive and Cancer Hazard Assessment Branch was responsible for the preparation of this document.

Authors (listed alphabetically by last name)

Sarah Elmore, Ph.D.
Associate Toxicologist

Neela Guha, Ph.D., M.P.H.
Research Scientist III

Jennifer C.Y. Hsieh, Ph.D., M.S., DABT
Staff Toxicologist

Kate Li, Ph.D., DABT
Staff Toxicologist

M. Elizabeth Marder, Ph.D.
Senior Environmental Scientist

Meltem Musa, Ph.D.
Staff Toxicologist

Gwendolyn Osborne, M.D., M.P.H.
Staff Toxicologist

Karin Ricker, Ph.D.
Staff Toxicologist

Rose Schmitz, M.S.
Research Scientist III

Feng C. Tsai, Ph.D., M.S.
Staff Toxicologist

Acknowledgment

The valuable contribution of Nancy Firchow, MLS in conducting the literature searches is acknowledged.

Internal OEHHA Reviewers

Meng Sun, Ph.D., M.S.
Chief, Cancer Toxicology and Epidemiology Section

Martha S. Sandy, Ph.D., M.P.H.
Chief, Reproductive and Cancer Hazard Assessment Branch

Vincent Cogliano, Ph.D.
Deputy Director, Division of Scientific Programs

David Edwards, Ph.D.
Chief Deputy Director

Director

Lauren Zeise, Ph.D.

PREFACE

Proposition 65[1] requires the publication of a list of chemicals "known to the state" to cause cancer or reproductive toxicity. The Office of Environmental Health Hazard Assessment (OEHHA) of the California Environmental Protection Agency maintains this list in its role as the lead agency for implementing Proposition 65. The Carcinogen Identification Committee (CIC) advises and assists OEHHA, and adds chemicals to the Proposition 65 list of chemicals that cause cancer, as required by Health and Safety Code section 25249.8. The CIC serves as the state's qualified experts for determining whether a chemical has been clearly shown to cause cancer.

The CIC also provides advice and consultation regarding which chemicals should receive their review. At their meeting in November 2020, the CIC recommended that "PFOS and its salts and transformation and degradation precursors" be placed in a 'high' priority group for future listing consideration. OEHHA selected PFOS and its salts and transformation and degradation precursors for consideration for listing by the CIC, and in March 2021 OEHHA solicited from the public information relevant to the assessment of the evidence on its carcinogenicity. OEHHA reviewed and considered the information received in preparing this document.

[1] The Safe Drinking Water and Toxic Enforcement Act of 1986 (California Health and Safety Code 25249.5 *et seq.*)

Table of Contents

LIST OF TABLES

LIST OF FIGURES

LIST OF ABBREVIATIONS

Abbreviation	Full name
µg/cm^3	Micrograms per cubic centimeter
µg/g	Micrograms per gram
µg/kg-day	Micrograms per kilogram per day
µg/l	Micrograms per liter
µg/m^3	Micrograms per cubic meter
µg/ml	Micrograms per milliliter
µM	Micromolar
8-OHdG	8-Hydroxydeoxyguanosine
AC_{50}	Active Concentration 50
ACE 1	Asian/Pacific Islander community exposures 1
ACE 2	Asian/Pacific Islander community exposures 2
ACOX	palmitoyl CoA oxidase
ADME	Absorption, distribution, metabolism, and excretion
AFB_1	Aflatoxin B1
AhR	Aryl hydrocarbon receptor
AM	Arithmetic mean
AR	Androgen receptor
ATSDR	Agency for Toxic Substances and Disease Registry
BEST	Biomonitoring exposures study
BLOC-1	Biogenesis of lysome-related organelles complex-1
BMI	Body mass index
BRCA	Breast cancer gene
BW	Body weight
CA	Chromosomal aberrations
CalEPA	California Environmental Protection Agency
CAR	Constitutive androstane receptor
CARE-2	California regional exposure study 2

Abbreviation	Full name
CARE-LA	California regional exposure study, Los Angeles county
CAS RN	CAS registry number
CAT	Catalase
CHARGE	Childhood autism risk from genetics and environmental study
CHDS	Child health and development studies
CHO	Chinese hamster ovary
CI	Confidence interval
CIC	Carcinogen Identification Committee
CompTox Chemical Dashboard	Computational Toxicology Chemicals Dashboard
COMT	Catechol-O-methyltransferase
ConA	Concanavalin A
CpG	cytosine-phosphate-guanine
CTS	California teachers study
CYP450	Cytochrome P450
DHT	Dihydrotestosterone
DMP	Differentially methylated position
DMR	Differentially methylated region
DNA	Deoxyribonucleic acid
DNBC	Danish National Birth Cohort
DNMT	DNA methyltransferase
E2	17β-Estradiol
ECF	Electrochemical fluorination
EFSA	European Food Safety Authority
ER	Estrogen receptor
EtPFOSA/EtFOSA	N-Ethyl perfluorooctane sulfonamide
EtPFOSAA/EtFOSAA	N-Ethyl perfluorooctane sulfonamido acetic acid
EtPFOSE/EtFOSE	N-Ethyl perfluorooctane sulfonamidoethanol

Abbreviation	Full name
FOX	Firefighter occupational exposures project
GD	Gestational day
GI	Gastrointestinal
GJIC	Gap junction intercellular communication
GM	Geometric mean
GPx	Glutathione peroxidase
GR	Glutathione reductase
GSH	Reduced glutathione
GSSG	Glutathione disulfide
GST	Glutathione-S-transferase
Gstm3	Glutathione-S-transferase Mu 3
GSTP	Glutathione-S-transferase Pi
GVIN1	GTPase, very large interferon inducible pseudogene 1
HAWC	Health Assessment Workspace Collaborative
HO-1	Heme oxygenase-1
HTS	High-throughput screening
IARC	International Agency for Research on Cancer
IFN-γ	Interferon gamma
IGF1R	Insulin-like growth factor 1 receptor
IgG	Immunoglobulin G
IgM	Immunoglobulin M
IGR	Intergenic region
IL	Interleukin
iNOS	Inducible nitric oxide synthase
IRR	Incidence rate ratio
JEM	Job exposure matrix
KCs	Key characteristics
KEEP	Korean Elderly Environmental Panel
kg	Kilogram

Abbreviation	Full name
LBD	Ligand-binding domain
L-FABP	Liver fatty acid-binding protein
LINE1	Long interspersed element 1
lncRNA	Long non-coding RNA
Kow	Octanol-water partition coefficient
LTL	leukocyte telomere length
m^3/day	Cubic meters per day
MAMAS	Measuring analytes in maternal archived samples
MDA	Malondialdehyde
MEF	Mouse embryonic fibroblast
MeFOSSA	N-Methylperfluorooctane sulfonamide acetic acid
MePFOSAA	N-Methyl perfluorooctane sulfonamide acetic acid
MePFOSE	N-Methyl perfluorooctane sulfonamidoethanol
mg/kg	Milligrams per kilogram
mg/kg-bw	Milligrams per kilogram body weight
mg/kg-day	Milligrams per kilogram per day
mg/m^3	Milligrams per cubic meter
MIEEP	Maternal and infant environmental exposure project
miRNA	MicroRNA
mmHg	Millimeters of mercury
MMTV-LTR	Mouse mammary tumor virus long terminal repeat
MN	Micronuclei
mol/l	Moles per liter
MPO	Myeloperoxidase
NCI	National Cancer Institute
ng/ml	Nanograms per milliliter
NHANES	National Health and Nutrition Examination Survey
NICNAS	National Industrial Chemicals Notification and Assessment Scheme
NK cells	Natural killer cells

Abbreviation	Full name
NO	Nitric oxide
Nrf2	Nuclear factor erythroid 2–related factor 2
NS	No significant changes
NTP	National Toxicology Program
ºC	Degrees Celsius
OECD	Organisation for Economic Co-operation and Development
OEHHA	Office of Environmental Health Hazard Assessment
OHAT	Office of Health Assessment and Translation
OR	Odds ratio
OTD	Oregon test diet
PBPK	Physiologically-based pharmacokinetic
PCK1	Phosphoenolpyruvate carboxykinase 1
PCR	Polymerase chain reaction
PFASs	Per- and poly-fluoroalkyl substances
PFNA	Perfluorononanoic acid
PFOA	Perfluorooctanoic acid
PFOS	Perfluorooctane sulfonic acid
PFOS anion	Perfluorooctane sulfonate
PFOSA	Perfluorooctane sulfonamide
PFOSAA	Perfluorooctane sulfonamide acetic acid
PFOSAmS	Perfluorooctanesulfonamido ammonium salt
PFOSE alcohol	*N*-(2-hydroxyethyl)perfluorooctanesulfonamide
PFOSF (or FOSF)	Perfluorooctane sulfonyl fluoride
$PFOSK^+$	Perfluorooctane sulfonate potassium salt
PFUA	Perfluoroundecanoic acid
pH	Scale used to specify the acidity or basicity of an aqueous solution
PHG	Public Health Goal
pKa	Negative base-10 logarithm of the acid dissociation constant (Ka)

Abbreviation	Full name
PND	Post-natal day
POK	POZ/BTB and Kruppel
POP	Persistent organic pollutants
PPAR	Peroxisome proliferator activated receptor
ppb	Parts per billion
ppm	Parts per million
PPRE	Peroxisome proliferator response element
ppt	Parts per trillion
PR	Progesterone receptor
PRKCA	Protein kinase C alpha
PXR	Pregnane X receptor
QSAR	Quantitative structure activity relationship
RNA	Ribonucleic acid
RNS	Reactive nitrogen species
RoC	Report on Carcinogens
ROS	Reactive oxygen species
RR	Relative risk
s.c.	Subcutaneous injection
SCEs	Sister chromatid exchanges
SD rats	Sprague-Dawley rats
SERPINA1	Serpin family A member 1
SHE	Syrian hamster embryo
SINE	Short interspersed element
SIR	Standardized incidence ratio
SMR	Standardized mortality ratio
SNARE	Soluble N-ethylmaleimide-sensitive fusion protein attachment protein receptor
SNP	Single nucleotide polymorphism
SOD	Superoxide dismutase

Abbreviation	Full name
SRBC	Sheep red blood cell
SSB	Single strand breaks
T1/2	Half-life
TAD	Total administered dose
T-AOC	Total antioxidant capacity
TDAR	T cell dependent antibody response
TETs	Ten-eleven translocation
TFF1	Trefoil factor 1
TGF-β	Transforming growth factor beta
TIAR	T cell independent antibody response
TNF-α	Tumor necrosis factor alpha
TNP	Trinitrophenyl
Tox21	Toxicology in the 21st Century
ToxCast	US EPA Toxicity Forecaster
TSH	Thyroid stimulating hormone
UDS	Unscheduled DNA synthesis
UK	United Kingdom
US EPA	United States Environmental Protection Agency
US FDA	United States Food and Drug Administration
Vtg	Vitellogenin
ZFL	Zebrafish liver
γ-H2AX	Phosphorylated histone 2AX (serine 139)

EXECUTIVE SUMMARY

This document presents evidence relevant to the evaluation of the cancer hazard of perfluorooctane sulfonic acid (PFOS) and its salts and transformation and degradation precursors. These chemicals were placed in a 'high' priority group for future listing consideration by the Carcinogen Identification Committee (CIC) at their November 2020 meeting.

PFOS is one of the most extensively produced and studied members of a class of chemicals called per- and poly-fluoroalkyl substances (PFASs). PFOS is ubiquitous, with levels measured in environmental media, biota, and humans. Humans are exposed to PFOS through contaminated food and drinking water, ingestion of dust, and inhalation of indoor and outdoor air. Recent data from Biomonitoring California (https://biomonitoring.ca.gov) have shown that PFOS is readily detected in Californians. See Section 1.3 for additional information on PFOS exposure, and Appendix C for biomonitoring studies in California.

The evidence summarized in this document includes studies of PFOS, as well as studies of PFOS salts, which dissociate to release the perfluorooctane sulfonate ion. Additionally, the evidence includes a few studies of PFOS transformation and degradation precursors that provide information relevant to the evaluation of the effects of PFOS. In this document, "PFOS and its salts and precursors" is used to represent this group of chemicals (See Appendix A for more information).

Systematic Literature Review Approach

Using a systematic approach similar to that recommended by the National Toxicology Program (NTP) Handbook for Preparing Report on Carcinogens (RoC) Monographs (NTP 2015), the Office of Environmental Health Hazard Assessment (OEHHA) conducted literature searches on the carcinogenicity of PFOS and its salts and precursors (last comprehensive search, February 2021). The literature searches were supplemented with a data call-in period from March 26 to May 10, 2021[2], and with references cited in the Proposed Public Health Goals (PHGs) for perfluorooctanoic acid (PFOA) and PFOS in drinking water (OEHHA 2021). The latter document included references cited by previous comprehensive reviews such as the United States Environmental Protection Agency (US EPA 2016a, b), the European Food Safety Authority (EFSA 2008, 2018, 2020), and the Agency for Toxic Substances and Disease

[2] See https://oehha.ca.gov/proposition-65/crnr/chemical-selected-consideration-listing-carcinogen-identification-committee-and

Registry (ATSDR 2021). An overview of the systematic literature review approach is presented in Section 2 of this document, and more detailed information can be found in Appendix B.

Carcinogenicity Studies in Humans

The majority of the published epidemiologic studies reported on breast cancer. The results were mixed, regardless of whether PFOS levels were measured before or after breast cancer diagnosis. The studies that measured PFOS levels at or after breast cancer diagnosis may be susceptible to reverse causation bias; PFOS internal levels could have been affected by the onset and/or treatment of breast cancer. The inconsistencies may also reflect differences in the levels of PFOS exposure and genetic susceptibilities across study populations. The possibility that positive findings were due to chance, publication bias, or reverse causation could not be ruled out. There were too few studies for other cancer sites to draw conclusions. See Section 3 for more detailed information on carcinogenicity studies in humans.

Carcinogenicity Studies in Animals

Long-term carcinogenicity studies of PFOS potassium salt were conducted in male and female Crl:CD (SD) BR rats by Thomford (2002) and were reported by Butenhoff et al. (2012a). Liver hepatocellular tumors were increased in male (adenoma) and female (adenoma and carcinoma combined) rats treated with PFOS in these two-year feeding studies (statistically significant by pairwise comparison with control and by trend test). One hepatocellular carcinoma was observed in the high-dose female rats; this is a rare tumor type in this strain. An increase in pancreatic islet cell carcinomas (statistically significant by trend test) was observed in male rats. Mammary gland fibroadenomas were increased in female rats administered 0.5 parts per million (ppm) PFOS in feed for two years (statistically significant by pairwise comparison with control). Thyroid follicular cell adenomas were increased in male rats administered 20 ppm PFOS in feed for one year then fed basal diet for an additional year (statistically significant by pairwise comparison with control). Thyroid follicular cell adenomas and one carcinoma were observed in female rats treated for two years, and one thyroid follicular cell adenoma was observed in a female rat administered 20 ppm PFOS in feed for one year then fed basal diet for an additional year; thyroid follicular cell adenomas and carcinomas are rare in female rats of this strain.

In a tumor promotion study, six-month dietary exposure to PFOS as a promoter after initiation with aflatoxin B1 in rainbow trout resulted in increased liver tumor incidence (adenoma and carcinoma combined; statistically significant by logistic regression analysis performed by the study authors) (Benninghoff et al. 2012).

See Section 4 for more detailed information on carcinogenicity studies in animals.

Mechanistic Considerations and Other Relevant Data

Pharmacokinetics

Review of pharmacokinetic data shows interspecies similarities in the absorption and distribution of PFOS, and some interspecies differences in the excretion and serum half-life. PFOS is not known to be metabolized in animals or humans. PFOS is well absorbed with oral administration in animals and is widely distributed throughout the body in both humans and animals. PFOS half-life is significantly longer in humans (3.4 years) versus rodents (24-83 days) and monkeys (110-200 days). The highest PFOS levels are generally detected in the liver, plasma, and kidney in both humans and animals. PFOS can cross the blood-brain barrier and the placenta, and PFOS and several precursors have been detected in breast milk or paired maternal and cord serum samples taken after delivery. PFOS excretion pathways in humans include urinary and fecal excretion and incorporation into nails and hair. Additional PFOS elimination routes include pregnancy-related losses, elimination via breast milk, and menstrual blood loss in females. Several precursors (*e.g.*, perfluorooctane sulfonamide) have been shown to form PFOS via biotransformation in *in vivo* or *in vitro* studies. Isomeric differences in transformation rates and/or elimination half-lives were observed in some PFOS and PFOS precursor studies. See Section 5.1 for more detailed information on pharmacokinetics.

Key characteristics of carcinogens

The 10 key characteristics (KCs) of carcinogens were used to organize the data relevant to carcinogenicity from mechanistic studies of PFOS. KCs are characteristics of agents that cause cancer, and can encompass many types of mechanistic endpoints. OEHHA uses this approach to systematically identify, organize, and summarize information on mechanisms of carcinogenesis. Most of the evidence relates to seven of the 10 KCs and is summarized here. See Section 5.3 for more detailed summaries of data relevant to the KCs.

Is genotoxic

Overall, there is some evidence of mutagenicity and suggestive evidence of chromosomal effects and DNA damage induced by PFOS. PFOS is not mutagenic in bacterial assays, but induced mutations in transgenic mice and fish, and in rodent cells *in vitro*. Several *in vivo* and *in vitro* rodent studies found induction of micronuclei, although one study showed negative results in a human cell line. One study reported

no effect on chromosomal aberrations (CA) in human peripheral blood cells while another reported increased CA in onion. Positive evidence of induction of DNA strand breaks was observed in various cell types from treated rats, primary mouse cells, and various organisms including zebrafish and carp, with no effects observed in human sperm cells or Syrian hamster embryo cells. One study reported increased γ-H2AX in transgenic mouse cells *in vitro*. Two human studies from Korea and Taiwan reported a positive association between serum PFOS and urinary 8-OHdG (a biomarker for oxidative DNA damage), while another study from Taiwan reported no association.

Induces epigenetic alterations

Studies show that PFOS can induce epigenetic changes, including altered methylation of regions associated with specific genes, global methylation changes, miRNA changes, and alterations in expression of DNA methyltransferases (DNMTs). Many of these effects have been correlated with processes involved in the development of cancer. Associations with altered gene expression, altered phenotype, and cancer, however, are not always clear.

Induces oxidative stress

Studies of oxidative stress responses in humans, rodents, zebrafish and plants indicate that PFOS can induce oxidative DNA damage, generation of reactive oxygen species (ROS) or reactive nitrogen species (RNS), and lipid peroxidation. In observational studies in humans, higher serum PFOS levels were associated with significant dose-dependent increases of oxidative DNA damage (in two of three studies), lipid peroxidation, and ROS. Significant increases of ROS/RNS and lipid peroxidation were reported in multiple experimental test systems. Significant decreases in total antioxidant capacity were reported in one rodent study *in vivo*, but no change was reported in one human observational study and one zebrafish study. PFOS exposure in multiple experimental systems induced changes in antioxidant enzyme activities/levels and glutathione status. Changes in the protein or gene expression of Nrf2 have also been observed. Evidence from genomic and metabolomic studies also provide some evidence for the induction of oxidative stress by PFOS.

Induced chronic inflammation

The effects of PFOS on pro-inflammatory cytokine production have been tested in multiple human cell types *in vitro*. Increases of interleukin-1 (IL-1), and decreases of IL-10, interferon gamma (IFN-γ), and tumor necrosis factor alpha (TNF-α) have each been reported in a few of these *in vitro* studies. The effects of PFOS on other human cytokines, such as IL-2, IL-4, IL-6, and IL-8, remain unclear. Animal studies reported increased IL-1 and IL-6 production in zebrafish and several cell types in rodents, with inconsistent results for IL-6 production by mouse peritoneal macrophages. The effects

of PFOS on other cytokines, such as IL-4, IL-5, IL-10, IFN-γ and TNF-α, remain unclear from animal studies.

Is immunosuppressive

PFOS suppressed immunoglobulin M (IgM) responses in four mouse studies following an antigen challenge, and in one study without antigen challenge. Two studies in mice reported no change in IgM response, and one study in rats reported an increase. PFOS has also been shown to reduce the number and proliferation of thymocytes and splenocytes in mice in multiple studies. Two additional studies reported no change; a third study reported an increase in proliferation of dolphin CD4+ and CD8+ T lymphocytes exposed *in vitro*. Several studies have shown that PFOS suppresses natural killer (NK) cell activity, including one study in cultured human blood cells and four studies in mice, although two other mouse studies reported an increase in NK cell activity. Taken together, these studies suggest that PFOS can suppress the immune system in ways that would allow neoplastic cells to escape immune surveillance, survive, and replicate to form tumors.

Modulates receptor-mediated effects

Several animal studies have shown that PFOS alters the expression of genes that are regulated by estrogen receptor alpha (ERα), peroxisome proliferator activated receptor alpha (PPARα), PPARγ, pregnane X receptor (PXR), and constitutive androstane receptor (CAR), and one reporter gene study shows PFOS activates murine PPARβ/δ *in vitro*. The evidence for estrogenic effects of PFOS also comes from increased ER reporter activity in human cell lines, increased proliferation of estrogen-responsive human breast cancer cell lines in several studies, weak binding to ER in fish, and similar gene expression patterns between PFOS and estradiol (E2) in fish. PFOS altered androgen receptor (AR) expression in rats, and one reporter gene study indicates PFOS inhibited AR activation by dihydrotestosterone (DHT). There is also evidence from animal studies that PFOS can decrease thyroid hormone levels and increase estradiol levels.

Alters cell proliferation, cell death or nutrient supply

Two studies in rats provide evidence that PFOS increases cell proliferation or inhibits apoptosis in the liver, with the effect on apoptosis being long-lived. A third rat study reported early transcriptional changes related to cell cycle control, apoptosis, and proliferation in the liver of rats exposed to PFOS *in utero* and via lactation. Multiple *in vitro* studies of human fetal liver, breast and ovarian cell lines showed an increase in cell proliferation with PFOS treatment. PFOS also altered the expression of proteins linked to cell proliferation, including increased levels of regulatory cell cycle proteins and growth factors in a human fetal liver cell line. One study reported that PFOS inhibits

gap junctional intercellular communications (GJICs), which regulate cell growth and proliferation via contact inhibition, in a rat liver epithelial cell line. An *in vitro* study in primary salmon hepatocytes reported a significant decrease in caspase 3B, an important marker for apoptosis, with a slight decrease in apoptosis.

1. INTRODUCTION

1.1 Chemical Identity of Perfluorooctane Sulfonic Acid and Its Salts and Transformation and Degradation Precursors

Perfluorooctane sulfonic acid (PFOS) is a member of a class of chemicals called per- and poly-fluoroalkyl substances (PFASs). It is a synthetic aliphatic chemical with a fully-fluorinated eight-carbon chain and a sulfonic acid functional group attached to carbon number eight. PFOS has been used to refer to the anion perfluorooctane sulfonate, as well as perfluorooctane sulfonic acid, since the anion and acid forms exist in equilibrium in aqueous solution. Salts of PFOS will dissociate in solution, releasing the PFOS anion. PFOS can also be formed by the transformation or degradation of a variety of PFOS precursors. In this document, the term "PFOS and its salts and precursors" is used to represent this group of chemicals.

1.1.1 Chemical identity of PFOS and its salts

PFOS exists in an equilibrium with perfluorooctane sulfonate, with the anion being the more predominant form, with low pKa (< 1) in the wide range of environmental and physiologically relevant pH values, 5 to 9 (ATSDR 2021; Cheng et al. 2009). The structure and CAS registry number (CAS RN) of the linear PFOS and its anion form are shown in Figure 1. PFOS can also exist as branched chain isomers (Table A1 in Appendix A).

PFOS is a solid at room temperature (*e.g.*, white powder for PFOS potassium salt). It is not volatile. It can be transported in the atmosphere in a particle-bound, non-gaseous state (UNEP 2006). PFOS is both hydrophobic and lipophobic, leading to its popular uses as a surfactant (Buck et al. 2011). Selected chemical properties of PFOS are listed in Table 1.

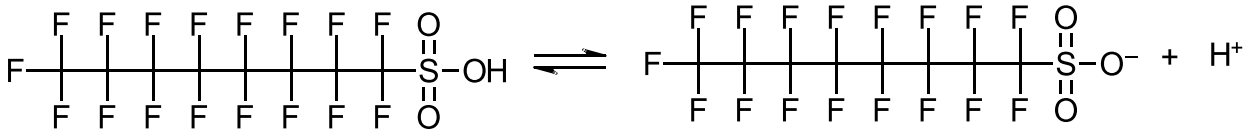

Perfluorooctane sulfonic acid (PFOS);
CAS RN: 1763-23-1

Perfluorooctane sulfonate;
CAS RN: 45298-90-6

Figure 1 Chemical structures of perfluorooctane sulfonic acid (PFOS) and perfluorooctane sulfonate

Table 1 Chemical properties of perfluorooctane sulfonic acid[a]

Chemical name	Perfluorooctane sulfonic acid
CAS RN	1763-23-1
Molecular formula	$C_8F_{17}SO_3H$
Molecular weight (g/mol)	500.13
Solubility in water at 25°C (mol/L)	$1.14*10^{(-3)}$
Boiling Point (ºC)	169
Vapor pressure (mmHg)	$2.48 * 10^{(-6)}$
Melting point (ºC)	84[b]
Octanol-water coefficient (Log K_{ow})	5.61
Acid dissociation constant (pKa)	<1[c]

[a] Values are from US EPA's CompTox Chemical Dashboard unless otherwise specified.
[b] Predicted value
[c] This empirical data (pKa < 1) measured by electrospray ionization mass spectrometry (Cheng et al. 2009) is consistent with predicted pKa values of 0.14 (ATSDR 2021) and -3.27 (Brooke et al. 2004).

Manufactured PFOS products contain both linear and branched isomers. Branched PFOS isomers may contain linear perfluoroisopropyl and *t*-perfluorobutyl structures with monomethyl (CF_3-) or multiple methyl-substituted groups attached to different carbon positions. Commercial grade PFOS produced using the historical electrochemical fluorination (ECF) process contains a mixture of around 30% branched and 70% linear isomers (Arsenault et al. 2008; Buck et al. 2011), whereas commercial grade PFOS produced using the newer telomerization process is comprised of nearly 100% linear PFOS isomer (Kato et al. 2011; Schulz et al. 2020). The chemical structures of ten identified branched PFOS isomers (*e.g.*, CF_3 isopropyl branched PFOS isomers) are shown in Table A1 (Appendix A). The structural differences between linear and branched isomers may result in differences in pharmacokinetics (*e.g.*, partition, distribution, and bioaccumulation within the body) and pharmacodynamics (Benskin et al. 2009b; Schulz et al. 2020).

Table A2 (Appendix A) also includes 17 PFOS salts, of which the four most common are the ammonium, diethanolamine, potassium, and lithium salts. Similar to PFOS, PFOS salts may also exist as a mixture of linear and branched isomers.

1.1.2 Chemical identity of PFOS precursors

In this document, "transformation and degradation precursors of PFOS" ("PFOS precursors" for short), are defined as substances containing the PFOS moiety ($C_8F_{17}SO_2$) that may transform or degrade to PFOS.

A non-exhaustive list of 169 PFOS precursors is given in Table A3 and Table A4 (Appendix A). This list was compiled primarily based on information from several published lists of potential PFOS precursors, namely by Environment Canada (2006), OECD (2007), and Australia's National Industrial Chemicals Notification and Assessment Scheme (NICNAS) (NICNAS 2019a, 2019b). Several additional precursors were identified from the peer-reviewed literature and from the US EPA Computational Toxicology (CompTox) Chemicals Dashboard (https://comptox.epa.gov/dashboard/chemical_lists/pfasmaster). The ability of the chemicals included in Tables A3 and A4 to transform or degrade to PFOS was evaluated either through the use of 11 quantitative structure-activity relationship (QSAR)-based metabolic simulators embedded in the OECD Toolbox v.4 (https://qsartoolbox.org/) or knowledge-based expert judgment (personal communication with Dr. K. Durkin, UC Berkeley). The approaches used to identify these PFOS precursors are briefly described in Appendix A.

For most PFOS precursors, there is a lack of data relevant to carcinogenicity from studies in humans, animals, cultured cells or other types of model systems (*e.g.*, high throughput screening (HTS) systems). A quick screening of the published scientific literature and of the bioactivity modules on the US EPA CompTox Chemicals Dashboard site (https://comptox.epa.gov/dashboard, accessed in February 2021) was performed on each listed PFOS precursor, and seven were identified as having some data relevant to carcinogenicity. These seven PFOS precursors are shown in Table 2 below.

Table 2 Seven PFOS precursors with cancer-related toxicity data

Chemical name	Abbreviation	CAS RN	Chemical structure
Perfluorooctane sulfonyl fluoride	PFOSF	307-35-7	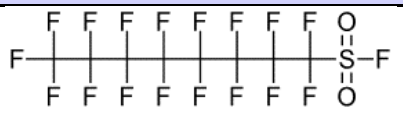
Perfluorooctane sulfonamide	PFOSA	754-91-6	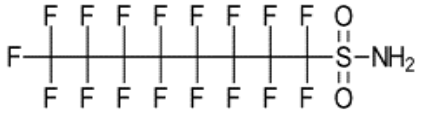
N-Methyl perfluorooctane sulfonamide acetic acid	MePFOSAA	2355-31-9	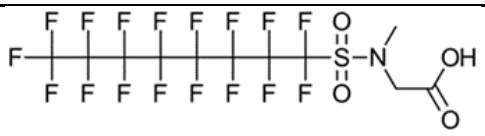
N-Methyl perfluorooctane sulfonamidoethanol	MePFOSE	2448-09-7	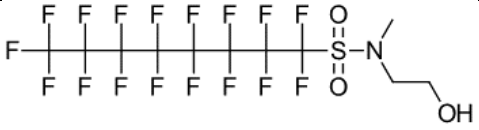
N-Ethyl perfluorooctane sulfonamide	EtPFOSA	4151-50-2	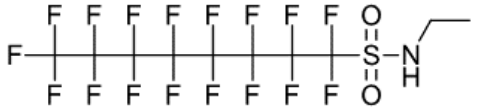
N-Ethyl perfluorooctane sulfonamido acetic acid	EtPFOSAA	2991-50-6	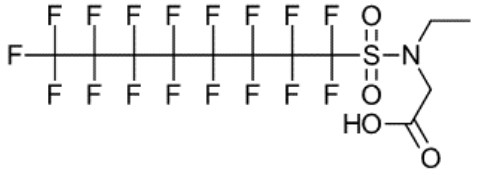
N-Ethyl perfluorooctane sulfonamidoethanol	EtPFOSE	1691-99-2	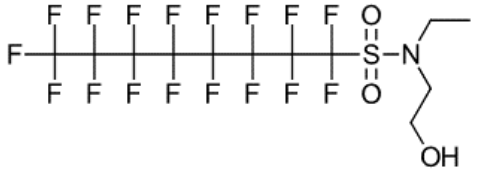

1.2 Production, Sources, and Use

The 3M Company (3M, St. Paul, MN, USA) was the major manufacturer of PFOS in the US until the company voluntarily phased out production by approximately 2002 (De Silva et al. 2009). In the US, ECF was used for commercial production of PFOS, in which perfluorooctane sulfonyl fluoride (PFOSF; $C_8H_{17}SO_2F$; a PFOS precursor) was the primary intermediate (Schulz et al. 2020; UNEP 2006). The ECF process generates a mixture comprised of branched (~30%) and linear (~70%) PFOS isomers (Buck et al. 2011). Commercial grade PFOS produced by 3M was used as the test substance in the animal cancer bioassays (see section 4.1).

PFOSF may also be used to make other PFASs, many of which can either be transformed or degraded to PFOS, or contain residual amounts of unreacted PFOS or PFOS precursors. For example, PFOSF can be reacted with methyl- or ethyl-amine to form N-ethyl- or N-methyl-perfluorooctane sulfonamide (EtPFOSA or MePFOSA, respectively; PFOS precursors). Further reaction of these N-alkyl perfluorooctane sulfonamides (PFOSAs) with ethylene carbonate results in the formation of N-ethyl- or N-methyl-perfluorooctane sulfonamidoethanol (EtPFOSE or MePFOSE, respectively; PFOS precursors), two additional PFASs manufactured in large volumes by 3M before the voluntary phase-out (Martin et al. 2010). EtPFOSE and MePFOSE can be used to manufacture acetates, phosphorus esters, acrylate esters and their respective copolymers. These products may contain up to 1-2% of unreacted residuals, including PFOS precursors.

Direct sources of PFOS include emissions from its manufacture and use in various applications, and releases from products containing PFOS, while indirect sources of PFOS include numerous precursor compounds that can undergo degradation or transformation to form PFOS (Buck et al. 2011). PFOS precursors contain the perfluorooctane moiety and can degrade or transform to PFOS abiotically or biotically under industrial, environmental, or metabolic conditions (Buck et al. 2011; Martin et al. 2010). Major precursor degradation mechanisms that can form PFOS have been reviewed by Martin et al. (2010) and Buck et al. (2011), including abiotic hydrolysis, photolysis, and oxidation. Microbial degradation of PFOS precursors has also been demonstrated (Benskin et al. 2013; Liu and Mejia Avendaño 2013; Zhang et al. 2017a). In addition, the *in vivo* biotransformation of PFOS precursors to form PFOS has been observed in earthworms (Zhao et al. 2019; Zhao et al. 2020) and rats (Chang et al. 2017), while an intermediate step in the biotransformation of one PFOS precursor (*i.e.*, metabolism of EtPFOSA to PFOSA) has been observed to occur in sheep (Martin et al. 2010). The degradation or transformation processes may involve multiple steps and can be complicated. For example, PFOS precursors such as EtPFOSE may undergo serial reactions by microbial degradation in different environmental media (such as in sediment or activated sludge) to form several intermediate biotransformation products such as EtPFOSAA (N-ethyl perfluorooctane sulfonamide acetic acid), EtPFOSA, and PFOSA, which ultimately form PFOS under both abiotic and biotic conditions (Zhao et al. 2019). In addition, higher PFOS levels in water effluent (compared to influent) were reported after water treatment with chlorine or ozone, suggesting contributions from transformation of PFOS precursors present in the untreated water, such as MePFOSE, EtPFOSE, and PFOSAmS (perfluorooctanesulfonamido ammonium salt) (Eriksson et al. 2017; Xiao et al. 2018).

PFOS and its salts and precursors have been used in a wide array of industrial materials and consumer products to confer properties such as stain-, grease-, heat-, and water-resistance (D'Eon J and Mabury 2011; Paul et al. 2009; Prevedouros et al.

2006). As summarized in OEHHA (2021), consumer applications include nonstick coatings for cookware, water-repellant treatments for fabrics and leather, stain- and dirt-resistant treatments for carpets, and oil- and grease-repellant treatments for paper and packaging. Industrial applications include production of firefighting foams, pesticides, surfactants, fume suppressants, semiconductors, photoresist and antireflective coatings, and hydraulic fluids. Though 3M voluntarily discontinued its production and use of PFOS in the US from the early 2000s, and seven other companies participating in the US Environmental Protection Agency (US EPA) PFOA Stewardship Program[3] agreed to phase out PFOA and PFOA-related chemicals (including PFOS) by 2015, some companies may have continued to import or produce PFOS for use in the US (ATSDR 2021). In 2009, PFOS, its salts and PFOSF were added to the Stockholm Convention's list of globally restricted Persistent Organic Pollutants (POPs)[4]. However, some critical uses, such as fume suppression, were exempted and substantial production has continued in countries other than the US, including China (ATSDR 2021; Liu et al. 2017; OECD 2015). Some PFOS precursors are still manufactured globally for a variety of uses, such as EtPFOSE in paper and board packaging applications and MePFOSE in surface treatment applications (*e.g.*, carpets, upholstery and textiles). Another PFOS precursor, EtPFOSA, is an active ingredient in the pesticide sulfluramid, which is not currently registered for use in the US but is used extensively in South America for management of leaf-cutting ants and other ants and termites (Pinas et al. 2020).

1.3 Occurrence and Exposure

PFOS and its salts and precursors are ubiquitous, with levels measured in environmental media, biota, and humans. PFOS is very stable in the environment and resistant to biodegradation, photooxidation, direct photolysis, and hydrolysis given the strength of the carbon-fluorine bonds (ATSDR 2021; Buck et al. 2011). Environmental occurrence of PFOS is discussed in detail in OEHHA (2021). Briefly, PFOS has been identified in soils with and without known emission sources nearby, including soil samples from California (Rankin et al. 2016; Sepulvado et al. 2011; Strynar et al. 2012). PFOS has been identified in drinking water, groundwater, and surface waters, including in California[5] (Hu et al. 2016). PFOS is readily taken up by plants and has been shown to accumulate in animals, including domestic livestock and wildlife (de Wit et al. 2020;

[3] https://www.epa.gov/assessing-and-managing-chemicals-under-tsca/fact-sheet-20102015-pfoa-stewardship-program [Accessed June 11, 2021]

[4] http://www.pops.int/Implementation/IndustrialPOPs/PFOS/Overview/tabid/5221/Default.aspx [Accessed June 11, 2021]

[5] https://www.waterboards.ca.gov/pfas/drinking_water.html [Accessed June 11, 2021]

Gebbink et al. 2016; Ghisi et al. 2019; Kratzer et al. 2011; Lechner and Knapp 2011; Stahl et al. 2014; Stahl et al. 2009). PFOS has been detected in the US in samples of fish and ground turkey (Fair et al. 2019; FDA 2019a, 2019b) and has been detected in additional foods in other countries, with the highest levels occurring in fish and meat (Domingo and Nadal 2017; EFSA 2020; Trudel et al. 2008). PFOS has been detected in indoor dust in multiple studies, including a recent study of childcare centers in California in which all carpet and dust samples were found to contain PFOS (Goosey and Harrad 2011; Kato et al. 2009; Strynar and Lindstrom 2008; Wu et al. 2020b). In addition to the wide variety of older consumer products known to contain PFOS, some newer products tested in Europe (including imported products), such as outdoor clothing, leather products, carpets, and certain food contact materials, have been shown to have detectable levels of PFOS (Kotthoff et al. 2015; Surma et al. 2015; Vestergren et al. 2015).

Environmental occurrence of PFOS precursors as reported in studies published through late 2015 have been reviewed by Land et al. (2018). More recent studies report the presence of PFOS precursors, including MePFOSE, EtPFOSE, MePFOSA, and EtPFOSA in indoor dust, including in California household dust (Hall et al. 2020; Shin et al. 2020; Winkens et al. 2018). PFOS precursors are also present in foods; PFOSA and PFOSAA (perfluorooctane sulfonamide acetic acid) were detected in meat, fish and/or eggs in a Swedish market basket study (Gebbink et al. 2015). A recent study of US cosmetic products (including foundations, lip products, and mascaras) reported detectable levels of PFOS precursors such as PFOSA and EtPFOSA (Whitehead et al. 2021). Human exposure to PFOS precursors has been confirmed by biomonitoring. Specifically, measurements of PFOSA and PFOSAA in Californians have been reported in serum samples of highly-exposed firefighters (Dobraca et al. 2015; Shaw et al. 2013; Trowbridge et al. 2020), general populations (Hurley et al. 2018a, 2018b; Wang et al. 2011), and pregnant women and their newborns (in cord blood) (Cohn et al. 2020; Kim et al. 2020; Morello-Frosch et al. 2016).

Humans are exposed to PFOS through contaminated food and drinking water, ingestion of dust, and inhalation of indoor and outdoor air. Studies investigating the relative contribution of exposure pathways have consistently identified ingestion of contaminated food and drinking water as the predominant contributors to exposure for most individuals, although there can be considerable variation amongst individuals (Egeghy and Lorber 2011; Harrad et al. 2019; Haug et al. 2011; Poothong et al. 2020; Shan et al. 2016; Sunderland et al. 2019; Trudel et al. 2008). PFOS has also been detected in breast milk in the US and other countries, which contributes to dietary intake for infants and toddlers (Tao et al. 2008; Zheng et al. 2021). PFOS precursors are thought to generally contribute less than 10% to PFOS exposures within the general population (Fromme et al. 2009; Gebbink et al. 2015; Vestergren et al. 2008). However,

PFOS precursors may contribute up to 60-80% to PFOS exposures for certain highly exposed individuals (Vestergren et al. 2008).

PFOS exposure can be directly assessed using biomonitoring data in matrices such as blood, urine, nails, and hair (Wang et al. 2018b). Serum is considered the most appropriate exposure matrix for measurement of PFOS and is commonly used in epidemiologic studies (Calafat et al. 2019). In the 2013-2014 US National Health and Nutrition Examination Survey (NHANES), all serum samples from participants had detectable PFOS, with a weighted average serum concentration of 4.1 ng/ml (Jain 2018), whereas less than 0.1% of urine samples tested had detectable PFOS (Calafat et al. 2019). Several biomonitoring studies have reported PFOS serum levels in California residents, including studies conducted by the Biomonitoring California program. Generally, PFOS serum levels in Californians have decreased from earlier peaks (Kim et al. 2020; Olsen et al. 2012; Wang et al. 2011), consistent with nationally representative data including studies conducted as part of NHANES, which show an appreciable decline in serum levels in residents of the US since the phase-out of PFOS began in the early 2000s. Table C1 in Appendix C presents reported PFOS levels in Californians. The most recent data, from Biomonitoring California analyses of samples collected from adults in Riverside, San Bernardino, Imperial, Mono, and Inyo counties in 2019 and from adults in Los Angeles county in 2018, report average serum levels of 2.40 ng/ml (95th percentile, 8.72 ng/ml) and 2.13 ng/ml (95th percentile, 8.33 ng/ml), respectively (https://biomonitoring.ca.gov).

1.4 Reviews by CalEPA or Other Health Agencies

1.4.1 Reviews by CalEPA

On July 22, 2021, OEHHA announced the release of the first public review draft of the "Proposed Public Health Goals for Perfluorooctanoic Acid and Perfluorooctane Sulfonic Acid in Drinking Water" (OEHHA 2021) and published the draft technical support document on the OEHHA website. A PHG is the level of a drinking water contaminant at which adverse health effects are not expected to occur from a lifetime of exposure.

The proposed PHG (1 part per trillion, or 1 ppt) is based on liver and pancreatic tumors in laboratory animals, and is set at a level of risk of one additional cancer case per one million persons exposed over a lifetime. The draft document also presents health-protective drinking water concentrations for noncancer health effects. The proposed noncancer health-protective concentration is 2 ppt for PFOS, based on increased total cholesterol in humans.

In developing this hazard identification document, the OEHHA (2021) draft PHG document served as a recent, comprehensive review of relevant literature and is cited in various sections.

1.4.2 Reviews by other health agencies

PFOS has not been reviewed or classified as to its potential carcinogenicity by the International Agency for Research on Cancer (IARC), the National Institute for Occupational Safety and Health, the National Toxicology Program (NTP) Report on Carcinogens, or the US Food and Drug Administration (US FDA).

In 2016, the US EPA evaluated PFOS in drinking water and concluded that there is "suggestive evidence of the carcinogenic potential of PFOS in humans" (US EPA 2016b).

In 2016, Health Canada (2016) reviewed PFOS in drinking water and acknowledged that "[c]hronic exposure to PFOS has been associated with both cancer and non-cancer effects in animals and humans". Regarding the epidemiologic evidence for carcinogenicity, Health Canada noted "[a]lthough some evidence of an association between PFOS and the risk of cancer has been observed, the effects were equivocal, and no clear trend could be determined due to limitations in the studies (small number of cases, confounding, and participant selection bias)".

In 2018, the European Food Safety Authority (EFSA) concluded that "human epidemiological studies provide insufficient support for carcinogenicity of PFOS" (EFSA 2018). In 2020, EFSA reviewed additional epidemiologic and mechanistic studies related to cancer published since the 2018 review and reaffirmed their prior conclusion (EFSA 2020).

In 2021, the Agency for Toxic Substances and Disease Registry (ATSDR) evaluated PFOS for its toxicity to humans but did not issue its own conclusion regarding the chemical's carcinogenic potential. ATSDR included the US EPA's conclusion in its report (ATSDR 2021).

2. OVERVIEW OF SYSTEMATIC LITERATURE REVIEW APPROACH

2.1 Literature Search Process

Literature searches on the carcinogenicity of PFOS, its salts, and transformation and degradation precursors were conducted in February 2021. The goal was to identify peer-reviewed journal articles, print and digital books, reports, and gray literature that reported toxicological and epidemiological information on the carcinogenicity of this chemical.

As described below, we used an approach similar to that recommended by the National Toxicology Program (NTP) Handbook for Preparing Report on Carcinogens (RoC) Monographs (NTP 2015; https://ntp.niehs.nih.gov/ntp/roc/handbook/roc_handbook_508.pdf).

Three searches were conducted:

- Primary searches in major biomedical databases (PubMed, Embase, and Scopus), conducted by OEHHA librarian Nancy Firchow, MLS
- Searches in other data sources, including authoritative reviews and reports, and databases or web resources, conducted by OEHHA scientists
- Additional focused searches, conducted by OEHHA scientists

In addition to data identified from these searches, OEHHA also considered the following information:

- One submission received from the data call-in period
- OEHHA (2021), "Proposed Public Health Goals for Perfluorooctanoic Acid and Perfluorooctane Sulfonic Acid in Drinking Water"

Primary searches for PFOS and its salts were executed using chemical synonyms in combination with search terms for human cancer studies, animal cancer studies, toxicokinetic studies, and mechanistic studies such for as genotoxicity and other key characteristics. There were no restrictions in the searches on exposure route or duration of exposure on cancer studies in humans, cancer studies in animals or mechanistic studies, or on publication language. Primary searches for the PFOS precursors were executed with chemical terms only without further restrictions.

For detailed information on the literature search process, please see Appendix B.

2.2 Literature Screening Process

HAWC (Health Assessment Workspace Collaborative, https://hawcproject.org) was used as a tool in the systematic review of the literature following the guidance provided in NTP (2015). One HAWC project was created for PFOS and its salts, and one for PFOS precursors. The same literature screening processes were applied to both HAWC projects. Citations retrieved from literature searches were uploaded to EndNote libraries, and duplicates were removed. Next, the EndNote libraries were uploaded to HAWC for multi-level screening using specific inclusion and exclusion criteria (see Appendix B). For example, certain citations identified by the literature search as epidemiological studies were later excluded, and the reasons for exclusion are provided in Appendix D.

In Level 1 screening, each citation was first screened independently by two OEHHA scientists, based solely on titles and abstracts, to eliminate studies or articles that do not contain information on PFOS or its precursors on any of the key topics covered in this cancer hazard identification document, such as cancer studies in humans and animals, toxicokinetics, metabolism, genotoxicity, or other cancer-associated mechanisms. The initial screen was intended to identify all studies deemed to have a reasonable possibility of containing information that could be useful for the review process. Papers identified for inclusion during Level 1 screening were tagged in HAWC according to key topics.

In Level 2 screening, full-text papers for all citations that passed the Level 1 screening were obtained and screened independently by two OEHHA scientists, using similar inclusion/exclusion criteria as was used in the Level 1 screening.

Following Level 2 screening, the tagging of articles according to key topics was updated in HAWC. Level 1 and 2 screenings were repeated and HAWC search results were updated if additional relevant studies in addition to those cited in the original set of publications ("secondary citations") were identified.

Table Builder (Shapiro et al. 2018), a web-based application, was applied to systematically extract and analyze the data that were included in Section 3, Carcinogenicity studies in humans. Additionally, Table Builder was used as a custom-made database to generate Word tables in this document.

More than 1400 references, including peer-reviewed journal articles and government reports, were identified for inclusion through these search strategies. Among these, around 500 references were cited in this document.

3. CARCINOGENICITY STUDIES IN HUMANS

3.1 Introduction

The epidemiologic literature on the carcinogenicity of PFOS and its salts was identified through a systematic search of several databases. A systematic search for cancer epidemiology studies on precursors of PFOS (see Section 2.1) was also conducted. Appendix B provides a description of the details of the literature search strategy, including the search question, literature search terms by database searched, and the literature decision tree. A similar analysis of the literature on PFOS and cancer was conducted by the OEHHA Public Health Goals (PHG) program; the methods are presented in OEHHA (2021), the proposed PHGs for PFOA and PFOS.

3.1.1 Methods

All human epidemiologic studies of PFOS and cancer presenting results as relative risks, mean differences, regression or correlation coefficients, or other appropriate outcome metrics were eligible for inclusion. No restrictions were placed on the methods used to evaluate PFOS exposure levels although almost all studies we identified assessed exposure using blood concentrations of these chemicals. Studies that estimated PFOS intake based on industrial hygiene records were also considered eligible for inclusion.

We included studies that were of cohort, case-cohort, nested case-control and case-control designs. Cross-sectional studies were excluded due to the potential for reverse causation or exposure misclassification. Similar concerns about reverse causation may also apply to case-control studies with cross-sectional designs. Furthermore, since cross-sectional studies measure prevalent rather than incident cases, the data reflect determinants of survival as well as etiology (Hennekens et al. 1987). Ecologic studies without exposure data on the individual level were excluded due to the potential for ecologic fallacy and confounding. We excluded case-reports because of the lack of a comparison group, and conference abstracts because the results are considered preliminary as they have not been subject to peer review for journal publication. Studies without original data (*e.g.,* reviews or editorials) were also excluded but reviewed to identify publications with primary data that may have been missed in the literature search. There were no exclusions based on study location, language, or statistical adjustments. When screening articles for inclusion, we first screened based on title and abstract and then full article review.

Our literature search identified 23 epidemiologic studies (cohort (n=7), case-control (n=6), nested case-control (n=6), and cross-sectional designs with long latency periods

studies (n=4)) that investigated associations between exposure to PFOS and cancer, 18 of which met the eligibility criteria described above for inclusion (see Appendix B). For several cancer endpoints, where there was sparse literature and the results were inconsistent, the published data are described briefly. For certain cancer endpoints with more published data (*e.g.,* breast cancer), a more detailed review of the studies as well as tables are presented. Studies that were not included in this section are listed in Appendix D.

The quality of each study identified for inclusion was evaluated as well as the major aspects of causal inference using an updated version of the Bradford Hill criteria (Hill 1965). The criteria used to assess the quality of studies is similar to those described in the NTP Report on Carcinogens Handbook (NTP 2015) and the IARC Monographs Programme Preamble (IARC 2019). In assessing study quality, special attention was given to the assessment of biases, which in observational studies are usually grouped into 1) selection bias, 2) information bias, and 3) confounding (Rothman et al. 2015). We also assessed features of study design, temporality of the association, statistical significance, magnitude of association, and dose-response. There were also several considerations specific to assessing the epidemiologic literature on PFOS and cancer, which are discussed briefly below.

3.1.2 Key issues in the consideration of the epidemiologic data on PFOS and cancer

Reverse causation and timing of exposure assessment

Reverse causation may be a concern in some epidemiologic studies where serum PFOS levels were measured at or near the time of cancer diagnosis. Hormonal or other physiological changes as well as behavioral changes associated with the onset of disease and treatment may alter serum PFAS levels (Dhingra et al. 2017; Hurley et al. 2018b; Steenland and Winquist 2021), which may be of concern for assessing studies of PFOS and cancer. Therefore serum PFOS levels measured at or after the time of diagnosis might not accurately reflect PFOS levels at a time that would be relevant to cancer causation, given the latency period between the occurrence of exposure and the development/detection of cancer (Steenland and Winquist 2021).

Estimates of the half-life of PFOS in human blood have been reported to range from 1.7-8.7 years (see Section 5.1 Pharmacokinetics and Appendix E). If the latency period were short (*e.g.*, shorter than the half-life of PFOS), then PFOS levels measured at or near the time of diagnosis could potentially be a relevant measure. However, given the long latency that is usually associated with environmentally-related adult cancers, there is the possibility that cancer diagnosis or treatment could lead to changes in physiology

or personal habits (medication use, behaviors) that could affect PFOS levels (reverse causation).

Another concern is that epidemiologic studies generally measured PFOS levels in the blood at a single time point. Although the estimated half-life of PFOS in human blood is fairly long, assessing exposure based on a single serum sample or samples collected only during a single short window of time could miss long-term exposure fluctuations or relevant exposure periods (Steenland and Winquist 2021).

Confounding

Confounding by other co-occurring chemical exposures, especially other PFASs present in the same environment, can be a specific problem in studies of PFOS and cancer (Steenland and Winquist 2021). Strong correlations between exposures to multiple PFASs, particularly collinear exposures, can result in an inability to distinguish effects of specific PFASs and difficulty in controlling for concurrent exposures (Joseph 2007, 2010).

3.1.3 Descriptions of cohorts with multiple cancer outcomes

Two cohorts reported on PFOS exposure and multiple cancer outcomes: an occupational cohort from Decatur, Alabama (Alexander et al. 2003) and a case-cohort analysis within the Danish general population (Eriksen et al. 2009). These cohorts are described in detail below and their results are presented elsewhere in the document when data are summarized by cancer site.

Occupational cohort from Decatur, Alabama

An occupational cohort from a 3M manufacturing facility in Decatur, Alabama assessed the association between PFOS and multiple cancers in multiple analyses and follow-ups (Alexander et al. 2003; Alexander and Olsen 2007; Grice et al. 2007; Olsen et al. 2004). This facility consisted of two plants: a film plant (considered unexposed to PFOS) and a chemical plant (considered exposed to PFOS) (Alexander et al. 2003). Chemical production began in 1961; the major sulfonated fluorochemical manufactured at the chemical plant was perfluorooctanesulfonyl fluoride (PFOSF, reported as POSF in the publication), which can degrade or be metabolized to PFOS (Olsen et al. 2003b). Although PFOSF-based chemicals were the primary fluorochemicals produced at this plant, exposure to other fluorochemicals was likely, including PFOA, due to production of the chemicals themselves (PFOA production began at the site in 1998) or as by-products of PFOSF production (Alexander et al. 2003). Indeed, biologic monitoring conducted to assess exposure in this cohort showed that serum levels of PFOA were slightly lower than PFOS but correlated.

PFOS exposure was measured in serum samples collected from a random sample of employees in 1998 (126 chemical plant employees and 60 film plant employees). The geometric mean serum PFOS levels were 941 ng/ml (95% confidence interval (CI), 787-1126 or 0.941 ppm; 95%CI, 0.787–1.126) and 136 ng/ml (95%CI, 114-161 or 0.136 ppm; 95%CI, 0.114–0.161) for chemical and film plant employees, respectively (Olsen et al. 2003b) (One ppm is equivalent to 1000 ng/ml). Olsen et al. (2003b) noted that the serum fluorochemical data correlated with industrial hygiene measurements among 3M employees.

An industrial hygienist and epidemiologist developed a job exposure matrix (JEM) by using the cumulative work history of employees, information on PFOS levels for specific jobs, and classifying the jobs into three subgroups of PFOS exposure: no workplace exposure (includes film plant jobs); low potential workplace exposure (includes chemical plant workers such as engineers, administrative assistants and managers); and high potential workplace exposure (includes chemical plant workers such as cell operators, chemical operators, and maintenance workers) (Alexander et al. 2003).

PFOS exposures in this cohort, even in the film plant workers considered to be non-exposed, were higher than in the other studies of PFOS and breast cancer and possibly also for other cancers (see Table 3). This would bias risk estimates towards the null when comparing exposed workers to those considered to be unexposed but who were actually exposed and could result in failure of the study to detect a true effect.

The studies conducted in this cohort assessed cancer outcomes by three methods: mortality data obtained from the National Death Index up to 1998 (Alexander et al. 2003), episodes of care from claims data records collected between 1993 and 1998 (Olsen et al. 2004), and cancer incidence determined from self-administered questionnaires supplemented by tracing mortality records in 2002 (Alexander and Olsen 2007; Grice et al. 2007). All analyses adjusted for age and gender, and Alexander et al. (2003) additionally adjusted for calendar period. There may have been overlap of cases between these studies, but the extent of overlap was not possible to assess. There was indication of a healthy worker effect: the standardized mortality ratio (SMR) for all deaths was 0.63 (95%CI, 0.53–0.74) when comparing the entire cohort to the general population of Alabama (Alexander et al. 2003).

In this cohort, exposure was assessed prior to disease ascertainment, thus reducing the possibility of reverse causation. However, the interpretation of these studies is limited mainly by the small numbers of cancer cases, and also by the lack of control for exposure to other chemicals (*e.g.*, PFOA), absence of information on potential confounders and possible selection bias (healthy worker effect). The analyses that determined cancer incidence from self-administered questionnaire followed by tracing mortality records may have under-ascertained cases (Alexander and Olsen 2007; Grice et al. 2007). Although there was high exposure to PFOS among certain job positions

that could potentially increase the ability to detect an effect, PFOS levels were also high among those considered to be non-exposed, which would bias risk estimates towards the null. In addition, there were small numbers of exposed cases for each cancer; therefore dose-response analyses were uninformative and there was limited power to detect an effect (Thomas 2009).

Case-cohort analysis within the Danish general population

Eriksen et al. (2009) conducted a case-cohort analysis within the Danish general population to investigate the association between plasma levels of PFOS and cancer risk. This analysis from the Danish prospective cohort study, "Diet, Cancer and Health", is part of the European Prospective Investigation into Nutrition and Cancer (EPIC) (Tjønneland et al. 2007). Plasma samples were taken at recruitment, and cases of prostate, bladder, pancreatic, and liver cancers were identified through the Danish Cancer Registry and the Danish Pathology Data Bank. Data were sampled according to a case-cohort design, and incidence rate ratios (IRRs) were estimated by the Cox proportional hazards model. The median plasma concentrations of PFOS were 35.0 ng/ml (95%CI, 16.8–62.4) and 29.3 ng/ml (95%CI, 14.2–55.6) for men and women, respectively, within the subcohort comparison group. The authors noted that plasma concentrations in this study were considerably lower than those measured in the occupational cohort from Decatur, AL (Alexander et al. 2003; Alexander and Olsen 2007), and therefore may have been too low to detect an effect.

3.2 Human Epidemiology Studies by Cancer Site

3.2.1 Breast cancer

It is estimated that among women in the US, breast cancer will be responsible for approximately 281,550 new diagnoses of invasive cancer cases, 49,290 new cases of ductal carcinoma *in situ*, and 43,600 deaths in 2021 (ACS 2021). Of the risk factors for breast cancer, several are also associated with PFOS exposure and therefore may be considered potential confounders. There is evidence that PFOS exposure is associated with obesity (Karlsen et al. 2017; Lauritzen et al. 2018; Maisonet et al. 2012; Tian et al. 2019b), perturbations in sex hormones (Wang et al. 2021), menopausal status (Ding et al. 2020), and reproductive factors (Bach et al. 2015; Fei et al. 2009; Zhou et al. 2017). Female hormone use, not being physically active, and alcohol use are important risk factors for breast cancer, although their association with PFOS exposure is unknown (ACS 2021; IARC 2020a).

For breast cancer, the results were inconsistent, which may be partially explained by differences in study design, the method or timing of exposure assessment, levels of PFOS exposure, and genetic differences. The studies as well as their unique

characteristics are discussed below. Several studies reported co-occurrence of PFASs; however, none accounted for the correlation between PFASs in the analyses of PFOS.

A number of studies that assessed PFOS and breast cancer were excluded due to limitations in their utility for causal inference, as stated above (see also Appendix D). Among these, two studies for which reverse causation was of potential concern were excluded: a case-control study from Taiwan with prevalent cancers that both recruited participants and assessed PFOS after diagnosis (Tsai et al. 2020) and a cross-sectional study (Omoike et al. 2020). Studies of cohort and case-control design that enrolled incident cases of breast cancer were included.

Characteristics of the epidemiologic studies that reported on breast cancer, including PFOS levels and exposure assessment methods, are displayed in tables below. Table 3 summarizes the exposure characterization, and Table 4 and Table 5 report details and results for studies that assessed exposure before and after breast cancer diagnosis, respectively.

Table 3 Exposure characterization of studies evaluating the association of PFOS with breast cancer

Reference and location	PFOS levels	Exposure assessment method/ matrix	Exposure assessment timing
PFOS assessed before diagnosis			
Alexander et al. (2003) and Olsen et al. (2003b); USA: Decatur, Alabama	Maximum: 10.6 ppm; geometric mean of chemical plant workers: 0.9 ppm (95%CI, 0.8–1.1); geometric mean of film plant workers: 0.136 ppm (95%CI, 0.114–0.161; range, 0.015–0.946) 1 ppm = 1000 ng/ml	Job exposure matrix (JEM) developed using cumulative employment history and serum PFOS levels measured in a random sample of employees	Before diagnosis; serum sampled in 1998; 1961-1997 for job history
Bonefeld-Jørgensen et al. (2014); Ghisari et al. (2017); Denmark	Mean levels among controls were 30.6 ng/ml for PFOS and 3.5 ng/ml for its precursor PFOSA.	Serum	Before diagnosis; 1996-2002
Mancini et al. (2020); France	Median (min–max) levels were 17.51 ng/ml (5.83–85.26 ng/ml) overall, 17.62 ng/ml (5.84–85.29 ng/ml) in breast cancer cases, and 17.32 ng/ml (6.61–59.12 ng/ml) in controls.	Serum	Before diagnosis; 1994-1999

Reference and location	PFOS levels	Exposure assessment method/ matrix	Exposure assessment timing
Cohn et al. (2020); USA: California	Median levels were similar in cases (30.5 ng/ml) and controls (32.1 ng/ml).	Maternal serum	Before diagnosis (in offspring); 1959-1967; collected generally 1–3 days after delivery.
PFOS assessed after diagnosis			
Bonefeld-Jørgensen et al. (2011); Ghisari et al. (2014); Greenland	Median: 45.6 ng/ml (95%CI, 45.7–69.3 ng/ml); range: 11.6–124 ng/ml	Serum	At diagnosis; 2000-2003
Wielsøe et al. (2017); Wielsøe et al. (2018); Greenland	Levels were significantly higher in the 77 breast cancer cases (median = 35.50 ng/ml; range: 4.23–187.0 ng/ml) than in the 81 controls (median = 18.2 ng/ml; range: 1.70–133.00 ng/ml) (p=0.001)	Serum	At enrollment; 2000–2003 and 2011–2014
Hurley et al. (2018b); USA, California	Levels did not significantly differ (p-value = 0.14) between cases (mean = 8.021 ng/ml; median = 6.695 ng/ml; range: 0.046–39.400 ng/ml) and controls (mean = 8.320 ng/ml; median = 6.950 ng/ml; range: 0.046–99.800 ng/ml)	Serum	After diagnosis and after treatment; 2011-2015. Blood specimens were collected an average of 35 months after case diagnosis (range of interval between diagnosis date and date of specimen collection = 9 months to 8.5 years).

Studies where PFOS exposure was determined by samples collected before breast cancer diagnosis

Five publications assessed PFOS exposure in samples collected prior to breast cancer diagnosis (Alexander et al. 2003; Bonefeld-Jørgensen et al. 2014; Cohn et al. 2020; Ghisari et al. 2017; Mancini et al. 2020).

The only occupational cohort study to report on breast cancer documented high PFOS exposure among workers at a chemical plant within a manufacturing facility in Decatur, Alabama (Alexander et al. 2003) (see above for a detailed description of this study). The SMR for breast cancer adjusted for age and calendar period was 1.57 (95%CI,

0.19–5.66); however, this was based on only two deaths from breast cancer occurring in the group classified as non-exposed, which is the major limitation to interpreting these findings.

Two publications from a case-control study nested within the Danish National Birth Cohort (DNBC) evaluated the association between serum PFOS levels in pregnant Danish women (collected between the 6th and 14th gestation weeks, prospectively) and their subsequent risk of premenopausal breast cancer (Bonefeld-Jørgensen et al. 2014; Ghisari et al. 2017). Significant correlation coefficients were found between PFOS and PFOA (0.69), PFOSA (0.58), PFNA (0.42), and PFHxS (0.15), and between PFOSA and PFOA (0.36) (Bonefeld-Jørgensen et al. 2014). In both publications, multivariable models were adjusted for age at blood draw, body mass index (BMI) before pregnancy, total number of gravidities, oral contraceptive use, age of menarche, smoking status and alcohol intake during pregnancy, physical activity, and maternal education.

The first publication from the DNBC analyzed PFAS levels as continuous variables and as quintiles, decided *a priori* (Bonefeld-Jørgensen et al. 2014). Analyses were stratified by mean age of diagnosis (≤40 or >40 years) due to the influence of age on breast cancer risk. The associations with PFOS or PFOSA exposure were inconsistent across analyses. PFOS, analyzed as a continuous variable, was not associated with breast cancer risk: relative risk (RR), 0.99 (95%CI, 0.98–1.01) in adjusted analyses (for each log ng/ml increase in serum PFOS level). However, when PFOS was analyzed as a categorical variable, there were some non-significant increases (RRs near 1.5) in the second and third quintiles. The magnitude of the RRs was greater in those >40 years of age at diagnosis; the RRs were around 2, although not statistically significant, for all but the highest quintile of PFOS exposure. There was no evidence of an exposure-response relationship, although tests for linear trend were not reported.

There were some positive associations observed with PFOSA, for which levels in cases were significantly higher than in the controls (p=0.04). When analyzed as a continuous variable, the unadjusted RR for PFOSA was 1.03 (95%CI 1.00–1.07) and the adjusted RR was 1.04 (95%CI 0.99–1.08). When analyzed using the first (lowest) quintile as the reference, the adjusted RR in the fifth quintile was 1.89 (95%CI, 1.01–3.54). The associations were stronger among those diagnosed <40 years of age; the adjusted RR for PFOSA in the highest quintile was 2.45 (95%CI, 1.00–6.00) and 1.07 (95%CI, 1.00–1.14) for a 1 ng/ml increase in PFOSA analyzed as a continuous variable. There was no evidence of an exposure-response relationship, although tests for linear trend were not reported.

A subsequent analysis within this study population from the DNBC investigated the interaction between breast cancer, serum PFAS levels (including PFOS and PFOSA), and single nucleotide polymorphisms (SNPs) in genes with known involvement in steroid hormone and xenobiotic metabolism (Ghisari et al. 2017). PFAS exposure was

dichotomized into “low” or “high”, based on median levels in the controls. Genotyping was conducted for the following genes and polymorphisms: cytochrome P4501A1 (CYP1A1: Ile462Val; rs1048943), CYP1B1 (Leu432Val; rs1056836), catechol-O-methyltransferase (COMT: Val158Met; rs4680), CYP17A1(A1→A2; rs743572), and CYP19A1(C→T; rs10046). P-values for deviation from the multiplicative interactions were obtained by fitting models with an interaction term for the gene and PFAS exposure (continuous variable). Interactions on an additive scale, which may be more biologically relevant, were not assessed.

RRs were presented for the association between log-transformed, continuous PFAS variables and breast cancer, stratified by genotype for each SNP. Positive associations were reported between PFOSA exposure and breast cancer in individuals with polymorphisms in genes involved in estrogen biosynthesis and metabolism, notably CYP1B1 wild type low activity Leu/Leu genotype (RR, 1.70; 95%CI, 1.03–2.82) and the higher 17β-estradiol hydroxylation activity variant Val/Val (RR, 1.95; 95%CI, 1.10–3.47), COMT low activity variant Met/Met (RR, 2.04; 95%CI, 1.27–3.28), CYP17 homozygous wild type A1/A1 (RR, 2.02; 95%CI, 1.29–3.16), and CYP19 homozygous wild type C/C (RR, 2.08; 95%CI, 1.06–4.09). The RR increased with increasing number of risk alleles for COMT, CYP17 and CYP19. For PFOSA, the p-value for multiplicative interaction was only statistically significant for COMT (p-interaction= 0.048). For PFOS, a positive association between exposure and breast cancer was observed only in individuals with the CYP19 homozygous wild type CC genotype (adjusted RR, 6.42; 95%CI, 1.08-38.3; p-interaction= 0.055).

Strengths of these analyses within the DNBC were the prospective data collection of PFAS levels within a well-defined cohort, minimizing concerns regarding possible information bias or reverse causation. This study adjusted for a large number of risk factors for breast cancer, which reduced the precision of the risk estimates. Multiple testing may be a concern due to the large numbers of genotypes studied.

In a case-control study of postmenopausal breast cancer nested in a large cohort of French women, referred to as the E3N cohort (Mancini et al. 2020), there were several ORs for PFOS exposure above 1.0 and statistically significant; however there were no clear dose-response trends overall. Statistical models were adjusted for smoking, exercise, diet, and several reproductive and development factors.

Dose-response trends were more consistent for hormone receptor positive tumors. There was a positive association between PFOS concentrations and ER+ tumors (third quartile, OR, 2.22; 95%CI, 1.05–4.69; fourth quartile: OR, 2.33; 95%CI, 1.11–4.90; p-trend= 0.04). For PR+ tumors, positive associations were found with the 3rd quartile (OR, 2.47; 95%CI 1.07–5.65) and fourth quartile of exposure (OR, 2.76; 95%CI, 1.21–6.30) with a significant exposure-response trend (p-trend = 0.01 reported in the text or 0.02 reported in the table of Mancini et al. 2020). For hormone receptor negative

tumors, positive associations were found for the second quartile of PFOS exposure and ER− tumors (OR, 15.40; 95%CI, 1.84–129.19) and the second quartile and PR− tumors (OR, 3.47; 95%CI, 1.29–9.15). Strengths of this study were the long follow-up of the E3N cohort, which allowed prospective investigation of long-term health effects of PFOS and collection of extensive information on the main breast cancer risk factors. Limitations include limited power when stratifying on hormone receptor status (due to this information being missing for a large number of cases and the low prevalence of ER−/PR− tumors in this population), the wide confidence intervals, and the single measurement of PFOS.

No association was observed between maternal perinatal serum PFOS levels and risk of breast cancer in daughters within a nested case-control study in California (the risk estimate for the main effects analysis between PFOS and breast cancer was not reported) (Cohn et al. 2020). Within the Child Health and Development Studies pregnancy cohort in California, a 54-year follow-up of 9300 daughters born 1959–1967, PFOS levels were measured in archived maternal perinatal serum (generally collected postpartum 1-3 days after delivery). The authors stated that "Total cholesterol and PFASs were measured in archived maternal perinatal serum for 102 daughter breast cancer cases diagnosed by age 52, and 310 controls matched on birth year and blood draw trimester."

Confounding factors considered in the statistical model were several maternal factors (serum levels of *p*,*p*′-DDT, *o*,*p*′-DDT, *p*,*p*′-DDE, cholesterol, and triglycerides, maternal age, race, early pregnancy weight, height, and history of breast cancer) and whether the daughter was breastfed. For maternal PFOS and breast cancer in daughters, the OR and 95%CI bounds were less than one and presented only in a forest plot. Exposure-response was not assessed. The authors stated that the joint association between PFOS, total cholesterol and EtFOSAA (a PFOS precursor) was assessed because PFASs have been correlated with higher serum cholesterol and metabolic outcomes in pregnancy and with breast cancer risk. Therefore, serum cholesterol levels would be an intermediate in the causal pathway between PFOS and breast cancer and may complicate interpretation of the findings. High maternal EtFOSAA, in combination with high maternal total cholesterol, was associated with an increased risk of breast cancer in daughters (OR, 3.6; 95%CI, 1.1–11.6; p-interaction < 0.05). EtFOSAA is a precursor to PFOS and therefore both PFASs were included in the same model.

Strengths of the study were that it was conducted within a large cohort, exposure information was collected prospectively, and case ascertainment was nearly complete through linkage to the cancer registry. This study assessed breast cancer diagnosed before age 52 and therefore the findings may not be generalizable to breast cancers in older women.

Table 4 Epidemiologic studies of breast cancer and PFOS assessed before diagnosis

Reference, study-design, location, and year	Population description & exposure assessment method	Exposure category or level	Risk estimate (95% CI)	Exposed cases/ deaths	Co-variates controlled	Comments, strengths, and limitations
Alexander et al. (2003) Cohort Decatur, Alabama **Enrollment or follow-up:** 1961-1997	**Population:** 2083 workers employed in two plants. To be eligible for inclusion in the cohort, a worker had to accrue at least 365 days of cumulative employment at the site by 31 December 1997. **Exposure assessment method:** job exposure matrix (JEM)	**Deaths: SMR**			Age, sex, calendar period	**Exposure information:** Median 13.2 years of employment (3.4-25.3 interquartile range) **Strengths:** Prospective collection of PFOS exposure assessed using a JEM with expert assessment. **Limitations:** No data on breast cancer incidence. Analyses were underpowered - only 2 breast cancer deaths were reported and both were in the non-exposed group. Data on breast cancer risk factors/potential confounders were not available. Evidence of healthy worker effect.
		All cohort members	1.57 (0.19–5.66)	2		
		Only worked in jobs characterized as "non-exposed"	5.11 (0.62–18.45)	2		
Bonefeld-Jørgensen et al. (2014) Nested Case-Control Denmark **Enrollment or follow-up:** enrolled 1996-2002; followed-up until 2010	**Population:** Danish National Birth Cohort Cases: 250; Controls: 233 **Exposure assessment method:** serum	**Relative Risk PFOS (ng/ml)**			Age at blood sampling, BMI before pregnancy, gravidity, menarche age, smoking during pregnancy, alcohol intake, maternal education, physical activity, oral contraceptive use	**Exposure information:** Mean serum levels for controls: PFOS = 30.6 ng/ml **Strengths:** Exposure data was prospectively collected and outcome was obtained from population-based cancer registries, minimizing concerns over information bias and reverse causation. Population was representative of Denmark, minimizing concerns over selection bias. Plasma was taken up to 15 years before diagnosis of breast cancer, providing an adequate latency period. **Limitations:** Lack of consistency in the findings made it difficult to interpret the data; few positive associations could be due to chance or multiple testing. The cases were heterogeneous, which may have compromised the power of the study if the exposure is only causal for subtypes of breast cancer. There was no information on
		Any PFOS	0.99 (0.98–1.01)	221		
		Less than 20.42	1	42		
		20.42-25.31	1.51 (0.81–2.71)	52		
		25.31-30.20	1.51 (0.82–2.84)	49		
		30.20-39.07	1.13 (0.59–2.04)	43		
		Greater than 39.07	0.9 (0.47–1.7)	35		
		Relative Risk PFOS (ng/ml), age 40 years or less			Age at blood sampling, BMI before pregnancy, gravidity, menarche age, smoking during pregnancy, alcohol intake, maternal education, physical activity, oral contraceptive use	
		Any PFOS	0.99 (0.97–1.02)	132		
		Less than 20.42	1	26		
		20.42-25.31	1.22 (0.52–2.88)	28		
		25.31-30.20	1.38 (0.58–3.3)	30		
		30.20-39.07	0.79 (0.33–1.88)	22		
		Greater than 39.07	1.01 (0.41–2.5)	26		

Table 4 Epidemiologic studies of breast cancer and PFOS assessed before diagnosis

Reference, study-design, location, and year	Population description & exposure assessment method	Exposure category or level	Risk estimate (95% CI)	Exposed cases/ deaths	Co-variates controlled	Comments, strengths, and limitations
		Relative Risk PFOS (ng/ml), age greater than 40 years			Age at blood sampling, BMI before pregnancy, gravidity, menarche age, smoking during pregnancy, alcohol intake, maternal education, physical activity, oral contraceptive use	case characteristics, e.g., regarding tumor size, nodal status, in situ versus invasive, and immune histochemical markers (i.e., estrogen receptor, progesterone receptor, or HER2/neu) or the family history of breast cancer. Cohort consists mostly of premenopausal women, limiting generalizability of the findings. **Comments:** For PFOSA, relative risk was 2.45 (1.00–6.00) in the highest exposed group for those <40 years of age at diagnosis, but no association in those >40 years of age.
		Any PFOS	1 (0.98–1.02)	118		
		Less than 20.42	1	22		
		20.42-25.31	2.3 (0.94–5.64)	27		
		25.31-30.20	1.9 (0.73–4.97)	26		
		30.20-39.07	2.22 (0.87–5.69)	25		
		Greater than 39.07	0.88 (0.33–2.38)	18		
		Relative Risk PFOSA (ng/ml)			Age at blood sampling, BMI before pregnancy, gravidity, menarche age, smoking during pregnancy, alcohol intake, maternal education, physical activity, oral contraceptive use	
		Any PFOSA	1.04 (0.99–1.08)	221		
		Less than 0.93	1	43		
		0.93-1.70	1.38 (0.75–2.52)	48		
		1.70-2.83	0.91 (0.49–1.66)	38		
		2.83-5.75	1.11 (0.6–2.05)	41		
		Greater than 5.75	1.89 (1.01–3.54)	51		
		Relative Risk PFOSA (ng/ml), age 40 years or less			Age at blood sampling, BMI before pregnancy, gravidity, menarche age, smoking during pregnancy, alcohol intake, maternal education, physical activity, oral contraceptive use	
		Any PFOSA	1.07 (1–1.14)	132		
		Less than 0.93	1	29		
		0.93-1.70	1.53 (0.7–3.32)	32		
		1.70-2.83	1.04 (0.45–2.4)	22		
		2.83-5.75	1.1 (0.46–2.59)	22		
		Greater than 5.75	2.45 (1–6)	27		
		Relative Risk PFOSA (ng/ml), age greater than 40 years			Age at blood sampling, BMI before pregnancy, gravidity, menarche age, smoking	
		Any PFOSA	1.01 (0.97–1.07)	118		
		Less than 0.93	1	19		

Table 4 Epidemiologic studies of breast cancer and PFOS assessed before diagnosis

Reference, study-design, location, and year	Population description & exposure assessment method	Exposure category or level	Risk estimate (95% CI)	Exposed cases/ deaths	Co-variates controlled	Comments, strengths, and limitations
		0.93-1.70	1.3 (0.48–3.56)	21	during pregnancy, alcohol intake, maternal education, physical activity, oral contraceptive use	
		1.70-2.83	0.96 (0.37–2.51)	22		
		2.83-5.75	1.37 (0.52–3.61)	24		
		Greater than 5.75	1.62 (0.61–4.29)	32		
Ghisari et al. (2017) Nested Case-Control Denmark **Enrollment or follow-up:** 1996-2002; followed-up until 2010	**Population:** Cases: 178; Controls: 233 **Exposure assessment method:** serum	**Relative Risk natural log-transformed PFOS, by genotype**			Age at blood sampling, BMI before pregnancy, gravidities, oral contraceptive use, age at menarche, smoking status during pregnancy, alcohol intake during pregnancy, physical activity, maternal education	**Exposure information:** Median PFOS serum levels: controls = 28.77 ng/ml; cases = 27.80 ng/ml **Strengths:** Prospective design; availability of DNA and genotype data on a nested sample. **Limitations:** Heterogeneity of the cases may have compromised the power of the study if the exposure is only causal for subtypes of breast cancer. No information on case characteristics such as tumor size, nodal status, in situ versus invasive, and immunohistochemical markers, i.e. ER, PR, and family history. Small size limits the power for certain analyses (e.g. gene-environment interactions). **Comments:** Subset of population in Bonefeld-Jørgensen et al. (2014).
		All	1.15 (0.64–2.08)	158		
		CYP1A1 Ile/Ile	1.22 (0.62–2.4)	NR		
		CYP1B1 Leu/Leu	1.39 (0.45–3.42)	45		
		CYP1B1 Leu/Val	0.85 (0.24–3.01)	46		
		CYP1B1 Val/Val	1.25 (0.28–5.62)	31		
		CYP1B1 Leu/Val + Val/Val	0.89 (0.36–2.2)	77		
		COMT Val/Val	0.82 (0.14–4.9)	27		
		COMT Val/Met	0.76 (0.27–2.29)	51		
		COMT Met/Met	1.91 (0.6–6.1)	45		
		COMT Val/Met + Met/Met	1.35 (0.64–2.87)	96		
		CYP17 (-34T>C) A1A1	1.79 (0.61–5)	44		
		CYP17 (-34T>C) A1A2	0.68 (0.22–2.4)	61		
		CYP17 (-34T>C) A2A2	0.15 (0.14–5.77)	21		
		CYP17 (-34T>C) A1A2 + A2A2	0.92 (0.36–2.36)	82		
		CYP19 (C>T) CC	6.42 (1.08–38.3)	35		
		CYP19 (C>T) CT	1.16 (0.44–3.1)	59		
		CYP19 (C>T) TT	0.45 (0.1–1.97)	34		
		CYP19 (C>T) CT+TT	0.78 (0.36–1.72)	93		
		Relative Risk natural log-transformed PFOSA, by genotype			Age at blood sampling, BMI	
		PFOSA - All	1.25 (1.01–1.56)	158		

Table 4 Epidemiologic studies of breast cancer and PFOS assessed before diagnosis

Reference, study-design, location, and year	Population description & exposure assessment method	Exposure category or level	Risk estimate (95% CI)	Exposed cases/ deaths	Co-variates controlled	Comments, strengths, and limitations
		CYP1A1 Ile/Ile	1.2 (0.94–1.54)	NR	before pregnancy, gravidities, oral contraceptive use, age at menarche, smoking status during pregnancy, alcohol intake during pregnancy, physical activity, maternal education	
		CYP1B1 Leu/Leu	1.7 (1.03–2.82)	45		
		CYP1B1 Leu/val	0.96 (0.66–1.5)	46		
		CYP1B1 Val/val	1.95 (1.1–3.47)	31		
		CYP1B1 Leu/val+Val/Val	1.21 (0.89–1.66)	77		
		COMT Val/Val	0.96 (0.57–1.65)	27		
		COMT Val/Met	1.2 (0.81–1.77)	51		
		COMT Met/Met	2.04 (1.27–3.28)	45		
		COMT Val/Met+Met/Met	1.46 (1.09–1.93)	96		
		CYP17 (-34T>C) A1A1	2.02 (1.29–3.16)	44		
		CYP17 (-34T>C) A1A2	1.11 (0.75–1.64)	61		
		CYP17 (-34T>C) A2A2	0.73 (0.36–1.49)	21		
		CYP17 (-34T>C) A1A2+A2A2	1.06 (0.77–1.46)	82		
		CYP19 (C>T) CC	2.08 (1.06–4.09)	35		
		CYP19 (C>T) CT	1.25 (0.89–1.74)	59		
		CYP19 (C>T) TT	1.06 (0.64–1.75)	34		
		CYP19 (C>T) CT+TT	1.17 (0.89–1.52)	93		
Cohn et al. (2020) Nested Case-Control Northern California **Enrollment or follow-up:** 1959-1967; 54	**Population:** Cases: 102; Controls: 310 **Exposure assessment method:** serum	**Odds ratio**			Maternal age at pregnancy, maternal history of breast cancer, African American, primipara, maternal overweight at first prenatal visit, maternal serum log2-transformed	**Exposure information:** Perinatal maternal serum samples were taken; median PFOS levels: controls = 32.1 ng/ml; cases = 30.5 ng/ml. median EtFOSAA levels: controls = 0.3 ng/ml; cases = 0.3 ng/ml **Strengths:** Prospective data collection (maternal serum and breast cancer in daughters). Long follow-up period.
		Log2 PFOS, low cholesterol (Q1)	0.3 (0.1–0.9)	NR		
		Log2 PFOS, high cholesterol (Q4)	0.3 (0.1–0.9)	NR		
		Log2 PFOS, low EtFOSAA (Q1)	0.3 (0.1–0.9)	NR		
		Log2 PFOS, high EtFOSAA (Q4)	0.3 (0.1–0.9)	NR		

Table 4 Epidemiologic studies of breast cancer and PFOS assessed before diagnosis

Reference, study-design, location, and year	Population description & exposure assessment method	Exposure category or level	Risk estimate (95% CI)	Exposed cases/ deaths	Co-variates controlled	Comments, strengths, and limitations
year follow-up		Log2 EtFOSAA, low cholesterol (Q1)	0.9 (0.3–2.7)	NR	*p*,*p*′-DDE, maternal serum log2-transformed *o*,*p*′-DDT, whether daughter was breastfed	**Limitations:** No information presented on main effects of PFOS and breast cancer; only stratified analyses presented. Number of exposed cases not presented. Outcome window may not be sufficient (only assessed breast cancer diagnosed before age 52). No data on alcohol consumption or breast cancer subtypes.
		Log2 EtFOSAA, high cholesterol (Q4)	3.6 (1.1–11.6)	NR		
		Log2 cholesterol, low EtFOSAA (Q1)	0.8 (0.4–1.9)	NR		
		Log2 cholesterol, high EtFOSAA (Q4)	3.3 (1.2–8.9)	NR		
		Log2 (EtFOSAA : PFOS), low cholesterol (Q1)	1 (0.3–2.9)	NR		
		Log2 (EtFOSAA : PFOS), high cholesterol (Q4)	3.8 (1.4–10.6)	NR		
		Log2 cholesterol, low EtFOSAA : PFOS (Q1)	0.8 (0.3–1.8)	NR		
		Log2 cholesterol, high EtFOSAA : PFOS (Q4)	3.1 (1.2–8.2)	NR		
		Odds ratio			Maternal age at pregnancy, maternal history of breast cancer, African American, primipara, maternal overweight at first prenatal visit, maternal serum log2-transformed *p*,*p*′-DDE, maternal serum log2-transformed *o*,*p*′-DDT, whether daughter was breastfed	
		EtFOSAA : PFOS, cholesterol ≤ median	0.6 (0.2–1.4)	NR		
		EtFOSAA : PFOS, cholesterol > median	2.5 (1.2–5.6)	NR		
		Cholesterol, EtFOSAA : PFOS ≤ median	0.6 (0.3–1.4)	NR		
		Cholesterol, EtFOSAA : PFOS > median	2.8 (1.3–6.1)	NR		

Table 4 Epidemiologic studies of breast cancer and PFOS assessed before diagnosis

Reference, study-design, location, and year	Population description & exposure assessment method	Exposure category or level	Risk estimate (95% CI)	Exposed cases/ deaths	Co-variates controlled	Comments, strengths, and limitations
Mancini et al. (2020) Nested Case-Control France **Enrollment or follow-up:** 1990	**Population:** E3N (Etude Epidémiologique auprès de femmes de l'Education Nationale) is a prospective cohort study involving 98,995 French women, aged 40–65 years at inclusion in 1990 and insured by a national health insurance covering workers from the French National Education System (Mutuelle Générale de l'Education Nationale, MGEN). Cases: 194; Controls: 194 **Exposure assessment method:** serum	**Post-menopausal: Unadjusted Odds Ratio PFOS (ng/ml)**			Model 0: none	**Exposure information:** Median serum PFOS concentrations: all participants=17.51 ng/ml (5.83–85.26); breast cancer cases=17.62 ng/ml (5.84–85.29); controls=17.32 ng/ml (6.61–59.12). **Strengths:** Prospective collection of serum PFOS within the cohort, before diagnosis. One of the only studies to conduct analyses by hormone receptor status (pathology reports obtained for 93% of cases). **Limitations:** Potential for incomplete outcome assessment or misclassification for a small proportion of cases for whom outcome was obtained from self-report and mortality data.
		Quartile 1 (5.8-13.6)	1	80		
		Quartile 2 (13.6-17.3)	1.8 (1.01–3.21)	109		
		Quartile 3 (17.3-22.5)	1.59 (0.88–2.9)	99		
		Quartile 4 (22.5-85.3)	1.53 (0.85–2.74)	100		
		Trend-test *p*-value: 0.38				
		Post-menopausal: Adjusted Odds Ratio PFOS (ng/ml)			Model 1: total serum lipids, smoking status, physical activity, education level, personal history of benign breast disease, family history of breast cancer	
		Quartile 1 (5.8-13.6)	1	80		
		Quartile 2 (13.6-17.3)	1.8 (0.98–3.28)	109		
		Quartile 3 (17.3-22.5)	1.78 (0.95–3.34)	99		
		Quartile 4 (22.5-85.3)	1.67 (0.9–3.1)	100		
		Trend-test *p*-value: 0.23				
		Post-menopausal: Adjusted Odds Ratio PFOS (ng/ml)			Model 2: model 1 + parity/age at first full-term pregnancy, total breastfeeding duration, age at menarche, age at menopause, use of oral contraceptives, current use of menopausal hormone therapy	
		Quartile 1 (5.8-13.6)	1	80		
		Quartile 2 (13.6-17.3)	1.93 (1.01–3.7)	109		
		Quartile 3 (17.3-22.5)	1.96 (1–3.84)	99		
		Quartile 4 (22.5-85.3)	1.7 (0.88–3.28)	100		
		Trend-test *p*-value: 0.26				
		Post-menopausal: Adjusted Odds Ratio PFOS (ng/ml)			Model 3: model 2 + score of adherence to the Western diet and to the Mediterranean diet	
		Quartile 1 (5.8-13.6)	1	80		
		Quartile 2 (13.6-17.3)	1.94 (1–3.78)	109		
		Quartile 3 (17.3-22.5)	2.03 (1.02–4.04)	99		
		Quartile 4 (22.5-85.3)	1.72 (0.88–3.36)	100		

Table 4 Epidemiologic studies of breast cancer and PFOS assessed before diagnosis

Reference, study-design, location, and year	Population description & exposure assessment method	Exposure category or level	Risk estimate (95% CI)	Exposed cases/ deaths	Co-variates controlled	Comments, strengths, and limitations
		Trend-test *p*-value: 0.25				
		Post-menopausal; Estrogen Receptor-positive (n=132): Adjusted Odds Ratio PFOS (ng/ml)			Model 3	
		Quartile 1 (5.8-13.6)	1	NR		
		Quartile 2 (13.6-17.3)	1.85 (0.9–3.82)	NR		
		Quartile 3 (17.3-22.5)	2.22 (1.05–4.69)	NR		
		Quartile 4 (22.5-85.3)	2.33 (1.11–4.9)	NR		
		Trend-test *p*-value: 0.04				
		Post-menopausal; Estrogen Receptor-negative (n=26): Adjusted Odds Ratio PFOS (ng/ml)			Model 3	
		Quartile 1 (5.8-13.6)	1	NR		
		Quartile 2 (13.6-17.3)	15.4 (1.84–129.19)	NR		
		Quartile 3 (17.3-22.5)	4.74 (0.45–49.62)	NR		
		Quartile 4 (22.5-85.3)	7.07 (0.73–68.03)	NR		
		Trend-test *p*-value: 0.72				
		Post-menopausal; Missing Estrogen Receptor status (n=36): Adjusted Odds Ratio PFOS (ng/ml)			Model 3	
		Quartile 1 (5.8-13.6)	1	NR		
		Quartile 2 (13.6-17.3)	0.67 (0.23–1.97)	NR		
		Quartile 3 (17.3-22.5)	1.25 (0.45–3.43)	NR		
		Quartile 4 (22.5-85.3)	0.41 (0.12–1.44)	NR		
		Trend-test *p*-value: 0.27				
		Post-menopausal; Progesterone Receptor-positive (n=98): Adjusted Odds Ratio PFOS (ng/ml)			Model 3	
		Quartile 1 (5.8-13.6)	1	NR		
		Quartile 2 (13.6-17.3)	1.84 (0.82–4.14)	NR		
		Quartile 3 (17.3-22.5)	2.47 (1.07–5.65)	NR		
		Quartile 4 (22.5-85.3)	2.76 (1.21–6.3)	NR		
		Trend-test *p*-value: 0.02				

Table 4 Epidemiologic studies of breast cancer and PFOS assessed before diagnosis

Reference, study-design, location, and year	Population description & exposure assessment method	Exposure category or level	Risk estimate (95% CI)	Exposed cases/ deaths	Co-variates controlled	Comments, strengths, and limitations
		Post-menopausal; Progesterone Receptor-negative (n=57): Adjusted Odds Ratio PFOS (ng/ml)			Model 3	
		Quartile 1 (5.8-13.6)	1	NR		
		Quartile 2 (13.6-17.3)	3.47 (1.29–9.15)	NR		
		Quartile 3 (17.3-22.5)	1.82 (0.61–5.45)	NR		
		Quartile 4 (22.5-85.3)	1.71 (0.57–5.1)	NR		
		Trend-test *p*-value: 0.93				
		Post-menopausal; Missing Progesterone Receptor status (n=39): Adjusted Odds Ratio PFOS (ng/ml)			Model 3	
		Quartile 1 (5.8-13.6)	1	NR		
		Quartile 2 (13.6-17.3)	0.78 (0.27–2.21)	NR		
		Quartile 3 (17.3-22.5)	1.3 (0.47–3.56)	NR		
		Quartile 4 (22.5-85.3)	0.64 (0.2–2.01)	NR		
		Trend-test *p*-value: 0.58				

NR, not reported

Studies where PFOS exposure was determined by samples collected at or after breast cancer diagnosis

Several studies collected PFOS exposure at or after breast cancer diagnosis (Bonefeld-Jørgensen et al. 2011; Hurley et al. 2018b; Wielsøe et al. 2017; Wielsøe et al. 2018). These studies are included and described briefly below because incident breast cancers were assessed; however, limitations in their utility for causal inference should be noted. The designs of these studies do not ensure that the PFOS levels measured are reflective of exposures that preceded the disease (*e.g.* temporality) and reverse causation bias cannot be fully ruled out. Given the relatively long half-life of PFOS in human blood, the exposure levels measured in these studies could represent exposures that occurred prior to cancer development. However, it is currently difficult to evaluate since data on the latency of PFOS-related cancers is not available and it is unknown how serum PFOS levels could have been affected by the onset and/or treatment of breast cancer (Hurley et al. 2018b).

There were three published case-control analyses, partially overlapping in study subjects, conducted within the Greenland Inuit population. In all three studies, PFOS in serum was collected at breast cancer diagnosis for cases, and at enrollment for controls.

In the first case-control study among women of Greenlandic Inuit descent (Bonefeld-Jørgensen et al. 2011) conducted during 2000-2003, a 1 ng/ml increase in serum PFOS level (analyzed as a continuous variable) was associated with an OR of 1.03 (95%CI, 1.001–1.07; p= 0.05) for breast cancer, after adjusting for several risk factors.

In a second case-control analysis of breast cancer among Greenland Inuit women (Wielsøe et al. 2017), an additional 66 cases and 62 controls were enrolled during 2011-2014, and analyzed together with the earlier set of cases and controls enrolled in 2000-2003 and studied by Bonefeld-Jørgensen et al. (2011). The adjusted OR for PFOS exposure analyzed as a continuous variable was 1.02 (95%CI, 1.01–1.03); the risk of breast cancer was increased in the second (OR, 3.13; 95%CI, 1.20–8.15) and third (OR, 5.50; 95%CI, 2.19–13.84) tertile of exposure. The p-value for the test for trend for the categorical analysis was not presented.

Gene-environment interactions were investigated by Ghisari et al. (2014) among the participants in the first case-control study of Bonefeld-Jørgensen et al. (2011), and by Wielsøe et al. (2018) for the participants in the second case-control study of Wielsøe et al. (2017).

In Ghisari et al. (2014), interactions between serum PFOS levels and genes with known involvement in steroid hormone and xenobiotic metabolism were investigated in 31 breast cancer cases and 115 matched controls, among a subset of the study participants investigated by Bonefeld-Jørgensen et al. (2011). Genotyping was

conducted for CYP1A1 (Ile462Val; rs1048943), CYP1B1 (Leu432Val; rs1056836), COMT (Val158Met; rs4680), CYP17A1 (A1> A2; rs743572); CYP19A1 (C> T; rs10046) and CYP19A1 ((TTTA)n repeats) polymorphisms. Three models were presented: crude analyses, adjustment for age, and adjustment for age and serum cotinine as continuous variables, since smoking can affect the gene expression of CYP450 genes (Crofts et al. 1994). Analyses were conducted stratified by genotype, *i.e.* within a certain genotype, comparing women with low (reference category) versus high PFOS exposure. Compared with women with low PFOS levels, an increased risk was observed for women with high serum PFOS levels and at least one of the following alleles: one CYP1A1 variant Val allele (high activity), one variant COMT Met allele (low activity), or the common CYP17A1 allele. However, the interaction terms in the model between the PFOS variable and genetic polymorphisms were not significant. The addition of cotinine to the age adjusted models generally increased the magnitude of the risk estimates, although not significantly, as evidenced by the overlapping 95%CIs. The sample size was small, there were few exposed cases in each stratum, and the analyses may have been underpowered to draw firm conclusions from the gene-environment interaction analyses, as evidenced by the wide confidence intervals.

Wielsøe et al. (2018) also investigated interactions between PFAS levels (including PFOS) and polymorphisms in genes with known involvement in steroid hormone and xenobiotic metabolism (*CYP17A1, CYP19A1, CYP1A1, CYP1B1* and *COMT*) in women of Greenlandic Inuit descent, using a subset of study participants investigated by Wiesloe et al (2017). The reference category for each analysis was low PFOS exposure (≤ median) and the homozygous wild type genotype for each gene assessed. There was a significantly increased risk of breast cancer in those with high PFOS exposure (> median) and at least one of the following genotypes or alleles: the CYP17A1 -34 TT homozygous wild type genotype (OR, 12.7; 95%CI, 2.50–64.2); CYP19A1 *19C>T heterozygous or homozygous variants with the CT or TT genotype (OR, 3.82; 95%CI, 1.33–10.9); CYP1A1 Ile462Val homozygous wild type Ile/Ile genotype (OR, 6.33; 95%CI, 1.41–28.4) or those carrying a variant allele OR, 2.19; 95%CI, 1.02–4.70) for the Ile/Val+Val/Val genotypes; CYP1B1Leu432Val Leu/Leu genotype (OR, 2.08, 95%CI, 1.01–4.29) or Leu/Val+Val/Val genotype (OR,11.3, 95%CI, 1.86–68.1); or the COMTIle462Val Val/Met+Met/Met genotype (OR 2.14, 95%CI, 1.51–6.53). Although statistically significant associations were observed for the interaction between high PFOS exposure and several genotypes, the role of chance could not be excluded as there was no correction for multiple testing. The sample size was also relatively small. Furthermore, only unadjusted analyses were presented because it was noted that addition of covariates to the model did not change the effect estimate more than 10%. Had *a priori* confounders been added to the statistical models, the precision of the risk estimates may have been reduced, rendering some of these results statistically non-significant. Although significant associations were observed between

high PFOS exposure and variations in several of the genes assessed, CYP1B1 Leu432Val was the only SNP not in Hardy–Weinberg equilibrium among the cases. This could reflect either a genotyping error or true association with disease (Robertson and Williams 2017). The associations of PFOS with increased breast cancer risk in women with specific genetic polymorphisms observed in this study, in a population highly exposed to POPs, merits further investigation in other, differently exposed populations.

A nested case-control analysis within the California Teacher's Study (CTS) reported that PFOS exposure was inversely associated with risk of invasive breast cancer (Hurley et al. 2018b). There were statistically significant positive correlations between PFASs; the Spearman Rank Correlation was 0.63 for PFOS and PFOA. Hurley et al. (2018b) also stated that correlations between the PFASs were generally similar among cases and controls, although no data were shown in the publication.

Exposure to PFASs, including PFOS, were modelled as categorical and continuous variables. The adjusted OR associated with log PFOS serum concentration analyzed as a continuous variable was 0.934 (95%CI, 0.683–1.277); similarly, inverse associations were observed for the second and third tertiles of PFOS exposure. There appeared to be no dose-response relationship using log PFOS serum concentration as a continuous or categorical variable (p-trend = 0.67 or 0.41, respectively).

The analyses were stratified by menopausal and hormone receptor status. Increasing PFOS exposure was inversely associated with post-menopausal breast cancer (adjusted OR for log[PFOS, ng/ml], 0.885; 95%CI, 0.641–1.223), but the ORs were above 1 (not statistically significant) in pre- or peri-menopausal women with medium and high serum PFOS concentrations.

There was also some suggestion of an inverse association between serum PFOS level and breast cancer risk among those with ER-/PR- tumors (adjusted OR [log PFOS ng/ml], 0.573; 95%CI, 0.323–1.016; p = 0.06) and no association with ER+ or PR+ tumors (adjusted OR [log PFOS ng/ml], 1.054; 95%CI, 0.744–1.493; p = 0.77).

This study also reported on MeFOSAA, a precursor to PFOS. MeFOSAA was generally not associated with invasive breast cancer (OR for log [MeFOSAA, ng/ml], 0.960; 95%CI, 0.774–1.191) nor were there any significant associations when stratified by hormone receptor or menopausal status.

Therefore, chance or artifacts of study design could not be ruled out as potential explanations for any of the observed associations. Although this study collected data prospectively within an ongoing cohort study, blood was collected post-diagnosis and sometimes post-treatment. Therefore, reverse causation is a concern. The effects of breast cancer treatment, if any, on levels of serum PFAS are unknown. Complete information on treatment was not available for the CTS cohort. If breast cancer treatment caused declines in PFAS levels, this would have limited the ability to detect

an effect and could have resulted in spurious inverse associations. Most women in this study were born before the widespread introduction of PFOS in the early 1950s.

Table 5 Epidemiologic studies of breast cancer and PFOS assessed after diagnosis

Reference, study-design, location, and year	Population description & exposure assessment method	Exposure category or level	Risk estimate (95% CI)	Exposed cases/ deaths	Co-variates controlled	Comments, strengths, and limitations
Bonefeld-Jørgensen et al. (2011) Case-Control Greenland **Enrollment or follow-up:** 2000-2003	**Population:** Inuit women from Greenland Cases: 31; Controls: 115 **Exposure assessment method:** serum	**Odds ratio Continuous PFOS (ng/ml)**			None	**Exposure information:** Cases: median=45.6 ng/ml (range 11.6-124); Controls: median=21.9 ng/ml (range 1.5-172) **Strengths:** Conducted in a population highly exposed to PFOS. **Limitations:** Reverse causality could not be ruled out as PFOS was assessed after diagnosis. This population is highly exposed to a number of chemicals (e.g. polychlorinated biphenyls [PCBs] and organochlorine [OC] pesticides), making it difficult to disentangle the effect of individual compounds.
		PFOS, unadjusted data for full number of samples	1.01 (1.003–1.02)	31		
		PFOS, unadjusted data for subset having all adjustment variables	1.01 (0.99–1.03)	9		
		Odds ratio Continuous PFOS (ng/ml)			Age, BMI, pregnancy, cotinine, breastfeeding, menopausal status	
		PFOS, adjusted	1.03 (1.001–1.07)	9		
Ghisari et al. (2014) Case-Control Greenland **Enrollment or follow-up:** 2000-2003	**Population:** Inuit women from Greenland Cases: 31; Controls: 115 **Exposure assessment method:** serum	**Odds ratio Low vs high PFOS exposure, by genotype**			Age	**Exposure information:** Cases: median=45.6 ng/ml (range 11.6-124); Controls: median=21.9 ng/ml (range 1.5-172) **Strengths:** Conducted in a population highly exposed to PFOS. **Limitations:** Reverse causality could not be ruled out as PFOS was assessed after diagnosis. This population is highly exposed to a number of
		CYP1A1 Ile/Ile; low PFOS	1	1		
		CYP1A1 Ile/Ile; high PFOS	6.33 (0.35–114.1)	3		
		CYP1A1 Ile/Val + Val/Val; low PFOS	1	2		
		CYP1A1 Ile/Val + Val/Val; high PFOS	12.4 (2.57–59.9)	24		
		CYP1B1 Leu/Leu; low PFOS	1	3		
		CYP1B1 Leu/Leu; high PFOS	7.3 (1.8–29.4)	23		
		COMT Val/Val; low PFOS	1	1		
		COMT Val/Val; high PFOS	7.13 (0.65–77.6)	6		

Table 5 Epidemiologic studies of breast cancer and PFOS assessed after diagnosis

Reference, study-design, location, and year	Population description & exposure assessment method	Exposure category or level	Risk estimate (95% CI)	Exposed cases/ deaths	Co-variates controlled	Comments, strengths, and limitations
		COMT Val/Met + Met/Met; low PFOS	1	2		chemicals (e.g. PCBs, OC pesticides), making it difficult to disentangle the effect of individual compounds. **Comments:** Same Inuit population as Bonefeld-Jørgensen et al. (2011).
		COMT Val/Met + Met/Met; high PFOS	15.36 (3.02–78.2)	22		
		CYP17 A1/A2 + A2/A2; low PFOS	1	3		
		CYP17 A1/A2 + A2/A2; high PFOS	5.67 (1.38–23.4)	15		
		CYP19_CT CC; low PFOS	1	3		
		CYP19_CT CC; high PFOS	8.85 (2.15–36.4)	20		
		CYP19_TTTA $(TTTA)_{8-10}$; low PFOS	1	3		
		CYP19_TTTA $(TTTA)_{8-10}$; high PFOS	8.92 (2.33–34.2)	24		
		Odds Ratio Natural log transformed PFOS as continuous variable, by genotype			Age	
		CYP1A1 Ile/Ile	1.71 (0.47–6.32)	4		
		CYP1A1 Ile/Val+Val/Val	2.63 (1.46–4.75)	26		
		CYP1B1 Leu/Leu	1.95 (1.09–3.48)	26		
		CYP1B1 Leu/Val+Val/Val	8.67 (1.33–56.6)	5		
		COMT Val/Val	2.7 (0.83–8.79)	7		
		COMT Val/Met+Met/Met	2.65 (1.44–4.89)	24		
		CYP17 A1A1	4.89 (1.28–18.7)	12		
		CYP17 A1A2+A2A2	2.21 (1.19–4.12)	18		
		CYP19 CC	2.65 (1.39–5.06)	23		
		CYP19 CT+TT	2.54 (0.92–7.04)	8		
		CYP19_TTTA $(TTTA)_{8-10}$	2.58 (1.4–4.75)	27		
		CYP19_TTTA $(TTTA)_{11-13}$	41.9 (0.42–4203)	4		

Table 5 Epidemiologic studies of breast cancer and PFOS assessed after diagnosis

Reference, study-design, location, and year	Population description & exposure assessment method	Exposure category or level	Risk estimate (95% CI)	Exposed cases/ deaths	Co-variates controlled	Comments, strengths, and limitations
Wielsøe et al. (2017) Case-Control Greenland **Enrollment or follow-up:** 2000–2003 and 2011–2014	**Population:** Inuit women from Greenland Cases: 77; Controls: 84 **Exposure assessment method:** serum	**Odds ratio**			None	**Exposure information:** Cases: median=35.50 ng/ml (range 4.23-187); Controls: median=18.2 ng/ml (range 1.70-133) **Strengths:** Conducted in a population highly exposed to PFOS. **Limitations:** Reverse causality could not be ruled out as PFOS was assessed after diagnosis. This population is highly exposed to a number of chemicals (e.g. PCBs, OC pesticides), making it difficult to disentangle the effect of individual compounds. **Comments:** Cases and controls from the 2000-2003 time period were the same as cases and controls reported in Wielsøe et al. (2018). Partial overlap with Bonefeld-Jørgensen et al. (2011).
		Unadjusted continuous PFOS (ng/ml serum)	1.02	77[a]		
		Odds ratio			Age, BMI, cotinine levels, parity, breastfeeding	
		Adjusted continuous PFOS (ng/ml serum)	1.02 (1.01–1.03)	77[a]		
		Tertile 1	1	8		
		Tertile 2	3.13 (1.2–8.15)	25		
		Tertile 3	5.5 (2.19–13.84)	44		
Wielsøe et al. (2018) Case-Control Greenland **Enrollment or follow-up:** 2000–2003 and 2011–2014	**Population:** Inuit women from Greenland Cases: 77; Controls: 84 **Exposure assessment method:** serum	**Unadjusted Odds Ratio CYP17A1 -34T>C genotype**			None	**Exposure information:** Cases: median=35.50 ng/ml (range 4.23-187 ng/ml); Controls: median=18.2 ng/ml (range 1.70-133 ng/ml) **Strengths:** Conducted in a population highly exposed to PFOS. **Limitations:**
		TT; low PFOS	1	5		
		TT; high PFOS	12.7 (2.5–64.2)	19		
		TC + CC; low PFOS	1.23 (0.38–4.04)	24		
		TC + CC; high PFOS	2 (0.6–6.63)	27		
		Unadjusted Odds Ratio CYP17A1 -34T>C genotype			None	
		TC + CC; low PFOS	1	24		

Table 5 Epidemiologic studies of breast cancer and PFOS assessed after diagnosis

Reference, study-design, location, and year	Population description & exposure assessment method	Exposure category or level	Risk estimate (95% CI)	Exposed cases/ deaths	Co-variates controlled	Comments, strengths, and limitations
		TC + CC; high PFOS	1.63 (0.78–3.4)	27		Reverse causality could not be ruled out as PFOS was assessed after diagnosis. This population is highly exposed to a number of chemicals (e.g. PCBs, OC pesticides), making it difficult to disentangle the effect of individual compounds. **Comments:** Same population as Wielsøe et al. (2017) and partial overlap with Bonefeld-Jørgensen et al. (2011). Cases and controls from the 2000-2003 time period were the same as cases and controls reported in Bonefeld-Jørgensen et al. (2011).
		Unadjusted Odds Ratio CYP19A1 *19C>T genotype			None	
		CC; low PFOS	1	18		
		CC; high PFOS	1.94 (0.84–4.48)	25		
		CT + TT; low PFOS	0.82 (0.32–2.09)	11		
		CT + TT; high PFOS	3.11 (1.19–8.15)	20		
		Unadjusted Odds Ratio CYP19A1 *19C>T genotype			None	
		CT + TT; low PFOS	1	11		
		CT + TT; high PFOS	3.82 (1.33–10.9)	20		
		Unadjusted Odds Ratio CYP1A1 Ile462Val genotype			None	
		Ile/Ile; low PFOS	1	10		
		Ile/Ile; high PFOS	6.33 (1.41–28.4)	10		
		Ile/Val + Val/Val; low PFOS	1.2 (0.46–3.13)	19		
		Ile/Val + Val/Val; high PFOS	2.63 (1.05–6.58)	36		
		Unadjusted Odds Ratio CYP1A1 Ile462Val genotype			None	
		Ile/Val + Val/Val; low PFOS	1	19		
		Ile/Val + Val/Val; high PFOS	2.19 (1.02–4.7)	36		
		Unadjusted Odds Ratio CYP1B1 Leu432Val genotype			None	
		Leu/Leu; low PFOS	1	23		
		Leu/Leu; high PFOS	2.08 (1.01–4.29)	38		
		Leu/Val + Val/Val; low PFOS	0.59 (0.2–1.75)	6		
		Leu/Val + Val/Val; high PFOS	6.65 (1.32–33.6)	9		
		Unadjusted Odds Ratio CYP1B1 Leu432Val genotype			None	
		Leu/Val + Val/Val; low PFOS	1	6		
		Leu/Val + Val/Val; high PFOS	11.3 (1.86–68.1)	9		
		Unadjusted Odds Ratio COMT Val158Met genotype			None	

Table 5 Epidemiologic studies of breast cancer and PFOS assessed after diagnosis

Reference, study-design, location, and year	Population description & exposure assessment method	Exposure category or level	Risk estimate (95% CI)	Exposed cases/ deaths	Co-variates controlled	Comments, strengths, and limitations
		Val/Val; low PFOS	1	7		
		Val/Val; high PFOS	1.43 (0.32–6.32)	10		
		Val/Met + Met/Met; low PFOS	0.44 (0.13–1.46)	22		
		Val/Met + Met/Met; high PFOS	1.38 (0.41–4.62)	37		
		Unadjusted Odds Ratio COMT Val158Met genotype			None	
		Val/Met + Met/Met; low PFOS	1	22		
		Val/Met + Met/Met; high PFOS	3.14 (1.51–6.53)	37		
Hurley et al. (2018) Nested Case-Control California **Enrollment or follow-up:** 1995-96	**Population:** Cases: 902; Controls: 858 **Exposure assessment method:** serum	**Invasive breast cancer: Adjusted Odds Ratio**			Age at baseline enrollment, race/ethnicity, region of residence, blood draw date, season of blood draw, total pack-years smoking, BMI, family history of breast cancer, age at first full-term pregnancy, pork consumption, menopausal status at blood draw	**Exposure information:** Cases: median=6.695 ng/ml (range 0.046-39.4 ng/ml); Controls: median=6.950 ng/ml (range 0.046-99.8 ng/ml) **Strengths:** Detailed analyses for PFOS and its precursor, MeFOSAA, using categorical and continuous analyses, stratifying by menopausal status and hormone receptor status. **Limitations:** Potential for reverse causality could not be ruled out because PFOS was measured in blood collected post-diagnosis and sometimes post-treatment. Most women in this study were born before the widespread introduction of PFOS in the early 1950s, limiting the ability to detect
		Low PFOS	1	318		
		Medium PFOS	0.883 (0.691–1.129)	297		
		High PFOS	0.898 (0.695–1.161)	287		
		Log_{10} [PFOS, ng/ml]	0.934 (0.683–1.277)	902		
		Trend-test *p*-value: 0.41				
		Postmenopausal: Adjusted Odds Ratio			Age at baseline enrollment, race/ethnicity, region of residence, blood draw date, season of blood draw, total pack-years smoking, BMI, family history of breast cancer, age at first full-term pregnancy, pork consumption	
		Low PFOS	1	293		
		Medium PFOS	0.843 (0.653–1.088)	284		
		High PFOS	0.86 (0.661–1.118)	282		
		Log_{10} [PFOS, ng/ml]	0.885 (0.641–1.223)	859		
		Trend-test *p*-value: 0.26				
		Pre- or peri-menopausal: Adjusted Odds Ratio			Age at baseline enrollment, race/ethnicity, region of residence, season of blood draw, total red meat consumption	
		Low PFOS	1	25		
		Medium PFOS	1.796 (0.493–6.546)	13		
		High PFOS	1.208 (0.163–8.944)	5		
		Log_{10} [PFOS, ng/ml]	0.9 (0.166–4.876)	43		

Table 5 Epidemiologic studies of breast cancer and PFOS assessed after diagnosis

Reference, study-design, location, and year	Population description & exposure assessment method	Exposure category or level	Risk estimate (95% CI)	Exposed cases/ deaths	Co-variates controlled	Comments, strengths, and limitations
		Trend-test *p*-value: 0.57				potential effects from early life exposure.
		Estrogen Receptor-positive or Progesterone Receptor-positive: Adjusted Odds Ratio			Age at baseline enrollment, race/ethnicity, region of residence, date of blood draw, season of blood draw, total smoking pack-years, BMI, family history of breast cancer, age at first full-term pregnancy, menopausal status at blood draw, pork consumption	
		Low PFOS	1	250		
		Medium PFOS	0.937 (0.721–1.218)	247		
		High PFOS	0.967 (0.737–1.27)	246		
		Log_{10} [PFOS, ng/ml]	1.054 (0.744–1.493)	743		
		Trend-test *p*-value: 0.81				
		Estrogen Receptor-negative and Progesterone Receptor-negative: Adjusted Odds Ratio			Age at baseline enrollment, race/ethnicity, region of residence, date of blood draw, season of blood draw, physical activity	
		Low PFOS	1	47		
		Medium PFOS	0.628 (0.378–1.041)	32		
		High PFOS	0.615 (0.357–1.059)	28		
		Log_{10} [PFOS, ng/ml]	0.573 (0.323–1.016)	107		
		Trend-test *p*-value: 0.06				
		Invasive breast cancer: Adjusted Odds Ratio			Age at baseline enrollment, race/ethnicity, region of residence, blood draw date, season of blood draw, total pack-years smoking, BMI, family history of breast cancer, age at first full-term pregnancy, pork consumption, menopausal status at blood draw	
		Low MePFOSAA	1	349		
		Medium MePFOSAA	0.847 (0.663–1.083)	278		
		High MePFOSAA	0.877 (0.682–1.126)	275		
		Log_{10} [MePFOSAA, ng/ml]	0.96 (0.774–1.191)	902		
		Trend-test *p*-value: 0.29				

NR, not reported

[a] Reported as 81 cases in Wielsøe et al. (2018), which is believed to be a typo since there were 77 cases in Wielsøe et al. (2017), which are the same study participants.

3.2.2 Pediatric germ cell tumors

A hospital-based case-control study reported significantly higher serum PFOS and PFOSA concentrations in pediatric patients with germ cell tumors compared to age- and sex-matched tumor-free pediatric patients (Lin et al. 2020b). The authors do not state whether incident or prevalent cancer cases were enrolled. PFOS was measured in blood samples, which were collected one week following the pathological identification of the cases and on the day of discharge in the control group. The median (interquartile) concentrations in cases compared to controls were 5.202 (3.237–10.126) vs. 3.888 (1.976–6.944) ng/ml, $p = 0.036$ for PFOS and 0.115 (0.099–0.129) vs. 0.095 (0.093–0.113) ng/ml, $p < 0.001$ for PFOSA. The study reported an OR of 1.08 (95%CI, 0.96–1.21) for a 1 ng/ml increase in serum PFOS concentrations, after adjustment for infectious disease, cosmetics usage, barbecued food consumption, filtered water use, indoor decorating, and living near farmland. Reverse causation could not be ruled out, although concerns were minimized in this pediatric population compared to adult populations since the latency period between time of exposure and development of cancer was short (generally less than 3 years). The ages (in months (range)) for cases (29 (13–48)) and controls (22 (11–47)) did not differ significantly ($p = 0.558$).

3.2.3 All cancer mortality

Among participants aged 60 years and older from the 1999–2006 US National Health and Nutrition Examination Surveys (NHANES), 1043 individuals were analyzed for PFASs (Fry and Power 2017). Mortality status was obtained from public-use, linked mortality files until December 31, 2011. PFOS was one of the PFASs detected in greater than 90% of the population: the median serum concentration of PFOS was 4.3 ng/g (standard error, 0.2). The PFAS analytes were not strongly correlated; correlation coefficients ranged from 0.22 ($p < 0.0001$) to 0.63 ($p < 0.0001$). The hazard ratio (HR) for a one standard deviation unit increase in serum PFOS for all cancer mortality was 1.01 (95%CI, 0.86–1.19; p-value = 0.88) and was 0.91 (95%CI, 0.80–1.03; p-value = 0.12) for all-cause mortality, indicating no major concerns over selection bias. The HRs were adjusted for age, gender, race/ethnicity, education, and smoking status and were materially unchanged when further adjusted for alcohol consumption, BMI, and poverty income ratio.

3.2.4 Prostate cancer

Three studies reported on PFOS exposure and prostate cancer. A Swedish population-based case-control study of prostate cancer (Hardell et al. 2014) reported no association with PFOS exposure overall (OR, 1.0; 95%CI, 0.6–1.5) nor when stratified

by gleason score or prostate specific antigen level, but an increased risk in a subset of cases with at least one first-degree relative with prostate cancer and PFOS level above the median (OR, 2.7; 95%CI, 1.04–6.8). However, serum samples were collected at the time of diagnosis and the potential for reverse causation could not be ruled out. No significant associations were observed between prostate cancer and PFOS-exposed jobs (chemical plant workers) within the occupational cohort in Decatur, Alabama (see above for a detailed description of this occupational cohort) (Grice et al. 2007). The OR for high PFOS exposure (>1 yr) was 1.08 (95%CI, 0.44–2.69); the OR for low or high PFOS exposure (≥1 yr) was 1.36 (95%CI, 0.61–3.02) (Grice et al. 2007).

In the case-cohort analysis within the Danish general population, an increase in prostate cancer was observed for the three upper quartiles of PFOS serum levels compared with the lowest quartile (Eriksen et al. 2009). For the lowest vs the fourth quartile, the incidence rate ratio (IRR) was 1.38 (95%CI, 0.99–1.93). When PFOS was analyzed as a continuous variable, the IRR was 1.05 (95%CI, 0.97–1.14). None of the prostate cancer studies adjusted for prostate cancer screening. Although this could have potentially confounded some of the associations reported above, there is currently no evidence that PFOS exposure is strongly related to cancer screening.

3.2.5 Bladder cancer

The association between PFOS exposure and risk of bladder cancer was reported in three published studies. Two studies were from the occupational cohort from Decatur, Alabama. Bladder cancer mortality was elevated in the most highly exposed workers compared to Alabama state rates (SMR, 12.77; 95%CI, 2.63–37.35), although this involved only three deaths and adjusted only for age, sex, and calendar period (Alexander et al. 2003). Information on potential confounders such as smoking was not available; however, the SMRs for lung cancer and other smoking related cancers were not increased in this cohort, suggesting that the cohort as a whole did not smoke more than the general population. In a follow-up study, current and past employees were sent a questionnaire in 2002 in an attempt to identify incident cases of bladder cancer (Alexander and Olsen 2007). The response rate was 74%, and 11 cases of bladder cancer were identified. The standardized incidence ratio (SIR) for the cohort overall compared to the US population was 1.28 (95%CI, 0.64–2.29) for men and women combined. The SIR for those ever working in a high-exposure job was 1.74 (95%CI, 0.64–3.79; 6 cases) (adjusted for age and sex).

In the case-cohort analysis within the Danish general population, Eriksen et al. (2009) reported an inverse association between PFOS exposure and bladder cancer, which was not statistically significant in analyses of the lowest vs the highest quartile (IRR, 0.70; 95%CI, 0.46–1.07; 82 cases) or PFOS as a continuous variable (IRR, 0.93; 95%CI, 0.83–1.03; 332 cases). Plasma concentrations in this study were considerably

lower than those measured in the occupational cohort studies from Decatur, Alabama, and therefore may be too low to detect an effect.

3.2.6 Urinary tract cancers

Besides bladder cancer, two studies reported associations of PFOS with cancer of one or more organs in the urinary tract. The occupational cohort from Decatur, Alabama reported an SMR of 4.02 (95%CI, 0.83–11.75; 3 deaths) for mortality from cancer of the 'urinary organs' in workers ever employed in a high exposure job (Alexander et al. 2003). A case-control study nested within the National Cancer Institute's (NCI) Prostate, Lung, Colorectal, and Ovarian Screening Trial reported a statistically significant positive trend in risk of renal cell carcinoma with pre-diagnostic serum levels of PFOS (OR, 2.51; 95%CI, 1.28–4.92 for the highest vs lowest quartiles; p-trend = 0.009) (Shearer et al. 2020). However, this association with PFOS was attenuated after adjusting for other PFASs (OR, 1.14; 95%CI, 0.45–2.88; p-trend = 0.64), indicating potential confounding by correlated PFAS exposures. This study has several strengths and is reviewed in greater detail in the draft PHG document (OEHHA 2021).

3.2.7 Liver cancer

In the occupational cohort from Decatur, Alabama, only two deaths from liver cancer were identified in the entire cohort, for an SMR of 1.61 (95%CI, 0.20–5.82) (Alexander et al. 2003). One case was employed in a high exposure job and the other was in a low exposure job. The study was limited by the potential for selection bias (healthy worker effect) and wide confidence intervals due to the small number of liver cancer deaths. In the case-cohort analysis within the Danish general population, Eriksen et al. (2009) reported an inverse association between PFOS exposure and liver cancer in a comparison between the lowest vs the highest quartile, which was not statistically significant (IRR, 0.59; 95%CI, 0.27–1.27). No association was observed in the trend analysis (IRR, 0.97; 95%CI, 0.79–1.19).

3.2.8 Pancreatic cancer

In the case-cohort analysis within the Danish general population by Eriksen et al. (2009), a 10 ng/ml increase in PFOS plasma concentration was not associated with pancreatic cancer (IRR, 0.99; 95%CI, 0.86–1.14).

3.2.9 Gastrointestinal tract cancers

The publications reporting on cancers of the gastrointestinal tract come from the occupational cohort from Decatur, Alabama. Alexander et al. (2003) reported SMRs of 0.51 (95%CI, 0.06–1.85; 2 deaths) for mortality from cancer of the 'digestive organs and peritoneum' in workers ever employed in a high exposure job, 0.30 (95%CI, 0.01–1.66; 1 death) for mortality from cancer of the large intestine in the total cohort, and 2.16 (95%CI, 0.05–12.02; 1 death) for mortality from esophageal cancer in those ever employed in a high exposure job. A study evaluating episodes of care from claims data records collected between 1993 and 1998 reported increased risks of malignant neoplasms of the colon (RR, 5.4; 95%CI, 0.5 – 100+; 4 cases) and rectum (RR, 1.8; 95%CI, 0.3–12.4; 4 cases) (Olsen et al. 2004). Grice et al. (2007) conducted a follow-up study by questionnaire in 2002 and reported an increased risk of colon cancer in workers with high cumulative exposure to PFOS, although it was not statistically significant (OR, 1.69; 95%CI, 0.68–4.17; 7 cases). These studies had few exposed cases and wide confidence intervals, which limit the interpretation of the findings.

3.2.10 Respiratory tract cancers

The only publications reporting respiratory tract cancers were from the occupational cohort in Decatur, Alabama. There were few exposed cases and wide confidence intervals, which limit the interpretation of the findings. Alexander et al. (2003) reported an SMR of 0.85 (95%CI, 0.34–1.75; 7 deaths) for respiratory system cancer mortality and 0.88 (95%CI, 0.35–1.81; 7 deaths) for "bronchus, trachea, lung" cancer mortality in workers ever employed in a high exposure job. Olsen et al. (2004) reported an RR of 2.7 (95%CI, 0.1 – 100+; 2 cases) for incident malignant neoplasms of the lower respiratory tract identified through episodes of care from claims data records.

3.2.11 Malignant melanoma

The three studies on melanoma come from the occupational cohort in Decatur, Alabama. There were few exposed cases and wide confidence intervals, which limit the interpretation of the findings. Alexander et al. (2003) reported an SMR of 2.62 (95%CI, 0.32–9.46; 2 deaths) for malignant melanoma mortality in those ever employed in a high exposure job. In the study by Olsen et al. (2004), an RR of 12 (95%CI, 1.0 – 100+; 5 cases) was observed for malignant melanoma of the skin. The study by Grice et al. (2007) reported no association of PFOS with melanoma in workers with high cumulative exposure (OR, 1.01; 95%CI, 0.25–4.11; 4 cases).

3.2.12 Lymphohematopoietic cancers

The only study that reported on PFOS and lymphatic and hematopoetic cancers was the occupational cohort from Decatur, Alabama. The SMR for lymphatic and hematopoietic cancers was 0.70 (95%CI, 0.19–1.80; 4 deaths) for the entire cohort, 0.43 (95%CI, 0.01–2.40; 1 death) for ever employment in a high exposure job, 0.56 (95%CI, 0.01–3.08; 1 death) for employment in a high exposure job for at least one year, and 1.37 (95%CI, 0.28–4.00; 3 deaths) among workers in non-exposed jobs (Alexander et al. 2003).

4. CARCINOGENICITY STUDIES IN ANIMALS

Two-year dietary bioassays of PFOS potassium salt (K^+PFOS) were identified in rats by Thomford (2002), reported as Butenhoff et al. (2012a). One tumor promotion study of K^+PFOS, conducted in trout, was also identified (Benninghoff et al. 2012).

No peer-reviewed publications of long-term bioassays were identified for PFOS precursors. Short-term inhalation studies of a PFOS precursor, PFOSF, were conducted in male and female rats exposed for 13 weeks, with or without an unexposed four-week observation period (Butenhoff et al. 2017). No tumors were observed in any of the treated groups. These studies of PFOSF were not considered informative because of the short exposure duration and observation period.

4.1 Carcinogenicity Studies Conducted in Rats

4.1.1 Two-year carcinogenicity studies in male and female Sprague Dawley rats

Two-year carcinogenicity studies of K^+PFOS in male and female rats were conducted and reported by the 3M Company (Thomford 2002), and the data were later published in a peer-reviewed article (Butenhoff et al. 2012a). In these studies, 41-day-old male and female Sprague Dawley [Crl:CD(SD)IGS BR] rats (50 animals/group/sex) were administered K^+PFOS (PFOS potassium salt, 86.9% purity), produced by 3M Company (Saint Paul, MN), in the diet at doses of 0, 0.5, 2, 5, or 20 ppm for two years. The K^+PFOS used in these studies (Lot 217) contained 70% linear and 30% branched isomers (Arsenault et al. 2008). The impurities in this lot included 4.73% perfluorohexane sulfonate (C6 homolog, PFHxS), 0.71% perfluorinated carboxylic acids (C4, C5, and C8), 1.45% metals (calcium, magnesium, sodium, nickel, and iron), and 0.59% inorganic fluoride (Seacat et al. 2003).

In these studies, 5 additional animals/sex/dosed group were sacrificed at 4 weeks for blood chemistry/proliferation rate, and another 5 animals/sex/dosed group were sacrificed at 14 weeks for histopathology analysis. An additional 10 animals/sex in each of the control and 20 ppm groups were sacrificed at 53 weeks for interim evaluation (*e.g.*, liver weight, clinical pathology and histopathology). The studies also included a "20 ppm recovery" group (40 animals/sex) in which the animals were administered 20 ppm K^+PFOS in the diet for 52 weeks, and then received basal diet for 52 weeks before study termination.

Males

In the two-year study in male rats, mortality in the 5 and 20 ppm groups was significantly decreased compared to the control group; a statistically significant dose-related trend in survival was observed. The average body weight in the 20 ppm group was statistically significantly lower than that in the control group during 9 to 37 weeks of K^+PFOS treatment. Among the animals alive at 105 weeks, average body weight in the treated groups were similar to the control group. From weeks 1 to 24, a decrease in feed consumption was observed in the 20 ppm group when compared with the controls. Food consumption was similar among all groups from 28 weeks through study termination at 104 weeks.

Achieved intakes of K^+PFOS were reported to be 0, 0.024, 0.098, 0.242, or 0.984 mg/kg-day in males. Serum PFOS concentrations at various time points were reported by Butenhoff et al. (2012a). OEHHA calculated the achieved lifetime average daily serum PFOS concentrations as 0.014, 2.64, 12.1, 32.3 and 121 mg/l for the 0, 0.5, 2, 5, and 20 ppm groups, respectively (see Section 5.7.2, OEHHA (2021)).

Tumors observed in the two-year male rat study are presented in Table 6. A statistically significant increase in hepatocellular adenomas was observed in the 20 ppm group compared to the control group, with a positive dose-related trend. Spontaneous tumors of the liver are relatively rare in rats (Bannasch and Zerban 1990), although incidence may vary by rat strain and by tumor type. In SD rats, spontaneous hepatocellular adenomas occurred at a rate of 2.3% (32/1389) in males in studies initiated between 1995 and 2002 (Charles River Laboratories 2004). Hepatocellular adenomas and carcinomas originate from the same cell type, and adenomas can progress to carcinomas with the potential to metastasize (Maronpot et al. 1986).

In the pancreas, islet cell carcinomas were increased with a statistically significant dose-related trend. One animal in the 5 ppm group developed islet cell carcinoma that metastasized to the liver. There was no treatment related increase in islet cell adenoma, or combined islet cell adenoma and carcinoma. Pancreatic islet cell adenomas occur more frequently than carcinomas (Mense and Rosol 2018). The rates of pancreatic islet cell tumors are reported to be 7.9% (109/1385) for adenomas and 3.4% (47/1385) for carcinomas in untreated male SD rats based on studies initiated between 1995-2002 and reported by Charles River Laboratories (2004). Pancreatic islet cell adenomas and carcinomas arise from the same cell type in rats, and adenomas can progress to carcinomas (McConnell et al. 1986).

Table 6 Tumor incidence in male Crl:CD (SD) IGS BR rats exposed to K^+PFOS in feed for up to two years (Butenhoff et al. 2012a)

Tumor site	Tumor type	Day of first tumor	Administered dose in feed (ppm)					Trend test p-value
			0	0.5	2	5	20	
Liver	Hepatocellular adenoma	512	0/41	3/42	3/47	1/44	7/43**	0.006
Pancreas	Islet cell adenoma	465	4/44	3/44	4/48	4/46	4/44	NS
	Islet cell carcinoma	542	1/38	2/41	2/44	5/44	5/40	0.048
	Combined adenoma and carcinoma	465	5/44	5/44	6/48	8/46	9/44	NS

NS, not significant, $p \geq 0.05$. Tumor incidence is expressed as the number of tumor-bearing animals over the number of animals alive at the time of first occurrence of the tumor and examined at the site. Treatment group tumor incidences with asterisks indicate significant results from Fisher pairwise comparison with controls (conducted by OEHHA): ** $p < 0.01$. Exact trend test conducted by OEHHA.

In the group of male rats fed 20 ppm K^+PFOS in the diet for one year followed by basal diet for another year (the "20 ppm recovery" group), a statistically significant increase ($p = 0.04$) in thyroid follicular cell adenomas was observed compared to the control group (Table 7). The incidence was 3/31 in controls and 9/29 in the "20 ppm recovery" group, with the first occurrence of follicular cell adenoma on day 566. A follicular cell carcinoma was observed in one terminally sacrificed animal in the same treatment group. Thyroid follicular cell adenomas occur at a rate of 2.6% (36/1384) in untreated male SD rats based on studies initiated from 1995 to 2002 and reported by Charles River Laboratories (2004). Thyroid gland follicular cell adenomas and carcinomas arise from the same cell type (Botts et al. 1991). Follicular cell adenomas are expected to progress to carcinomas (McConnell et al. 1986). No increase in follicular cell adenomas or carcinomas was observed in the study's two-year continuous treatment groups.

Table 7 Tumor incidence in male Crl:CD (SD) IGS BR rats exposed to K^+PFOS in feed for one year and observed for an additional year (Thomford 2002)

Tumor site	Tumor type	Administered dose in feed (ppm)	
		0	20 ppm for one year and basal diet for another year
Thyroid	Follicular cell adenoma (Day of first tumor: 566)	3/31	9/29*

Tumor incidence is expressed as the number of tumor-bearing animals over the number of animals alive at the time of first occurrence of the tumor and examined at the site. Treatment group tumor incidences with asterisks indicate significant results from Fisher pairwise comparison with controls (conducted by OEHHA): * $p < 0.05$.

Non-neoplastic pathology findings

Some non-neoplastic findings were observed in the liver, pancreas, and thyroid gland of treated males.

At the 14-week and 53-week interim sacrifices, liver weights in the 20 ppm group were significantly higher compared to controls. Centrilobular hepatocellular hypertrophy and vacuolation were observed at the 14-week (5 and 20 ppm groups) and 53-week (20 ppm group) interim sacrifices. At terminal sacrifice, hepatocellular hypertrophy, eosinophilic granules, pigment, and vacuolation in the centrilobular region were each significantly increased in the 5 and 20 ppm groups. Increases in centrilobular cystic degeneration were observed in all dosed groups. Increases of altered basophilic foci and liver coagulative necrosis were observed in the 5 ppm group. In the pancreas, increases in interstitial fat infiltration were reported at terminal sacrifice in the 2 ppm group. Thyroid/parathyroid weights were decreased in the 20 ppm group at the 53-week interim sacrifice compared to controls.

Females

In the two-year study in females, a statistically significant increase in mortality was observed in the 2 ppm K^+PFOS group compared to controls from week 80 onwards and animals in this dose group were placed on basal diet at 103 weeks. No significant differences in mortality were observed in other dose groups compared to controls. The average body weight in the 20 ppm group was statistically significantly lower than that in the control group, starting at 3 weeks, and a statistically significant reduction in feed consumption was observed from weeks 2 to 36 in this dose group compared with the controls. Feed consumption and mean body weight were similar among all other treated groups compared to the control group.

Achieved intakes of K^+PFOS were reported to be 0, 0.029, 0.120, 0.299, or 1.251 mg/kg-day in females. Serum PFOS concentrations in these animals at various time points were reported by Butenhoff et al. (2012a). OEHHA (2021) calculated the achieved lifetime average daily serum PFOS concentrations as 0.841, 5.49, 23.0, 66.4 and 215 mg/l, for the 0.5, 2, 5, and 20 ppm groups, respectively.

As shown in Table 8, statistically significant increases in hepatocellular adenoma and adenoma or carcinoma combined were observed in females at the highest dose (20 ppm). Positive trends for hepatocellular adenoma and adenoma or carcinoma combined were also observed. One hepatocellular carcinoma was seen in the 20 ppm group and none in any other groups. Hepatocellular carcinoma is a rare tumor in female Sprague Dawley rats. Specifically in female Crl:CD (SD) BR rats, reported historical control incidences are 0/765 (Baldrick 2005) and 4/1389 (0.29%) (Charles River Laboratories 2004)[6]. In SD rats, spontaneous hepatocellular adenomas occurred at a rate of 1.2% in females (16/1389) in studies initiated between 1995 and 2002 (Charles River Laboratories 2004). Hepatocellular adenomas and carcinomas originate from the same cell type, and adenomas can progress to carcinomas with the potential to metastasize (Maronpot et al. 1986).

There were two thyroid gland follicular cell adenomas and one carcinoma in the 5 ppm group and one adenoma in the 20 ppm group. These tumors are rare, with reported historical control incidences of 0.55% (8/1467) (Baldrick 2005) and 0.86% (12/1388) (Charles River Laboratories 2004) for adenomas, and 0/1530 (Baldrick 2005) and 0.50% (7/1388) (Charles River Laboratories 2004) for carcinomas. Thyroid gland follicular cell adenomas and carcinomas arise from the same cell type (Botts et al. 1991). Follicular cell adenomas are expected to progress to carcinomas (McConnell et al. 1986).

Additionally, increased incidence of mammary fibroadenoma was observed in the low-dose (0.5 ppm) group. Transition from mammary gland fibroadenomas to malignant carcinomas has been observed in SD rats (McConnell et al. 1986; van Zwieten 1984).

[6] Charles River Laboratories (2004) includes studies that were initiated or published between 1989 and 2002. In general, the more relevant historical control data are provided by studies conducted within 2-3 years of the Thomford (2002) study. The Thomford (2002) study started in 1998 and lasted two years. Therefore, a subset of studies from Charles River Laboratories (2004), initiated or published between 1995 and 2002, was used in OEHHA's analysis.

Table 8 Tumor incidence in female Crl:CD (SD) IGS BR rats exposed to K^+PFOS in feed for up to two years (Butenhoff et al. 2012a; Thomford 2002)

Tumor site	Tumor type	Day of first tumor	Administered dose in feed (ppm)					Trend test *p*-value
			0	0.5	2[c]	5	20	
Liver	Adenoma	666	0/28	1/26	1/15	1/28	5/31*	$p < 0.01$
	Carcinoma	653	0/28	0/29	0/16	0/31	1/32	NS
	Combined adenoma and carcinoma	653	0/28	1/29	1/16	1/31	6/32*	$p < 0.01$
Thyroid[a]	Follicular cell adenoma[a]	671	0/26	0/25	0/14	2/26	1/30	NS
	Follicular cell carcinoma[a]	731	0/24	0/15	0/9	1/15	0/25	NS
	Combined adenoma and carcinoma[a]	671	0/26	0/25	0/14	3/26	1/30	NS
Mammary	Fibroadenoma[b]	229[b]	20/60	27/50*	20/48	24/49	11/60	NS

Tumor incidence is expressed as the number of tumor-bearing animals over the number of animals alive at the time of first occurrence of the tumor and examined at the site (first occurrence of follicular cell carcinoma was at terminal sacrifice). Treatment group tumor incidences with asterisks indicate significant results from Fisher pairwise comparison with controls (conducted by OEHHA): * $p < 0.05$. Exact trend test conducted by OEHHA. NS, not significant ($p \geq 0.05$).

[a] Thyroid follicular cell adenomas and carcinomas are both rare in female Crl:CD (SD) BR rats, with reported historical control incidences of 0.55% (Baldrick 2005) and 0.84% (based on studies conducted between 1995-2002 by Charles River Laboratories (2004)) for adenoma, and 0 (Baldrick 2005) and 0.53% (based on studies conducted between 1995-2002 by Charles River Laboratories (2004)) for carcinoma.

[b] The first occurrence of mammary gland fibroadenoma happened within the first year on day 229, therefore, incidence of mammary gland fibroadenoma for the control and 20 ppm groups includes 10 animals each from the one-year interim sacrifice group. For the 0.5, 2, and 5 ppm groups, there were no interim sacrifices at one year.

[C] Dosing stopped at week 103.

In the group fed 20 ppm K^+PFOS in the diet for one year followed by basal diet for another year (the "20 ppm recovery" group), one rare thyroid follicular cell adenoma was observed, compared to none in controls (Table 9).

Table 9 Tumor incidence in female Crl:CD (SD) IGS BR rats exposed to K^+PFOS in feed for one year and observed for an additional year (Thomford 2002)

Tumor site	Tumor type	Administered dose in feed (ppm)	
		0	20
Thyroid[a]	Follicular cell adenoma (day of first tumor: 736)	0/24	1/17

Tumor incidence is expressed as the number of tumor-bearing animals over the number of animals alive at the time of first occurrence of the tumor and examined at the site (first occurrence of follicular cell adenoma was at terminal sacrifice). Fisher pairwise comparison conducted by OEHHA showed no significant difference between control and treatment group tumor incidences.

[a] Thyroid follicular cell adenomas are rare in female Crl:CD (SD) BR rats, with reported historical control incidences of 0.55% (Baldrick 2005) and 0.84% (based on studies conducted between 1995-2002 by Charles River Laboratories (2004)).

Non-neoplastic pathology findings

Statistically significant increases of centrilobular hepatocellular hypertrophy were observed in the 5 and 20 ppm treatment groups, with a dose-related trend. Additionally, an increase in smooth endoplasmic reticulum was observed in the hepatocytes of rats in the 20 ppm treatment group.

4.2 Tumor Promotion Study Conducted In Trout

4.2.1 Six-month dietary exposure to K^+PFOS as a promoter after initiation with aflatoxin B_1 in rainbow trout

In this two-stage carcinogenesis study (Benninghoff et al. 2012), PFOS was tested to determine if it is a carcinogen or could act as a tumor promoter after initiation with the known carcinogen aflatoxin B_1 (AFB_1). K^+PFOS used in this study was purchased from Fluka Chemical Corp. (St Louis, MO), and was comprised of 78.9% linear and 21.1% branched isomers (Benskin et al. 2010). K^+PFOS dissolved in dimethyl sulfoxide (DMSO) was added directly to the oil portion of the Oregon Test Diet (OTD), a semipurified casein-based diet.

Approximately 500 trout per group were initiated with 10 parts per billion (ppb) AFB_1 for 30 minutes at 15 weeks (approximately 3.5 months) of age; controls were exposed to

0.01% ethanol. After initiation, fish were fed standard OTD for one month. After one month, trout (250 fish/treatment) were fed *ad libitum* OTD containing either 100 ppm K^+PFOS or 0.01% DMSO, 5 days per week for 6 months.

After the 6-month promotion period, animals were once again fed standard OTD (without K^+PFOS) for the remainder of the study (approximately two additional months). Histological evaluations of tumors were conducted at 12.5 months of age and were completed within one week.

As shown in Table 10, initiation with AFB_1 followed by promotion with dietary K^+PFOS (100 ppm) resulted in a statistically significant increase in liver adenomas and carcinomas combined compared to fish receiving AFB_1 initiation alone only (AFB_1/PFOS, 13%; AFB_1 only, 1%) ($p = 0.0014$). Of the liver tumors observed in the group initiated with AFB_1 and treated with dietary PFOS (100 ppm), 5% were hepatocellular adenoma, 10% were hepatocellular carcinoma, 5% were "mixed" adenoma, 68% were "mixed" carcinoma, 3% were cholangiocellular adenoma, and 10% were cholangiocellular carcinoma. Of the liver tumors observed in the "AFB_1 only" group, 29% were hepatocellular carcinoma and 71% were "mixed" carcinoma. No liver tumors were observed in the untreated control group (0 ppb AFB_1, 0 ppm PFOS) or in the "PFOS-only" group (0 ppb AFB_1, 100 ppm PFOS).

Table 10 Liver tumor incidence[a] in rainbow trout treated with AFB_1 as an initiator, K^+PFOS in diet for 6 months as a promoter, and observed for two additional months (Benninghoff et al. 2012)

Tumor site	Tumor type	AFB_1 0 ppb		AFB_1 10 ppb	
		PFOS 0 ppm	PFOS 100 ppm	PFOS 0 ppm	PFOS 100 ppm
Liver	Adenoma and carcinoma combined	0	0	1%	13%**

[a] Tumor incidence is reported as the percentage of fish with tumors.

** $p < 0.01$ compared with AFB_1 10 ppb/PFOS 0 ppm as determined by logistic regression analysis performed by Benninghoff et al. (2012) (LOGISTIC procedure, SAS version 9.2; SAS Institute, Cary, NC).

5. MECHANISTIC CONSIDERATIONS AND OTHER RELEVANT DATA

5.1 Pharmacokinetics and Metabolism

Much of the following information on the pharmacokinetics of PFOS appears in the OEHHA (2021) document "Proposed Public Health Goals for Perfluorooctanoic Acid and Perfluorooctane Sulfonic Acid in Drinking Water". Additional relevant information identified via OEHHA's literature search for this document (see Appendix B for literature search strategy) has been reviewed and included here, such as information on the transformation of PFOS precursors.

Overall, pharmacokinetic data demonstrate interspecies similarities in the absorption and distribution of PFOS, and some interspecies differences in the excretion and serum half-life. The half-life ($T_{1/2}$) estimates of PFOS are shorter in rats (24-83 days) and mice (30-43 days), and longer (110-200 days) in Cynomolgus monkeys [see Table 4.1.1. of OEHHA (2021); Pizzurro et al. (2019)]. The human PFOS $T_{1/2}$ is significantly longer compared to rodents and Cynomolgus monkeys. As reviewed in OEHHA (2021), estimated half-lives for PFOS in humans (highly exposed workers or general population) range from 1.7 to 8.7 years (see Table E1 in Appendix E of this document). OEHHA's drinking water program selected the human $T_{1/2}$ estimate of 3.4 years, a value from a study on a highly-exposed population due to drinking water contamination by PFASs, in development of the public health goal for PFOS (Li et al. 2018b; OEHHA 2021). US EPA (2016b) uses the $T_{1/2}$ estimate of 5.4 years for PFOS, based on data from a 5 year follow-up study of retired workers (Olsen et al. 2007).

5.1.1 Absorption

No empirical studies of PFOS oral absorption in humans were identified. PFOS is well absorbed with oral administration in animal studies. PFOS was fully absorbed in female white New Zealand rabbits following an oral gavage dose of 0.2 µg/kg (Tarazona et al. 2016). When 2 mg/kg PFOS was administered by intravenous (*i.v.)* injection or oral gavage to male or female Sprague-Dawley rats, the plasma concentration curves overlapped at ≥ 2 hours in either sex, indicating 100% absorption by the oral route in both sexes (Huang et al. 2019b).

5.1.2 Distribution

PFOS is widely distributed in the human body with preferential accumulation in the liver, plasma, and kidney, but it has also been detected in the lung, brain, gonads, bone, and other tissues (Koskela et al. 2017; Maestri et al. 2006; Olsen et al. 2003a; Pérez et al.

2013; Pizzurro et al. 2019). Detection in the brain indicates that PFOS crosses the blood-brain barrier. Similarly, studies in rodents show distribution throughout the body with the highest PFOS levels usually detected in the liver (Chang et al. 2012; Cui et al. 2009; De Silva et al. 2009; Huang et al. 2019b; Pizzurro et al. 2019). OEHHA (2021) provides a detailed overview regarding tissue distribution in its Appendix on Toxicokinetics (Table 6.5 in Appendix 6 of that document).

PFOS can cross the placenta and accumulate in the fetus, with accumulation in the fetal liver being observed in humans (Mamsen et al. 2019). PFOS and several precursors (*i.e.* PFOSA, MePFOSAA and EtPFOSAA) were detected in 50 paired maternal and cord serum samples taken after delivery (Yang et al. 2016). Significant correlation between maternal and cord blood levels was found for PFOS (Pearson correlation coefficient, r = 0.882). Maternal serum PFOSA was significantly correlated with PFOS in cord serum with a smaller correlation (r = 0.361) (but not with maternal PFOS or cord serum PFOSA), suggesting maternal PFOSA could be a potential indirect source of PFOS in fetuses (Yang et al. 2016). PFOS is also distributed into breastmilk in animals (Kowalczyk et al. 2012; Kowalczyk et al. 2013) and humans, resulting in decreased body burden in the mothers and increased blood concentrations in the infants (reviewed in Pizzurro et al. (2019); (Zheng et al. 2021)). Increases of serum PFOS levels by up to 29.2% per month have been reported in infants and toddlers (through age 18 months) during periods of exclusive breastfeeding (Mogensen et al. 2015). In a cross-sectional study of 300 children in Texas, plasma concentrations of PFOS steadily increased for the following age groups: 0-3, 3-6, 6-9 and 9-13 years old, indicating that the PFOS burden due to *in utero* or lactational exposure becomes less significant starting at 3 years of age, if not earlier, as the child is exposed to PFOS from other sources such as dust or food (Schecter et al. 2012). Several recent kinetic and physiologically based pharmacokinetic (PBPK) models have addressed infant kinetics of PFASs (Brochot et al. 2019; Goeden et al. 2019; Verner et al. 2016).

The distribution and bioaccumulation pattern of PFOS in the body is thought to be driven by its binding to proteins, such as serum albumin and the liver fatty acid-binding protein (L-FABP), which is an intracellular lipid-carrier protein (Cheng and Ng 2017; Kennedy et al. 2004). PFOS protein binding studies are summarized in OEHHA (2021) (Table 6.2 in Appendix 6 of that document).

At physiological pH, PFOS exists predominantly in the anionic form and therefore would not be able to cross membranes via passive transport. Several transporter proteins are likely to be involved in PFOS transport. Relevant studies have been detailed in OEHHA (2021) (Table 6.3 in Appendix 6 of that document).

Human biomonitoring data show that the percentage of branched PFOS isomers measured in serum can range between 24.4% to 50.8% of total PFOS in different populations (Schultes et al. 2020; Zhou et al. 2014). The different composition of linear

and branched PFOS isomers observed in biomonitoring studies can be the result of a variety of factors, including different sources of exposure (Schultes et al. 2020; Zhou et al. 2014), differential transformation of specific PFOS precursors (Xu et al. 2004), and different accumulation or excretion patterns between linear and branched isomers (Gao et al. 2015). The linear PFOS isomer can be enriched in serum relative to the percentage present in commercial ECF-produced PFOS, which typically consists of approximately 70% linear PFOS. The percentage of the linear isomer can reach up to 75.6% in cord blood (Schulz et al. 2020), and up to 78.4% in occupationally exposed workers (Zhou et al. 2014). Longer retention of the linear PFOS isomer could be due to differences in excretion and/or tighter binding to proteins (*e.g.*, albumin) (Beesoon and Martin 2015; Gao et al. 2015; Zhang et al. 2013b). Studies of isomer-specific binding affinity of PFOS to serum proteins have shown that linear PFOS has a stronger interaction with human serum albumin than branched isomers (Beesoon and Martin 2015; Gao et al. 2015).

There are some animal studies that have reported on the distribution of PFOS structural isomers (Benskin et al. 2009a; De Silva et al. 2009). When administered orally as a mixture of isomers to rats, PFOS demonstrated organ-specific and sex-specific differences between linear and branched isomers after 38 days following a single dose or after 38 daily treatments (Benskin et al. 2009a; De Silva et al. 2009). Tissue-specific isomer distribution has also been reported in polar bears and several aquatic organisms (Fang et al. 2014; Greaves and Letcher 2013).

5.1.3 Metabolism

PFOS is not known to be metabolized in animals or humans (EFSA 2018). While metabolism studies in humans are lacking, it is generally assumed that PFOS is inert to metabolism and is excreted intact (US EPA 2016b). PFOS can be formed in the body from various PFOS precursors (discussed further below).

5.1.4 Excretion

PFOS excretion pathways in humans include urinary and fecal excretion and incorporation into nails and hair, although overall the rate of elimination for PFOS is slow. Additional PFOS elimination routes include pregnancy-related losses, elimination via breast milk, and menstrual blood loss in females (Gomis et al. 2017; Wong et al. 2014).

In humans, multiple reports directly measured PFOS renal clearance in occupationally exposed subjects and in the general population (see OEHHA (2021); Table 4.5.1 of that document). In addition to its presence in the serum and urine, PFOS was detected in the nails and hair of the general population (Wang et al. 2018b). All studies were in

Asia (China, Japan). Despite a wide range of observed PFOS serum concentrations, the average renal clearance values from each study were generally narrowly distributed, ranging from 0.01 to 0.031 ml/kg-day with a geometric mean of 0.016 ml/kg-day from six studies.

Measurements of PFOS in feces were below the detection limit in two human studies (Beesoon et al. 2012; Genuis et al. 2013). However, PFOS could be detected in stool samples following treatment with cholestyramine in eight highly exposed individuals (Genuis et al. 2013), providing evidence for the presence of enterohepatic circulation of PFOS. Cholestyramine is a resin used to immobilize certain lipophilic compounds in the gastrointestinal tract, preventing their reabsorption and therefore, interrupting their enterohepatic cycle. A study using NHANES data indicates that dietary fiber intake may also increase the gastrointestinal excretion of PFOS (Dzierlenga et al. 2021).

Further evidence for enterohepatic circulation of PFOS comes from measurements of its biliary clearance in humans. Harada et al. (2007) measured PFOS in bile samples from four elderly patients, and estimated mean biliary clearance as 2.98 ml/kg-day, which is higher than the urinary clearance, and would also greatly exceed the overall plasma clearance given the kinetic assumptions used in that study. Therefore, the authors concluded that a large fraction of PFOS secreted with bile would be reabsorbed via an enterohepatic circulation mechanism, and estimated that the reabsorbed fraction was 0.97.

Animal studies indicate that excretion rates and amounts can vary amongst species, with ruminants and fish excreting more via feces compared to rodents. Overall, urinary and fecal excretion of PFOS in rodents is minimal (Chang et al. 2012; Kowalczyk et al. 2012; Lupton et al. 2014; Vidal et al. 2019).

A study in rats indicated that approximately similar amounts of PFOS were excreted in the urine and feces over the first 10 days of the study, in which rats received daily doses of either 5 or 20 mg/kg-day via gavage for 28 days, with progressively relatively higher amounts of PFOS excreted in urine at 10+ days (Cui et al. 2010). The amounts excreted in urine and feces during the first 24 hours amounted to 2.6-2.8% of the total dose. In another study, rats excreted a mean cumulative 30.2% of the administered dose in urine by day 89 post-dosing, and 12.6% in feces by day 64. Excretion in 24 hours in urine and feces was 1.55% and 1.57%, respectively (Chang et al. 2012). Similar to reports in human studies discussed above, fecal excretion of PFOS in rats can be increased via administration of cholestyramine (Johnson et al. 1984).

In Cynomolgus monkeys, urinary excretion was less than 0.07% of the administered dose 24 hours post-dosing (Chang et al. 2012).

In cattle and sheep, feces is the major route of excretion, amounting to 11% of the administered dose in cattle (Lupton et al. 2014) and 4-5% in sheep (Kowalczyk et al.

2012); only minimal (0.5%) urinary excretion is reported in cattle (Lupton et al. 2014). Similarly, in fish PFOS is primarily eliminated in the feces while urine is a minor excretion route (Vidal et al. 2019).

PFOS is also excreted into milk in animals. Dairy cows had a cumulative secretion into milk of 14% after 28 days when fed a diet containing 7.6 µg/kg-day of PFOS for 21 days (Kowalczyk et al. 2013). In sheep exposed to 1.16 and 1.45 µg/kg-day of PFOS for 21 days, the median milk concentrations for PFOS ranged from 2.6 to 7.0 µg/l, with a calculated transfer rate of ≤ 2% in a period of 21 days (Kowalczyk et al. 2012).

PFOS structural isomers may vary in their excretion pathways and rates. When examining the elimination of PFOS isomers in rats, Benskin et al. (2009a) reported that urine, but not feces, had preferential enrichment of branched PFOS isomers. Branched PFOS isomers were generally cleared more rapidly from the blood in females than in males (De Silva et al. 2009). Branched PFOS isomers were also eliminated faster than the linear isomer in fish (*Pseudogobius sp.*) (Hassell et al. 2020). The elimination of linear and branched isomers of one PFOS precursor, PFOSA, has been studied in rats. After administration of PFOSA via food for 77 days, branched PFOSA isomers were eliminated faster than the linear form in rats (Ross et al. 2012).

5.1.5 Biotransformation of precursors to PFOS

Studies have been conducted on three PFOS precursors, *i.e.,* PFOSA, EtPFOSE and PFOSAmS (perfluorooctanesulfonamido ammonium salt), demonstrating *in vivo* biotransformation to PFOS. These *in vivo* biotransformation studies are discussed below, followed by a brief summary of biotransformation studies conducted using *in vitro* systems. In one study, male SD rats were fed PFOSA (synthesized by ECF and containing linear and various branched isomers) via food for 77 days (Ross et al. 2012), and the blood levels of linear and branched PFOS isomers (*e.g.*, 1m-, 3m- and 5m-PFOS; see Table A1 in Appendix A for isomer definitions) were measured and compared to the isomeric pattern of PFOS (synthesized by ECF). Various PFOS isomers were detected in blood following exposure to PFOS, indicating *in vivo* biotransformation of PFOSA in rats. Among all PFOS isomers detected, the authors observed a significantly higher percentage of branched 5m-PFOS and significantly lower percentages of 1m-, 3m- and 4m-PFOS, compared to the isomeric composition of ECF PFOS. PFOSA elimination half-lives in blood were shorter for branched isomers compared to the linear isomer (2.5-3.7 vs. 5.9 days), and the authors suggested this was possibly due to preferential transformation of certain branched PFOSA isomers to PFOS rather than faster excretion, since there was no enrichment in urinary or fecal excretion of branched PFOSA isomers. PFOSA has also been shown to be transformed to PFOS in carp (Chen et al. 2015) and earthworms (Zhao et al. 2020).

Another precursor, EtPFOSE, was shown to be biotransformed to PFOS in female SD rats treated orally with EtPFOSE for 21 days (Xie et al. 2009). Several metabolites (including PFOSE, PFOSA and PFOS) were detected in the liver and serum. PFOS was the major EtPFOSE metabolite, accounting for 9.5% of the administered EtPFOSE dose in the serum and liver. Another study of EtPFOSE in male SD rats estimated that 12% of the inhaled EtPFOSE dose was transformed to PFOS (Chang et al. 2017). PFOS was detected in the serum immediately after the 6-hour exposure and reached a peak concentration in serum between 8-14 days post-exposure (Chang et al. 2017). EtPFOSE was not detected in any serum samples 24 hours post-exposure. Et-PFOSE can be transformed to PFOS in earthworms (Zhao et al. 2019), as can PFOSAmS (Jin et al. 2020).

Several *in vitro* studies have examined the transformation of various PFOS precursors to more immediate precursors (such as PFOSA) or to PFOS itself. *In vitro* evidence shows that human liver microsomes and isolated CYP enzymes (2C9 and 2C19) transformed EtPFOSA to PFOSA, a more immediate precursor of PFOS (Benskin et al. 2009b). Branched EtPFOSA isomers can be transformed faster than the linear isomer. Xu et al. (2004) carried out *in vitro* studies on the transformation of various PFOS precursors, and reported that one PFOS precursor, EtPFOSE, can be transformed to *N*-(2-hydroxyethyl)perfluorooctanesulfonamide (PFOSE alcohol) and subsequently to perfluorooctanesulfonamide (PFOSA) by male SD rat liver slices, liver microsomes, or cytosol. These biotransformations were catalyzed mainly by rat P450 2C11 and 3A2, and by human P450 2C19 and 3A4/5 (Xu et al. 2004). Interestingly, Xu et al. (2004) found that PFOSA was transformed to PFOS in rat liver slices at a low rate, but PFOS was not detected in liver slices treated with any of the other PFOS precursors. Transformation of PFOSA (or any of the other precursors) to PFOS was not detected with microsomal, cytosolic or 9000 g supernatant fractions. Similarly, Benskin et al. (2009b) did not observe any transformation of PFOSA to PFOS by human liver microsomes. *In silico* prediction indicated that transformation pathways for PFOS precursors are isomeric-specific (Fu et al. 2015), which is consistent with the *in vivo* findings reported by Ross et al. (2012) in male SD rats that branched PFOSA isomers are more rapidly converted to PFOS than linear PFOSA.

5.2 Toxcast High-Throughput Screening Assays

ToxCast (US EPA Toxicity Forecaster) is a chemical prioritization research program developed by the US EPA (Dix et al. 2007; Judson et al. 2010; Kavlock et al. 2012). ToxCast includes data generated by the Tox21 (Toxicology in the 21st Century) program, which is a multi-agency collaboration between the National Institute of Environmental Health Sciences/National Toxicology Program, the National Center for Advancing Translational Sciences, the US Food and Drug Administration, and US EPA's National Center for Computational Toxicology. ToxCast utilizes various *in vitro* and zebrafish systems to identify chemical activity in a battery of high-throughput screening (HTS) assays. OEHHA explored ToxCast data on PFOS and its salts and transformation and degradation precursors using information that is publicly available on the Computational Toxicology (CompTox) Chemicals Dashboard (https://comptox.epa.gov/dashboard, accessed on May 3, 2021).

The ToxCast database on the CompTox Chemicals Dashboard reported that:

- PFOS was active in 260 of the 1,165 assays it was tested in
- PFOS potassium salt was active in 179 of the 895 assays it was tested in
- PFOS lithium salt was active in 26 of the 238 assays it was tested in
- PFOSA was active in 260 of the 894 assays it was tested in (excluding cell-free assays)
- EtFOSA was active in 139 of the 797 assays it was tested in (excluding cell-free assays)

ToxCast assays in which PFOS, PFOS potassium salt, PFOS lithium salt, PFOSA, and EtFOSA were active are shown in Appendix F, Table F1– F5, respectively. For purposes of this document, the activity of PFOS precursors is only relevant for those assays where cellular biotransformation of the precursor to PFOS may have occurred; therefore, cell-free assays for PFOSA and EtFOSA were excluded from consideration (and Table F1-F5). Although there were curve-fitting flags (flags not shown in Appendix F) associated with some ToxCast assays in which PFOS and its salts, PFOSA and EtFOSA were active, we did not exclude assays with flags for the following reasons. First, these curve-fitting flags are subject to change as the ToxCast data analysis pipeline evolves (Thomas et al. 2019). Second, completely filtering out all active assay calls that have curve-fitting flags is not recommended because potential biological signals could be omitted (Judson et al. 2016). The most up-to-date flags for these assays can be found on the CompTox Chemicals Dashboard and the implications of individual flags should be interpreted in the context of the specific assay and data chart.

There are several limitations that exist in the ToxCast datasets for PFOS, its salts, PFOSA, and EtFOSA. First, the purity grades of the PFOS, PFOS potassium salt, PFOS lithium salt, and EtFOSA used in the ToxCast assays were not reported, and the purity grades of the test substances used in the Tox21 assays are reported as "unknown/inconclusive", based on the Tox21 quality control analyses (https://tripod.nih.gov/tox21/samples, accessed on May 3, 2021). While the purity grade of PFOSA used in the Tox21 assays is reported as "more than 90%" and considered adequate, the purity grade of PFOSA used in the ToxCast assays was not reported. Another limitation of the ToxCast data on PFOS precursors is the uncertainty regarding the extent to which biotransformation of EtFOSA or PFOSA to PFOS may have occurred in these *in vitro* or zebrafish assays, *i.e.*, it remains unknown if and how much the observed effects were due to their transformation into PFOS.

Given all of the above, the ToxCast data provide limited information on the carcinogenicity of PFOS. Also, PFOS, its salts, and precursors are surfactants, and the *in vitro* disposition of these chemicals in ToxCast assay systems (other than the zebrafish assays) remains uncertain. It has been acknowledged that chemical disposition and partitioning can greatly affect the accuracy of predictions from *in vitro* test systems[7]. Additionally, the surfactant properties of PFOS, its salts, and precursors may cause cell lysis and cytotoxicity at high concentrations in cell-based assays, *e.g.*, in human bronchial epithelial cells (Sørli et al. 2020).

[7] Tox21 Cross-Partner Projects. 4. *In vitro* Chemical Disposition. Available: https://tox21.gov/projects/. Crizer D, Sipes N, Waidyananthaet S et al (2020): *In Vitro* Disposition of Tox21 Chemicals: Initial Results and Next Steps. Available: https://www.epa.gov/sites/production/files/2020-10/documents/7_david_crizer_epa_nams_conference_2020_508c.pdf

5.3 Key Characteristics of Carcinogens

A comprehensive review of the more than 100 agents known to cause cancer in humans identified 10 key characteristics (KCs) of carcinogens (Table 11) (IARC 2020b; Smith et al. 2016). As the name implies, KCs are characteristics of agents that cause cancer, in contrast to the hallmarks of cancer (Hanahan and Weinberg 2000, 2011), which are properties of cancer cells and neoplasms, and also in contrast to modes of action, which are sequences of key events that transform normal cells into malignant tumors. Mode of action analysis depends on prior knowledge sufficient to hypothesize how an agent might cause cancer, knowledge that too often is incomplete. The KCs can encompass many types of mechanistic endpoints and are not constrained to previously formulated hypotheses, allowing a broader consideration of multiple mechanistic pathways and hypotheses. OEHHA uses this approach to systematically identify, organize, and summarize information on mechanisms of carcinogenesis.

For this assessment on PFOS and its salts and precursors, OEHHA reviewed the evidence identified through literature searches on all 10 KCs and found evidence for 8 of them (few data were identified for KC1 and KC3). Data on PFOS precursors were identified but not considered relevant for the hazard identification of PFOS, as there is considerable uncertainty regarding whether the effects seen were due to their transformation/degradation into PFOS.

Table 11 Ten key characteristics of carcinogens

Key characteristic	Example of relevant evidence
1. Is electrophilic or can be metabolically activated	Parent compound or metabolite with an electrophilic structure (*e.g.,* epoxide, quinone), formation of DNA and protein adducts
2. Is genotoxic	DNA damage (DNA strand breaks, DNA–protein cross-links, UDS), intercalation, gene mutations, cytogenetic changes (*e.g.,* CAs, MN)
3. Alters DNA repair or causes genomic instability	Alterations of DNA replication or repair (*e.g.,* topoisomerase II, base-excision or double-strand break repair)
4. Induces epigenetic alterations	DNA methylation, histone modification, microRNA expression
5. Induces oxidative stress	Oxygen radicals, oxidative stress, oxidative damage to macromolecules (*e.g.,* DNA, lipids)
6. Induces chronic inflammation	Elevated white blood cells, myeloperoxidase activity, altered cytokine and/or chemokine production
7. Is immunosuppressive	Decreased immunosurveillance, immune system dysfunction
8. Modulates receptor-mediated effects	Receptor inactivation/activation (*e.g.,* ER, PPAR, AhR) or modulation of endogenous ligands (including hormones)
9. Causes immortalization	Inhibition of senescence, cell transformation
10. Alters cell proliferation, cell death, or nutrient supply	Increased proliferation, decreased apoptosis, changes in growth factors, energetics and signaling pathways related to cellular replication or cell cycle control, angiogenesis

Source: Smith et al. (2016) and IARC (2020b)

AhR, aryl hydrocarbon receptor; ER, estrogen receptor; PPAR, peroxisome proliferator–activated receptor. Any of the 10 characteristics in this table could interact with any other (*e.g.*, oxidative stress, DNA damage, and chronic inflammation), which when combined provides stronger evidence for a cancer mechanism than would oxidative stress alone.

5.3.1 Is electrophilic or can be metabolically activated

The literature search identified few data for this key characteristic.

5.3.2 Is genotoxic

Genotoxicity refers to the ability of a chemical or other type of agent or biological process to damage DNA or induce changes in the DNA sequence. The link between genotoxicity and carcinogenesis is well established (Smith et al. 2016; Smith et al. 2020). Changes in the DNA sequence include gene or point mutations such as base substitutions, frameshifts, and small deletions or insertions, and chromosomal effects such as chromosomal aberrations, micronuclei, and aneuploidy. Examples of DNA damage include DNA adducts, DNA strand breaks, and DNA-DNA and DNA-protein crosslinks.

Studies on the genotoxicity of PFOS have been reviewed and summarized in detail by the European Food Safety Authority (EFSA 2008, 2018). EFSA (2018) concluded "the available data are inconclusive", noting that there is "some evidence that the observed effects [of genotoxicity] are related to oxidative stress", and that, "[f]rom *in vitro* and *in vivo* genotoxicity studies, there is no evidence for a direct genotoxic mode of action for both PFOS and PFOA, however, genotoxicity cannot be excluded."

Based on the literature search conducted for this hazard identification document, additional genotoxicity publications on PFOS were identified that were not included in the EFSA (2008, 2018) reviews of genotoxicity (Chen et al. 2016b; Eke et al. 2017; Emerce and Çetin 2018; Jernbro et al. 2007; Kim et al. 2016; Kim et al. 2010; Lin et al. 2016; Liu et al. 2016; Logeshwaran et al. 2021; Lu et al. 2012, 2013a; Lu et al. 2013b; Nalbantlar and Çakal Arslan 2017; NTP 2019; Oda et al. 2007; Shao et al. 2019; Sivaram et al. 2020; Wang et al. 2013; Zhang et al. 2013a; Zheng et al. 2013; Zheng et al. 2016). These additional studies are briefly discussed below, followed by Table 12 to Table 15 that summarize all of the studies identified as relevant to the genotoxicity of PFOS.

Three studies analyzing biomarkers of genotoxicity in human urine (Kim et al. 2016; Lin et al. 2016; Lin et al. 2020a) were identified. Serum PFOS levels correlated with urinary levels of the oxidative DNA damage marker 8-OHdG in a dose-dependent manner in two studies, one conducted in 126 Korean seniors over 60 years of age (Kim et al. 2016) and another in 597 adults (22-63 years old) in Taiwan (Lin et al. 2020a). No association was reported in a third study of 848 individuals (12-30 years old) in Taiwan (Lin et al. 2016).

One rat study conducted by Eke et al. (2017) reported that PFOS administered at doses of 0, 0.6, 1.25, or 2.5 mg/kg every 48 hours via oral gavage over a four-week period increased micronuclei (MN) and DNA damage (DNA strand breaks, as measured in the comet assay) in a dose-dependent manner in hepatocytes of male rats.

In 28-day studies conducted by NTP in male and female rats, a statistically significant increase in MN was observed in polychromatic erythrocytes in the peripheral blood of female rats in the high dose group, with a significant dose-related trend, following exposure to PFOS (NTP 2019). However, the increases in MN were within the historical control range, and thus NTP considered the findings in female rats to be equivocal. No increase in MN was observed in similarly exposed male rats (NTP 2019). Dose dependent decreases in the percentages of polychromatic erythrocytes in peripheral blood were observed in rats of both sexes, suggesting that the bone marrow is a target of PFOS cytotoxicity (NTP 2019).

Four *in vitro* studies investigating PFOS and genotoxicity using a variety of cell types/lines were identified. One study using sperm cells obtained from 3 healthy men found no increase of DNA strand breaks via comet assay after one hour of PFOS treatment (100, 300, and 1000 µM) (Emerce and Çetin 2018). One study in human-hamster hybrid cells (full set of hamster chromosomes and a single copy of human chromosome 11) found no induction of mutations at the *CD59* locus on human chromosome 11 after 1, 4, 8, or 16 days of PFOS treatment (1-200 µM) (Wang et al. 2013). A single PFOS concentration (12.5 µg/ml) and exposure time point (4 hours) did not show any effect on MN formation in hamster lung V9 cells (Jernbro et al. 2007). Using the comet assay, Zhang et al. (2013a) observed increased DNA damage in primary mouse Leydig cells treated with 12.5-62.5 µg/ml of PFOS for 24, 48, or 72 hours in a dose- and time-dependent manner, although no p-value from the statistical analysis was reported. In addition to these studies using cells/cell lines, one electrochemical study of the interaction of PFOS with calf thymus DNA immobilized on a specially prepared carbon electrode found that PFOS binds to the groove in the DNA double helix, intercalates into the DNA, and forms hydrogen bonds with DNA bases, perturbing base pair stacking and reducing DNA charge transport (Lu et al. 2012). Similar findings were reported by the same laboratory using a cadmium selenide quantum dot electrochemiluminescence sensor (Lu et al. 2013b) and a nano-gold embedded nanoporous poly-pyrrole film (Lu et al. 2013a).

In non-mammalian test systems, several studies investigating mutations or DNA damage caused by PFOS were identified. A set of studies conducted by NTP reported findings from bacterial mutagenicity assays (NTP 2019). PFOS was not mutagenic in two strains of *Salmonella* (TA98, TA100) or in the *E. coli* strain WP2 *uvrA*/pkM101, in either the presence or absence of metabolic activation (S9). One *in vivo* transgenic medaka fish study showed that a 30-day exposure to PFOS, followed by a 15-day

exposure to clean water induced mutations in the *cII* target gene in the liver (Chen et al. 2016b). These authors noted that PFOS induced "a distinct mutational spectrum dominated by +1 frameshift mutations" in the target gene in the livers of exposed fish. Nalbantlar and Çakal Arslan (2017) and Sivaram et al. (2020) detected a significant increase in MN formation in mussels and onion roots, respectively. DNA strand breaks as detected by the comet assay were observed with PFOS exposure in carp (50-50,000 µg/l for 4 days) (Kim et al. 2010), earthworms (50-470 mg/kg for 14 days) (Zheng et al. 2016), earthworms (10-250 mg/kg for 14 days) (Zheng et al. 2013), a type of planarian, *Dugesia japonica* (5 mg/l for 4 days) (Shao et al. 2019), water flea (0.001-10 mg/l) (Logeshwaran et al. 2021) and onion (1-100 mg/l for 48 hours) (Sivaram et al. 2020) . The mRNA expression of DNA repair genes, *uvrA* and *recA*, was increased in *E. coli* treated with 400 mg/l K^+PFOS for 3 hours, suggesting a treatment-related increase in DNA damage (Liu et al. 2016). No effect on DNA damage was reported for *Salmonella* with or without metabolic activation (S9) after 3 or 5 hours of 30-1000 µM of PFOS exposure in the umu gene expression test (Oda et al. 2007).

Table 12 Genotoxicity studies of PFOS in humans

Test endpoint	Study population (sample size)	PFOS exposure metric	Results	Reference
Oxidative DNA damage (urinary 8-OHdG)	Urine and serum sampled from Korean Elderly Environmental Panel (KEEP) study (n = 126)	Mean levels of PFOS measured in serum: 10.04 ng/ml (14 other PFASs also measured)	PFOS levels were positively associated with 8-OHdG levels (p = 0.001); does not seem to be adjusted for creatinine	Kim et al. (2016)
Oxidative DNA damage (urinary 8-OHdG)	Taiwanese adults aged 22 to 63 years old in a case-control study of cardiovascular disease (n = 597)	Serum levels of PFOS (GM = 12.92 ng/ml for linear PFOS, and 0.44 ng/ml for branched PFOS)	Increasing linear PFOS (but not branched PFOS) levels were associated with urinary 8-OHdG (in natural log) (p trend = 0.016)	Lin et al. (2020a)
Oxidative DNA damage (urinary 8-OHdG)	Urine and serum sampled from male and female university students in Taiwan from the Young Taiwanese Cohort 1992-2000 (n = 848)	Geometric mean levels of PFOS measured in serum: 6.44 ng/ml (PFOA, PFNA, and PFUA also measured)	Negative	Lin et al. (2016)

PFOA, perfluorooctanoic acid; PFNA, perfluorononanoic acid; PFUA, perfluoroundecanoic acid

Table 13 *In vivo* genotoxicity studies of PFOS in mammals

Test endpoint	Species assayed	Route, duration, dosing regimen	Results	Reference
Mutation	Mouse: male *gpt* delta transgenic (6/dose)	0, 1.5, 4, or 10 mg/kg via gavage for 28 days	Increase of the *red/gam* locus mutation frequencies in the liver at ≥4 mg/kg	Wang et al. (2015c), also reviewed in EFSA (2018)
Micronuclei	Mouse: male and female	A single oral dose of 237.5, 450, or 950 mg/kg, with sampling at 24, 48, or 72 hours	Negative	Corning Hazleton, Inc. (1993), as reported by EFSA (2008)[1]
Micronuclei	Mouse: male *gpt* delta transgenic (6/dose)	0, 1.5, 4, or 10 mg/kg via gavage for 28 days	Non-significant increase of MN frequency in the liver at ≥ 4 mg/kg	Wang et al. (2015c), also reviewed in EFSA (2018)
Micronuclei	Rat: male Swiss albino (Wistar) (6/dose)	0, 0.6, 1.25, or 2.5 mg/kg via gavage every 48 hours over a 4-week period	Increased MN frequency of polychromatic erythrocytes in bone marrow at ≥ 1.25 mg/kg	Çelik et al. (2013), also reviewed in EFSA (2018)
Micronuclei	Rat: male Swiss albino (Wistar) (6/dose)	0, 0.6, 1.25, or 2.5 mg/kg via gavage every 48 hours over a 4-week period	Increased MN frequency in peripheral blood cells at ≥ 0.6 mg/kg	Eke and Çelik (2016), also reviewed in Chen et al. (2016b); EFSA (2018)
Micronuclei	Rat: male Swiss albino (Wistar) (6/dose)	0, 0.6, 1.25, or 2.5 mg/kg via gavage every 48 hours over a 4-week period	Dose-dependent increases in MN frequency in hepatocytes at ≥ 0.6 mg/kg	Eke et al. (2017)
Micronuclei	Rat: female Sprague Dawley (10/dose)	0, 0.312, 0.625, 1.25, 2.5, or 5 mg/kg-day via gavage for 28 days	Dose-dependent increases in MN in polychromatic erythrocytes in peripheral blood; increases are within historical control range. Also reported a dose-dependent decrease in percentage of polychromatic erythrocytes in peripheral blood.	NTP (2019)

Test endpoint	Species assayed	Route, duration, dosing regimen	Results	Reference
Micronuclei	Rat: male Sprague Dawley (10/dose)	0, 0.312, 0.625, 1.25, 2.5, or 5 mg/kg-day via gavage for 28 days	No increase in MN in polychromatic erythrocytes in peripheral blood; dose-dependent decrease in percentage of polychromatic erythrocytes in peripheral blood	NTP (2019)
DNA strand breaks (comet assay)	Rat: male Swiss albino (Wistar) (6/dose)	0, 0.6, 1.25, or 2.5 mg/kg via gavage every 48 hours over a 4-week period	Increased DNA damage (strand breaks) in bone marrow at ≥ 0.6 mg/kg	Çelik et al. (2013); Wang et al. (2015c), also reviewed in EFSA (2018)
DNA strand breaks (comet assay)	Rat: male Swiss albino (Wistar) (6/dose)	0, 0.6, 1.25, or 2.5 mg/kg via gavage every 48 hours over a 4-week period	Increased DNA damage (strand breaks) in peripheral blood cells at ≥ 0.6 mg/kg	Eke and Çelik (2016); Wang et al. (2015c), also reviewed in EFSA (2018)
DNA strand breaks (comet assay)	Rat: male Swiss albino (Wistar) (6/dose)	0, 0.6, 1.25, or 2.5 mg/kg via gavage every 48 hours over a 4-week period	Increased DNA damage (strand breaks) in hepatocytes at ≥ 0.6 mg/kg	Eke et al. (2017)

[1] OEHHA has no access to Corning Hazleton, Inc. (1993), which was summarized by EFSA (2008). The EFSA (2008) summary of the study did not include information on the number of animals per treatment group.

Table 14 *In vitro* genotoxicity studies of PFOS in mammalian cells

Test endpoint	Species/cell line	Concentration/ duration	Results/comments	Reference
Mutation [*redBA/gam gene locus* (Spi^- assay)]	*gpt* delta transgenic mouse embryonic fibroblasts	0, 1-20 µM, 24 hours	Positive at ≥ 10 µM	Wang et al. (2015c), also reviewed in EFSA (2018)
Mutation (CD59 locus)	Human-hamster hybrid cells (full set of hamster chromosomes and a single copy of human chromosome 11)	0, 1-200 µM for 1, 4, 8, and 16 days	Negative	Wang et al. (2013)
Micronuclei	Human hepatoma HepG2 cells	0, 5-300 µM, 24 hours	Negative; significant cytotoxicity at ≥ 300 µM in a separate viability assay	Florentin et al. (2011), also reviewed in EFSA (2018)
Micronuclei	Hamster lung V9 cells	12.5 µg/ml with S9, 4 hours	Negative	Jernbro et al. (2007)

Test endpoint	Species/cell line	Concentration/ duration	Results/comments	Reference
Chromosomal aberrations	Human peripheral blood lymphocytes	Up to 599 µg/ml (-S9); up to 449 µg/ml (+S9)	Negative with or without S9	Cifone (1999), as reported by EFSA (2008)[1]
DNA strand breaks (comet assay)	Sperm cells obtained from 3 nonsmoker healthy men from Turkey, *in vitro*	0, 100, 300, 1000 µM	Negative	Emerce and Çetin (2018)
DNA strand breaks (comet assay)	Human hepatoma HepG2 cells	0, 5-300 µM, 24 hours	Negative; significant cytotoxicity at ≥ 300 µM in a separate viability assay	Florentin et al. (2011), also reviewed in EFSA (2018)
DNA strand breaks (comet assay)	Human hepatoma HepG2 cells	0, 0.2-20 µM, 24 hours	Positive at ≥ 0.2 µM	Wielsøe et al. (2015), also reviewed in EFSA (2018)
DNA strand breaks and FPG-sensitive sites (comet assay)	Human hepatoma HepG2 cells	0, 100, 400 µM, 24 hours	Negative; 400 µM for 24 hours resulted in cytotoxicity	Eriksen et al. (2010), also reviewed in EFSA (2018)
DNA strand breaks (comet assay)	Syrian hamster embryo cells	0, 0.00037-93 µM, 5 or 24 hours	Negative	Jacquet et al. (2012); Wang et al. (2015c), also reviewed in EFSA (2018)
DNA strand breaks (comet assay)	Primary mouse Leydig cells	0, 12.5, 25, 37.5, 50, 62.5 µg/ml, 24, 48 or 72 hours	Positive at > 50 µg/ml for 24 hours, > 37.5 µg/ml for 48 hours, > 25 µg/ml for 72 hours	Zhang et al. (2013a)
DNA damage (γ-H2AX)	*gpt* delta transgenic mouse embryonic fibroblasts	0, 0-20 µM, 24 hours	Positive at 20 µM	Wang et al. (2015c), also reviewed in EFSA (2018)
Unscheduled DNA synthesis	Primary cultured rat liver cells	Up to 4,000 µg/ml	Negative	Cifone (1999), as reported by EFSA (2008)[1]

[1] OEHHA has no access to Cifone (1999), which was summarized by EFSA (2008). The EFSA (2008) summary of the study did not report the numeric results for chromosomal aberrations or unscheduled DNA synthesis observed at each treatment concentration.

Table 15 Genotoxicity studies of PFOS in non-mammalian systems

Test endpoint	Test system	Concentration	Results/comments	Reference
Mutation [c*II* gene locus]	Fish: λ transgenic medaka (7-12/conc.)	0, 6.7, 27.6, or 87.6 µg/l in water for 30 days	Dose-dependent increase in mutations in liver, as measured in the *cII* transgene, with a distinct mutational spectrum dominated by +1 frameshift mutations at ≥ 6.7 µg/l	Chen et al. (2016b)
Reverse mutation assay (Ames test)	*S. typhimurium* TA98, TA100, TA1535, TA1537	Up to 5,000 µg/plate	Negative with or without S9	Mecchi (1999), as reported by EFSA (2008)[1]
Reverse mutation assay (Ames test)	*S. typhimurium* TA09, TA100, TA1535, TA1537, TA1538	0.01-500 µg/plate (-S9); 0.1-500 µg/plate (+S9)	Negative with or without S9	Litton Bionetics, Inc. (1978), as reported by EFSA (2008)[2]
Reverse mutation assay (Ames test)	*S. typhimurium* TA98 and TA100	0-10,000 µg/plate with or without 10% rat liver S9	Negative with or without S9	NTP (2019)
Reverse mutation assay	*E. coli* (WP2 *uvrA* pKM101)	0-5,000 µg/plate with or without 10% rat liver S9	Negative with or without S9	NTP (2019)
Reverse mutation assay	*E. coli* (WP2 *uvrA*)	Up to 5,000 µg/plate	Negative with or without S9	Mecchi (1999), as reported by EFSA (2008)[1]
Mitotic recombination	*Saccharomyces cerevisiae* (D4)	Not reported	Negative	Litton Bionetics, Inc. (1978), as reported by EFSA (2008)[2]
Micronuclei	Zebrafish	0, 0.4-1.6 mg/l, 30 days incubation of embryos	Positive at ≥ 0.8 mg/l in peripheral blood cells	Du et al. (2014), also reviewed in EFSA (2018)
Micronuclei	Mussel (*Mytilus galloprouinciulus*)	0, 2-6 mg/l, 30 days	Positive at all doses in gill cells; positive at ≥ 3 mg/l in hemolymph cells	Nalbantlar and Çakal Arslan (2017)
Micronuclei	Onion *(Allium cepa)*	0, 1-100 mg/l, 48 hours	Positive at ≥ 25 mg/l in meristematic root cells; cytotoxicity noted at ≥ 25 mg/l	Sivaram et al. (2020)
Chromosomal aberrations	Onion *(Allium cepa)*	0, 1-100 mg/l, 48 hours	Positive at ≥ 10 mg/l in meristematic root tip cells	Sivaram et al. (2020)
DNA strand breaks (comet assay)	Zebrafish	0, 0.4-1.6 mg/l, 30 days incubation of embryos	Positive at ≥ 0.4 mg/l in peripheral blood cells	Du et al. (2014), also reviewed in EFSA (2018)

Test endpoint	Test system	Concentration	Results/comments	Reference
DNA strand breaks (comet assay)	Carp, (*Cyprius carpio*)	0, 50- 50,000 µg/l, for 4 days	Positive at ≥ 5,000 µg/l in blood cells	Kim et al. (2010)
DNA strand breaks (comet assay)	Gull eggs (*Larus michahellis*)	0, 100, 200 ng/g egg (injected)	Negative	Parolini et al. (2016), also reviewed in EFSA (2018)
DNA strand breaks (comet assay)	Green mussel (*Perna viridis*)	0, 0.01-1,000 µg/l for 7 days	Positive at ≥ 1,000 µg/l	Liu et al. (2014), also reviewed in EFSA (2018)
DNA strand breaks (comet assay)	Earthworms (*Eisenia fetida*)	0, 0.25-8 µg/cm^3, 48 hours	Positive at ≥ 0.25 µg/cm^3	Wang et al. (2015c); Xu et al. (2013b), also reviewed in EFSA (2018)
DNA strand breaks (comet assay)	Earthworms (*Eisenia fetida*)	0, 50-470 mg/kg deionized water, 14 days	Positive≥ 50 mg/kg; significant dose trend	Zheng et al. (2016)
DNA strand breaks (comet assay)	Earthworms (*Eisenia fetida*)	0, 10, 50, 250 mg/kg, 14 days	Positive ≥ 10 mg/kg	Zheng et al. (2013)
DNA strand breaks (comet assay)	Flatworms *(Dugesia japonica)*	5 mg/l, 4 days	Positive	Shao et al. (2019)
DNA strand break (comet assay)	Water flea *(Daphnia carinata)*	0, 0.001-10 mg/l, 94 hours	Positive; significant increase at 1.0 and 10.0 mg/l, with 10 mg/l above the LC_{50}	Logeshwaran et al. (2021)
DNA strand breaks (comet assay)	*Paramecium caudatum*	0, 10, 30, 100 µM (1, 3 hours); 0, 10, 30 µM (24 hours)	Negative	Kawamoto et al. (2010), also reviewed in EFSA (2018)
DNA strand breaks (comet assay)	Onion *(Allium cepa)*	0, 1-100 mg/l, 48 hours	Positive at ≥ 25 mg/l in meristematic root cells; cytotoxicity noted at ≥ 25 mg/l	Sivaram et al. (2020)
DNA damage (Hus-1: GFP Focus)	*Caenorhabditis elegans*	0, 0.25-25 µM (12-60 hours)	Positive at ≥ 0.25 µM, 24 hours, in germ cell nuclei	Guo et al. (2016), also reviewed in EFSA (2018)
DNA damage (umu assay)	*S. typhimurium* TA1535/psk1002	0, 30-1000 µM without S9 for 5 hours; 0, 30-1000 µM with S9 for 5 hours	Negative	Oda et al. (2007)

Test endpoint	Test system	Concentration	Results/comments	Reference
Altered DNA structure (DNA charge transfer)	Cell-free; calf thymus DNA	10 µmol/l, 30 minutes, 37ºC	Positive, increased DNA charge transfer resistance. Authors interpret this as an indication of the loosening of duplex DNA structure and change in DNA base pair stacking	Lu et al. (2012)
Altered DNA structure (DNA charge transfer)	DNA on nano-gold particles embedded in a nano-porous overoxidized polypyrrole film	10 µmol/l, 5, 10, 15, 20, and 30 minutes, 37ºC	Positive; incubation time dependent intercalation of PFOS into DNA as measured by DNA charge transfer	Lu et al. (2013a)
Altered DNA structure (DNA charge transfer)	DNA immobilized on CdS quantum dots	10 µM, 30 minutes, 37ºC	Positive; DNA binding, increased DNA charge transfer resistance.	Lu et al. (2013b)
Altered expression of DNA damage and repair genes (real-time PCR)	*E. coli K12*	400 mg/l, 3 hours	Positive; increased expression of *uvrA* and *recA* genes	Liu et al. (2016)

[1] OEHHA has no access to Mecchi (1999), which was summarized by EFSA (2008). The EFSA (2008) summary of the studies did not report the numeric results for mutations observed at each treatment concentration.
[2] OEHHA has no access to Litton Bionetics, INC. (1978), which was summarized by EFSA (2008). The EFSA (2008) summary of the studies did not report the numeric results for mutations or recombination events at each treatment concentration.

Summary of evidence for KC2

Overall, there is some evidence of mutagenicity and suggestive evidence of chromosomal effects and DNA damage induced by PFOS.

PFOS is not mutagenic in bacterial assays conducted in multiple strains of *S. typhimurium* and *E. coli*. PFOS induced mutations in the livers of *gpt* delta transgenic mice at the *redBA/gam* locus (Wang et al. 2015c) and transgenic fish at the c*II* gene locus (Chen et al. 2016b) *in vivo* after long-term exposure (28 and 30 days, respectively), and at the *redBA/gam* locus in *gpt* delta transgenic mouse embryonic fibroblast cells *in vitro* (Wang et al. 2015c).

With regard to chromosomal effects, in addition to the positive MN tests in mussels and onion (Jernbro et al. 2007; Nalbantlar and Çakal Arslan 2017; Sivaram et al. 2020) and the positive CA test in onion by Sivaram et al. (2020), a number of *in vivo* studies in rodents and one *in vivo* study in fish have reported increases in micronuclei following

long-term exposure (28 or 30 days) to PFOS. Twenty-eight day exposure to PFOS increased MN in male Wistar rat bone marrow polychromatic erythrocytes (Çelik et al. 2013), peripheral blood cells (Eke and Çelik 2016), and hepatocytes (Eke et al. 2017), and in female SD rat polychromatic erythrocytes (increases in female rats were dose-dependent, although levels were within the historical control range), but not in male SD rat polychromatic erythrocytes (NTP 2019). Twenty-eight day exposure to PFOS in male transgenic mice increased MN in hepatocytes, although the increase did not reach statistical significance (Wang et al. 2015c), whereas a single oral dose of PFOS did not increase MN in mouse bone marrow (EFSA 2008). A 30-day exposure to PFOS increased MN in peripheral blood cells of zebrafish (Du et al. 2014). PFOS did not increase MN in human hepatoma HepG2 cells (Yao and Zhong 2005), chromosomal aberrations (CA) in human peripheral blood lymphocytes exposed *in vitro* (Buhrke et al. 2013; IARC 2017), or mitotic recombination in *S. cerevisae*.

In addition to the several positive comet assays in fish, earthworms, flatworms, water flea, and onion described earlier (Kim et al. 2010; Logeshwaran et al. 2021; Shao et al. 2019; Sivaram et al. 2020; Zheng et al. 2013; Zheng et al. 2016), there is a substantial amount of evidence of PFOS-induced-DNA damage, measured as increases in DNA strand breaks, γ-H2AX, and foci of Hus-1. In male Wistar rats, exposure to PFOS for 28 days significantly increased DNA strand breaks as measured in the comet assay in bone marrow (Çelik et al. 2013), peripheral blood cells (Eke and Çelik 2016), and hepatocytes (Eke et al. 2017). PFOS also increased DNA strand breaks as measured in the comet assay in the peripheral blood cells of zebrafish following a 30-day exposure, and in green mussels and earthworms, but not in gull eggs or *Paramecium caudatum* (EFSA 2018). *In vitro*, PFOS increased DNA strand breaks in one of three studies conducted in human hepatoma HepG2 cells. The lowest concentration tested in two HepG2 studies (Eriksen et al. 2010; Florentin et al. 2011), which did not cause any increases in DNA strand breaks, was higher than the highest concentration tested in the one HepG2 study (Wielsøe et al. 2015) that did observe increases. PFOS increased DNA strand breaks in primary mouse Leydig cells following 24-, 48-, or 72-hour treatments (Zhang et al. 2013a). PFOS did not increase any DNA strand breaks in sperm cells obtained from human volunteers treated with PFOS *in vitro* (Emerce and Çetin 2018) or in Syrian hamster embryo cells (Jacquet et al. 2012). PFOS increased γ-H2AX, a marker for DNA damage, in transgenic mouse embryonic fibroblasts *in vitro* (Wang et al. 2015c), and increased the number of foci of the DNA damage checkpoint protein Hus-1 in germ cells of *C. elegans* (strain *hus-1:gfp*) (Guo et al. 2016). No increase in unscheduled DNA synthesis was observed in primary liver cell cultures (EFSA 2008). Two human studies from Korea and Taiwan reported a positive association between serum PFOS and urinary 8-OHdG (a biomarker for oxidative DNA damage), while another study from Taiwan reported no association.

5.3.3 Alters DNA repair or causes genomic instability

The literature search identified one study for this key characteristic. PFOS did not cause impairment of DNA mismatch repair function in zebrafish at the concentrations tested (up to 0.5 µM) (Chen et al. 2016c).

5.3.4 Induces epigenetic alterations

The potential for exposure to PFOS to result in epigenetic effects or effects on gene or protein expression that may be caused by epigenetic changes has been investigated in human and animal *in vivo* and *in vitro* studies. Epigenetic changes are "hypothesized to serve as mediators of cancer etiology and progression, in many cases preceding cancer" (Smith et al. 2020). "The epigenome of a cancer cell is characterized by site-specific DNA hypermethylation, a global pattern of DNA hypomethylation, alterations in miRNA [microRNA] profile, and histone modifications" (Kanwal et al. 2015). Table 16 briefly describes some of the terms and concepts relevant to evaluating epigenetic studies, and Table 17 lists the genes evaluated in the human studies reviewed in this section, along with brief descriptions of the functions of the genes.

Table 16 Epigenetic terminology

Term	Definition	Reference(s)
DNA methylation	Occurs when a methyl group is added at a cytosine nucleotide that precede guanines (CpG dinucleotides); influences DNA function by activating or repressing transcriptional activity of a gene and by altering chromatin accessibility and remodeling. Alterations in DNA methylation include hypermethylation, hypomethylation, and loss of imprinting. • DNA hypermethylation occurs mainly in promoter CpG islands. Modifications are catalyzed by the enzyme DNA methyltransferase (DNMT). • DNA hypomethylation is associated with genomic instability and cancer progression. • Loss of imprinting is the loss of parental allele-specific monoallelic expression of	Kanwal et al. (2015)

Term	Definition	Reference(s)
	genes due to altered DNA hypomethylation and can increase risk of cancer.	
Altered expression of microRNA	MicroRNAs (miRNAs) are a class of noncoding RNAs that modulate chromatin regulation and gene expression. It has been hypothesized that miRNAs regulate the translation rate of more than 60% of protein-coding genes and participate in the regulation of cellular processes. Altered miRNAs are involved in cancer initiation and metastasis and can act as either oncogenes or tumor suppressors.	Kanwal et al. (2015); Li et al. (2019); Wang et al. (2015b)
Histone modifications	Histones are large groups of protein complexes that help DNA condense into chromatin. Modifications includes methylation and acetylation of lysine residues on histone tails, which can affect gene expression by altering chromatin structure and accessibility.	Wen et al. (2016a)
Nucleosome positioning	The assembly, mobilization and disassembly of nucleosomes can influence the regulation of gene expression and development of cancer.	Kanwal et al. (2015)

Table 17 Function of genes (human) evaluated in the human studies reviewed in this section

Gene/Element	Full Name	Gene Expression Product and Function/Function of Element
CXADRP3	Coxsackie virus and adenovirus receptor pseudogene 3	• Encodes a long non-coding RNA (lncRNA). • Altered in gene expression profiles of gallbladder cancer (Zhang et al. 2018a); ovarian cancer (Auer et al. 2015; Dong et al. 2019); myelodysplastic syndrome, which increases the risk for transformation to acute myeloid leukemia (Szikszai et al. 2020); and *BRCA*-positive breast cancer (Chen et al. 2020).

Gene/Element	Full Name	Gene Expression Product and Function/Function of Element
CYP2E1	Cytochrome P450 family 2 subfamily E member 1	• Encodes a member of the cytochrome P450 superfamily of enzymes that catalyze many reactions involved in drug metabolism and synthesis of cholesterol, steroids and other lipids (NCBI 2021d). • *CYP2E1* polymorphisms have been implicated in many types of cancer, including oral cavity, nasopharyngeal, esophageal, lung, gastric, colorectal, liver, bladder, and others (MalaCards 2021e).
EBF1	Early B-cell factor 1	• Encodes a novel transcription factor that is strongly expressed in early stages of B cell development. • Down-regulation of EBF1 has been found in many tumors and is hypothesized to play a role in tumor promotion and progression (Armartmuntree et al. 2018).
GVIN1	GTPase, very large interferon inducible pseudogene 1 (*GVINP1*; *GVIN1*).	• Is primarily involved in immune function but has been found to be altered in a few cancer types, including lung, breast, and pancreas (Liao et al. 2017; Sui et al. 2019; Wang et al. 2020b; Zhou et al. 2019).
HLA-DPA1	Major histocompatibility complex, class II, DP alpha 1	• Class II molecule that is expressed in antigen presenting cells (macrophages, dendritic cells, B lymphocytes) • Plays a central role in the immune system by presenting peptides derived from extracellular proteins (NCBI 2021a) • Expression altered in many cancers, including lymphohematopoietic, lung, liver, and breast (MalaCards 2021f)

Gene/Element	Full Name	Gene Expression Product and Function/Function of Element
HOOK2	Hook microtubule tethering protein 2	• Encodes hook proteins, *i.e.*, cytosolic coiled-coil proteins that contain conserved N-terminal domains, which attach to microtubules (OMIM 2021). • Also encode more divergent C-terminal domains, which mediate binding to organelles (OMIM 2021). • Expression of *HOOK2* has been altered in some cancers, for example, ovarian (Onkes et al. 2013; Wang et al. 2014), colon (Helmke et al. 2012), esophageal (Shimada et al. 2005), and gastrointestinal (Kobayashi et al. 2018).
IGF2	Insulin like growth factor 2	• Encodes a member of the insulin family of polypeptide growth factors that are involved in development and growth (NCBI 2021c). • Altered in many types of cancer, including colorectal, breast, liver, lung, prostate, gastric, ovarian, and eye (MalaCards 2021d).
KLHL35	Kelch like family member 35	• Function is not well characterized but other members of the family are involved in ubiquitination. • *KLHL35* has been found in a few cancers, including kidney (Morris et al. 2011), liver (Shitani et al. 2012), lung, ovarian, and colon (Xiang et al. 2021).
LINE1	Long interspersed element 1	• Methylation of LINE1 is correlated with DNA methylation across the entire genome and can be used as a surrogate for global DNA methylation (Kobayashi et al. 2017).
Alu	Alu Short Interspersed Element (SINE)	• Belongs to a class of SINEs; has wide-ranging influence on gene expression (Deininger 2011). • Marker of global DNA hypomethylation. • Variants associated with several cancer types (Payer et al. 2017).

Gene/Element	Full Name	Gene Expression Product and Function/Function of Element
Satα	Alpha satellite DNA	• Repetitive satellite DNA sequences often found in centromeres or centromere-adjacent heterochromatin (Leter et al. 2014). • Marker of global DNA hypomethylation. • Altered in some cancers (Choi et al. 2009).
PRKCA	Protein kinase C alpha	• Encodes a protein that plays a role in many different signaling pathways and cellular processes. • Has been found to be altered in many types of cancers (CDC 2021; KEGG 2021; NCBI 2021b).
PTBP1	Polypyrimidine tract binding protein 1	• Encodes for a ribonucleoprotein located in the nucleus which is involved in pre-mRNA splicing and mRNA transport. • Expression is related to progression in multiple cancers (Robinson et al. 2020; Sayed et al. 2019; Zhu et al. 2020).
SERPINA1	Serpin family A member 1	• Encodes a serine protease inhibitor whose targets include elastase, plasmin, thrombin, trypsin, chymotrypsin, and plasminogen activator (NCBI 2021e). • Has been implicated in several different cancers (MalaCards 2021a).
SLC17A9	Solute carrier family 17 member 9	• Encodes a vesicular nucleotide transporter; its main function is to participate in vesicle uptake, storage and secretion of ATP and other nucleotides. • Plays an important role in the ATP transport of airway epithelium and neutrophils, astrocytes, adrenal chromaffin cells and pancreatic cells. • Has been shown to drive colorectal tumor progression and has been shown to play a role in other cancers (Wu et al. 2020a).

Gene/Element	Full Name	Gene Expression Product and Function/Function of Element
SMAD3	SMAD family member 3	• Encodes a protein that functions in the transforming growth factor-beta signaling pathway and transmits signals from the cell surface to the nucleus, regulating gene activity and cell proliferation. • Also functions as a tumor suppressor (GeneCards 2021a). • Altered in many different cancers (MalaCards 2021b).
SNAPIN	SNAP associated protein	• Encodes a coiled-coil-forming protein that associates with the SNARE (soluble N-ethylmaleimide-sensitive fusion protein attachment protein receptor) complex of proteins and the BLOC-1 (biogenesis of lysosome-related organelles complex-1). • Required for vesicle docking and fusion and regulates neurotransmitter release as part of the SNARE complex. • The BLOC-1 complex is required for the biogenesis of specialized organelles (GeneCards 2021c). • Has been found to be altered in breast, pancreatic, and prostate cancer (MalaCards 2021c).
ZBTB7A	Zinc finger and BTB domain containing 7A	• Encodes a "transcription factor that represses the transcription of a wide range of genes involved in cell proliferation and differentiation" (GeneCards 2021b). • A member of the POZ/BTB and Kruppel (POK) family that directly and specifically binds to short DNA recognition sites located near their target genes thereby acting as a transcriptional activator or repressor. • Overexpression has been associated with tumorigenesis and metastasis in various human cancer types, including breast, prostate, lung, ovarian, and colon cancer (Singh et al. 2021).

Gene/Element	Full Name	Gene Expression Product and Function/Function of Element
ZNF26	Zinc finger protein 26	• Encodes a DNA-binding transcription factor and involved in regulation of transcription by RNA polymerase II. • Expressed in T cells (Thiesen 1990). • No associations with cancers have been identified.

Epigenetic and related observations in human studies

Ten studies evaluated epigenetic effects in PFOS-exposed individuals; all ten focused on changes in DNA methylation. Altered DNA methylation is understood to be a major early event in tumor development characterized by widespread genome hypomethylation that leads to chromosome instability and localized DNA hypermethylation. "This unique pattern of individual gene methylation is the characteristic commonly observed in various tumor suppressor genes in most types of human cancers and serve as a surrogate for point mutations or deletions that cause transcriptional silencing of tumor-suppressor genes" (Kanwal et al. 2015). The first part of this section describes the six studies that reported effects on individual genes (Kobayashi et al. 2017; Leung et al. 2018; Miura et al. 2018; Ouidir et al. 2020; Robinson et al. 2020; van den Dungen et al. 2017a), while the following section describes the five studies that reported global methylation effects (Guerrero-Preston et al. 2010; Kobayashi et al. 2017; Leter et al. 2014; Liu et al. 2018a; Watkins et al. 2014).

Effects on individual genes

Epigenetic alterations were measured in human umbilical cord blood (Kobayashi et al. 2017; Leung et al. 2018; Miura et al. 2018), placenta (Ouidir et al. 2020), newborn dried blood spots (Robinson et al. 2020), and serum from adult men (van den Dungen et al. 2017a).

DNA methylation changes were measured in cord blood samples from 177 mother-child pairs from the Hokkaido Study on Environment and Children's Health (Kobayashi et al. 2017). Prenatal PFOS exposure was not associated with significantly altered methylation of the insulin-like growth factor 2 (*IGF2*) differentially methylated region (DMR) or H19 DMR. Miura et al. (2018) analyzed 190 cord blood samples from the same Japanese cohort in addition to 37 samples from Taiwan and found that several DMRs were associated with prenatal PFOS exposure (Miura et al. 2018). The top 5 DMRs associated with PFOS exposure were *CYP2E1, KLHL35, SMAD3, HOOK2,* and *SLC17A9* (see Table 17 for more information on these genes). Miura et al. (2018) observed a global up-methylation shift in cord blood associated with prenatal PFOS exposure. They found epigenome-wide significant associations between PFOS exposure and DNA methylation for two CpGs: one located in the intergenic region (IGR) of *CXADRP3* (cg02044327), and another mapped to *SNAPIN* (cg25705526). They also found a differentially methylated position (DMP): cg16242615, mapped to the 5′ untranslated region (5′-UTR) of *ZBTB7A*. Leung et al. (2018) measured DNA methylation in cord blood from 72 participants in a Faroese birth cohort. The study reported that significant CpG sites were associated with 10 genes related to cancer etiology/progression in male offspring exposed to PFOS (pathway analysis to determine key physiological functions/diseases and methylation changes was not performed with females). The specific genes that were mapped to cancer as a disease outcome were not reported. Ouidir et al. (2020) measured PFOS in maternal plasma and DNA methylation in placental samples from 312 pregnant women. PFOS was associated with DNA hypermethylation of CpG sites within genes *PRKCA* and *EBF1* and hypomethylation of a CpG site within the gene *SERPINA1.*

Robinson et al. (2020) measured PFOS and DNA methylation in dried blood spots from 597 neonates in the Upstate KIDS cohort. After false discovery rate correction, the highest decile of PFOS concentration was associated lower DNA methylation at one CpG site among boys (within gene *GVIN1*) and with higher DNA methylation at another site among girls (within gene *ZNF26*). Log-transformed continuous PFOS was also inversely related to DNA methylation at one CpG site (within the gene *PTBP1*) in the total samples and among boys. PFOS above the 90th percentile was also inversely related to a CpG site within *HLA-DPA1*.

van den Dungen et al. (2017a) measured DNA methylation in serum samples from 34 Dutch men with high levels of PFOS. After correction for multiple testing, no significant DMRs or DMPs were detected.

Effects on global methylation

Global methylation was measured in five studies in humans (Guerrero-Preston et al. 2010; Kobayashi et al. 2017; Leter et al. 2014; Liu et al. 2018a; Watkins et al. 2014). No association was observed between PFOS levels and global DNA hypomethylation in cord blood samples from a cohort in Baltimore, MD (Guerrero-Preston et al. 2010) or in the Hokkaido Study on Environment and Children's Health (Kobayashi et al. 2017). A birth-cohort study examining epigenetic changes in LINE1 and Alu methylation in cord blood samples from Taiwan reported that increasing concentrations of PFOS were associated with decreased LINE1 and Alu global methylation in a crude unadjusted model (Liu et al. 2018a). In the adjusted model, PFOS was statistically significantly associated with hypomethylation of Alu, but not LINE1. Similarly, serum PFOS concentrations were associated with LINE1 global DNA hypomethylation in peripheral blood leukocytes from adults in the C8 Health Project (Watkins et al. 2014). No associations between PFOS exposure and global DNA methylation (as measured by methylation levels of LINE1 loci, Alu elements, and Satα repeats) in sperm DNA from adults were found in a cross-sectional study in three populations combined (from Greenland, Poland and Ukraine) (Leter et al. 2014). Analysis of each population separately revealed a negative association between PFOS and overall sperm DNA global methylation level in the population in Poland, but not Ukraine or Greenland. In Ukraine, a positive association was detected with Satα methylation.

Epigenetic and related observations in animal studies

Epigenetic alterations were analyzed in four studies in rats (Dong et al. 2016; Tian et al. 2019a; Wan et al. 2010; Wang et al. 2015b) and one study in mice (Yan et al. 2014). Two of the studies examined epigenetic effects of PFOS on DNA methylation, and three examined effects on miRNAs. miRNAs play crucial roles in the regulation of cancer-associated processes, including proliferation, differentiation, and apoptosis (Aure et al. 2021). Effects on miRNAs depend on exposure time and dose, and vary across species, tissues and developmental stages (Dong et al. 2016).

Female SD rats were exposed to 0, 0.1, 0.6 or 2.0 mg/kg-day PFOS via gavage from gestation days 2 to 21, and liver samples were collected at postnatal day (PND) 21 (Wan et al. 2010). The offspring of PFOS-treated dams exhibited a slight decrease in global DNA methylation and methylation of LINE1 regulatory region in liver tissue from the high-dose group, as well as increased methylation of several critical sites of the glutathione-S-transferase Pi (GSTP) promoter in the mid- and high-dose groups. GSTP mRNA expression was also significantly increased in the high-dose group; the GSTP

gene is a known tumor biomarker and altered methylation of its promoter has been hypothesized to be involved in liver carcinogenesis (Chatterjee and Gupta 2018). Wan et al. (2010) also observed an increase in DNA methyltransferase 3a (*DNMT3a*) expression (but not *DNMT1* or *DNMT3b*) in groups treated with PFOS, but the authors speculated that this increase may be a compensatory reaction to decreased global methylation. DNMTs are key enzymes that regulate the DNA methylation machinery, and overexpression can lead to a reduced expression of tumor suppressor genes (Hegde and Joshi 2021). No change was observed in methylation of the cyclin-dependent kinase inhibitor 2A (p16) gene promoter, which encodes a cell cycle regulatory protein and controls cellular differentiation, cell cycle arrest and apoptosis (Wan et al. 2010). Similar findings were observed in male Sprague-Dawley rats orally exposed to 5 mg/kg-d PFOS from PND 6 to 60 (Tian et al. 2019a). Expression of *Dnmt3a* mRNA was increased in treated animals, but there was no effect on *Dnmt1* and *DNMT3b* mRNA levels.

Wang et al. (2015b) exposed rats to 0 or 3.2 mg/kg PFOS in feed from day 1 of gestation through PND 7 in order to measure alterations in the expression of miRNAs in rat livers. Exposure to PFOS resulted in alterations in 46 and 9 miRNAs at PND 1 and 7, respectively. Several of these are cancer-related, such as miR-125a, miR-192, miR-199a-3p, miR-26a, miR-200c, and miR-494, and regulate tumor suppressors (Wang et al. 2015b). The authors' pathway analysis revealed genes associated with several different cancers, including melanoma, pancreatic cancer, colorectal cancer, and glioma. The analysis also identified genes associated with a number of biological processes, including regulation of cell proliferation, cell death, and apoptosis.

In another study in rats, adult male Sprague-Dawley rats were exposed to 0 or 50 mg PFOS/kg diet for 28 days, after which liver samples were analyzed for expression of miRNAs (Dong et al. 2016). Changes in 38 miRNA profiles were observed in rats treated with PFOS. The three with the greatest fold changes were miR-200a-3p, miR-200b-3p, and miR-429. The authors explain that up-regulation of the miR-200 family has been observed in the livers of rats exposed to known hepatocarcinogens. The miR200 family of miRNAs are direct targets of P53 and regulate the epithelial to mesenchymal transition, which plays an important role in tumor development, progression, and metastasis (Dong et al. 2016).

Alterations in miRNAs were also measured in an experiment in male mice treated with 0, 1.25, or 5 mg/kg-day PFOS via gavage for 28 days (Yan et al. 2014). Several miRNAs (miR-28-5p, miR-32-5p, miR-200c-3p, miR-122-5p, miR-192-5p) showed a significantly increased fold-change in the high-dose group compared to controls. Expression levels of miR-34a-5p and miR-26b-5p were significantly increased in the high dose group. Several of these miRNAs have been associated with tumor formation

and mechanisms of carcinogenesis in other studies (miR-200c-3p, miR-28-5p, miR-34a-5p, miR-32-5p, miR-26b-5p) (Yan et al. 2014).

Epigenetic and related observations in human cells in vitro

Seven studies exposed human cells to various concentrations of PFOS *in vitro* to measure epigenetic effects (Guo et al. 2017; Jabeen et al. 2020; Li et al. 2015; Peng et al. 2012; Pierozan et al. 2020; Sonkar et al. 2019; van den Dungen et al. 2017b).

Two studies examined the effect of PFOS on the expression of enzymes related to methylation/demethylation in human cells. Human A549 lung carcinoma cells were exposed to 0, 10, 200, or 400 µM PFOS (Jabeen et al. 2020). PFOS increased mRNA expression of *DNMT1* in the low-dose group and decreased expression in the high-dose group, decreased expression of *DNMT3a* in the mid-dose group, and decreased expression of *DNMT3b* in the high-dose group. DNMT1 is a maintenance enzyme that methylates the hemi-methylated DNA, while DNMT3a and DNMT3b are *de novo* enzymes that catalyze the formation of 5-methylcytosine to establish new methylated CpG sites. PFOS also caused a significant decrease in mRNA expression of *TET1* (ten-eleven translocation) at all doses, an increase in expression of *TET2* at all doses, and an increase in expression of *TET3* at the mid- and high doses. TETs are a family of enzymes that play a crucial role in demethylation. Overall, the decrease in expression of DNMTs and increase in TETs suggests that PFOS may cause hypomethylation in this lung carcinoma cell line, particularly at higher doses (Jabeen et al. 2020).

In a study of adipocyte differentiation, human mesenchymal stem cells (hMSCs) were exposed to 10 µM PFOS (van den Dungen et al. 2017b). Analysis of the entire genome revealed 440 DMRs; the authors' pathway analysis revealed that the most significant pathways were 'molecular mechanisms of cancer', 'G1/S checkpoint regulation', 'GADD45 signaling', and 'IGF-1 signaling'. Additionally, 45 DMPs were identified in cells exposed to PFOS, although the differences were not statistically significant after correction for multiple testing. The top 1000 DMPs with the lowest unadjusted p-values were predominantly hypomethylated, which may lead to genomic instability if it occurs in intergenic regions (van den Dungen et al. 2017b).

Global DNA methylation increased in human breast epithelial MCF-10A cells exposed to 10 µM PFOS and first generation daughter cells (D1) (Pierozan et al. 2020). The effect did not persist in second generation daughter cells (D2). Levels of acetylated H3K9 decreased in PFOS-treated cells and D1 cells, but not D2 cells. H3K9 acetylation levels have been shown to be reduced in breast and other cancers and are correlated with tumor progression and poor clinical outcomes. H3K9 is generally associated with open chromatin structure and active gene transcription. PFOS did not alter dimethylated H3K9, acetylated H3K27, or trimethylated H3K4 (Pierozan et al. 2020).

In a first trimester human trophoblast cell line (HTR-8/SV_{neo}), global DNA methylation and global acetylation of protein significantly decreased in response to treatment with PFOS compared to DMSO controls (Sonkar et al. 2019). PFOS significantly decreased gene and protein expression of DNA methyltransferases *DNMT1*, *DNMT3A*, and *DNMT3B* and of sirtuins *SIRT1* and *SIRT3*. PFOS significantly increased *miRNA-29b* expression at 24 hours. Altered methylation, acetylation, and expression of the DNA methyltransferases were shown to be dependent on expression of *miRNA-29b* through the use of knockout models (Sonkar et al. 2019). *miRNA-29b* has been shown to regulate multiple mechanisms of carcinogenesis (Kwon et al. 2019).

In a human neuroblastoma cell line, SK-N-SH, PFOS increased the mRNA levels of *miRNA-16*, *miRNA-22*, *miRNA-30a-5p*, and *DNMT3a* (at high dose), and decreased expression of *DMNT1* (Guo et al. 2017). PFOS also altered the methylation status of brain-derived neurotrophic factor promoter I and IV. A similar study conducted in SH-SY5Y human neuroblastoma cells found that PFOS decreased *miRNA-16* expression and increased *miRNA-22* expression, the latter of which may suppress *BDNF* gene expression (Li et al. 2015).

Bastos Sales et al. (2013) did not observe an alteration in global DNA methylation status in human neuroblastoma SK-N-AS cells exposed to PFOS for 72 hours. Peng et al. (2012) exposed human liver L-02 cells to PFOS for 72 hours and observed a reduction in global DNA methylation compared to controls.

Epigenetic and related observations in animal cells in vitro

Three publications studied epigenetic changes in animal cells exposed to PFOS *in vitro* (Bastos Sales et al. 2013; Xu et al. 2013a; Xu et al. 2015). In mouse embryonic stem cells exposed to PFOS for 24 hours, expression of both miRNA-145 and miR-490-3p increased in a dose-dependent manner (Xu et al. 2013a). Xu et al. (2015) exposed mouse embryoid bodies to PFOS for up to 6 days and observed a decrease in expression levels of miRNA-134, miRNA-145, and miRNA-490-3p. miRNA-145 and miR-490-3p are known tumor suppressors (Cui et al. 2014; Yu et al. 2019; Zhang et al. 2019). It seems that dose, timing of exposure and cell type modify the effects of PFOS in miRNA expression. Mouse neuroblastoma N2A cells exposed to PFOS for 48 hours did not exhibit an alteration in global DNA methylation status (Bastos Sales et al. 2013).

Epigenetic and related observations in zebrafish and sea urchins

Zhang et al. (2011) exposed zebrafish embryos to 1 µg/ml PFOS or DMSO control for 24 or 120 hours, then analyzed the expression profiles of 219 known zebrafish miRNAs. Thirty-nine and 81 miRNAs demonstrated significantly altered expression after 24 and 120 hours of PFOS exposure, respectively. The authors' functional analysis revealed that many of these differentially expressed miRNAs are involved in cancer-related

processes, including development, apoptosis and cell signal pathway (n=9), cell cycle progression and proliferation (n=14), and oncogenesis (n=26).

Another study investigated the effects of PFOS on epigenetic-related effects in two models: zebrafish embryos and the Zebrafish Liver (ZFL) cell line (Blanc et al. 2019). Embryos were exposed to 35 µM PFOS for 24 or 96 hours, and ZFL cells were exposed to 93 µM PFOS for 48 hours. Of the seven epigenetic regulators measured, significant downregulation in transcriptional levels of *dnmt3ab* and *kdm5ba* (regulators of histone demethylation) were observed in embryos and ZFL cells, respectively. Both regulators were significantly upregulated in daughter cells (of parent cells exposed to PFOS). ZFL cells showed a significant increase in global methylation after PFOS exposure.

Ding et al. (2015) exposed adult sea urchins to 0, 0.01, 0.1, or 1 mg/l PFOS for 21 days, followed by a 7-day depuration period. Both DNA methylation and demethylation rates increased in a dose-dependent manner with exposure time, followed by a decrease after the depuration period.

Summary of evidence for KC4

Overall, these studies show that PFOS can induce epigenetic changes, including altered methylation of regions associated with specific genes, global methylation changes, miRNA changes, and alterations in expression of DNMTs. Many of these effects have been correlated with processes involved in the development of cancer. Associations with altered gene expression, altered phenotype, and cancer, however, are not always clear.

5.3.5 Induces oxidative stress

Oxidative stress refers to a condition of an imbalance between the production and elimination of reactive oxygen and nitrogen species (ROS, RNS). Oxidative stress may contribute to the carcinogenic process by causing DNA mutations, chromosomal damage, genomic instability, and altered cell cycle regulation (Reuter et al. 2010).

There are a number of studies that investigated whether PFOS induces oxidative stress, including observational studies in humans, studies using cultured human cells, and *in vivo* and *in vitro* animal studies. Findings from these studies are briefly summarized below, including studies that measured 8-OHdG (8-hydroxydeoxyguanosine, a marker of oxidative DNA damage that is linked to mutagenesis and carcinogenesis, also discussed in Section 5.3.2 KC2), ROS or RNS production, malondialdehyde (MDA, a marker of lipid peroxidation), total antioxidant capacity (T-AOC), antioxidant enzyme activities [*e.g.*, superoxide dismutase (SOD), catalase (CAT), inducible nitric oxide synthase (iNOS)], glutathione status [*e.g.*, reduced glutathione (GSH), glutathione disulfide (GSSG), GSH/GSSG ratio; glutathione-S-transferase (GST), glutathione

reductase (GR), glutathione peroxidase (GPx)], and expression of Nrf2 (nuclear factor erythroid 2–related factor 2, regulating cellular resistance to oxidative stress). Some non-mammalian studies are also presented. Several omics studies, including one metabolomics study in humans and several transciptomics studies in rodents, are also informative with regard to the ability of PFOS to induce oxidative stress. Details of individual studies discussed in this section, such as study design and lowest effective doses, are provided in tables in Appendix G, organized by experimental system as follows.

- Table G1: Oxidative stress in human observational studies
- Table G2: Oxidative stress in studies using human cells *in vitro*
- Table G3: Oxidative stress in rodent studies *in vivo*
- Table G4: Oxidative stress in rodent studies *in vitro*
- Table G5: Oxidative stress in zebrafish studies *in vivo/ex vivo*

Oxidative DNA damage

Human observational studies

- Serum PFOS levels correlated with urinary levels of the oxidative DNA damage marker 8-OHdG in a dose-dependent manner in two studies, one conducted in 126 Korean seniors over 60 years of age (Kim et al. 2016) and another in 597 adults (22-63 years old) in Taiwan (Lin et al. 2020a). No association was reported in a third study of 848 individuals (12-30 years old) in Taiwan (Lin et al. 2016).

Studies using human cells in vitro

- Oxidative DNA damage, measured as formamidopyrimidine-DNA-glycosylase (FPG)-sensitive sites in the comet assay, was not significantly increased in HepG2 cells treated at up to 400 µM PFOS for 24 hours (Eriksen et al. 2010).

Studies using rodent cells in vitro

- A study in *gpt* delta transgenic mouse embryonic fibroblast cells showed that treatment of PFOS at 20 µM for 24 hours induced increases in phosphorylated histone H2AX (γ-H2AX), a biomarker of DNA double strand breaks. PFOS also increased the mutation frequencies at the *redBA/gam* loci (a marker gene for determining point and deletion mutations induced by a genotoxic agent) in transgenic mouse embryo fibroblast cells. Concurrent treatment with CAT significantly decreased the formation of both γ-H2AX foci and mutation frequencies induced by PFOS, suggesting that the effects were mediated by the induction of the reactive oxygen species H_2O_2 (Wang et al. 2015c).

Plant study

- 8-OHdG was significantly increased in lettuce seedlings (*Lactuca sativa*) exposed to PFOS at concentrations of 500 or 5000 ng/l for 28 days (Li et al. 2020b).

ROS or RNS production

Human observational studies

- In a cohort of 581 newborns from China, significantly higher levels of serum ROS levels were reported in the group with the highest levels of PFOS (the fourth quartile) in cord blood plasma compared with the lowest quartile, after adjusting for potential confounders (Liu et al. 2018b).

Studies using human cells in vitro

- Significant increases of ROS or RNS (*i.e.* NO, nitric oxide) were reported in several human cell types after exposure to PFOS, including in HepG2 cells (Eriksen et al. 2010; Hu and Hu 2009; Wielsøe et al. 2015), human umbilical vein endothelial cells (Liao et al. 2012; Liao et al. 2013), human microvascular endothelial cells (Qian et al. 2010) , human-hamster hybrid cells (Wang et al. 2013), and human lymphocytes (Zarei et al. 2018). Two of these studies showed time-dependent increases of ROS with PFOS exposure (Liao et al. 2012; Qian et al. 2010). In other studies dose-dependent increases in ROS in SH-SY5Y cells treated with PFOS at 25-200 µM were reported in the absence of statistical analysis (Sun et al. 2019), and non-significant increases of ROS were observed in HepG2 cells treated with PFOS at concentrations of up to 300 µM for 24 hours (Florentin et al. 2011), in contrast with the significant increases of ROS reported in HepG2 cells treated with 0.2 µM for 24 hours (Wielsøe et al. 2015).

Rodent studies in vivo

- Significant increases in ROS (*e.g.*, H_2O_2) in liver were reported in Kunming mice and in an unspecified strain of mice treated by intragastric injection (*i.e.*, gavage) at 10 mg/kg/d for three weeks (Huang et al. 2020; Lv et al. 2018), and in splenocytes and thymocytes of C57BL/6 mice treated by gavage at 5 mg/kg/d for 7 days (Zhang et al. 2013c). In another study, dose-dependent increases of ROS were reported (in the absence of statistical analysis) in the liver of male SD rats treated with daily oral doses of 1 or 10 mg/kg-day for 28 days (Han et al. 2018).

Rodent studies in vitro

- Significant increases in ROS following PFOS exposure were observed in various cell types exposed *in vitro*, including rat and mouse hepatocytes (Khansari et al. 2017; Xu et al. 2019), rat proximal renal tubular cells (Wen et al. 2021), neuronal

cells (Dong et al. 2015; Lee et al. 2012; Reistad et al. 2013; Wang et al. 2015a), mouse macrophages (Qian et al. 2010), mouse Leydig cells and Leydig tumor cells (Zhang et al. 2015a; Zhao et al. 2017), embryonic stem-cell derived mouse cardiomyocytes (Cheng et al. 2013) and transgenic mouse embryonic fibroblast cells (Wang et al. 2015c). Studies conducted with rat liver mitochondria and rat cerebellar granule neurons reported no significant changes in ROS following incubation with PFOS (Berntsen et al. 2017; O'Brien and Wallace 2004).

- PFOS induced concentration-dependent NO production, along with a concomitant increase in iNOS levels, in rat HAPI microglia cells (Wang et al. 2015a).

Zebrafish studies in vivo/ex vivo

- In zebrafish, significant increases in ROS production were observed in embryo tissues exposed to PFOS (Du et al. 2017; Shi and Zhou 2010). Increases also occurred in zebrafish liver tissues (Guo et al. 2019; Li et al. 2017). No increase in ROS production was observed in zebrafish larvae (Zou et al. 2021).

Invertebrate studies in vivo

- Significant dose-dependent increases in ROS levels were also observed in *Caenorhabditis elegans (C. elegans)* following PFOS exposure (0.25 to 25 µM) (Guo et al. 2016).

Lipid peroxidation

Human observational studies

- Dose-dependent increases of MDA in urine associated with increasing PFOS levels in serum were reported in a Korean cohort of seniors (Kim et al. 2016).

Studies using human cells in vitro

- Significant increases in MDA were reported in human lung cancer A549 cells (Mao et al. 2013) and human lymphocytes following *in vitro* exposure to PFOS (Zarei et al. 2018).

Rodent studies in vivo

- Significant increases in MDA were reported in the liver of Kunming mice treated by gavage (Huang et al. 2020; Lv et al. 2018), in the liver of male SD rats by gavage (Han et al. 2018), and in the lung of rats of an unspecified strain by gavage (Chen et al. 2012). Non-significant changes in MDA levels were observed in the brain and liver of Kunming mice treated with a single subcutaneous injection of 50 mg/kg/d at different postnatal days (Liu et al. 2009).

Rodent studies in vitro

- MDA was significantly increased in rat liver hepatocytes following 3-hour incubation with PFOS (Khansari et al. 2017) and in rat PC12 cells following 24-hour and 4-day exposure to PFOS (Slotkin et al. 2008). Lipid peroxidation was significantly reduced after exposure to PFOS compared to controls in rat cerebellar granule neurons in one study (Berntsen et al. 2017). However, PFOS significantly increased cumene hydroperoxide-induced lipid peroxidation in the same study.

Zebrafish studies in vivo/ex vivo

- Lipid peroxidation (measured as MDA) was significantly increased in two studies in zebrafish embryos and larvae (Du et al. 2017; Shi and Zhou 2010). In a third study an increase of MDA was observed in zebrafish larvae during the uptake phase, with a significant decrease in the depuration phase, indicating possible adaptation to the oxidative damage by the zebrafish (Zou et al. 2021).

Total antioxidant capacity (T-AOC)

Studies using human cells in vitro

- No significant change in total antioxidant capacity (T-AOC) was found in HepG2 cells treated with PFOS at concentrations of up to 20 µM for 24 hours (Wielsøe et al. 2015).

Rodent studies in vivo

- Significant decreases in T-AOC were observed in Kunming mice treated with one subcutaneous dose of PFOS at 50 mg/kg (Liu et al. 2009) and in C57BL/6 mice treated with 0.075 g/kg-day for 30 days by gavage (Xing et al. 2016).

Zebrafish studies in vivo/ex vivo

- No change in T-AOC was observed in zebrafish larvae exposed to PFOS (Zou et al. 2021).

Changes in antioxidant enzyme activities or levels

Studies using human cells in vitro

- Significant increases in antioxidant enzyme activities, *e.g.*, SOD or CAT, were reported in HepG2 cells treated with 150 µM PFOS for 48 hours (Hu and Hu 2009) and in human lung cancer A549 cells treated with 50 µM PFOS for 24 hours (Mao et al. 2013).

Rodent studies in vivo

- Significant changes in various antioxidant enzyme activities (SOD, CAT and myeloperoxidase, MPO) were reported in PFOS exposed Kunming and C57BL/6 mice (Huang et al. 2020; Liu et al. 2009; Lv et al. 2018; Xing et al. 2016; Zhang et al. 2013c), and SD rats (Chen et al. 2012; Han et al. 2018). Specifically,
    - A significant increase in MPO activity was reported in rat offspring of dams treated with 2 mg/kg-day PFOS from gestational day (GD) 1 to GD 22 (Chen et al. 2012).
    - There are no consistent patterns for changes in SOD or CAT activities following *in vivo* PFOS exposure of rodents, with some studies showing significant increases while others showing significant decreases or no changes. Significant increases of SOD activities were reported in mice (Zhang et al. 2013c) and, in contrast, significant decreases of SOD activities were seen in Kunming mice (Huang et al. 2020; Liu et al. 2009), C57BL/6 mice (Xing et al. 2016), SD rats (Han et al. 2018), and one unspecified strain of rats (Chen et al. 2012). No significant change in SOD activity was reported in CD-1 mice (Lee et al. 2015).

Rodent studies in vitro

- PFOS induced significant increases in SOD activity (0.5 mM) and significant decreases of CAT activity (0.01 mM) in mouse hepatocytes (Xu et al. 2019).

Zebrafish in vivo/ex vivo

- SOD and CAT activities were significantly increased in two studies in zebrafish embryo (Du et al. 2017; Shi and Zhou 2010). While no change in the activity level of either SOD or CAT was observed in larvae, the protein expression levels of SOD and CAT increased significantly following exposure to PFOS (10 µg/l) during the uptake period; SOD protein expression levels were also significantly increased during the depuration period (Zou et al. 2021). Activities of both enzymes were also increased in zebrafish liver tissues, and CAT activity was additionally increased in zebrafish intestinal and brain tissues (Li et al. 2017).

Changes in glutathione status

Studies using human cells in vitro

- PFOS induced significant increases of GR activity and GSSG levels, and significant decreases of GST and GPx activities and GSH levels in treated human lymphocytes or HepG2 cells under varying conditions (Hu and Hu 2009; Zarei et al. 2018).

Rodent studies in vivo

- Significant increases in GR activity and GSSG levels, and significant decreases in GPx and GST activities and GSH levels were observed following exposure to PFOS in mice (Kunming, C57BL/6 and one unspecified strain) (Lv et al. 2018; Xing et al. 2016; Zhang et al. 2013c) and rats (SD and one unspecified strain) (Chen et al. 2012; Han et al. 2018).

Rodent studies in vitro

- GSH levels were increased in mouse hepatocytes following exposure to PFOS (Xu et al. 2019).

Zebrafish studies in vivo/ex vivo

- GPx activity was increased in two zebrafish embryo studies following PFOS exposure (Du et al. 2017; Shi and Zhou 2010).
- GSSG levels were increased in wild type, but not Nrf2 mutant (impaired function) zebrafish embryos following exposure to PFOS (Sant et al. 2018).
- No changes in GSH levels were observed in wild type or Nrf2 mutant zebrafish embryos following exposure to PFOS (Sant et al. 2018).

Changes in Nrf2 expression

Rodent studies in vivo

- Significantly reduced Nrf2 protein expression was reported in male mice treated by gavage at 10 mg/kg-day for three weeks (Lv et al. 2018).

Zebrafish studies in vivo/ex vivo

- Statistically significantly increased gene expression of *Nrf2* and heme oxygenase-1 (*HO-1*, an Nrf2-regulated gene and a key enzyme in the maintenance of antioxidant homeostasis during cellular stress) was observed in zebrafish treated with PFOS at concentrations of 0.4 mg/l or above (Shi and Zhou 2010). In zebrafish larvae treated with 10 µg/l PFOS for 48 hours and followed by a 24-hour depuration period, Nrf2 protein expression was significantly increased in the uptake phase and decreased in the depuration phase (Zou et al. 2021).

Omics studies

- Metabolomics: Low level exposure to PFOS (average serum level: 13.39 nM) in humans may disrupt pathways related to oxidative stress (Wang et al. 2017). PFOS exposure was associated with significant increases of hydroxybutyric acid and significant decreases of pyroglutamic acid (both related to the glutathione cycle), and tetrahydrobiopterin (related to nitric oxide generation).

- Transcriptomics: Global gene expression in the spleen of BALB/c mice exposed to PFOS by gavage (10 mg/kg-day, for three weeks) was studied (Lv et al. 2015). Microarray and bioinformatics analyses show that several pathways were significantly enriched in the PFOS-treated group. Down-regulated expression of genes involved in cell cycle regulation and the Nrf2-mediated oxidative stress response were identified. Genes down-regulated in the Nrf2-mediated pathway include *Gstm3* (Glutathione-S-transferase Mu 3) and microsomal GST (*Mgst3)*.
- Transcriptomics: Martin et al. (2007) applied microarray technology in the liver of male SD rats treated with PFOS by gavage (10 mg/kg-day for one, three and five consecutive days; three rats per dosing group). Significant changes in several genes related to the oxidative stress response via the Nrf2-mediated pathway were identified; including upregulation of glutathione reductase, glutamate-cysteine ligase, HO-1, and thioredoxin reductase 1.
- Transcriptomics: Gene expression in the liver of female SD rats treated by gavage (daily dose of 5 mg/kg-day PFOS for 3 days or 3 weeks) was studied using the Affymetrix rat genome U34A genechip array (Hu et al. 2005). Expression of multiple genes was significantly altered by *in vivo* PFOS exposure, including upregulation (> 3-fold changes) of three genes involved in peroxisomal fatty acid β-oxidation, which generates H_2O_2 and causes oxidative stress or damage.

Summary of evidence for KC5

Studies of oxidative stress responses in humans, rodents, zebrafish and plants indicate that PFOS can induce oxidative DNA damage, generation of ROS or RNS, and lipid peroxidation. Notably, in human observational studies, significant dose-dependent increases of oxidative DNA damage (8-OHdG) (in two of three studies), lipid peroxidation (MDA), and ROS were associated with higher serum PFOS levels. Significant increases of ROS/RNS and lipid peroxidation were reported in multiple experimental test systems, with several studies showing dose-dependent responses. Significant decreases in T-AOC were reported in one rodent study *in vivo*, but no change was reported in one human observational study and in one zebrafish study. Following PFOS exposure, in multiple experimental systems, changes occurred in antioxidant enzyme activities/levels and glutathione status (*e.g.*, GSH, GSSG, GSH/GSSG ratio, GST, GR, and GPx). Changes in the protein or gene expression of Nrf2 have also been observed, with one mouse study reporting reduced levels of Nrf2 protein following PFOS exposure, and two studies in zebrafish reporting increases in Nrf2 gene or protein expression during the uptake phase but decreased expression during the depuration phase. Evidence from genomic and metabolomic studies also provide some evidence for the induction of oxidative stress by PFOS.

5.3.6 Induces chronic inflammation

Chronic inflammation associated with the development of cancer is a prolonged response to persistent infections or irritants that inflict cell death and tissue injury. For example, chronic inflammation, if linked with inflammatory bowel disease such as ulcerative colitis and Crohn's disease, can increase the risk of colorectal cancer by 10-fold, whereas the control of colitis by certain anti-inflammatory agents reduces colon cancer incidence (reviewed by (Lu et al. 2006)).

Chronic inflammation can trigger cellular events associated with carcinogenesis, such as cellular transformation, promotion and survival of transformed cells, proliferation, invasion, angiogenesis, and metastasis (Aggarwal et al. 2006; Sethi et al. 2008; Smith et al. 2020).

Several pro-inflammatory molecules have been identified, including the cytokines tumor necrosis factor-alpha (TNF-α), transforming growth factor-β (TGF-β) and several interleukins (IL) such as IL-1, IL-6, IL-8, IL-18, chemokines, and others (Aggarwal et al. 2006; Landskron et al. 2014). Cytokines mediate cell-to-cell communication and regulate proliferation, cell survival, differentiation, immune cell activation, cell migration, and death. During chronic inflammation, cytokines can induce cell transformation and malignancy, conditional on the balance of pro- and anti-inflammatory cytokines, their relative concentrations, cytokine receptor expression levels, and the activation state of surrounding cells (Landskron et al. 2014). For example, during acute inflammation macrophages and leukocytes can generate high levels of reactive oxygen and nitrogen species; however, if inflammation becomes prolonged, these infection-fighting reactive species (*e.g.*, peroxynitrate) can produce cellular damage and mutagens (reviewed in Lu et al. (2006)). Macrophages and T lymphocytes may also release pro-inflammatory molecules like TNF-α and macrophage migration inhibitory factor to exacerbate DNA damage. Migration inhibitory factor impairs p53-dependent protective responses, thus causing the accumulation of oncogenic mutations (Lu et al. 2006).

In experimental settings, the release of cytokines is frequently measured using whole blood or human peripheral blood leukocytes, splenocytes, liver homogenate and other cell types (see tables in Appendix H), either non-stimulated or stimulated with reagents like lipopolysaccharide (LPS), plant lectins and others. Different stimulating reagents and treatments may result in the production of different types of cytokines, and in varying amounts (Ai et al. 2013). Thus, effects of chemicals of interest can be measured as increasing or decreasing levels of specific cytokines.

Table 18 Common cytokines and chemokines involved in chronic inflammation and carcinogenesis

Cytokine or Chemokine	Roles in chronic inflammation and carcinogenesis	References
Tumor necrosis factor alpha (TNF-α)	TNF-α is a multifunctional cytokine that plays a role in cell survival, proliferation, differentiation, and death; it can either enhance or inhibit tumor progression. • TNF-α activates other inflammatory actors which in turn participate in the inflammatory response. • TNF-α has been linked to all steps involved in tumorigenesis, including cellular transformation, promotion, survival, proliferation, invasion, angiogenesis, and metastasis. • TNF-α may contribute to immune escape and tumor progression by facilitating the biological activity and/or expansion of immune-suppressive cells such as regulatory T cells, B cells, and myeloid-derived suppressor cells. • TNF-α activates Nuclear Factor kB (NF-κB), which in turn leads to the expression of inflammatory genes, including cyclooxygenase-2 (COX-2), lipoxygenase-2 (LOX-2), cell-adhesion molecules, anti-apoptotic proteins, inflammatory cytokines, chemokines, and inducible nitric oxide synthase (iNOS). • TNF-α can activate other signaling pathways such as nuclear factor p38 and c-Jun N-terminal kinase (JNK), which can result in the induction of oncoproteins. For example, TNF-α up-regulated the oncoprotein HBXIP, resulting in the enhanced growth of breast cancer cells. • TNF-α has also been shown to stimulate reactive oxygen species (ROS) *in vitro*.	Aggarwal (2003); Aggarwal et al. (2006); Cai et al. (2017); Cruceriu et al. (2020); Montfort et al. (2019); Sethi et al. (2008); Wang and Lin (2008); Woo et al. (2000)

Cytokine or Chemokine	Roles in chronic inflammation and carcinogenesis	References
Interleukin (IL)-1 (including IL-1α and IL-1β)	IL-1 induces the recruitment of tumor-associated macrophages (TAMs) and tumor immunosuppressive myeloid-derived suppressor cells (MDSCs), which may promote tumor development in breast cancer. In human breast cancer, higher expression of IL-1β has been associated with tumor invasiveness and aggressiveness. Expression of IL-1α, IL-1β, and their receptors in human breast cancer tissues results in the activation of a population of cells and subsequently contributes to angiogenesis, tumor proliferation, and tumor invasion in the microenvironment.	Kaneko et al. (2019)
IL-2	IL-2 plays a critical role in the differentiation of CD4+ regulatory T cells into a variety of subsets. It can promote CD8+ T-cell and natural killer (NK) cell cytotoxicity activity, and modulate T-cell differentiation in response to antigen, promoting naive CD4+ T-cell differentiation into T helper-1 (Th1) and T helper-2 (Th2) cells while inhibiting T helper-17 (Th17) differentiation.	Jiang et al. (2016)
IL-4	IL-4 acts directly on tumor cells as a tumor promoting cytokine. It also contributes to the establishment and maintenance of Th2-polarized immune responses, reduces the tumoricidal activity of CD8+ T cells and indirectly impairs the antitumor immunity in tumor bearing animals or cancer patients.	Li et al. (2020c)
IL-6	IL-6 is involved in the activation of T helper cells, the inhibition of T-regulatory cells, and the differentiation of B cells. IL-6 can affect tumor cell proliferation. In some cancers such as lung cancer, IL-6 can have both a preventative role in tumor initiation but it has also been linked to tumor progression.	Unver and McAllister (2018)
IL-8	IL-8 has been reported to promote growth, angiogenesis, and metastasis of several types of tumors. Additionally, polymorphisms in the IL-8 gene are associated with a higher risk of some cancers in specific populations.	Aggarwal et al. (2006)

Cytokine or Chemokine	Roles in chronic inflammation and carcinogenesis	References
IL-10	IL-10 can suppress antigen presentation by myeloid cells and inhibit the production of interferon gamma (IFN-γ)-promoting cytokines, especially IL-12, thereby hindering the induction of strong anti-tumor immunity by these cells. IL-10 can inhibit the synthesis of IL-1, IL-6, and TNF-α and can also inhibit NF-κB signaling, leading to a downregulation of pro-inflammatory cytokine expression.	Kumar and Creery (2000); Landskron et al. (2014); Ouyang and O'Garra (2019)
IL-15	IL-15 is involved in the development, differentiation, and survival of NK cells; it also stimulates the production and secretion of IL-8 by neutrophils through the activation of the NF-κB transcription factor. In macrophages IL-15 functions as a potent autocrine regulator of pro-inflammatory cytokine production by these cells, with high concentrations of IL-15 favoring TNF-α, IL-1, and IL-6 production, whereas very low concentrations of IL-15 favor IL-10 production.	Perera et al. (2012)
Interferon gamma (IFN-γ)	IFN-γ is critical to both innate and adaptive immunity and plays a pivotal function in cancer immune surveillance, stimulating antitumor immunity and promoting tumor recognition and elimination. It is a primary activator of macrophages. However, recent studies suggest that IFN-γ may also be a tumor promoter.	Castro et al. (2018)

Changes in pro-inflammatory markers: human in vitro studies

The effects of PFOS on pro-inflammatory cytokine production have been tested in multiple human cell types *in vitro*, including peripheral blood leukocytes, lymphocytes, primary CD4+ T cells, colon myofibroblasts, bronchial epithelial cells, THP-1 (human promyelocytic cell line) cells, Jurkat T cells, and splenocytes. Here we provide a short summary of reported significant increases, decreases or no changes of relevant cytokines (compared to controls with or without stimulation) following treatment with PFOS. A more detailed description of the individual study results and experimental conditions can be found in Table H1 in Appendix H.

Increases of IL-1α and IL-1β levels were observed in bronchial epithelial cells treated with 10 μM PFOS with an immune stimulant (Sørli et al. 2020). In human peripheral

blood lymphocytes, production of IL-1 was significantly increased following exposure to 50 µM PFOS (Li et al. 2020c).

IL-2 production was decreased following treatment with PFOS in human primary T cells and in Jurkat T cells (an immortalized human T lymphocytes cell line) stimulated with phytohemagglutinin (PHA)/phorbol myristate acetate (PMA), and in Jurkat T cells stimulated with anti-CD3 or anti-CD3 plus anti-CD28. Significant decrease of IL-2 production was observed in primary CD4+ T cells stimulated with PHA/PMA. Significant decrease of IL-2 was also observed in Jurkat cells stimulated with anti-CD3, but no significant changes were observed when Jurkat T cells were stimulated with both anti-CD3 and anti-CD28. The decrease in Jurkat T cells stimulated with PHA/PMA was independent of peroxisome proliferator-activated receptor alpha (PPARα) activity, as it was still observed in cells treated with a PPARα antagonist (Midgett et al. 2015). In human peripheral blood lymphocytes, no significant change in IL-2 was observed following exposure to 50 µM PFOS (Li et al. 2020c).

IL-4 secretion by human peripheral blood leucocytes was decreased following PHA stimulation (Corsini et al. 2011). In another study using human peripheral blood lymphocytes, IL-4 production was significantly increased following exposure to 50 µM PFOS (Li et al. 2020c).

IL-6 production was significantly increased in human peripheral blood lymphocytes following exposure to 50 µM PFOS (Li et al. 2020c). IL-6 secretion by peripheral blood leukocytes and human colon myofibroblasts was decreased compared to controls following stimulation with LPS or IL-1β (Corsini et al. 2011; Corsini et al. 2012; Giménez-Bastida et al. 2015). In contrast, no change in IL-6 production was observed in peripheral blood leukocytes stimulated with PHA or LPS (Brieger et al. 2011) or in bronchial epithelial cells following stimulation with Poly I:C (Sørli et al. 2020).

IL-8 production showed no change in peripheral blood leukocytes in the presence of LPS (Corsini et al. 2011) and a decrease in LPS-stimulated THP-1 cells (Corsini et al. 2011). A decrease was observed in bronchial epithelial cells following stimulation with Poly I:C (Sørli et al. 2020). IL-8 secretion by human peripheral blood lymphocytes was significantly increased following exposure to 50 µM PFOS (Li et al. 2020c).

IL-10 production was decreased in peripheral blood leukocytes with PHA as stimulant (Corsini et al. 2011; Corsini et al. 2012).

TNF-α secretion was decreased in human peripheral blood leukocytes and THP-1 cells following stimulation with LPS (Brieger et al. 2011; Corsini et al. 2011) but not with PHA (Brieger et al. 2011). Corsini et al (2011) also reported a decrease in TNF-α mRNA expression in THP-1 cells with PFOS treatment.

IFN-γ production was decreased in peripheral blood leukocytes with PHA as stimulant (Corsini et al. 2011; Corsini et al. 2012).

C-X-C motif chemokine ligand 10 (CXCL-10) production was decreased in bronchial epithelial cells following stimulation with poly I:C (Sørli et al. 2020).

Changes in pro-inflammatory markers- Animal in vivo/ex vivo and in vitro studies

Studies in animals were conducted in different strains of mice (C57BL/6, C57BL/6J, B6C3F1, and one unspecified strain); one study was conducted in male SD rats. Here is a short summary of reported significant increases, decreases or no changes of relevant cytokines (compared to controls with or without stimulation) following treatment with PFOS. A more detailed description of the individual study results and experimental conditions can be found in Table H2 in Appendix H.

Increases in IL-1β levels were observed in splenic and colonic cells and peritoneal fluid of PFOS-treated C57BL/6 or C57BL/6J mice (Dong et al. 2012; Wang et al. 2020a), in rat astrocytes (Chen et al. 2018a), and IL-1β mRNA expression was increased in zebrafish liver after 14 or 21 days exposure (Guo et al. 2019).

Decrease of the quantity of IL-2 secreting splenocytes was observed in PFOS treated C57BL/6 mice at 20 mg/kg-day) in one study (Zheng et al. 2011) and at 50 mg/kg total administered dose (total administered dose (TAD), 0.8333 mg/kg-day for 60 days) in another study (Dong et al. 2011).

IL-4 production was increased by PFOS in C57BL/6 mice in splenocytes (Dong et al. 2011; Zheng et al. 2011), decreased in liver cells (Qazi et al. 2010a), and not affected in splenic CD4+ T cells in B6C3F1 mice (Fair et al. 2011). In chicken embryo fibroblasts, a decrease in IL-4 mRNA expression following PFOS treatment was observed (Castaño-Ortiz et al. 2019).

No change was reported for IL-5 production in splenic CD4+ T cells in B6C3F1 mice (Fair et al. 2011).

IL-6 production was examined in several studies in mice. In B6C3F1 mice, increases were observed in splenic B cells (Fair et al. 2011), serum and peritoneal macrophages (with *in vivo* stimulation using 25 µg LPS) (Mollenhauer et al. 2011); no change was observed for peritoneal macrophages (with *in vitro* stimulation using 0.1 µg/ml LPS) while a decreasing trend was seen in peritoneal lavage fluid (with *in vivo* stimulation using 25 µg LPS) (Mollenhauer et al. 2011). In C57BL/6 mice, increases were observed in splenic cells and peritoneal macrophages in one study (Dong et al. 2012) but not in a second study (Qazi et al. 2009a). An increase was observed in bone marrow cells (with LPS) and peritoneal cavity fluid (with or without LPS) (Qazi et al. 2009a). In one study using male mice of an unspecified strain, expression of IL-6 in the liver of PFOS treated mice was significantly increased (Lv et al. 2018), while no change was observed in the liver of PFOS treated C57BL/6 mice (Qazi et al. 2010a). IL-6 was also significantly increased in zebrafish following PFOS exposure for 7, 14, or 21 days (Guo et al. 2019).

In chicken embryo fibroblasts following PFOS treatment, a decrease of IL-8 mRNA expression was observed (Castaño-Ortiz et al. 2019).

The number of IL-10 secreting cells was increased in PFOS-treated C57BL/6 mice (Dong et al. 2011), and an increase was observed in colon cells in C57BL/6J mice (Wang et al. 2020a). No change was observed in the quantity of IL-10 secreting splenocytes of PFOS treated C57BL/6 mice (Zheng et al. 2011).

IL-15 mRNA expression was increased in zebrafish liver following exposure to PFOS for 7, 14, or 21 days (Guo et al. 2019).

TNF-α was measured in rats (SD) and mice (C57BL/6, B6C3F1, and one unspecified strain), rat C6 glia cells, chicken embryo fibroblasts, and zebrafish. Increases in TNF-α was observed in liver homogenate and serum in SD rats (Han et al. 2018) and in rat C6 glia cells exposed to PFOS (Chen et al. 2018b). In C57BL/6 or C57BL/6J mice, levels were decreased in liver (Qazi et al. 2010a; Wang et al. 2020a), increased or decreased in splenic cells (Dong et al. 2012; Qazi et al. 2009a); increased in bone marrow cells (Qazi et al. 2009a), peritoneal macrophages (Dong et al. 2012), and peritoneal cavity (Qazi et al. 2009a). In B6C3F1 mice, the following results were observed regarding TNF-α production: no changes in blood serum, no change in peritoneal macrophages with *in vivo* stimulation using 25 µg LPS, an increase at the highest dose in peritoneal macrophages stimulated with 0.1 µg/ml LPS *in vitro*, and a decreasing trend in peritoneal lavage fluid with *in vivo* stimulation using 25 µg LPS (Mollenhauer et al. 2011). In chicken embryo fibroblasts, a decrease of TNF-α mRNA expression following PFOS treatment was observed (Castaño-Ortiz et al. 2019). TNF-α and TGF-β mRNA expression was significantly increased in zebrafish following PFOS exposure for 7, 14, or 21 days (Guo et al. 2019).

No change in production of IFN-γ was observed in intrahepatic immune cells of C57BL/6 mice, but a decrease was observed in liver homogenate (Qazi et al. 2010a). A decrease in IFN-γ secretion by splenic cells was observed in the same strain (Dong et al. 2011; Zheng et al. 2011). An increase in IFN-γ secretion was observed in dolphin peripheral blood leukocytes when exposed to PFOS *in vitro* (Soloff et al. 2017).

Summary of evidence for KC6

The effects of PFOS on pro-inflammatory cytokine production have been tested in multiple human cell types *in vitro*, including peripheral blood leukocytes, lymphocytes, primary CD4+ T cells, colon myofibroblasts, bronchial epithelial cells, THP-1 cells, Jurkat T cells, and neuronal cells. IL-1 production has been shown to be increased with PFOS treatment in two studies using human bronchial epithelial cells and lymphocytes. IL-10 and IFN-γ levels were both decreased in two studies conducted by the same research group using human peripheral blood leukocytes. Two studies reported a decrease in TNF-α secretion and mRNA expression in human blood cells. The effect of

PFOS on IL-2, IL-4, IL-6, and IL-8 production remains unclear, as different results have been observed in different studies. A single study has reported a decrease of CXCL-10 production.

Studies in animals were conducted in different strains of mice, and in SD rats, zebrafish, and chicken embryo fibroblasts. Increases of IL-1 production have been observed in mice, rats and zebrafish. Two studies in mice reported a decrease in the number of splenocytes secreting IL-2. The effect of PFOS on IL-4, IL-5, IL-6, IL-10, TNF-α and IFN-γ production remains unclear, as different results have been observed from different studies. Single studies have reported no change of IL-5 production by mouse splenic T cells, a decrease of IL-8 mRNA in chicken embryo fibroblasts, and an increase of IL-15 and TGF-β mRNA in zebrafish liver.

5.3.7 Is Immunosuppressive

Immunosuppression can result in a reduction in the capacity of the immune system to respond effectively to tumor cells. Immunosuppression may allow neoplastic cells to escape immune surveillance and permit the survival and replication of these cells to form tumors (Smith et al. 2020). Both the innate and adaptive parts of the immune system participate in immune surveillance, *i.e.*, recognition and removal of malignant cells. The innate immune system is the first line of defense, and key components of the innate (or natural) immune system include natural immunoglobulin M (IgM) antibody-producing B1 or $CD5^+$ cells, macrophages, mast cells, dendritic cells, and natural killer (NK) cells (Vollmers and Brändlein 2009). The adaptive immune system consists of a heterogeneous population of infiltrating lymphocytes such as T cells and other immune cells to modulate the anti-tumor response (Neeve et al. 2019).

Both natural IgM (produced by B1 cells and marginal zone cells) and adaptive IgM (synthesized by B2 cells) play important roles in the cancer immune response. Natural IgM eliminates tumor cells when they begin to transform; adaptive IgM eliminates tumor cells during growth (Díaz-Zaragoza et al. 2015). Natural IgM antibodies recognize and bind to tumor-specific surface antigens and induce apoptosis via induction of cellular stress, for example by cross-linking of modified anti-complement receptors, blocking of growth-factor receptors, or by increasing the intracellular level of neutral lipids (Vollmers and Brändlein 2009). NK cells are effector lymphocytes that control several types of tumors and microbial infections by limiting their spread and subsequent tissue damage. Functions of NK cells, including the control of tumor development, can be dependent on their interaction with dendritic cells, macrophages, T cells and endothelial cells (Vivier et al. 2008). NK cells have been observed to induce tumor cell apoptosis through interferon gamma (IFN-γ) and perforin release (Neeve et al. 2019). Dendritic cells are antigen-presenting cells (*i.e.*, they capture tumor antigen) and are capable of activating

naive T cells to differentiate into tumor antigen-specific CD4+ helper T cells or to $CD8^+$ cytotoxic T cells. Neutrophils are key cellular mediators of the innate immune response (Qazi et al. 2009a). Results from various studies suggest that tumor-associated neutrophils have anti-tumor properties, including the ability to induce cytotoxicity and inhibit metastasis. Conversely, other studies point to a tumor-supporting role of neutrophils (Shaul and Fridlender 2019; Uribe-Querol and Rosales 2015).

This section summarizes data for only the immunosuppressive effects of PFOS that are relevant to carcinogenesis.

Effects on T cell dependent and independent antibody response (TDAR/TIAR)

The T cell dependent antibody response (TDAR) assesses immune function in rodents. TDAR focuses on the humoral arm of adaptive immunity and a response requires antigen recognition and presentation, T and B cell signaling, and class switching (DeWitt et al. 2012). TDAR can detect immunosuppression across a range of cell types and signals, usually measured as changes in levels of IgM or IgG production (DeWitt et al. 2012).

The response of IgM, which peaks at days 7 to 14, precedes the response of IgG, which peaks at days 14 to 21 (Lebrec et al. 2011). Assessing IgM TDAR to an antigen is a sensitive measure of immune function, as it requires T cells, B cells, and antigen-presenting cells to function properly to elicit an antibody response (DeWitt et al. 2008). T cell dependent release of IgM (also known as adaptive IgM) has been associated with recognition of breast cancer antigens and priming of the subsequent adaptive immune response (Díaz-Zaragoza et al. 2015). While TDAR measures antibody production resulting from the combined action of T and B cells, another assay, T cell independent IgM antibody response (TIAR), assesses B cell-specific antibody production (DeWitt et al. 2012).

Here, relevant results from animal studies using TDAR and TIAR to assess immune function after PFOS administration are briefly described.

TDAR-IgM and TIAR-IgM responses were suppressed in several studies in mice following administration of PFOS and subsequent antigen challenge. One study without antigen challenge reported IgM suppression (in mice), while another study without antigen challenge reported an increase in IgM (in rats).

- Suppression of TDAR: Suppression (by 53%) of sheep red blood cell (SRBC)-specific IgM production in male B6C3F1 pups following maternal exposure to

PFOS (5 mg/kg-day) during gestation and challenge with SRBCs; no suppression was observed in female pups (Keil et al. 2008).

- Suppression of TDAR/TIAR: Dose-dependent suppression of IgM production in male and female B6C3F1 mice exposed to PFOS daily via gavage for 28 days (0, 0.005, 0.05, 0.1, 0.5, 1, or 5 mg/kg total administered dose (TAD)) and challenged with SRBC (males responded at lower doses), and suppression of trinitrophenyl (TNP)-specific IgM following a challenge with TNP conjugated to lipopolysaccharide (LPS) (T cell independent) (Peden-Adams et al. 2008).
- Suppression of TDAR: Dose-dependent suppression of IgM production in adult male C57BL/6 mice following gavage with PFOS for 60 days (0, 0.5, 5, 25, 50, or 125 mg PFOS/kg body weight TAD) and SRBC challenge; response was observed at 5 mg PFOS/kg body weight and above (Dong et al. 2009; Dong et al. 2011).
- Suppression of TIAR: Suppression of total immunoglobulin formation (measured as response to ovalbumin) and IgM formation (measured as TNP response) in female BALB/c mice exposed to PFOS via gavage (20 mg/kg-day) and challenged with ovalbumin or TNP (Vetvicka and Vetvickova 2013).
- No changes in TDAR/TIAR: no difference in level of IgM antibodies in male B6C3F1 mice following PFOS exposure via diet for 28 days (250 µg PFOS/kg body weight/day) and SRBC challenge on day 23 (TDAR) or challenge with 100 µg TNP–LPS on day 23 (TIAR) (Qazi et al. 2010b).
- IgM levels without antigen challenge:
    - Dose-dependent suppression of total IgM in adult male C57BL/6 mice (oral gavage for 7 days; 0, 5, or 20 mg/kg-day); no consistent effect on IgG levels (Zheng et al. 2011).
    - Increase of IgM was observed at the highest dose and by trend (p-trend < 0.001) in female (but not male) SD rats exposed to PFOS in the diet for 28 days (0, 2, 20, 50, or 100 mg/kg diet per day) (Lefebvre et al. 2008).

Effects on T cell and B cell cellularity or proliferation

PFOS has been shown to reduce the number and proliferation of thymocytes and splenocytes in mice in multiple studies. Two studies reported no change (one in mice, and one in rats). In a study using dolphin peripheral blood leucocytes, PFOS induced dose-dependent CD4+ and CD8+ T cell proliferation.

- Reduced total number of thymocytes and splenocytes, as well as the ratio of thymocytes expressing both CD4 and CD8 to total thymocytes in male C57BL/6 mice following exposure via diet to PFOS (0.02%) (Qazi et al. 2009b).
- Reduced proliferation of T cells and decreased cellularity in the thymus (by more than 50%) and in the spleen in BALB/c mice following exposure to

PFOS via gavage (20 mg/kg-day for seven days) (Vetvicka and Vetvickova 2013).

- Reductions in splenic and thymic cellularity by up to 51% and 61%, respectively, in male C57BL/6 mice treated with 20 and 40 mg/kg-day PFOS; and decreases of 28% and 21%, respectively, in the relative $CD4^{+}CD8^{-}$ and $CD4^{-}CD8^{+}$ populations in the highest dose group (Zheng et al. 2009).
- Reductions in splenic and thymic cellularity in male C57BL/6 mice at 25, 50, and 125 mg PFOS/kg TAD (0, 0.5, 5, 25, 50 or 125 mg PFOS/kg body weight TAD via gavage over the course of 60 days); Reduction at the highest dose reached 55 and 70% for splenic and thymic cellularity, respectively (Dong et al. 2009).
- Modulation (decrease) of splenic and thymic CD4 and CD8 T-lymphocyte subpopulations in male C57BL/6 mice at doses of 25 mg PFOS/kg TAD and above (0, 0.5, 5, 25, 50, 125 mg PFOS/kg body weight TAD via gavage over the course of 60 days). Decreased B cells with increasing PFOS exposure at doses of 25 mg PFOS/kg TAD and above (Dong et al. 2009).
- Modulation of T cell subpopulations in male B6C3F1 mice, with increased $CD4^{-}CD8^{-}$ subpopulation at all doses; minimal alteration of splenic T cell immune phenotypes in females and no alteration of lymphocyte proliferation in either sex following exposure up to 5 mg/kg-day PFOS via gavage (Peden-Adams et al. 2008).
- Decreased splenic B220 cells at 4 weeks (but not 8 weeks) in female (but not male) B6C3F1 pups exposed to 5 mg/kg-day PFOS *in utero*; however, male pups exposed to this dose *in utero* had a 25% decrease in CD3+ and a 28% decrease in $CD4^{+}$ thymocytes at 8 weeks, and a reduction in thymocyte CD4:CD8 ratio to 3.5 (as compared to 4.2 in controls) (Keil et al. 2008).
- Decreased splenic lymphocyte proliferation of cells from male C57BL/6 mice exposed at 50 and 125 mg PFOS/kg TAD (0, 0.5, 5, 25, 50, or 125 mg PFOS/kg body weight TAD via gavage over the course of 60 days); cells were stimulated with concanavalin A (ConA) or LPS for 48 hours after harvest (Dong et al. 2009).
- No change in absolute numbers of CD4+/CD154+ T-helper cells, CD4+/CD154− or CD4−/CD154+ cells in female B6C3F1 mice following gavage with PFOS for 28 days (TAD of 0, 0.1, 0.5, 1, or 5 mg/kg body weight) (Fair et al. 2011).
- No significant effect of PFOS exposure to male or female SD rats (0, 2, 20, 50, or 100 mg PFOS/kg diet for 28 days) on splenocyte proliferation with either LPS or ConA stimulation (Note: data not shown) (Lefebvre et al. 2008).

- Increased proliferation of CD4+ and CD8+ cells with increasing PFOS concentration in cultured peripheral blood leucocytes from bottle nosed dolphins (Soloff et al. 2017).

Additional effects of PFOS on immune system cellularity (as described in Section 5.1 Immunotoxicity of OEHHA 2021) include decreased absolute spleen weight (Xing et al. 2016; Zhong et al. 2016) and decreased absolute thymus weight and cellularity (Zhong et al. 2016) in C57BL/6 mice, decreased relative thymus weight in Sprague-Dawley rats (NTP 2019), and decreased white blood cells, neutrophils, and eosinophils in male Sprague-Dawley rats (NTP 2019).

Effects on NK cells

NK cell activity was assessed in one human *in vitro* study and in seven animal studies. The human study and four studies in mice reported decreases in NK cell activity following exposure to PFOS. Two studies reported an increase in NK cell activity in male mice. A study in rats reported no changes.

- Decreased NK cell activity in human peripheral blood mononuclear cells cultured for 24 hours in the presence of PFOS (Brieger et al. 2011).
- Decreased NK cell activity in 8-week-old male and female B6C3F1 pups following maternal oral exposure to PFOS at the two highest doses (1 and 5 mg/kg-day) (Keil et al. 2008).
- Decreased NK cell activity in adult male C57BL/6 mice at the two highest doses (20 and 40 mg/kg-day) (Zheng et al. 2009).
- Decreased splenic NK cell activity in C57BL/6 mice of both sexes exposed *in utero (*1.0 and 5.0 mg/kg-day maternal dose) (Zhong et al. 2016).
- Decreased splenic NK cell activity in male C57BL/6 mice exposed to 50 and 125 mg PFOS/kg TAD (0, 0.5, 5, 25, 50, or 125 mg PFOS/kg body weight TAD via gavage over the course of 60 days) (Dong et al. 2009).
- Increased splenic NK cell activity in male C57BL/6 mice exposed to 5 mg PFOS/kg TAD (0, 0.5, 5, 25, 50, or 125 mg PFOS/kg body weight TAD via gavage over the course of 60 days) (Dong et al. 2009).
- A 2–2.5-fold increase in splenic NK activity in male (but not female) B6C3F1 mice treated via gavage (at 0.5, 1, and 5 mg/kg total administered dose); no change in lymphocyte proliferation in either sex (Peden-Adams et al. 2008).
- No significant changes in CD161+ NK cell activity in male or female SD rats following PFOS exposure via diet for 28 days (0, 2, 20, 50, or 100 mg PFOS/kg diet) (Note: data not shown) (Lefebvre et al. 2008).

Summary of evidence for KC7

PFOS suppressed IgM responses in four mouse studies following an antigen challenge; one additional study observed a decrease without antigen challenge. Two studies in mice reported no change in IgM response (one with and one without antigen challenge, and one study in rats reported an increase in IgM response (without antigen challenge). PFOS has also been shown to reduce the number and proliferation of thymocytes and splenocytes in mice in multiple studies. Two additional studies reported no change (one mouse, one rat study); a third study reported an increase in proliferation of dolphin CD4+ and CD8+ T-lymphocytes exposed *in vitro*.

Several studies have shown that PFOS suppresses NK cell activity, including one study in cultured human blood cells and four studies in mice, although two other mouse studies reported an increase in NK cell activity. Taken together, these studies suggest that PFOS can suppress the immune system in ways that would allow neoplastic cells to escape immune surveillance, survive, and replicate to form tumors.

5.3.8 Modulates receptor-mediated effects

Chemicals may modulate receptor-mediated effects in a variety of ways, including binding to and either activating or inactivating a receptor, altering receptor levels or function, altering levels of endogenous ligands that are available to bind to the receptor, or otherwise altering receptor-mediated gene expression or intracellular signaling. Many cellular receptors regulate critical cellular pathways, such as those involved in differentiation and proliferation, the disruption of which can contribute to carcinogenic processes. For example, activation of certain growth factor receptors, or estrogen, androgen, or progesterone receptors can lead to the development of various types of cancer in humans and animals. As another example, activation of the aryl hydrocarbon receptor is involved in the development of a number of different types of cancers in humans and animals. Activation of other nuclear receptors, including peroxisome proliferator activated receptor alpha (PPARα) and the constitutive androstane receptor (CAR), also has been associated with carcinogenesis (Smith et al. 2020).

Estrogen receptors

A number of studies provide evidence that PFOS has ER activity. In human cells *in vitro*, PFOS increased ERα reporter activity in several cell lines and ERβ in one cell line, increased cell proliferation in breast epithelial cells, and downregulated gene expression of estrogen-responsive genes. In rodents *in vivo*, PFOS increased expression of ERα and altered the estrous cycle in female rats, induced a gene expression profile similar to an ERα agonist in mice, and induced ERβ in male mice. PFOS increased vitellogenin (Vtg) expression and altered expression of ERα and ERβ in several species of fish.

Differences in ER expression and responses between studies may reflect varying sensitivities of different species and cell lines, the use of different doses, or the composition of the test chemical, as suggested by *in silico* studies. Findings from these studies are briefly summarized below.

Human observational studies

- In a cross-sectional study conducted in Italy, levels of gene expression of nuclear receptors were measured in serum samples of 111 infertile women and 44 fertile women. No significant correlations between PFOS levels and expression of ERα or ERβ were observed in either group of women (Caserta et al. 2013).

Studies using human cells in vitro

- PFOS increased ERα reporter activity in human embryonic kidney (HEK293T) cells transfected with a human ERα reporter gene in one study (Benninghoff et al. 2011) but did not increase ERα or ERβ reporter activity in another (Behr et al. 2018).
- PFOS increased cell proliferation and cell cycle progression in human breast epithelial MCF-10A cells and had no effect on cellular protein levels of either ERα or ERβ. PFOS-induced cell proliferation was partially blocked by the ER antagonist ICI 182,780, indicating that the effect of PFOS on cell proliferation was partially due to activation of ER (Pierozan and Karlsson 2018).
- In the E-SCREEN assay, PFOS induced estrogenic responses in human MCF-7 cells in one study (Henry and Fair 2013) but not in two other studies (Behr et al. 2018; Maras et al. 2006).
- PFOS induced anti-estrogenic activity when MCF-7 cells were co-exposed to PFOS and 17β-estradiol (E2) in two studies. PFOS with E2 induced a small but significant downregulation in gene expression of three estrogen-responsive genes, *TFF1* (trefoil factor 1, also known as *pS2*), *ESR1* (estrogen receptor 1), and *EGR3* (early growth response 3) (Henry and Fair 2013; Li et al. 2020a). Without E2, PFOS induced the expression of *TFF1* (Li et al. 2020a).
- In MVLN cells (MCF-7 cells transfected with a luciferase reporter gene plasmid), PFOS demonstrated agonistic ER transactivation activity in one study (Li et al. 2020a) but not another (Kang et al. 2016). In the presence of E2, PFOS showed a weak antagonistic ER transactivation response in two studies (Kang et al. 2016; Li et al. 2020a).
- PFOS weakly induced an estrogenic response in ER-MMV-Luc cells (MCF-7 cells transformed with a vector containing the luciferase gene controlled by a Vtg promoter) (Doan et al. 2020).

- In T47D human breast cancer cells, PFOS alone did not induce estrogen response element (ERE) activation in the ERE luciferase reporter assay or alter expression of the estrogen-responsive genes progesterone (*PR)* and *TFF1*. Co-exposure of cells to PFOS and E2 induced ERE activation and *pS2* mRNA expression, but not PR expression, demonstrating that PFOS did not have estrogenic activity in this assay but enhanced the effects of E2 (Sonthithai et al. 2016).
- ERα expression was significantly upregulated in human umbilical vein endothelial cells exposed to PFOS (Liao et al. 2012).
- PFOS (10 μM) induced ERβ expression in HepG2 cells (Xu et al. 2017).

Rodent studies in vivo

- The gene expression profiles in the liver of wild-type 129S1/SvlmJ mice treated with PFOS by gavage for seven days were compared to those of wild-type or ERα-null mice treated with a known ERα agonist. The data show that the gene expression profile in the liver of PFOS-treated wild-type mice was similar to that of wild-type mice treated with a known ERα agonist, and different from the gene expression profile in the liver of ERα-null mice treated with the known ERα agonist, indicating that the effects of PFOS on gene expression in the liver are mediated through ERα (Rosen et al. 2017).
- In female SD rats, daily administration of PFOS (at doses of 1 or 10 mg/kg bw by i.p. injection for two weeks) resulted in dose-dependent changes in estrous cyclicity (irregular cycles/persistent diestrus) that were statistically significant at the high dose (Austin et al. 2003). A similar effect was reported in female ICR mice exposed to 0.1 mg/kg-day PFOS via gavage for 4 months (Feng et al. 2015).
- In female SD rats, administration of 15 mg/kg-day PFOS in drinking water for 28 days resulted in an increase in expression of ERα in the uterus compared to controls (Qiu et al. 2020).
- In the testis of male C57 mice administered 0, 0.5, or 10 mg/kg PFOS via gavage, a significant decrease in expression of ERα in the high-dose group and significant increases in expression of ERβ in the mid- and high-dose groups were observed (Qu et al. 2016).
- Exposure to 5 mg/kg PFOS via gavage for 28 days induced ERβ but not ERα expression in the livers of wild-type male C57BL/6 mice. PFOS-induced hepatotoxicity (liver injury and decreased hepatic cholesterol and bile acid content) in wild-type mice was shown to be partly mediated by ERβ, since no

pathological changes were observed in the livers of ERβ-knockout mice (Xu et al. 2017).

Animal studies in vitro

- In a reporter gene assay in CV-1 cells (African green monkey kidney cells), PFOS acted additively to E2 as an ERα agonist (Du et al. 2013).

Fish studies in vivo/ex vivo

- In rainbow trout, PFOS in the diet had no effect on plasma levels of Vtg, an estrogen-responsive biomarker protein (Benninghoff et al. 2011).
- In male swordtail fish, 0.1, 0.5 and 2.5 mg/l PFOS significantly inhibited Vtg mRNA expression after one or two weeks and stimulated Vtg at three weeks. Vtg remained stimulated after a recovery period only in the high-dose group (Han and Fang 2010).
- In zebrafish, exposure to 0.6 µg/l PFOS significantly increased levels of Vtg in F1 and F2 males at 90 days post-fertilization, and 100 µg/l PFOS significantly increased Vtg levels in F2 males at 180 days post-fertilization (Keiter et al. 2012).
- In zebrafish, PFOS exposure altered genes related to estrogen receptor production, *i.e.*, an increase in expression of *esr1* and a decrease in expression of *esr2b* (Du et al. 2013).
- PFOS competitively binds (weakly) to trout liver ER in a study with liver cytosol homogenates (Benninghoff et al. 2011).
- In toxicogenomic studies in rainbow trout, the hepatic gene expression profile of fish exposed to PFOS (200 ppm) for two weeks in the diet was similar overall to that of fish exposed to E2 for two weeks (Benninghoff et al. 2012).
- In liver tumor promotion studies in rainbow trout initiated with aflatoxin B1, PFOS promoted liver tumors in a manner similar to that of E2 (Benninghoff et al. 2012) (see Section 4.2 Tumor Promotion Study Conducted in Trout).
- In marine medaka embryos exposed to PFOS at two days post-fertilization; mRNA expression levels of ERα were significantly decreased in the high-dose group in early development and increased at all doses in late development. ERβ expression levels were increased in the mid- and high-dose groups in early development and in the high-dose group in late development (Fang et al. 2012).
- Atlantic salmon embryos (at the egg stage) were exposed to PFOS for a period of 52 days. A significant decrease in ERα mRNA was observed at day 21 in head tissues after PFOS exposure, differences in expression from controls were no longer observed in head tissues from day 35 onwards. Minor non-significant

alterations in ERα mRNA were observed in body tissues. Significant increases in ERβ were observed at day 21 in both head and body tissues that were restored to control levels thereafter (Spachmo and Arukwe 2012).

In silico studies

- Analyses using *in silico* computational models indicate that PFOS can efficiently dock with human ERα in the ligand-binding domain (LBD) and form a hydrogen bond at residue Arg394 in a manner similar to that of estrogens (Benninghoff et al. 2011; Gao et al. 2013; Qiu et al. 2020). Of eight PFASs tested, PFOS was estimated as having the highest binding affinity to ERα (Qiu et al. 2020).
- A comparison of species-specific binding characterizations between PFOS and ERα indicates that PFOS is predicted to bind most strongly to human ERα, followed by rat and rainbow trout ERα. Linear PFOS is predicted to bind much more strongly to ERα than branched PFOS (Qu et al. 2019).

Androgen receptor

Overall, few studies have examined the effects of PFOS on AR activity. PFOS correlated with AR expression in women in one study and antagonized AR activity in a human breast cancer cell line. PFOS did not have an effect on other human cell lines. PFOS altered AR gene expression in male rats, and antagonized AR activity in Chinese hamster cells. Findings from these studies are briefly summarized below.

Human observational studies

- In the cross-sectional study of fertile and infertile women in Italy, serum PFOS concentration positively correlated with AR expression ($r = 0.236$; $p<0.05$) in infertile women. A weak, not statistically significant, negative correlation was observed in fertile women ($r = -0.031$; $p\geq0.05$) (Caserta et al. 2013).

Studies using human cells in vitro

- In a human breast cancer cell line (MDA-kb2) that expresses endogenous AR and a transfected AR-dependent luciferase reporter, PFOS significantly antagonized dihydrotestosterone (DHT)-induced AR activity in one study (Behr et al. 2018), but had no detectable androgenic or antiandrogenic activity in another study (Du et al. 2013).
- PFOS did not have any effect on AR expression or targeted androgen-responsive gene expression in LNCaP cells (human prostate adenocarcinoma cells) (Behr et al. 2018).
- PFOS did not induce any androgen receptor response in TARM-Luc cells (human mammary gland carcinoma T47D cells transformed with a vector

containing the MMTV (mouse mammary tumor virus)-LTR (long terminal repeat) promoter and an expression vector coding for human AR) (Doan et al. 2020).

- Neither agonistic nor antagonistic effects on AR transactivation were observed in 22Rv1/MVLN cells (22Rv1 cells, a human prostate carcinoma cell line, transfected with a luciferase reporter gene plasmid) (Kang et al. 2016).

Rodent studies in vivo

- In male SD rats administered 0, 1.0, 3.0, or 6.0 mg/kg-day PFOS via gavage for 28 days, an increase in AR gene expression was observed in the hypothalamus and pituitary gland, with a decrease in AR protein expression in those tissues. In the testis, both gene and protein expression of AR were significantly decreased (López-Doval et al. 2016).

Rodent studies in vitro

- PFOS significantly antagonized DHT-induced AR activity in a concentration-dependent manner in a Chinese hamster ovary cell line (CHO-K1) transfected with AR and a reporter vector (Kjeldsen and Bonefeld-Jorgensen 2013).

PPARα

Overall, PFOS induces PPARα activity in several test systems, including human cells *in vitro*, rodents *in vivo*, animal cells *in vitro,* and several species of fish. It seems that PFOS is a weaker agonist of human PPARα compared to rat or mouse PPARα (Behr et al. 2020), yet PFOS did activate PPARα-mediated gene expression in human hepatocytes in two studies. Additionally, studies with PPARα-knockout mice demonstrate that PFOS can exert effects via PPARα-independent mechanisms, although PPARα appears to be the primary nuclear receptor target of PFOS in rodents (Elcombe et al. 2012a). Findings from these studies are briefly summarized below.

Studies using human cells in vitro (and mammalian cells transfected with human PPARα)

- In human HepG2 cells transfected with human PPARα and a luciferase reporter gene, PFOS at concentrations up to 100 µM did not induce PPARα activity (Rosenmai et al. 2018). However, cellular uptake of PFOS was less than 0.05% (approximately 6-fold lower than the cellular uptake of PFOA in the same study); thus, the lack of PPARα activity observed with PFOS may have been due to the limited uptake by the cells.
- In human HepRG cells, PFOS at concentrations up to 100 µM activated PPARα-mediated gene expression, as demonstrated by upregulation of the PPAR signaling pathway that includes mRNA expression of the genes *PCK1*, *PLIN4*,

PLIN1, *PLIN2*, and *SLC27A2* (Louisse et al. 2020). PFOS at concentrations up to 250 µM also upregulated *PLIN2* in primary human hepatocytes in another study (Rosen et al. 2013).

- PFOS at a concentration of 25 µM did not induce increased expression of PPARα-dependent genes in human primary hepatocytes (Bjork and Wallace 2009; Bjork et al. 2011) or human hepatoma HepG2/C3A cells (Bjork and Wallace 2009).
- In human HEK293T cells transfected with a reporter gene, PFOS induced a 1.8-fold PPARα activation at the highest test concentration of 100 µM but no activation was observed at concentrations at or below 50 µM (Behr et al. 2020).
- PFOS activated PPARα in mouse 3T3-L1 fibroblasts transfected with the LBD of human PPARα (Vanden Heuvel et al. 2006).
- PFOS induced PPARα activity in COS-1 cells (a fibroblast-like cell line derived from African green monkey kidney tissue) transfected with a human PPARα receptor-luciferase reporter plasmid in two studies (Shipley et al. 2004; Wolf et al. 2008).

Rodent studies in vivo

- Two studies demonstrated that effects of PFOS can be independent of PPARα. Male wild-type and PPARα-null C57BL/6 mice were fed diets containing 0, 0.001%, 0.005%, or 0.02% PFOS for 10 days. Effects such as hepatomegaly were found to be independent of PPARα, thymic changes were partially dependent on PPARα, and splenic changes were entirely dependent on PPARα (Qazi et al. 2009b). In another study, wild-type 129S1/SvlmJ mice and PPARα-null 129S4/SvJae-*Ppara*^{tm1Gonz}/J mice were administered 0, 3, or 10 mg/kg PFOS via gavage for seven days. Some changes were observed in expression of markers of PPARα transactivation in the livers of wild-type mice, but were less robust than Wy14,643, a PPARα agonist. In wild-type mice, PFOS modified the expression of genes related to several PPARα-regulated functions (*e.g.,* lipid metabolism, inflammation, peroxisome biogenesis, and proteosome activation), indicative of a weak PPARα activator. Genes related to lipid metabolism, inflammation, and xenobiotic metabolism were affected in both wild-type and PPARα-null mice, and several categories of genes were upregulated only by PPARα-null mice. Thus, PFOS induced both PPARα-dependent and PPARα-independent effects in mouse liver (Rosen et al. 2010).
- Significant increases in expression of *Acox1* and *Cyp4a1*, markers of PPARα activity, were observed in male SD rats exposed to PFOS by gavage for 28 days (NTP 2019).

- Significant increases in markers for PPARα activation, liver palmitoyl CoA oxidase (ACOX) activity and hepatic lauric acid 12-hydroxylation activity (a marker for CYP4A), were observed in male SD rats in two studies at different doses and time points (Elcombe et al. 2012a; Elcombe et al. 2012b). Increases in hepatic CYP4A1 protein levels were also observed in Elcombe et al. (2012a).
- Increased expression of PPARα was observed in the livers of male SD rats treated with PFOS via i.p. injection, but no increase was observed in the liver of neonatal rats exposed *in utero* (Bjork et al. 2008).
- PFOS exposure in the diet to male SD rats resulted in changes in expression of 48 genes in the PPARα pathway, which is approximately 10% of all PPARα target genes in the Target Explorer Database (Dong et al. 2016).
- Adult SD rat dams were exposed to 0, 5, or 20 mg/kg-day PFOS from gestational days (GD) 12-18. Animals were euthanized on day 18.5 and fetal lung tissue was analyzed for RNA profiling. PFOS exposure dose-dependently upregulated expression of five PPARα target genes in offspring (Ye et al. 2012).
- Male C57BL/6 J mice were fed normal diet, high-fat diet, normal diet + PFOS, or high-fat diet + PFOS for 6 weeks. No changes were observed in PPARα expression in any groups (Huck et al. 2018).
- Transcript profiling of fetal liver and lung tissues collected from offspring of CD-1 mouse dams exposed to 0, 5, or 10 mg/kg PFOS on GD 1-17 demonstrated that PFOS upregulated a number of markers of PPARα activity in the fetal liver, but fewer in the fetal lung (Rosen et al. 2009).

Animal studies in vitro

- Exposure of rat brain capillaries to 1 or 10 nM PFOS increased transport activity of three ATP-driven drug efflux transporters (P-glycoprotein [Abcb1], breast cancer resistance protein [Bcrp/Abcg2], and multidrug resistance-associated protein 2 [Mrp2/Abcc2]). Effects were blocked by the PPARα antagonist GW6471 (More et al. 2017).
- PFOS activated PPARα in mouse 3T3-L1 fibroblasts transfected with the LDB of mouse PPARα and in those transfected with the LBD of rat PPARα (Vanden Heuvel et al. 2006).
- PFOS induced PPARα in monkey kidney fibroblast-like COS-1 cells transfected with a mouse PPARα receptor-luciferase reporter plasmid in three studies (Shipley et al. 2004; Wolf et al. 2008; Wolf et al. 2014).

- In primary rat hepatocytes, PFOS at a concentration of 25 µM increased mRNA expression of several genes regulated by PPARα (Bjork and Wallace 2009; Bjork et al. 2011).
- In primary mouse hepatocytes, PFOS at concentrations up to 250 µM did not alter expression of genes associated with PPARα, including *Acox1, Hadha, Me1, Acaa1a, Hmgcs1,* and *Slc27a1* (Rosen et al. 2013).
- In an *in vitro* reporter gene assay of an African green monkey kidney CV-1 cell line transfected with Baikal seal PPARα plasmid, treatment with PFOS induced PPARα-mediated transcriptional activity in two studies (Ishibashi et al. 2008; Ishibashi et al. 2011). (Additionally, PFOS was positively, but not statistically significantly, correlated with PPARα levels in livers of Baikal seals (Ishibashi et al. 2008))
- Chicken embryos exposed to 0, 0.1, 5, or 100 µg/g PFOS via injection into the egg prior to incubation did not demonstrate alterations in transcriptional activity of any of the measured PPARα-regulated genes (O'Brien et al. 2009).
- Primary chicken embryonic hepatocytes were exposed to 10 or 40 µM manufactured technical product PFOS or linear PFOS for 24 hours. Of the genes dysregulated by PFOS, few interacted with PPARα, and PPARα did not occur in any of the interaction networks generated by ingenuity pathway analysis of genes affected by PFOS (O'Brien et al. 2011).

Fish studies in vivo/ex vivo/in vitro

- PFOS upregulated PPARα in thicklip grey mullets exposed to 2 ppm PFOS dissolved in sea water for 16 days, as demonstrated by an increase in PPARα mRNA expression and upregulation of the PPARα-responsive gene AOX1 (Bilbao et al. 2010).
- Marine medaka embryos were exposed to 0, 1, 4, or 16 mg/l PFOS starting on the second day after fertilization; transcriptional responses were measured at the early and late developmental stages. The mRNA expression levels of PPARα were decreased at all doses in early development and increased in mid- and high-dose groups in late development (Fang et al. 2012).
- In Atlantic salmon administered PFOS in feed, PPARα mRNA levels in the liver significantly increased at day 2, then decreased to control levels through the recovery period. In the kidney, PPARα significantly decreased at day 2, returned to control level at days 5 and 8, then decreased again after the recovery period (Arukwe and Mortensen 2011).

- Isolated hepatocytes from Atlantic salmon were exposed to 0, 2.1, 6.2, 15.1, or 25.0 mg/l for 24 and 48 hours. After both exposure times, there was a significant induction of PPARα in the high-dose group compared to controls (Krøvel et al. 2008).

Other nuclear receptors, i.e., PPARγ, PXR, CAR, and PPARβ/δ

Besides effects on PPARα, a number of studies show that PFOS can modulate other receptors such as PPARγ, PXR, CAR, and possibly PPARβ/δ, through measurement of receptor activation-induced luciferase reporter activity, and increased expression of target gene and/or protein levels (cytochrome P450 isoforms) from translation of downstream regulated genes in rodents. Mice treated with PFOS had increased gene expression of PPARγ and CAR transcriptional targets. In human cells *in vitro*, PFOS has also been shown to activate PPARγ, PXR, and CAR. Findings from these studies are briefly summarized below.

Human observational studies

- In the cross-sectional study of fertile and infertile women in Italy, there were no significant correlations ($p < 0.05$) between serum PFOS and expression of PPARγ or PXR in either group of women (Caserta et al. 2013).

Studies using human cells in vitro (and mammalian cells transfected with human nuclear receptors)

- PPARγ expression was significantly upregulated in human umbilical vein endothelial cells exposed to PFOS (Liao et al. 2012).
- In a reporter gene assay of HepG2 cells transfected with human PXR (hPXR), PFOS induced hPXR activity (Zhang et al. 2017b).
- In primary human hepatocytes, exposure to 25 μM PFOS significantly increased gene expression of the measured PXR and CAR activation markers, *CYP2B6*, *CYP2C19*, and *CYP3A4* (Bjork et al. 2011).
- In human HEK293T cells transfected with a reporter gene for CAR, PXR, PPARγ, or PPARδ, PFOS at concentrations up to 100 μM did not induce activation of any of these receptors (Behr et al. 2020).
- PFOS activated human PPARγ transfected into mouse 3T3-L1 fibroblasts (Vanden Heuvel et al. 2006).
- In studies conducted in COS-1 cells (a monkey kidney fibroblast-like cell line) transfected with plasmids containing various human PPAR genes and a luciferase reporter, PFOS did not transactivate human PPARβ/δ or PPARγ (Takacs and Abbott 2007).

Rodent studies in vivo

- Male and female SD rats exposed to PFOS by gavage for 28 days exhibited significant increases in expression of *Cyp2b1* and *Cyp2b2* compared to controls, an indication of increased CAR activity (NTP 2019).
- In a study of male SD rats exposed to PFOS in the diet at concentrations of 0, 20 or 100 ppm for 1, 7 or 28 days, increases in liver activity and protein levels of CYP2B and CYP3A, target cytochrome P450 isoforms of CAR and PXR activation, respectively, were observed (Elcombe et al. 2012a).
- Male SD rats were exposed to PFOS in the diet at concentrations of 0, 20 or 100 ppm for 7 days, and then fed basal diet for up to an additional 84 days. Increases in liver activity and protein levels of CYP3A (PXR marker) persisted throughout the additional 84-day period on basal diet in the 100-ppm dose group, whereas liver activity and protein levels of CYP2B (CAR marker) remained elevated after 1 and 28 days on basal diet, were equivalent to levels in untreated animals after 56 days, and were decreased compared to untreated animals after 84 days (Elcombe et al. 2012b).
- PFOS exposure in the diet to male SD rats resulted in altered expression of 29 genes downstream of CAR/PXR, which is approximately 14% of all curated target genes of CAR/PXR. Expression of CAR target genes *Aldh1a7* and *Cyp2b* and PXR target gene *Cyp3a* were increased by PFOS (Dong et al. 2016).
- Male C57BL/6 J mice were fed normal diet, high-fat diet, normal diet + PFOS, or high-fat diet + PFOS for 6 weeks. There was a significant increase in PPARγ in the high-fat diet group and the normal diet + PFOS group compared to the normal diet group, but no change in the high-fat diet + PFOS group (Huck et al. 2018). It is unclear why PFOS suppressed expression of these genes in animals fed a high-fat diet.

Animal studies in vitro

- In primary rat hepatocytes, PFOS exposure significantly increased gene expression of the measured PXR and CAR activation markers *Cyp2b2*, *Cyp2c6*, and *Cyp3a23/3a1* (Bjork et al. 2011).
- In studies conducted in COS-1 cells (a monkey kidney fibroblast-like cell line) transfected with plasmids containing various murine PPAR genes and a luciferase reporter, PFOS transactivated mouse PPARβ/δ, but not PPARγ (Takacs and Abbott 2007).
- PFOS activated mouse and rat PPARγ transfected into mouse 3T3-L1 fibroblasts (Vanden Heuvel et al. 2006).

- In a rat renal proximal tubular epithelial cell line (NRK-52E) transfected with a peroxisome proliferator response element (PPRE)-luciferase vector, PFOS reduced the PPRE-driven transactivational activity of luciferase, which could be rescued by a PPARγ agonist (rosiglitazone) and deteriorated by a PPARγ antagonist (GW9662), demonstrating that PFOS inactivated PPARγ (Wen et al. 2016b).
- Primary chicken embryonic hepatocytes were exposed to 10 or 40 μM manufactured technical product PFOS or linear PFOS for 24 hours. Pathway and interactome analysis suggested that PFOS affected genes through the PPARγ receptor, and to a much greater extent than PPARα (O'Brien et al. 2011).

Fish studies in vivo/ex vivo

- PFOS downregulated PPARγ in grey mullets exposed to 2 ppm PFOS in dissolved sea water for 2 days (Bilbao et al. 2010).
- Marine medaka embryos were exposed to 0, 1, 4, or 16 mg/l PFOS at two days post-fertilization; transcriptional responses were measured at the early and late developmental stages. The mRNA expression levels of PPARβ were decreased in the high-dose group in early development but increased at all doses in late development. PPARγ expression was unchanged at all doses in both stages of development (Fang et al. 2012).
- Isolated hepatocytes from Atlantic salmon were exposed to 0, 2.1, 6.2, 15.1, or 25.0 mg/l PFOS for 24 and 48 hours. After 24 hours, there was a significant induction of PPARγ in the 15.1 mg/l group compared to controls. There were no significant differences for PPARβ after exposure to PFOS (Krøvel et al. 2008).
- In Atlantic salmon administered PFOS in feed, PPARβ and PPARγ mRNA levels in the liver significantly increased at day 2, then decreased to control levels through the recovery period. In the kidney, PPARβ significantly increased at day 8, then returned to control levels after the recovery period, and PPARγ decreased at day 2, returned to control levels, then significantly decreased after the recovery period (Arukwe and Mortensen 2011).

In silico studies

- A molecular docking analysis predicts that PFOS can dock in the binding pocket of hPXR in a way that suggests high potential for hPXR activation (Zhang et al. 2017b).

Modulation of endogenous hormones

Estradiol

Overall, the evidence for an association between PFOS and E2 levels is limited and not consistent. PFOS was negatively associated with E2 in women and girls in several studies. Several studies did not find an association with E2; however, the majority of these are cross-sectional studies and the temporal relationship between exposure and outcome could not be determined (*e.g.*, temporality). In human cells *in vitro*, PFOS reduced E2 in placental cells and increased E2 in adrenal cells. PFOS also increased E2 in female rats, decreased E2 in female mice, and had no effect in male mice. Findings from these studies are briefly summarized below.

Human observational studies

- In prospective cohort studies conducted in Denmark, PFOS was measured in maternal serum, and hormones were measured in male and female offspring at approximately 20 years of age. Maternal PFOS concentration was not associated with E2 levels in daughters or sons (Kristensen et al. 2013; Vested et al. 2013).
- In a prospective cohort study conducted in Japan, maternal serum PFOS levels were associated with increased cord blood E2 in male infants but not female infants (Itoh et al. 2016).
- In a cross-sectional study conducted using data from the National Health and Nutrition Examination Survey (NHANES) database, no associations of PFOS with E2 were observed in men or women (Xie et al. 2021).
- In two cross-sectional studies of healthy men from the general Danish population conducted in 2003 and in 2008-2009, PFOS levels were not associated with serum E2 (Joensen et al. 2009; Joensen et al. 2013).
- In a cross-sectional study of men in the Faroe Islands, serum PFOS was not associated with E2 (Petersen et al. 2018).
- In a cross-sectional study conducted in women in Norway in 2000-2002, PFOS concentrations were associated with decreased E2 in nulliparous, but not parous, women (Barrett et al. 2015).
- In a cross-sectional study of women from the C8 Health Project, PFOS was negatively associated with E2 concentrations in perimenopausal (43–51 year-old) and menopausal (52–65 year-old) women (Knox et al. 2011).
- In a cross-sectional analysis of children aged 6–9 years-old from the C8 Health Project, serum PFOS concentrations were associated with decreased E2 levels in boys but not girls (Lopez-Espinosa et al. 2016).

- In a cross-sectional study of adolescents in Taiwan, PFOS was not significantly associated with E2 in boys or girls (Zhou et al. 2016).
- In a study of Chinese women, serum PFOS was associated with decreased levels of E2 in patients with primary ovarian insufficiency (Zhang et al. 2018b).
- In a cross-sectional study of men in North Carolina, PFOS in semen or plasma was not associated with E2 levels (Raymer et al. 2012).

Studies using human cells in vitro

- Primary human placental cytotrophoblasts exposed to 0.0001 to 1 µM PFOS had significantly reduced E2 levels (Zhang et al. 2015b).
- PFOS significantly increased the levels of E2 in H295R cells (a human adrenal corticocarcinoma cell line) in four studies (Du et al. 2013; Kang et al. 2016; Kraugerud et al. 2011; van den Dungen et al. 2015).

Rodent studies in vivo

- PFOS significantly increased serum E2 in female SD rats exposed via subcutaneous injection on PND 1-5 at all doses and in the low and medium dose groups exposed on PND 26-30 (Du et al. 2019).
- In female SD rats, administration of 15 mg/kg-day PFOS in drinking water for 28 days resulted in an increase in serum E2 levels compared to controls (Qiu et al. 2020).
- PFOS significantly decreased levels of serum E2 in female ICR mice exposed via gavage for 4 months (Feng et al. 2015) or via oral administration for up to 30 days (Wang et al. 2018a).
- PFOS did not affect serum E2 levels in male C57 mice administered 0, 0.5, or 10 mg/kg-bw PFOS per day via gavage for five weeks (Qu et al. 2016).
- Serum and testicular E2 levels were not altered in male ICR mice exposed to 0, 0.5, 5, or 10 mg/kg-bw PFOS per day via gavage for four weeks (Qiu et al. 2021).

Fish studies in vivo/ex vivo

- In zebrafish exposed to 250 µg/l PFOS for five months, E2 levels were significantly elevated compared to controls in females but not males (Chen et al. 2016a).

Testosterone

Several observational studies in humans found significant associations of PFOS with testosterone levels. Many, but not all, of these were inverse associations (*i.e.*, higher levels of PFOS were associated with lower levels of testosterone). In a human adrenal

cell line, PFOS increased the levels of testosterone in two studies and decreased the levels of testosterone in one study. In rodents *in vivo*, PFOS administration decreased testosterone in male mice and rats. PFOS also decreased testosterone secretion in mouse Leydig cells *in vitro* and increased testosterone levels in zebrafish. Findings from these studies are briefly summarized below.

Human observational studies

- A prospective cohort study in the UK (the Avon Longitudinal Study of Parents and Children) linked PFAS concentrations measured in pregnant women with their daughters' serum concentrations of total testosterone at 15 years old. Testosterone concentrations were higher in the group of daughters with prenatal PFOS concentrations in the upper tertile compared to those in the lower tertile (Maisonet et al. 2015).
- In a cross-sectional study conducted using data from the NHANES database, PFOS was significantly associated with increased total and free serum testosterone concentrations in all men in the third and fourth quartiles of PFOS exposure. There was a negative association between total testosterone and the second quartile of PFOS in 12–19-year-old women and a positive association between free testosterone and the second quartile of PFOS in 20–49-year-old women. No associations were observed in women overall (Xie et al. 2021).
- In a cross-sectional study of healthy men from the general Danish population conducted from 2008-2009, PFOS levels were negatively associated with serum testosterone (Joensen et al. 2013). Another study of Danish men conducted in 2003 found no significant associations with testosterone (Joensen et al. 2009).
- In a cross-sectional study of men in the Faroe Islands, serum PFOS was not associated with testosterone (Petersen et al. 2018).
- In a study of Chinese women, serum PFOS was not associated with levels of testosterone in patients with primary ovarian insufficiency (Zhang et al. 2018b).
- In a cross-sectional analysis of children aged 6–9 years-old from the C8 Health Project, serum PFOS concentrations were associated with decreased testosterone levels in boys and girls (Lopez-Espinosa et al. 2016).
- In a cross-sectional study of adolescents in Taiwan, PFOS was negatively associated with testosterone in boys, with a significant trend, but not girls (Zhou et al. 2016). In another cross-sectional study of adolescents in Taiwan, PFOS was negatively associated with testosterone in 12–17-year-old girls (Tsai et al. 2015).

- In a prospective cohort in Denmark, maternal serum concentration of PFOS was not associated with serum testosterone in male offspring (mean age of 3.9 months) (Jensen et al. 2020).
- In a cross-sectional analysis of maternal amniotic fluid of patients from the Danish National Patient Registry, the highest tertile of PFOS exposure was associated with an increased level of testosterone (Toft et al. 2016).
- In a prospective cohort study conducted in Japan, maternal serum PFOS levels were not associated with cord blood testosterone in male or female infants (Itoh et al. 2016).
- In two prospective cohort studies conducted in Denmark, PFOS was measured in maternal serum, and hormones were measured in sons and daughters at approximately 20 years of age. Maternal PFOS concentration was not associated with testosterone levels in daughters or sons (Kristensen et al. 2013; Vested et al. 2013).

Studies using human cells in vitro

- In H295R cells (a human adrenal corticocarcinoma cell line), PFOS increased the levels of testosterone in two studies (Kraugerud et al. 2011; van den Dungen et al. 2015) and decreased the levels of testosterone in one study (Du et al. 2013).

Rodent studies in vivo

- PFOS administered via gavage significantly decreased serum testosterone levels in male C57 mice in one study (Qu et al. 2016) and in male SD rats in two studies (Li et al. 2018a; López-Doval et al. 2014).
- PFOS exposure to male SD rats *in utero* resulted in decreased testosterone production on GD 20.5 (Zhao et al. 2014) and when measured 1, 35, and 90 days after birth (Zhang et al. 2020).
- Serum and testicular testosterone levels were significantly decreased in male ICR mice exposed to 0, 0.5, 5, or 10 mg/kg-bw PFOS per day via gavage for four weeks (Qiu et al. 2021).

Rodent studies in vitro

- Primary mouse Leydig cells exposed to PFOS demonstrated significant decreases in the secretion of testosterone (Qiu et al. 2021).

Fish studies in vivo

- In zebrafish exposed to 250 µg/l PFOS for five months, testosterone levels were significantly elevated compared to controls in males but not females (Chen et al. 2016a).

Thyroid Hormones

The effect of PFOS on thyroid hormones has been discussed in detail in Section 5.4 of the PHG (OEHHA 2021). In the general human population, OEHHA did not find consistent trends across the different studies reviewed by US EPA (2016b) and studies published after this review. In pregnant women, US EPA (2016b) identified three studies that reported positive associations between PFOS and thyroid stimulating hormone (TSH). However, the four studies published since US EPA's review (US EPA 2016b) (or otherwise not included in that review) reported essentially opposite findings. In animals, the overall body of evidence from the literature, including studies summarized by (US EPA 2016b) and recent studies newly identified and reviewed in Section 5.4 of the PHG (OEHHA 2021), suggests that PFOS decreases thyroid hormone levels. Recent mechanistic studies suggest that PFOS may interact with thyroid hormone transporters and receptors in animals, which is similar to results reported in mechanistic studies with human thyroid hormone transporters and receptors (US EPA 2016b).

Summary of evidence for KC8

A number of animal studies have shown that PFOS alters the expression of genes that are regulated by ERα, PPARα, PPARγ, PXR, and CAR, and one reporter gene study shows PFOS activates murine PPARβ/δ *in vitro*. The evidence for the estrogenic effect of PFOS also comes from increased ER reporter activity in human cell lines, increased proliferation of estrogen-responsive human breast cancer cell lines in several studies, weak binding to ER in fish, and similar gene expression patterns between PFOS and E2 in fish. PFOS altered AR expression in rats, and one reporter gene study indicates PFOS inhibited AR activation by DHT. There is also evidence from animal studies that PFOS can decrease thyroid hormone levels and increase estradiol levels.

5.3.9 Causes immortalization

Carcinogens have been shown to increase the frequency of cell transformation from normal to malignant phenotypes and to extend telomere length, which are key elements that lead to immortalization (Smith et al. 2020). Information on PFOS and its salts identified through OEHHA's literature search relevant to this KC is summarized below.

PFOS showed significant increases of cell transformation frequency in Syrian hamster embryo (SHE) cells at 0.37 and 3.7 µM, but not at higher concentrations (Jacquet et al. 2012). Both 0.37 and 3.7 µM are considered non-cytotoxic (non-cytotoxic dose range: 0.000037-93 µM) by Jacquet et al. (2012) and are similar to the serum PFOS concentrations observed in PFOS-exposed workers.

Treatment with 10 µM PFOS for 72 hours stimulated the migration (transwell assay) and invasion (Matrigel assay) of the normal human breast epithelial cell line MCF-10A, indicating PFOS induced malignant transformation of these cells (Pierozan and Karlsson 2018). This study also reported that the same PFOS treatment significantly decreased protein levels of p21 and p53 in MCF-10A cells (Pierozan and Karlsson 2018). Both p53 and p21 are important regulators of senescence (Dodig et al. 2019; Mijit et al. 2020).

In studies in humans, associations between PFOS levels and telomere length from blood cells have been examined in mothers and newborns from a birth cohort in California (Eick et al. 2021), in newborns from Shanghai, China (Liu et al. 2018b), in an adult population in the US (Huang et al. 2019a), and in a Belgian population (50-65 years old) (Vriens et al. 2019). In the California study, PFOS was weakly associated with increased maternal blood telomere length, but was not associated with newborn telomere length (Eick et al. 2021). In an adult population from the US (NHANES participants from 1999-2000), serum PFOS was significantly associated with increased leukocyte telomere length (LTL) in females (but not males) and in the 40-50 age group of both females and males (Huang et al. 2019a). In contrast, inverse associations were reported between PFOS and LTL in female newborns in a Chinese birth cohort study (Liu et al. 2018b) and in older adults in a Belgian population (Vriens et al. 2019). A study in wild Arctic seabirds found a statistically significant correlation between total plasma concentrations of six PFASs, including PFOS, and elongated telomere length in four birds (23.5% of the birds studied) with relatively high levels of PFAS (Blévin et al. 2017). Interpretation of this study is limited by several aspects of study design, including small sample size, analysis focusing on the summed plasma concentrations of six PFASs instead of individual chemicals, and absence of adjustment for age as a confounding factor.

Summary of evidence for KC9

There are a few studies available on PFOS and its potential to cause immortalization. Inconsistent results have been reported for the association between serum PFOS levels and telomere lengths from human blood samples, with positive associations in females and the 40-50 year old age group in a US population, a weakly positive association with maternal telomere length in a California birth cohort, no association with newborn telomere length in the same California birth cohort, and inverse associations in female newborns from China and 50-65 year olds in a Belgian population. One study reported that PFOS increased the transformation frequency of SHE cells and another reported that PFOS induced malignant transformation of a normal human breast epithelial cell line.

5.3.10 Alters cell proliferation, cell death or nutrient supply

Examples of the types of effects indicative of KC10 include increased cell proliferation, decreased apoptosis, changes in growth factors, energetics and signaling pathways related to cellular replication or cell cycle control, and increased angiogenesis, as described by Smith et al. (2016).

This section summarizes data on the effects of PFOS on cell proliferation, apoptosis, growth factors, and signaling pathways related to cellular replication and cell cycle control observed in rats *in vivo* and various cell types *in vitro*.

PFOS (20 or 100 ppm in diet) increased cell proliferation and decreased apoptosis in the livers of Sprague Dawley rats. The effects were observed after 1, 7 and 28 days of exposure to 100 ppm and after 7 days of exposure to 20 ppm PFOS (Elcombe et al. 2012a). In a follow-up study in which Sprague Dawley rats were similarly fed PFOS in the diet for 7 days, a sustained decrease in apoptosis in the liver was observed 84 days after cessation of exposure (20 or 100 ppm) (Elcombe et al. 2012b). In Sprague Dawley rats treated with PFOS via gavage for 28 days, hepatocyte hypertrophy was observed; however, no hyperplasia in the liver or any other organ was observed (NTP 2019). PFOS also resulted in miRNA expression changes in the developing rat liver (Wang et al. 2015b). Pregnant Wistar rats were treated with 3.2 mg/kg PFOS in feed from gestational day 1 to PND 1 or 7. Livers from neonatal rats exposed to PFOS gestationally and via lactation for 1 or 7 days exhibited miRNA expression changes associated with cell cycle control, apoptosis, and cell proliferation. Specifically, the expression of miR-494, a suppressor of cellular proliferation and a modulator of apoptosis, was significantly lower than control on PND 1 and significantly higher on PND 7. The expression levels of miR-21, a down-regulator of tumor suppressor genes that affect cellular growth and proliferation, and miR-215, an inducer of cell cycle arrest, were both significantly higher than control on PND 1 with no difference from control on PND 7. A more detailed reviewed of the miRNA changes is discussed in KC4.

In a human fetal hepatic cell line (HL-7702), 50, 100, or 200 µM PFOS stimulated cell proliferation and altered expression of 27 proteins associated with cell proliferation, including hepatoma-derived growth factor, the proliferation biomarker Ki67, Cyclin D1, Cyclin E2, Cyclin A2, Cyclin B1, c-Myc, and p53 (Cui et al. 2015).

In human breast epithelial cells (MCF-10A), PFOS increased cell proliferation at concentrations of 1 or 10 µM after 72-hour treatment (Pierozan and Karlsson 2018). PFOS also induced MCF-10A cell-cycle progression at 10 µM with 24, 48, or 72-hour treatment (Pierozan and Karlsson 2018). The ER blocker “ICI 182, 780” partially blocked PFOS-induced cell proliferation, indicating stimulation of proliferation was at

least in part driven by ER activation (Pierozan and Karlsson 2018). Additionally, PFOS at 0.01 µg/ml (~0.025 µM) and 30 µg/ml (~75 µM) was shown to be estrogenic and to induce cell proliferation in the E-SCREEN assay in estrogen-sensitive human breast adenocarcinoma (MCF-7) cells (Henry and Fair 2013). In the presence of E2, PFOS significantly decreased cell proliferation in the E-SCREEN assay compared with E2 alone. However, PFOS (1 to 100 µM) did not affect MCF-7 cell proliferation in another E-SCREEN assay (Maras et al. 2006). PFOS increased cell proliferation in two human ovarian granulosa cell tumor cell lines, COV434 and KGN, after 72-hour treatment with PFOS concentrations as low as 0.08 ng/ml. Proliferation was inhibited by pretreatment of KGN cells with an insulin-like growth factor 1 receptor (IGF1R) antagonist, suggesting that PFOS acts through the IGF1R in KGN cells (Gogola et al. 2019).

WB-F344 cells, a rat liver epithelial cell line, were treated with PFOS at various concentrations (0 to 250 µM) for 20 minutes and analyzed for gap junctional intercellular communication (GJIC) (Upham et al. 1998). A significant dose-dependent inhibition in GJIC was observed at PFOS concentrations ≤ 75 µM within 5-10 minutes of exposure, and the authors stated that PFOS was not cytotoxic at concentrations up to 375 µM. Inhibition of GJIC can result in abnormal cell growth, such as a lack of contact inhibition (Trosko and Ruch 1998). In another study, primary salmon hepatocytes were treated with 2.1, 6.2, 15.1, or 25 mg/l PFOS for 24 or 48 hours and assayed for viability and apoptosis (Krøvel et al. 2008). A slight decrease in apoptosis was observed at the three highest doses. After 48 hours of exposure to 25 mg/l PFOS, the mRNA expression of the apoptotic marker caspase 3B was significantly down-regulated compared to the control group.

Summary of evidence for KC10

Two studies in rats provide evidence that PFOS increases cell proliferation or inhibits apoptosis in the liver, with the effect on apoptosis being long-lived. A third rat study reported early transcriptional changes related to cell cycle control, apoptosis, and proliferation in the liver of PND 1 and 7 rats exposed to PFOS *in utero* and via lactation. Multiple *in vitro* studies of human fetal liver, breast and ovarian cell lines showed an increase in cell proliferation with PFOS treatment. PFOS also altered the expression of proteins linked to cell proliferation, including increased levels of regulatory cell cycle proteins and growth factors in a human fetal liver cell line. One study reported that PFOS inhibits GJIC, which regulates cell growth and proliferation via contact inhibition, in a rat liver epithelial cell line. An *in vitro* study in primary salmon hepatocytes reported a significant decrease in caspase 3B, an important marker for apoptosis, with a slight decrease in apoptosis.

5.4 Comparison of PFOS and PFOA with a Focus on Data-Rich Endpoints

PFOS and perfluorooctanoic acid (PFOA) are two of the most studied PFASs. Both chemicals are fully fluorinated organic acids that consist of an eight-carbon chain ("C8"). PFOS has a sulfonic acid functional group attached to carbon number eight, while carbon eight of PFOA is a carboxylic acid (see Table 19). OEHHA compared data on the carcinogenicity of PFOS to PFOA using data summarized in OEHHA (2021) for PFOA. This section summarizes the tumor findings in rodent carcinogenicity studies, followed by comparisons of other effects that may be related to carcinogenicity for which there are ample data. Further details and discussion of these studies are available in OEHHA (2021) for PFOA, and Section 5.3 (Key characteristics of carcinogens) of this document for PFOS.

5.4.1 Carcinogenicity studies in rodents

PFOS and PFOA induced tumors in rats at several similar sites, as summarized in Table 19. Specifically, PFOA induced liver tumors (hepatocellular adenomas and/or carcinomas) and pancreatic tumors (acinar cell adenomas and/or carcinomas) in male and female rats (Biegel et al. 2001; NTP 2020). It also induced testicular tumors (Leydig cell adenomas) in male rats [(Biegel et al. 2001; Butenhoff et al. 2012b), data from Sibinsky (1987)] and mammary gland tumors (fibroadenomas) and uterine endometrial tumors (adenomas/adenocarcinomas) in female rats (Butenhoff et al. 2012b; NTP 2020).

Similar to PFOA, PFOS also induced liver tumors in male (hepatocellular adenoma) and female (adenoma and carcinoma combined) rats, pancreatic tumors (islet cell carcinomas) in male rats, and mammary gland tumors (fibroadenomas) in female rats (Butenhoff et al. 2012a; Thomford 2002). In addition, PFOS induced thyroid tumors in male (follicular cell adenomas) and female (rare follicular cell adenomas and one rare carcinoma) rats (Butenhoff et al. 2012a; Thomford 2002).

PFOA was also tested in one study in mice. It induced hepatocellular adenomas and hepatic hemangiosarcomas in female mice exposed prenatally (the liver was the only organ examined) (Filgo et al. 2015). The carcinogenicity of PFOS has not been studied in mice.

Table 19 Structures and comparison of treatment-related tumors induced by PFOS and PFOA in rat cancer bioassays

Chemical	PFOS	PFOA
Structure	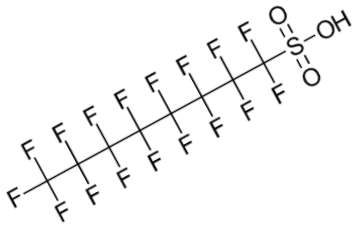	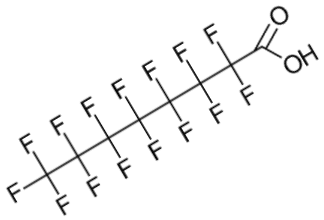
Thyroid follicular cell adenoma and/or carcinoma	**M**, **F**	Not Observed
Liver hepatocellular adenoma and/or carcinoma	**M**[a], **F**	**M**, **F**
Pancreatic tumors	**M**[b]	**M**[c], **F**[c]
Testicular Leydig cell adenoma	Not Observed	**M**
Mammary gland fibroadenoma	**F**	**F**
Uterine adenoma and/or adenocarcinoma	Not Observed	**F**

M, tumors observed in male rats; F, tumors observed in female rats

[a] Only adenomas were observed in male rats

[b] Pancreatic islet cell carcinoma in males; no increase of pancreatic tumors in females

[c] Pancreatic acinar cell adenoma and/or carcinoma

5.4.2 Genotoxic effects

PFOS and PFOA have been tested in many genotoxicity test systems that have assessed numerous endpoints indicative of mutagenicity, chromosomal effects, or DNA damage. Several studies provide evidence that PFOA is not mutagenic, some studies provide evidence that PFOA may have chromosomal effects, while others do not, and several studies provide evidence that PFOA causes DNA damage – measured as increases in DNA strand breaks (in human cell lines and in non-mammalian species), γ-H2AX (a marker for DNA damage, measured in a human cell line), and 8-hydroxydeoxyguanosine (8-OHdG, a marker of oxidative DNA damage, in human cell lines and in rodent liver) (OEHHA 2021). Regarding PFOS, some studies provide

evidence of mutagenicity (in transgenic mice and fish and in transgenic mouse cells *in vitro*), several studies provide evidence of chromosomal effects (*e.g.*, induction of micronuclei (MN) in rodents and zebrafish), and several studies provide evidence of DNA damage (*e.g.*, induction of DNA strand breaks in rats, zebrafish, and other non-mammalian species) (see Section 5.3.2, Is genotoxic).

5.4.3 Effects related to oxidative stress and carcinogenesis

As reviewed in OEHHA (2021), two studies in rodents and two studies in human cells have shown that PFOA exposure increased 8-OHdG, while one study in human cells reported mixed results and two studies (one in exposed humans and one in a unicellular organism) found no effect. Several studies, including one in mice, four in human HepG2 cells, and one in a mouse cell line, have shown that PFOA increased intracellular production of ROS, while a study in human-hamster hybrid cells showed increased intracellular production of both ROS and RNS. Increased lipid peroxidation was observed in mice, in human erythrocytes exposed *in vitro*, and in a rat cell line. PFOA also has been shown to alter total antioxidant capacity, antioxidant enzyme content or activity, and glutathione levels in mice, fish, and in *in vitro* studies of human erythrocytes and human HepG2 cells.

Similar to PFOA, studies of oxidative stress responses in humans, rodents, zebrafish and plants indicate that PFOS can induce oxidative DNA damage, generation of ROS or RNS, and lipid peroxidation (see Section 5.3.5, Induces oxidative stress). Notably, in human observational studies, significant dose-dependent increases of oxidative DNA damage (8-OHdG), lipid peroxidation (MDA), and ROS were associated with higher serum PFOS levels. Significant increases of ROS/RNS and lipid peroxidation were reported in multiple experimental test systems, with several studies showing dose-dependent responses. Significant decreases in T-AOC were reported in one rodent study *in vivo*, but no change was reported in one human observational study and in one zebrafish study. Following PFOS exposure, in multiple experimental systems, changes occurred in antioxidant enzyme activities/levels and glutathione status (*e.g.*, GSH, GSSG, GSH/GSSG ratio, GST, GR, and GPx). Changes in the protein or gene expression of Nrf2 have also been observed, with one mouse study reporting reduced levels of Nrf2 protein following PFOS exposure, and two studies in zebrafish reporting increases in Nrf2 gene or protein expression during the uptake phase but decreased expression during the depuration phase. Genomic and metabolomic studies also provide some evidence for the induction of oxidative stress by PFOS.

5.4.4 Immunosuppressive effects related to carcinogenesis

Several animal studies have shown that PFOA suppresses IgM production as either a T cell dependent antibody response (TDAR) or T cell independent antibody response (TIAR), reduces cellularity and proliferation of T cells and B cells, and reduces the number of neutrophils (OEHHA 2021). PFOS has also been shown to suppress TDAR/TIAR IgM production and reduce cellularity and proliferation of T cells and B cells in animal studies. In addition, PFOS has been shown to suppress NK cell activity in cultured human blood cells and in four studies in mice, although two other mouse studies reported an increase in NK cell activity (see Section 5.3.7, Is immunosuppressive). Thus, both PFOA and PFOS can suppress the immune system in ways that would allow neoplastic cells to escape immune surveillance, survive, and replicate to form tumors.

5.4.5 Receptor-mediated effects related to carcinogenesis

Several animal studies have shown that PFOA alters gene expression in the liver, and that these effects are mediated through estrogen receptor alpha (ERα), peroxisome proliferator-activated receptor alpha and gamma (PPARα and PPARγ), pregnane X receptor (PXR), and constitutive active/androstane receptor (CAR). Evidence that PFOA can bind to or activate ERα, PPARα, and possibly PPARβ/δ comes from *in silico* modeling studies (human ERα), studies in human cells or cell lines (ERα, PPARα), and studies in animal tissue preparations or cell lines (ERα, PPARβ/δ) (OEHHA 2021). PFOS has also been shown to alter expression of genes that are regulated by ERα, PPARα, PPARγ, PXR, and CAR. Evidence for the estrogenic effect of PFOS comes from increased ER reporter activity in human cells *in vitro*, increased proliferation of estrogen-responsive human breast cancer cell lines in several studies, weak binding to ER in fish, and similar gene expression patterns between PFOS and E2 in fish. Reporter gene studies indicate that PFOS can also activate murine PPARβ/δ *in vitro* and inhibit AR activation by dihydrotestosterone (DHT) (see Section 5.3.8, Modulates receptor-mediated effects).

There is also evidence from studies in animals that both PFOS and PFOA can modulate levels of endogenous hormones, including estradiol, testosterone, and thyroid hormones.

6. SUMMARY OF EVIDENCE

6.1 Epidemiological Studies

6.1.1 Breast cancer

In summary, the results were inconsistent in the published studies on PFOS exposure and breast cancer. Five publications collected data on PFOS exposure prior to breast cancer diagnosis (Alexander et al. 2003; Bonefeld-Jørgensen et al. 2014; Cohn et al. 2020; Ghisari et al. 2017; Mancini et al. 2020) and five measured PFOS levels at or after breast cancer diagnosis (Bonefeld-Jørgensen et al. 2011; Ghisari et al. 2014; Hurley et al. 2018b; Wielsøe et al. 2017; Wielsøe et al. 2018). In the latter publications, reverse causation bias cannot be fully ruled out due to the fact that PFOS internal levels could have been affected by the onset and/or treatment of breast cancer.

Studies in which PFOS levels were measured before breast cancer diagnosis showed mixed results. The only occupational cohort study (Alexander et al. 2003) reported high serum PFOS levels, and elevated breast cancer mortality, based on 2 breast cancer deaths in unexposed workers. Interpretation of this study was limited by the small number of breast cancer deaths, the potential for selection bias (healthy worker effect) and the lack of data on potential confounders or breast cancer risk factors other than age. PFOS level was generally not associated with breast cancer risk in the Danish National Birth Cohort (DNBC) (Bonefeld-Jørgensen et al. 2014; Ghisari et al. 2017), although there were some non-significant increases in the second and third quintiles of PFOS exposure, in those >40 years of age at diagnosis, and in those with polymorphisms in genes involved in steroid hormone and xenobiotic metabolism, notably the CYP19A1 (rs10046) homozygous wild type CC genotype. These results require replication in further studies and in different populations. In a case-control study of breast cancer nested in a large cohort of French women, there were several ORs for PFOS exposure above 1.0 and statistically significant, particularly in those exposed to PFOS at higher levels and with hormone receptor positive tumors (Mancini et al. 2020). Although there was no clear dose-response trend overall, the trends were more consistent in hormone receptor positive tumors. The only study to assess maternal perinatal serum PFOS levels on daughter's risk of breast cancer – in California – found no association (Cohn et al. 2020); however, the risk estimate for the main effects analysis was not reported and the study included only women younger than 52 years of age, which does not capture breast cancers that could be diagnosed in older women. Although exposures to PFASs may have been correlated with one another, the studies presented analyses for PFOS or other PFASs alone, without adjustment for other co-

occurring PFASs in the statistical models. Therefore, potential confounding by other PFASs could not be ruled out.

There were also mixed results in the five publications where PFOS was collected after breast cancer diagnosis: the four studies (Bonefeld-Jørgensen et al. 2011; Ghisari et al. 2014; Wielsøe et al. 2017; Wielsøe et al. 2018) that were conducted within Greenland Inuits showed some positive associations while a study (Hurley et al. 2018b) conducted within a cohort of teachers in California reported null or inverse associations. Among Greenland Inuits, there were some positive interactions reported between PFOS exposure and polymorphisms in genes with known involvement in steroid hormone and xenobiotic metabolism.

In the studies that investigated gene-environment interactions, the CYP19A1 (rs10046) homozygous wild type CC genotype was associated with increased breast cancer risk in Danish (Ghisari et al. 2017) and Greenland Inuit populations (Ghisari et al. 2014; Wielsøe et al. 2018). These results need replication in independent populations.

The studies from France (Mancini et al. 2020) and California (Hurley et al. 2018b) both stratified by hormone receptor status, but found inconsistent results.

The inconsistencies across these studies may reflect differences in the levels of PFOS exposure and genetic susceptibilities in these study populations. The PFOS exposure levels in the DNBC were less than half of those reported in Greenland Inuits; therefore, exposures in the Danish population may have been too low to detect an effect. However, the Inuit population was highly exposed to PFOS and a number of other POPs (*e.g.*, PCBs, OC pesticides), making it difficult to disentangle the effect of individual compounds. Exposure assessment methods also varied across studies – the studies from California (Hurley et al. 2018b) and Greenland (Bonefeld-Jørgensen et al. 2011) assessed serum PFOS concentrations measured in blood collected after diagnosis. The possibility of positive findings due to chance, publication bias, or reverse causation could not be ruled out.

6.1.2 Cancers at other sites

The data from epidemiology studies were too sparse to draw conclusions for a number of other cancer sites: pediatric germ cell tumors, prostate, urinary bladder, liver, pancreas, malignant melanoma, lymphohematopoietic system, urinary tract, respiratory tract, and gastrointestinal tract.

6.2 Animal Studies

Long-term dietary carcinogenicity studies of K^+PFOS have been conducted in male and female Sprague Dawley (Crl:CD(SD)IGS BR) rats. Significant tumor findings are as follows:

6.2.1 Liver tumors

- In PFOS-treated male rats, the incidence of hepatocellular adenoma was significantly increased in the high-dose (20 ppm) group by pairwise comparison with controls, with a significant dose-related trend.
- In PFOS-treated female rats, the incidences of hepatocellular adenoma and adenoma or carcinoma combined were significantly increased in the high-dose (20 ppm) group by pairwise comparison with controls, with significant dose-related trends. One rare hepatocellular carcinoma was observed in the 20 ppm group.

6.2.2 Pancreatic tumors

- In PFOS-treated male rats, the incidence of islet cell carcinoma was significantly increased with a statistically significant dose-related trend.

6.2.3 Thyroid tumors

- In PFOS-treated male rats, the incidence of thyroid gland follicular cell adenoma was significantly increased by pairwise comparison with controls in the “20 ppm recovery” group, that is, exposure for 12 months followed by 12 months on the basal diet.
- In PFOS-treated female rats, two rare thyroid gland follicular cell adenomas and one rare follicular cell carcinoma were observed in the 5 ppm group, and one rare follicular cell adenoma was observed in the 20 ppm group. Additionally, one rare follicular cell adenoma was observed in the “20 ppm recovery” group.

6.2.4 Mammary tumors

- In PFOS-treated female rats, the incidence of mammary fibroadenoma was significantly increased in the low-dose (0.5 ppm) group by pairwise comparison with controls.

In a six-month tumor promotion study in rainbow trout, the percentage of fish bearing liver adenomas and carcinomas combined were significantly higher in the group initiated with AFB_1 and promoted with PFOS, compared to fish receiving AFB_1 initiation alone.

6.3 Mechanistic Studies

6.3.1 Pharmacokinetics

Review of pharmacokinetic data shows interspecies similarities in the absorption and distribution of PFOS, and some interspecies differences in the excretion and serum half-life. PFOS is not known to be metabolized in animals or humans. PFOS is well absorbed with oral administration in animals, and is widely distributed throughout the body in both humans and animals. PFOS half-life is significantly longer in humans (3.4 years) versus rodents (24-83 days) and monkeys (110-200 days). The highest PFOS levels are generally detected in the liver, plasma, and kidney in both humans and animals. PFOS can cross the blood-brain barrier and the placenta, and PFOS and several precursors have been detected in breastmilk or paired maternal and cord serum samples taken after delivery. PFOS excretion pathways in humans include urinary and fecal excretion and incorporation into nails and hair, although overall the elimination rate of PFOS is slow. Additional PFOS elimination routes include pregnancy-related losses, elimination via breast milk, and menstrual blood loss in females. Several precursors (*e.g.*, PFOSA) have been shown to form PFOS via biotransformation in *in vivo* or *in vitro* studies. Isomeric differences in transformation rates and/or elimination half-lives were observed in some PFOS and PFOS precursor studies.

6.3.2 Key characteristics of carcinogens

The 10 key characteristics (KCs) of carcinogens were used to organize the data relevant to carcinogenicity from mechanistic studies of PFOS and its salts. KCs are characteristics of agents that cause cancer, and can encompass many types of mechanistic endpoints. OEHHA uses this approach to systematically identify, organize, and summarize information on mechanisms of carcinogenesis. Most of the evidence relates to 7 of the 10 KCs and is summarized here.

Is genotoxic

Overall, there is some evidence of mutagenicity and suggestive evidence of chromosomal effects and DNA damage induced by PFOS.

- PFOS is not mutagenic in bacterial assays conducted in multiple strains of *S. typhimurium* and *E. coli*
- PFOS induced mutations in the livers of *gpt* delta transgenic mice and transgenic fish at the c*II* gene locus *in vivo* after long-term exposure, and at the *redBA/gam* locus in *gpt* delta transgenic mouse embryonic fibroblast cells *in vitro*
- PFOS showed the following effects on micronuclei (MN) formation
    - Did not increase MN in human hepatoma HepG2 cells

    - Increased MN in a number of *in vivo* studies in rats, including tests in bone marrow and peripheral blood polychromatic erythrocytes in rats by several studies, and hepatocytes in rats in one study
    - Did not increase MN in one study in male SD rat polychromatic erythrocytes (NTP 2019)
    - Increased MN in hepatocytes of treated transgenic mice (albeit not statistically significant)
    - Did not increase of MN in bone marrow from treated mice
    - Increased MN in one study in peripheral blood cells of zebrafish
    - Increased MN in mussels and onion
- PFOS had the following effects on chromosomal aberrations (CA)
    - Had no effect on CA in human peripheral blood lymphocytes exposed *in vitro*
    - Increased CA in onion
- PFOS had the following effects on DNA damage, measured as increases in DNA strand breaks, γ-H2AX, foci of Hus-1, and the oxidative DNA damage marker 8-OHdG
    - DNA strand breaks
        - Increased DNA strand breaks in one of three studies conducted in human hepatoma HepG2 cells *in vitro*
        - Did not increase DNA strand breaks in sperm cells obtained from human volunteers treated with PFOS *in vitro*
        - Increased DNA strand breaks (Comet assay) in bone marrow, peripheral blood cells, and hepatocytes of treated rats
        - Did not increase DNA strand breaks in Syrian hamster embryo cells *in vitro*
        - Increased DNA strand breaks in primary mouse Leydig cells
        - Increased DNA strand breaks (Comet assay) in peripheral blood cells of zebrafish and carp, in green mussels, flatworms, water flea, earthworms, and onion, but not in gull eggs or *Paramecium caudatum*
    - Increased γ-H2AX in transgenic mouse embryonic fibroblasts *in vitro*
    - Increased the number of foci of the DNA damage checkpoint protein Hus-1 in germ cells of *C. elegans*
    - Did not increase unscheduled DNA synthesis (UDS) in rat primary liver cell cultures
    - Serum level of PFOS was associated with the level of 8-OHdG in human urine samples in two out of three studies

Induces epigenetic alterations

Overall, these studies show that PFOS can induce epigenetic changes, including altered methylation of regions associated with specific genes, global methylation changes, miRNA changes, and alterations in expression of DNA methyltransferases

(DNMTs). Many of these effects have been correlated with processes involved in the development of cancer. Associations with altered gene expression, altered phenotype, and cancer, however, are not always clear.

Induces oxidative stress

Studies of oxidative stress responses in humans, rodents, zebrafish and plants indicate that PFOS can induce oxidative DNA damage, generation of ROS or RNS, and lipid peroxidation. Notably, in human observational studies, significant dose-dependent increases of oxidative DNA damage (8-OHdG) (in two of three studies), lipid peroxidation (MDA), and ROS were associated with higher serum PFOS levels. Significant increases of ROS/RNS and lipid peroxidation were reported in multiple experimental test systems, with several studies showing dose-dependent responses. Significant decreases in total antioxidant capacity (T-AOC) were reported in one rodent study *in vivo*, but no change was reported in one human observational study and in one zebrafish study. Following PFOS exposure, in multiple experimental systems, changes occurred in antioxidant enzyme activities/levels and glutathione status [*e.g.*, reduced glutathione (GSH), glutathione disulfide (GSSG), GSH/GSSG ratio, glutathione-S-transferase (GST), glutathione reductase (GR), and glutathione peroxidase (GPx)). Changes in the protein or gene expression of nuclear factor erythroid 2–related factor 2 (Nrf2, a regulator of cellular resistance to oxidative stress) have also been observed, with one mouse study reporting reduced levels of Nrf2 protein following PFOS exposure, and two studies in zebrafish reporting increases in Nrf2 gene or protein expression during the uptake phase but decreased expression during the depuration phase. Evidence from genomic and metabolomic studies also provide some evidence for the induction of oxidative stress by PFOS.

Induces chronic inflammation

The effects of PFOS on pro-inflammatory cytokine production have been tested in multiple human cell types *in vitro*, including peripheral blood leukocytes, lymphocytes, primary CD4+ T cells, colon myofibroblasts, bronchial epithelial cells, THP-1 cells, Jurkat T cells, and neuronal cells. Interleukin-1 (IL-1) production has been shown to be increased with PFOS treatment in two studies using human bronchial epithelial cells and lymphocytes. IL-10 and interferon gamma (IFN-γ) levels were both decreased in two studies conducted by the same research group using human peripheral blood leukocytes. Two studies reported a decrease in tumor necrosis factor alpha (TNF-α) secretion and mRNA expression in human blood cells. The effect of PFOS on IL-2, IL-4, IL-6, and IL-8 production remains unclear, as different results have been observed from different studies. A single study has reported a decrease of C-X-C motif chemokine ligand 10 (CXCL-10) production.

Studies in animals were conducted in different strains of mice, and in SD rats, zebrafish, and chicken embryo fibroblasts. Increases of IL-1 production have been observed in mice, rats and zebrafish. Two studies in mice reported a decrease in the number of splenocytes secreting IL-2. The effect of PFOS on IL-4, IL-5, IL-6, IL-10, TNF-α and IFN-γ production remains unclear, as different results have been observed from different studies. Single studies have reported no change of IL-5 production by mouse splenic T cells, a decrease of IL-8 mRNA in chicken embryo fibroblasts, and an increase of IL-15 and transforming growth factor beta (TGF-β) mRNA in zebrafish liver.

Is immunosuppressive

PFOS suppressed immunoglobulin M (IgM) responses in four mouse studies following an antigen challenge; one additional study observed a decrease without antigen challenge. Two studies in mice reported no change in IgM response (one with and one without antigen challenge), and one study in rats reported an increase in IgM response (without antigen challenge). PFOS has also been shown to reduce the number and proliferation of thymocytes and splenocytes in mice in multiple studies. Two additional studies reported no change (one mouse, one rat study); a third study reported an increase in proliferation of dolphin CD4+ and CD8+ T-lymphocytes exposed *in vitro*.

Several studies have shown that PFOS suppresses natural killer (NK) cell activity, including one study in cultured human blood cells and four studies in mice, although two other mouse studies reported an increase in NK cell activity.

Taken together, these studies suggest that PFOS can suppress the immune system in ways that would allow neoplastic cells to escape immune surveillance, survive, and replicate to form tumors.

Modulates receptor-mediated effects

A number of animal studies have shown that PFOS alters the expression of genes that are regulated by estrogen receptor alpha (ERα), peroxisome proliferator activated receptor alpha (PPARα), PPARγ, pregnane X receptor (PXR), and constitutive androstane receptor (CAR), and one reporter gene study shows PFOS activates murine PPARβ/δ *in vitro*. The evidence for the estrogenic effect of PFOS also comes from increased ER reporter activity in human cell lines, increased proliferation of estrogen-responsive human breast cancer cell lines in several studies, weak binding to ER in fish, and similar gene expression patterns between PFOS and estradiol (E2) in fish. PFOS altered AR expression in rats, and one reporter gene study indicates PFOS inhibited AR activation by dihydrotestosterone (DHT). There is also evidence from animal studies that PFOS can decrease thyroid hormone levels and increase estradiol levels.

Alters cell proliferation, cell death or nutrient supply

Two studies in rats provide evidence that PFOS increases cell proliferation or inhibits apoptosis in the liver, with the effect on apoptosis being long-lived. A third rat study reported early transcriptional changes related to cell cycle control, apoptosis, and proliferation in the liver of postnatal day (PND) 1 and 7 rats exposed to PFOS *in utero* and via lactation. Multiple *in vitro* studies of human fetal liver, breast and ovarian cell lines showed an increase in cell proliferation with PFOS treatment. PFOS also altered the expression of proteins linked to cell proliferation, including increased levels of regulatory cell cycle proteins and growth factors in a human fetal liver cell line. One study reported that PFOS inhibits gap junctional intercellular communications (GJICs), which regulates cell growth and proliferation via contact inhibition, in a rat liver epithelial cell line. An *in vitro* study in primary salmon hepatocytes reported a significant decrease in caspase 3B, an important marker for apoptosis, with a slight decrease in apoptosis.

6.4 Comparison of PFOS and PFOA with a Focus on Data-Rich Endpoints

A comparison of carcinogenicity studies in rodents and several other data-rich endpoints was made between PFOS and PFOA, two of the most studied PFASs. Data from carcinogenicity studies in rats show that both chemicals induced liver tumors in male and female rats, pancreatic tumors in male rats, and mammary gland fibroadenomas in female rats. With regard to KCs, there is evidence of genotoxicity for both chemicals (*e.g.*, both cause chromosomal effects and DNA damage), with the evidence of mutagenicity being stronger for PFOS than PFOA, and both chemicals have shown activities related to oxidative stress, immunosuppressive effects, and receptor-mediated effects related to carcinogenesis.

7. REFERENCES

ACS. 2021. Breast Cancer. Available: https://www.cancer.org/cancer/breast-cancer.html.

Aggarwal BB. 2003. Signalling pathways of the TNF superfamily: a double-edged sword. Nature reviews immunology 3:745-756.

Aggarwal BB, Shishodia S, Sandur SK, Pandey MK, Sethi G. 2006. Inflammation and cancer: how hot is the link? Biochemical pharmacology 72:1605-1621.

Ai W, Li H, Song N, Li L, Chen H. 2013. Optimal method to stimulate cytokine production and its use in immunotoxicity assessment. International journal of environmental research and public health 10:3834-3842.

Alexander BH, Olsen GW, Burris JM, Mandel JH, Mandel JS. 2003. Mortality of employees of a perfluorooctanesulphonyl fluoride manufacturing facility. Occupational and environmental medicine 60:722-729.

Alexander BH, Olsen GW. 2007. Bladder cancer in perfluorooctanesulfonyl fluoride manufacturing workers. Annals of epidemiology 17:471-478.

Armartmuntree N, Murata M, Techasen A, Yongvanit P, Loilome W, Namwat N, et al. 2018. Prolonged oxidative stress down-regulates Early B cell factor 1 with inhibition of its tumor suppressive function against cholangiocarcinoma genesis. Redox Biol 14:637-644.

Arsenault G, Chittim B, Gu J, McAlees A, McCrindle R, Robertson V. 2008. Separation and fluorine nuclear magnetic resonance spectroscopic (19F NMR) analysis of individual branched isomers present in technical perfluorooctanesulfonic acid (PFOS). Chemosphere 73:S53-59.

Arukwe A, Mortensen AS. 2011. Lipid peroxidation and oxidative stress responses of salmon fed a diet containing perfluorooctane sulfonic- or perfluorooctane carboxylic acids. Comparative biochemistry and physiology Toxicology & pharmacology : CBP 154:288-295.

ATSDR. 2021. Toxicological Profile for Perfluoroalkyls. Atlanta, GA. Available: https://www.atsdr.cdc.gov/ToxProfiles/tp200.pdf [accessed on May 5 2021].

Auer K, Bachmayr-Heyda A, Aust S, Sukhbaatar N, Reiner AT, Grimm C, et al. 2015. Peritoneal tumor spread in serous ovarian cancer-epithelial mesenchymal status and outcome. Oncotarget 6:17261-17275.

Aure MR, Fleischer T, Bjørklund S, Ankill J, Castro-Mondragon JA, Børresen-Dale AL, et al. 2021. Crosstalk between microRNA expression and DNA methylation drives the hormone-dependent phenotype of breast cancer. Genome medicine 13:72.

Austin ME, Kasturi BS, Barber M, Kannan K, MohanKumar PS, MohanKumar SM. 2003. Neuroendocrine effects of perfluorooctane sulfonate in rats. Environmental health perspectives 111:1485-1489.

Bach CC, Liew Z, Bech BH, Nohr EA, Fei C, Bonefeld-Jorgensen EC, et al. 2015. Perfluoroalkyl acids and time to pregnancy revisited: An update from the Danish National Birth Cohort. Environmental health : a global access science source 14:59.

Baldrick P. 2005. Carcinogenicity evaluation: comparison of tumor data from dual control groups in the Sprague–Dawley rat. Toxicologic pathology 33:283-291.

Bannasch P, Zerban H. 1990. Pathology of tumours in laboratory animals. Tumours of the liver in rat. IARC scientific publications I:199-240.

Barrett ES, Chen C, Thurston SW, Haug LS, Sabaredzovic A, Fjeldheim FN, et al. 2015. Perfluoroalkyl substances and ovarian hormone concentrations in naturally cycling women. Fertil Steril 103:1261-1270.e1263.

Bastos Sales L, Kamstra JH, Cenijn PH, van Rijt LS, Hamers T, Legler J. 2013. Effects of endocrine disrupting chemicals on in vitro global DNA methylation and adipocyte differentiation. Toxicology in vitro : an international journal published in association with BIBRA 27:1634-1643.

Beesoon S, Genuis SJ, Benskin JP, Martin JW. 2012. Exceptionally high serum concentrations of perfluorohexanesulfonate in a Canadian family are linked to home carpet treatment applications. Environmental science & technology 46:12960-12967.

Beesoon S, Martin JW. 2015. Isomer-specific binding affinity of perfluorooctanesulfonate (PFOS) and perfluorooctanoate (PFOA) to serum proteins. Environmental Science and Technology 49:5722-5731.

Behr AC, Lichtenstein D, Braeuning A, Lampen A, Buhrke T. 2018. Perfluoroalkylated substances (PFAS) affect neither estrogen and androgen receptor activity nor steroidogenesis in human cells in vitro. Toxicology letters 291:51-60.

Behr AC, Plinsch C, Braeuning A, Buhrke T. 2020. Activation of human nuclear receptors by perfluoroalkylated substances (PFAS). Toxicology in vitro : an international journal published in association with BIBRA 62:104700.

Benninghoff AD, Bisson WH, Koch DC, Ehresman DJ, Kolluri SK, Williams DE. 2011. Estrogen-like activity of perfluoroalkyl acids in vivo and interaction with human and rainbow trout estrogen receptors in vitro. Toxicological sciences : an official journal of the Society of Toxicology 120:42-58.

Benninghoff AD, Orner GA, Buchner CH, Hendricks JD, Duffy AM, Williams DE. 2012. Promotion of hepatocarcinogenesis by perfluoroalkyl acids in rainbow trout. Toxicological sciences : an official journal of the Society of Toxicology 125:69-78.

Benskin JP, De Silva AO, Martin LJ, Arsenault G, McCrindle R, Riddell N, et al. 2009a. Disposition of perfluorinated acid isomers in Sprague-Dawley rats; part 1: single dose. Environmental toxicology and chemistry 28:542-554.

Benskin JP, Holt A, Martin JW. 2009b. Isomer-specific biotransformation rates of a perfluorooctane sulfonate (PFOS)-precursor by cytochrome P450 isozymes and human liver microsomes. Environmental science & technology 43:8566-8572.

Benskin JP, De Silva AO, Martin JW. 2010. Isomer profiling of perfluorinated substances as a tool for source tracking: a review of early findings and future applications. Reviews of environmental contamination and toxicology 208:111-160.

Benskin JP, Ikonomou MG, Gobas FA, Begley TH, Woudneh MB, Cosgrove JR. 2013. Biodegradation of N-ethyl perfluorooctane sulfonamido ethanol (EtFOSE) and EtFOSE-based phosphate diester (SAmPAP diester) in marine sediments. Environmental science & technology 47:1381-1389.

Berntsen HF, Bjørklund CG, Audinot JN, Hofer T, Verhaegen S, Lentzen E, et al. 2017. Time-dependent effects of perfluorinated compounds on viability in cerebellar granule neurons: Dependence on carbon chain length and functional group attached. Neurotoxicology 63:70-83.

Biegel LB, Hurtt ME, Frame SR, O'Connor JC, Cook JC. 2001. Mechanisms of extrahepatic tumor induction by peroxisome proliferators in male CD rats. Toxicological sciences : an official journal of the Society of Toxicology 60:44-55.

Bilbao E, Raingeard D, de Cerio OD, Ortiz-Zarragoitia M, Ruiz P, Izagirre U, et al. 2010. Effects of exposure to Prestige-like heavy fuel oil and to perfluorooctane sulfonate on conventional biomarkers and target gene transcription in the thicklip grey mullet Chelon labrosus. Aquatic toxicology (Amsterdam, Netherlands) 98:282-296.

Bjork JA, Lau C, Chang SC, Butenhoff JL, Wallace KB. 2008. Perfluorooctane sulfonate-induced changes in fetal rat liver gene expression. Toxicology 251:8-20.

Bjork JA, Wallace KB. 2009. Structure-activity relationships and human relevance for perfluoroalkyl acid-induced transcriptional activation of peroxisome proliferation in liver cell cultures. Toxicological sciences : an official journal of the Society of Toxicology 111:89-99.

Bjork JA, Butenhoff JL, Wallace KB. 2011. Multiplicity of nuclear receptor activation by PFOA and PFOS in primary human and rodent hepatocytes. Toxicology 288:8-17.

Blanc M, Rüegg J, Scherbak N, Keiter SH. 2019. Environmental chemicals differentially affect epigenetic-related mechanisms in the zebrafish liver (ZF-L) cell line and in zebrafish embryos. Aquatic toxicology (Amsterdam, Netherlands) 215:105272.

Blévin P, Angelier F, Tartu S, Bustamante P, Herzke D, Moe B, et al. 2017. Perfluorinated substances and telomeres in an Arctic seabird: Cross-sectional and longitudinal approaches. Environmental Pollution 230:360-367.

Bonefeld-Jørgensen EC, Long M, Bossi R, Ayotte P, Asmund G, Krüger T, et al. 2011. Perfluorinated compounds are related to breast cancer risk in Greenlandic Inuit: A case control study. Environmental Health: A Global Access Science Source 10.

Bonefeld-Jørgensen EC, Long M, Fredslund SO, Bossi R, Olsen J. 2014. Breast cancer risk after exposure to perfluorinated compounds in Danish women: a case–control study nested in the Danish National Birth Cohort. Cancer Causes and Control 25:1439-1448.

Botts S, Jokinen M, Isaacs K, Meuten D, Tanaka N. 1991. Proliferative lesions of the thyroid and parathyroid glands. Guides for Toxicologic Pathology:1-12.

Brieger A, Bienefeld N, Hasan R, Goerlich R, Haase H. 2011. Impact of perfluorooctanesulfonate and perfluorooctanoic acid on human peripheral leukocytes. Toxicology in vitro : an international journal published in association with BIBRA 25:960-968.

Brochot C, Casas M, Manzano-Salgado C, Zeman FA, Schettgen T, Vrijheid M, et al. 2019. Prediction of maternal and foetal exposures to perfluoroalkyl compounds in a Spanish birth cohort using toxicokinetic modelling. Toxicology and applied pharmacology 379:114640.

Brooke D, Footitt A, Nwaogu TA. 2004. Environmental Risk Evaluation Report: Perfluorooctanesulphonate (PFOS). Environment Agency, UK. Available: https://www.gov.uk/government/uploads/system/uploads/attachment_data/file/290857/scho1009brbl-e-e.pdf.

Buck RC, Franklin J, Berger U, Conder JM, Cousins IT, de Voogt P, et al. 2011. Perfluoroalkyl and polyfluoroalkyl substances in the environment: terminology, classification, and origins. Integrated environmental assessment and management 7:513-541.

Buhrke T, Kibellus A, Lampen A. 2013. In vitro toxicological characterization of perfluorinated carboxylic acids with different carbon chain lengths. Toxicology letters 218:97-104.

Butenhoff JL, Chang SC, Olsen GW, Thomford PJ. 2012a. Chronic dietary toxicity and carcinogenicity study with potassium perfluorooctanesulfonate in Sprague Dawley rats. Toxicology 293:1-15.

Butenhoff JL, Kennedy Jr GL, Chang SC, Olsen GW. 2012b. Chronic dietary toxicity and carcinogenicity study with ammonium perfluorooctanoate in Sprague-Dawley rats. Toxicology 298:1-13.

Butenhoff JL, Olsen GW, Chang S. 2017. Toxicological response of Sprague Dawley rats from inhalation exposure to perfluorooctane sulfonyl fluoride (POSF). Toxicology letters 271:38-49.

Cai X, Cao C, Li J, Chen F, Zhang S, Liu B, et al. 2017. Inflammatory factor TNF-α promotes the growth of breast cancer via the positive feedback loop of TNFR1/NF-κB (and/or p38)/p-STAT3/HBXIP/TNFR1. Oncotarget 8:58338.

Calafat AM, Kato K, Hubbard K, Jia T, Botelho JC, Wong LY. 2019. Legacy and alternative per- and polyfluoroalkyl substances in the U.S. general population: Paired serum-urine data from the 2013–2014 National Health and Nutrition Examination Survey. Environment international 131.

Caserta D, Ciardo F, Bordi G, Guerranti C, Fanello E, Perra G, et al. 2013. Correlation of endocrine disrupting chemicals serum levels and white blood cells gene expression of nuclear receptors in a population of infertile women. International journal of endocrinology 2013:510703.

Castaño-Ortiz JM, Jaspers VLB, Waugh CA. 2019. PFOS mediates immunomodulation in an avian cell line that can be mitigated via a virus infection. BMC veterinary research 15:214.

Castro F, Cardoso AP, Gonçalves RM, Serre K, Oliveira MJ. 2018. Interferon-gamma at the crossroads of tumor immune surveillance or evasion. Frontiers in immunology 9:847.

CDC. 2021. Genopedia: PRKCA. Available: https://phgkb.cdc.gov/PHGKB/huGEPedia.action?firstQuery=PRKCA&geneID=5578&typeOption=gene&which=2&pubOrderType=pubD&typeSubmit=GO&check=y, accessed on May 19, 2021.

Çelik A, Eke D, Ekinci SY, Yıldırım S. 2013. The protective role of curcumin on perfluorooctane sulfonate-induced genotoxicity: single cell gel electrophoresis and micronucleus test. Food and chemical toxicology : an international journal published for the British Industrial Biological Research Association 53:249-255.

Chang S, Mader BT, Lindstrom KR, Lange CC, Hart JA, Kestner TA, et al. 2017. Perfluorooctanesulfonate (PFOS) Conversion from N-Ethyl-N-(2-hydroxyethyl)-perfluorooctanesulfonamide (EtFOSE) in male Sprague Dawley rats after inhalation exposure. Environmental research 155:307-313.

Chang SC, Ehresman DJ, Noker PE, Gorman GS, Hart JA, John TN, et al. 2012. Comparative pharmacokinetics of perfluorooctanesulfonate (PFOS) in rats, mice, and monkeys. Reproductive Toxicology 33:607.

Charles River Laboratories. 2004. Compilation of Spontaneous Neoplastic Lesions and Survival in Crl: CD (SD) Rats from Control Groups® [Prepared by Giknis M and Clifford

C]. Available: https://www.criver.com/products-services/find-model/cd-sd-igs-rat?region=3611.

Chatterjee A, Gupta S. 2018. The multifaceted role of glutathione S-transferases in cancer. Cancer letters 433:33-42.

Chen J, Wang X, Ge X, Wang D, Wang T, Zhang L, et al. 2016a. Chronic perfluorooctanesulphonic acid (PFOS) exposure produces estrogenic effects in zebrafish. Environmental Pollution 218:702-708.

Chen M, Qiang L, Pan X, Fang S, Han Y, Zhu L. 2015. In Vivo and in Vitro Isomer-Specific Biotransformation of Perfluorooctane Sulfonamide in Common Carp (Cyprinus carpio). Environmental science & technology 49:13817-13824.

Chen T, Zhang L, Yue JQ, Lv ZQ, Xia W, Wan YJ, et al. 2012. Prenatal PFOS exposure induces oxidative stress and apoptosis in the lung of rat off-spring. Reproductive toxicology (Elmsford, NY) 33:538-545.

Chen X, Nie X, Mao J, Zhang Y, Yin K, Sun P, et al. 2018a. Perfluorooctane sulfonate mediates secretion of IL-1β through PI3K/AKT NF-κB pathway in astrocytes. Neurotoxicology and teratology 67:65-75.

Chen X, Nie X, Mao J, Zhang Y, Yin K, Jiang S. 2018b. Perfluorooctanesulfonate induces neuroinflammation through the secretion of TNF-α mediated by the JAK2/STAT3 pathway. Neurotoxicology 66:32-42.

Chen X, Zheng J, Zhuo ML, Zhang A, You Z. 2020. A six-gene-based signature for breast cancer radiotherapy sensitivity estimation. Bioscience reports 40.

Chen Y, Hu W, Huang C, Hua S, Wei Q, Bai C, et al. 2016b. Subchronic perfluorooctanesulfonate (PFOS) exposure induces elevated mutant frequency in an in vivo λ transgenic medaka mutation assay. Scientific reports 6:38466.

Chen Y, Huang C, Bai C, Du C, Liao J, Dong Q. 2016c. In vivo DNA mismatch repair measurement in zebrafish embryos and its use in screening of environmental carcinogens. Journal of hazardous materials 302:296-303.

Cheng J, Psillakis E, Hoffmann MR, Colussi AJ. 2009. Acid dissociation versus molecular association of perfluoroalkyl oxoacids: environmental implications. The journal of physical chemistry A 113:8152-8156.

Cheng W, Yu Z, Feng L, Wang Y. 2013. Perfluorooctane sulfonate (PFOS) induced embryotoxicity and disruption of cardiogenesis. Toxicology in Vitro 27:1503-1512.

Cheng W, Ng CA. 2017. A permeability-limited physiologically based pharmacokinetic (PBPK) model for perfluorooctanoic acid (PFOA) in male rats. Environmental science & technology 51:9930-9939.

Choi SH, Worswick S, Byun H-M, Shear T, Soussa JC, Wolff EM, et al. 2009. Changes in DNA methylation of tandem DNA repeats are different from interspersed repeats in cancer. International journal of cancer 125:723-729.

Clarity C, Trowbridge J, Gerona R, Ona K, McMaster M, Bessonneau V, et al. 2020. Associations between polyfluoroalkyl substance and organophosphate flame retardant exposures and telomere length in a cohort of women firefighters and office workers in San Francisco. medRxiv : the preprint server for health sciences.

Cohn BA, La Merrill MA, Krigbaum NY, Wang M, Park JS, Petreas M, et al. 2020. In utero exposure to poly- and perfluoroalkyl substances (PFASs) and subsequent breast cancer. Reproductive toxicology (Elmsford, NY) 92:112-119.

Corsini E, Avogadro A, Galbiati V, dell'Agli M, Marinovich M, Galli CL, et al. 2011. In vitro evaluation of the immunotoxic potential of perfluorinated compounds (PFCs). Toxicology and applied pharmacology 250:108-116.

Corsini E, Sangiovanni E, Avogadro A, Galbiati V, Viviani B, Marinovich M, et al. 2012. In vitro characterization of the immunotoxic potential of several perfluorinated compounds (PFCs). Toxicology and applied pharmacology 258:248-255.

Crofts F, Taioli E, Trachman J, Cosma GN, Currie D, Toniolo P, et al. 1994. Functional significance of different human CYP1A1 genotypes. Carcinogenesis 15:2961–2963.

Cruceriu D, Baldasici O, Balacescu O, Berindan-Neagoe I. 2020. The dual role of tumor necrosis factor-alpha (TNF-α) in breast cancer: molecular insights and therapeutic approaches. Cellular Oncology 43:1-18.

Cui L, Zhou QF, Liao CY, Fu JJ, Jiang GB. 2009. Studies on the toxicological effects of PFOA and PFOS on rats using histological observation and chemical analysis. Archives of environmental contamination and toxicology 56:338-349.

Cui L, Liao C-y, Zhou Q-f, Xia T-m, Yun Z-j, Jiang G-b. 2010. Excretion of PFOA and PFOS in male rats during a subchronic exposure. Archives of environmental contamination and toxicology 58:205-213.

Cui R, Zhang H, Guo X, Cui Q, Wang J, Dai J. 2015. Proteomic analysis of cell proliferation in a human hepatic cell line (HL-7702) induced by perfluorooctane sulfonate using iTRAQ. Journal of hazardous materials 299:361-370.

Cui S-Y, Wang R, Chen L-B. 2014. MicroRNA-145: a potent tumour suppressor that regulates multiple cellular pathways. J Cell Mol Med 18:1913-1926.

D'Eon J C, Mabury SA. 2011. Is indirect exposure a significant contributor to the burden of perfluorinated acids observed in humans? Environmental science & technology 45:7974-7984.

De Silva AO, Benskin JP, Martin LJ, Arsenault G, McCrindle R, Riddell N, et al. 2009. Disposition of perfluorinated acid isomers in Sprague-Dawley rats; part 2: subchronic dose. Environmental toxicology and chemistry 28:555-567.

de Wit CA, Bossi R, Dietz R, Dreyer A, Faxneld S, Garbus SE, et al. 2020. Organohalogen compounds of emerging concern in Baltic Sea biota: Levels, biomagnification potential and comparisons with legacy contaminants. Environment international.

Deininger P. 2011. Alu elements: know the SINEs. Genome Biology 12:236.

DeWitt JC, Copeland CB, Strynar MJ, Luebke RW. 2008. Perfluorooctanoic Acid-Induced Immunomodulation in Adult C57BL/6J or C57BL/6N Female Mice. Environmental Health Perspectives 116:644-650.

DeWitt JC, Peden-Adams MM, Keller JM, Germolec DR. 2012. Immunotoxicity of perfluorinated compounds: recent developments. Toxicologic pathology 40:300-311.

Dhingra R, Winquist A, Darrow LA, Klein M, Steenland K. 2017. A Study of Reverse Causation: Examining the Associations of Perfluorooctanoic Acid Serum Levels with Two Outcomes. Environmental health perspectives 125:416-421.

Díaz-Zaragoza M, Hernández-Ávila R, Viedma-Rodríguez R, Arenas-Aranda D, Ostoa-Saloma P. 2015. Natural and adaptive IgM antibodies in the recognition of tumor-associated antigens of breast cancer (Review). Oncol Rep 34:1106-1114.

Ding G, Wang L, Zhang J, Wei Y, Wei L, Li Y, et al. 2015. Toxicity and DNA methylation changes induced by perfluorooctane sulfonate (PFOS) in sea urchin Glyptocidaris crenularis. Chemosphere 128:225-230.

Ding N, Harlow SD, Randolph JF, Calafat AM, Mukherjee B, Batterman S, et al. 2020. Associations of Perfluoroalkyl Substances with Incident Natural Menopause: The Study of Women's Health Across the Nation. The Journal of clinical endocrinology and metabolism 105:e3169-3182.

Dix DJ, Houck KA, Martin MT, Richard AM, Setzer RW, Kavlock RJ. 2007. The ToxCast program for prioritizing toxicity testing of environmental chemicals. Toxicological sciences 95:5-12.

Doan T, Connolly L, Igout A, Nott K, Muller M, Scippo MI. 2020. In vitro profiling of the potential endocrine disrupting activities affecting steroid and aryl hydrocarbon receptors of compounds and mixtures prevalent in human drinking water resources. Chemosphere 258.

Dobraca D, Israel L, McNeel S, Voss R, Wang M, Gajek R, et al. 2015. Biomonitoring in California firefighters: metals and perfluorinated chemicals. Journal of occupational and environmental medicine 57:88-97.

Dodig S, Čepelak I, Pavić I. 2019. Hallmarks of senescence and aging. Biochemia medica 29:483-497.

Domingo JL, Nadal M. 2017. Per- and Polyfluoroalkyl Substances (PFASs) in Food and Human Dietary Intake: A Review of the Recent Scientific Literature. Journal of agricultural and food chemistry 65:533-543.

Dong GH, Zhang YH, Zheng L, Liu W, Jin YH, He QC. 2009. Chronic effects of perfluorooctanesulfonate exposure on immunotoxicity in adult male C57BL/6 mice. Archives of toxicology 83:805-815.

Dong GH, Liu MM, Wang D, Zheng L, Liang ZF, Jin YH. 2011. Sub-chronic effect of perfluorooctanesulfonate (PFOS) on the balance of type 1 and type 2 cytokine in adult C57BL6 mice. Archives of toxicology 85:1235-1244.

Dong GH, Zhang YH, Zheng L, Liang ZF, Jin YH, He QC. 2012. Subchronic effects of perfluorooctanesulfonate exposure on inflammation in adult male C57BL/6 mice. Environmental toxicology 27:285-296.

Dong H, Curran I, Williams A, Bondy G, Yauk CL, Wade MG. 2016. Hepatic miRNA profiles and thyroid hormone homeostasis in rats exposed to dietary potassium perfluorooctanesulfonate (PFOS). Environmental toxicology and pharmacology 41:201-210.

Dong L, Yang X, Gu W, Zhao K, Ge H, Zhou J, et al. 2015. Connexin 43 mediates PFOS-induced apoptosis in astrocytes. Chemosphere 132:8-16.

Dong S, Wang R, Wang H, Ding Q, Zhou X, Wang J, et al. 2019. HOXD-AS1 promotes the epithelial to mesenchymal transition of ovarian cancer cells by regulating miR-186-5p and PIK3R3. Journal of experimental & clinical cancer research : CR 38:110.

Du G, Hu J, Huang H, Qin Y, Han X, Wu D, et al. 2013. Perfluorooctane sulfonate (PFOS) affects hormone receptor activity, steroidogenesis, and expression of endocrine-related genes in vitro and in vivo. Environmental toxicology and chemistry 32:353-360.

Du G, Hu J, Huang Z, Yu M, Lu C, Wang X, et al. 2019. Neonatal and juvenile exposure to perfluorooctanoate (PFOA) and perfluorooctane sulfonate (PFOS): Advance puberty onset and kisspeptin system disturbance in female rats. Ecotoxicology and environmental safety 167:412-421.

Du J, Wang S, You H, Jiang R, Zhuang C, Zhang X. 2014. Developmental toxicity and DNA damage to zebrafish induced by perfluorooctane sulfonate in the presence of ZnO nanoparticles. Environmental toxicology 31:360-371.

Du L, Wu Y, Zhang X, Zhang F, Chen X, Cheng Z, et al. 2017. Preparation of magnetic molecularly imprinted polymers for the rapid and selective separation and enrichment of perfluorooctane sulfonate. Journal of separation science 40:2819-2826.

Dzierlenga MW, Keast DR, Longnecker MP. 2021. The concentration of several perfluoroalkyl acids in serum appears to be reduced by dietary fiber. Environment international 146:106292.

EFSA. 2008. Perfluorooctane Sulfonate (PFOS), Perfluorooctaonic Acid (PFOA) and their salts. Scientific Opinion of the Panel on Contaminants in the Food Chain. Parma, Italy: European Food Safety Authority. Available: https://efsa.onlinelibrary.wiley.com/doi/abs/10.2903/j.efsa.2008.653.

EFSA. 2018. Risk to human health related to the presence of perfluorooctane sulfonic acid and perfluorooctanoic acid in food. (EFSA Journal). 1831-4732. Available: https://efsa.onlinelibrary.wiley.com/doi/pdfdirect/10.2903/j.efsa.2018.5194?download=true.

EFSA. 2020. Risk to human health related to the presence of perfluoroalkyl substances in food. EFSA Journal. Available: https://efsa.onlinelibrary.wiley.com/doi/pdfdirect/10.2903/j.efsa.2020.6223?download=true.

Egeghy PP, Lorber M. 2011. An assessment of the exposure of Americans to perfluorooctane sulfonate: A comparison of estimated intake with values inferred from NHANES data. Journal of Exposure Science and Environmental Epidemiology 21:150-168.

Eick SM, Goin DE, Cushing L, DeMicco E, Park J-S, Wang Y, et al. 2021. Mixture effects of prenatal exposure to per- and polyfluoroalkyl substances and polybrominated diphenyl ethers on maternal and newborn telomere length. Environmental Health 20:76.

Eke D, Çelik A. 2016. Curcumin prevents perfluorooctane sulfonate-induced genotoxicity and oxidative DNA damage in rat peripheral blood. Drug and chemical toxicology 39:97-103.

Eke D, Çelik A, Yilmaz MB, Aras N, Kocatürk Sel S, Alptekin D. 2017. Apoptotic gene expression profiles and DNA damage levels in rat liver treated with perfluorooctane sulfonate and protective role of curcumin. International journal of biological macromolecules 104:515-520.

Elcombe CR, Elcombe BM, Foster JR, Chang SC, Ehresman DJ, Butenhoff JL. 2012a. Hepatocellular hypertrophy and cell proliferation in Sprague-Dawley rats from dietary exposure to potassium perfluorooctanesulfonate results from increased expression of xenosensor nuclear receptors PPARα and CAR/PXR. Toxicology 293:16-29.

Elcombe CR, Elcombe BM, Foster JR, Chang SC, Ehresman DJ, Noker PE, et al. 2012b. Evaluation of hepatic and thyroid responses in male Sprague Dawley rats for up to eighty-four days following seven days of dietary exposure to potassium perfluorooctanesulfonate. Toxicology 293:30-40.

Emerce E, Çetin Ö. 2018. Genotoxicity assessment of perfluoroalkyl substances on human sperm. Toxicology and industrial health 34:884-890.

Environment Canada. 2006. Canadian Environmental Protection Act, 1999 (CEPA 1999): Ecological Screening Assessment Report on Perfluorooctane Sulfonate, Its Salts and Its Precursors that Contain the C8F17SO2 or C8F17SO3, or C8F17SO2N Moiety. Available: https://www.ec.gc.ca/lcpe-cepa/documents/substances/spfo-pfos/ecological_sar_pfos_eng.pdf.

Eriksen KT, Sørensen M, McLaughlin JK, Lipworth L, Tjønneland A, Overvad K, et al. 2009. Perfluorooctanoate and perfluorooctanesulfonate plasma levels and risk of cancer in the general Danish population. Journal of the National Cancer Institute 101:605-609.

Eriksen KT, Raaschou-Nielsen O, Sørensen M, Roursgaard M, Loft S, Møller P. 2010. Genotoxic potential of the perfluorinated chemicals PFOA, PFOS, PFBS, PFNA and PFHxA in human HepG2 cells. Mutation research 700:39-43.

Eriksson U, Haglund P, Karrman A. 2017. Contribution of precursor compounds to the release of per- and polyfluoroalkyl substances (PFASs) from waste water treatment plants (WWTPs). Journal of environmental sciences (China) 61:80-90.

Fair PA, Driscoll E, Mollenhauer MA, Bradshaw SG, Yun SH, Kannan K, et al. 2011. Effects of environmentally-relevant levels of perfluorooctane sulfonate on clinical parameters and immunological functions in B6C3F1 mice. Journal of immunotoxicology 8:17-29.

Fair PA, Wolf B, White ND, Arnott SA, Kannan K, Karthikraj R, et al. 2019. Perfluoroalkyl substances (PFASs) in edible fish species from Charleston Harbor and tributaries, South Carolina, United States: Exposure and risk assessment. Environmental research 171:266-277.

Fang C, Wu X, Huang Q, Liao Y, Liu L, Qiu L, et al. 2012. PFOS elicits transcriptional responses of the ER, AHR and PPAR pathways in Oryzias melastigma in a stage-specific manner. Aquatic toxicology (Amsterdam, Netherlands) 106-107:9-19.

Fang S, Zhao S, Zhang Y, Zhong W, Zhu L. 2014. Distribution of perfluoroalkyl substances (PFASs) with isomer analysis among the tissues of aquatic organisms in Taihu Lake, China. Environmental pollution (Barking, Essex : 1987) 193:224-232.

FDA. 2019a. Analytical Results for PFAS in 2019 Total Diet Study Sampling (Parts per Trillion)- Dataset-1. Available: https://www.fda.gov/media/127852/download [accessed on April 29, 2021].

FDA. 2019b. Analytical Results for PFAS in 2019 Total Diet Study Sampling (Parts per Trillion)- Dataset-2. Available: https://www.fda.gov/media/133693/download [accessed on April 29, 2021].

Fei C, McLaughlin JK, Lipworth L, Olsen J. 2009. Maternal levels of perfluorinated chemicals and subfecundity. Human reproduction (Oxford, England) 24:1200-1205.

Feng X, Wang X, Cao X, Xia Y, Zhou R, Chen L. 2015. Chronic Exposure of Female Mice to an Environmental Level of Perfluorooctane Sulfonate Suppresses Estrogen Synthesis Through Reduced Histone H3K14 Acetylation of the StAR Promoter Leading to Deficits in Follicular Development and Ovulation. Toxicological Sciences 148:368-379.

Filgo AJ, Quist EM, Hoenerhoff MJ, Brix AE, Kissling GE, Fenton SE. 2015. Perfluorooctanoic Acid (PFOA)-induced Liver Lesions in Two Strains of Mice Following Developmental Exposures: PPARalpha Is Not Required. Toxicologic pathology 43:558-568.

Florentin A, Deblonde T, Diguio N, Hautemaniere A, Hartemann P. 2011. Impacts of two perfluorinated compounds (PFOS and PFOA) on human hepatoma cells: cytotoxicity but no genotoxicity? International journal of hygiene and environmental health 214:493-499.

Fromme H, Tittlemier SA, Volkel W, Wilhelm M, Twardella D. 2009. Perfluorinated compounds--exposure assessment for the general population in Western countries. International journal of hygiene and environmental health 212:239-270.

Fry K, Power MC. 2017. Persistent organic pollutants and mortality in the United States, NHANES 1999-2011. Environmental Health: A Global Access Science Source 16.

Fu Z, Wang Y, Wang Z, Xie H, Chen J. 2015. Transformation pathways of isomeric perfluorooctanesulfonate precursors catalyzed by the active species of P450 enzymes: in silico investigation. Chemical research in toxicology 28:482-489.

Gao Y, Li X, Guo LH. 2013. Assessment of estrogenic activity of perfluoroalkyl acids based on ligand-induced conformation state of human estrogen receptor. Environmental Science and Technology 47:634-641.

Gao Y, Fu J, Cao H, Wang Y, Zhang A, Liang Y, et al. 2015. Differential accumulation and elimination behavior of perfluoroalkyl acid isomers in occupational workers in a manufactory in China. Environmental Science and Technology 49:6953-6962.

Gebbink WA, Glynn A, Darnerud PO, Berger U. 2015. Perfluoroalkyl acids and their precursors in Swedish food: The relative importance of direct and indirect dietary exposure. Environmental Pollution 198:108-115.

Gebbink WA, Bignert A, Berger U. 2016. Perfluoroalkyl Acids (PFAAs) and Selected Precursors in the Baltic Sea Environment: Do Precursors Play a Role in Food Web Accumulation of PFAAs? Environmental Science and Technology 50:6354-6362.

GeneCards. 2021a. SMAD3 Gene. Available: https://www.genecards.org/cgi-bin/carddisp.pl?gene=SMAD3, accessed on May 19, 2021.

GeneCards. 2021b. ZBTB7A Gene. Available: https://www.genecards.org/cgi-bin/carddisp.pl?gene=ZBTB7A&keywords=zbtb7a, accessed on May 19, 2021.

GeneCards. 2021c. SNAPIN Gene. Available: https://www.genecards.org/cgi-bin/carddisp.pl?gene=SNAPIN&keywords=snapin), accessed on May 19, 2021.

Genuis SJ, Curtis L, Birkholz D. 2013. Gastrointestinal elimination of perfluorinated compounds using cholestyramine and Chlorella pyrenoidosa. ISRN toxicology 2013.

Ghisari M, Eiberg H, Long M, Bonefeld-Jørgensen EC. 2014. Polymorphisms in phase I and phase II genes and breast cancer risk and relations to persistent organic pollutant exposure: a case-control study in Inuit women. Environmental health : a global access science source 13:19.

Ghisari M, Long M, Røge DM, Olsen J, Bonefeld-Jørgensen EC. 2017. Polymorphism in xenobiotic and estrogen metabolizing genes, exposure to perfluorinated compounds and subsequent breast cancer risk: A nested case-control study in the Danish National Birth Cohort. Environmental research 154:325-333.

Ghisi R, Vamerali T, Manzetti S. 2019. Accumulation of perfluorinated alkyl substances (PFAS) in agricultural plants: A review. Environmental research 169:326-341.

Giménez-Bastida JA, Surma M, Zieliński H. 2015. In vitro evaluation of the cytotoxicity and modulation of mechanisms associated with inflammation induced by perfluorooctanesulfonate and perfluorooctanoic acid in human colon myofibroblasts CCD-18Co. Toxicology in vitro : an international journal published in association with BIBRA 29:1683-1691.

Goeden HM, Greene CW, Jacobus JA. 2019. A transgenerational toxicokinetic model and its use in derivation of Minnesota PFOA water guidance. Journal of exposure science & environmental epidemiology 29:183-195.

Gogola J, Hoffmann M, Ptak A. 2019. Persistent endocrine-disrupting chemicals found in human follicular fluid stimulate the proliferation of granulosa tumor spheroids via GPR30 and IGF1R but not via the classic estrogen receptors. Chemosphere 217:100-110.

Gomis MI, Vestergren R, MacLeod M, Mueller JF, Cousins IT. 2017. Historical human exposure to perfluoroalkyl acids in the United States and Australia reconstructed from biomonitoring data using population-based pharmacokinetic modelling. Environ Int 108:92-102.

Goosey E, Harrad S. 2011. Perfluoroalkyl compounds in dust from Asian, Australian, European, and North American homes and UK cars, classrooms, and offices. Environment international 37:86-92.

Greaves AK, Letcher RJ. 2013. Linear and branched perfluorooctane sulfonate (PFOS) isomer patterns differ among several tissues and blood of polar bears. Chemosphere 93:574-580.

Grice MM, Alexander BH, Hoffbeck R, Kampa DM. 2007. Self-reported medical conditions in perfluorooctanesulfonyl fluoride manufacturing workers. Journal of occupational and environmental medicine 49:722-729.

Guerrero-Preston R, Goldman LR, Brebi-Mieville P, Ili-Gangas C, Lebron C, Witter FR, et al. 2010. Global DNA hypomethylation is associated with in utero exposure to cotinine and perfluorinated alkyl compounds. Epigenetics 5:539-546.

Guo J, Wu P, Cao J, Luo Y, Chen J, Wang G, et al. 2019. The PFOS disturbed immunomodulatory functions via nuclear Factor-κB signaling in liver of zebrafish (Danio rerio). Fish & shellfish immunology 91:87-98.

Guo X, Li Q, Shi J, Shi L, Li B, Xu A, et al. 2016. Perfluorooctane sulfonate exposure causes gonadal developmental toxicity in Caenorhabditis elegans through ROS-induced DNA damage. Chemosphere 155:115-126.

Guo XX, He QZ, Li W, Long DX, Pan XY, Chen C, et al. 2017. Brain-Derived Neurotrophic Factor Mediated Perfluorooctane Sulfonate Induced-Neurotoxicity via Epigenetics Regulation in SK-N-SH Cells. International journal of molecular sciences 18.

Hall SM, Patton S, Petreas M, Zhang S, Phillips AL, Hoffman K, et al. 2020. Per- and Polyfluoroalkyl Substances in Dust Collected from Residential Homes and Fire Stations in North America. Environmental science & technology 54:14558-14567.

Han J, Fang Z. 2010. Estrogenic effects, reproductive impairment and developmental toxicity in ovoviparous swordtail fish (Xiphophorus helleri) exposed to perfluorooctane sulfonate (PFOS). Aquatic toxicology (Amsterdam, Netherlands) 99:281-290.

Han R, Hu M, Zhong Q, Wan C, Liu L, Li F, et al. 2018. Perfluorooctane sulphonate induces oxidative hepatic damage via mitochondria-dependent and NF-κB/TNF-α-mediated pathway. Chemosphere 191:1056-1064.

Hanahan D, Weinberg RA. 2000. The hallmarks of cancer. cell 100:57-70.

Hanahan D, Weinberg RA. 2011. Hallmarks of cancer: the next generation. cell 144:646-674.

Harada KH, Hashida S, Kaneko T, Takenaka K, Minata M, Inoue K, et al. 2007. Biliary excretion and cerebrospinal fluid partition of perfluorooctanoate and perfluorooctane sulfonate in humans. Environmental toxicology and pharmacology 24:134-139.

Hardell E, Kärrman A, van Bavel B, Bao J, Carlberg M, Hardell L. 2014. Case-control study on perfluorinated alkyl acids (PFAAs) and the risk of prostate cancer. Environment international 63:35-39.

Harrad S, Wemken N, Drage DS, Abdallah MA, Coggins AM. 2019. Perfluoroalkyl Substances in Drinking Water, Indoor Air and Dust from Ireland: Implications for Human Exposure. Environmental science & technology 53:13449-13457.

Hassell KL, Coggan TL, Cresswell T, Kolobaric A, Berry K, Crosbie ND, et al. 2020. Dietary Uptake and Depuration Kinetics of Perfluorooctane Sulfonate, Perfluorooctanoic Acid, and Hexafluoropropylene Oxide Dimer Acid (GenX) in a Benthic Fish. Environmental toxicology and chemistry 39:595-603.

Haug LS, Huber S, Schlabach M, Becher G, Thomsen C. 2011. Investigation on per- and polyfluorinated compounds in paired samples of house dust and indoor air from Norwegian homes. Environmental science & technology 45:7991-7998.

Health Canada. 2016. Perfluorooctane Sulfonate (PFOS) in Drinking Water. Available: https://www.canada.ca/en/health-canada/programs/consultation-perfluorooctane-sulfonate-pfos-in-drinking-water/document.html.

Hegde M, Joshi MB. 2021. Comprehensive analysis of regulation of DNA methyltransferase isoforms in human breast tumors. Journal of cancer research and clinical oncology 147:937-971.

Helmke BM, Markowski DN, Meyer A, Bullerdiek J. 2012. The expression of HMGA2 varies strongly among colon carcinomas. Anticancer research 32:1589-1593.

Hennekens CH, Buring JE, Mayrent SL. 1987. Epidemiology in medicine. Boston, Massachusetts:Little, Brown.

Henry ND, Fair PA. 2013. Comparison of in vitro cytotoxicity, estrogenicity and anti-estrogenicity of triclosan, perfluorooctane sulfonate and perfluorooctanoic acid. Journal of applied toxicology : JAT 33:265-272.

Hill AB. 1965. The environment and disease: Association or causation? Proceedings of the Royal Society of Medicine 58:295-300.

Hu W, Jones PD, Celius T, Giesy JP. 2005. Identification of genes responsive to PFOS using gene expression profiling. Environmental toxicology and pharmacology 19:57-70.

Hu XC, Andrews DQ, Lindstrom AB, Bruton TA, Schaider LA, Grandjean P, et al. 2016. Detection of Poly- and Perfluoroalkyl Substances (PFASs) in U.S. Drinking Water Linked to Industrial Sites, Military Fire Training Areas, and Wastewater Treatment Plants. Environmental science & technology letters 3:344-350.

Hu XZ, Hu DC. 2009. Effects of perfluorooctanoate and perfluorooctane sulfonate exposure on hepatoma Hep G2 cells. Archives of toxicology 83:851-861.

Huang H, Wang Q, He X, Wu Y, Xu C. 2019a. Association between polyfluoroalkyl chemical concentrations and leucocyte telomere length in US adults. Science of the Total Environment 653:547-553.

Huang MC, Dzierlenga AL, Robinson VG, Waidyanatha S, DeVito MJ, Eifrid MA, et al. 2019b. Toxicokinetics of perfluorobutane sulfonate (PFBS), perfluorohexane-1-sulphonic acid (PFHxS), and perfluorooctane sulfonic acid (PFOS) in male and female Hsd:Sprague Dawley SD rats after intravenous and gavage administration. Toxicol Rep 6:645-655.

Huang T, Zhang Y, Zhang W, Lin T, Chen L, Yang B, et al. 2020. Attenuation of Perfluorooctane Sulfonate-Induced Steatohepatitis by Grape Seed Proanthocyanidin Extract in Mice. BioMed research international 2020:8818160.

Huck I, Beggs K, Apte U. 2018. Paradoxical Protective Effect of Perfluorooctanesulfonic Acid Against High-Fat Diet-Induced Hepatic Steatosis in Mice. International journal of toxicology 37:383-392.

Hurley S, Houtz E, Goldberg D, Wang M, Park J, Nelson D, et al. 2016. Preliminary Associations between the Detection of Perfluoroalkyl Acids (PFAAs) in Drinking Water and Serum Concentrations in a Sample of California Women. Environmental Science and Technology Letters 3:6.

Hurley S, Goldberg D, Wang M, Park JS, Petreas M, Bernstein L, et al. 2018a. Time Trends in Per- and Polyfluoroalkyl Substances (PFASs) in California Women: Declining Serum Levels, 2011-2015. Environmental science & technology 52:277-287.

Hurley S, Goldberg D, Wang M, Park JS, Petreas M, Bernstein L, et al. 2018b. Breast cancer risk and serum levels of per- and poly-fluoroalkyl substances: a case-control study nested in the California Teachers Study. Environmental health : a global access science source 17:83.

IARC. 2017. Perfluorooctanoic Acid. (IARC Monographs on the evaluation of carcinogenic risks to humans). International Agency for Research on Cancer, Volume 110. Available: https://monographs.iarc.who.int/wp-content/uploads/2018/06/mono110-01.pdf.

IARC. 2019. Preamble to the IARC Monographs on the Idenfication of Carcinogenic Hazards to Humans. Lyon, France. Available: https://monographs.iarc.who.int/iarc-monographs-preamble-preamble-to-the-iarc-monographs/.

IARC. 2020a. List of classifications by cancer sites with sufficient or limited evidence in humans, IARC Monographs Volumes 1-129. Lyon, France: International Agency for Research on Cancer, World Health Organization. Available: https://monographs.iarc.who.int/wp-content/uploads/2019/07/Classifications_by_cancer_site.pdf.

IARC. 2020b. The IARC Monographs: Updated procedures for modern and transparent evidence synthesis in cancer hazard identification. JNCI: Journal of the National Cancer Institute 112:30-37.

Ishibashi H, Iwata H, Kim EY, Tao L, Kannan K, Tanabe S, et al. 2008. Contamination and effects of perfluorochemicals in Baikal seal (Pusa sibirica). 2. Molecular characterization, expression level, and transcriptional activation of peroxisome proliferator-activated receptor alpha. Environmental science & technology 42:2302-2308.

Ishibashi H, Kim EY, Iwata H. 2011. Transactivation potencies of the Baikal seal (Pusa sibirica) peroxisome proliferator-activated receptor α by perfluoroalkyl carboxylates and sulfonates: estimation of PFOA induction equivalency factors. Environmental science & technology 45:3123-3130.

Itoh S, Araki A, Mitsui T, Miyashita C, Goudarzi H, Sasaki S, et al. 2016. Association of perfluoroalkyl substances exposure in utero with reproductive hormone levels in cord blood in the Hokkaido Study on Environment and Children's Health. Environment international 94:51-59.

Jabeen M, Fayyaz M, Irudayaraj J. 2020. Epigenetic Modifications, and Alterations in Cell Cycle and Apoptosis Pathway in A549 Lung Carcinoma Cell Line upon Exposure to Perfluoroalkyl Substances. Toxics 8.

Jacquet N, Maire MA, Landkocz Y, Vasseur P. 2012. Carcinogenic potency of perfluorooctane sulfonate (PFOS) on Syrian hamster embryo (SHE) cells. Archives of toxicology 86:305-314.

Jain RB. 2018. Time trends over 2003-2014 in the concentrations of selected perfluoroalkyl substances among US adults aged >/=20years: Interpretational issues. The Science of the total environment 645:946-957.

Jensen RC, Glintborg D, Gade Timmermann CA, Nielsen F, Kyhl HB, Frederiksen H, et al. 2020. Prenatal exposure to perfluorodecanoic acid is associated with lower circulating concentration of adrenal steroid metabolites during mini puberty in human female infants. The Odense Child Cohort. Environmental research 182:109101.

Jernbro S, Rocha PS, Keiter S, Skutlarek D, Färber H, Jones PD, et al. 2007. Perfluorooctane sulfonate increases the genotoxicity of cyclophosphamide in the micronucleus assay with V79 cells. Further proof of alterations in cell membrane properties caused by PFOS. Environmental science and pollution research international 14:85-87.

Jiang T, Zhou C, Ren S. 2016. Role of IL-2 in cancer immunotherapy. Oncoimmunology 5:e1163462.

Jin B, Mallula S, Golovko SA, Golovko MY, Xiao F. 2020. In Vivo Generation of PFOA, PFOS, and Other Compounds from Cationic and Zwitterionic Per- And Polyfluoroalkyl

Substances in a Terrestrial Invertebrate (Lumbricus terrestris). Environmental Science and Technology 54:7378-7387.

Joensen UN, Bossi R, Leffers H, Jensen AA, Skakkebaek NE, Jørgensen N. 2009. Do perfluoroalkyl compounds impair human semen quality? Environmental health perspectives 117:923-927.

Joensen UN, Veyrand B, Antignac JP, Blomberg Jensen M, Petersen JH, Marchand P, et al. 2013. PFOS (perfluorooctanesulfonate) in serum is negatively associated with testosterone levels, but not with semen quality, in healthy men. Human reproduction (Oxford, England) 28:599-608.

Johnson JD, Gibson SJ, Ober RE. 1984. Cholestyramine-enhanced fecal elimination of carbon-14 in rats after administration of ammonium [14C]perfluorooctanoate or potassium [14C]perfluorooctanesulfonate. Fundamental and Applied Toxicology 4:972-976.

Joseph L. 2007. Confounding and Collinearity in Multivariate Logistic Regression.McGill University.

Joseph L. 2010. Confounding and Collinearity in Multiple Linear Regression.McGill University.

Judson R, Houck K, Martin M, Richard AM, Knudsen TB, Shah I, et al. 2016. Analysis of the Effects of Cell Stress and Cytotoxicity on In Vitro Assay Activity Across a Diverse Chemical and Assay Space. Toxicological sciences : an official journal of the Society of Toxicology 153:409.

Judson RS, Houck KA, Kavlock RJ, Knudsen TB, Martin MT, Mortensen HM, et al. 2010. In vitro screening of environmental chemicals for targeted testing prioritization: The toxcast project. Environmental Health Perspectives 118:485-492.

Kaneko N, Kurata M, Yamamoto T, Morikawa S, Masumoto J. 2019. The role of interleukin-1 in general pathology. Inflammation and regeneration 39:1-16.

Kang JS, Choi JS, Park JW. 2016. Transcriptional changes in steroidogenesis by perfluoroalkyl acids (PFOA and PFOS) regulate the synthesis of sex hormones in H295R cells. Chemosphere 155:436-443.

Kanwal R, Gupta K, Gupta S. 2015. Cancer epigenetics: an introduction. Methods in molecular biology (Clifton, NJ) 1238:3-25.

Karlsen M, Grandjean P, Weihe P, Steuerwald U, Oulhote Y, Valvi D. 2017. Early-life exposures to persistent organic pollutants in relation to overweight in preschool children. Reproductive toxicology (Elmsford, NY) 68:145-153.

Kato K, Calafat AM, Needham LL. 2009. Polyfluoroalkyl chemicals in house dust. Environmental research 109:518-523.

Kato K, Wong LY, Jia LT, Kuklenyik Z, Calafat AM. 2011. Trends in exposure to polyfluoroalkyl chemicals in the U.S. Population: 1999-2008. Environmental science & technology 45:8037-8045.

Kavlock R, Chandler K, Houck K, Hunter S, Judson R, Kleinstreuer N, et al. 2012. Update on EPA's ToxCast program: providing high throughput decision support tools for chemical risk management. Chemical research in toxicology 25:1287-1302.

Kawamoto K, Oashi T, Oami K, Liu W, Jin Y, Saito N, et al. 2010. Perfluorooctanoic acid (PFOA) but not perfluorooctane sulfonate (PFOS) showed DNA damage in comet assay on Paramecium caudatum. The Journal of toxicological sciences 35:835-841.

KEGG. 2021. Homo sapiens (human): 5578. Available: https://www.genome.jp/dbget-bin/www_bget?hsa:5578, accessed on May 18, 2021.

Keil DE, Mehlmann T, Butterworth L, Peden-Adams MM. 2008. Gestational exposure to perfluorooctane sulfonate suppresses immune function in B6C3F1 mice. Toxicological Sciences 103:77-85.

Keiter S, Baumann L, Färber H, Holbech H, Skutlarek D, Engwall M, et al. 2012. Long-term effects of a binary mixture of perfluorooctane sulfonate (PFOS) and bisphenol A (BPA) in zebrafish (Danio rerio). Aquatic toxicology (Amsterdam, Netherlands) 118-119:116-129.

Kennedy GL, Butenhoff JL, Olsen GW, O'Connor JC, Seacat AM, Perkins RG, et al. 2004. The toxicology of perfluorooctanoate. Critical reviews in toxicology 34:351-384.

Khansari MR, Yousefsani BS, Kobarfard F, Faizi M, Pourahmad J. 2017. In vitro toxicity of perfluorooctane sulfonate on rat liver hepatocytes: probability of distructive binding to CYP 2E1 and involvement of cellular proteolysis. Environmental science and pollution research international 24:23382-23388.

Kim JH, Park HY, Jeon JD, Kho Y, Kim SK, Park MS, et al. 2016. The modifying effect of vitamin C on the association between perfluorinated compounds and insulin resistance in the Korean elderly: a double-blind, randomized, placebo-controlled crossover trial. European journal of nutrition 55:1011-1020.

Kim K, Bennett DH, Calafat AM, Hertz-Picciotto I, Shin HM. 2020. Temporal trends and determinants of serum concentrations of per- and polyfluoroalkyl substances among Northern California mothers with a young child, 2009-2016. Environmental research 186:109491.

Kim WK, Lee SK, Jung J. 2010. Integrated assessment of biomarker responses in common carp (Cyprinus carpio) exposed to perfluorinated organic compounds. Journal of hazardous materials 180:395-400.

Kjeldsen LS, Bonefeld-Jorgensen EC. 2013. Perfluorinated compounds affect the function of sex hormone receptors. Toxicology Letters 221:S156.

Knox SS, Jackson T, Javins B, Frisbee SJ, Shankar A, Ducatman AM. 2011. Implications of Early Menopause in Women Exposed to Perfluorocarbons. The Journal of Clinical Endocrinology & Metabolism 96:1747-1753.

Kobayashi S, Azumi K, Goudarzi H, Araki A, Miyashita C, Kobayashi S, et al. 2017. Effects of prenatal perfluoroalkyl acid exposure on cord blood IGF2/H19 methylation and ponderal index: The Hokkaido Study. Journal of exposure science & environmental epidemiology 27:251-259.

Kobayashi S, Hiwasa T, Arasawa T, Kagaya A, Ishii S, Shimada H, et al. 2018. Identification of specific and common diagnostic antibody markers for gastrointestinal cancers by SEREX screening using testis cDNA phage library. Oncotarget 9:18559-18569.

Koskela A, Koponen J, Lehenkari P, Viluksela M, Korkalainen M, Tuukkanen J. 2017. Perfluoroalkyl substances in human bone: concentrations in bones and effects on bone cell differentiation. Scientific reports 7:6841.

Kotthoff M, Muller J, Jurling H, Schlummer M, Fiedler D. 2015. Perfluoroalkyl and polyfluoroalkyl substances in consumer products. Environmental science and pollution research international 22:14546-14559.

Kowalczyk J, Ehlers S, Fürst P, Schafft H, Lahrssen-Wiederholt M. 2012. Transfer of perfluorooctanoic acid (PFOA) and perfluorooctane sulfonate (PFOS) from contaminated feed into milk and meat of sheep: pilot study. Archives of environmental contamination and toxicology 63:288-298.

Kowalczyk J, Ehlers S, Oberhausen A, Tischer M, Fürst P, Schafft H, et al. 2013. Absorption, distribution, and milk secretion of the perfluoroalkyl acids PFBS, PFHxS, PFOS, and PFOA by dairy cows fed naturally contaminated feed. Journal of agricultural and food chemistry 61:2903-2912.

Kratzer J, Ahrens L, Roos A, Backlin BM, Ebinghaus R. 2011. Temporal trends of polyfluoroalkyl compounds (PFCs) in liver tissue of grey seals (Halichoerus grypus) from the Baltic Sea, 1974-2008. Chemosphere 84:1592-1600.

Kraugerud M, Zimmer KE, Ropstad E, Verhaegen S. 2011. Perfluorinated compounds differentially affect steroidogenesis and viability in the human adrenocortical carcinoma (H295R) in vitro cell assay. Toxicology letters 205:62-68.

Kristensen SL, Ramlau-Hansen CH, Ernst E, Olsen SF, Bonde JP, Vested A, et al. 2013. Long-term effects of prenatal exposure to perfluoroalkyl substances on female reproduction. Human reproduction (Oxford, England) 28:3337-3348.

Krøvel AV, Søfteland L, Torstensen B, Olsvik PA. 2008. Transcriptional effects of PFOS in isolated hepatocytes from Atlantic salmon Salmo salar L. Comparative biochemistry and physiology Toxicology & pharmacology : CBP 148:14-22.

Kumar A, Creery WD. 2000. The therapeutic potential of interleukin 10 in infection and inflammation. Arch Immunol Ther Exp (Warsz) 48:529-538.

Kwon JJ, Factora TD, Dey S, Kota J. 2019. A Systematic Review of miR-29 in Cancer. Molecular therapy oncolytics 12:173-194.

Land M, de Wit CA, Bignert A, Cousins IT, Herzke D, Johansson JH, et al. 2018. What is the effect of phasing out long-chain per- and polyfluoroalkyl substances on the concentrations of perfluoroalkyl acids and their precursors in the environment? A systematic review. Environmental Evidence 7:4.

Landskron G, De la Fuente M, Thuwajit P, Thuwajit C, Hermoso MA. 2014. Chronic inflammation and cytokines in the tumor microenvironment. Journal of immunology research 2014.

Lauritzen HB, Larose TL, Øien T, Sandanger TM, Odland J, van de Bor M, et al. 2018. Prenatal exposure to persistent organic pollutants and child overweight/obesity at 5-year follow-up: a prospective cohort study. Environmental health : a global access science source 17:9.

Lebrec H, Cowan L, Lagrou M, Krejsa C, Neradilek MB, Polissar NL, et al. 2011. An inter-laboratory retrospective analysis of immunotoxicological endpoints in non-human primates: T-cell-dependent antibody responses. Journal of immunotoxicology 8:238-250.

Lechner M, Knapp H. 2011. Carryover of perfluorooctanoic acid (PFOA) and perfluorooctane sulfonate (PFOS) from soil to plant and distribution to the different plant compartments studied in cultures of carrots (Daucus carota ssp. Sativus), potatoes (Solanum tuberosum), and cucumbers (Cucumis Sativus). Journal of agricultural and food chemistry 59:11011-11018.

Lee HG, Lee YJ, Yang JH. 2012. Perfluorooctane sulfonate induces apoptosis of cerebellar granule cells via a ROS-dependent protein kinase C signaling pathway. Neurotoxicology 33:314-320.

Lee YY, Wong CK, Oger C, Durand T, Galano JM, Lee JC. 2015. Prenatal exposure to the contaminant perfluorooctane sulfonate elevates lipid peroxidation during mouse fetal development but not in the pregnant dam. Free radical research 49:1015-1025.

Lefebvre DE, Curran I, Armstrong C, Coady L, Parenteau M, Liston V, et al. 2008. Immunomodulatory effects of dietary potassium perfluorooctane sulfonate (PFOS) exposure in adult Sprague-Dawley rats. Journal of toxicology and environmental health Part A 71:1516-1525.

Leter G, Consales C, Eleuteri P, Uccelli R, Specht IO, Toft G, et al. 2014. Exposure to perfluoroalkyl substances and sperm DNA global methylation in Arctic and European populations. Environmental and molecular mutagenesis 55:591-600.

Leung YK, Ouyang B, Niu L, Xie C, Ying J, Medvedovic M, et al. 2018. Identification of sex-specific DNA methylation changes driven by specific chemicals in cord blood in a Faroese birth cohort. Epigenetics 13:290-300.

Li J, Cao H, Feng H, Xue Q, Zhang A, Fu J. 2020a. Evaluation of the Estrogenic/Antiestrogenic Activities of Perfluoroalkyl Substances and Their Interactions with the Human Estrogen Receptor by Combining in Vitro Assays and in Silico Modeling. Environmental Science and Technology 54:14514-14524.

Li L, Li X, Chen X, Chen Y, Liu J, Chen F, et al. 2018a. Perfluorooctane sulfonate impairs rat Leydig cell development during puberty. Chemosphere 190:43-53.

Li M, Huo X, Davuljigari CB, Dai Q, Xu X. 2019. MicroRNAs and their role in environmental chemical carcinogenesis. Environmental geochemistry and health 41:225-247.

Li P, Oyang X, Xie X, Li Z, Yang H, Xi J, et al. 2020b. Phytotoxicity induced by perfluorooctanoic acid and perfluorooctane sulfonate via metabolomics. Journal of hazardous materials 389:121852.

Li R, Guo C, Lin X, Chan TF, Lai KP, Chen J. 2020c. Integrative omics analyses uncover the mechanism underlying the immunotoxicity of perfluorooctanesulfonate in human lymphocytes. Chemosphere 256:127062.

Li W, He QZ, Wu CQ, Pan XY, Wang J, Tan Y, et al. 2015. PFOS Disturbs BDNF-ERK-CREB Signalling in Association with Increased MicroRNA-22 in SH-SY5Y Cells. BioMed research international 2015:302653.

Li Y, Men B, He Y, Xu H, Liu M, Wang D. 2017. Effect of single-wall carbon nanotubes on bioconcentration and toxicity of perfluorooctane sulfonate in zebrafish (Danio rerio). The Science of the total environment 607-608:509-518.

Li Y, Fletcher T, Mucs D, Scott K, Lindh CH, Tallving P, et al. 2018b. Half-lives of PFOS, PFHxS and PFOA after end of exposure to contaminated drinking water. Occupational and environmental medicine 75:46-51.

Liao X, Huang K, Huang R, Liu X, Han C, Yu L, et al. 2017. Genome-scale analysis to identify prognostic markers in patients with early-stage pancreatic ductal adenocarcinoma after pancreaticoduodenectomy. OncoTargets and therapy 10:4493-4506.

Liao Y, Wang J, Huang QS, Fang C, Kiyama R, Shen H, et al. 2012. Evaluation of cellular response to perfluorooctane sulfonate in human umbilical vein endothelial cells. Toxicology in vitro : an international journal published in association with BIBRA 26:421-428.

Liao Y, Dong S, Kiyama R, Cai P, Liu L, Shen H. 2013. Flos lonicerae extracts and chlorogenic acid protect human umbilical vein endothelial cells from the toxic damage of perfluorooctane sulphonate. Inflammation 36:767-779.

Lin CY, Chen PC, Lo SC, Torng PL, Sung FC, Su TC. 2016. The association of carotid intima-media thickness with serum Level of perfluorinated chemicals and endothelium-platelet microparticles in adolescents and young adults. Environment international 94:292-299.

Lin CY, Lee HL, Hwang YT, Su TC. 2020a. The association between total serum isomers of per- and polyfluoroalkyl substances, lipid profiles, and the DNA oxidative/nitrative stress biomarkers in middle-aged Taiwanese adults. Environmental research 182:109064.

Lin HW, Feng HX, Chen L, Yuan XJ, Tan Z. 2020b. Maternal exposure to environmental endocrine disruptors during pregnancy is associated with pediatric germ cell tumors. Nagoya journal of medical science 82:323-333.

Liu C, Gin KY, Chang VW. 2014. Multi-biomarker responses in green mussels exposed to PFCs: effects at molecular, cellular, and physiological levels. Environmental science and pollution research international 21:2785-2794.

Liu CY, Chen PC, Lien PC, Liao YP. 2018a. Prenatal Perfluorooctyl Sulfonate Exposure and Alu DNA Hypomethylation in Cord Blood. Int J Environ Res Public Health 15.

Liu G, Zhang S, Yang K, Zhu L, Lin D. 2016. Toxicity of perfluorooctane sulfonate and perfluorooctanoic acid to Escherichia coli: Membrane disruption, oxidative stress, and DNA damage induced cell inactivation and/or death. Environmental pollution (Barking, Essex : 1987) 214:806-815.

Liu H, Chen Q, Lei L, Zhou W, Huang L, Zhang J, et al. 2018b. Prenatal exposure to perfluoroalkyl and polyfluoroalkyl substances affects leukocyte telomere length in female newborns. Environmental Pollution 235:446-452.

Liu J, Mejia Avendaño S. 2013. Microbial degradation of polyfluoroalkyl chemicals in the environment: A review. Environment international 61:98-114.

Liu L, Liu W, Song J, Yu H, Jin Y, Oami K, et al. 2009. A comparative study on oxidative damage and distributions of perfluorooctane sulfonate (PFOS) in mice at different postnatal developmental stages. The Journal of toxicological sciences 34:245-254.

Liu Z, Lu Y, Wang P, Wang T, Liu S, Johnson AC, et al. 2017. Pollution pathways and release estimation of perfluorooctane sulfonate (PFOS) and perfluorooctanoic acid (PFOA) in central and eastern China. The Science of the total environment 580:1247-1256.

Logeshwaran P, Sivaram AK, Surapaneni A, Kannan K, Naidu R, Megharaj M. 2021. Exposure to perfluorooctanesulfonate (PFOS) but not perflurorooctanoic acid (PFOA) at

ppb concentration induces chronic toxicity in Daphnia carinata. The Science of the total environment 769:144577.

López-Doval S, Salgado R, Pereiro N, Moyano R, Lafuente A. 2014. Perfluorooctane sulfonate effects on the reproductive axis in adult male rats. Environmental Research 134:158-168.

López-Doval S, Salgado R, Lafuente A. 2016. The expression of several reproductive hormone receptors can be modified by perfluorooctane sulfonate (PFOS) in adult male rats. Chemosphere 155:488-497.

Lopez-Espinosa MJ, Mondal D, Armstrong BG, Eskenazi B, Fletcher T. 2016. Perfluoroalkyl substances, sex hormones, and insulin-like growth factor-1 at 6-9 years of age: A cross-sectional analysis within the C8 Health Project. Environmental Health Perspectives 124:1269-1275.

Louisse J, Rijkers D, Stoopen G, Janssen A, Staats M, Hoogenboom R, et al. 2020. Perfluorooctanoic acid (PFOA), perfluorooctane sulfonic acid (PFOS), and perfluorononanoic acid (PFNA) increase triglyceride levels and decrease cholesterogenic gene expression in human HepaRG liver cells. Archives of toxicology 94:3137-3155.

Lu H, Ouyang W, Huang C. 2006. Inflammation, a key event in cancer development. Molecular cancer research 4:221-233.

Lu L, Xu L, Kang T, Cheng S. 2012. Investigation of DNA damage treated with perfluorooctane sulfonate (PFOS) on ZrO2/DDAB active nano-order film. Biosensors & bioelectronics 35:180-185.

Lu L, Xu L, Kang T, Cheng S. 2013a. DNA damage due to perfluorooctane sulfonate based on nano-gold embedded in nano-porous poly-pyrrole film. Applied Surface Science 284:258-262.

Lu LP, Xu LH, Kang TF, Cheng SY. 2013b. DNA damage detection by Electrochemiluminescence sensor of CdS quantum dots. Fenxi Huaxue/ Chinese Journal of Analytical Chemistry 41:805-810.

Lupton SJ, Huwe JK, Smith DJ, Dearfield KL, Johnston JJ. 2014. Distribution and excretion of perfluorooctane sulfonate (PFOS) in beef cattle (Bos taurus). Journal of agricultural and food chemistry 62:1167-1173.

Lv QY, Wan B, Guo LH, Yang Y, Ren XM, Zhang H. 2015. In vivo immunotoxicity of perfluorooctane sulfonate in BALB/c mice: Identification of T-cell receptor and calcium-mediated signaling pathway disruption through gene expression profiling of the spleen. Chemico-biological interactions 240:84-93.

Lv Z, Wu W, Ge S, Jia R, Lin T, Yuan Y, et al. 2018. Naringin protects against perfluorooctane sulfonate-induced liver injury by modulating NRF2 and NF-κB in mice. International immunopharmacology 65:140-147.

Maestri L, Negri S, Ferrari M, Ghittori S, Fabris F, Danesino P, et al. 2006. Determination of perfluorooctanoic acid and perfluorooctanesulfonate in human tissues by liquid chromatography/single quadrupole mass spectrometry. Rapid Communications in Mass Spectrometry: An International Journal Devoted to the Rapid Dissemination of Up-to-the-Minute Research in Mass Spectrometry 20:2728-2734.

Maisonet M, Terrell ML, McGeehin MA, Christensen KY, Holmes A, Calafat AM, et al. 2012. Maternal concentrations of polyfluoroalkyl compounds during pregnancy and fetal and postnatal growth in British girls. Environmental health perspectives 120:1432-1437.

Maisonet M, Calafat AM, Marcus M, Jaakkola JJ, Lashen H. 2015. Prenatal Exposure to Perfluoroalkyl Acids and Serum Testosterone Concentrations at 15 Years of Age in Female ALSPAC Study Participants. Environmental health perspectives 123:1325-1330.

MalaCards. 2021a. Search results for serpina1. Available: https://www.malacards.org/search/results?query=serpina1, accessed on May 18, 2021.

MalaCards. 2021b. Search results for SMAD3. Available: https://www.malacards.org/search/results/SMAD3, accessed on May 18, 2021.

MalaCards. 2021c. Search results for SNAPIN. Available: https://www.malacards.org/search/results/SNAPIN, accessed on May 18, 2021.

MalaCards. 2021d. Search results for igf2. Available: https://www.malacards.org/search/results?query=igf2, accessed on August 30, 2021.

MalaCards. 2021e. Search results for CYP2E1. Available: https://www.malacards.org/search/results/CYP2E1, accessed on May 18, 2021.

MalaCards. 2021f. Search results for hla-dpa1. Available: https://www.malacards.org/search/results?query=hla-dpa1, accessed on August 30, 2021.

Mamsen LS, Björvang RD, Mucs D, Vinnars M-T, Papadogiannakis N, Lindh CH, et al. 2019. Concentrations of perfluoroalkyl substances (PFASs) in human embryonic and fetal organs from first, second, and third trimester pregnancies. Environment international 124:482-492.

Mancini FR, Cano-Sancho G, Gambaretti J, Marchand P, Boutron-Ruault MC, Severi G, et al. 2020. Perfluorinated alkylated substances serum concentration and breast cancer risk: Evidence from a nested case-control study in the French E3N cohort. International journal of cancer 146:917-928.

Mao Z, Xia W, Wang J, Chen T, Zeng Q, Xu B, et al. 2013. Perfluorooctane sulfonate induces apoptosis in lung cancer A549 cells through reactive oxygen species-mediated mitochondrion-dependent pathway. Journal of applied toxicology : JAT 33:1268-1276.

Maras M, Vanparys C, Muylle F, Robbens J, Berger U, Barber JL, et al. 2006. Estrogen-like properties of fluorotelomer alcohols as revealed by mcf-7 breast cancer cell proliferation. Environmental health perspectives 114:100-105.

Maronpot RR, Montgomery Jr CA, Boorman GA, McConnell EE. 1986. National Toxicology Program nomenclature for hepatoproliferative lesions of rats. Toxicologic pathology 14:263-273.

Martin JW, Asher BJ, Beesoon S, Benskin JP, Ross MS. 2010. PFOS or PreFOS? Are perfluorooctane sulfonate precursors (PreFOS) important determinants of human and environmental perfluorooctane sulfonate (PFOS) exposure? Journal of environmental monitoring : JEM 12:1979-2004.

Martin MT, Brennan RJ, Hu W, Ayanoglu E, Lau C, Ren H, et al. 2007. Toxicogenomic study of triazole fungicides and perfluoroalkyl acids in rat livers predicts toxicity and categorizes chemicals based on mechanisms of toxicity. Toxicological sciences : an official journal of the Society of Toxicology 97:595-613.

McConnell EE, Solleveld HA, Swenberg JA, Boorman GA. 1986. Guidelines for combining neoplasms for evaluation of rodent carcinogenesis studies. Journal of the National Cancer Institute 76:283-289.

Mense MG, Rosol TJ. 2018. Endocrine pancreas. . In: Boorman's pathology of the rat: reference and atlas, (Suttie AW, Leininger JR, Bradley AE, eds):Academic press by Elsevier.

Midgett K, Peden-Adams MM, Gilkeson GS, Kamen DL. 2015. In vitro evaluation of the effects of perfluorooctanesulfonic acid (PFOS) and perfluorooctanoic acid (PFOA) on IL-2 production in human T-cells. Journal of applied toxicology : JAT 35:459-465.

Mijit M, Caracciolo V, Melillo A, Amicarelli F, Giordano A. 2020. Role of p53 in the Regulation of Cellular Senescence. Biomolecules 10:420.

Miura R, Araki A, Miyashita C, Kobayashi S, Kobayashi S, Wang SL, et al. 2018. An epigenome-wide study of cord blood DNA methylations in relation to prenatal perfluoroalkyl substance exposure: The Hokkaido study. Environment international 115:21-28.

Mogensen UB, Grandjean P, Nielsen F, Weihe P, Budtz-Jørgensen E. 2015. Breastfeeding as an exposure pathway for perfluorinated alkylates. Environmental science & technology 49:10466-10473.

Mollenhauer MA, Bradshaw SG, Fair PA, McGuinn WD, Peden-Adams MM. 2011. Effects of perfluorooctane sulfonate (PFOS) exposure on markers of inflammation in

female B6C3F1 mice. Journal of environmental science and health Part A, Toxic/hazardous substances & environmental engineering 46:97-108.

Montfort A, Colacios C, Levade T, Andrieu-Abadie N, Meyer N, Ségui B. 2019. The TNF paradox in cancer progression and immunotherapy. Frontiers in immunology 10:1818.

More VR, Campos CR, Evans RA, Oliver KD, Chan GN, Miller DS, et al. 2017. PPAR-α, a lipid-sensing transcription factor, regulates blood-brain barrier efflux transporter expression. Journal of cerebral blood flow and metabolism : official journal of the International Society of Cerebral Blood Flow and Metabolism 37:1199-1212.

Morello-Frosch R, Cushing LJ, Jesdale BM, Schwartz JM, Guo W, Guo T, et al. 2016. Environmental Chemicals in an Urban Population of Pregnant Women and Their Newborns from San Francisco. Environmental science & technology 50:12464-12472.

Morris MR, Ricketts CJ, Gentle D, McRonald F, Carli N, Khalili H, et al. 2011. Genome-wide methylation analysis identifies epigenetically inactivated candidate tumour suppressor genes in renal cell carcinoma. Oncogene 30:1390-1401.

Nalbantlar B, Çakal Arslan Ö. 2017. Determination of the perflorooctane sulfonate-induced genotoxic response in Mytilus galloprovincialis using a micronucleus assay. Zoology and Ecology 27:161-167.

NCBI. 2021a. HLA-DPA1 major histocompatibility complex, class II, DP alpha 1 [Homo sapiens (human)]. Available: https://www.ncbi.nlm.nih.gov/gene/3113, accessed on August 30, 2021.

NCBI. 2021b. PRKCA protein kinase C alpha [Homo sapiens (human)]. Available: https://www.ncbi.nlm.nih.gov/gene/5578, accessed on May 18, 2021.

NCBI. 2021c. IGF2 insulin like growth factor 2 [Homo sapiens (human)]. Available: https://www.ncbi.nlm.nih.gov/gene/3481, accessed on August 30, 2021.

NCBI. 2021d. CYP2E1 cytochrome P450 family 2 subfamily E member 1 [Homo sapiens (human)]. Available: https://www.ncbi.nlm.nih.gov/gene/1571, accessed on May 18, 2021.

NCBI. 2021e. Homo sapiens gene SERPINA1, encoding serpin peptidase inhibitor, clade A (alpha-1 antiproteinase, antitrypsin), member 1. Available: https://www.ncbi.nlm.nih.gov/IEB/Research/Acembly/av.cgi?c=geneid&org=9606&l=5265, accessed on May 18, 2021.

Neeve SC, Robinson BW, Fear VS. 2019. The role and therapeutic implications of T cells in cancer of the lung. Clinical & Translational Immunology 8:e1076.

NICNAS. 2019a. Direct precursors to perfluorooctanesulfonate (PFOS): Environment tier II assessment. Australia's National Industrial Chemicals Notification and Assessment Scheme (NICNAS). Available:

https://www.industrialchemicals.gov.au/sites/default/files/Direct%20precursors%20to%20perfluorooctanesulfonate%20%28PFOS%29_%20Environment%20tier%20II%20assessment.pdf.

NICNAS. 2019b. Indirect precursors to perfluorooctanesulfonate (PFOS): Environment tier II assessment. Australia's National Industrial Chemicals Notification and Assessment Scheme (NICNAS). Available: https://www.industrialchemicals.gov.au/sites/default/files/Indirect%20precursors%20to%20perfluorooctanesulfonate%20%28PFOS%29_%20Environment%20tier%20II%20assessment.pdf.

NTP. 2015. Handbook for Preparing Report on Carcinogens Monographs. National Toxicology Program. Available: https://ntp.niehs.nih.gov/go/rochandbook.

NTP. 2019. NTP Technical Report on the Toxicity Studies of Perfluoroalkyl Sulfonates (Perfluorobutane Sulfonic Acid, Perfluorohexane Sulfonate Potassium Salt, and Perfluorooctane Sulfonic Acid) Administered by Gavage to Sprague Dawley (Hsd: Sprague Dawley SD) Rats. Research Triangle Park, North Carolina: National Toxicology Program. Available: https://ntp.niehs.nih.gov/ntp/htdocs/st_rpts/tox096_508.pdf?utm_source=direct&utm_medium=prod&utm_campaign=ntpgolinks&utm_term=tox096.

NTP. 2020. NTP Technical Report on the Toxicology and Carcinogenesis Studies of Perfluorooctanoic Acid (CASRN 335-67-1) Administered in Feed to Sprague Dawley (HSD:Sprague Dawley SD) Rats. Research Triangle Park, North Carolina. Available: https://ntp.niehs.nih.gov/ntp/htdocs/lt_rpts/tr598_508.pdf?utm_source=direct&utm_medium=prod&utm_campaign=ntpgolinks&utm_term=tr598.

O'Brien JM, Carew AC, Chu S, Letcher RJ, Kennedy SW. 2009. Perfluorooctane sulfonate (PFOS) toxicity in domestic chicken (Gallus gallus domesticus) embryos in the absence of effects on peroxisome proliferator activated receptor alpha (PPARalpha)-regulated genes. Comparative biochemistry and physiology Toxicology & pharmacology : CBP 149:524-530.

O'Brien JM, Austin AJ, Williams A, Yauk CL, Crump D, Kennedy SW. 2011. Technical-grade perfluorooctane sulfonate alters the expression of more transcripts in cultured chicken embryonic hepatocytes than linear perfluorooctane sulfonate. Environmental toxicology and chemistry 30:2846-2859.

O'Brien TM, Wallace KB. 2004. Mitochondrial permeability transition as the critical target of N-acetyl perfluorooctane sulfonamide toxicity in vitro. Toxicological Sciences 82:333-340.

Oda Y, Nakayama S, Harada KH, Koizumi A. 2007. Negative results ofumu genotoxicity test of fluorotelomer alcohols and perfluorinated alkyl acids. Environmental health and preventive medicine 12:217-219.

OECD. 2007. Lists of PFOS, PFAS, PFOA, PFCA, Related Compounds and Chemicals that may degrade to PFCA. Available: http://www.oecd.org/ehs/.

OECD. 2015. Working Towards a Global Emission Inventory of PFASs. Available: https://www.oecd.org/chemicalsafety/risk-management/Working%20Towards%20a%20Global%20Emission%20Inventory%20of%20PFASS.pdf.

OEHHA. 2021. Proposed Public Health Goals for Perfluorooctanoic Acid and Perfluorooctane Sulfonic Acid in Drinking Water.

Olsen GW, Hansen KJ, Stevenson LA, Burris JM, Mandel JH. 2003a. Human donor liver and serum concentrations of perfluorooctanesulfonate and other perfluorochemicals. Environmental science & technology 37:888-891.

Olsen GW, Logan PW, Hansen KJ, Simpson CA, Burris JM, Burlew MM, et al. 2003b. An occupational exposure assessment of a perfluorooctanesulfonyl fluoride production site: biomonitoring. AIHA journal : a journal for the science of occupational and environmental health and safety 64:651-659.

Olsen GW, Burlew MM, Marshall JC, Burris JM, Mandel JH. 2004. Analysis of episodes of care in a perfluorooctanesulfonyl fluoride production facility. Journal of occupational and environmental medicine 46:837-846.

Olsen GW, Burris JM, Ehresman DJ, Froelich JW, Seacat AM, Butenhoff JL, et al. 2007. Half-life of serum elimination of perfluorooctanesulfonate, perfluorohexanesulfonate, and perfluorooctanoate in retired fluorochemical production workers. Environmental Health Perspectives 115:1298-1305.

Olsen GW, Lange CC, Ellefson ME, Mair DC, Church TR, Goldberg CL, et al. 2012. Temporal trends of perfluoroalkyl concentrations in American Red Cross adult blood donors, 2000-2010. Environmental science & technology 46:6330-6338.

OMIM. 2021. Hook microtubule tethering protein 2; HOOK2. Available: https://omim.org/entry/607824, accessed on May 18, 2021.

Omoike OE, Pack RP, Mamudu HM, Liu Y, Wang L. 2020. A cross-sectional study of the association between perfluorinated chemical exposure and cancers related to deregulation of estrogen receptors. Environmental research:110329.

Onkes W, Fredrik R, Micci F, Schönbeck BJ, Martin-Subero JI, Ullmann R, et al. 2013. Breakpoint characterization of the der(19)t(11;19)(q13;p13) in the ovarian cancer cell line SKOV-3. Genes, chromosomes & cancer 52:512-522.

Ouidir M, Mendola P, Buck Louis GM, Kannan K, Zhang C, Tekola-Ayele F. 2020. Concentrations of persistent organic pollutants in maternal plasma and epigenome-wide placental DNA methylation. Clinical epigenetics 12:103.

Ouyang W, O'Garra A. 2019. IL-10 family cytokines IL-10 and IL-22: from basic science to clinical translation. Immunity 50:871-891.

Parolini M, Colombo G, Valsecchi S, Mazzoni M, Possenti CD, Caprioli M, et al. 2016. Potential toxicity of environmentally relevant perfluorooctane sulfonate (PFOS) concentrations to yellow-legged gull Larus michahellis embryos. Environmental science and pollution research international 23:426-437.

Paul AG, Jones KC, Sweetman AJ. 2009. A first global production, emission, and environmental inventory for perfluorooctane sulfonate. Environmental science & technology 43:386-392.

Payer LM, Steranka JP, Yang WR, Kryatova M, Medabalimi S, Ardeljan D, et al. 2017. Structural variants caused by Alu insertions are associated with risks for many human diseases. Proc Natl Acad Sci U S A 114:E3984-E3992.

Peden-Adams MM, Keller JM, Eudaly JG, Berger J, Gilkeson GS, Keil DE. 2008. Suppression of humoral immunity in mice following exposure to perfluorooctane sulfonate. Toxicological sciences : an official journal of the Society of Toxicology 104:144-154.

Peng S-Y, Zhang J, Tian M-P, Wang Z-L, Shen H-Q. 2012. Determination of Global DNA Methylation in Biological Samples by Liquid Chromatography-Tandem Mass Spectrometry. Chinese Journal of Analytical Chemistry 40:1201-1206.

Perera P-Y, Lichy JH, Waldmann TA, Perera LP. 2012. The role of interleukin-15 in inflammation and immune responses to infection: implications for its therapeutic use. Microbes and infection 14:247-261.

Pérez F, Nadal M, Navarro-Ortega A, Fàbrega F, Domingo JL, Barceló D, et al. 2013. Accumulation of perfluoroalkyl substances in human tissues. Environment international 59:354-362.

Petersen MS, Halling J, Jørgensen N, Nielsen F, Grandjean P, Jensen TK, et al. 2018. Reproductive Function in a Population of Young Faroese Men with Elevated Exposure to Polychlorinated Biphenyls (PCBs) and Perfluorinated Alkylate Substances (PFAS). Int J Environ Res Public Health 15.

Pierozan P, Karlsson O. 2018. PFOS induces proliferation, cell-cycle progression, and malignant phenotype in human breast epithelial cells. Archives of toxicology 92:705-716.

Pierozan P, Cattani D, Karlsson O. 2020. Perfluorooctane sulfonate (PFOS) and perfluorooctanoic acid (PFOA) induce epigenetic alterations and promote human breast cell carcinogenesis in vitro. Archives of toxicology 94:3893-3906.

Pinas V, Van Dijk C, Weber R. 2020. Inventory and action plan for PFOS and related substances in Suriname as basis for Stockholm Convention implementation. Emerging Contaminants 6:11.

Pinney SM, Biro FM, Windham GC, Herrick RL, Yaghjyan L, Calafat AM, et al. 2014. Serum biomarkers of polyfluoroalkyl compound exposure in young girls in Greater Cincinnati and the San Francisco Bay Area, USA. Environmental pollution (Barking, Essex : 1987) 184:327-334.

Pizzurro DM, Seeley M, Kerper LE, Beck BD. 2019. Interspecies differences in perfluoroalkyl substances (PFAS) toxicokinetics and application to health-based criteria. Regulatory toxicology and pharmacology : RTP 106:239-250.

Poothong S, Papadopoulou E, Padilla-Sánchez JA, Thomsen C, Haug LS. 2020. Multiple pathways of human exposure to poly- and perfluoroalkyl substances (PFASs): From external exposure to human blood. Environment international 134:105244.

Prevedouros K, Cousins IT, Buck RC, Korzeniowski SH. 2006. Sources, fate and transport of perfluorocarboxylates. Environmental science & technology 40:32-44.

Qazi MR, Bogdanska J, Butenhoff JL, Nelson BD, DePierre JW, Abedi-Valugerdi M. 2009a. High-dose, short-term exposure of mice to perfluorooctanesulfonate (PFOS) or perfluorooctanoate (PFOA) affects the number of circulating neutrophils differently, but enhances the inflammatory responses of macrophages to lipopolysaccharide (LPS) in a similar fashion. Toxicology 262:207-214.

Qazi MR, Xia Z, Bogdanska J, Chang SC, Ehresman DJ, Butenhoff JL, et al. 2009b. The atrophy and changes in the cellular compositions of the thymus and spleen observed in mice subjected to short-term exposure to perfluorooctanesulfonate are high-dose phenomena mediated in part by peroxisome proliferator-activated receptor-alpha (PPARα). Toxicology 260:68-76.

Qazi MR, Abedi MR, Nelson BD, DePierre JW, Abedi-Valugerdi M. 2010a. Dietary exposure to perfluorooctanoate or perfluorooctane sulfonate induces hypertrophy in centrilobular hepatocytes and alters the hepatic immune status in mice. International immunopharmacology 10:1420-1427.

Qazi MR, Nelson BD, Depierre JW, Abedi-Valugerdi M. 2010b. 28-Day dietary exposure of mice to a low total dose (7 mg/kg) of perfluorooctanesulfonate (PFOS) alters neither the cellular compositions of the thymus and spleen nor humoral immune responses: does the route of administration play a pivotal role in PFOS-induced immunotoxicity? Toxicology 267:132-139.

Qian Y, Ducatman A, Ward R, Leonard S, Bukowski V, Lan Guo N, et al. 2010. Perfluorooctane sulfonate (PFOS) induces reactive oxygen species (ROS) production in human microvascular endothelial cells: role in endothelial permeability. Journal of toxicology and environmental health Part A 73:819-836.

Qiu L, Wang H, Dong T, Huang J, Li T, Ren H, et al. 2021. Perfluorooctane sulfonate (PFOS) disrupts testosterone biosynthesis via CREB/CRTC2/StAR signaling pathway in Leydig cells. Toxicology 449:152663.

Qiu Z, Qu K, Luan F, Liu Y, Zhu Y, Yuan Y, et al. 2020. Binding specificities of estrogen receptor with perfluorinated compounds: A cross species comparison. Environment international 134:105284.

Qu JH, Lu CC, Xu C, Chen G, Qiu LL, Jiang JK, et al. 2016. Perfluorooctane sulfonate-induced testicular toxicity and differential testicular expression of estrogen receptor in male mice. Environmental toxicology and pharmacology 45:150-157.

Qu K, Song J, Zhu Y, Liu Y, Zhao C. 2019. Perfluorinated compounds binding to estrogen receptor of different species: a molecular dynamic modeling. Journal of Molecular Modeling 25:1.

Rankin K, Mabury SA, Jenkins TM, Washington JW. 2016. A North American and global survey of perfluoroalkyl substances in surface soils: Distribution patterns and mode of occurrence. Chemosphere 161:333-341.

Raymer JH, Michael LC, Studabaker WB, Olsen GW, Sloan CS, Wilcosky T, et al. 2012. Concentrations of perfluorooctane sulfonate (PFOS) and perfluorooctanoate (PFOA) and their associations with human semen quality measurements. Reproductive toxicology (Elmsford, NY) 33:419-427.

Reistad T, Fonnum F, Mariussen E. 2013. Perfluoroalkylated compounds induce cell death and formation of reactive oxygen species in cultured cerebellar granule cells. Toxicology letters 218:56-60.

Reuter S, Gupta SC, Chaturvedi MM, Aggarwal BB. 2010. Oxidative stress, inflammation, and cancer: how are they linked? Free radical biology and medicine 49:1603-1616.

Robertson D, Williams GH. 2017. Clinical and Translational Science: Principles of Human Research. 2nd ed. Amsterdam:Elsevier/Academic Press.

Robinson SL, Zeng X, Guan W, Sundaram R, Mendola P, Putnick DL, et al. 2020. Perfluorooctanoic acid (PFOA) or perfluorooctane sulfonate (PFOS) and DNA methylation in newborn dried blood spots in the Upstate KIDS cohort. Environmental research 194:110668.

Rosen MB, Schmid JE, Das KP, Wood CR, Zehr RD, Lau C. 2009. Gene expression profiling in the liver and lung of perfluorooctane sulfonate-exposed mouse fetuses: Comparison to changes induced by exposure to perfluorooctanoic acid. Reproductive Toxicology 27:278-288.

Rosen MB, Schmid JR, Corton JC, Zehr RD, Das KP, Abbott BD, et al. 2010. Gene Expression Profiling in Wild-Type and PPARα-Null Mice Exposed to Perfluorooctane Sulfonate Reveals PPARα-Independent Effects. PPAR research 2010.

Rosen MB, Das KP, Wood CR, Wolf CJ, Abbott BD, Lau C. 2013. Evaluation of perfluoroalkyl acid activity using primary mouse and human hepatocytes. Toxicology 308:129-137.

Rosen MB, Das KP, Rooney J, Abbott B, Lau C, Corton JC. 2017. PPARα-independent transcriptional targets of perfluoroalkyl acids revealed by transcript profiling. Toxicology 387:95-107.

Rosenmai AK, Ahrens L, le Godec T, Lundqvist J, Oskarsson A. 2018. Relationship between peroxisome proliferator-activated receptor alpha activity and cellular concentration of 14 perfluoroalkyl substances in HepG2 cells. Journal of applied toxicology : JAT 38:219-226.

Ross MS, Wong CS, Martin JW. 2012. Isomer-specific biotransformation of perfluorooctane sulfonamide in Sprague-Dawley rats. Environmental science & technology 46:3196-3203.

Rothman KJ, Greenland S, Lash TL. 2015. Modern Epidemiology:Wolters Kluwer Health/Lippincott Williams & Wilkins.

Sant KE, Sinno PP, Jacobs HM, Timme-Laragy AR. 2018. Nrf2a modulates the embryonic antioxidant response to perfluorooctanesulfonic acid (PFOS) in the zebrafish, Danio rerio. Aquatic toxicology (Amsterdam, Netherlands) 198:92-102.

Sayed ME, Yuan L, Robin JD, Tedone E, Batten K, Dahlson N, et al. 2019. NOVA1 directs PTBP1 to hTERT pre-mRNA and promotes telomerase activity in cancer cells. Oncogene 38:2937-2952.

Schecter A, Malik-Bass N, Calafat AM, Kato K, Colacino JA, Gent TL, et al. 2012. Polyfluoroalkyl compounds in Texas children from birth through 12 years of age. Environmental health perspectives 120:590-594.

Schultes L, Sandblom O, Broeg K, Bignert A, Benskin JP. 2020. Temporal Trends (1981–2013) of Per- and Polyfluoroalkyl Substances and Total Fluorine in Baltic cod (Gadus morhua). Environmental toxicology and chemistry 39:300-309.

Schulz K, Silva MR, Klaper R. 2020. Distribution and effects of branched versus linear isomers of PFOA, PFOS, and PFHxS: A review of recent literature. Science of The Total Environment 733:139186.

Seacat AM, Thomford PJ, Hansen KJ, Clemen LA, Eldridge SR, Elcombe CR, et al. 2003. Sub-chronic dietary toxicity of potassium perfluorooctanesulfonate in rats. Toxicology 183:117-131.

Sepulvado JG, Blaine AC, Hundal LS, Higgins CP. 2011. Occurrence and fate of perfluorochemicals in soil following the land application of municipal biosolids. Environmental science & technology 45:8106-8112.

Sethi G, Sung B, Aggarwal BB. 2008. TNF: a master switch for inflammation to cancer. Front biosci 13:5094-5107.

Shan G, Wang Z, Zhou L, Du P, Luo X, Wu Q, et al. 2016. Impacts of daily intakes on the isomeric profiles of perfluoroalkyl substances (PFASs) in human serum. Environment international 89-90:62-70.

Shao X, Zhao B, Wang B, Zhao B, Zhu Y, Yuan Z, et al. 2019. Neuroprotective effects of blueberry anthocyanins against perfluorooctanoic sulfonate on planarian Dugesia japonica. Ecotoxicology and environmental safety 175:39-47.

Shapiro AJ, Antoni S, Guyton KZ, Lunn RM, Loomis D, Rusyn I, et al. 2018. Software tools to facilitate systematic review used for cancer hazard identification. Environmental health perspectives 126:104501.

Shaul ME, Fridlender ZG. 2019. Tumour-associated neutrophils in patients with cancer. Nature Reviews Clinical Oncology 16:601-620.

Shaw SD, Berger ML, Harris JH, Yun SH, Wu Q, Liao C, et al. 2013. Persistent organic pollutants including polychlorinated and polybrominated dibenzo-p-dioxins and dibenzofurans in firefighters from Northern California. Chemosphere 91:1386-1394.

Shearer JJ, Callahan CL, Calafat AM, Huang WY, Jones RR, Sabbisetti VS, et al. 2020. Serum concentrations of per- and polyfluoroalkyl substances and risk of renal cell carcinoma. Journal of the National Cancer Institute.

Shi X, Zhou B. 2010. The role of Nrf2 and MAPK pathways in PFOS-induced oxidative stress in zebrafish embryos. Toxicological sciences : an official journal of the Society of Toxicology 115:391-400.

Shimada H, Nakashima K, Ochiai T, Nabeya Y, Takiguchi M, Nomura F, et al. 2005. Serological identification of tumor antigens of esophageal squamous cell carcinoma. International journal of oncology 26:77-86.

Shin HM, Moschet C, Young TM, Bennett DH. 2020. Measured concentrations of consumer product chemicals in California house dust: Implications for sources, exposure, and toxicity potential. Indoor Air 30:60-75.

Shipley JM, Hurst CH, Tanaka SS, DeRoos FL, Butenhoff JL, Seacat AM, et al. 2004. Trans-activation of PPARα and induction of PPARα target genes by perfluorooctane-based chemicals. Toxicological Sciences 80:151-160.

Shitani M, Sasaki S, Akutsu N, Takagi H, Suzuki H, Nojima M, et al. 2012. Genome-wide analysis of DNA methylation identifies novel cancer-related genes in hepatocellular

carcinoma. Tumour biology : the journal of the International Society for Oncodevelopmental Biology and Medicine 33:1307-1317.

Sibinsky LJ. 1987. Two Year Oral <Diet> Toxicity/Carcinogenicity Study of Fluorochemical FC-143 in Rats. St. Paul, MN: 3M.

Singh AK, Verma S, Kushwaha PP, Prajapati KS, Shuaib M, Kumar S, et al. 2021. Role of ZBTB7A zinc finger in tumorigenesis and metastasis. Molecular biology reports.

Sivaram AK, Logeshwaran P, Surapaneni A, Shah K, Crosbie N, Rogers Z, et al. 2020. Evaluation of Cyto-genotoxicity of Perfluorooctane Sulfonate (PFOS) to Allium cepa. Environmental toxicology and chemistry.

Slotkin TA, MacKillop EA, Melnick RL, Thayer KA, Seidler FJ. 2008. Developmental neurotoxicity of perfluorinated chemicals modeled in vitro. Environmental health perspectives 116:716-722.

Smith MT, Guyton KZ, Gibbons CF, Fritz JM, Portier CJ, Rusyn I, et al. 2016. Key characteristics of carcinogens as a basis for organizing data on mechanisms of carcinogenesis. Environmental health perspectives 124:713-721.

Smith MT, Guyton KZ, Kleinstreuer N, Borrel A, Cardenas A, Chiu WA, et al. 2020. The Key Characteristics of Carcinogens: Relationship to the Hallmarks of Cancer, Relevant Biomarkers, and Assays to Measure Them. Cancer Epidemiol Biomarkers Prev 29:1887-1903.

Soloff AC, Wolf BJ, White ND, Muir D, Courtney S, Hardiman G, et al. 2017. Environmental perfluorooctane sulfonate exposure drives T cell activation in bottlenose dolphins. Journal of applied toxicology : JAT 37:1108-1116.

Sonkar R, Kay MK, Choudhury M. 2019. PFOS Modulates Interactive Epigenetic Regulation in First-Trimester Human Trophoblast Cell Line HTR-8/SV(neo). Chemical research in toxicology 32:2016-2027.

Sonthithai P, Suriyo T, Thiantanawat A, Watcharasit P, Ruchirawat M, Satayavivad J. 2016. Perfluorinated chemicals, PFOS and PFOA, enhance the estrogenic effects of 17β-estradiol in T47D human breast cancer cells. Journal of applied toxicology : JAT 36:790-801.

Sørli JB, Låg M, Ekeren L, Perez-Gil J, Haug LS, Da Silva E, et al. 2020. Per- and polyfluoroalkyl substances (PFASs) modify lung surfactant function and pro-inflammatory responses in human bronchial epithelial cells. Toxicology in vitro : an international journal published in association with BIBRA 62:104656.

Spachmo B, Arukwe A. 2012. Endocrine and developmental effects in Atlantic salmon (Salmo salar) exposed to perfluorooctane sulfonic or perfluorooctane carboxylic acids. Aquatic toxicology (Amsterdam, Netherlands) 108:112-124.

Stahl LL, Snyder BD, Olsen AR, Kincaid TM, Wathen JB, McCarty HB. 2014. Perfluorinated compounds in fish from U.S. urban rivers and the Great Lakes. The Science of the total environment 499:185-195.

Stahl T, Heyn J, Thiele H, Huther J, Failing K, Georgii S, et al. 2009. Carryover of perfluorooctanoic acid (PFOA) and perfluorooctane sulfonate (PFOS) from soil to plants. Archives of environmental contamination and toxicology 57:289-298.

Steenland K, Winquist A. 2021. PFAS and cancer, a scoping review of the epidemiologic evidence. Environmental research 194:110690.

Strynar MJ, Lindstrom AB. 2008. Perfluorinated compounds in house dust from Ohio and North Carolina, USA. Environmental science & technology 42:3751-3756.

Strynar MJ, Lindstrom AB, Nakayama SF, Egeghy PP, Helfant LJ. 2012. Pilot scale application of a method for the analysis of perfluorinated compounds in surface soils. Chemosphere 86:252-257.

Sui J, Yang S, Liu T, Wu W, Xu S, Yin L, et al. 2019. Molecular characterization of lung adenocarcinoma: A potential four-long noncoding RNA prognostic signature. Journal of cellular biochemistry 120:705-714.

Sun P, Gu L, Luo J, Qin Y, Sun L, Jiang S. 2019. ROS-mediated JNK pathway critically contributes to PFOS-triggered apoptosis in SH-SY5Y cells. Neurotoxicology and teratology 75:106821.

Sunderland EM, Hu XC, Dassuncao C, Tokranov AK, Wagner CC, Allen JG. 2019. A review of the pathways of human exposure to poly- and perfluoroalkyl substances (PFASs) and present understanding of health effects. Journal of exposure science & environmental epidemiology 29:131-147.

Surma M, Wiczkowski W, Zieliński H, Cieslik E. 2015. Determination of Selected Perfluorinated Acids (PFCAs) and Perfluorinated Sulfonates (PFASs) in Food Contact Materials Using LC-MS/MS. Packaging Technology and Science 28:11.

Szikszai K, Krejcik Z, Klema J, Loudova N, Hrustincova A, Belickova M, et al. 2020. LncRNA Profiling Reveals That the Deregulation of H19, WT1-AS, TCL6, and LEF1-AS1 Is Associated with Higher-Risk Myelodysplastic Syndrome. Cancers 12.

Takacs ML, Abbott BD. 2007. Activation of mouse and human peroxisome proliferator-activated receptors (alpha, beta/delta, gamma) by perfluorooctanoic acid and perfluorooctane sulfonate. Toxicological sciences : an official journal of the Society of Toxicology 95:108-117.

Tao L, Kannan K, Wong CM, Arcaro KF, Butenhoff JL. 2008. Perfluorinated compounds in human milk from Massachusetts, U.S.A. Environmental science & technology 42:3096-3101.

Tarazona JV, Rodríguez C, Alonso E, Sáez M, González F, San Andrés MD, et al. 2016. Toxicokinetics of perfluorooctane sulfonate in rabbits under environmentally realistic exposure conditions and comparative assessment between mammals and birds. Toxicology letters 241:200-206.

Thiesen HJ. 1990. Multiple genes encoding zinc finger domains are expressed in human T cells. The New biologist 2:363-374.

Thomas DC. 2009. Chapter 5: Some special-purpose designs. In: Statistical Methods in Environmental Epidemiology. New York:Oxford University Press, 92-109.

Thomas RS, Bahadori T, Buckley TJ, Cowden J, Deisenroth C, Dionisio KL, et al. 2019. The next generation blueprint of computational toxicology at the US Environmental Protection Agency. Toxicological Sciences 169:317-332.

Thomford PJ. 2002. 104-Week Dietary Chronic Toxicity and Carcinogenicity Study with Perfluorooctane Sulfonic Acid Potassium Salt (PFOS; T-6295) in Rats. In: 3M T-6295. Madison, WI.: Covance Laboratories.

Tian J, Xu H, Zhang Y, Shi X, Wang W, Gao H, et al. 2019a. SAM targeting methylation by the methyl donor, a novel therapeutic strategy for antagonize PFOS transgenerational fertilitty toxicity. Ecotoxicology and environmental safety 184:109579.

Tian YP, Zeng XW, Bloom MS, Lin S, Wang SQ, Yim SHL, et al. 2019b. Isomers of perfluoroalkyl substances and overweight status among Chinese by sex status: Isomers of C8 Health Project in China. Environment international 124:130-138.

Tjønneland A, Olsen A, Boll K, Stripp C, Christensen J, Engholm G, et al. 2007. Study design, exposure variables, and socioeconomic determinants of participation in Diet, Cancer and Health: a population-based prospective cohort study of 57,053 men and women in Denmark. Scandinavian journal of public health 35:432-441.

Toft G, Jönsson BA, Bonde JP, Nørgaard-Pedersen B, Hougaard DM, Cohen A, et al. 2016. Perfluorooctane Sulfonate Concentrations in Amniotic Fluid, Biomarkers of Fetal Leydig Cell Function, and Cryptorchidism and Hypospadias in Danish Boys (1980-1996). Environmental health perspectives 124:151-156.

Trosko JE, Ruch RJ. 1998. Cell-cell communication in carcinogenesis. Front Biosci 3:d208-236.

Trowbridge J, Gerona RR, Lin T, Rudel RA, Bessonneau V, Buren H, et al. 2020. Exposure to Perfluoroalkyl Substances in a Cohort of Women Firefighters and Office Workers in San Francisco. Environmental Science and Technology 54:3363-3374.

Trudel D, Horowitz L, Wormuth M, Scheringer M, Cousins IT, Hungerbühler K. 2008. Estimating consumer exposure to PFOS and PFOA. Risk Analysis 28:251-269.

Tsai MS, Lin CY, Lin CC, Chen MH, Hsu SH, Chien KL, et al. 2015. Association between perfluoroalkyl substances and reproductive hormones in adolescents and young adults. International journal of hygiene and environmental health 218:437-443.

Tsai MS, Chang SH, Kuo WH, Kuo CH, Li SY, Wang MY, et al. 2020. A case-control study of perfluoroalkyl substances and the risk of breast cancer in Taiwanese women. Environment international 142:105850.

UNEP. 2006. PERFLUOROOCTANE SULFONATE RISK PROFILE; Adopted by the Persistent Organic Pollutants Review Committee at its second meeting (United Nations Environment Programme). Available: http://chm.pops.int/Portals/0/download.aspx?d=UNEP-POPS-POPRC.2-17-Add.5.English.pdf.

Unver N, McAllister F. 2018. IL-6 family cytokines: Key inflammatory mediators as biomarkers and potential therapeutic targets. Cytokine & growth factor reviews 41:10-17.

Upham BL, Deocampo ND, Wurl B, Trosko JE. 1998. Inhibition of gap junctional intercellular communication by perfluorinated fatty acids is dependent on the chain length of the fluorinated tail. International journal of cancer 78:491-495.

Uribe-Querol E, Rosales C. 2015. Neutrophils in Cancer: Two Sides of the Same Coin. Journal of Immunology Research 2015:983698.

US EPA. 2016a. Drinking Water Health Advisory for Perfluorooctane Sulfonate (PFOS). Washington DC: United States Environmental Protection Agency. Available: https://www.epa.gov/sites/default/files/2016-05/documents/pfos_health_advisory_final-plain.pdf.

US EPA. 2016b. Health Effects Support Document for Perfluorooctane Sulfonate (PFOS). EPA Document Number: 822-R-16-002. Available: https://www.epa.gov/sites/production/files/2016-05/documents/pfos_hesd_final_508.pdf.

van den Dungen MW, Rijk JC, Kampman E, Steegenga WT, Murk AJ. 2015. Steroid hormone related effects of marine persistent organic pollutants in human H295R adrenocortical carcinoma cells. Toxicology in vitro : an international journal published in association with BIBRA 29:769-778.

van den Dungen MW, Murk AJ, Kampman E, Steegenga WT, Kok DE. 2017a. Association between DNA methylation profiles in leukocytes and serum levels of persistent organic pollutants in Dutch men. Environmental epigenetics 3:dvx001.

van den Dungen MW, Murk AJ, Kok DE, Steegenga WT. 2017b. Persistent organic pollutants alter DNA methylation during human adipocyte differentiation. Toxicology in vitro : an international journal published in association with BIBRA 40:79-87.

van Zwieten MJ. 1984. The rat as animal model in breast cancer research: a histopathological study of radiation-and hormone-induced rat mammary tumors.

Vanden Heuvel JP, Thompson JT, Frame SRSR, Gillies PJ. 2006. Differential activation of nuclear receptors by perfluorinated fatty acid analogs and natural fatty acids: A comparison of human, mouse, and rat peroxisome proliferator-activated receptor-α, -β, and -γ, liver X receptor-β, and retinoid X receptor-α. Toxicological Sciences 92:476-489.

Verner M-A, Ngueta G, Jensen ET, Fromme H, Völkel W, Nygaard UC, et al. 2016. A Simple Pharmacokinetic Model of Prenatal and Postnatal Exposure to Perfluoroalkyl Substances (PFASs). Environmental science & technology 50:978-986.

Vested A, Ramlau-Hansen CH, Olsen SF, Bonde JP, Kristensen SL, Halldorsson TI, et al. 2013. Associations of in utero exposure to perfluorinated alkyl acids with human semen quality and reproductive hormones in adult men. Environmental health perspectives 121:453-458.

Vestergren R, Cousins IT, Trudel D, Wormuth M, Scheringer M. 2008. Estimating the contribution of precursor compounds in consumer exposure to PFOS and PFOA. Chemosphere 73:1617-1624.

Vestergren R, Herzke D, Wang T, Cousins IT. 2015. Are imported consumer products an important diffuse source of PFASs to the Norwegian environment? Environmental pollution (Barking, Essex : 1987) 198:223-230.

Vetvicka V, Vetvickova J. 2013. Reversal of perfluorooctanesulfonate-induced immunotoxicity by a glucan-resveratrol-vitamin C combination. Oriental Pharmacy and Experimental Medicine 13:77-84.

Vidal A, Babut M, Garric J, Beaudouin R. 2019. Elucidating the fate of perfluorooctanoate sulfonate using a rainbow trout (Oncorhynchus mykiss) physiologically-based toxicokinetic model. The Science of the total environment 691:1297-1309.

Vivier E, Tomasello E, Baratin M, Walzer T, Ugolini S. 2008. Functions of natural killer cells. Nature Immunology 9:503-510.

Vollmers HP, Brändlein S. 2009. Natural antibodies and cancer. New Biotechnology 25:294-298.

Vriens A, Nawrot TS, Janssen BG, Baeyens W, Bruckers L, Covaci A, et al. 2019. Exposure to environmental pollutants and their association with biomarkers of aging: A multipollutant approach. Environmental science & technology 53:5966-5976.

Wan YJ, Li YY, Xia W, Chen J, Lv ZQ, Zeng HC, et al. 2010. Alterations in tumor biomarker GSTP gene methylation patterns induced by prenatal exposure to PFOS. Toxicology 274:57-64.

Wang C, Nie X, Zhang Y, Li T, Mao J, Liu X, et al. 2015a. Reactive oxygen species mediate nitric oxide production through ERK/JNK MAPK signaling in HAPI microglia after PFOS exposure. Toxicology and applied pharmacology 288:143-151.

Wang F, Liu W, Jin Y, Wang F, Ma J. 2015b. Prenatal and neonatal exposure to perfluorooctane sulfonic acid results in aberrant changes in miRNA expression profile and levels in developing rat livers. Environmental toxicology 30:712-723.

Wang G, Sun S, Wu X, Yang S, Wu Y, Zhao J, et al. 2020a. Intestinal environmental disorders associate with the tissue damages induced by perfluorooctane sulfonate exposure. Ecotoxicology and environmental safety 197.

Wang L, Wenners A, Hilpert F, Fredrik R, Micci F, Onkes W, et al. 2014. Frequent translocations of 11q13.2 and 19p13.2 in ovarian cancer. Genes, chromosomes & cancer 53:447-453.

Wang M, Park JS, Petreas M. 2011. Temporal changes in the levels of perfluorinated compounds in California women's serum over the past 50 years. Environmental science & technology 45:7510-7516.

Wang X, Lin Y. 2008. Tumor necrosis factor and cancer, buddies or foes? 1. Acta Pharmacologica Sinica 29:1275-1288.

Wang X, Zhao G, Liang J, Jiang J, Chen N, Yu J, et al. 2013. PFOS-induced apoptosis through mitochondrion-dependent pathway in human-hamster hybrid cells. Mutation research 754:51-57.

Wang X, Liu L, Zhang W, Zhang J, Du X, Huang Q, et al. 2017. Serum metabolome biomarkers associate low-level environmental perfluorinated compound exposure with oxidative /nitrosative stress in humans. Environmental pollution (Barking, Essex : 1987) 229:168-176.

Wang X, Bai Y, Tang C, Cao X, Chang F, Chen L. 2018a. Impact of Perfluorooctane Sulfonate on Reproductive Ability of Female Mice through Suppression of Estrogen Receptor α-Activated Kisspeptin Neurons. Toxicological sciences : an official journal of the Society of Toxicology 165:475-486.

Wang Y, Zhang X, Wang M, Cao Y, Wang X, Liu Y, et al. 2015c. Mutagenic Effects of Perfluorooctanesulfonic Acid in gpt Delta Transgenic System Are Mediated by Hydrogen Peroxide. Environmental science & technology 49:6294-6303.

Wang Y, Zhong Y, Li J, Zhang J, Lyu B, Zhao Y, et al. 2018b. Occurrence of perfluoroalkyl substances in matched human serum, urine, hair and nail. Journal of environmental sciences (China) 67:191-197.

Wang Y, Zhu M, Guo F, Song Y, Fan X, Qin G. 2020b. Identification of Tumor Microenvironment-Related Prognostic Biomarkers in Luminal Breast Cancer. Frontiers in genetics 11:555865.

Wang Y, Aimuzi R, Nian M, Zhang Y, Luo K, Zhang J. 2021. Perfluoroalkyl substances and sex hormones in postmenopausal women: NHANES 2013-2016. Environment international 149:106408.

Watkins DJ, Wellenius GA, Butler RA, Bartell SM, Fletcher T, Kelsey KT. 2014. Associations between serum perfluoroalkyl acids and LINE-1 DNA methylation. Environment international 63:71-76.

Wen KX, Miliç J, El-Khodor B, Dhana K, Nano J, Pulido T, et al. 2016a. The Role of DNA Methylation and Histone Modifications in Neurodegenerative Diseases: A Systematic Review. PloS one 11:e0167201.

Wen LL, Lin CY, Chou HC, Chang CC, Lo HY, Juan SH. 2016b. Perfluorooctanesulfonate Mediates Renal Tubular Cell Apoptosis through PPARgamma Inactivation. PloS one 11:e0155190.

Wen LL, Chen YT, Lee YG, Ko TL, Chou HC, Juan SH. 2021. Perfluorooctane sulfonate induces autophagy-associated apoptosis through oxidative stress and the activation of extracellular signal-regulated kinases in renal tubular cells. PloS one 16:e0245442.

Whitehead HD, Venier M, Wu Y, Eastman E, Urbanik S, Diamond ML, et al. 2021. Fluorinated Compounds in North American Cosmetics. Environmental science & technology letters.

Wielsøe M, Long M, Ghisari M, Bonefeld-Jørgensen EC. 2015. Perfluoroalkylated substances (PFAS) affect oxidative stress biomarkers in vitro. Chemosphere 129:239-245.

Wielsøe M, Kern P, Bonefeld-Jørgensen EC. 2017. Serum levels of environmental pollutants is a risk factor for breast cancer in Inuit: a case control study. Environmental health : a global access science source 16:56.

Wielsøe M, Eiberg H, Ghisari M, Kern P, Lind O, Bonefeld-Jorgensen EC. 2018. Genetic Variations, Exposure to Persistent Organic Pollutants and Breast Cancer Risk - A Greenlandic Case-Control Study. Basic & clinical pharmacology & toxicology 123:335-346.

Winkens K, Giovanoulis G, Koponen J, Vestergren R, Berger U, Karvonen AM, et al. 2018. Perfluoroalkyl acids and their precursors in floor dust of children's bedrooms - Implications for indoor exposure. Environment international 119:493-502.

Wolf CJ, Takacs ML, Schmid JE, Lau C, Abbott BD. 2008. Activation of mouse and human peroxisome proliferator-activated receptor alpha by perfluoroalkyl acids of different functional groups and chain lengths. Toxicological sciences : an official journal of the Society of Toxicology 106:162-171.

Wolf CJ, Rider CV, Lau C, Abbott BD. 2014. Evaluating the additivity of perfluoroalkyl acids in binary combinations on peroxisome proliferator-activated receptor-α activation. Toxicology 316:43-54.

Wong F, MacLeod M, Mueller JF, Cousins IT. 2014. Enhanced elimination of perfluorooctane sulfonic acid by menstruating women: evidence from population-based pharmacokinetic modeling. Environmental science & technology 48:8807-8814.

Woo C-H, Eom Y-W, Yoo M-H, You H-J, Han HJ, Song WK, et al. 2000. Tumor necrosis factor-α generates reactive oxygen species via a cytosolic phospholipase A2-linked cascade. Journal of Biological Chemistry 275:32357-32362.

Wu J, Yang Y, Song J. 2020a. Expression of SLC17A9 in hepatocellular carcinoma and its clinical significance. Oncology letters 20:182.

Wu Y, Romanak K, Bruton T, Blum A, Venier M. 2020b. Per- and polyfluoroalkyl substances in paired dust and carpets from childcare centers. Chemosphere 251:126771.

Xiang S, Shi X, Chen P, Chen Y, Bing S, Jin X, et al. 2021. Targeting Cul3-scaffold E3 ligase complex via KLHL substrate adaptors for cancer therapy. Pharmacological research 169:105616.

Xiao F, Hanson RA, Golovko SA, Golovko MY, Arnold WA. 2018. PFOA and PFOS Are Generated from Zwitterionic and Cationic Precursor Compounds During Water Disinfection with Chlorine or Ozone. Environmental Science and Technology Letters:7.

Xie W, Wu Q, Kania-Korwel I, Tharappel JC, Telu S, Coleman MC, et al. 2009. Subacute exposure to N-ethyl perfluorooctanesulfonamidoethanol results in the formation of perfluorooctanesulfonate and alters superoxide dismutase activity in female rats. Archives of toxicology 83:909-924.

Xie X, Weng X, Liu S, Chen J, Guo X, Gao X, et al. 2021. Perfluoroalkyl and polyfluoroalkyl substance exposure and association with sex hormone concentrations: results from the NHANES 2015–2016. Environmental sciences Europe 33:69.

Xing J, Wang G, Zhao J, Wang E, Yin B, Fang D, et al. 2016. Toxicity assessment of perfluorooctane sulfonate using acute and subchronic male C57BL/6J mouse models. Environmental pollution (Barking, Essex : 1987) 210:388-396.

Xu B, Chen X, Mao Z, Chen M, Han X, Du G, et al. 2013a. Perfluorooctane sulfonate disturbs Nanog expression through miR-490-3p in mouse embryonic stem cells. PloS one 8:e74968.

Xu B, Ji X, Chen X, Yao M, Han X, Chen M, et al. 2015. Effect of perfluorooctane sulfonate on pluripotency and differentiation factors in mouse embryoid bodies. Toxicology 328:160-167.

Xu C, Jiang ZY, Liu Q, Liu H, Gu A. 2017. Estrogen receptor beta mediates hepatotoxicity induced by perfluorooctane sulfonate in mouse. Environmental science and pollution research international 24:13414-13423.

Xu D, Li C, Wen Y, Liu W. 2013b. Antioxidant defense system responses and DNA damage of earthworms exposed to perfluorooctane sulfonate (PFOS). Environmental pollution (Barking, Essex : 1987) 174:121-127.

Xu L, Krenitsky DM, Seacat AM, Butenhoff JL, Anders MW. 2004. Biotransformation of N-ethyl-N-(2-hydroxyethyl)perfluorooctanesulfonamide by rat liver microsomes, cytosol, and slices and by expressed rat and human cytochromes P450. Chemical research in toxicology 17:767-775.

Xu M, Wan J, Niu Q, Liu R. 2019. PFOA and PFOS interact with superoxide dismutase and induce cytotoxicity in mouse primary hepatocytes: A combined cellular and molecular methods. Environmental research 175:63-70.

Yan S, Wang J, Zhang W, Dai J. 2014. Circulating microRNA profiles altered in mice after 28 d exposure to perfluorooctanoic acid. Toxicology letters 224:24-31.

Yang L, Wang Z, Shi Y, Li J, Wang Y, Zhao Y, et al. 2016. Human placental transfer of perfluoroalkyl acid precursors: levels and profiles in paired maternal and cord serum. Chemosphere 144:1631-1638.

Yao X, Zhong L. 2005. Genotoxic risk and oxidative DNA damage in HepG2 cells exposed to perfluorooctanoic acid. Mutation research 587:38-44.

Ye L, Zhao B, Yuan K, Chu Y, Li C, Zhao C, et al. 2012. Gene expression profiling in fetal rat lung during gestational perfluorooctane sulfonate exposure. Toxicology letters 209:270-276.

Yu H, Sun J, Jiang S, Xu Y. 2019. MicroRNA-490-3p regulates cell proliferation and apoptosis in gastric cancer via direct targeting of AKT1. Exp Ther Med 17:1330-1336.

Zarei MH, Hosseini Shirazi SF, Aghvami M, Pourahmad J. 2018. Perfluorooctanesulfonate (PFOS) induces apoptosis signaling and proteolysis in human lymphocytes through ROS mediated mitochondrial dysfunction and lysosomal membrane labialization. Iranian journal of pharmaceutical research : IJPR 17:995-1007.

Zhang DY, Xu XL, Shen XY, Wang L, Lu Y, Xu HY, et al. 2013a. The effects of perfluorooctane sulfonate(PFOS) on proliferation of mouse leydig cells in vitro. In: Advanced Materials Research, Vol. 726-731, 824-828.

Zhang DY, Xu XL, Shen XY, Ruan Q, Hu WL. 2015a. Analysis of apoptosis induced by perfluorooctane sulfonates (PFOS) in mouse Leydig cells in vitro. Toxicology mechanisms and methods 25:21-25.

Zhang H, Bao J, Zhao S, Huo Z, Li B. 2019. MicroRNA-490-3p suppresses hepatocellular carcinoma cell proliferation and migration by targeting the aurora kinase A gene (AURKA). Arch Med Sci 16:395-406.

Zhang H, Lu H, Chen P, Chen X, Sun C, Ge RS, et al. 2020. Effects of gestational Perfluorooctane Sulfonate exposure on the developments of fetal and adult Leydig cells in F1 males. Environmental Pollution 262.

Zhang L, Li YY, Zeng HC, Wei J, Wan YJ, Chen J, et al. 2011. MicroRNA expression changes during zebrafish development induced by perfluorooctane sulfonate. Journal of applied toxicology : JAT 31:210-222.

Zhang L, Ren XM, Guo LH. 2013b. Structure-based investigation on the interaction of perfluorinated compounds with human liver fatty acid binding protein. Environmental Science and Technology 47:11293-11301.

Zhang L, Lee LS, Niu J, Liu J. 2017a. Kinetic analysis of aerobic biotransformation pathways of a perfluorooctane sulfonate (PFOS) precursor in distinctly different soils. Environmental pollution (Barking, Essex : 1987) 229:159-167.

Zhang L, Geng Z, Meng X, Meng F, Wang L. 2018a. Screening for key lncRNAs in the progression of gallbladder cancer using bioinformatics analyses. Molecular medicine reports 17:6449-6455.

Zhang N, Wang WS, Li WJ, Liu C, Wang Y, Sun K. 2015b. Reduction of progesterone, estradiol and hCG secretion by perfluorooctane sulfonate via induction of apoptosis in human placental syncytiotrophoblasts. Placenta 36:575-580.

Zhang S, Tan R, Pan R, Xiong J, Tian Y, Wu J, et al. 2018b. Association of Perfluoroalkyl and Polyfluoroalkyl Substances With Premature Ovarian Insufficiency in Chinese Women. The Journal of Clinical Endocrinology & Metabolism 103:2543-2551.

Zhang YH, Wang J, Dong GH, Liu MM, Wang D, Zheng L, et al. 2013c. Mechanism of perfluorooctanesulfonate (PFOS)-induced apoptosis in the immunocyte. Journal of immunotoxicology 10:49-58.

Zhang YM, Dong XY, Fan LJ, Zhang ZL, Wang Q, Jiang N, et al. 2017b. Poly- and perfluorinated compounds activate human pregnane X receptor. Toxicology 380:23-29.

Zhao B, Li L, Liu J, Li H, Zhang C, Han P, et al. 2014. Exposure to perfluorooctane sulfonate in utero reduces testosterone production in rat fetal Leydig cells. PloS one 9:e78888.

Zhao S, Liu T, Wang B, Fu J, Liang T, Zhong Z, et al. 2019. Accumulation, biodegradation and toxicological effects of N-ethyl perfluorooctane sulfonamidoethanol on the earthworms Eisenia fetida exposed to quartz sands. Ecotoxicology and environmental safety 181:138-145.

Zhao S, Wang B, Zhong Z, Liu T, Liang T, Zhan J. 2020. Contributions of enzymes and gut microbes to biotransformation of perfluorooctane sulfonamide in earthworms (Eisenia fetida). Chemosphere 238:124619.

Zhao W, Cui R, Wang J, Dai J. 2017. Inhibition effects of perfluoroalkyl acids on progesterone production in mLTC-1. Journal of environmental sciences (China) 56:272-280.

Zheng G, Schreder E, Dempsey JC, Uding N, Chu V, Andres G, et al. 2021. Per- and Polyfluoroalkyl Substances (PFAS) in Breast Milk: Concerning Trends for Current-Use PFAS. Environmental science & technology.

Zheng L, Dong GH, Jin YH, He QC. 2009. Immunotoxic changes associated with a 7-day oral exposure to perfluorooctanesulfonate (PFOS) in adult male C57BL/6 mice. Archives of toxicology 83:679-689.

Zheng L, Dong GH, Zhang YH, Liang ZF, Jin YH, He QC. 2011. Type 1 and Type 2 cytokines imbalance in adult male C57BL/6 mice following a 7-day oral exposure to perfluorooctanesulfonate (PFOS). Journal of immunotoxicology 8:30-38.

Zheng X, Shi Y, Lü Y, Xu X. 2013. Effects of perfluorooctane sulfonate on antioxidant and metabolic enzymes and DNA damage of earthworms (Eisenia fetida). Huanjing Kexue Xuebao/Acta Scientiae Circumstantiae 33:3153-3159.

Zheng XQ, Shi YJ, Lu YL, Xu XB. 2016. Growth inhibition and DNA damage in the earthworm (Eisenia fetida) exposed to perfluorooctane sulphonate and perfluorooctanoic acid. Chemistry and Ecology 32:103-116.

Zhong S-Q, Chen Z-X, Kong M-L, Xie Y-Q, Zhou Y, Qin X-D, et al. 2016. Testosterone-mediated endocrine function and TH1/TH2 cytokine balance after prenatal exposure to Perfluorooctane Sulfonate: by sex status. International journal of molecular sciences 17:1509.

Zhou W, Zhang L, Tong C, Fang F, Zhao S, Tian Y, et al. 2017. Plasma Perfluoroalkyl and Polyfluoroalkyl Substances Concentration and Menstrual Cycle Characteristics in Preconception Women. Environmental health perspectives 125:067012.

Zhou W, Liu T, Saren G, Liao L, Fang W, Zhao H. 2019. Comprehensive analysis of differentially expressed long non-coding RNAs in non-small cell lung cancer. Oncology letters 18:1145-1156.

Zhou Y, Hu LW, Qian ZM, Chang JJ, King C, Paul G, et al. 2016. Association of perfluoroalkyl substances exposure with reproductive hormone levels in adolescents: By sex status. Environment international 94:189-195.

Zhou Z, Shi Y, Vestergren R, Wang T, Liang Y, Cai Y. 2014. Highly elevated serum concentrations of perfluoroalkyl substances in fishery employees from Tangxun Lake, China. Environmental Science and Technology 48:3864-3874.

Zhu W, Zhou BL, Rong LJ, Ye L, Xu HJ, Zhou Y, et al. 2020. Roles of PTBP1 in alternative splicing, glycolysis, and oncogensis. J Zhejiang Univ Sci B 21:122-136.

Zou Y, Wu Y, Wang Q, Wan J, Deng M, Tu W. 2021. Comparison of toxicokinetics and toxic effects of PFOS and its novel alternative OBS in zebrafish larvae. Chemosphere 265.

Appendix A. PFOS Branched Isomers, PFOS Salts, and Major Groups of PFOS Precursors

Ten branched PFOS isomers are presented in Table A1 and seventeen salts of PFOS (linear and branched isomers) are presented in Table A2 PFOS salts. A non-exhaustive set of 169 PFOS precursors is presented in Table A3 (Major groups of PFOS precursors, excluding telomers, polymers, fatty acid derivatives and mixtures) and Table A4 (PFOS precursors: telomers, polymers, fatty acid derivatives, and mixtures). Chemical names follow Organisation for Economic Co-operation and Development (OECD) nomenclature; the International Union of Pure and Applied Chemistry (IUPAC) name is given in brackets for some chemicals. The ability of the chemicals included in Table A3 and Table A4 to transform and/or degrade to PFOS was evaluated either through the use of 11 quantitative structure-activity relationship (QSAR)-based metabolic simulators embedded in the OECD Toolbox v.4 (https://qsartoolbox.org/) or by knowledge-based expert judgment (personal communication with Dr. K. Durkin, UC Berkeley).

The approaches used to identify PFOS branched isomers, salts and precursors are briefly described as follows:

- These tables were compiled primarily based on information from four published lists of potential PFOS precursors, namely
    - Environment Canada (2006)
    - OECD (2007)
    - Direct PFOS precursors from Australia's National Industrial Chemicals Notification and Assessment Scheme (NICNAS) (NICNAS 2019a).
    - Indirect PFOS precursors from (NICNAS 2019b)
- Additional PFOS branched isomers, salts, and precursors were identified from peer-reviewed literature or from the PFAS master list in US Environmental Protection Agency (US EPA)'s CompTox Chemicals Dashboard (https://comptox.epa.gov/dashboard/chemical_lists/pfasmaster, accessed on February 9th, 2021).
- In Table A3 and Table A4, the precursors were grouped into 11 major categories proposed by Martin et al. (2010) or Buck et al. (2011) or NICNAS (2019b) or knowledge-based expert judgment (personal communication with Dr. K. Durkin, UC Berkeley). Several computational tools, *i.e.,* ChemDoodle 2D (https://www.chemdoodle.com), ChemoTyper (download from https://chemotyper.org/wiki), and ChemoType Editor Version 0.0.9 (download

from https://chemotyper.org/wiki) were applied to validate and draw the 2-dimensional chemical structures based on chemical names, and to group the 11 major PFOS precursor categories. For Table A3, 82 chemical structures were prepared by ChemDoodle 2D and saved either as picture (enhanced metafile) files for visual presentation in Table A3 or as a SDF (standard data file) file for grouping purposes in ChemoTyper. Six major PFOS precursor categories, proposed by Martin et al. (2010) or Buck et al. (2011), were created in ChemoType Editor for grouping in ChemoTyper. For the grouping of the remaining 87 chemicals in Table A4, knowledge-based expert judgment and grouping rationale reported in NICNAS (2019b) were used. The names of the PFOS precursor categories included in Table A3, the number of chemicals identified in each of those categories and examples of core chemical structures within those categories are presented below, followed by similar information for the PFOS precursor categories included in Table A4.

Table A3 includes:

- Perfluoroalkane sulfonamides (PFOSA) or salts: 16 chemicals

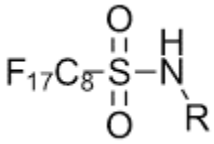

- Perfluoroalkane sulfonamide acetic acids (PFOSAA) or salts: 10 chemicals

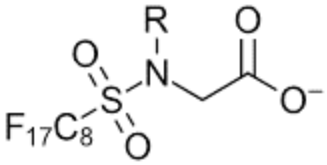

- Perfluoroalkane sulfonamidoethanols (PFOSE): 7 chemicals

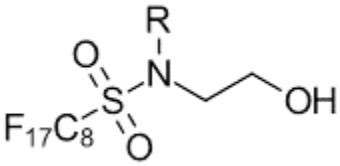

- Perfluoroalkane sulfonamidoethanol phosphates (PFOSE phosphate): 8 chemicals

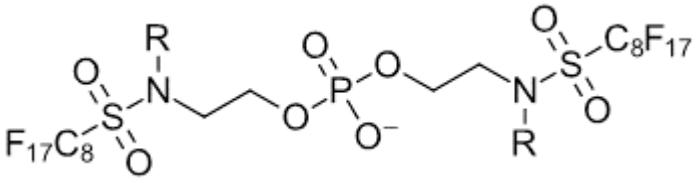

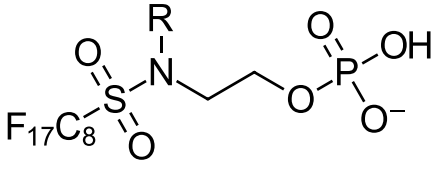

- Perfluoroalkane sulfonamidoethanol acrylate esters (PFOSE acrylate esters): 9 chemicals

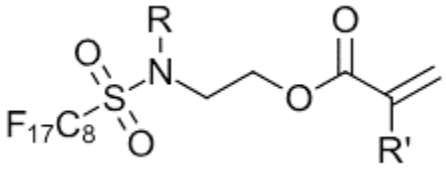

- Perfluoroalkane sulfonamido amine or amine oxide salts or propanimium salts: 14 chemicals

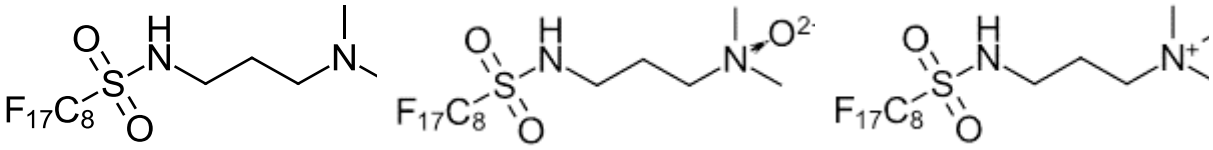

- Miscellaneous perfluorooctanesulfonyl derivatives: 18 chemicals

Table A4 includes:

- Telomers: 8 chemicals
- Polymers: 42 chemicals
- Fatty acid derivatives: 4 chemicals
- Mixtures, including reaction products: 33 chemicals

- These precursors were validated by 11 quantitative structure-activity relationship (QSAR)-based metabolic simulators embedded in the OECD Toolbox v.4 (https://qsartoolbox.org/) or by knowledge-based expert judgment (personal communication with Dr. K. Durkin, UC Berkeley). These 11 QSAR-based metabolic simulators are built based on knowledge-based rules generated from a training set of chemicals to produce the simulating algorithm for metabolite and metabolism pathway predictions and consist of:
  - 7 non-enzymatic-based simulators: autoxidation, autoxidation (alkaline medium), dissociation, hydrolysis (acidic), hydrolysis (basic), hydrolysis (neutral), and tautomerism simulators
  - 4 enzymatic-based simulators: microbial, *in vivo* rat, rat liver S9, and skin metabolism simulators
- Chemicals in Table A3 were validated using these 11 metabolic simulators. For each of the chemicals, PFOS was predicted as a metabolite by at least one simulator, except for one polyglycol derivative of perfluorooctanesulfonamides (CAS RN 52032-20-9), which is included as a PFOS precursor based on expert

judgment and supported by QSAR analysis of the predicted glycol perfluorooctanesulfonamide monomer.

- Chemicals in Table A4 were mainly validated and predicted to be metabolized to PFOS by knowledge-based expert judgment (expert judgment reported in environment Canada (2006) or personal communication with Dr. K. Durkin, UC Berkeley) and some were further supported by QSAR analysis of starting reactants (in the case of some mixtures) or predicted monomers in the case of some telomers and polymers. In general, per expert judgement provided by Dr. Durkin, most telomers and polymers in Table A4 can be hydrolyzed at the polymerization backbone, *e.g.*, at a carboxylic ester bond, to release a monomer that can be further metabolized or degraded (*e.g.*, by microbial metabolism of carbon-nitrogen or sulfur-nitrogen bonds to form PFOS).

Table A1 PFOS branched isomers

Chemical name	Abbreviation	CAS RN[b]	Chemical structure
Heptadecafluorooctane-2-sulfonic acid	*1m*-PFOS; Alpha CF_3 branched PFOS at C1[a]	927670-12-0	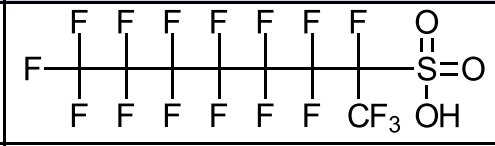
1,1,2,3,3,4,4,5,5,6,6,7,7,7-tetradecafluoro-2-(trifluoromethyl)heptane-1-sulfonic acid	*2m*-PFOS; CF_3 branched PFOS at C2[a]	NOCAS_ 1019148	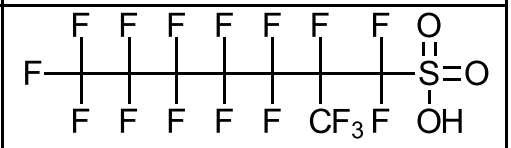
1,1,2,2,3,4,4,5,5,6,6,7,7,7-tetradecafluoro-3-(trifluoromethyl)heptane-1-sulfonic acid	*3m*-PFOS: CF_3 branched PFOS at C3[a]	NOCAS_ 1019147	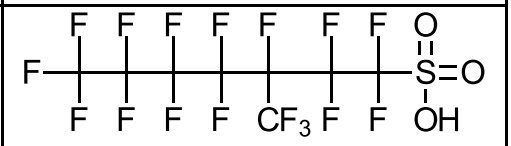
1,1,2,2,3,3,4,5,5,6,6,7,7,7-tetradecafluoro-4-(trifluoromethyl)heptane-1-sulfonic acid	*4m*-PFOS; CF_3 branched PFOS at C4[a]	NOCAS_ 1019146	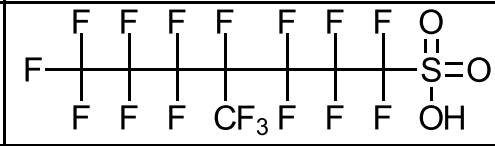
1,1,2,2,3,3,4,4,5,6,6,7,7,7-tetradecafluoro-5-(trifluoromethyl)heptane-1-sulfonic acid	*5m*-PFOS; CF_3 branched PFOS at C5[a]	NOCAS_ 1019145	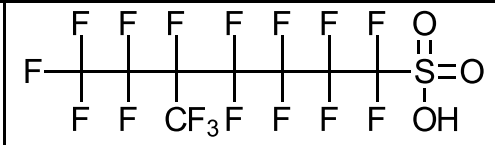
1,1,2,2,3,3,4,4,6,6,6-Undecafluoro-5,5-bis(trifluoromethyl)-1-hexanesulfonic acid	CF_3 *t*-butyl branched PFOS at C5[a]	NA	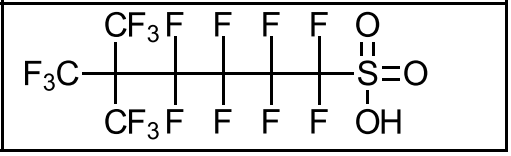

Chemical name	Abbreviation	CAS RN[b]	Chemical structure
1,1,2,2,3,3,4,4,5,5,6,7,7,7-Tetradecafluoro-6-(trifluoromethyl)heptane-1-sulfonic acid	*iso*-PFOS; CF_3 Isopropyl branched PFOS at C6[a]	NOCAS_ 1019144	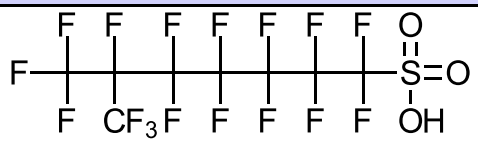
1,1,2,2,3,3,5,5,6,6,6-undecafluoro-4,4-bis(trifluoromethyl)hexane-1-sulfonic acid	*4,4m2*-PFOS; gem-di-CF3 branched PFOS at C4[a]	NOCAS_ 1019149	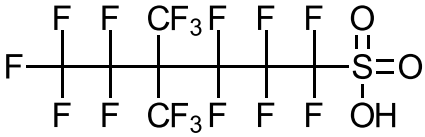
1,1,2,2,3,3,4,5,6,6,6-Undecafluoro-4,5-bis(trifluoromethyl)-1-hexanesulfonic acid	*5,4m2*-PFOS: di-CF3 branched PFOS at C4 and C5[a]	NA	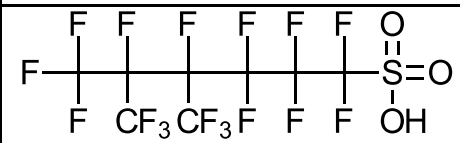
1,1,2,2,3,4,4,5,6,6,6-Undecafluoro-3,5-bis(trifluoromethyl)-1-hexanesulfonic acid	*5,3m2*-PFOS; di-CF3 branched PFOS at C3 and C5[a]	NA	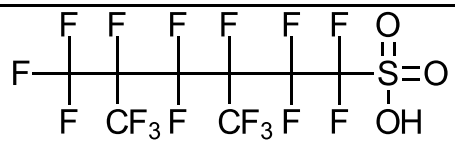

[a] The abbreviations of various perfluoromonomethyl isomers were defined in Figure S-1 in Benskin et al (2009) or Arsenault et al (2008). The numbering of the carbon chain for PFOS branched isomers is as follows: C(7)–C(6)–C(5)–C(4)–C(3)–C(2)–C(1)–R (R = SO_2OH) (Arsenault et al. 2008).
[b] "NOCAS_" numbers are assigned by US EPA when there is no CAS RN available (Williams et al., 2017) ; NA, Neither CAS RN or NOCAS is available.

Table A2 PFOS salts

Chemical name	Abbreviation	CAS RN	Chemical structure
Salts of linear PFOS			
1-Octanesulfonic acid, 1,1,2,2,3,3,4,4,5,5,6,6,7,7,8,8,8-heptadecafluoro-, potassium salt	PFOS potassium (K+) salt	2795-39-3	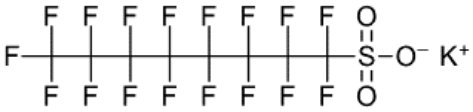
1-Octanesulfonic acid, 1,1,2,2,3,3,4,4,5,5,6,6,7,7,8,8,8-heptadecafluoro-, ammonium salt	PFOS ammonium (NH4+) salt	29081-56-9	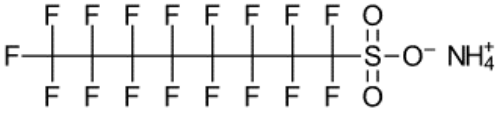
1-Octanesulfonic acid, 1,1,2,2,3,3,4,4,5,5,6,6,7,7,8,8,8-heptadecafluoro-, lithium salt	PFOS lithium (Li+) salt	29457-72-5	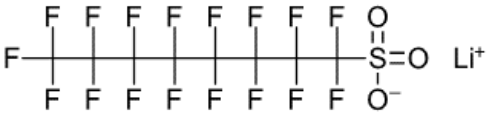
1-Octanesulfonic acid, 1,1,2,2,3,3,4,4,5,5,6,6,7,7,8,8,8-heptadecafluoro-, sodium salt	PFOS sodium (Na+) salt	4021-47-0	

Chemical name	Abbreviation	CAS RN	Chemical structure
1-Octanesulfonic acid, 1,1,2,2,3,3,4,4,5,5,6,6,7,7,8,8,8-heptadecafluoro-, compd. with 2,2-iminobis[ethanol] (1:1)	PFOS diethanolamine (DEA) salt	70225-14-8	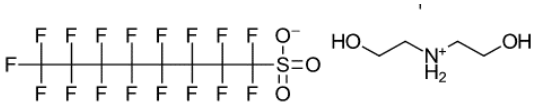
1-Octanesulfonic acid, 1,1,2,2,3,3,4,4,5,5,6,6,7,7,8,8,8-heptadecafluoro-, compd. With piperidine (1:1)	PFOS piperidinium salt	71463-74-6	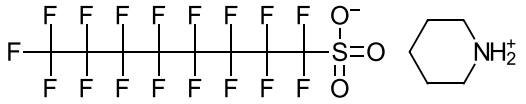
Ethanaminium,N,N,N-triethyl-,salt with 1,1,2,2,3,3,4,4,5,5,6,6,7,7,8,8,8-heptadecafluoro-1-octanesulfonicacid (1:1)	PFOS tetra-ethylammonium salt	56773-42-3	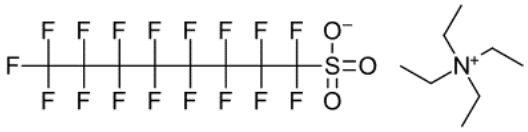
1-Decanaminium, N-decyl-N,N-dimethyl-, salt with 1,1,2,2,3,3,4,4,5,5,6,6,7,7,8,8,8-heptadecafluoro-1-octanesulfonic acid (1:1)	PFOS N-decyl-N,N-dimethyl-1-decanaminium salt	251099–16–8	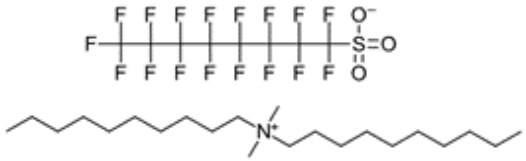
N,N-Dibutyl-N-methylbutan-1-aminium heptadecafluorooctane-1-sulfonate	PFOS N,N-dibutyl-N-methylbutan-1-aminium	124472-68-0	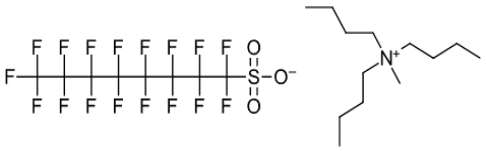
N,N,N-Tripropylpentan-1-aminium heptadecafluorooctane-1-sulfonate	PFOS N,N,N-tripropylpentan-1-aminium salt	56773-56-9	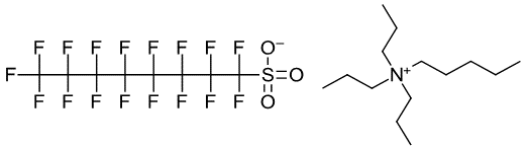
Tetrabutylammonium perfluorooctanesulfonate	PFOS tetra-butylammonium salt	111873-33-7	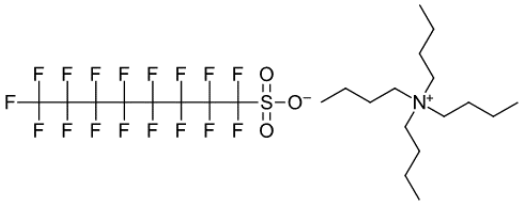
N,N,N-Triethyldecan-1-aminium heptadecafluorooctane-1-sulfonate	PFOS N,N,N-triethyldecan-1-aminium salt	773895-92-4	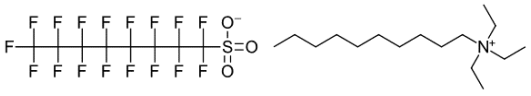

Chemical name	Abbreviation	CAS RN	Chemical structure
Magnesium bis [heptadecafluorooctane sulphonate]	PFOS magnesium salt	91036-71-4	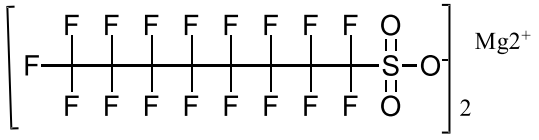
Salts of PFOS branched isomers			
1-Octanesulfonic acid, 1,1,2,2,3,3,4,4,5,5,6,6,7,7 ,8,8,8-heptadecafluoro-, branched, potassium salt	Potassium salt, CF_3 branched PFOS	90480-49-2	Unknown
Isooctanesulfonic acid, heptadecafluoro-, potassium salt	Potassium salt, CF_3 isopropyl branched PFOS	93894-68-9	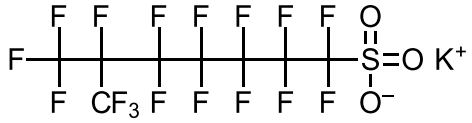
Lithium heptadecafluoroisooctane sulphonate	Lithium salt, CF_3 isopropyl branched PFOS	93894-67-8	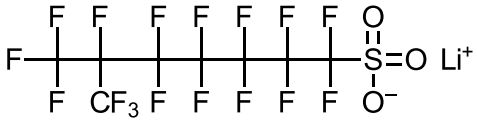
Magnesium heptadecafluoroisooctane sulphonate	Magnesium salt, CF_3 isopropyl branched PFOS	93894-73-6	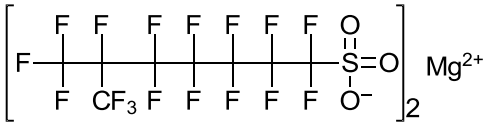

Table A3 Major groups of PFOS precursors, excluding telomers, polymers, fatty acid derivatives and mixtures

Chemical name[a]	Abbreviation	CAS RN	Chemical structure	Source	Inclusion criteria (QSAR or expert)
Perfluoroalkane sulfonamides (PFOSA) or salts					
Heptadecafluorooctanesulphonamide or Perfluorooctane sulfonamide	PFOSA, FOSA	754–91–6	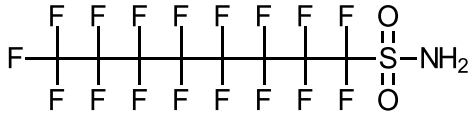	OECD, Literature (Xie et al 2009)	QSAR
Heptadecafluorooctane-1-sulphonamide, compound with triethylamine (1:1)	PFOSA triethylamine salt	76752-82-4	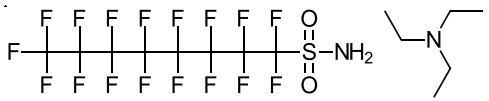	OECD	QSAR
CompTox: Perfluorooctanesulfonamide ammonium salt (1:1)	PFOSA ammonium salt; PFOSAmS	76752-72-2	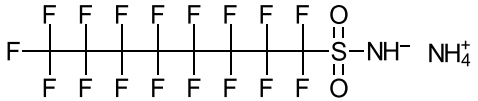	CompTox	QSAR
CompTox: Perfluorooctanesulfonamide lithium salt (1:1)	PFOSA lithium salt	76752-79-9	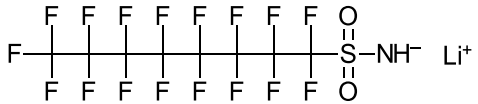	CompTox	QSAR
CompTox: Perfluorooctanesulfonamide sodium salt (1:1)	PFOSA sodium salt	76752-78-8	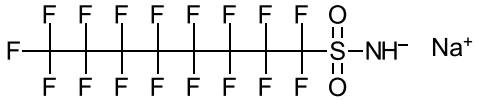	CompTox	QSAR
CompTox: Perfluorooctanesulfonamide potassium salt (1:1)	PFOSA potassium salt	76752-70-0	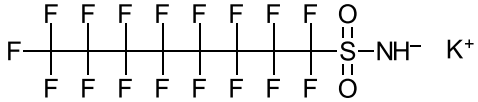	CompTox	QSAR

Chemical name[a]	Abbreviation	CAS RN	Chemical structure	Source	Inclusion criteria (QSAR or expert)
Heptadecafluoroisooctanesulphonamide	Branched PFOSA	93894-56-5	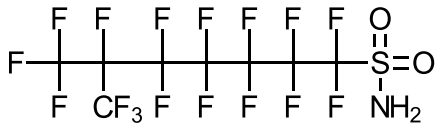	OECD	QSAR
Heptadecafluoroisooctanesulphonamide, compound with triethylamine(1:1)	Branched PFOSA with triethylamine salt	93894-57-6	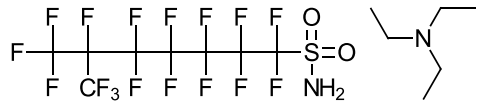	OECD	QSAR
1-Octanesulfonamide, 1,1,2,2,3,3,4,4,5,5,6,6,7,7,8,8,8-heptadecafluoro-N-methyl-	MePFOSA	31506-32-8	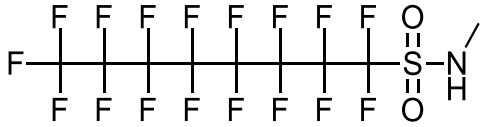	Environment Canada, OECD, NICNAS indirect	QSAR
Heptadecafluoro-N-methylisooctanesulphonamide	Branched MePFOSA	93894-71-4	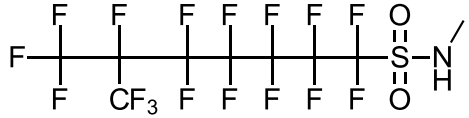	OECD	QSAR
Buck et al (2011): N,N-Dimethyl perfluorooctane sulfonamide	Me2PFOSA	213181-78-3	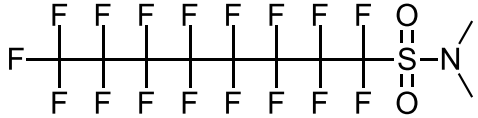	Literature (Buck et al. 2011)	QSAR
1-Octanesulfonamide, N-ethyl-1,1,2,2,3,3,4,4,5,5,6,6,7,7,8,8,8-heptadecafluoro- or N-Ethyl perfluorooctane sulfonamide	EtPFOSA	4151-50-2	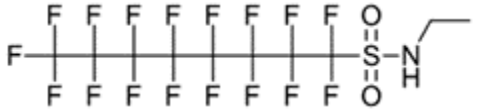	Environment Canada, OECD	QSAR

Chemical name[a]	Abbreviation	CAS RN	Chemical structure	Source	Inclusion criteria (QSAR or expert)
1-Octanesulfonamide, 1,1,2,2,3,3,4,4,5,5,6,6,7,7,8,8,8-heptadecafluoro-N-2-propenyl-	NA	423-86-9	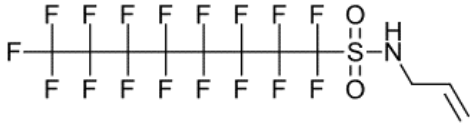	OECD	QSAR
Buck et al (2011): N,N-Diethyl perfluorooctane sulfonamide	Et2PFOSA	87988-61-2	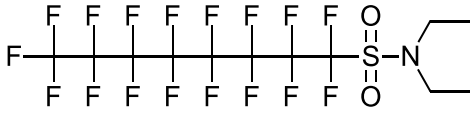	Literature (Buck et al. 2011)	QSAR
1-Octanesulfonamide, N-ethyl-1,1,2,2,3,3,4,4,5,5,6,6,7,7,8,8,8-heptadecafluoro-N-2-propenyl-	NA	24924-36-5	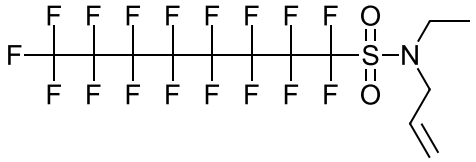	OECD	QSAR
1-Octanesulfonamide, 1,1,2,2,3,3,4,4,5,5,6,6,7,7,8,8,8-heptadecafluoro-N-(phenylmethyl)-	NA	50598-29-3	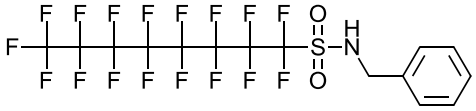	OECD	QSAR
Perfluoroalkane sulfonamide acetic acids (PFOSAA) or salts					
Buck et al (2011): N-[(1,1,2,2,3,3,4,4,5,5,6,6,7,7,8,8,8-Heptadecafluorooctyl)sulfonyl] glycine	PFOSAA	2806-24-8	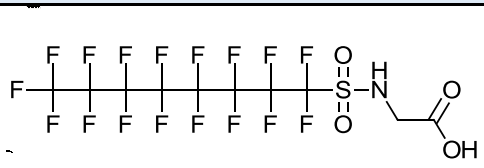	Literature (Buck et al. 2011; Benskin et al. 2012; Gebbink et al. 2016)	QSAR

Chemical name[a]	Abbreviation	CAS RN	Chemical structure	Source	Inclusion criteria (QSAR or expert)
NICNAS indirect: Glycine, N-[(heptadecafluoroctyl)sulfonyl]-, monopotassium salt	PFOSAA potassium salt	75260-69-4	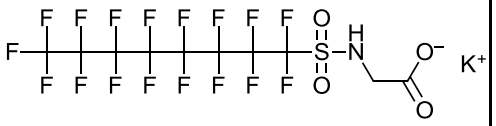	NICNAS indirect	QSAR
Buck et al (2011): N-methylperfluorooctane sulfonamido acetic acid	MePFOSAA	2355-31-9	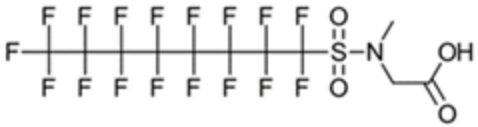	Literature (Buck et al. 2011; Benskin et al. 2012; Gebbink et al. 2016)	QSAR
CompTox: 2-(N-Methylperfluorooctanesulfonamido) acetate	MePFOSA acetate	909405-48-7	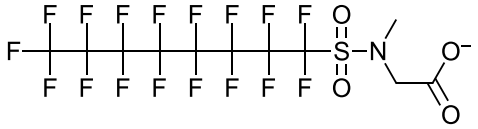	CompTox	QSAR
CompTox: Potassium N-((heptadecafluorooctyl)sulphonyl)-N-methylglycinate	MePFOSAA potassium salt	70281-93-5	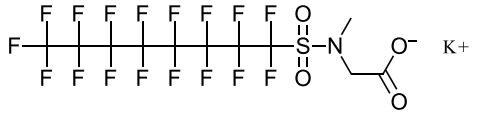	CompTox	QSAR
Glycine, N-ethyl-N-[(heptadecafluorooctyl)sulfonyl]- [IUPAC: N-Ethyl perfluorooctane sulfonamido acetic acid]	EtPFOSAA	2991-50-6	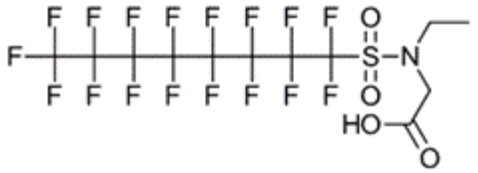	OECD	QSAR

Chemical name[a]	Abbreviation	CAS RN	Chemical structure	Source	Inclusion criteria (QSAR or expert)
CompTox: 2-(N-Ethyl-perfluorooctanesulfonamido) acetate	EtPFOSA acetate	909405-49-8	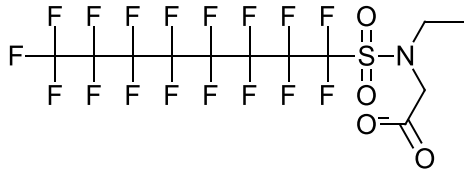	CompTox	QSAR
Glycine, N-ethyl-N-[(heptadecafluorooctyl)sulfonyl]-, potassium salt	EtPFOSAA potassium salt	2991-51-7	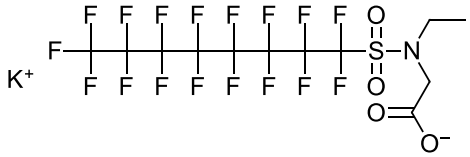	Environment Canada, OECD, NICNAS indirect	QSAR
Glycine, N-ethyl-N-[(heptadecafluorooctyl)sulfonyl]-, sodium salt	EtPFOSAA sodium salt	3871-50-9	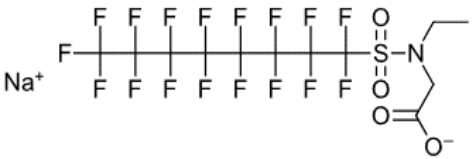	OECD	QSAR
Glycine, N-[(heptadecafluorooctyl)sulfonyl]-N-propyl-, potassium salt	PrPFOSAA potassium salt	55910-10-6	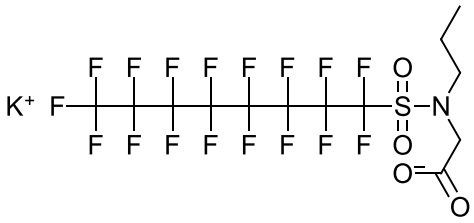	OECD	QSAR

Chemical name[a]	Abbreviation	CAS RN	Chemical structure	Source	Inclusion criteria (QSAR or expert)
Perfluoroalkane sulfonamidoethanols (PFOSE)					
1-Octanesulfonamide, 1,1,2,2,3,3,4,4,5,5,6,6,7,7,8,8,8-heptadecafluoro-N-(2-hydroxyethyl)-N-methyl- [IUPAC: N-Methyl perfluorooctane sulfonamidoethanol]	MePFOSE	24448-09-7	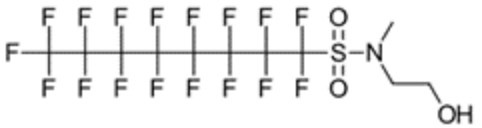	Environment Canada, OECD, NICNAS indirect	QSAR
Heptadecafluoro-N-(2-hydroxyethyl)-N-methylisooctanesulphonamide	Branched MePFOSE	93894-65-6	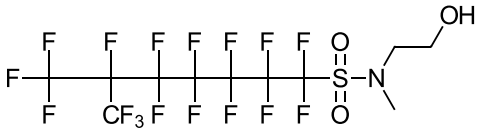	OECD	QSAR
1-Octanesulfonamide, N-ethyl-1,1,2,2,3,3,4,4,5,5,6,6,7,7,8,8,8-heptadecafluoro-N-(2-hydroxyethyl)- [IUPAC: N-Ethyl perfluorooctane sulfonamidoethanol]	EtPFOSE	1691-99-2	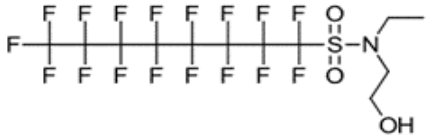	Environment Canada, OECD, NICNAS indirect	QSAR
Heptadecafluoro-N-(2-hydroxyethyl)-N-propyloctanesulphonamide	PrPFOSE	4236-15-1	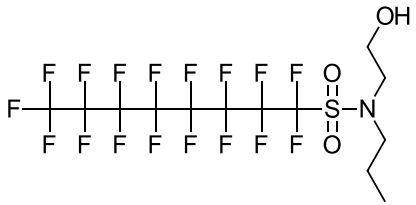	OECD	QSAR
1-Octanesulfonamide, N-butyl-1,1,2,2,3,3,4,4,5,5,6,6,7,7,8,8,8-heptadecafluoro-N-(2-hydroxyethyl)- [IUPAC: N-Butyl-1,1,2,2,3,3,4,4,5,5,6,6,7,7,8,8,8-heptadecafluoro-N-(2-hydroxyethyl)octane-1-sulfonamide]	BuPFOSE	2263-09-4	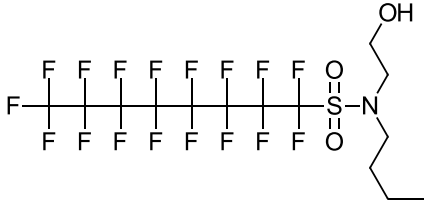	OECD	QSAR

Chemical name[a]	Abbreviation	CAS RN	Chemical structure	Source	Inclusion criteria (QSAR or expert)
Heptadecafluoro-N,N-bis(2-hydroxyethyl)octanesulphonamide	NA	40630-61-3	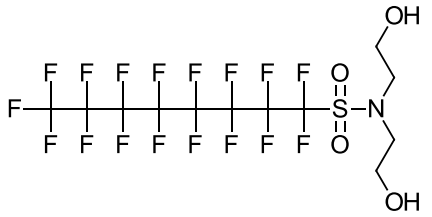	OECD, NICNAS indirect	QSAR
Heptadecafluoro-N,N-bis(2-hydroxyethyl) isooctanesulphonamide	NA	93894-66-7	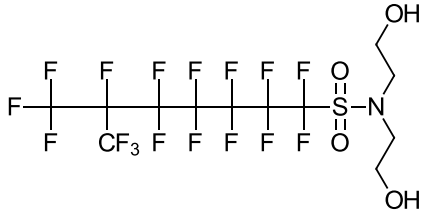	OECD	QSAR
Perfluoroalkane sulfonamidoethanol phosphates (PFOSE phosphate)					
Phosphonic acid, [3-[ethyl[(heptadecafluorooctyl)sulfonyl]amino]propyl]-	NA	71463-78-0	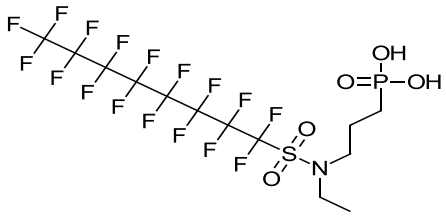	OECD	QSAR

Chemical name[a]	Abbreviation	CAS RN	Chemical structure	Source	Inclusion criteria (QSAR or expert)
Heptadecafluoro-N-[2-(phosphonooxy)ethyl]-N-propyloctanesulphonamide	NA	64264-44-4	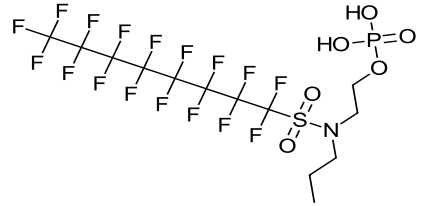	OECD	QSAR
1-Octanesulfonamide, N-ethyl-1,1,2,2,3,3,4,4,5,5,6,6,7,7,8,8,8-heptadecafluoro-N-[2-(phosphonooxy)ethyl]- [IUPAC: 2-[Ethyl(1,1,2,2,3,3,4,4,5,5,6,6,7,7,8,8,8-heptadecafluorooctane-1-sulfonyl)amino]ethyl dihydrogen phosphate]	SAmPAP	3820-83-5	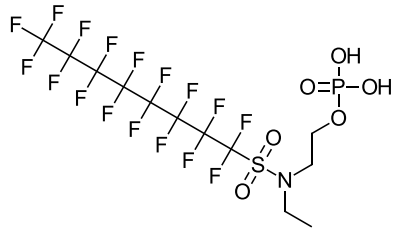	OECD, NICNAS indirect	QSAR
1-Octanesulfonamide, N-ethyl-1,1,2,2,3,3,4,4,5,5,6,6,7,7,8,8,8-heptadeca-fluoro-N-[2-(phosphonooxy)ethyl]-, diammonium salt	SAmPAPdiammonium salt	67969-69-1	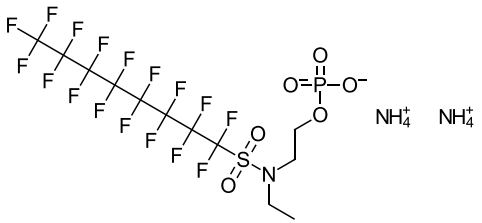	Environment Canada, OECD, NICNAS indirect	QSAR
1-Octanesulfonamide, N,N'-[phosphinicobis(oxy-2,1-ethanediyl)]bis[N-ethyl-1,1,2,2,3,3,4,4,5,5,6,6,7,7,8,8,8-heptadecafluoro-	diSAmPAP	2965-52-8	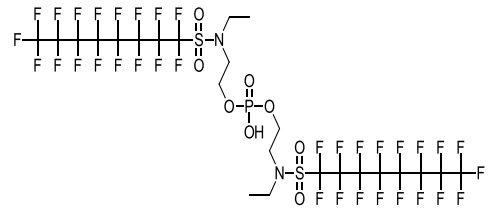	OECD	QSAR

Chemical name[a]	Abbreviation	CAS RN	Chemical structure	Source	Inclusion criteria (QSAR or expert)
1-Octanesulfonamide, N,N'-[phosphinicobis(oxy-2,1-ethanediyl)]bis[N-ethyl-1,1,2,2,3,3,4,4,5,5,6,6,7,7,8,8,8-heptadecafluoro-, ammonium salt	diSAmPAP ammonium salt	30381-98-7	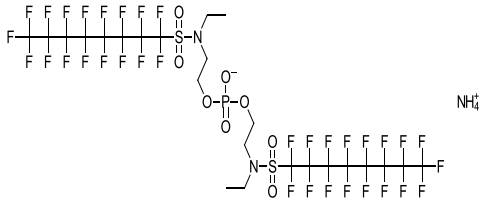	Environment Canada, OECD, NICNAS indirect	QSAR
1-Octanesulfonamide, N,N',N"-[phosphinylidynetris(oxy-2,1-ethanediyl)]tris[N-ethyl-1,1,2,2,3,3,4,4,5,5,6,6,7,7,8,8,8-heptadecafluoro- [IUPAC: Tris{2-[ethyl(1,1,2,2,3,3,4,4,5,5,6,6,7,7,8,8,8-heptadecafluorooctane-1-sulfonyl)amino]ethyl phosphate]	triSAmPAP	2250-98-8	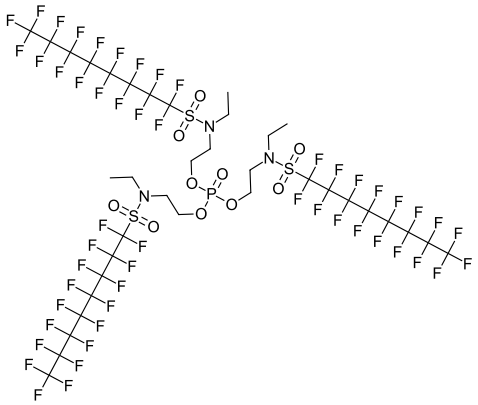	Environment Canada, OECD, NICNAS indirect	QSAR
Phosphonic acid, [3-[ethyl[(heptadecafluorooctyl)sulfonyl]amino]propyl]-, diethyl ester	NA	71463-80-4	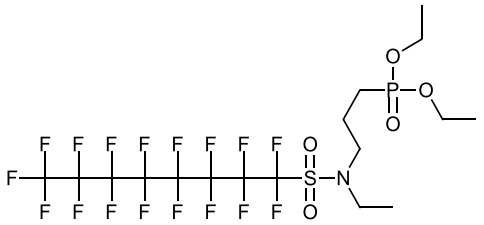	OECD	QSAR

Chemical name[a]	Abbreviation	CAS RN	Chemical structure	Source	Inclusion criteria (QSAR or expert)
Perfluoroalkane sulfonamidoethanol acrylate esters (PFOSE acrylate esters)					
2-Propenoic acid, 2-[[(heptadecafluorooctyl)sulfonyl] methylamino]ethyl ester	MePFOSEA	25268–77–3	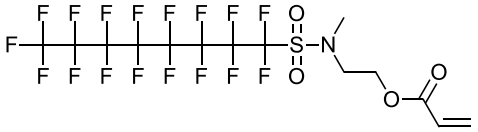	OECD, Environment Canada	QSAR
2-Propenoic acid, 2-methyl-, 2-[[(heptadecafluorooctyl)sulfonyl]methylamino] ethyl ester	MePFOSMAC	14650–24–9	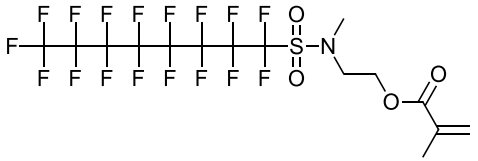	OECD, Environment Canada	QSAR
2-Propenoic acid, 2-[ethyl[(heptadecafluorooctyl)sulfonyl] amino]ethyl ester	EtPFOSEA	423–82–5	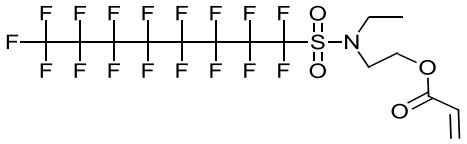	OECD, Environment Canada, NICNAS indirect	QSAR
2-Propenoic acid, 2-methyl-, 2-[ethyl[(heptadecafluorooctyl)sulfonyl] amino] ethyl ester [IUPAC: N-ethylperfluorooctane sulfonamidoethyl methacrylate]	EtPFOSMAC	376–14–7	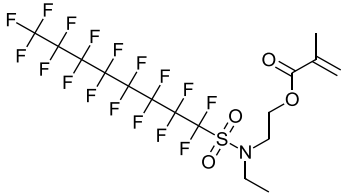	OECD, Environment Canada, NICNAS indirect	QSAR
2-[[(Heptadecafluorooctyl)sulphonyl] propylamino]ethyl acrylate [IUPAC: 2-[(1,1,2,2,3,3,4,4,5,5,6,6,7,7,8,8,8-Heptadecafluorooctane-1-sulfonyl)(propyl)amino]ethyl prop-2-enoate]	PrPFOSEA	2357-60-0	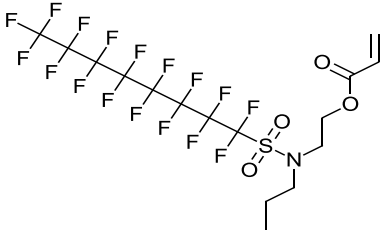	OECD	QSAR

Chemical name[a]	Abbreviation	CAS RN	Chemical structure	Source	Inclusion criteria (QSAR or expert)
2-[[(Heptadecafluorooctyl)sulphonyl] propylamino]ethyl methacrylate [IUPAC: 2-[(1,1,2,2,3,3,4,4,5,5,6,6,7,7, 8,8,8-Heptadecafluorooctane-1-sulfonyl) (propyl)amino]ethyl 2-methylprop-2-enoate]	PrFOSMAC	13285-40-0	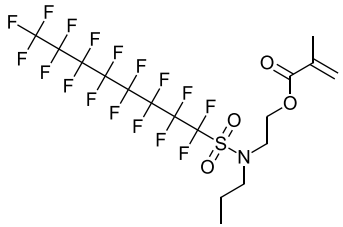	OECD	QSAR
2-Propenoic acid, 2-[butyl[(heptadecafluorooctyl)sulfonyl] amino]ethyl ester [IUPAC: 2-(N-Butylperfluorooctane sulfonamido)ethyl acrylate]	BuPFOSEA	383-07-3	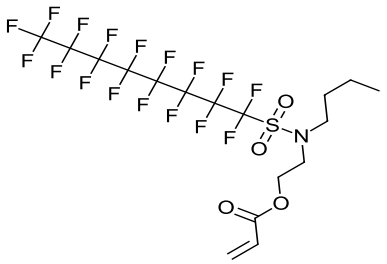	OECD	QSAR
2-Propenoic acid, 4-[[(heptadecafluorooctyl)sulfonyl]methylamino]butyl ester	POLYFLGSID_880493	58920-31-3	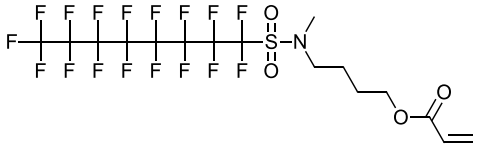	OECD	QSAR
2-Propenoic acid, 2-methyl-, 4-[[(heptadecafluorooctyl)sulfonyl] methylamino]butyl ester	POLYFLGSID_880525	61577-14-8	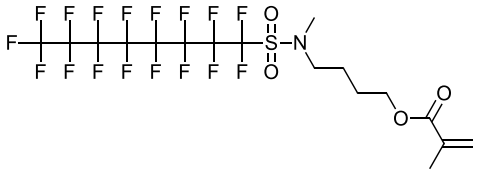	OECD	QSAR

Chemical name[a]	Abbreviation	CAS RN	Chemical structure	Source	Inclusion criteria (QSAR or expert)
Perfluoroalkane sulfonamido amine or amine oxide salts or propanimium salts					
1-Octanesulfonamide, N-[3-(dimethylamino)propyl]-1,1,2,2,3,3,4,4,5,5,6,6,7,7, 8,8,8-heptadecafluoro-	PFOSaAm	13417-01-1	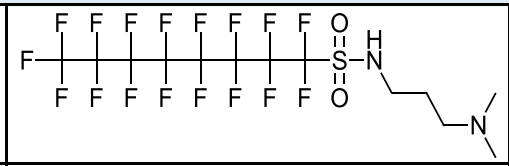	OECD	QSAR
1-Octanesulfonamide, N-[3-(dimethylamino)propyl]-1,1,2,2,3,3,4,4,5,5,6,6,7,7, 8,8,8-heptadecafluoro-, monohydrochloride	PFOSaAm HCl salt	67939-88-2	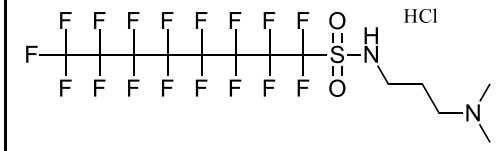	Environment Canada, OECD, NICNAS indirect	QSAR
1-Propanesulfonic acid, 3-[[3-(dimethylamino)propyl][(heptadecafluoro octyl) sulfonyl]amino]-2-hydroxy-, monosodium salt	NA	94133-90-1	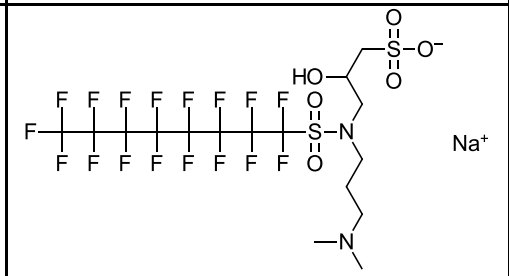	Environment Canada, OECD, NICNAS indirect	QSAR
1-Octanesulfonamide, N-[3-(dimethyloxidoamino)propyl]-1,1,2,2,3,3,4,4,5,5, 6,6,7,7,8,8,8-heptadecafluoro-	PFOSNO	30295-51-3	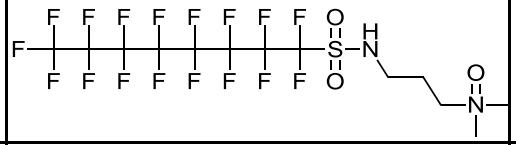	Environment Canada, OECD	QSAR
1-Octanesulfonamide, N-[3-(dimethyloxidoamino)propyl]-1,1,2,2,3,3,4,4, 5,5,6,6,7,7,8,8,8-heptadecafluoro-, potassium salt (1:1)	PFOSNO potassium salt	178094-69-4	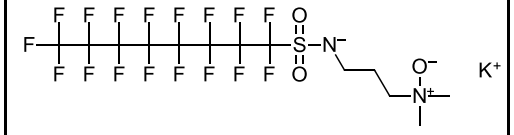	Environment Canada, OECD	QSAR

Chemical name[a]	Abbreviation	CAS RN	Chemical structure	Source	Inclusion criteria (QSAR or expert)
CompTox: Perfluorooctanesulfonamido ammonium	PFOSaAms	70225-25-1	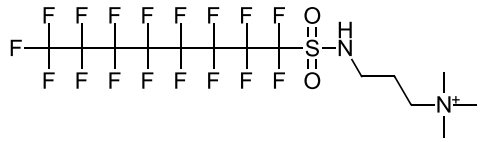	CompTox	QSAR
1-Propanaminium, 3-[[(heptadecafluorooctyl)sulfonyl]amino]-N,N,N-trimethyl-, chloride	PFOSaAms chloride salt	38006-74-5	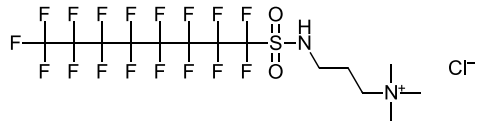	Environment Canada, OECD, NICNAS indirect	QSAR
1-Propanaminium, 3-[[(heptadecafluorooctyl)sulfonyl]amino]-N,N,N-trimethyl-, iodide	Fluorotenside -134	1652-63-7	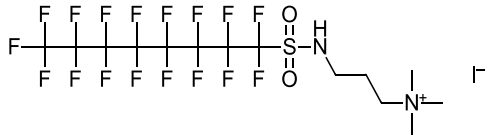	OECD, NICNAS indirect	QSAR
1-Propanaminium, 3-[[(heptadecafluorooctyl)sulfonyl]amino]-N,N,N-trimethyl-, iodide, ammonium salt	PFOSaAms iodide, ammonium salt	68310-75-8	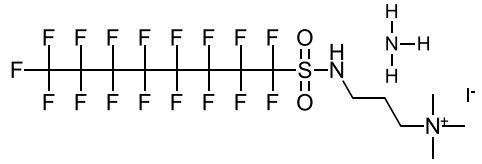	OECD	QSAR

Chemical name[a]	Abbreviation	CAS RN	Chemical structure	Source	Inclusion criteria (QSAR or expert)
1-Propanaminium, 3-[[(heptadecafluorooctyl)sulfonyl]amino]-N,N,N-trimethyl-, sulfate (2:1)	NA	70225-26-2	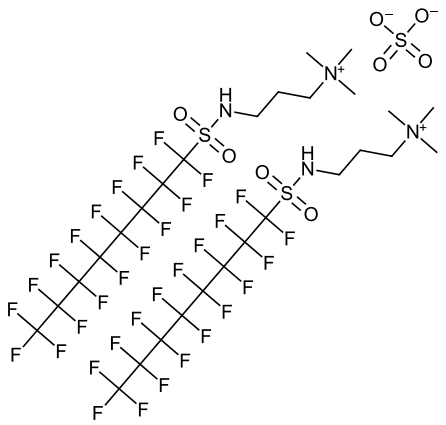	OECD	QSAR
1-Propanaminium, 3-[(carboxymethyl)[(heptadecafluorooctyl)sulfonyl]amino]-N,N,N-trimethyl-, inner salt	NA	68318-36-5	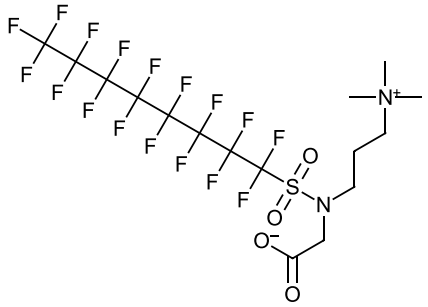	OECD	QSAR
CompTox: Perfluorooctanesulfonamido betaine	PFOSB	75046-16-1	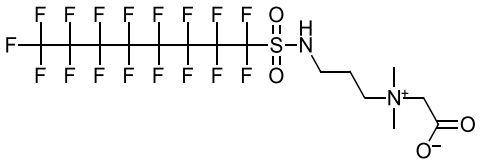	CompTox	QSAR

Chemical name[a]	Abbreviation	CAS RN	Chemical structure	Source	Inclusion criteria (QSAR or expert)
1-Propanaminium, 3-[[(heptadecafluorooctyl)sulfonyl](3-sulfopropyl)amino]-N-(2-hydroxyethyl)-N,N-dimethyl-, inner salt	NA	68298-11-3	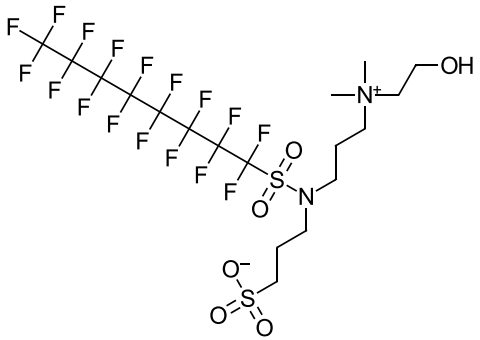	Environment Canada, OECD, NICNAS indirect	QSAR
NICNAS indirect: 1-Propanaminium, 3-[[(heptadecafluorooctyl)sulfonyl](2-hydroxy-3-sulfopropyl)amino]-N-(2-hydroxyethyl)-N,N-dimethyl-, hydroxide, monosodium salt	POLYFLGSID_882929	94133-91-2	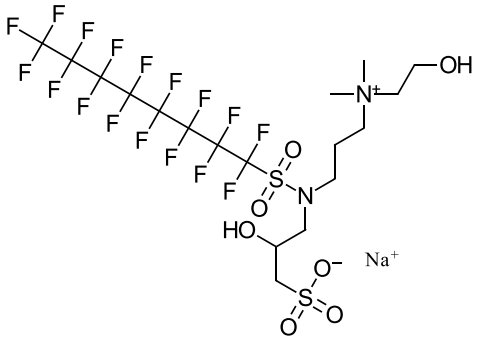	NICNAS indirect	QSAR
Miscellaneous perfluorooctanesulfonyl derivatives					
1-Octanesulfonyl fluoride, 1,1,2,2,3,3,4,4,5,5,6,6,7,7,8,8,8-heptadecafluoro- or Perfluorooctane sulfonyl fluoride	POSF	307-35-7	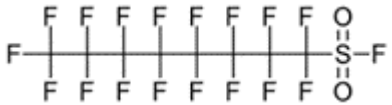	OECD, Environment Canada, NICNAS direct	QSAR
1-Octanesulfonyl fluoride, 1,1,2,2,3,3,4,4,5,5,6,6,7,7,8,8,8-heptadecafluoro-, branched	POSF, branched	90480-50-5	NA	OECD	QSAR

Chemical name[a]	Abbreviation	CAS RN	Chemical structure	Source	Inclusion criteria (QSAR or expert)
Buck et al (2011): Perfluorooctane sulfinic acid or Perfluorooctanesulfinate	PFOSI	647-29-0	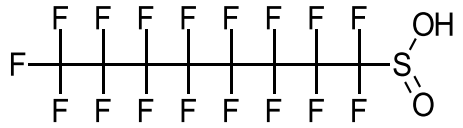	Literature (Buck et al. 2011, Martin et al. 2010)	QSAR
1-Octanesulfonamide, 1,1,2,2,3,3,4,4,5,5,6,6,7,7,8,8,8-heptadecafluoro-N-(4-hydroxybutyl)-N-methyl-	NA	68239-73-6	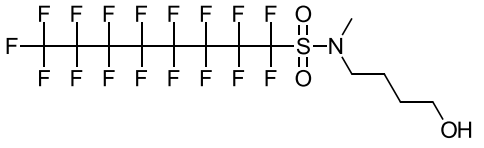	OECD	QSAR
1,3-Benzenedicarboxamide, N3-[2-[[(heptadecafluorooctyl)sulfonyl] methylamino]ethyl]-N1-[2-[[(heptadecafluorooctyl)sulfonyl]propylamino]ethyl]-4-methyl-	NA	73019-20-2	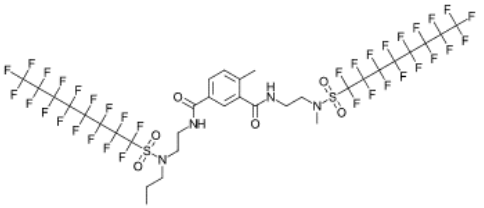	OECD	QSAR
Carbamic acid, (4-methyl-1,3-phenylene)bis-, bis[2-[ethyl [(heptadecafluorooctyl) sulfonyl]amino]ethyl] ester	NA	21055-88-9	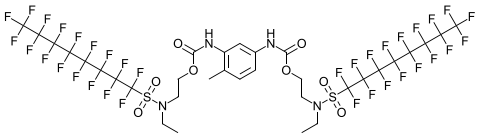	OECD	QSAR
Benzenesulfonic acid, [[[(heptadecafluorooctyl)sulfonyl]amino]methyl]-, monosodium salt	POLYFLGSID_880427	51032-47-4	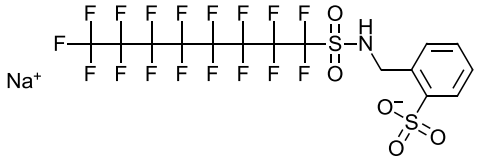	OECD	QSAR

Chemical name[a]	Abbreviation	CAS RN	Chemical structure	Source	Inclusion criteria (QSAR or expert)
Benzoic acid, 2,3,4,5-tetrachloro-6-[[[3-[[(heptadecafluorooctyl)sulfonyl]oxy] phenyl]amino] carbonyl]-, monopotassium salt	POLYFLGSID_880488	57589-85-2	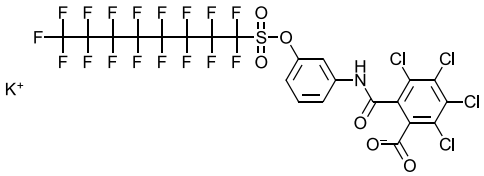	Environment Canada, OECD, NICNAS indirect	QSAR
1-Octanesulfonamide, N-ethyl-1,1,2,2,3,3,4,4,5,5,6,6,7,7,8,8,8-heptadecafluoro-N-[3-(trimethoxysilyl)propyl]-	NA	61660-12-6	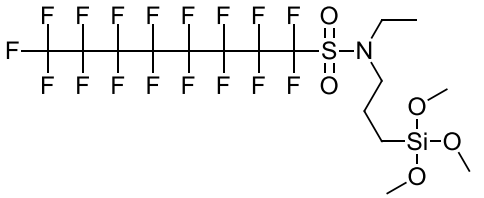	OECD	QSAR
1-Octanesulfonamide, N-ethyl-1,1,2,2,3,3,4,4,5,5,6,6,7,7,8,8,8-heptadecafluoro-N-[3-(trichlorosilyl)propyl]-	NA	67939-42-8	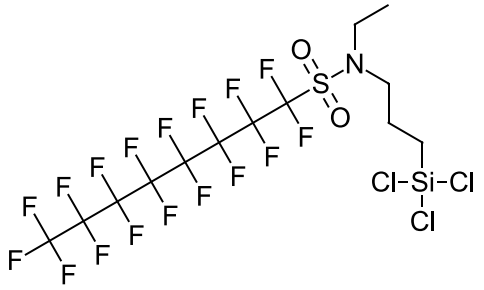	OECD	QSAR
Glycine, N-ethyl-N-[(heptadecafluorooctyl)sulfonyl]-, ethyl ester	NA	1869-77-8	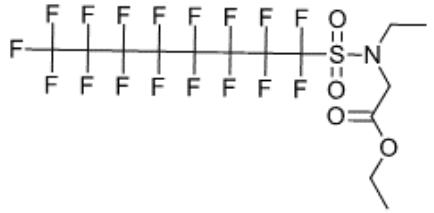	OECD	QSAR

Chemical name[a]	Abbreviation	CAS RN	Chemical structure	Source	Inclusion criteria (QSAR or expert)
Polyglycol Derivatives of Perfluorooctanesulfonamides: Poly(oxy-1,2-ethanediyl), a-[2-[ethyl[(heptadecafluorooctyl)sulfonyl] amino]ethyl]-w-hydroxy- or N-ethylperfluorooctanesulfonamide poly(ethylene glycol)	NA	29117-08-6	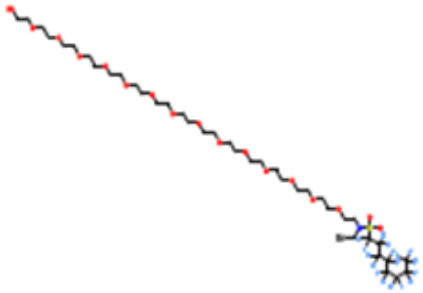	Environment Canada, OECD, NICNAS indirect	QSAR
Polyglycol Derivatives of Perfluorooctanesulfonamides: Poly[oxy(methyl-1,2-ethanediyl)], alpha-[2-[ethyl[(heptadecafluorooctyl) sulfonyl]amino]ethyl]-omega-hydroxy-	NA	37338-48-0	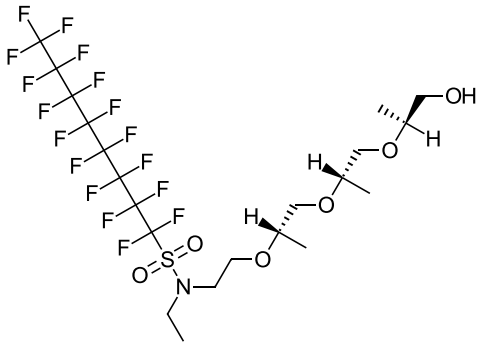	OECD, NICNAS indirect	QSAR
Polyglycol Derivatives of Perfluorooctanesulfonamides: Poly(oxy-1,2-ethanediyl), alpha-[[[(heptadecafluorooctyl)sulfonyl] methylamino] carbonyl]-omega-butoxy-	NA	52032-20-9	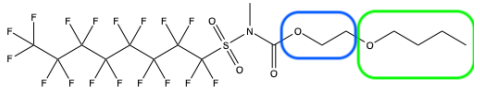	OECD	Expert judgment (supported by QSAR analysis of monomer)

Chemical name[a]	Abbreviation	CAS RN	Chemical structure	Source	Inclusion criteria (QSAR or expert)
Carbamic acid, [5-[[[2-[[(heptadecafluorooctyl)sulfonyl]methylamino]ethoxy] carbonyl]amino]-2-methylphenyl]-, 9-octadecenyl ester, (Z)-	NA	94313-84-5	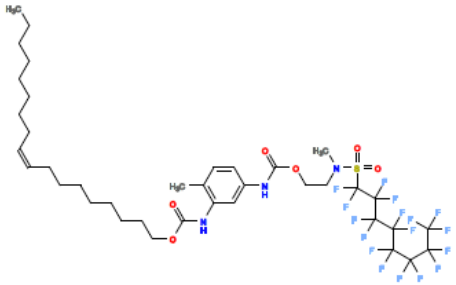	Environment Canada, OECD, NICNAS indirect	QSAR
Chromium, diaquatetrachloro[m-[N-ethyl-N-[(heptadecafluorooctyl)sulfonyl] glycinato-kO:kO']]-m-hydroxybis(2-methyl-1-propanol)di-	NA	68891–96–3	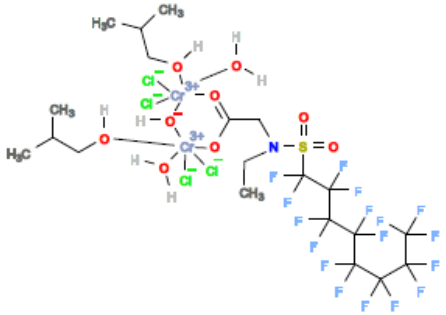	Environment Canada, OECD, NICNAS indirect	QSAR

Chemical name[a]	Abbreviation	CAS RN	Chemical structure	Source	Inclusion criteria (QSAR or expert)
1-Propanesulfonic acid, 3-[[3-(dimethylamino)propyl][(heptadecafluorooctyl) sulfonyl]amino]-	NA	72785-08-1	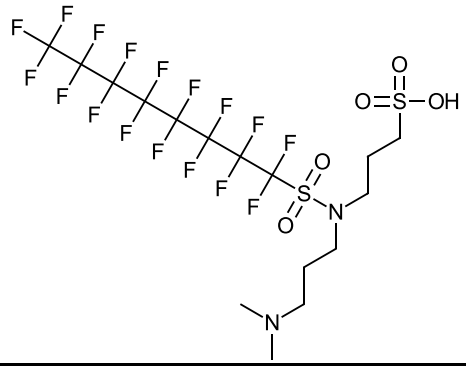	OECD	QSAR
Benzamide, 4-[[4-[[[2-[[(heptadecafluorooctyl)sulfonyl]propylamino]ethyl] amino]carbonyl]phenyl]methyl]-N-octadecyl-	NA	73019-19-9	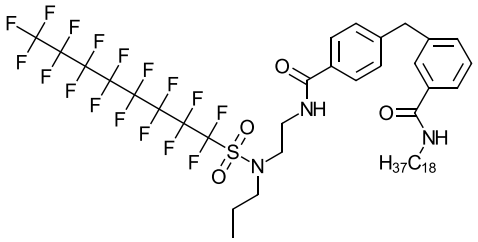	OECD	QSAR

[a] Chemical names are defined by OECD unless otherwise specified.
NA, Neither CAS RN or abbreviation is available.

Table A4 PFOS precursors: telomers, polymers, fatty acid derivatives, and mixtures

Chemical name[a]	CAS RN	Chemical structure description	Source	Inclusion criteria (QSAR or expert)
Telomers				
2-Propenoic acid, 2-methyl-, 2-[ethyl[(heptadecafluorooctyl) sulfonyl] amino]ethyl ester, telomer with 2-[ethyl[(nonafluorobutyl)sulfonyl] amino]ethyl 2-methyl-2-propenoate, 2-[ethyl [(pentadecafluoroheptyl) sulfonyl]amino]ethyl 2-methyl-2-propenoate, 2-[ethyl[(tridecafluorohexyl) sulfonyl]amino]ethyl 2-methyl-2-propenoate, 2-[ethyl[(undecafluoropentyl) sulfonyl]amino]ethyl 2-methyl-2-propenoate, methyloxirane polymer with oxirane di-2-propenoate, methyloxirane polymer with oxirane mono-2-propenoate and 1-octanethiol	68227-87-2	Methacrylate and acrylate telomers with perfluorooctane sulfonamide side chains and PFOS like precursor here is 2-Propenoic acid, 2-methyl-, 2-[ethyl[(heptadecafluorooctyl)sulfonyl] amino]ethyl ester	OECD, NICNAS indirect	Expert judgment (supported by QSAR analysis of monomer)
2-Propenoic acid, butyl ester, telomer with 2-[[(heptadecafluorooctyl) sulfonyl]methylamino]ethyl 2-propenoate, 2-[methyl[(nonafluorobutyl) sulfonyl]amino] ethyl 2-propenoate, alpha-(2-methyl-1-oxo-2-propenyl)-omega-hydroxypoly(oxy-1,4-butanediyl), alpha-(2-methyl-1-oxo-2-propenyl)-omega-[(2-methyl-1-oxo-2-propenyl)oxy]poly(oxy-1,4-butanediyl), 2-[methyl[(pentadecafluoroheptyl)sulfonyl] amino]ethyl 2-propenoate, 2-[methyl[(tridecafluorohexyl)sulfonyl]amino]ethyl 2-propenoate, 2-[methyl[(undecafluoropentyl)sulfonyl]amino]ethyl 2-propenoate and 1-octanethiol	68227-96-3	PFOS like precursor here is: 2-[[(heptadeca fluorooctyl)sulfonyl] methylamino]ethyl 2-propenoate	OECD	Expert judgment (supported by QSAR analysis of monomer)
2-Propenoic acid, 2-[butyl[(heptadecafluorooctyl)sulfonyl]amino] ethyl ester, telomer with 2-[butyl[(pentadecafluoroheptyl) sulfonyl]amino]ethyl 2-propenoate, methyloxirane polymer with oxirane di-2-propenoate, methyloxirane polymer with oxirane mono-2-propenoate and 1-octanethiol	68298-62-4	Methacrylate and acrylate polymers with perfluorooctane sulfonamide side chains	Environment Canada, OECD, NICNAS indirect	Environment Canada Expert

Chemical name[a]	CAS RN	Chemical structure description	Source	Inclusion criteria (QSAR or expert)
2-Propenoic acid, 2-methyl-, 2-[[[[5-[[[2-[ethyl[(heptadecafluorooctyl) sulfonyl]amino]ethoxy]carbonyl]amino]-2-methylphenyl]amino]carbonyl] oxy]propyl ester, telomer with butyl 2-propenoate, 2-[[[[5-[[[2-[ethyl [(nonafluorobutyl) sulfonyl]amino] ethoxy]carbonyl]amino]-2-methylphenyl]amino]carbonyl]oxy]propyl 2-methyl-2-propenoate, 2-[[[[5-[[[2-[ethyl[(pentadecafluoroheptyl) sulfonyl]amino]ethoxy] carbonyl] amino]-2-methylphenyl]amino]carbonyl] oxy]propyl 2-methyl-2-propenoate, 2-[[[[5-[[[2-[ethyl[(tridecafluorohexyl) sulfonyl]amino]ethoxy] carbonyl] amino]-2-methylphenyl]amino]carbonyl] oxy]propyl 2-methyl-2-propenoate, 2-[[[[5-[[[2-[ethyl[(undecafluoropentyl) sulfonyl]amino]ethoxy] carbonyl]amino]-2-methylphenyl]amino]carbonyl] oxy]propyl 2-methyl-2-propenoate, 2-[[(heptadecafluorooctyl)sulfonyl] methylamino]ethyl 2-propenoate, 2-[methyl[(nonafluorobutyl)sulfonyl] amino]ethyl 2-propenoate, 2-[methyl[(pentadecafluoroheptyl)sulfonyl] amino]ethyl 2-propenoate, 2-[methyl[(tridecafluorohexyl)sulfonyl]amino]ethyl 2-propenoate, 2-[methyl[(undecafluoropentyl)sulfonyl]amino]ethyl 2-propenoate and 1-octanethiol	68298-78-2	Methacrylate and acrylate telomers with perfluorooctane sulfonamide side chains	Environment Canada, OECD, NICNAS indirect	Environment Canada, Expert
2-Propenoic acid, 2-methyl-, 4-[[(heptadecafluorooctyl) sulfonyl] methylamino] butyl ester, telomer with butyl 2-propenoate, 2-[[(heptadecafluorooctyl) sulfonyl]methylamino]ethyl 2-propenoate, 4-[methyl[(nonafluorobutyl) sulfonyl]amino]butyl 2-methyl-2-propenoate, 2-[methyl[(nonafluorobutyl) sulfonyl]amino]ethyl 2-propenoate, alpha-(2-methyl-1-oxo-2-propenyl)-omega-hydroxypoly(oxy-1,4-butanediyl), alpha-(2-methyl-1-oxo-2-propenyl)-omega-[(2-methyl-1-oxo-2-propenyl)oxy] poly(oxy-1,4-butanediyl), 4-[methyl[(pentadecafluoroheptyl) sulfonyl] amino]butyl 2-methyl-2-propenoate, 2-[methyl [(pentadecafluoroheptyl) sulfonyl]amino]ethyl 2-propenoate, 4-[methyl [(tridecafluorohexyl) sulfonyl]amino]butyl 2-methyl-2-propenoate, 2-[methyl [(trideca fluorohexyl)sulfonyl]amino]ethyl 2-propenoate, 4-[methyl [(undeca fluoropentyl)sulfonyl]amino]butyl 2-methyl-2-propenoate, 2-[methyl [(undecafluoropentyl)sulfonyl]amino]ethyl 2-propenoate and 1-octanethiol	68299-39-8	Methacrylate and acrylate telomers with perfluorooctane sulfonamide side chains and 2 PFOS precursors here are 2-Propenoic acid, 2-methyl-, 4-[[(heptadeca fluorooctyl)sulfonyl] methylamino] butyl ester and 2-[[(hepta decafluorooctyl) sulfonyl]methylamino] ethyl 2-propenoate	OECD, NICNAS indirect	Expert judgment (supported by QSAR analysis of 2 monomers)

Chemical name[a]	CAS RN	Chemical structure description	Source	Inclusion criteria (QSAR or expert)
2-Propenoic acid, 2-[[(heptadecafluorooctyl)sulfonyl]methylamino]ethyl ester, telomer with 2-[methyl[(nonafluorobutyl)sulfonyl]amino]ethyl 2-propenoate, a-(2-methyl-1-oxo-2-propenyl)-w-hydroxypoly(oxy-1,2-ethanediyl), a-(2-methyl-1-oxo-2-propenyl)-w-[(2-methyl-1-oxo-2-propenyl)oxy]poly(oxy-1,2-ethanediyl), 2-[methyl[(pentadecafluoroheptyl) sulfonyl]amino]ethyl 2-propenoate, 2-[methyl[(tridecafluorohexyl) sulfonyl]amino]ethyl 2-propenoate, 2-[methyl[(undecafluoropentyl) sulfonyl]amino]ethyl 2-propenoate and 1-octanethiol	68586-14-1	Methacrylate and acrylate telomers with perfluorooctane sulfonamide side chains	Environment Canada, OECD, NICNAS indirect	Environment Canada Expert
2-Propenoic acid, 2-methyl-, 2-[ethyl[(heptadecafluorooctyl)sulfonyl] amino]ethyl ester, telomer with 2-[ethyl[(nonafluorobutyl)sulfonyl]amino] ethyl 2-methyl-2-propenoate, 2-[ethyl[(pentadecafluoroheptyl) sulfonyl]amino]ethyl 2-methyl-2-propenoate, 2-[ethyl[(tridecafluorohexyl) sulfonyl]amino]ethyl 2-methyl-2-propenoate, 2-[ethyl[(undecafluoropentyl) sulfonyl]amino]ethyl 2-methyl-2-propenoate, 1-octanethiol and a-(1-oxo-2-propenyl)-w-methoxypoly(oxy-1,2-ethanediyl)	68867-62-9	Methacrylate and acrylate telomers with perfluorooctane sulfonamide side chains	Environment Canada, OECD, NICNAS indirect	Environment Canada Expert
2-Propenoic acid, 2-methyl-, 2-[[[[5-[[[4-[[(heptadecafluorooctyl)sulfonyl] methylamino]butoxy]carbonyl]amino]-2-methylphenyl]amino]carbonyl] oxy]propyl ester, telomer with butyl 2-propenoate, 2-[[(heptadeca fluorooctyl)sulfonyl]methylamino]ethyl 2-propenoate, 2-[[[[2-methyl-5-[[[4-[methyl [(nonafluorobutyl)sulfonyl]amino]butoxy]carbonyl]amino] phenyl]amino] carbonyl]oxy]propyl 2-methyl-2-propenoate, 2-[[[[2-methyl-5-[[[4-[methyl [(pentadecafluoroheptyl)sulfonyl]amino]butoxy] carbonyl]amino]phenyl]amino]carbonyl]oxy]propyl 2-methyl-2-propenoate, 2-[[[[2-methyl-5-[[[4-[methyl[(tridecafluorohexyl)sulfonyl]amino]butoxy] carbonyl]amino]phenyl]amino]carbonyl]oxy]propyl 2-methyl-2-propenoate, 2-[[[[2-methyl-5-[[[4-[methyl[(undecafluoropentyl)sulfonyl]amino]butoxy] carbonyl]amino]phenyl]amino]carbonyl]oxy]propyl 2-methyl-2-propenoate, 2-[methyl[(nonafluorobutyl) sulfonyl]amino]ethyl 2-propenoate, 2-[methyl [(pentadecafluoroheptyl) sulfonyl]amino]ethyl 2-propenoate, 2-[methyl [(tridecafluorohexyl) sulfonyl]amino]ethyl 2-propenoate, 2-[methyl [(undecafluoropentyl)sulfonyl]amino]ethyl 2-propenoate and 1-octanethiol	70900-40-2	Methacrylate and acrylate telomers with perfluorooctane sulfonamide side chains and 2 PFOS precursors here are 2-Propenoic acid, 2-methyl-, 2-[[[[5-[[[4-[[(heptadecafluorooctyl) sulfonyl] methylamino] butoxy]carbonyl]amino]-2-methylphenyl]amino] carbonyl] oxy]propyl ester, and 2-[[(hepta decafluorooctyl)sulfonyl]methylamino]ethyl 2-propenoate	OECD, NICNAS indirect	Expert judgment (supported by QSAR analysis of 2 monomers)

Chemical name[a]	CAS RN	Chemical structure description	Source	Inclusion criteria (QSAR or expert)
Polymers				
2-Propenoic acid, 2-[[(heptadecafluorooctyl)sulfonyl]methylamino]ethyl ester, polymer with 2-[methyl[(nonafluorobutyl)sulfonyl]amino]ethyl 2-propenoate, alpha-(2-methyl-1-oxo-2-propenyl)-omega-hydroxypoly(oxy-1,2-ethanediyl), alpha-(2-methyl-1-oxo-2-propenyl)-omega-[(2-methyl-1-oxo-2-propenyl) oxy]poly(oxy-1,2-ethanediyl), 2-[methyl[(pentadecafluoroheptyl)sulfonyl] amino]ethyl 2-propenoate, 2-[methyl [(tridecafluorohexyl)sulfonyl]amino]ethyl 2-propenoate, 2-[methyl [(undecafluoropentyl)sulfonyl]amino]ethyl 2-propenoate and alpha-(1-oxo-2-propenyl)-omega-methoxypoly(oxy-1,2-ethanediyl)	68227-94-1	PFOS like precursor here is: 2-Propenoic acid, 2-[[(heptadeca fluorooctyl)sulfonyl]met hylamino]ethyl ester	OECD	Expert judgment (supported by QSAR analysis of monomer)
2-Propenoic acid, ethyl ester, polymer with 4-[[(heptadecafluorooctyl) sulfonyl]methylamino]butyl 2-propenoate, 4-[methyl[(nonafluorobutyl) sulfonyl]amino]butyl 2-propenoate, alpha-(2-methyl-1-oxo-2-propenyl)-omega-hydroxypoly(oxy-1,4-butanediyl), alpha-(2-methyl-1-oxo-2-propenyl)-omega-hydroxypoly(oxy-1,2-ethanediyl), alpha-(2-methyl-1-oxo-2-propenyl)-omega-[(2-methyl-1-oxo-2-propenyl)oxy]poly(oxy-1,4-butanediyl), alpha-(2-methyl-1-oxo-2-propenyl)-omega-[(2-methyl-1-oxo-2-propenyl)oxy]poly(oxy-1,2-ethanediyl), 4-[methyl[(pentadeca fluoroheptyl)sulfonyl]amino]butyl 2-propenoate, 4-[methyl[(trideca fluorohexyl)sulfonyl]amino]butyl 2-propenoate and 4-[methyl [(undecafluoropentyl)sulfonyl]amino]butyl 2-propenoate	68228-00-2	PFOS like precursor here is: 4-[[(heptadeca fluorooctyl) sulfonyl] methylamino]butyl 2-propenoate	OECD	Expert judgment (supported by QSAR analysis of monomer)
2-Propenoic acid, eicosyl ester, polymer with 2-[[(heptadecafluorooctyl) sulfonyl]methylamino]ethyl 2-propenoate, hexadecyl 2-propenoate, 2-[methyl [(nonafluorobutyl)sulfonyl]amino]ethyl 2-propenoate, 2-[methyl [(pentadeca-fluoroheptyl)sulfonyl]amino]ethyl 2-propenoate, 2-[methyl [(tridecafluorohexyl) sulfonyl]amino]ethyl 2-propenoate, 2-[methyl[(undeca fluoropentyl)sulfonyl] amino]ethyl 2-propenoate and octadecyl 2-propenoate	68329-56-6	Methacrylate and acrylate polymers with perfluorooctane sulfonamide side chains	Environment Canada, OECD, NICNAS indirect	Environment Canada Expert

Chemical name[a]	CAS RN	Chemical structure description	Source	Inclusion criteria (QSAR or expert)
2-Propenoic acid, polymer with 2-[ethyl[(heptadecafluorooctyl) sulfonyl]amino]ethyl 2-methyl-2-propenoate and octadecyl 2-propenoate	68541-80-0	PFOS like precursor here is: 2-[ethyl[(heptadecafluorooctyl)sulfonyl]amino] ethyl 2-methyl-2-propenoate	OECD	Expert judgment (supported by QSAR analysis of monomer)
2-Propenoic acid, butyl ester, polymer with 2-[[(heptadecafluorooctyl)sulfonyl] methylamino]ethyl 2-propenoate, 2-[methyl[(nonafluorobutyl)sulfonyl]amino] ethyl 2-propenoate, 2-[methyl[(pentadecafluoroheptyl)sulfonyl]amino]ethyl 2-propenoate, 2-[methyl[(tridecafluorohexyl)sulfonyl]amino]ethyl 2-propenoate and 2-[methyl [(undecafluoropentyl)sulfonyl]amino]ethyl 2-propenoate	68555-90-8	Methacrylate and acrylate polymers with perfluorooctane sulfonamide side chains	Environment Canada, OECD, NICNAS indirect	Environment Canada Expert
2-Propenoic acid, 2-methyl-, 2-[ethyl[(heptadecafluorooctyl)sulfonyl]amino] ethyl ester, polymer with 2-[ethyl[(nonafluorobutyl)sulfonyl]amino]ethyl 2-methyl-2-propenoate, 2-[ethyl[(pentadecafluoroheptyl)sulfonyl]amino]ethyl 2-methyl-2-propenoate, 2-[ethyl[(tridecafluorohexyl)sulfonyl]amino]ethyl 2-methyl-2-propenoate, 2-[ethyl[(undecafluoropentyl)sulfonyl]amino]ethyl 2-methyl-2-propenoate and octadecyl 2-methyl-2-propenoate	68555-91-9	Methacrylate and acrylate polymers with perfluorooctane sulfonamide side chains	Environment Canada, OECD, NICNAS indirect	Environment Canada Expert
2-Propenoic acid, 2-methyl-, 2-[[(heptadecafluorooctyl)sulfonyl]methylamino] ethyl ester, polymer with 2-[methyl[(nonafluorobutyl)sulfonyl]amino]ethyl 2-methyl-2-propenoate, 2-[methyl[(pentadecafluoroheptyl)sulfonyl]amino]ethyl 2-methyl-2-propenoate, 2-[methyl[(tridecafluorohexyl)sulfonyl]amino]ethyl 2-methyl-2-propenoate, 2-[methyl[(undecafluoropentyl)sulfonyl]amino]ethyl 2-methyl-2-propenoate and octadecyl 2-methyl-2-propenoate	68555-92-0	Methacrylate and acrylate polymers with perfluorooctane sulfonamide side chains	Environment Canada, OECD, NICNAS indirect	Environment Canada Expert

Chemical name[a]	CAS RN	Chemical structure description	Source	Inclusion criteria (QSAR or expert)
2-Propenoic acid, 2-methyl-, 2-[ethyl[(heptadecafluorooctyl)sulfonyl]amino] ethyl ester, polymer with 2-chloro-1,3-butadiene, 2-[ethyl[(nonafluorobutyl) sulfonyl]amino]ethyl 2-methyl-2-propenoate, 2-[ethyl[(pentadecafluoroheptyl) sulfonyl]amino]ethyl 2-methyl-2-propenoate, 2-[ethyl[(tridecafluorohexyl) sulfonyl]amino]ethyl 2-methyl-2-propenoate and 2-[ethyl[(undecafluoro-pentyl)sulfonyl]amino]ethyl 2-methyl-2-propenoate	68568-77-4	Methacrylate and acrylate polymers with perfluorooctane sulfonamide side chains and PFOS Precursor here is 2-Propenoic acid, 2-methyl-, 2-[ethyl[(heptadecafluorooctyl)sulfonyl]amino] ethyl ester	OECD, NICNAS indirect	Expert judgment (supported by QSAR analysis of monomer)
2-Propenoic acid, 2-methyl-, 2-ethylhexyl ester, polymer with 2-[[(heptadecafluorooctyl)sulfonyl]methylamino]ethyl 2-propenoate, 2-[methyl[(nonafluorobutyl)sulfonyl]amino]ethyl 2-propenoate, 2-[methyl[(pentadecafluoroheptyl)sulfonyl]amino]ethyl 2-propenoate, 2-[methyl[(tridecafluorohexyl)sulfonyl]amino]ethyl 2-propenoate, 2-[methyl[(undecafluoropentyl)sulfonyl]amino]ethyl 2-propenoate and oxiranylmethyl 2-methyl-2-propenoate	68797-76-2	Methacrylate and acrylate polymers with perfluorooctane sulfonamide side chains and PFOS Precursor here is 2-[[(heptadecafluorooctyl)sulfonyl]methylamino]ethyl 2-propenoate	OECD, NICNAS indirect	Expert judgment (supported by QSAR analysis of monomer)
2-Propenoic acid, 2-[[(heptadecafluorooctyl)sulfonyl]methylamino]ethyl ester, polymer with 2-[methyl[(nonafluorobutyl)sulfonyl]amino]ethyl 2-propenoate, 2-[methyl[(pentadecafluoroheptyl)sulfonyl]amino]ethyl 2-propenoate, 2-[methyl[(tridecafluorohexyl)sulfonyl]amino]ethyl 2-propenoate, 2-[methyl[(undecafluoropentyl)sulfonyl]amino]ethyl 2-propenoate and a-(1-oxo-2-propenyl)-w-methoxypoly(oxy-1,2-ethanediyl)	68867-60-7	Methacrylate and acrylate polymers with perfluorooctane sulfonamide side chains and PFOS Precursor here is 2-Propenoic acid, 2-[[(heptadecafluorooctyl)sulfonyl]methylamino] ethyl ester	OECD, NICNAS indirect	Expert judgment (supported by QSAR analysis of monomer)

Chemical name[a]	CAS RN	Chemical structure description	Source	Inclusion criteria (QSAR or expert)
2-Propenoic acid, 2-methyl-, 2-[ethyl[(heptadecafluorooctyl)sulfonyl] amino]ethyl ester, polymer with 2-[ethyl[(nonafluorobutyl)sulfonyl]amino]ethyl 2-methyl-2-propenoate, 2-[ethyl[(pentadecafluoroheptyl)sulfonyl]amino]ethyl 2-methyl-2-propenoate, 2-[ethyl[(tridecafluorohexyl)sulfonyl]amino]ethyl 2-methyl-2-propenoate, 2-[ethyl[(undecafluoropentyl)sulfonyl]amino]ethyl 2-methyl-2-propenoate and 2-methyl-1,3-butadiene	68877-32-7	PFOS like precursor here is: 2-Propenoic acid, 2-methyl-, 2-[ethyl [(heptadecafluorooctyl) sulfonyl] amino]ethyl ester	OECD, Environment Canada	Environment Canada Expert
2-Propenoic acid, eicosyl ester, polymers with branched octyl acrylate, 2-[[(heptadecafluorooctyl)sulfonyl]methylamino]ethyl acrylate, 2-[methyl [(nonafluorobutyl)sulfonyl]amino]ethyl acrylate, 2-[methyl[(pentadecafluoro-heptyl)sulfonyl]amino]ethyl acrylate, 2-[methyl[(tridecafluorohexyl)sulfonyl] amino]ethyl acrylate, 2-[methyl[(undecafluoropentyl)sulfonyl]amino]ethyl acrylate, polyethylene glycol acrylate Me ether and stearyl acrylate	68909-15-9	Methacrylate and acrylate polymers with perfluorooctane sulfonamide side chains	Environment Canada, OECD, NICNAS indirect	Environment Canada Expert
2-Propenoic acid, 2-methyl-, octadecyl ester, polymer with 1,1-dichloroethene, 2-[[(heptadecafluorooctyl)sulfonyl]methylamino]ethyl 2-propenoate, N-(hydroxymethyl)-2-propenamide, 2-[methyl[(nonafluorobutyl)sulfonyl] amino]ethyl 2-propenoate, 2-[methyl[(pentadecafluoroheptyl)sulfonyl] amino]ethyl 2-propenoate, 2-[methyl[(tridecafluorohexyl)sulfonyl]amino]ethyl 2-propenoate and 2-[methyl[(undecafluoropentyl)sulfonyl]amino]ethyl 2-propenoate	70776-36-2	Methacrylate and acrylate polymers with perfluorooctane sulfonamide side chains	Environment Canada, OECD, NICNAS indirect	Environment Canada Expert
2-Propenoic acid, 2-methyl-, methyl ester, polymer with ethenylbenzene, 2-[[(heptadecafluorooctyl)sulfonyl]methylamino]ethyl 2-propenoate, 2-[methyl[(nonafluorobutyl) sulfonyl]amino]ethyl 2-propenoate, 2-[methyl[(pentadecafluoroheptyl)sulfonyl]amino]ethyl 2-propenoate, 2-[methyl[(tridecafluorohexyl)sulfonyl]amino]ethyl 2-propenoate, 2-[methyl[(undecafluoropentyl)sulfonyl]amino]ethyl 2-propenoate and 2-propenoic acid	71487-20-2	PFOS like precursor here is: 2-[[(hepta decafluorooctyl)sulfonyl]methylamino]ethyl 2-propenoate	Environment Canada, OECD	Environment Canada Expert

Chemical name[a]	CAS RN	Chemical structure description	Source	Inclusion criteria (QSAR or expert)
2-Propenoic acid, 2-methyl-, 2-ethylhexyl ester, polymer with 2-[[(heptadecafluorooctyl)sulfonyl]methylamino]ethyl 2-propenoate	73018-93-6	PFOS like precursor here is: 2-[[(heptadecafluorooctyl)sulfonyl]methylamino]ethyl 2-propenoate	OECD	Expert judgment (supported by QSAR analysis of monomer)
2-Propenoic acid, 2-[[(heptadecafluorooctyl)sulfonyl]propylamino]ethyl ester, polymer with alpha-(2-methyl-1-oxo-2-propenyl)-omega-methoxypoly(oxy-1,2-ethanediyl)	73019-28-0	PFOS like precursor here is: 2-Propenoic acid, 2-[[(heptadecafluorooctyl)sulfonyl]propylamino]ethyl ester	OECD	Expert judgment (supported by QSAR analysis of monomer)
2-Propenoic acid, 2-[[(heptadecafluorooctyl)sulfonyl]propylamino]ethyl ester, polymer with methyloxirane polymer with oxirane mono(2-methyl-2-propenoate)	73038-33-2	PFOS like precursor here is: 2-Propenoic acid, 2-[[(heptadecafluorooctyl)sulfonyl]propylamino]ethyl ester	OECD	Expert judgment (supported by QSAR analysis of monomer)
2-Propenoic acid, 2-[[(heptadecafluorooctyl)sulfonyl]propylamino]ethyl ester, polymer with alpha-(2-methyl-1-oxo-2-propenyl)-omega-butoxypoly[oxy (methyl-1,2-ethanediyl)]	73275-59-9	PFOS like precursor here is: 2-Propenoic acid, 2-[[(heptadecafluorooctyl)sulfonyl]propylamino]ethyl ester	OECD	Expert judgment (supported by QSAR analysis of monomer)
Ethanaminium, N,N,N-trimethyl-2-[(2-methyl-1-oxo-2-propenyl)oxy]-, chloride, polymer with 2-ethoxyethyl 2-propenoate, 2-[[(heptadecafluorooctyl)sulfonyl] methylamino]ethyl 2-propenoate and oxiranylmethyl 2-methyl-2-propenoate	92265-81-1	Methacrylate and acrylate polymers with perfluorooctane sulfonamide side chains	Environment Canada, OECD, NICNAS indirect	Environment Canada Expert

Chemical name[a]	CAS RN	Chemical structure description	Source	Inclusion criteria (QSAR or expert)
2-Propenoic acid, 2-methyl-, 3-(trimethoxysilyl)propyl ester, polymer with ethenylbenzene, 2-[ethyl[(heptadecafluorooctyl)sulfonyl]amino]ethyl 2-propenoate and 2-hydroxyethyl 2-propenoate	95590-48-0	PFOS like precursor here is: 2-[ethyl[(heptadecafluorooctyl)sulfonyl]amino]ethyl 2-propenoate	OECD	Expert judgment (supported by QSAR analysis of monomer)
Sulfonamides, C7-8-alkane, perfluoro, N-methyl-N-[2-[(1-oxo-2-propenyl) oxy]ethyl], polymers with 2-ethoxyethyl acrylate, glycidyl methacrylate and N,N,N-trimethyl-2-[(2-methyl-1-oxo-2-propenyl)oxy]ethanaminium chloride	98999-57-6	PFOS like precursor here is: Sulfonamides, C8-alkane, perfluoro, N-methyl-N-[2-[(1-oxo-2-propenyl) oxy]ethyl]	Environment Canada, OECD	Environment Canada Expert
2-Propenoic acid, 2-methyl-, polymers with Bu methacrylate, lauryl methacrylate and 2-[methyl[(perfluoro-C4-8-alkyl)sulfonyl]amino]ethyl methacrylate	127133-66-8	Methacrylate and acrylate polymers with perfluorooctane sulfonamide side chains	OECD, Environment Canada, NICNAS indirect	Environment Canada Expert and CATABOL[b] prediction
Polymer(butyl acrylate-2-[N-methyl-N-[perfluoroalkyl[C=4-8]sulfonyl]amino] ethyl acrylate)	160336-17-4	PFOS like precursor here is: N-methyl-N-[perfluoroalkyl [C8] sulfonyl]amino]ethyl acrylate	OECD	QSAR analysis of a monomer
Sulfonamides, C4-8-alkane, perfluoro, N-ethyl-N-(hydroxyethyl), reaction products with 2-ethyl-1-hexanol and polymethylenepolyphenylene isocyanate	160901-25-7	PFOS like precursor here is: [(heptadecafluorooctyl)sulfonyl]amino] N-ethyl-N-(hydroxyethyl)	OECD	Expert judgment (supported by QSAR analysis of one of the ingredients)

Chemical name[a]	CAS RN	Chemical structure description	Source	Inclusion criteria (QSAR or expert)
Sulfonamides, C4-8-alkane, perfluoro, N-ethyl-N-(hydroxyethyl), polymers with 1,1'-methylenebis[4-isocyanatobenzene] and polymethylenepolyphenylene isocyanate, 2-ethylhexyl esters, Me Et ketone oxime-blocked	178535-22-3	PFOS like precursor here is: [(heptadeca fluorooctyl)sulfonyl]amino] N-ethyl-N-(hydroxyethyl)	OECD	Expert judgment (supported by QSAR analysis of one of the ingredients)
Siloxanes and Silicones, di-Me, mono[3-[(2-methyl-1-oxo-2-propenyl)oxy] propyl group]-terminated, polymers with 2-[methyl[(perfluoro-C4-8-alkyl) sulfonyl]amino]ethyl acrylate and stearyl methacrylate	306974-28-7	PFOS like precursor here is: 2-[methyl[(heptadecafluorooctyl) sulfonyl] amino]ethyl acrylate	OECD	Expert judgment (supported by QSAR analysis of monomer)
Propanoic acid, 3-hydroxy-2-(hydroxymethyl)-2-methyl-, polymer with 2-ethyl-2-(hydroxymethyl)-1,3-propanediol and N,N',2-tris(6-isocyanatohexyl) imidodicarbonic diamide, reaction products with N-ethyl-1,1,2,2,3,3,4,4,5,5, 6,6,7,7,8,8,8-heptadecafluoro-N-(2-hydroxyethyl)-1-octanesulfonamide and N-ethyl-1,1,2,2,3,3,4,4,5,5,6,6,7,7,7-pentadecafluoro-N-(2-hydroxyethyl)-1-heptanesulfonamide, compds. with triethylamine	306975-56-4	Urethane polymers incorporating perfluoro-octanesulfonamides	OECD, NICNAS indirect	QSAR prediction based on one of the ingredients
Propanoic acid, 3-hydroxy-2-(hydroxymethyl)-2-methyl-, polymer with 1,1'-methylenebis[4-isocyanatobenzene] and 1,2,3-propanetriol, reaction products with N-ethyl-1,1,2,2,3,3,4,4,5,5,6,6,7,7,8,8,8-heptadecafluoro-N-(2-hydroxyethyl)-1-octanesulfonamide and N-ethyl-1,1,2,2,3,3,4,4,5,5,6,6,7,7,7-pentadecafluoro-N-(2-hydroxyethyl)-1-heptanesulfonamide, compds. with morpholine	306975-57-5	PFOS like precursor here is: N-ethyl-1,1,2,2,3,3,4,4,5,5,6,6,7,7,8,8,8-heptadeca fluoro-N-(2-hydroxy ethyl)-1-octane sulfonamide	OECD	QSAR prediction based on one of the ingredients

Chemical name[a]	CAS RN	Chemical structure description	Source	Inclusion criteria (QSAR or expert)
2-Propenoic acid, 2-methyl-, dodecyl ester, polymers with 2-[methyl[(perfluoro-C4-8-alkyl)sulfonyl]amino]ethyl acrylate and vinylidene chloride	306975-62-2	PFOS like precursor here is: 2-[[(heptadecafluorooctyl)sulfonyl] methylamino]ethyl acrylate	OECD	Expert judgment (supported by QSAR analysis of monomer)
Poly(oxy-1,2-ethanediyl), a-hydro-w-hydroxy-, polymer with 1,6-diisocyanatohexane, N-(hydroxyethyl)-N-methylperfluoro-C4-8-alkanesulfonamides-blocked	306975–84–8	PFOS like precursor here is: N-(hydroxy ethyl)-N-methyl perfluoro octane sulfonamide and linked by 1,6-diisocyanato hexane moieties and ethyl hydroxy units.	OECD	Expert judgment (supported by QSAR analysis of monomer)
2-Propenoic acid, 2-methyl-, dodecyl ester, polymers with N-(hydroxymethyl)-2-propenamide, 2-[methyl[(perfluoro-C4-8-alkyl)sulfonyl]amino]ethyl methacrylate, stearyl methacrylate and vinylidene chloride	306975–85–9	PFOS like precursor here is: 2-methyl[[(heptadecafluorooctyl) sulfonyl]amino ethyl methacrylate	OECD	Expert judgment (supported by QSAR analysis of monomer)
1-Hexadecanaminium, N,N-dimethyl-N-[2-[(2-methyl-1-oxo-propenyl)oxy]ethyl]-, bromide, polymers with Bu acrylate, Bu methacrylate and 2-[methyl[(perfluoro-C4-8-alkyl)sulfonyl]amino]ethyl acrylate	306976–25–0	PFOS like precursor here is again: 2-[[(heptadecafluorooctyl)sulfonyl] methylamino]ethyl acrylate	OECD	Expert judgment (supported by QSAR analysis of monomer)
2-Propenoic acid, 2-methyl-, 2-methylpropyl ester, polymer with 2,4-diisocyanato-1-methylbenzene, 2-ethyl-2-(hydroxymethyl)-1,3-propanediol and 2-propenoic acid, N-ethyl-N-(hydroxyethyl)perfluoro-C4-8-alkanesulfonamides-blocked	306976–55–6	PFOS like precursor here is: 2-[ethyl[(heptadecafluorooctyl) sulfonyl]amino]ethyl 2-propenoate	OECD	Expert judgment (supported by QSAR analysis of monomer)

Chemical name[a]	CAS RN	Chemical structure description	Source	Inclusion criteria (QSAR or expert)
2-Propenoic acid, 2-methyl-, 2-(dimethylamino)ethyl ester, telomer with 2-[ethyl[(perfluoro-C4-8-alkyl)sulfonyl]amino]ethyl methacrylate and 1-octanethiol, N-oxides	306977–10–6	PFOS like precursor here is: 2-[ethyl[(perfluoro-C4-8-alkyl) sulfonyl]amino]ethyl methacrylate	OECD	Expert judgment (supported by QSAR analysis of one of the ingredients)
2-Propenoic acid, 2-methyl-, 3-(trimethoxysilyl)propyl ester, polymers with acrylic acid, 2-[methyl[(perfluoro-C4-8-alkyl)sulfonyl]amino]ethyl acrylate and propylene glycol monoacrylate, hydrolyzed, compds. with 2,2'-(methylimino)bis[ethanol]	306977–58–2	PFOS like precursor here is: 2-methyl[[(heptadecafluorooctyl)sulfonyl] amino]ethyl methacrylate	OECD	Expert judgment (supported by QSAR analysis of monomer)
2-Propenoic acid, butyl ester, polymers with acrylamide, 2-[methyl[(perfluoro-C4-8-alkyl)sulfonyl]amino]ethyl acrylate and vinylidene chloride	306978–04–1	PFOS like precursor here is: 2-[methyl[(heptadecafluorooctyl) sulfonyl] amino]ethyl acrylate	OECD	Expert judgment (supported by QSAR analysis of monomer)
Copolymer of 2-[N-ethylperfluoroalkane(C 4-8)sulfonamido]ethyl methacrylate and a-acryloyl-w-methoxypoly(n 10-25)(oxyethylene)	504396-13-8	PFOS like precursor here is 2-[N-ethyl (heptadecafluorooctyl) sulfonyl] amino] ethyl methacrylate	OECD	Expert judgment (supported by QSAR analysis of monomer)

Chemical name[a]	CAS RN	Chemical structure description	Source	Inclusion criteria (QSAR or expert)
2-Propenoic acid, butyl ester, polymer with 2[butyl[(heptadecafluorooctyl) sulfonyl]amino]ethyl 2-propenoate and 2-methylpropyl 2-propenoate	594864-11-6	Methacrylate and acrylate polymers with perfluorooctane sulfonamide side chains and PFOS Precursor here is 2 [butyl[(heptadecafluoro octyl) sulfonyl]amino] ethyl 2-propenoate	OECD, NICNAS indirect	Expert judgment (supported by QSAR analysis of monomer)
Oligomers of a substituted oxirane compd. with N-methyl-heptadecafluoro-N-(2-hydroxyethyl)-1-octanesulfonamide, N-methyl-pentadecafluoro-N-(2-hydroxyethyl)-1-heptanesulfoamide, N-methyl-tridecafluoro-N-(2-hydroxyethyl)-1-hexanesulfonamide, N-methyl-undecafluoro-N-(2-hydroxyethyl)-1-pentanesulfonamide, and N-methyl-nonafluoro-N-(2-hydroxyethyl)-1-butanesulfonamide	NA	PFOS like precursor here is: N-methyl-heptadecafluoro-N-(2-hydroxyethyl)-1-octanesulfonamide	OECD	QSAR prediction based on one of the ingredients
Polymer(2,3-epoxypropyl methacrylate/2-ethoxyethyl acrylate/[2-[methacryloyloxy]ethyl]trimethylammonium chloride/2-[N-methyl-N-[perfluoro-n-alkyl[C=4-8]sulfonyl]amino]ethyl acrylate	NA	PFOS like precursor here is: 2-[methyl[(heptadecafluorooctyl) sulfonyl] amino]ethyl acrylate	OECD	Expert judgment (supported by QSAR analysis of monomer)
Vegetable fatty acids, polymers with [[(heptadecafluorooctyl)sulfonyl] alkylamino]alkyl esters	NA	PFOS like precursor here is reasonably modeled as: 2-(((Hepta decafluorooctyl) sulphonyl)methylamino) ethyl acrylate	OECD	Expert judgment (supported by QSAR analysis of monomer)

Chemical name[a]	CAS RN	Chemical structure description	Source	Inclusion criteria (QSAR or expert)
2-Propenoic acid, 2-methyl-, butyl ester, polymer with 2-[ethyl[(heptadecafluorooctyl)sulfonyl]amino]ethyl 2-methyl-2-propenoate, 2-[ethyl[(nonafluorobutyl)sulfonyl]amino]ethyl 2-methyl-2-propenoate, 2-[ethyl[(pentadecafluoroheptyl)sulfonyl]amino]ethyl 2-methyl-2-propenoate, 2-[ethyl[(tridecafluorohexyl)sulfonyl]amino]ethyl 2-methyl-2-propenoate and 2-propenoic acid	L–92–0151	A polymer with a base units of:2-propenoic acid, 2-methyl-, butyl ester and its PFOS like precursor is 2-[ethyl[(heptadecafluorooctyl) sulfonyl]amino]ethyl 2-methyl-2-propenoate	OECD	Expert judgment (supported by QSAR analysis of monomer)
Fatty acid derivatives				
Fatty acids, C18-unsatd., trimers, 2-[[(heptadecafluorooctyl)sulfonyl] methylamino]ethyl esters	148240–78–2	PFOS like precursor here is: 2-[[(heptadecafluorooctyl)sulfonyl] methylamino]ethyl esters	OECD	QSAR analysis of a monomer
Fatty acids, linseed-oil, dimers, 2-[[(heptadecafluorooctyl)sulfonyl] methylamino]ethyl esters	306973–46–6	PFOS like precursor here is: 2-[[(heptadecafluorooctyl)sulfonyl] methylamino]ethyl esters	OECD	Expert judgment (supported by QSAR analysis of monomer)
Fatty acids, C18-unsatd., dimers, 2-[methyl[(perfluoro-C4-8-alkyl)sulfonyl] amino]ethyl esters	306974–63–0	PFOS like precursor here is again: 2-[[(heptadecafluorooctyl)sulfonyl] methylamino]ethyl acrylate	OECD	Expert judgment (supported by QSAR analysis of monomer)

Chemical name[a]	CAS RN	Chemical structure description	Source	Inclusion criteria (QSAR or expert)
Environment Canada: Fatty acids, C18-unsatd.,dimers, 2-[methyl[(perfluoro-C4-8-alkyl)sulfonyl]amino]ethyl esters	NA	PFOS like precursor here is: 2-[methyl[(perfluoro-C8-alkyl) sulfonyl]amino] ethyl esters	Environment Canada	Environment Canada Expert and CATABOL[b] prediction
Mixtures, including reaction products				
Sulfonic acids, C6-12-alkane, perfluoro, potassium salts	68391-09-3	PFOS like precursor here is: Sulfonic acids, C8-alkane, perfluoro, potassium salts	OECD	QSAR prediction based on one of the ingredients
Sulfonamides, C4-8-alkane, perfluoro, N-ethyl-N-(hydroxyethyl), reaction products with TDI	68608-13-9	Urethane polymers incorporating perfluoro-octanesulfonamides	OECD, NICNAS indirect	QSAR prediction based on one of the ingredients
Sulfonamides, C4-8-alkane, perfluoro, N-ethyl-N-(hydroxyethyl), reaction products with 1,1'-methylenebis[4-isocyanatobenzene]	68608–14-0	Urethane polymers incorporating perfluoro-octanesulfonamides	OECD, Environment Canada, NICNAS indirect	Environment Canada Expert and CATABOL[b] prediction

Chemical name[a]	CAS RN	Chemical structure description	Source	Inclusion criteria (QSAR or expert)
1-Octanesulfonamide, N-ethyl-1,1,2,2,3,3,4,4,5,5,6,6,7,7,8,8,8-heptadecafluoro-N-(2-hydroxyethyl)-, reaction products with N-ethyl-1,1,2,2,3,3,4,4,4-nonafluoro-N-(2-hydroxyethyl)-1-butanesulfonamide, N-ethyl-1,1,2,2,3,3,4,4,5,5,6,6,7,7,7-pentadecafluoro-N-(2-hydroxyethyl)-1-heptanesulfonamide, N-ethyl-1,1,2,2,3,3,4,4,5,5,6,6,6-tridecafluoro-N-(2-hydroxyethyl)-1-hexanesulfonamide, N-ethyl-1,1,2,2,3,3,4,4,5,5,5-undecafluoro-N-(2-hydroxyethyl)-1-pentanesulfonamide, polymethylenepolyphenylene isocyanate and stearyl alc.	68649-26-3	Urethane polymers incorporating perfluoro-octanesulfonamides	Environment Canada, OECD, NICNAS indirect	Environment Canada Expert
Sulfonamides, C4-8-alkane, perfluoro, N-(hydroxyethyl)-N-methyl, reaction products with epichlorohydrin, adipates (esters)	91081-99-1	Carboxylic acid, ester or amide derivatives of perfluorooctane sulfonamides present in the reaction mixtures	Environment Canada, OECD, NICNAS indirect	Environment Canada Expert
Sulfonic acids, C6-12-alkane, perfluoro	93572-72-6	PFOS like precursor here is: Sulfonic acids, C8-alkane, perfluoro	OECD	QSAR prediction based on one of the ingredients
Sulfonamides, C4-8-alkane, perfluoro, N-methyl-N-(oxiranylmethyl)	129813–71–4	PFOS like precursor here is: Sulfonamides, C8-alkane, perfluoro, N-methyl-N-(oxiranylmethyl)	OECD	QSAR prediction based on one of the ingredients
Sulfonamides, C4-8-alkane, perfluoro, N-(hydroxyethyl)-N-methyl, reaction products with 1,6-diisocyanatohexane homopolymer and ethylene glycol	148684-79-1	PFOS like precursor here is: Sulfonamides, C8-alkane, perfluoro, N-(hydroxyethyl)-N-methyl	Environment Canada, OECD	Environment Canada Expert

Chemical name[a]	CAS RN	Chemical structure description	Source	Inclusion criteria (QSAR or expert)
Potassium 3,4,5,6-tetrachloro-N-[3-((perfluoroalkyl(C=6-8)sulfonyloxy)) phenyl]phthalamate	160305-97-5	Mixtures of PFOSA	OECD	QSAR prediction based on one of the ingredients
Fatty acids, C18-unsatd. trimers, reaction products with 1,1,2,2,3,3,4,4,5,5, 6,6,7,7,8,8,8-heptadecafluoro-N-(2-hydroxyethyl)-N-methyl-1-octanesulfonamide, 1,1,2,2,3,3,4,4,4-nonafluoro-N-(2-hydroxyethyl)-N-methyl-1-butanesulfonamide, 1,1,2,2,3,3,4,4,5,5,6,6,7,7,7-pentadecafluoro-N-(2-hydroxyethyl)-N-methyl-1-heptanesulfonamide, 1,1,2,2,3,3,4,4,5,5,6,6,6-tridecafluoro-N-(2-hydroxyethyl)-N-methyl-1-hexanesulfonamide and 1,1,2,2,3,3,4,4,5,5,5-undecafluoro-N-(2-hydroxyethyl)-N-methyl-1-pentanesulfonamide	161074-58-4	C18-unsatd. Trimers fatty acids reacted with carboxylic acid, ester or amide derivatives of perfluorooctane sulfonamides	OECD, NICNAS indirect	QSAR prediction based on one of the ingredients
Sulfonamides, C4-8-alkane, perfluoro, N-[3-(dimethyloxidoamino)propyl], potassium salts	179005–06–2	PFOS like precursor here is: Sulfonamides, C8-alkane, perfluoro, N-[3-(dimethyloxido amino)propyl], potassium salts	OECD, Environment Canada	Environment Canada Expert
Sulfonamides, C4-8-alkane, perfluoro, N-[3-(dimethyloxidoamino)propyl]	179005-07-3	PFOS like precursor here is: Sulfonamides, C8-alkane, perfluoro, N-[3-(dimethyloxido amino)propyl]	Environment Canada, OECD	Environment Canada Expert
1-Octanesulfonamide, 1,1,2,2,3,3,4,4,5,5,6,6,7,7,8,8,8-heptadecafluoro-N-methyl-, reaction products with benzene-chlorine-sulfur chloride (S2Cl2) reaction products chlorides	182700–90–9	PFOS like precursor here is: 1-Octane sulfonamide, 1,1,2,2, 3,3,4,4,5,5,6,6,7,7,8,8,8 -heptadecafluoro-N-methyl-	OECD	QSAR prediction based on one of the ingredients

Chemical name[a]	CAS RN	Chemical structure description	Source	Inclusion criteria (QSAR or expert)
9-Octadecenoic acid (Z)-, reaction products with N-ethyl-1,1,2,2,3,3,4,4,5,5,6,6, 7,7,8,8,8-heptadecafluoro-N-(2-hydroxyethyl)-1-octanesulfonamide	185630-90-4	Carboxylic acid, ester or amide derivatives of perfluorooctane sulfonamides present in the reaction mixtures	OECD, NICNAS indirect	QSAR prediction based on one of the ingredients
Sulfonamides, C4-8-alkane, perfluoro, N-[3-(dimethylamino)propyl], reaction products with acrylic acid	192662-29-6	Carboxylic acid, ester or amide derivatives of perfluorooctane sulfonamides present in the reaction mixtures	OECD, NICNAS indirect	QSAR prediction based on one of the ingredients
2,5-Furandione, dihydro-, monopolyisobutylene derivatives reaction products with N-ethyl-1,1,2,2,3,3,4,4,5,5,6,6,7,7,8,8,8-heptadecaflouro-1-octanesulfonamide	253682-96-1	Carboxylic acid, ester or amide derivatives of perfluorooctane sulfonamides present in the reaction mixtures	OECD, NICNAS indirect	QSAR prediction based on one of the ingredients
Sulfonamides, C4-8-alkane, perfluoro, N-[3-(dimethylamino)propyl], reaction products with acrylic acid	306973-44-4	Sulfonamides, FOSA reaction products	OECD	QSAR prediction based on one of the ingredients

Chemical name[a]	CAS RN	Chemical structure description	Source	Inclusion criteria (QSAR or expert)
Sulfonamides, C4-8-alkane, perfluoro, N-(hydroxyethyl)-N-methyl, reaction products with 12-hydroxystearic acid and 2,4-TDI, ammonium salts	306973-47-7	Urethane polymers incorporating perfluoro-octanesulfonamides	OECD, NICNAS indirect	QSAR prediction based on one of the ingredients
Sulfonamides, C4-8-alkane, perfluoro, N-ethyl-N-(hydroxyethyl), reaction products with 2-ethyl-1-hexanol and polymethylenepolyphenylene isocyanate	306973-51-3	Sulfonamides reaction products	OECD	QSAR prediction based on one of the ingredients
Sulfonamides, C4-8-alkane, perfluoro, N-methyl-N-[(3-octadecyl-2-oxo-5-oxazolidinyl)methyl]	306974–19–6	Sulfonamides reaction products	OECD	QSAR prediction based on one of the ingredients
Sulfonic acids, C6-8-alkane, perfluoro, compds. with polyethylene-polypropylene glycol bis(2-aminopropyl) ether	306974–45–8	Mixtures of bis ether dimer of perfluoroalkane sulfonamides and PFOS like precursor here is likely PFOS itself	OECD	Expert judgment (supported by QSAR analysis of one of the ingredients)

Chemical name[a]	CAS RN	Chemical structure description	Source	Inclusion criteria (QSAR or expert)
Hexane, 1,6-diisocyanato-, homopolymer, N-(hydroxyethyl)-N-methylperfluoro-C4-8-alkanesulfonamides- and stearyl alc.-blocked	306978–65–4	PFOS like precursor here is N-(hydroxyethyl)-N-methyl (heptadecafluorooctyl) sulfonyl amino	OECD	Expert judgment (supported by QSAR analysis of one of the ingredients)
Poly(oxy-1,2-ethanediyl), a-[2-(methylamino)ethyl]-w-[(1,1,3,3-tetramethylbutyl) phenoxy]-, N-[(perfluoro-C4-8-alkyl)sulfonyl] derivs.	306979–40–8	PFOS like precursor here is (oxy-1,2-ethanediyl) 2-(methyl amino)ethyl (heptadeca fluorooctyl)sulfonyl amino-1,1,3,3-tetra methylbutyl) phenoxy, where the repeat unit is the short ether -C-C-O-	OECD	Expert judgment (supported by QSAR analysis of one of the ingredients)
Sulfonamides, C4-8-alkane, perfluoro, N,N'-[1,6-hexanediylbis[(2-oxo-3,5-oxazolidinediyl)methylene]]bis[N-methyl-	306980–27–8	PFOS like precursor here is: Sulfonamides, C8-alkane, perfluoro, N,N'-[1,6-hexanediyl bis[(2-oxo-3,5-oxa zolidinediyl)methylene]] bis[N-methyl-	OECD	QSAR prediction based on one of the ingredients
Reaction product of 2-butanone oxime with reaction product of a-isocyanato-w-isocyanatophenylpoly(phenylenemethylene), a-(3-hydroxypropyl-dimethylsilyl)- w-(3-hydroxypropyl)poly(n 10-15)(oxydimethylsilanediyl), poly(n 6-9)(oxy-2-methylethylene) and reaction product of 2-[N-methyl-N-perfluoroalkyl(C 3,4,5,6,7,8)sulfonylamino]ethyl acrylate with 2-mercaptoethanol (mole ratio 4:1)	507225-08-3	PFOS like precursor here is: 2-[N-methyl-N-perfluoroalkyl(C8) sulfonylamino] ethyl acrylate	OECD	QSAR prediction based on one of the ingredients

Chemical name[a]	CAS RN	Chemical structure description	Source	Inclusion criteria (QSAR or expert)
Reaction product of N-(3-aminopropyl)perfluorooctanesulfonamide, sodium 3-chloro-2-hydroxypropane-1-sulfonate and sodium 2-chloroacetate	512179-62-3	PFOS like precursor here is: N-(3-amino propyl)perfluoro octanesulfonamide, sodium 3-chloro-2-hydroxypropane-1-sulfonate	OECD	QSAR prediction based on one of the ingredients
Sodium 4-perfluoro (n 6-12) sulfoamidobenzenesulfonate	NA	PFOS like precursor here is: Sodium 4-perfluoro(n8)sulfoamido benzenesulfonate	OECD	QSAR prediction based on one of the ingredients
Sulfonamides, C7-8-alkane, perfluoro, N-ethyl-	NA	Mixtures of EtFOSA	OECD	QSAR prediction based on one of the ingredients
Sulfonamides, C7-8-alkane, perfluoro, N-ethyl-N-(hydroxyethyl), reaction products with substituted isocyanatobenzene	NA	Mixtures of EtFOSE reaction products	OECD	QSAR prediction based on one of the ingredients
Polymethylenepolyphenylene isocyanate and bis(4-NCO-phenyl)methane reaction products with 2-ethyl-1-hexanol, 2-butanone, oxime, N-ethyl-N-(2- hydroxyethyl)-1-C4-C8 perfluoroalkanesulfonamide	P–94–2205	Mixtures of EtFOSE reaction products	OECD	QSAR prediction based on one of the ingredients

Chemical name[a]	CAS RN	Chemical structure description	Source	Inclusion criteria (QSAR or expert)
NICNAS indirect: Sulfonamides, C4-8-alkane, perfluoro, N-[4,7-dimethyl-4-[[(1-methylpropylidene)amino]oxy]-3,5-dioxa-6-aza-4-silanon-6-en-1-yl]-N-ethyl	944578-05-6	Miscellaneous perfluorooctanesulfonyl derivatives present in the mixtures	NICNAS indirect	QSAR prediction based on one of the ingredients
Carbamic acid, (4-methyl-1,3-phenylene)bis-, bis[2-[ethyl[(perfluoro-C4-8-alkyl) sulfonyl]amino]ethyl] ester	68081-83-4	Mixture of carbamate esters of perfluorooctane sulfonamides	Environment Canada, OECD, NICNAS indirect	QSAR prediction based on one of the ingredients
Poly(oxy-1,2-ethanediyl), a-[2-[ethyl[(heptadecafluorooctyl)sulfonyl] amino]ethyl]-w-methoxy-	68958-61-2	It is a mixture of discrete chemicals. Representative chemical identity information is provided. However, it should be noted that this substance is expected to include a mixture of chemicals with polyethylene glycol chains containing between five and ten ethylene glycol units (average = 7.4) (Zou and Barton, 1994).	Environment Canada, OECD, NICNAS indirect	Environment Canada Expert

[a] Chemical names are defined by OECD unless otherwise specified.

[b] CATABOL is a QSAR-based biodegradation simulator and generates a microbial metabolic pathway tree, based upon each substance "query" structure, and a prediction for biodegradability. The metabolic pathway tree module is based on a training data set primarily from the University of Minnesota Biocatalysis/Biodegradation database (UM-BBD) and expert knowledge. The metabolic tree contains the products of microbial biodegradation from the parent compound down to PFOS, carbon dioxide and water or other stable metabolites.

NA, CAS RN is not available.

References cited in Appendix A

Arsenault G, Chittim B, Gu J, McAlees A, McCrindle R, Robertson V. 2008. Separation and fluorine nuclear magnetic resonance spectroscopic (19F NMR) analysis of individual branched isomers present in technical perfluorooctanesulfonic acid (PFOS). Chemosphere 73:S53-59.

Benskin JP, De Silva AO, Martin LJ, Arsenault G, McCrindle R, Riddell N, et al. 2009a. Disposition of perfluorinated acid isomers in Sprague-Dawley rats; part 1: single dose. Environmental toxicology and chemistry 28:542-554.

Benskin JP, Ikonomou MG, Gobas FA, Woudneh MB, Cosgrove JR. 2012. Observation of a novel PFOS-precursor, the perfluorooctane sulfonamido ethanol-based phosphate (SAmPAP) diester, in marine sediments. Environmental science & technology 46:6505-6514.

Buck RC, Franklin J, Berger U, Conder JM, Cousins IT, de Voogt P, et al. 2011. Perfluoroalkyl and polyfluoroalkyl substances in the environment: terminology, classification, and origins. Integrated environmental assessment and management 7:513-541.

Dimitrov S, Kamenska V, Walker JD, Windle W, Purdy R, Lewis M, et al. 2004. Predicting the biodegradation products of perfluorinated chemicals using CATABOL. SAR and QSAR in environmental research 15:69-82.

Environment Canada. 2006. Canadian Environmental Protection Act, 1999 (CEPA 1999): Ecological Screening Assessment Report on Perfluorooctane Sulfonate, Its Salts and Its Precursors that Contain the C8F17SO2 or C8F17SO3, or C8F17SO2N Moiety. Available: https://www.ec.gc.ca/lcpe-cepa/documents/substances/spfo-pfos/ecological_sar_pfos_eng.pdf.

Gebbink WA, Bignert A, Berger U. 2016. Perfluoroalkyl Acids (PFAAs) and Selected Precursors in the Baltic Sea Environment: Do Precursors Play a Role in Food Web Accumulation of PFAAs? Environmental Science and Technology 50:6354-6362.

Martin JW, Asher BJ, Beesoon S, Benskin JP, Ross MS. 2010. PFOS or PreFOS? Are perfluorooctane sulfonate precursors (PreFOS) important determinants of human and environmental perfluorooctane sulfonate (PFOS) exposure? Journal of environmental monitoring : JEM 12:1979-2004.

NICNAS. 2019a. Direct precursors to perfluorooctanesulfonate (PFOS): Environment tier II assessment. Australia's National Industrial Chemicals Notification and Assessment Scheme (NICNAS). Available: https://www.industrialchemicals.gov.au/sites/default/files/Direct%20precursors%20to%20perfluorooctanesulfonate%20%28PFOS%29_%20Environment%20tier%20II%20assessment.pdf.

NICNAS. 2019b. Indirect precursors to perfluorooctanesulfonate (PFOS): Environment tier II assessment. Australia's National Industrial Chemicals Notification and Assessment Scheme (NICNAS). Available: https://www.industrialchemicals.gov.au/sites/default/files/Indirect%20precursors%20to%20perfluorooctanesulfonate%20%28PFOS%29_%20Environment%20tier%20II%20assessment.pdf.

OECD. 2007. Lists of PFOS, PFAS, PFOA, PFCA, Related Compounds and Chemicals that may degrade to PFCA. Available: http://www.oecd.org/ehs/.

Williams AJ, Grulke CM, Edwards J, McEachran AD, Mansouri K, Baker NC, et al. 2017. The CompTox Chemistry Dashboard: a community data resource for environmental chemistry. Journal of cheminformatics 9:1-27.

Xie W, Wu Q, Kania-Korwel I, Tharappel JC, Telu S, Coleman MC, et al. 2009. Subacute exposure to N-ethyl perfluorooctanesulfonamidoethanol results in the formation of perfluorooctanesulfonate and alters superoxide dismutase activity in female rats. Archives of toxicology 83:909-924.

Appendix B. Literature Search on the Carcinogenicity of PFOS and Its Salts and Transformation and Degradation Precursors

Literature searches on the carcinogenicity of perfluorooctane sulfonic acid (PFOS), its salts, and transformation and degradation precursors were conducted in February 2021. The goal was to identify peer-reviewed journal articles, print and digital books, reports, and gray literature that potentially reported toxicological and epidemiological information on the carcinogenicity of this chemical.

As described below, we used an approach similar to that recommended by the National Toxicology Program (NTP) Handbook for Preparing Report on Carcinogens (RoC) Monographs (NTP 2015; https://ntp.niehs.nih.gov/ntp/roc/handbook/roc_handbook_508.pdf).

Three searches were conducted:

- Primary searches in major biomedical databases, conducted by OEHHA librarian Nancy Firchow, MLS
- Searches in other data sources, including authoritative reviews and reports, and databases or web resources, conducted by OEHHA scientists
- Additional focused searches, conducted by OEHHA scientists

In addition to data identified from these searches, OEHHA also considered the following information:

- One submission received from the data call-in period
- OEHHA (2021), "Proposed Public Health Goals for Perfluorooctanoic Acid and Perfluorooctane Sulfonic Acid in Drinking Water"

Primary Search Process

1) Data Sources

Table B1 lists the data sources that were searched to find information on PFOS, its salts, and its precursors. The list is adapted from the recommendation by the NTP Handbook for Preparing Report on Carcinogens (RoC) Monographs (NTP 2015), based on availability and suitability for this topic.

Table B1 Biomedical literature databases used in Primary Literature Search

PubMed (National Library of Medicine) (https://www.ncbi.nlm.nih.gov/pmc/)
Embase (https://www.embase.com/)
Scopus (https://www.scopus.com/)
SciFinder-n (https://scifinder-n.cas.org/)

2) Search Term Identification

The US EPA's Computational Toxicology (CompTox) Chemicals Dashboard (https://comptox.epa.gov/dashboard) was used to identify synonyms for PFOS, its salts, and its precursors, The PubMed MeSH database (https://www.ncbi.nlm.nih.gov/mesh/) was used to find subject headings and other index terms related to the chemicals.

The PubMed Cancer filter (https://www.nlm.nih.gov/bsd/pubmed_subsets/cancer_strategy.html) was used for cancer-related terminology.

NTP's Standard Search Strings for Literature Database Searches: Appendix to the Draft Handbook for Preparing Report on Carcinogens Monographs (https://ntp.niehs.nih.gov/ntp/roc/handbook/rochandbookappendix_508.pdf) was used to identify search strategies for ADME, Key Characteristics of Carcinogens, and other mechanistic concepts.

3) Primary Search Execution – PFOS and its Salts

Searches were executed in PubMed, Embase, and Scopus in February 2021. Four separate searches were done in each database, as follows.

- Human cancer studies
- Animal cancer studies
- ADME studies
- Studies on Key Characteristics of Carcinogens and other mechanistic concepts.

The basic search structure used for each of the four separate types of searches is presented in Table B3 through B5.

Table B2 Human cancer studies search structure

Search step	Search Concepts
#1	PFOS terms
#2	Cancer terms (PubMed Cancer Filter)
#3	#1 AND #2
#4	Limit #3 to humans

Table B3 Animal cancer studies search structure

Search step	Search Concepts
#1	PFOS terms
#2	Cancer terms (PubMed Cancer Filter)
#3	#1 AND #2
#4	Limit #3 to animals

Table B4 ADME studies search structure

Search step	Search Concepts
#1	PFOS terms
#2	RoC ADME strategy
#3	#1 AND #2

Table B5 Studies on key characteristics of carcinogens and other mechanistic concepts

Search step	Search Concepts
#1	PFOS terms
#2	RoC Key Characteristics of Carcinogens strategy
#3	RoC Other Mechanistic strategy
#4	#1 AND (#2 OR #3)

The searches were run first in PubMed. Then the search terms and syntax were tailored according to the search features unique to the other databases. For example, Embase uses different subject headings than PubMed, so the Emtree subject heading list was searched to identify equivalent terms to replace the MeSH terms used in the PubMed searches.

Results from all databases were uploaded to EndNote, maintaining separate libraries for each of the four concepts searched. Duplicates were removed. The results of the four primary searches for PFOS and its salts are shown in Table B6.

Table B6 PFOS and its salts search results

Search	PubMed Results	Embase Results	Scopus Results	Unique Results After Deduplication
Human Cancer	190	171	141	268
Animal Cancer	135	121	80	224
Human and animal cancer	325	292	221	379
ADME	655	632	810	1280
Studies on Key Characteristics of Carcinogens and other mechanistic concepts	569	752	626	943

4) Primary Search Execution – PFOS Precursors

As mentioned in section 1.1.2, a quick screening of the published scientific literature and of the bioactivity modules on the US EPA CompTox Chemicals Dashboard site (https://comptox.epa.gov/dashboard, accessed in February 2021) was performed on each listed PFOS precursor, and seven were identified as having some data relevant to carcinogenicity. Searches were executed in the four biomedical databases (Table B1) for seven PFOS precursors:

- PFOSF
- EtPFOSE
- EtPFOSA
- EtPFOSAA
- MePFOSE
- MePFOSAA
- PFOSA

In PubMed, Embase and Scopus, all searches were run using chemical terms and synonyms with no further limits. For PFOSA, an additional search was done using the chemical terms combined with the PubMed Cancer Filter. A final search was run using just the text term "PFOS precursor*".

In SciFinder-n searches were run using the precursor CAS Registry Number (CAS RN) combined with the keywords "cancer", "carcinogen*", "tumor*", "tumour*", and "neoplas*".

Table B7 outlines the basic search structures used in each database. Searches were executed in February 2021.

Table B7 PFOS precursor search structures

Search Topic	Database and Search Structure			
	PubMed	Embase	Scopus	SciFinder-n
PFOSF	PFOSF Terms	PFOSF Terms	PFOSF Terms	PFOSF CAS RN AND Cancer Keywords
EtPFOSE	EtPFOSE Terms	EtPFOSE Terms	EtPFOSE Terms	EtPFOSE CAS RN AND Cancer Keywords
EtPFOSA	EtPFOSA Terms	EtPFOSA Terms	EtPFOSA Terms	EtPFOSA CAS RN AND Cancer Keywords
EtPFOSAA	EtPFOSAA Terms	EtPFOSAA Terms	EtPFOSAA Terms	EtPFOSAA CAS RN AND Cancer Keywords
MePFOSE	MePFOSE Terms	EtPFOSAA Terms	EtPFOSAA Terms	MePFOSE CAS RN AND Cancer Keywords
MePFOSAA	MePFOSAA Terms	MePFOSAA Terms	MePFOSAA Terms	MePFOSAA CAS RN AND Cancer Keywords
PFOSA – Broad Search	PFOSA Terms	PFOSA Terms	PFOSA Terms	N/A[1]
PFOSA – Limited to Cancer	PFOSA Terms AND PubMed Cancer Filter	PFOSA Terms AND PubMed Cancer Filter	PFOSA Terms AND PubMed Cancer Filter	PFOSA CAS RN AND Cancer keywords
Precursor Text Search	"PFOS precursor*"	"PFOS precursor*"	"PFOS precursor*"	"PFOS precursor*"

[1] A broad PFOSA Search was not conducted in SciFinder-n.

As with PFOS and its salts, searches were done first in PubMed, then search terms and syntax were tailored for each additional database that was searched.

Results from all databases were uploaded to EndNote, maintaining separate libraries for each of the searches. Duplicates were removed. The results of the primary searches for PFOS precursors are shown in Table B8.

Table B8 PFOS precursors search results

Search	PubMed Results	Embase Results	Scopus Results	SciFinder-n Results	Unique Results After Deduplication
PFOSF	58	79	89	9	110
EtPFOSE	45	51	55	7	64
EtPFOSA	83	79	144	8	134
EtPFOSAA	68	42	44	8	54
MePFOSE	25	28	31	3	34
MePFOSAA	37	25	27	15	44
PFOSA – Broad Search	413	478	806	N/A[1]	892
PFOSA with cancer filter/terms	36	48	87	28	153
"PFOS precursor"[2]	57	91	100	60	111

[1] A broad PFOSA Search was not conducted in SciFinder-n.
[2] "PFOS precursor" was used as the only keyword for the search in the four databases listed.

Detailed PubMed search strategies for all primary searches are presented in Table B9 – Table B13. Detailed strategies translated for other databases (Embase, Scopus, SciFinder-n) are available upon request.

Other Data Source Searches

Several additional databases and websites of authoritative bodies were searched for data and additional references that may have been missed for our literature search pertaining to PFOS and its salts and precursors.

Authoritative reviews and reports:

- International Agency for Research on Cancer (IARC) publications, including but not limited to IARC Monographs on the Identification of Carcinogenic Hazards to Humans (https://monographs.iarc.fr/)
- NTP publications, including but not limited to, technical reports, nominations for toxicological evaluation documents, RoC monographs, RoC background documents or monographs, and NTP Office of Health Assessment and Translation (OHAT) monographs (https://ntp.niehs.nih.gov)
- US Environmental Protection Agency (US EPA) publications (https://www.epa.gov/)
- US Food and Drug Administration (US FDA) publications (https://www.fda.gov/)
- National Institute for Occupational Safety and Health (NIOSH) publications (https://www.cdc.gov/niosh/index.htm)

Other databases and web resources:

- Computational Toxicology (CompTox) Chemicals Dashboard, (https://www.epa.gov/chemical-research/comptox-chemicals-dashboard)
- Agency for Toxic Substances and Disease Registry (ATSDR) Toxicological Profiles (https://www.atsdr.cdc.gov/toxprofiles/index.asp)
- PubChem BioAssay (National Library of Medicine) (https://www.ncbi.nlm.nih.gov/pcassay)
- NCBI Gene (https://www.ncbi.nlm.nih.gov/gene/)
- OECD (for reference to toolbox and precursor list) (https://www.oecd.org/)
- Environment Canada (for precursor) (https://www.canada.ca/en/environment-climate-change.html)
- Australia (for precursors) (https://www.industrialchemicals.gov.au/)
- MalaCards (for gene functions) (https://www.malacards.org/)
- OMIM (for gene functions) (https://omim.org/)
- GeneCards (for gene functions) (https://www.genecards.org/)
- KEGG (for gene functions) (https://www.genome.jp/kegg/kegg2.html)
- CDC Public Health Genomics and Precision Health Knowledge Base (for gene functions) (https://phgkb.cdc.gov/PHGKB/phgHome.action?action=home)

Additional Focused Searches

In addition to the primary searches listed above, focused searches were conducted for epidemiology and ToxCast data. Additional relevant literature was identified from citations of individual articles.

Epidemiology

A focused search update in PubMed was conducted for human studies on June 17, 2021, using the same search strings as the primary search in PubMed and the built-in function in HAWC (Health Assessment Workspace Collaborative, see section below for information on HAWC). Based on the primary and focused searches, a total of 190 references were identified, screened and tagged accordingly.

ToxCast high-throughput screening assays

Focused searches for data on PFOS and its salts and precursors were conducted using the US EPA CompTox Chemicals Dashboard (https://comptox.epa.gov/dashboard, accessed on May 3, 2021). Chemical quality control data and assay descriptions for the

Tox21 assays (a subset of the ToxCast assays) were identified from the Tox21 Data Browser (https://tripod.nih.gov/tox21). An additional focused literature search was conducted on the interpretation and limitations of ToxCast data, including assay interferences and flags, in PubMed.

Use of Health Assessment Workspace Collaborative (HAWC)

HAWC (https://hawcproject.org/about/) was used as a tool in the systematic review of the literature on the carcinogenicity of PFOS, its salts, and its precursors, following the guidance provided in the NTP RoC Handbook (NTP 2015). Specifically:

- Importing the EndNote libraries into HAWC

The citations identified from all literature searches described above for each of the two HAWC projects (*i.e.*, PFOS and its salts, PFOS precursors) were uploaded into two corresponding EndNote libraries, and duplicates were removed. Next, the EndNote libraries were imported to HAWC for multi-level screening.

- Defining specific inclusion and exclusion criteria for multi-level literature tags in two HAWC projects.
- Screening and tagging references

In Level 1 screening, the citations were screened independently by two OEHHA scientists, based solely on titles and abstracts, to eliminate studies or articles that do not contain information on PFOS and its salts and precursors or on any of the key topics such as cancer studies in humans and animals, toxicokinetics, metabolism, genotoxicity, or cancer-associated mechanisms. The initial screen was intended to retrieve all studies deemed to have a reasonable possibility of containing information that could be useful for the review process. During the screening of each HAWC project, citations were added to the other project when appropriate. Specifically, when citations identified by the precursor HAWC project were determined to be more relevant for the PFOS project, they were moved to the PFOS HAWC project, and vice versa. Papers identified for inclusion during Level 1 screening were tagged in HAWC according to key topics. A paper can be assigned (or tagged) to one or more of the key topic(s). A positive response by only one of the reviewers was sufficient to pass a publication on to the next review level.

In Level 2 screening, the full papers were obtained for all citations that passed the Level 1 screen. These full papers were screened independently by two OEHHA scientists, using similar inclusion/exclusion criteria as was used in the Level 1 screening. However, Level 2 reviewers could make more accurate judgments about the relevance of the citations because they were reviewing the full text of the articles, in addition to the

title and abstract. Following Level 2 screening, the tagging of articles according to key topics was updated in HAWC.

Level 1 and 2 screenings were repeated and HAWC search results were updated if additional relevant studies cited in the original set of publications ("secondary citations") were identified.

There are a lot of references that overlap between the two HAWC projects. In developing this document, we used the PFOS and its salts HAWC project as our main project. See Figure B1 for the overview of the HAWC literature screening results (literature tagtree) for the PFOS and its salts HAWC project (including the references imported from the PFOS precursors HAWC project), and Figure B2 for the overview of the HAWC literature tagtree for the PFOS precursor HAWC project.

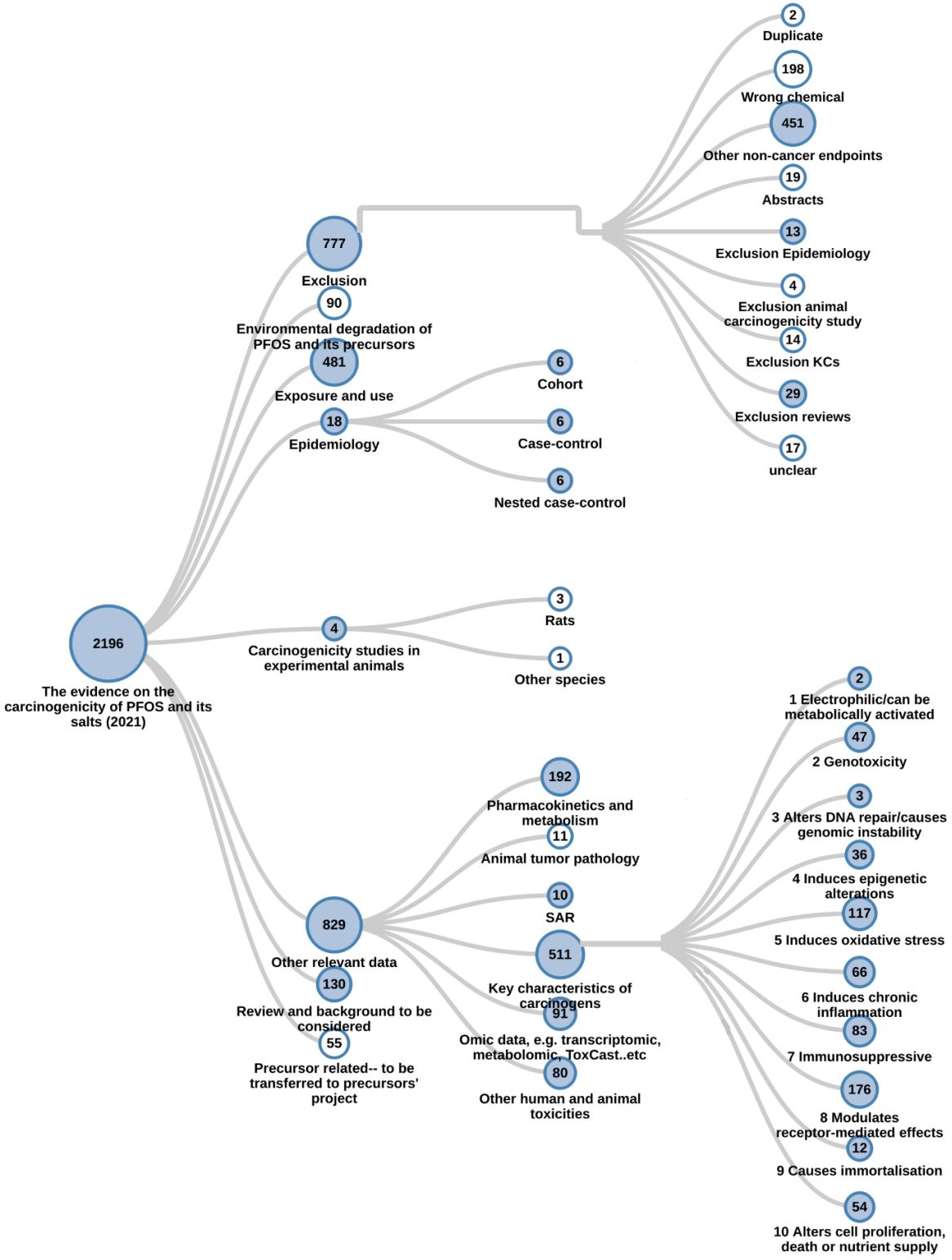

Figure B1 Overview of HAWC literature screening results (literature tagtree) for PFOS and its salts (number of citations in each tag is labelled in the node)

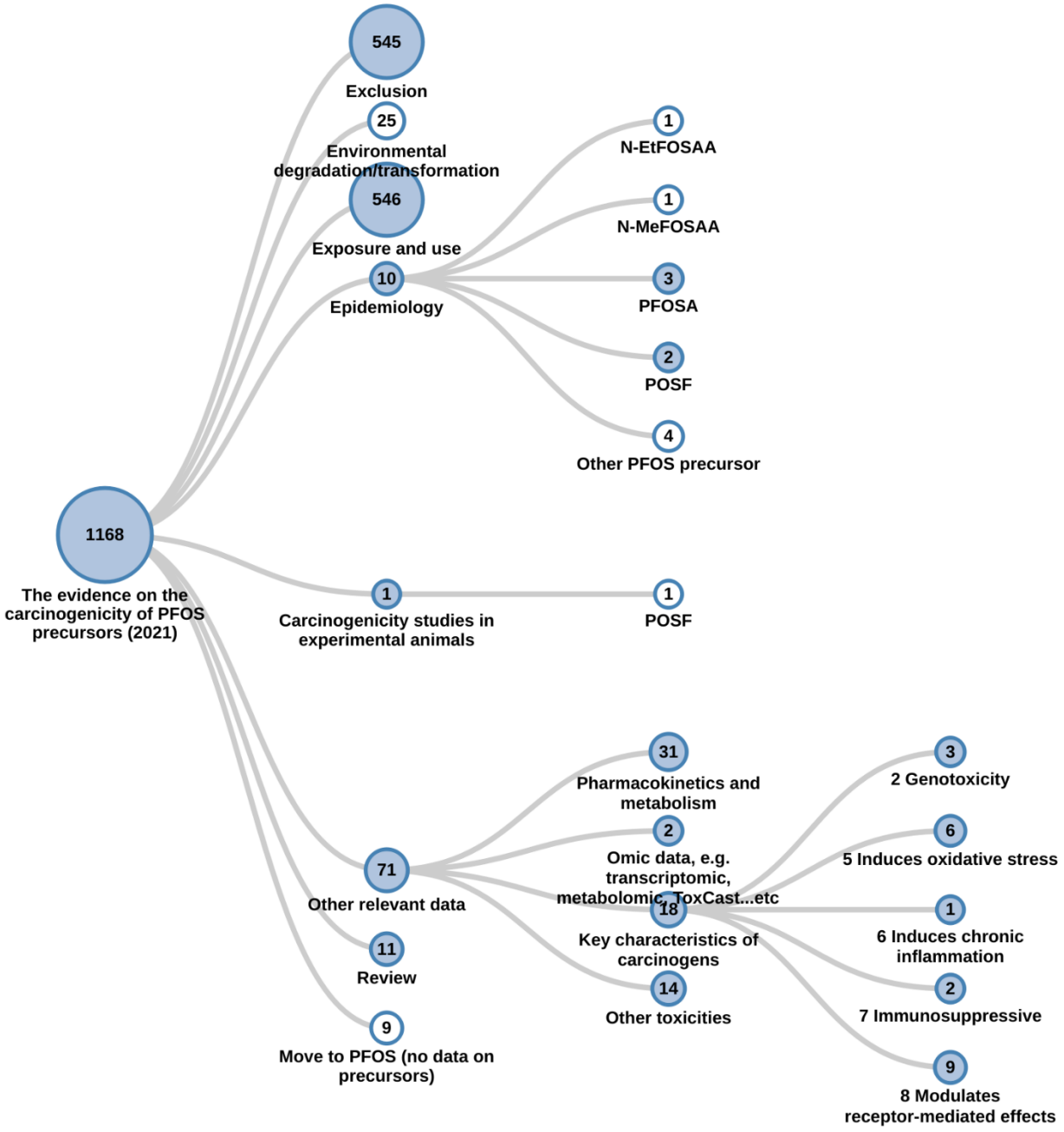

Figure B2 Overview of HAWC literature screening results (literature tagtree) for PFOS precursors (number of citations in each tag is labelled in the node).

Use of Table Builder in the organization of epidemiological data

Finally, Table Builder (Shapiro et al. 2018), a web-based application was applied to systematically extract and analyze the data that were included in Section 3.2 Carcinogenicity studies in humans. Additionally, Table Builder worked as a custom-made database to generate Word tables in this document.

Summary

In summary, approximately 2200 references, including government reports and peer-reviewed journal articles, were found through these search strategies for this HID. 1419 references were identified for inclusion and 777 references for exclusion. Among the 1419 references identified for inclusion, around 500 references were cited in this document. See Figure B3 for the overall literature search and screening process employed for this HID.

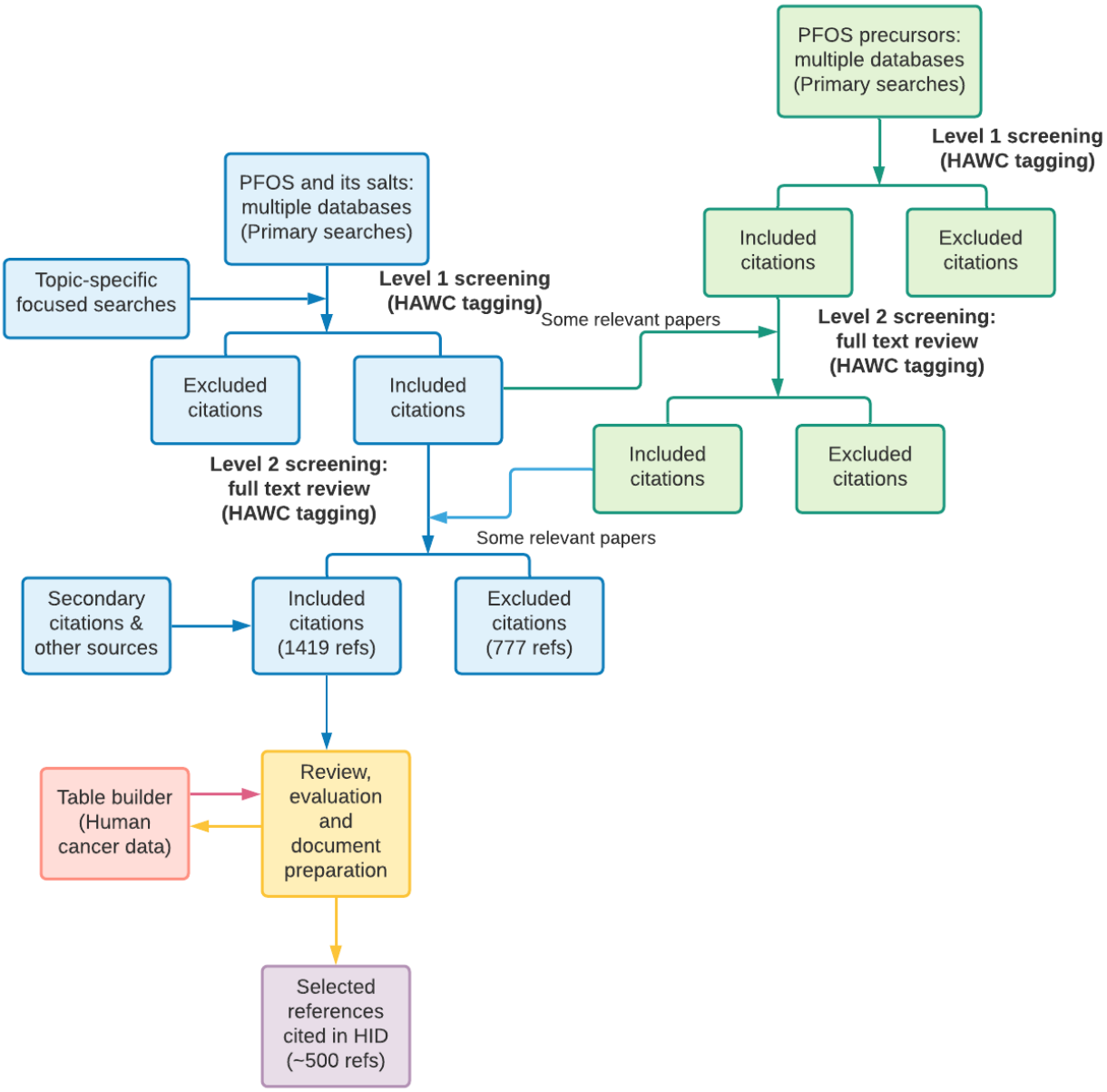

Figure B3 Overall literature search and screening process

Table B9 PubMed search strategy for human cancer studies

Set #	Search Terms	Number Retrieved	Concept
1	("perfluorooctane sulfonic acid"[nm] OR "PFOS"[Tiab] OR "PFOS anion"[Tiab] OR "PFOSH"[Tiab] OR "perfluoroalkyl sulphonate"[tiab] OR "perfluoro-n-octanesulfonic"[Tiab] OR "perfluoroctane sulfonic"[Tiab] OR "perfluorooctane sulfonic"[Tiab] OR "perfluoroctanesulfonic"[Tiab] OR "perfluorooctanesulfonic"[Tiab] OR "perfluorooctane sulphonic"[Tiab] OR "perfluoroctane sulphonic"[Tiab] OR "perfluoroctanesulphonic"[Tiab] OR "perfluorooctanesulphonic"[Tiab] OR "perfluorooctane sulfonate"[Tiab] OR "perfluoroctane sulfonate"[Tiab] OR "perfluorooctanesulfonate"[Tiab] OR "perfluoroctanesulfonate"[Tiab] OR "perfluorooctane sulphonate"[Tiab] OR "perfluoroctane sulphonate"[Tiab] OR "perfluoroctanesulphonate"[Tiab] OR "perfluorooctanesulphonate"[Tiab] OR "perfluorooctanyl sulfonate"[Tiab] OR "perfluorooctanyl sulphonate"[Tiab] OR "perfluoroctylsulfonic"[Tiab] OR "heptadecafluoro-1-octanesulfonic"[Tiab] OR "heptadecafluoro-1-octane sulfonic"[Tiab] OR "heptadecafluorooctane sulfonic"[Tiab] OR "heptadecafluoroctane sulfonic"[Tiab] OR "heptadecafluorooctane sulfonic"[Tiab] OR "heptadecafluorooctanesulfonic"[Tiab] OR "heptadecafluorooctane-1-sulphonic"[Tiab] OR "heptadecafluorooctane sulphonic"[Tiab] OR "heptadecafluorooctane-1-sulfonate"[tiab] OR "1-octanesulfonic acid"[Tiab] OR "1-octanesulphonic acid"[Tiab] OR "1-perfluoroctanesulfonic"[Tiab] OR "1-perfluorooctanesulfonic"[Tiab] OR "octanesulfonic acid"[Tiab] OR "octanesulphonic acid"[Tiab] OR "1-Octanesulfonic acid, 1,1,2,2,3,3,4,4,5,5,6,6,7,7,8,8,8-heptadecafluoro-"[tiab] OR "N,N-Dibutyl-N-methylbutan-1-aminium heptadecafluorooctane-1-sulfonate"[tiab] OR "N,N,N-Tripropylpentan-1-aminium heptadecafluorooctane-1-sulfonate"[tiab] OR "Tetrabutylammonium perfluorooctanesulfonate"[tiab] OR "N,N,N-Tributylbutan-1-aminium heptadecafluorooctane-1-sulfonate"[tiab] OR "N,N,N-Triethyldecan-1-aminium heptadecafluorooctane-1-sulfonate"[tiab] OR "isopfos"[tiab] OR "6-(Trifluoromethyl)tetradecafluoro-1-heptanesulfonic acid"[tiab]	3838	PFOS Terms

Set #	Search Terms	Number Retrieved	Concept
	OR "1,1,2,2,3,3,4,4,5,6,6,7,7,7-tetradecafluoro-5-(trifluoromethyl)heptane-1-sulfonic acid"[tiab] OR "1,1,2,2,3,3,4,5,5,6,6,7,7,7-tetradecafluoro-4-(trifluoromethyl)heptane-1-sulfonic acid"[tiab] OR "1,1,2,2,3,4,4,5,5,6,6,7,7,7-tetradecafluoro-3-(trifluoromethyl)heptane-1-sulfonic acid"[tiab] OR "1,1,2,2,3,3,5,5,6,6,6-undecafluoro-4,4-bis(trifluoromethyl)hexane-1-sulfonic acid"[tiab] OR 1763-23-1[rn] OR 45298-90-6[rn] OR 124472-68-0[rn] OR 56773-56-9[rn] OR 111873-33-7[rn] OR 773895-92-4[rn] OR 2795-39-3[rn] OR 29081-56-9[rn] OR 29457-72-5[rn] OR 4021-47-0[rn] OR 70225-14-8[rn] OR 56773-42-3[rn] OR 251099-16-8[rn] OR 71463-74-6[rn] OR 90480-49-2[rn] OR 93894-67-8[rn] OR 90480-49-2[rn] OR 93894-67-8[rn] OR "PFOS-K"[tiab] OR APFOS[tiab] OR "PFOS-li"[tiab] OR "heptadecafluorooctane-1-sulfonate "[tiab] OR "heptadecafluorooctanesulfonate "[tiab] OR "heptadecafluoro-1-octanesulfonate " OR "lsooctanesulfonic acid, heptadecafluoro-, lithium salt"[tiab])		
2	cancer[sb]	6590863	PubMed Cancer Filter
3	#1 AND #2	289	
4	#3 NOT (animal[mh] NOT human[mh])	190	Remove Animal Studies

Table B10 PubMed search strategy for animal cancer studies

Set #	Search Terms	Number Retrieved	Concept
1	("perfluorooctane sulfonic acid"[nm] OR "PFOS"[Tiab] OR "PFOS anion"[Tiab] OR "PFOSH"[Tiab] OR "perfluoroalkyl sulphonate"[tiab] OR "perfluoro-n-octanesulfonic"[Tiab] OR "perfluoroctane sulfonic"[Tiab] OR "perfluorooctane sulfonic"[Tiab] OR "perfluoroctanesulfonic"[Tiab] OR "perfluorooctanesulfonic"[Tiab] OR "perfluorooctane sulphonic"[Tiab] OR "perfluoroctane sulphonic"[Tiab] OR "perfluoroctanesulphonic"[Tiab] OR "perfluorooctanesulphonic"[Tiab] OR "perfluorooctane sulfonate"[Tiab] OR "perfluoroctane sulfonate"[Tiab] OR "perfluorooctanesulfonate"[Tiab] OR "perfluoroctanesulfonate"[Tiab] OR "perfluorooctane sulphonate"[Tiab] OR "perfluoroctane sulphonate"[Tiab] OR "perfluoroctanesulphonate"[Tiab] OR "perfluorooctanesulphonate"[Tiab] OR "perfluorooctanyl sulfonate"[Tiab] OR "perfluorooctanyl sulphonate"[Tiab] OR "perfluoroctylsulfonic"[Tiab] OR "heptadecafluoro-1-octanesulfonic"[Tiab] OR "heptadecafluoro-1-octane sulfonic"[Tiab] OR "heptadecafluorooctane sulfonic"[Tiab] OR "heptadecafluoroctane sulfonic"[Tiab] OR "heptadecafluorooctane sulfonic"[Tiab] OR "heptadecafluorooctanesulfonic"[Tiab] OR "heptadecafluorooctane-1-sulphonic"[Tiab] OR "heptadecafluorooctane sulphonic"[Tiab] OR "heptadecafluorooctane-1-sulfonate"[tiab] OR "1-octanesulfonic acid"[Tiab] OR "1-octanesulphonic acid"[Tiab] OR "1-perfluoroctanesulfonic"[Tiab] OR "1-perfluorooctanesulfonic"[Tiab] OR "octanesulfonic acid"[Tiab] OR "octanesulphonic acid"[Tiab] OR "1-Octanesulfonic acid, 1,1,2,2,3,3,4,4,5,5,6,6,7,7,8,8,8-heptadecafluoro-"[tiab] OR "N,N-Dibutyl-N-methylbutan-1-aminium heptadecafluorooctane-1-sulfonate"[tiab] OR "N,N,N-Tripropylpentan-1-aminium heptadecafluorooctane-1-sulfonate"[tiab] OR "Tetrabutylammonium perfluorooctanesulfonate"[tiab] OR "N,N,N-Tributylbutan-1-aminium heptadecafluorooctane-1-sulfonate"[tiab] OR "N,N,N-Triethyldecan-1-aminium heptadecafluorooctane-1-sulfonate"[tiab] OR "isopfos"[tiab] OR "6-(Trifluoromethyl)tetradecafluoro-1-heptanesulfonic acid"[tiab] OR "1,1,2,2,3,3,4,4,5,6,6,7,7,7-tetradecafluoro-5-	3838	PFOS Terms

Set #	Search Terms	Number Retrieved	Concept
	(trifluoromethyl)heptane-1-sulfonic acid"[tiab] OR "1,1,2,2,3,3,4,5,5,6,6,7,7,7-tetradecafluoro-4-(trifluoromethyl)heptane-1-sulfonic acid"[tiab] OR "1,1,2,2,3,4,4,5,5,6,6,7,7,7-tetradecafluoro-3-(trifluoromethyl)heptane-1-sulfonic acid"[tiab] OR "1,1,2,2,3,3,5,5,6,6,6-undecafluoro-4,4-bis(trifluoromethyl)hexane-1-sulfonic acid"[tiab] OR 1763-23-1[rn] OR 45298-90-6[rn] OR 124472-68-0[rn] OR 56773-56-9[rn] OR 111873-33-7[rn] OR 773895-92-4[rn] OR 2795-39-3[rn] OR 29081-56-9[rn] OR 29457-72-5[rn] OR 4021-47-0[rn] OR 70225-14-8[rn] OR 56773-42-3[rn] OR 251099-16-8[rn] OR 71463-74-6[rn] OR 90480-49-2[rn] OR 93894-67-8[rn] OR 90480-49-2[rn] OR 93894-67-8[rn] OR "PFOS-K"[tiab] OR APFOS[tiab] OR "PFOS-li"[tiab] OR "heptadecafluorooctane-1-sulfonate "[tiab] OR "heptadecafluorooctanesulfonate "[tiab] OR "heptadecafluoro-1-octanesulfonate " OR "Isooctanesulfonic acid, heptadecafluoro-, lithium salt"[tiab])		
2	cancer[sb]	6590863	PubMed Cancer Filter
3	#1 AND #2	289	
4	#3 NOT human[mh]	135	Remove Human Studies

Table B11 PubMed search strategy for ADME

Set #	Search Terms	Number Retrieved	Concept
1	("perfluorooctane sulfonic acid"[nm] OR "PFOS"[Tiab] OR "PFOS anion"[Tiab] OR "PFOSH"[Tiab] OR "perfluoroalkyl sulphonate"[tiab] OR "perfluoro-n-octanesulfonic"[Tiab] OR "perfluoroctane sulfonic"[Tiab] OR "perfluorooctane sulfonic"[Tiab] OR "perfluoroctanesulfonic"[Tiab] OR "perfluorooctanesulfonic"[Tiab] OR "perfluorooctane sulphonic"[Tiab] OR "perfluoroctane sulphonic"[Tiab] OR "perfluoroctanesulphonic"[Tiab] OR "perfluorooctanesulphonic"[Tiab] OR "perfluorooctane sulfonate"[Tiab] OR "perfluoroctane sulfonate"[Tiab] OR "perfluorooctanesulfonate"[Tiab] OR "perfluoroctanesulfonate"[Tiab] OR "perfluorooctane sulphonate"[Tiab] OR "perfluoroctane sulphonate"[Tiab] OR "perfluoroctanesulphonate"[Tiab] OR "perfluorooctanesulphonate"[Tiab] OR "perfluorooctanyl sulfonate"[Tiab] OR "perfluorooctanyl sulphonate"[Tiab] OR "perfluoroctylsulfonic"[Tiab] OR "heptadecafluoro-1-octanesulfonic"[Tiab] OR "heptadecafluoro-1-octane sulfonic"[Tiab] OR "heptadecafluorooctane sulfonic"[Tiab] OR "heptadecafluoroctane sulfonic"[Tiab] OR "heptadecafluorooctane sulfonic"[Tiab] OR "heptadecafluorooctanesulfonic"[Tiab] OR "heptadecafluorooctane-1-sulphonic"[Tiab] OR "heptadecafluorooctane sulphonic"[Tiab] OR "heptadecafluorooctane-1-sulfonate"[tiab] OR "1-octanesulfonic acid"[Tiab] OR "1-octanesulphonic acid"[Tiab] OR "1-perfluoroctanesulfonic"[Tiab] OR "1-perfluorooctanesulfonic"[Tiab] OR "octanesulfonic acid"[Tiab] OR "octanesulphonic acid"[Tiab] OR "1-Octanesulfonic acid, 1,1,2,2,3,3,4,4,5,5,6,6,7,7,8,8,8-heptadecafluoro-"[tiab] OR "N,N-Dibutyl-N-methylbutan-1-aminium heptadecafluorooctane-1-sulfonate"[tiab] OR "N,N,N-Tripropylpentan-1-aminium heptadecafluorooctane-1-sulfonate"[tiab] OR "Tetrabutylammonium perfluorooctanesulfonate"[tiab] OR "N,N,N-Tributylbutan-1-aminium heptadecafluorooctane-1-sulfonate"[tiab] OR "N,N,N-Triethyldecan-1-aminium heptadecafluorooctane-1-sulfonate"[tiab] OR "isopfos"[tiab] OR "6-(Trifluoromethyl)tetradecafluoro-1-heptanesulfonic acid"[tiab] OR "1,1,2,2,3,3,4,4,5,6,6,7,7,7-tetradecafluoro-5-	3838	PFOS Terms

Set #	Search Terms	Number Retrieved	Concept
	(trifluoromethyl)heptane-1-sulfonic acid"[tiab] OR "1,1,2,2,3,3,4,5,5,6,6,7,7,7-tetradecafluoro-4-(trifluoromethyl)heptane-1-sulfonic acid"[tiab] OR "1,1,2,2,3,4,4,5,5,6,6,7,7,7-tetradecafluoro-3-(trifluoromethyl)heptane-1-sulfonic acid"[tiab] OR "1,1,2,2,3,3,5,5,6,6,6-undecafluoro-4,4-bis(trifluoromethyl)hexane-1-sulfonic acid"[tiab] OR 1763-23-1[rn] OR 45298-90-6[rn] OR 124472-68-0[rn] OR 56773-56-9[rn] OR 111873-33-7[rn] OR 773895-92-4[rn] OR 2795-39-3[rn] OR 29081-56-9[rn] OR 29457-72-5[rn] OR 4021-47-0[rn] OR 70225-14-8[rn] OR 56773-42-3[rn] OR 251099-16-8[rn] OR 71463-74-6[rn] OR 90480-49-2[rn] OR 93894-67-8[rn] OR 90480-49-2[rn] OR 93894-67-8[rn] OR "PFOS-K"[tiab] OR APFOS[tiab] OR "PFOS-li"[tiab] OR "heptadecafluorooctane-1-sulfonate "[tiab] OR "heptadecafluorooctanesulfonate "[tiab] OR "heptadecafluoro-1-octanesulfonate " OR "Isooctanesulfonic acid, heptadecafluoro-, lithium salt"[tiab])		
2	(("microbiome"[tiab] OR "microbiota"[mh] OR Volume-of-Distribution[tiab] OR Toxicokinetics[mh] OR tissue-distribut*[tiab] OR Renal Elimination[mh] OR protein-bound[tiab] OR protein-bind*[tiab] OR plasma-protein[tiab] OR Pharmacokinetics[mh] OR Metabolism[mh] OR kinetic[tiab] OR Intestinal Elimination[mh] OR Hepatobiliary Elimination[mh] OR Hepatobiliary[tiab] OR enterohepatic[tiab] OR entero-hepatic[tiab] OR Distribution-volume[tiab] OR cellular-clearance[tiab] OR cell-clearance[tiab] OR Biotransformation[tiab] OR bioavailability[tiab] OR ADME[tiab] OR absorptive[tiab] OR (Skin[tiab] AND absorption[tiab]) OR (Oral[tiab] AND absorption[tiab]) OR (Injection[tiab] AND absorption[tiab]) OR (Gavage[tiab] AND absorption[tiab]) OR (Dietary[tiab] AND absorption[tiab]) OR (Dermal[tiab] AND absorption[tiab]))) OR ((urine[tiab] OR Urination[tiab] OR toxicokinetic*[tiab] OR Pharmacokinetic*[tiab] OR Metabolite*[tiab] OR metabolism[tiab] OR Metabolic* [tiab] OR feces[tiab] OR fecal[tiab] OR excretion[tiab] OR defecation[tiab] OR biliary[tiab] OR Bile[tiab]) NOT Medline[sb])	2918221	ADME Terms (RoC Strategy + 2 microbiome terms)
3	#1 AND #2	**655**	Final

Table B12 PubMed search strategy for key characteristics of carcinogens and mechanistic concepts

Set #	Search Terms	Number Retrieved	Concept
1	("perfluorooctane sulfonic acid"[nm] OR "PFOS"[Tiab] OR "PFOS anion"[Tiab] OR "PFOSH"[Tiab] OR "perfluoroalkyl sulphonate"[tiab] OR "perfluoro-n-octanesulfonic"[Tiab] OR "perfluoroctane sulfonic"[Tiab] OR "perfluorooctane sulfonic"[Tiab] OR "perfluoroctanesulfonic"[Tiab] OR "perfluorooctanesulfonic"[Tiab] OR "perfluorooctane sulphonic"[Tiab] OR "perfluoroctane sulphonic"[Tiab] OR "perfluoroctanesulphonic"[Tiab] OR "perfluorooctanesulphonic"[Tiab] OR "perfluorooctane sulfonate"[Tiab] OR "perfluoroctane sulfonate"[Tiab] OR "perfluorooctanesulfonate"[Tiab] OR "perfluoroctanesulfonate"[Tiab] OR "perfluorooctane sulphonate"[Tiab] OR "perfluoroctane sulphonate"[Tiab] OR "perfluoroctanesulphonate"[Tiab] OR "perfluorooctanesulphonate"[Tiab] OR "perfluorooctanyl sulfonate"[Tiab] OR "perfluorooctanyl sulphonate"[Tiab] OR "perfluoroctylsulfonic"[Tiab] OR "heptadecafluoro-1-octanesulfonic"[Tiab] OR "heptadecafluoro-1-octane sulfonic"[Tiab] OR "heptadecafluorooctane sulfonic"[Tiab] OR "heptadecafluoroctane sulfonic"[Tiab] OR "heptadecafluorooctane sulfonic"[Tiab] OR "heptadecafluorooctanesulfonic"[Tiab] OR "heptadecafluorooctane-1-sulphonic"[Tiab] OR "heptadecafluorooctane sulphonic"[Tiab] OR "heptadecafluorooctane-1-sulfonate"[tiab] OR "1-octanesulfonic acid"[Tiab] OR "1-octanesulphonic acid"[Tiab] OR "1-perfluoroctanesulfonic"[Tiab] OR "1-perfluorooctanesulfonic"[Tiab] OR "octanesulfonic acid"[Tiab] OR "octanesulphonic acid"[Tiab] OR "1-Octanesulfonic acid, 1,1,2,2,3,3,4,4,5,5,6,6,7,7,8,8,8-heptadecafluoro-"[tiab] OR "N,N-Dibutyl-N-methylbutan-1-aminium heptadecafluorooctane-1-sulfonate"[tiab] OR "N,N,N-Tripropylpentan-1-aminium heptadecafluorooctane-1-sulfonate"[tiab] OR "Tetrabutylammonium perfluorooctanesulfonate"[tiab] OR "N,N,N-Tributylbutan-1-aminium heptadecafluorooctane-1-sulfonate"[tiab] OR "N,N,N-Triethyldecan-1-aminium heptadecafluorooctane-1-sulfonate"[tiab] OR "isopfos"[tiab] OR "6-(Trifluoromethyl)tetradecafluoro-1-	3838	PFOS Terms

Set #	Search Terms	Number Retrieved	Concept
	heptanesulfonic acid"[tiab] OR "1,1,2,2,3,3,4,4,5,6,6,7,7,7-tetradecafluoro-5-(trifluoromethyl)heptane-1-sulfonic acid"[tiab] OR "1,1,2,2,3,3,4,5,5,6,6,7,7,7-tetradecafluoro-4-(trifluoromethyl)heptane-1-sulfonic acid"[tiab] OR "1,1,2,2,3,4,4,5,5,6,6,7,7,7-tetradecafluoro-3-(trifluoromethyl)heptane-1-sulfonic acid"[tiab] OR "1,1,2,2,3,3,5,5,6,6,6-undecafluoro-4,4-bis(trifluoromethyl)hexane-1-sulfonic acid"[tiab] OR 1763-23-1[rn] OR 45298-90-6[rn] OR 124472-68-0[rn] OR 56773-56-9[rn] OR 111873-33-7[rn] OR 773895-92-4[rn] OR 2795-39-3[rn] OR 29081-56-9[rn] OR 29457-72-5[rn] OR 4021-47-0[rn] OR 70225-14-8[rn] OR 56773-42-3[rn] OR 251099-16-8[rn] OR 71463-74-6[rn] OR 90480-49-2[rn] OR 93894-67-8[rn] OR 90480-49-2[rn] OR 93894-67-8[rn] OR "PFOS-K"[tiab] OR APFOS[tiab] OR "PFOS-li"[tiab] OR "heptadecafluorooctane-1-sulfonate "[tiab] OR "heptadecafluorooctanesulfonate "[tiab] OR "heptadecafluoro-1-octanesulfonate " OR "lsooctanesulfonic acid, heptadecafluoro-, lithium salt"[tiab])		
2	(("adduct-formation"[tiab] OR "DNA Adducts"[mh] OR "DNA-Adduct*"[tiab] OR "electrophile"[tiab] OR "electrophilic"[tiab] OR "dna-alkylating-agent*"[tiab] OR "Comet Assay"[mh] OR "Germ-line-mutation"[mh] OR "Mutagenesis"[mh] OR "Mutagenicity tests"[mh] OR "Sister-chromatid exchange"[mh] OR "Mutation"[mh] OR "Ames-Assay"[tiab] OR "Ames-test"[tiab] OR "Bacterial-Reverse-Mutation-Assay"[tiab] OR "Clastogen*"[tiab] OR "DNA-Repair*"[tiab] OR "Genetic-toxicology"[tiab] OR "hyperploid"[tiab] OR "micronucleus-test"[tiab] OR "tetraploid"[tiab] OR "Chromosome-aberrations"[tiab] OR	5655750	RoC key characteristics of carcinogens (includes genotoxicity)

Set #	Search Terms	Number Retrieved	Concept
	"DNA damage"[tiab] OR "Mutation"[tiab] OR "chromosome-translocations"[tiab] OR "DNA protein crosslinks"[tiab] OR "DNA-damag*"[tiab] OR "DNA-inhibit*"[tiab] OR "Micronuclei"[tiab] OR "Micronucleus"[tiab] OR "Mutagens"[tiab] OR "Strand-break*"[tiab] OR "Unscheduled-DNA-synthes*"[tiab] OR "chromosomal-aberration"[tiab] OR "chromosome-aberration"[tiab] OR "chromosomal-aberrations"[tiab] OR "chromosomal-abnormalit*"[tiab] OR "chromosome-abnormalit*"[tiab] OR "genotoxic"[tiab] OR "SOS Response, Genetics"[mh] OR "Polyploidy"[mh] OR "Genomic Instability"[mh] OR "DNA Repair"[mh] OR "Aneuploidy"[mh] OR ("DNA"[tiab] AND "Crosslink"[tiab]) OR "microsatellite-instability"[tiab] OR "chromosomal-instability"[tiab] OR "binucleation"[tiab] OR "binucleated"[tiab] OR "ubiquitination"[mh] OR "Gene Expression Regulation"[mh] OR "epigenomics"[mh] OR "DNA methylation"[mh] OR "gene silencing"[mh] OR "histone deacetylases"[mh] OR "RNA Interference"[mh] OR "microRNAs"[mh] OR "RNA, Small Interfering"[mh] OR "CpG-island-Methylator"[tiab] OR "CpG-island-Methylation"[tiab] OR "epigenotype"[tiab] OR "epimutation*"[tiab] OR "methylation-associated-silencing"[tiab] OR "histone-tail-modifications"[tiab] OR "histone-tail-modification"[tiab] OR "chromatin-organization"[tiab] OR "histone-modification"[tiab] OR "epigenetic*"[tiab] OR "epigenomic*"[tiab] OR "rna-interference"[tiab] OR "gene-activation"[tiab] OR "proteasome"[tiab] OR "Free Radicals"[mh] OR "Reactive Oxygen Species"[mh] OR "Oxidative stress"[mh] OR "Electron Transport"[mh] OR "Oxidative-damage*"[tiab] OR "reactive-nitrogen-species"[tiab] OR "superoxide-radical*"[tiab] OR "hydroxyl-radical"[tiab] OR "glutathione-deplet*"[tiab] OR "C-reactive protein"[mh] OR "eosinophils"[mh] OR ("fibrinogen"[tiab] AND "Inflammation"[tiab]) OR "chronic-inflammation"[tiab] OR "chronically-inflamed"[tiab] OR "infiltrating-leukocyt*"[tiab] OR "inflammatory-leukocyte"[tiab] OR "inflammatory-leukocytes"[tiab] OR "leukocyte-infiltrat*"[tiab] OR "pro-inflammatory"[tiab] OR "proinflammatory"[tiab] OR "macrophage-recruitment"[tiab] OR "Cytotoxicity,		

Set #	Search Terms	Number Retrieved	Concept
	Immunologic"[mh] OR "Immunologic Factors"[mh] OR "Immunomodulation"[mh] OR "B-Cell Activation Factor Receptor"[mh] OR Antigenic Modulation[mh] OR "B-Cell Activating Factor"[mh] OR "Immunologic Factors"[pa] OR "b-cell-activation"[tiab] OR "immune surveillance"[tiab] OR "immune-suppress*"[tiab] OR "immunostimulant"[tiab] OR "immune-activation"[tiab] OR "immunodeficien*"[tiab] OR "somatic-hypermutation"[tiab] OR "immune-activation"[tiab] OR "immune-system-activation"[tiab] OR "Chronic-antigenic-stimulation"[tiab] OR "immunosuppress*"[tiab] OR "Receptors, Aryl Hydrocarbon"[mh] OR "Transcriptional Activation"[mh] OR "Aryl-hydrocarbon-receptor*"[tiab] OR "receptor-mediat*"[tiab] OR "transcription-factor*"[tiab] OR "transcriptional-activat*"[tiab] OR "Xenobiotic-sensor*"[tiab] OR "xenosensor*"[tiab] OR "Ah-receptor*"[tiab] OR "alternative-lengthening-of-telomere*"[tiab] OR "cellular-Immortalization"[tiab] OR "p53-inactivat*"[tiab] OR "p53-inhibit*"[tiab] OR "p53-delet*"[tiab] OR "pRb-inactivat*"[tiab] OR "pRb-inhibit*"[tiab] OR "pRb-delet*"[tiab] OR "Rb/p16INK4a inactiv*"[tiab] OR "retinoblastoma-protein"[tiab] OR "senescent"[tiab] OR "senescence"[tiab] OR "Angiogenesis Modulating Agents"[mh] OR "Angiogenesis Inducing Agents"[pa] OR "Angiogenesis Inducing Agents"[mh] OR "Neovascularization, Pathologic"[mh] OR "Cell Hypoxia"[mh] OR "angiogenic"[tiab] OR "cellular-energetics"[tiab] OR "hypoxic-cell*"[tiab] OR "cell-hypoxia"[tiab] OR "cellular-hypoxia"[tiab] OR "Apoptosis"[mh] OR "Cytotoxicity, Immunologic"[mh] OR "Caspases"[mh] OR "autophagy"[mh] OR "necrosis" [mh] OR "Autolysis"[mh] OR "survivin"[tiab] OR "Cytotoxin"[tiab] OR "Caspases"[tiab] OR "Cell Proliferation"[mh] OR "homeostasis"[mh] OR "Cyclin-Dependent Kinases"[mh] OR "Cyclin-Dependent Kinase Inhibitor Proteins"[mh] OR "mitogens"[mh] OR "Mitogens"[pa] OR "cell-cycle-control*"[tiab] OR "mitotic-checkpoint*"[tiab] OR "hepatocellular-proliferation"[tiab] OR "Cytogenesis"[tiab] OR "Cytogenic"[tiab] OR "cellular-replication*"[tiab] OR "hyperplasia"[tiab] OR "Neoplasia"[tiab] OR "mitogenesis"[tiab])) OR (("Comet-assay"[tiab] OR		

Set #	Search Terms	Number Retrieved	Concept
	"Mutagenic"[tiab] OR "Mutagenicity"[tiab] OR "mutations"[tiab] OR "chromosomal-aberration-test"[tiab] OR "Sister-chromatid-exchange"[tiab] OR "SOS-response"[tiab] OR "Polyploid*"[tiab] OR "Genomic-Instability"[tiab] OR "DNA-Repair*"[tiab] OR "Aneuploid*"[tiab] OR "gene-silencer"[tiab] OR "gene-silencing"[tiab] OR "deacetylation"[tiab] OR "DNA-methylation"[tiab] OR "histone-deacetylase*"[tiab] OR "ubiquitination"[tiab] OR "gene-expression"[tiab] OR "microRNA*"[tiab] OR "miRNA*"[tiab] OR "non-coding-RNA*"[tiab] OR "SiRNA*"[tiab] OR "small-inhibitory-RNA*"[tiab] OR "Small-interfering-RNA*"[tiab] OR "electron-transport-chain*"[tiab] OR "reactive-oxygen-species"[tiab] OR "Oxidative-stress*"[tiab] OR "free-radical*"[tiab] OR "C-reactive-protein*"[tiab] OR "eosinophil*"[tiab] OR "autoimmunity"[tiab] OR "Immunomodulation"[tiab] OR "Immune-modulation"[tiab] OR "cellular-homeostasis"[tiab] OR "Cell-Proliferat*"[tiab] OR "Cellular-Proliferat*"[tiab] OR "cyclin-dependent-kinase*"[tiab] OR "cyclin-dependent-kinase-inhibit*"[tiab] OR "mitogens"[tiab] OR "mitogen"[tiab] OR "Apoptosis"[tiab] OR "autophagy"[tiab] OR "necrosis"[tiab] OR "autolysis"[tiab] OR "angiogenesis"[tiab]) NOT medline[sb])		
3	((("etiology"[sh] OR "Causality"[mh] OR "biomarkers, tumor"[mh] OR "oncogene fusion"[mh] OR "tumor necrosis factors"[mh] OR "adverse-outcome-pathway*"[tiab] OR "biological-marker"[tiab] OR "biological-markers"[tiab] OR "biomarkers"[tiab] OR "biomarker"[tiab] OR "Biotransformation"[tiab] OR "etiology"[tiab] OR "Key Event*"[tiab] OR "Mechanism-of-action"[tiab] OR "Mechanisms-of-action"[tiab] OR "Mode-of-action"[tiab] OR "modes-of-action"[tiab] OR "Molecular-Initiating-Event*"[tiab] OR "neoplastic-cell-transform*"[tiab] OR "Phosphorylation"[tiab] OR "Toxicity-Pathway*"[tiab] OR "toxicokinetic*"[tiab] OR "toxic-pathway*"[tiab]) AND (Cancer[sb])) OR ("tumor-inhibit*"[tiab] OR "tumor-promot*"[tiab] OR "tumour-inhibit*"[tiab] OR "tumour-promot*"[tiab] OR "Oncogenes"[tiab] OR	3533905	RoC Other Mechanistic

Set #	Search Terms	Number Retrieved	Concept
	"Oncogenesis"[tiab] OR "Oncogenic"[tiab] OR "pathogenesis"[tiab]))		
4	#1 AND (#2 OR #3)	**569**	Final

Table B13 PubMed search strategies for PFOS precursors

Search Terms	Number Retrieved	Concept
“Perfluorooctanesulfonyl fluoride"[tiab] OR “Perfluorooctane sulfonyl fluoride"[Tiab] OR “Perfluorooctyl sulfonyl fluoride"[Tiab] OR “Perfluorooctylsulfonyl fluoride"[Tiab] OR POSF[Tiab] OR PFOS-F[Tiab] OR PFOSF[tiab] OR “Heptadecafluorooctane-1-sulfonyl fluoride"[Tiab] OR “1-Octanesulfonyl fluoride, 1,1,2,2,3,3,4,4,5,5,6,6,7,7,8,8,8-heptadecafluoro-"[Tiab] OR “Heptadecafluoro-1-octanesulfonyl fluoride"[Tiab] OR “1,1,2,2,3,3,4,4,5,5,6,6,7,7,8,8,8-Heptadecafluoro-1-octanesulfonyl fluoride"[Tiab] OR “1-Octanesulfonyl fluoride, 1,1,2,2,3,3,4,4,5,5,6,6,7,7,8,8,8-heptadecafluoro-"[Tiab] OR “N-Perfluorooctanesulfonyl fluoride"[Tiab] OR “UNII-KPV81L86O0"[Tiab] OR 307-35-7[rn]	58	PFOSF
"2-(N-ethylperfluorooctanesulfonamido)ethyl alcohol"[nm] OR 1691-99-2 [rn] OR "N-ethyl perfluorooctanesulfonamido ethanol"[tiab] OR "N-EtPFOSE"[tiab] OR "N-EtFOSE"[tiab] OR "N-ethyl perfluorooctane sulfonamidoethanol" OR "NEtFOSE" [Tiab] OR "EtFOSE"[Tiab] OR “N-Ethyl-N-(2-hydroxyethyl) perfluorooctanesulfonamide"[tiab] OR “N-Ethyl-1,1,2,2,3,3,4,4,5,5,6,6,7,7,8,8,8-heptadecafluoro-N-(2-hydroxyethyl)octane-1-sulfonamide"[Tiab] OR “1-Octanesulfonamide, N-ethyl-1,1,2,2,3,3,4,4,5,5,6,6,7,7,8,8,8-heptadecafluoro-N-(2-hydroxyethyl)-"[Tiab] OR “l2-(N-Ethylperfluoro-1-octanesulfonamido)ethanol"[Tiab] OR “N-Ethyl-1,1,2,2,3,3,4,4,5,5,6,6,7,7,8,8,8-heptadecafluoro-N-(2-hydroxyethyl)-1-octanesulfonamide"[Tiab] OR “2-Perfluorooctylsulfonyl-N-ethylaminoethyl alcohol"[Tiab] OR “2-	45	EtPFOSE

Search Terms	Number Retrieved	Concept
[N-Ethyl-N-(perfluorooctylsulfonyl)amino]ethanol"[Tiab] OR "AI 3-29782"[Tiab] OR "Fluorad FC 10"[Tiab] OR "LE 011"[Tiab] OR "N-Ethyl perfluorooctanesulfonamidoethanol"[Tiab] OR "N-Ethylheptadecafluorooctanesulfonamidoethanol"[Tiab] OR "N-Ethylperfluorooctanesulfonamidoethanol"[Tiab] OR "N-Ethylperfluorooctanesulfonamidoethyl alcohol"[Tiab] OR "N-ethylheptadecafluoro-N-(2-hydroxyethyl)octanesulphonamide"[Tiab] OR "PERFLUOROALKYL (C8) SULFONAMIDO-(N-ETHYL) ETHYL ALCOHOL"[Tiab] OR "2-(N-Ethylperfluoro-1-Octanesulfonamido)-Ethanol"[Tiab]		
Sulfluramide[nm] OR "Sulfluramide"[tiab] OR "sulfluramid"[tiab] OR "Mirex S"[tiab] OR "N-Ethylperfluorooctanesulfonamide"[tiab] OR "N-Ethyl(perfluorooctane)sulfonamide"[tiab] OR "N-ethylperfluorooctane sulphonamide"[tiab] OR "N-ethylperfluorooctane-1-sulfonamide"[tiab] OR "N-Ethyl perfluorooctanesulfonamide"[tiab] OR "NEtFOSA"[tiab] OR "N-EtFOSA"[tiab] OR "EtFOSA"[tiab] OR "EtPFOSA"[tiab] OR "N-Ethyl-1,1,2,2,3,3,4,4,5,5,6,6,7,7,8,8,8-heptadecafluorooctane-1-sulfonamide"[tiab] OR "N-Ethyl-1,1,2,2,3,3,4,4,5,5,6,6,7,7,8,8,8-heptadecafluoro-1-octanesulfonamide"[tiab] OR "1-Octanesulfonamide, N-ethyl-1,1,2,2,3,3,4,4,5,5,6,6,7,7,8,8,8-heptadecafluoro-"[tiab] OR "N-Ethyl-1,1,2,2,3,3,4,4,5,5,6,6,7,7,8,8,8-heptadecafluorooctane-1-sulfonamide"[tiab] OR "1-Octanesulfonamide, N-ethyl-1,1,2,2,3,3,4,4,5,5,6,6,7,7,8,8,8-heptadecafluoro-"[tiab] OR "N-Ethylheptadecafluoroctansulfonamid"[tiab] OR "N-Ethylheptadecafluorooctanesulfonamide"[tiab] OR "N-ethylheptadecafluorooctanesulphonamide"[tiab] OR "N-Ethylperfluorooctylsulfonamide"[tiab]OR "octane sulfonamide, n-ethylperfluoro-"[tiab] OR 4151-50-2 [rn]	83	EtPFOSA
"N-ethyl perfluorooctane sulfonamido acetic acid"[tiab] OR "2-(N-Ethylperfluorooctanesulfonamido)acetic acid"[tiab] OR "N-Ethyl perfluorooctanesulfonamidoacetic acid"[tiab] OR "N-ethylperfluorooctane sulfonamidoacetic acid"[tiab] OR "NEtFOSAA"[tiab] OR "NEtPFOSAA"[tiab] OR "N-EtFOSAA"[tiab] OR "EtFOSAA"[tiab] OR "NEtPFOSA-AcOH"[tiab] OR "Et-PFOSA-AcOH"[tiab] OR "N-Ethyl-N-	68	EtPFOSAA

Search Terms	Number Retrieved	Concept
(1,1,2,2,3,3,4,4,5,5,6,6,7,7,8,8,8-heptadecafluorooctane-1-sulfonyl)glycine"[tiab] OR "Glycine, N-ethyl-N-[(1,1,2,2,3,3,4,4,5,5,6,6,7,7,8,8,8-heptadecafluorooctyl)sulfonyl]-"[tiab] OR "Glycine, N-ethyl-N-[(heptadecafluorooctyl)sulfonyl]-"[tiab] OR "Glycine, N-ethyl-N-[(1,1,2,2,3,3,4,4,5,5,6,6,7,7,8,8,8-heptadecafluorooctyl)sulfonyl]-"[tiab] OR "N-Ethyl-N-[(1,1,2,2,3,3,4,4,5,5,6,6,7,7,8,8,8-heptadecafluorooctyl)sulfonyl]glycine"[tiab] OR "2-(N-Ethylperfluorooctanesulfoamido) acetic acid"[tiab] OR "N-Ethyl-N-heptadecylfluorooctane sulfonyl glycine"[tiab] OR "2-(N-ethyl-perfluorooctane sulfonamido) acetic acid"[tiab] OR 2991-50-6[rn] OR 2991-52-8[rn] OR 3871-50-9[rn] OR 2991-51-7[rn] OR 909405-49-8[rn]		
"N-Methyl-N-(2-hydroxyethyl)perfluorooctanesulfonamide"[tiab] OR “1,1,2,2,3,3,4,4,5,5,6,6,7,7,8,8,8-Heptadecafluoro-N-(2-hydroxyethyl)-N-methyloctane-1-sulfonamide”[tiab] OR “1-Octanesulfonamide, 1,1,2,2,3,3,4,4,5,5,6,6,7,7,8,8,8-heptadecafluoro-N-(2-hydroxyethyl)-N-methyl-“[tiab] OR “1-Octanesulfonamide, 1,1,2,2,3,3,4,4,5,5,6,6,7,7,8,8,8-heptadecafluoro-N-(2-hydroxyethyl)-N-methyl-“[tiab] OR "2-(N-Methylperfluoro-1-octanesulfonamido)ethanol"[tiab] OR "MeFOSE"[tiab] OR "N-MeFOSE"[tiab] OR "NMeFOSE"[tiab] OR "N-(2-Hydroxyethyl)-N-methylperfluorooctanesulfonamide"[tiab] OR "N-Methyl-N-ethanolperfluorooctanesulfonamide"[tiab] OR "N-Methylperfluorooctanesulfonamide ethyl alcohol"[tiab] OR "N-Methyl perfluorooctanesulfonamidoethanol"[tiab] OR "N-Methyl perfluorooctane sulfonamide ethanol"[tiab] OR "N-Methyl perfluorooctane sulfonamido ethanol"[tiab] OR "N-methyl perfluorooctane sulfonamidoethanol"[tiab] OR "N-Methylheptadecafluorooctanesulfonamidoethanol"[tiab] OR "heptadecafluoro-N-(2-hydroxyethyl)-N-methyloctanesulphonamide"[tiab] OR "N-Methylperfluorooctanesulfonamidoethanol"[tiab] OR "2-(N-Methylperfluoro-1-octanesulfonamido)-ethanol"[tiab] OR “1,1,2,2,3,3,4,4,5,5,6,6,7,7,8,8,8-Heptadecafluoro-N-(2-hydroxyethyl)-N-methyl-1-octanesulfonamide”[tiab] OR 24448-09-7[rn]	25	MePFOSE

Search Terms	Number Retrieved	Concept
"2-(N-Methylperfluorooctanesulfonamido) acetic acid"[tiab] OR "2-(N-Methylperfluorooctanesulfonamido)acetic acid"[tiab] OR "N-(1,1,2,2,3,3,4,4,5,5,6,6,7,7,8,8,8-Heptadecafluorooctane-1-sulfonyl)-N-methylglycine"[tiab] OR "Glycine, N-[(1,1,2,2,3,3,4,4,5,5,6,6,7,7,8,8,8-heptadecafluorooctyl)sulfonyl]-N-methyl-"[tiab] OR "N-(1,1,2,2,3,3,4,4,5,5,6,6,7,7,8,8,8-Heptadecafluorooctane-1-sulfonyl)-N-methylglycine"[tiab] OR "N-Methyl perfluorooctanesulfonamidoacetic acid"[tiab] OR "2-(N-Methyl-perfluorooctane sulfonamido) acetate"[tiab] OR "Glycine, N-[(heptadecafluorooctyl)sulfonyl]-N-methyl-"[tiab] OR "Glycine, N-[(1,1,2,2,3,3,4,4,5,5,6,6,7,7,8,8,8-heptadecafluorooctyl)sulfonyl]-N-methyl-"[tiab] OR "N-[(1,1,2,2,3,3,4,4,5,5,6,6,7,7,8,8,8-Heptadecafluorooctyl)sulfonyl]-N-methylglycine"[tiab] OR "Sarcosine, N-[(heptadecafluorooctyl)sulfonyl]-"[tiab] OR "N-MeFOSAA"[tiab] OR "NMeFOSAA"[tiab] OR <eFOSAA"[tiab] OR "NMePFOSA-AcOH"[tiab] OR "Me-PFOSA-AcOH"[tiab] OR "N-(Heptadecafluorooctylsulfonyl)-N-methylglycine"[tiab] OR "N-methylperfluorooctane sulfonamidoacetic acid"[tiab] OR "N-methyl perfluorooctane sulfonamidoacetic acid"[tiab] OR "N-methyl perfluorooctanesulfonamidoacetic acid"[tiab] OR 2355-31-9[rn] OR 909405-48-7 [rn] OR 70281-93-5 [rn]	37	MePFOSAA
"Perfluorooctanesulfonamide"[nm] OR "Perfluorooctanesulfonamide"[tiab] OR "Perfluorooctane sulfonamide"[tiab] OR "Perfluoroctylsulfonamide"[tiab] OR "Perfluorooctanesulfonic acid amide"[tiab] OR (FOSA[tiab] NOT (Fosfomycin[tiab] OR gene[tiab] OR genes[tiab])) OR PFOSA[tiab] OR "1,1,2,2,3,3,4,4,5,5,6,6,7,7,8,8,8-Heptadecafluorooctane-1-sulfonamide"[tiab] OR "1-Octanesulfonamide, 1,1,2,2,3,3,4,4,5,5,6,6,7,7,8,8,8-heptadecafluoro-"[tiab] OR "1-Octanesulfonamide, 1,1,2,2,3,3,4,4,5,5,6,6,7,7,8,8,8-heptadecafluoro-"[tiab] OR "1,1,2,2,3,3,4,4,5,5,6,6,7,7,8,8,8-Heptadecafluoro-1-octanesulfonamide"[tiab] OR "Desethylsulfluramid"[tiab] OR "heptadecafluorooctanesulphonamide"[tiab] OR "heptadecafluorooctanesulfonamide"[tiab] OR "Heptadecafluoroctansulfonamid"[tiab] OR "heptadecafluorooctanosulfonamida"[tiab] OR "OCTANESULFONAMIDE, HEPTADECAFLUORO-"[tiab] OR "1,1,2,2,3,3,4,4,5,5,6,6,7,7,8,8,8-heptadecafluorooctane-1-	413	PFOSA - Broad

Search Terms	Number Retrieved	Concept
sulfonamide"[tiab] OR 754-91-6[rn] OR 76752-72-2[rn] OR 76752-79-9[rn] OR 76752-78-8[rn] OR 76752-70-0[rn] OR 76752-82-4[rn]		
"Perfluorooctanesulfonamide"[nm] OR "Perfluorooctanesulfonamide"[tiab] OR "Perfluorooctane sulfonamide"[tiab] OR "Perfluoroctylsulfonamide"[tiab] OR "Perfluorooctanesulfonic acid amide"[tiab] OR (FOSA[tiab] NOT (Fosfomycin[tiab] OR gene[tiab] OR genes[tiab])) OR PFOSA[tiab] OR "1,1,2,2,3,3,4,4,5,5,6,6,7,7,8,8,8-Heptadecafluorooctane-1-sulfonamide"[tiab] OR "1-Octanesulfonamide, 1,1,2,2,3,3,4,4,5,5,6,6,7,7,8,8,8-heptadecafluoro-"[tiab] OR "1-Octanesulfonamide, 1,1,2,2,3,3,4,4,5,5,6,6,7,7,8,8,8-heptadecafluoro-"[tiab] OR "1,1,2,2,3,3,4,4,5,5,6,6,7,7,8,8,8-Heptadecafluoro-1-octanesulfonamide"[tiab] OR "Desethylsulfluramid"[tiab] OR "heptadecafluorooctanesulphonamide"[tiab] OR "heptadecafluorooctanesulfonamide"[tiab] OR "Heptadecafluoroctansulfonamid"[tiab] OR "heptadecafluorooctanosulfonamida"[tiab] OR "OCTANESULFONAMIDE, HEPTADECAFLUORO-"[tiab] OR "1,1,2,2,3,3,4,4,5,5,6,6,7,7,8,8,8-heptadecafluorooctane-1-sulfonamide"[tiab] OR 754-91-6[rn] OR 76752-72-2[rn] OR 76752-79-9[rn] OR 76752-78-8[rn] OR 76752-70-0[rn] OR 76752-82-4[rn] AND cancer[sb]	36	PFOSA - Cancer
"pfos precursor*"[tiab]	57	

Appendix C. PFOS Biomonitoring Studies in California

Table C1 PFOS biomonitoring studies in California

Study	Area	Participants with PFOS analyses	Mean serum[a] PFOS concentration (ng/ml)	Reference
CHDS[b]	Northern California	Pregnant women, archived samples Overall (N=105) 1960s (N=40) 1980s (N=30) 2009 (N=35)	1960s: 45.90 (arithmetic mean) 1980s: 30.60 (arithmetic mean) 2009: 9.44 (arithmetic mean)	Wang et al. (2011)
CHARGE[b]	Northern California	Women (mothers) (N=450)	Overall (2009 – 2016): 3.29 2009: 4.86[c]; 2010: 4.1[c] 2011: 3.78[c]; 2012: 3.42[c] 2013: 3.02[c]; 2014: 2.8[c] 2015: 2.42[c]; 2016: 2.12[c]	Kim et al. (2020)
Red Cross plasma samples[b]	Los Angeles	Adult plasma donors (N=100)	2000/01: 35.0[c] 2006: 14.3[c] 2010: 7.7[c]	Olsen et al. (2012)
Kaiser Permanente Health Plan member serum samples[b]	San Francisco Bay Area	Girls aged 6-8 (N=351)	2005-2009: 13.2 (max: 104)	Pinney et al. (2014)
Firefighter serum samples[b]	San Francisco	Firefighters (N=12)	2009: 12 (arithmetic mean) (max: 59)	Shaw et al. (2013)
Women Firefighters Biomonitoring Collaborative Study[b]	San Francisco	Female firefighters and office workers (N=170)	2014-2015: 4.11 (95th pctl: 12.61; max: 81.02)	Trowbridge et al. (2020)
		Female firefighters (N=84)	2014-2015: 4.33	Clarity et al. (2020)
		Female office workers (N=79)	2014-2015: 4.03	
MIEEP	San Francisco	Pregnant women (N=77)	2010-2011: 2.55 (90th pctl: 4.9; 95th pctl: 7.25)	Biomonitoring California[d] Morello-Frosch et al. (2016)

Study	Area	Participants with PFOS analyses	Mean serum[a] PFOS concentration (ng/ml)	Reference
FOX	California	Firefighters (N=101)	2010-2011: 12.5 (95th pctl: 24.7; max 46.6)	Biomonitoring California[d] Dobraca et al. (2015)
CTS	California	Female teachers (N=1,759)	2011-ongoing: 6.80 (95th pctl: 19.5)	Biomonitoring California[d]
		Female teachers (N=1,257)	2011-2015: 8.539 (max: 99.800) (arithmetic mean)	Hurley et al. (2018a)
		Subset of CTS subjects with detectable PFOS in drinking water (N=93)	2011-2013: 8.51 (max: 39.4)	Hurley et al. (2016)
		Subset of CTS subjects with no detectable PFOS in drinking water (N=1,240)	2011-2013: 6.76 (max: 99.80)	
BEST-1	Central Valley	Adults (N=110)	2011-2012: 7.00 (95th pctl: 25.8)	Biomonitoring California[d]
BEST-2	Central Valley	Adults (N=337)	2013: 5.21 (95th pctl: 17.6)	
MAMAS	California	Pregnant women (N=200)	2012-2015: 4.2 (95th pctl: 12.3)	
ACE 1	San Francisco Bay Area	Chinese adults that have lived in the San Francisco Bay area for at least one year (N=96)	2016: 6.51 (90th pctl: 19.3)	
ACE 2	San Francisco Bay Area	Vietnamese adults (N=99)	2017: 7.47 (90th pctl: 22.9)	
CARE-LA	Los Angeles county	Adults (N=425)	2018: 2.13 (95th pctl: 8.33)	
CARE-2	Riverside, San Bernardino, Imperial, Mono, and Inyo counties	Adults (N=357)	2019: 2.40 (95th pctl: 8.72)	

ACE, Asian/Pacific Islander community exposures; BEST, biomonitoring exposures study; CARE-LA, California regional exposure study, Los Angeles county; CHARGE, childhood autism risk from genetics

and environment study; CHDS, child health and development studies; CTS, California teachers study; FOX, firefighter occupational exposures project; MAMAS, measuring analytes in maternal archived samples; MIEEP, maternal and infant environmental exposure project; max, maximum; pctl, percentile

[a] Geometric mean in serum samples, if not indicated otherwise

[b] CHDS (except for data for 2009), CHARGE, Olsen et al. (2012), Pinney et al. (2014), and Shaw et al. (2013) studies were not part of the Biomonitoring California program

[c] Geometric mean values for serum samples determined using GetData Graph Digitizer Software (version 2.26)

[d] https://biomonitoring.ca.gov/, accessed April 2021

Appendix D. Publications Initially Identified in the Literature Search as Epidemiologic Studies: Reasons for Exclusion

Table D1 Publications initially identified in the literature search as epidemiologic studies: Reasons for exclusion

Full Citation	Reason for Exclusion
Butenhoff JL. 2012. Translating toxicological information on perfluoroalkyls for human risk assessment. Reproductive Toxicology 33:594-595.	Conference abstract
Cohn B, Krigbaum N, Zimmermann L, Cirillo P. 2015. Findings from the first prospective womb to breast cancer study: New gestational biomarkers support proof of concept that gestation is a window of susceptibility for the breast. Cancer Research 75.	Conference abstract
Girardi P, Merler E. 2019. A mortality study on male subjects exposed to polyfluoroalkyl acids with high internal dose of perfluorooctanoic acid. Environmental Research 179:108743.	No risk estimate for PFOS and cancer
Innes KE, Wimsatt JH, Frisbee S, Ducatman AM. 2014. Inverse association of colorectal cancer prevalence to serum levels of perfluorooctane sulfonate (PFOS) and perfluorooctanoate (PFOA) in a large appalachian population. BMC Cncer 14:45.	Cross-sectional design
Mastrantonio M, Bai E, Uccelli R, Cordiano V, Screpanti A, Crosignani P. 2018. Drinking water contamination from perfluoroalkyl substances (PFAS): An ecological mortality study in the Veneto region, Italy. European Journal of Public Health 28:180-185.	No data for PFOS
Omoike OE, Pack RP, Mamudu HM, Liu Y, Wang L. 2020. A cross-sectional study of the association between perfluorinated chemical exposure and cancers related to deregulation of estrogen receptors. Environmental Research:110329.	Cross-sectional design
Petersen KU, Larsen JR, Deen L, Flachs EM, Hærvig KK, Hull SD, et al. 2020. Per- and polyfluoroalkyl substances and male reproductive health: A systematic review of the epidemiological evidence. Journal of Toxicology and Environmental Health - Part B: Critical Reviews 23:276-291.	No data for PFOS

Full Citation	Reason for Exclusion
Petrakis D, Vassilopoulou L, Mamoulakis C, Psycharakis C, Anifantaki A, Sifakis S, et al. 2017. Endocrine disruptors leading to obesity and related diseases. International Journal of Environmental Research and Public Health 14.	No data for PFOS
Rodprasert W, Main KM, Toppari J, Virtanen HE. 2019. Associations between male reproductive health and exposure to endocrine-disrupting chemicals. Current Opinion in Endocrine and Metabolic Research 7:49-61.	No data for PFOS
Roswall N, Larsen SB, Sørensen M, Tjønneland A, Raaschou-Nielsen O. 2018. Perfluorooctanoate and perfluorooctanesulfonate plasma concentrations and survival after prostate and bladder cancer in a population-based study. Environmental Epidemiology 2.	Cancer survival (cohort)
Tsai MS, Chang SH, Kuo WH, Kuo CH, Li SY, Wang MY, et al. 2020. A case-control study of perfluoroalkyl substances and the risk of breast cancer in Taiwanese women. Environment International 142:105850.	Cross-sectional design
Vassiliadou I, Costopoulou D, Ferderigou A, Leondiadis L. 2010. Levels of perfluorooctanesulfonate (PFOS) and perfluorooctanoate (PFOA) in blood samples from different groups of adults living in Greece. Chemosphere 80:1199-1206.	No risk estimate for PFOS and cancer
Yeung LW, Guruge KS, Taniyasu S, Yamashita N, Angus PW, Herath CB. 2013. Profiles of perfluoroalkyl substances in the liver and serum of patients with liver cancer and cirrhosis in Australia. Ecotoxicology and Environmental Safety 96:139-146.	Cross-sectional design. No comparison of exposed vs unexposed.

Appendix E. Human Half-Life Estimates for PFOS

Table E1 Human half-life estimates for PFOS (taken from OEHHA 2021)

Reference	Population	N	$T_{1/2}$ (years)	Method
Burris (2002), as cited in Harada et al. (2005a)	Occupational	9	8.7	3M study, unpublished
Olsen et al. (2007)	Occupational	26	5.4	Retired workers followed up for 5 years
Spliethoff et al. (2008)	General (infants)	2,640	4.4	Disappearance $T_{1/2}$ due to declining levels
D'Eon and Mabury (2011b)	Review of studies	NA	5.4	Disappearance $T_{1/2}$ due to declining levels
Glynn et al. (2012)	General	413	8.1	Disappearance $T_{1/2}$ due to declining levels
Olsen et al. (2012)	General	600	4.3	Cross-sectional, population based
Yeung et al. (2013b)	General	420	4.3-4.8	Disappearance $T_{1/2}$ due to declining levels
Zhang et al. (2013b)	General	66	22 (GM)	Calculated from urinary clearance
Fu et al. (2016)	Occupational	207	4.1 (GM)	Calculated from urinary clearance
Gomis et al. (2017)	General	120	3.3-5	Population-based cross-sectional model
Li et al. (2017e)	C8 Panel, 4y	455	3.7	Drinking water pollution, decline
Worley et al. (2017b)	Decatur	45	3.3	Probabilistic model of C8 Panel data
Li et al. (2018c)	Ronneby	106	3.4	Drinking water pollution, decline
Xu et al. (2020a)	Occupational	17	1.7-2.9	Airport workers followed for 5 months

GM, geometric mean; NA, not applicable.

References (as cited by OEHHA 2021)

D'eon JC and Mabury SA (2011b). Is indirect exposure a significant contributor to the burden of perfluorinated acids observed in humans? *Environmental science & technology* 45(19): 7974-7984.

Fu J, Gao Y, Cui L, et al. (2016). Occurrence, temporal trends, and half-lives of perfluoroalkyl acids (PFAAs) in occupational workers in China. *Sci Rep* 6: 38039.

Glynn A, Berger U, Bignert A, et al. (2012). Perfluorinated alkyl acids in blood serum from primiparous women in Sweden: serial sampling during pregnancy and nursing, and temporal trends 1996–2010. *Environmental science & technology* 46(16): 9071-9079.

Gomis MI, Vestergren R, MacLeod M, Mueller JF and Cousins IT (2017). Historical human exposure to perfluoroalkyl acids in the United States and Australia reconstructed from biomonitoring data using population-based pharmacokinetic modelling. *Environ Int* 108: 92-102.

Harada K, Inoue K, Morikawa A, Yoshinaga T, Saito N and Koizumi A (2005a). Renal clearance of perfluorooctane sulfonate and perfluorooctanoate in humans and their species-specific excretion. *Environ Res* 99(2): 253-261.

Li Y, Fletcher T, Mucs D, et al. (2018c). Half-lives of PFOS, PFHxS and PFOA after end of exposure to contaminated drinking water. *Occup Environ Med* 75(1): 46-51.

Li Y, Mucs D, Scott K, et al. (2017e). Half-lives of PFOS, PFHxS and PFOA after end of exposure to contaminated drinking water. *Technical Report, Gothenburg University* 2.

Olsen GW, Burris JM, Ehresman DJ, et al. (2007). Half-life of serum elimination of perfluorooctanesulfonate, perfluorohexanesulfonate, and perfluorooctanoate in retired fluorochemical production workers. *Environ Health Perspect* 115(9): 1298-1305.

Olsen GW, Lange CC, Ellefson ME, et al. (2012). Temporal trends of perfluoroalkyl concentrations in American Red Cross adult blood donors, 2000–2010. *Environmental science & technology* 46(11): 6330-6338.

Spliethoff HM, Tao L, Shaver SM, et al. (2008). Use of newborn screening program blood spots for exposure assessment: declining levels of perfluorinated compounds in New York State infants. *Environmental science & technology* 42(14): 5361-5367.

Worley RR, Moore SM, Tierney BC, et al. (2017b). Per- and polyfluoroalkyl substances in human serum and urine samples from a residentially exposed community. *Environ Int* 106: 135-143.

Xu Y, Fletcher T, Pineda D, et al. (2020a). Serum Half-Lives for Short-and Long-Chain Perfluoroalkyl Acids after Ceasing Exposure from Drinking Water Contaminated by Firefighting Foam. *Environmental health perspectives* 128(7): 077004.

Yeung LW, Robinson SJ, Koschorreck J and Mabury SA (2013b). Part II. A temporal study of PFOS and its precursors in human plasma from two German cities in 1982–2009. *Environmental science & technology* 47(8): 3875-3882.

Zhang Y, Beesoon S, Zhu L and Martin JW (2013b). Biomonitoring of perfluoroalkyl acids in human urine and estimates of biological half-life. *Environ Sci Technol* 47(18): 10619-10627.

Appendix F. Toxcast Data for PFOS, Its Potassium and Lithium Salts, and Its Precursors, PFOSA and EtPFOSA

OEHHA has organized the ToxCast HTS data for PFOS, PFOS potassium salt, PFOS lithium salt, PFOSA, and EtPFOSA (accessed on May 3, 2021) as follows:

- Table F1. 260 Active ToxCast assays for PFOS
- Table F2. 179 Active ToxCast assays for PFOS potassium salt
- Table F3. 26 Active ToxCast assays for PFOS lithium salt
- Table F4. 260 Active ToxCast assays for PFOSA (excluding cell-free assays)
- Table F5. 139 Active ToxCast assays for EtPFOSA (excluding cell-free assays)

For PFOSA and EtPFOSA, cell-free assays are excluded as there is no possibility of biotransformation into PFOS.

Table F1 260 Active ToxCast assays[1] for PFOS

Assay Name	Gene Symbol	Organism	Cells/Cell Lines	Intended Target Family	AC50 (µM)
LTEA_HepaRG_CAT_dn	CAT	human	HepaRG	catalase	82.1
BSK_hDFCGF_CollagenIII_ down	COL3A1	human	foreskin fibroblast	cell adhesion molecules	40.0
BSK_BE3C_HLADR_down	HLA-DRA	human	bronchial epithelial cells	cell adhesion molecules	10.0
BSK_hDFCGF_VCAM1_down	VCAM1	human	foreskin fibroblast	cell adhesion molecules	40.0
LTEA_HepaRG_BAX_up	BAX	human	HepaRG	cell cycle	33.4
LTEA_HepaRG_BCL2_up	BCL2	human	HepaRG	cell cycle	34.1
LTEA_HepaRG_CCND1_up	CCND1	human	HepaRG	cell cycle	21.3
APR_HepG2_OxidativeStress _24h_up	γH2AX	human	HepG2	cell cycle	108
APR_HepG2_OxidativeStress _72h_up	γH2AX	human	HepG2	cell cycle	7.98
APR_HepG2_MitoticArrest_ 24h_up	pH3	human	HepG2	cell cycle	109
APR_HepG2_MitoticArrest_ 72h_up	pH3	human	HepG2	cell cycle	8.10
APR_HepG2_CellLoss_24h_ dn	NA	human	HepG2	cell cycle	111
APR_HepG2_CellLoss_72h_ dn	NA	human	HepG2	cell cycle	111
BSK_3C_SRB_down	NA	human	umbilical vein endothelium	cell cycle	40.0
BSK_BE3C_SRB_down	NA	human	bronchial epithelial cells	cell cycle	40.0
BSK_hDFCGF_Proliferation_ down	NA	human	foreskin fibroblast	cell cycle	10.0
BSK_hDFCGF_SRB_down	NA	human	foreskin fibroblast	cell cycle	40.0
TOX21_TR_LUC_GH3_ Antagonist_viability	NA	rat	pituitary gland GH4	cell cycle	120
TOX21_FXR_BLA_antagonist _viability	NA	human	HEK293T	cell cycle	31.4
TOX21_PPARd_BLA_ antagonist_viability	NA	human	HEK293T	cell cycle	71.0
TOX21_DT40	NA	chicken	lymphoblast	cell cycle	115
LTEA_HepaRG_LDH_ cytotoxicity	NA	human	HepaRG	cell cycle	80.3

Assay Name	Gene Symbol	Organism	Cells/Cell Lines	Intended Target Family	AC50 (µM)
TOX21_ARE_BLA_agonist_ viability	NA	human	HepG2	cell cycle	54.2
TOX21_p53_BLA_p1_viability	NA	human	intestinal cells HCT116	cell cycle	78.1
TOX21_FXR_BLA_agonist_ viability	NA	human	HEK293T	cell cycle	30.1
TOX21_PPARd_BLA_Agonist _viability	NA	human	HEK293T	cell cycle	57.8
TOX21_p53_BLA_p3_viability	NA	human	intestinal cells HCT116	cell cycle	100
TOX21_p53_BLA_p4_viability	NA	human	intestinal cells HCT116	cell cycle	81.4
TOX21_VDR_BLA_Agonist_ viability	NA	human	HEK293T	cell cycle	37.3
NCCT_HEK293T_ CellTiterGLO	NA	human	HEK293T	cell cycle	49.9
TOX21_RXR_BLA_Agonist_ viability	NA	human	HEK293T	cell cycle	30.1
ACEA_AR_agonist_AUC_ viability	NA	human	prostate 22Rv1	cell cycle	80.0
ACEA_AR_antagonist_AUC_ viability	NA	human	prostate 22Rv1	cell cycle	33.7
TOX21_HRE_BLA_Agonist_ viability	NA	human	cervix ME-180	cell cycle	41.6
TOX21_RT_HEK293_FLO_ 08hr_viability	NA	human	HEK293T	cell cycle	30.7
TOX21_RT_HEK293_FLO_ 16hr_viability	NA	human	HEK293T	cell cycle	29.8
TOX21_RT_HEK293_FLO_ 24hr_viability	NA	human	HEK293T	cell cycle	28.1
TOX21_RT_HEK293_FLO_ 32hr_viability	NA	human	HEK293T	cell cycle	27.9
TOX21_RT_HEK293_FLO_ 40hr_viability	NA	human	HEK293T	cell cycle	27.7
TOX21_RT_HEK293_GLO_ 08hr_viability	NA	human	HEK293T	cell cycle	71.7
TOX21_RT_HEK293_GLO_ 16hr_viability	NA	human	HEK293T	cell cycle	70.5
TOX21_RT_HEK293_GLO_ 24hr_viability	NA	human	HEK293T	cell cycle	73.4

Assay Name	Gene Symbol	Organism	Cells/Cell Lines	Intended Target Family	AC50 (µM)
TOX21_RT_HEK293_GLO_ 32hr_viability	NA	human	HEK293T	cell cycle	66.4
TOX21_RT_HEK293_GLO_ 40hr_viability	NA	human	HEK293T	cell cycle	68.5
NIS_HEK293T_CTG_ Cytotoxicity	NA	human	HEK293T	cell cycle	0.100
TOX21_ERb_BLA_Agonist_ viability	NA	human	HEK293T	cell cycle	25.4
TOX21_ERb_BLA_Antagonist _viability	NA	human	HEK293T	cell cycle	30.3
TOX21_PR_BLA_Agonist_ viability	NA	human	PR-UAS-bla-HEK293T	cell cycle	27.7
TOX21_PR_BLA_Antagonist_ viability	NA	human	PR-UAS-bla-HEK293T	cell cycle	32.8
TOX21_DT40_657	NA	chicken	lymphoblast	cell cycle	67.0
TOX21_PXR_viability	NA	human	PXR-Luc HepG2 cells	cell cycle	99.4
APR_HepG2_MitoMass_24h_ dn	NA	human	HepG2	cell morphology	114
APR_HepG2_MitoMass_72h_ dn	NA	human	HepG2	cell morphology	17.5
APR_HepG2_NuclearSize_ 72h_dn	NA	human	HepG2	cell morphology	8.10
BSK_3C_Vis_down	NA	human	umbilical vein endothelium	cell morphology	40.0
TOX21_MMP_ratio_up	NA	human	HepG2	cell morphology	33.2
LTEA_HepaRG_CYP1A2_dn	CYP1A2	human	HepaRG	cyp	20.8
LTEA_HepaRG_CYP3A4_up	CYP3A4	human	HepaRG	cyp	10.1
LTEA_HepaRG_CYP3A7_up	CYP3A7	human	HepaRG	cyp	10.2
LTEA_HepaRG_CYP4A11_dn	CYP4A11	human	HepaRG	cyp	82.5
LTEA_HepaRG_CYP4A11_up	CYP4A11	human	HepaRG	cyp	10.8
LTEA_HepaRG_CYP4A22_dn	CYP4A22	human	HepaRG	cyp	88.2
LTEA_HepaRG_CYP4A22_up	CYP4A22	human	HepaRG	cyp	8.70
LTEA_HepaRG_CYP7A1_dn	CYP7A1	human	HepaRG	cyp	84.1
NVS_ADME_hCYP19A1	CYP19A1	human	NA	cyp	4.14
LTEA_HepaRG_CYP2B6_dn	CYP2B6	human	HepaRG	cyp	90.7
LTEA_HepaRG_CYP2B6_up	CYP2B6	human	HepaRG	cyp	5.52
CLD_CYP2B6_24hr	CYP2B6	human	primary hepatocyte	cyp	34.5

Assay Name	Gene Symbol	Organism	Cells/Cell Lines	Intended Target Family	AC50 (µM)
LTEA_HepaRG_CYP2C8_up	CYP2C8	human	HepaRG	cyp	16.7
NVS_ADME_hCYP2C8	CYP2C8	human	NA	cyp	4.70
LTEA_HepaRG_CYP2C9_dn	CYP2C9	human	HepaRG	cyp	85.4
NVS_ADME_hCYP2C9	CYP2C9	human	NA	cyp	2.17e-2
NVS_ADME_rCYP2C11	Cyp2c11	rat	NA	cyp	9.27e-2
NVS_ADME_hCYP2C18	CYP2C18	human	NA	cyp	0.822
LTEA_HepaRG_CYP2C19_up	CYP2C19	human	HepaRG	cyp	11.8
NVS_ADME_hCYP2C19	CYP2C19	human	NA	cyp	4.91
LTEA_HepaRG_CYP2E1_dn	CYP2E1	human	HepaRG	cyp	30.9
NVS_ADME_hCYP4F12	CYP4F12	human	NA	cyp	1.53
BSK_SAg_CD40_down	CD40	human	umbilical vein endothelium and peripheral blood mononuclear cells	cytokine	40.0
BSK_LPS_IL8_up	CXCL8	human	umbilical vein endothelium and peripheral blood mononuclear cells	cytokine	10.0
BSK_BE3C_IP10_down	CXCL10	human	bronchial epithelial cells	cytokine	10.0
BSK_KF3CT_IP10_down	CXCL10	human	keratinocytes and foreskin fibroblasts	cytokine	10.0
BSK_hDFCGF_IP10_down	CXCL10	human	foreskin fibroblast	cytokine	40.0
BSK_BE3C_IL1a_down	IL1A	human	bronchial epithelial cells	cytokine	40.0
BSK_BE3C_PAI1_down	SERPINE1	human	bronchial epithelial cells	cytokine	40.0
LTEA_HepaRG_FAS_up	FAS	human	HepaRG	cytokine receptor	17.4
LTEA_HepaRG_IL6R_dn	IL6R	human	HepaRG	cytokine receptor	85.3
NHEERL_MED_hDIO2_dn	NA	human	NA	deiodinase	93.2
NHEERL_MED_hDIO3_dn	NA	human	NA	deiodinase	173
LTEA_HepaRG_DDIT3_up	DDIT3	human	HepaRG	dna binding	33.9

Assay Name	Gene Symbol	Organism	Cells/Cell Lines	Intended Target Family	AC50 (µM)
LTEA_HepaRG_EGR1_dn	EGR1	human	HepaRG	dna binding	10.4
ATG_AP_1_CIS_up	FOS	human	HepG2	dna binding	33.7
LTEA_HepaRG_FOXO1_up	FOXO1	human	HepaRG	dna binding	23.8
LTEA_HepaRG_FOXO3_up	FOXO3	human	HepaRG	dna binding	27.3
LTEA_HepaRG_HSPA1A_up	HSPA1A	human	HepaRG	dna binding	19.3
ATG_MRE_CIS_up	MTF1	human	HepG2	dna binding	42.0
LTEA_HepaRG_MYC_up	MYC	human	HepaRG	dna binding	32.3
ATG_NRF2_ARE_CIS_up	NFE2L2	human	HepG2	dna binding	5.82
LTEA_HepaRG_NFE2L2_up	NFE2L2	human	HepaRG	dna binding	14.1
TOX21_ARE_BLA_agonist_ratio	NFE2L2	human	HEK293T	dna binding	25.2
ATG_Pax6_CIS_up	PAX6	human	HepG2	dna binding	84.0
ATG_Sp1_CIS_up	SP1	human	HepG2	dna binding	34.0
APR_HepG2_p53Act_24h_up	TP53	human	HepG2	dna binding	109
APR_HepG2_p53Act_72h_up	TP53	human	HepG2	dna binding	5.43
LTEA_HepaRG_TP53_up	TP53	human	HepaRG	dna binding	302
ATG_p53_CIS_dn	TP53	human	HepG2	dna binding	69.1
TOX21_p53_BLA_p4_ratio	TP53	human	intestinal cells HCT116	dna binding	159
LTEA_HepaRG_LIPC_dn	LIPC	human	HepaRG	esterase	47.2
NVS_ENZ_hPDE4A1	PDE4A	human	NA	esterase	9.62
NVS_ENZ_hPDE5	PDE5A	human	NA	esterase	25.6
LTEA_HepaRG_KRT19_up	KRT19	human	HepaRG	filaments	30.9
NVS_GPCR_hAdoRA2a	ADORA2A	human	NA	gpcr	5.17
NVS_GPCR_hAdra2C	ADRA2C	human	NA	gpcr	16.8
NVS_GPCR_hAdrb1	ADRB1	human	NA	gpcr	31.2
NVS_GPCR_gLTD4	Cysltr1	guinea pig	NA	gpcr	27.2
NVS_GPCR_hDRD4.4	DRD4	human	NA	gpcr	19.3
NVS_GPCR_h5HT5A	HTR5A	human	NA	gpcr	16.7
NVS_GPCR_h5HT6	HTR6	human	NA	gpcr	24.0
NVS_GPCR_h5HT7	HTR7	human	NA	gpcr	7.26
NVS_GPCR_hLTB4_BLT1	LTB4R	human	NA	gpcr	24.3
NVS_GPCR_gLTB4	Ltb4r	guinea pig	NA	gpcr	21.8
NVS_GPCR_hNPY2	NPY2R	human	NA	gpcr	28.0
NVS_GPCR_hOpiate_D1	OPRD1	human	NA	gpcr	12.6

Assay Name	Gene Symbol	Organism	Cells/Cell Lines	Intended Target Family	AC50 (µM)
NVS_GPCR_hPY2	P2RY1	human	NA	gpcr	11.8
NVS_GPCR_hTXA2	TBXA2R	human	NA	gpcr	16.1
LTEA_HepaRG_IGF1_dn	IGF1	human	HepaRG	growth factor	34.7
LTEA_HepaRG_TGFA_up	TGFA	human	HepaRG	growth factor	13.4
ATG_TGFb_CIS_up	TGFB1	human	HepG2	growth factor	70.7
BSK_BE3C_TGFb1_down	TGFB1	human	bronchial epithelial cells	growth factor	40.0
BSK_KF3CT_TGFb1_down	TGFB1	human	keratinocytes and foreskin fibroblasts	growth factor	40.0
LTEA_HepaRG_THRSP_dn	THRSP	human	HepaRG	growth factor	48.2
TOX21_SBE_BLA_Antagonist_ratio	NA	human	SBE-bla HEK 293T cell line	growth factor receptor	71.6
NVS_ENZ_hHDAC3	HDAC3	human	NA	hydrolase	9.92
NVS_ENZ_hSIRT2	SIRT2	human	NA	hydrolase	7.58
NVS_ENZ_hSIRT3_Activator	SIRT3	human	NA	hydrolase	7.55
NVS_ENZ_hAKT1	AKT1	human	NA	kinase	38.3
NVS_ENZ_hAKT2	AKT2	human	NA	kinase	26.2
NVS_ENZ_hAurA	AURKA	human	NA	kinase	26.8
NVS_ENZ_hBTK	BTK	human	NA	kinase	21.9
NVS_ENZ_hCDK6	CDK6	human	NA	kinase	20.0
NVS_ENZ_hIKKa	CHUK	human	NA	kinase	30.4
NVS_ENZ_hCSF1R	CSF1R	human	NA	kinase	23.0
NVS_ENZ_hCSF1R_Activator	CSF1R	human	NA	kinase	0.406
NVS_ENZ_hCK1a	CSNK1A1	human	NA	kinase	24.2
NVS_ENZ_hCK1D	CSNK1D	human	NA	kinase	26.4
NVS_ENZ_hDYRK1a	DYRK1A	human	NA	kinase	20.7
NVS_ENZ_hEGFR	EGFR	human	NA	kinase	19.1
NVS_ENZ_hEphA2	EPHA2	human	NA	kinase	20.8
NVS_ENZ_hFGFR1	FGFR1	human	NA	kinase	20.8
NVS_ENZ_hFGFR3	FGFR3	human	NA	kinase	33.3
NVS_ENZ_hVEGFR1	FLT1	human	NA	kinase	8.92
NVS_ENZ_hVEGFR3	FLT4	human	NA	kinase	8.36
NVS_ENZ_hFyn	FYN	human	NA	kinase	41.0
NVS_ENZ_hGSK3b	GSK3B	human	NA	kinase	25.5

Assay Name	Gene Symbol	Organism	Cells/Cell Lines	Intended Target Family	AC50 (µM)
NVS_ENZ_hInsR	INSR	human	NA	kinase	12.5
NVS_ENZ_hInsR_Activator	INSR	human	NA	kinase	40.9
NVS_ENZ_hVEGFR2	KDR	human	NA	kinase	32.2
NVS_ENZ_hLck	LCK	human	NA	kinase	40.9
NVS_ENZ_hLynA_Activator	LYN	human	NA	kinase	27.8
NVS_ENZ_hMARK1	MARK1	human	NA	kinase	32.5
NVS_ENZ_hMAPK1	MAPK1	human	NA	kinase	30.4
NVS_ENZ_hMAPK3	MAPK3	human	NA	kinase	31.5
NVS_ENZ_hMAPKAPK5	MAPKAPK5	human	NA	kinase	36.4
NVS_ENZ_hMet	MET	human	NA	kinase	25.7
NVS_ENZ_hTrkA	NTRK1	human	NA	kinase	30.2
NVS_ENZ_hPAK4	PAK4	human	NA	kinase	26.5
LTEA_HepaRG_PDK4_up	PDK4	human	HepaRG	kinase	24.2
NVS_ENZ_hPI3Ka	PIK3CA	human	NA	kinase	7.42
NVS_ENZ_hAMPKa1	PRKAA1	human	NA	kinase	5.47
NVS_ENZ_hPKA	PRKACA	human	NA	kinase	26.4
NVS_ENZ_hRAF1	RAF1	human	NA	kinase	24.4
NVS_ENZ_hROCK1	ROCK1	human	NA	kinase	33.9
NVS_ENZ_hMsk1	RPS6KA5	human	NA	kinase	29.7
NVS_ENZ_hSGK1	SGK1	human	NA	kinase	29.8
NVS_ENZ_hTie2	TEK	human	NA	kinase	8.69
NVS_ENZ_hZAP70	ZAP70	human	NA	kinase	13.5
LTEA_HepaRG_ACLY_dn	ACLY	human	HepaRG	lyase	32.2
LTEA_HepaRG_FASN_dn	FASN	human	HepaRG	lyase	45.0
LTEA_HepaRG_HMGCS2_dn	HMGCS2	human	HepaRG	lyase	83.6
Tanguay_ZF_120hpf_MORT_up	NA	zebrafish	dechorionated zebrafish embryo	malformation	0.547
Tanguay_ZF_120hpf_YSE_up	NA	zebrafish	dechorionated zebrafish embryo	malformation	8.65
Tanguay_ZF_120hpf_AXIS_up	NA	zebrafish	dechorionated zebrafish embryo	malformation	2.39

Assay Name	Gene Symbol	Organism	Cells/Cell Lines	Intended Target Family	AC50 (µM)
Tanguay_ZF_120hpf_SNOU_up	NA	zebrafish	dechorionated zebrafish embryo	malformation	26.0
Tanguay_ZF_120hpf_JAW_up	NA	zebrafish	dechorionated zebrafish embryo	malformation	29.2
Tanguay_ZF_120hpf_PE_up	NA	zebrafish	dechorionated zebrafish embryo	malformation	28.7
Tanguay_ZF_120hpf_TRUN_up	NA	zebrafish	dechorionated zebrafish embryo	malformation	16.8
Tanguay_ZF_120hpf_TR_up	NA	zebrafish	dechorionated zebrafish embryo	malformation	1.92
NHEERL_ZF_144hpf_TERATOSCORE_up	NA	zebrafish	zebrafish embryo	malformation	42.3
Tanguay_ZF_120hpf_ActivityScore	NA	zebrafish	dechorionated zebrafish embryo	malformation	3.45
LTEA_HepaRG_EZR_up	EZR	human	HepaRG	membrane protein	56.5
LTEA_HepaRG_MIR122_dn	MIR122	human	HepaRG	microrna	72.0
ACEA_AR_antagonist_80hr	AR	human	prostate 22Rv1	nuclear receptor	39.0
NVS_NR_hAR	AR	human	NA	nuclear receptor	12.6
NVS_NR_cAR	AR	chimpanzee	NA	nuclear receptor	7.31
NVS_NR_rAR	AR	rat	NA	nuclear receptor	4.27
ATG_ERE_CIS_up	ESR1	human	HepG2	nuclear receptor	18.1
ATG_ERa_TRANS_up	ESR1	human	HepG2	nuclear receptor	38.9
NVS_NR_hER	ESR1	human	NA	nuclear receptor	27.2
TOX21_ERa_BLA_Antagonist_ratio	ESR1	human	HEK293T	nuclear receptor	86.5
OT_ER_ERaERb_0480	ESR2	human	HEK293T	nuclear receptor	87.4
TOX21_ERb_BLA_Antagonist_ratio	ESR2	human	HEK293T	nuclear receptor	62.2
ATG_PXRE_CIS_up	NR1I2	human	HepG2	nuclear receptor	9.42
ATG_PXR_TRANS_up	NR1I2	human	HepG2	nuclear receptor	19.7
NVS_NR_hPXR	NR1I2	human	NA	nuclear receptor	40.9
NVS_NR_hCAR_Antagonist	NR1I3	human	NA	nuclear receptor	17.6

Assay Name	Gene Symbol	Organism	Cells/Cell Lines	Intended Target Family	AC50 (µM)
NVS_NR_hGR	NR3C1	human	NA	nuclear receptor	2.27
ATG_DR4_LXR_CIS_dn	NR1H3	human	HepG2	nuclear receptor	23.8
TOX21_PR_BLA_Antagonist_ratio	PGR	human	PR-UAS-bla-HEK293T	nuclear receptor	35.5
NVS_NR_hPR	PGR	human	NA	nuclear receptor	22.6
NVS_NR_bPR	PGR	bovine	NA	nuclear receptor	22.2
ATG_PPRE_CIS_up	PPARA	human	HepG2	nuclear receptor	33.9
ATG_PPARa_TRANS_up	PPARA	human	HepG2	nuclear receptor	58.9
ATG_PPARg_TRANS_up	PPARG	human	HepG2	nuclear receptor	26.7
NVS_NR_hPPARg	PPARG	human	NA	nuclear receptor	5.94
NVS_NR_hRAR_Antagonist	RARA	human	NA	nuclear receptor	28.4
NVS_NR_hTRa_Antagonist	THRA	human	NA	nuclear receptor	14.6
TOX21_TR_LUC_GH3_Antagonist	Thrb	rat	pituitary gland GH3	nuclear receptor	86.5
LTEA_HepaRG_ACOX1_up	ACOX1	human	HepaRG	oxidase	14.7
LTEA_HepaRG_FMO3_dn	FMO3	human	HepaRG	oxidoreductase	86.3
NVS_ENZ_oCOX2	PTGS2	sheep	NA	oxidoreductase	11.9
NVS_ENZ_hACP1	ACP1	human	NA	phosphatase	24.1
LTEA_HepaRG_ALPP_up	ALPP	human	HepaRG	phosphatase	40.4
NVS_ENZ_hDUSP3	DUSP3	human	NA	phosphatase	26.0
NVS_ENZ_hPPP1CA	PPP1CA	human	NA	phosphatase	16.1
NVS_ENZ_hPPP2CA	PPP2CA	human	NA	phosphatase	5.39
NVS_ENZ_hPTEN	PTEN	human	NA	phosphatase	7.66
NVS_ENZ_hPTPN1	PTPN1	human	NA	phosphatase	5.33e-2
NVS_ENZ_hPTPN2	PTPN2	human	NA	phosphatase	26.6
NVS_ENZ_hPTPN6	PTPN6	human	NA	phosphatase	23.3
NVS_ENZ_hPTPN11	PTPN11	human	NA	phosphatase	24.3
NVS_ENZ_hPTPN12	PTPN12	human	NA	phosphatase	21.8
NVS_ENZ_hPTPN13	PTPN13	human	NA	phosphatase	10.5
NVS_ENZ_hPTPRB	PTPRB	human	NA	phosphatase	25.4
NVS_ENZ_hPTPRC	PTPRC	human	NA	phosphatase	16.0
NVS_ENZ_hPTPRF	PTPRF	human	NA	phosphatase	11.1
NVS_ENZ_hPTPRM	PTPRM	human	NA	phosphatase	31.0
NVS_ENZ_hBACE	BACE1	human	NA	protease	0.471
LTEA_HepaRG_CASP3_up	CASP3	human	HepaRG	protease	21.1

Assay Name	Gene Symbol	Organism	Cells/Cell Lines	Intended Target Family	AC50 (μM)
NVS_ENZ_hCASP5	CASP5	human	NA	protease	13.6
LTEA_HepaRG_CASP8_up	CASP8	human	HepaRG	protease	18.5
NVS_ENZ_hMMP3	MMP3	human	NA	protease	18.8
NVS_ENZ_hMMP7	MMP7	human	NA	protease	1.73
NVS_ENZ_hMMP9	MMP9	human	NA	protease	18.4
BSK_KF3CT_MMP9_down	MMP9	human	keratinocytes and foreskin fibroblasts	protease	10.0
LTEA_HepaRG_MMP10_up	MMP10	human	HepaRG	protease	83.4
NVS_ENZ_hMMP13	MMP13	human	NA	protease	8.08
BSK_BE3C_tPA_down	PLAT	human	bronchial epithelial cells	protease	40.0
BSK_BE3C_uPA_down	PLAU	human	bronchial epithelial cells	protease	40.0
LTEA_HepaRG_GSTA2_dn	GSTA2	human	HepaRG	transferase	41.2
LTEA_HepaRG_UGT1A1_up	UGT1A1	human	HepaRG	transferase	15.3
LTEA_HepaRG_UGT1A6_dn	UGT1A6	human	HepaRG	transferase	56.1
LTEA_HepaRG_ABCB1_up	ABCB1	human	HepaRG	transporter	21.2
LTEA_HepaRG_ABCB11_dn	ABCB11	human	HepaRG	transporter	44.4
LTEA_HepaRG_ABCC2_up	ABCC2	human	HepaRG	transporter	11.6
LTEA_HepaRG_ABCG2_up	ABCG2	human	HepaRG	transporter	6.93
LTEA_HepaRG_FABP1_dn	FABP1	human	HepaRG	transporter	85.9
LTEA_HepaRG_IGFBP1_up	IGFBP1	human	HepaRG	transporter	57.5
NIS_RAIU_inhibition	SLC5A5	human	HEK293T	transporter	11.2
LTEA_HepaRG_SLC22A1_dn	SLC22A1	human	HepaRG	transporter	85.1
LTEA_HepaRG_SLCO1B1_dn	SLCO1B1	human	HepaRG	transporter	82.9

[1] Assays are alphabetically ordered by “intended target family”, and within each “intended target family” assays are ordered alphabetically by “gene symbol”. This table does not include assays classified by the US EPA CompTox Chemicals Dashboard as ‘background measurement’ assays (*e.g.*, artifact fluorescence, baseline controls, and internal markers).
AC50: the concentration that induces a half-maximal assay response.
NA, not applicable. This notation is used when no specific target genes are reported by the US EPA CompTox Chemicals Dashboard, and used for cell-free assays such as cell-free systems utilizing enzymes or receptors extracted from tissues or cells of various organisms.

Table F2 179 Active ToxCast assays[1] for PFOS potassium salt

Assay Name	Gene Symbol	Organism	Cells/Cell Lines	Intended Target Family	AC50 (µM)
LTEA_HepaRG_CAT_dn	CAT	human	HepaRG	catalase	87.0
BSK_BE3C_HLADR_down	HLA-DRA	human	bronchial epithelial cells	cell adhesion molecules	10.0
BSK_LPS_Eselectin_up	SELE	human	umbilical vein endothelium and peripheral blood mononuclear cells	cell adhesion molecules	40.0
BSK_4H_Pselectin_up	SELP	human	umbilical vein endothelium	cell adhesion molecules	40.0
APR_HepG2_CellLoss_24h_dn	NA	human	HepG2	cell cycle	115
APR_HepG2_MitoticArrest_24h_up	pH3	human	HepG2	cell cycle	110
APR_HepG2_OxidativeStress_24h_up	γH2AX	human	HepG2	cell cycle	121
APR_HepG2_CellLoss_72h_dn	NA	human	HepG2	cell cycle	111
APR_HepG2_MitoticArrest_72h_up	pH3	human	HepG2	cell cycle	107
APR_HepG2_OxidativeStress_72h_up	γH2AX	human	HepG2	cell cycle	111
APR_HepG2_StressKinase_72h_up	NA	human	HepG2	cell cycle	112
BSK_KF3CT_SRB_down	NA	human	keratinocytes and foreskin fibroblasts	cell cycle	40.0
BSK_BE3C_SRB_down	NA	human	bronchial epithelial cells	cell cycle	40.0
TOX21_TR_LUC_GH3_Antagonist_viability	NA	rat	pituitary gland GH4	cell cycle	49.4
LTEA_HepaRG_BAX_up	BAX	human	HepaRG	cell cycle	53.6
LTEA_HepaRG_BCL2_up	BCL2	human	HepaRG	cell cycle	43.0
LTEA_HepaRG_CCND1_up	CCND1	human	HepaRG	cell cycle	11.4
TOX21_FXR_BLA_antagonist_viability	NA	human	HEK293T	cell cycle	31.9
TOX21_PPARd_BLA_antagonist_viability	NA	human	HEK293T	cell cycle	43.2
TOX21_DT40	NA	chicken	lymphoblast	cell cycle	44.9

Assay Name	Gene Symbol	Organism	Cells/Cell Lines	Intended Target Family	AC50 (µM)
LTEA_HepaRG_LDH_ cytotoxicity	NA	human	HepaRG	cell cycle	83.4
TOX21_ARE_BLA_agonist_ viability	NA	human	HepG2	cell cycle	76.2
TOX21_FXR_BLA_agonist_ viability	NA	human	HEK293T	cell cycle	29.1
TOX21_PPARd_BLA_Agonist _viability	NA	human	HEK293T	cell cycle	32.4
TOX21_p53_BLA_p3_viability	NA	human	intestinal cells HCT116	cell cycle	54.1
TOX21_p53_BLA_p4_viability	NA	human	intestinal cells HCT116	cell cycle	45.4
TOX21_VDR_BLA_Agonist_ viability	NA	human	HEK293T	cell cycle	18.8
TOX21_AP1_BLA_Agonist_vi ability	NA	human	cervix cell line	cell cycle	50.2
ACEA_AR_agonist_AUC_ viability	NA	human	prostate 22Rv1	cell cycle	69.3
ACEA_AR_antagonist_AUC_ viability	NA	human	prostate 22Rv1	cell cycle	56.0
TOX21_ERR_viability	NA	human	ERR-HEK293T	cell cycle	38.3
TOX21_HRE_BLA_Agonist_ viability	NA	human	cervix ME-180	cell cycle	26.3
TOX21_RT_HEK293_FLO_ 08hr_viability	NA	human	HEK293T	cell cycle	28.5
TOX21_RT_HEK293_FLO_ 16hr_viability	NA	human	HEK293T	cell cycle	24.0
TOX21_RT_HEK293_FLO_ 24hr_viability	NA	human	HEK293T	cell cycle	29.2
TOX21_RT_HEK293_FLO_ 32hr_viability	NA	human	HEK293T	cell cycle	28.8
TOX21_RT_HEK293_FLO_ 40hr_viability	NA	human	HEK293T	cell cycle	29.1
TOX21_RT_HEPG2_FLO_16h r_ctrl_viability	NA	human	HEK293T	cell cycle	14.3
TOX21_RT_HEPG2_FLO_24h r_viability	NA	human	HEK293T	cell cycle	13.4
TOX21_RT_HEPG2_FLO_32h r_ctrl_viability	NA	human	HEK293T	cell cycle	15.7
TOX21_RT_HEPG2_FLO_40h r_ctrl_viability	NA	human	HEK293T	cell cycle	14.8

Assay Name	Gene Symbol	Organism	Cells/Cell Lines	Intended Target Family	AC50 (µM)
TOX21_RT_HEPG2_GLO_00 hr_ctrl_viability	NA	human	HEK293T	cell cycle	43.6
NIS_HEK293T_CTG_ Cytotoxicity	NA	human	HEK293T	cell cycle	10.3
TOX21_ERb_BLA_Agonist_ viability	NA	human	HEK293T	cell cycle	42.2
TOX21_ERb_BLA_Antagonist _viability	NA	human	HEK293T	cell cycle	42.5
TOX21_PR_BLA_Agonist_ viability	NA	human	PR-UAS-bla-HEK293T	cell cycle	40.5
TOX21_PR_BLA_Antagonist_ viability	NA	human	PR-UAS-bla-HEK293T	cell cycle	55.9
TOX21_DT40_100	NA	chicken	lymphoblast	cell cycle	43.3
TOX21_DT40_657	NA	chicken	lymphoblast	cell cycle	65.3
TOX21_PXR_viability	NA	human	PXR-Luc HepG2 cells	cell cycle	88.4
APR_HepG2_MitoMass_24h_ dn	NA	human	HepG2	cell morphology	120
APR_HepG2_MitoMass_72h_ dn	NA	human	HepG2	cell morphology	113
TOX21_MMP_ratio_up	NA	human	HepG2	cell morphology	72.5
LTEA_HepaRG_CYP1A2_dn	CYP1A2	human	HepaRG	cyp	202
LTEA_HepaRG_CYP3A4_up	CYP3A4	human	HepaRG	cyp	8.63
LTEA_HepaRG_CYP3A5_dn	CYP3A5	human	HepaRG	cyp	90.0
LTEA_HepaRG_CYP3A7_up	CYP3A7	human	HepaRG	cyp	9.25
LTEA_HepaRG_CYP4A11_dn	CYP4A11	human	HepaRG	cyp	87.0
LTEA_HepaRG_CYP4A22_dn	CYP4A22	human	HepaRG	cyp	85.8
LTEA_HepaRG_CYP7A1_dn	CYP7A1	human	HepaRG	cyp	82.2
LTEA_HepaRG_CYP2B6_dn	CYP2B6	human	HepaRG	cyp	86.4
LTEA_HepaRG_CYP2B6_up	CYP2B6	human	HepaRG	cyp	3.31
LTEA_HepaRG_CYP2C8_dn	CYP2C8	human	HepaRG	cyp	89.2
LTEA_HepaRG_CYP2C8_up	CYP2C8	human	HepaRG	cyp	21.2
LTEA_HepaRG_CYP2C9_dn	CYP2C9	human	HepaRG	cyp	86.3
NVS_ADME_hCYP2C9	CYP2C9	human	NA	cyp	1.30e-2
NVS_ADME_hCYP2C19	CYP2C19	human	NA	cyp	6.09
LTEA_HepaRG_CYP2C19_dn	CYP2C19	human	HepaRG	cyp	81.9
LTEA_HepaRG_CYP2C19_up	CYP2C19	human	HepaRG	cyp	11.1

Assay Name	Gene Symbol	Organism	Cells/Cell Lines	Intended Target Family	AC50 (µM)
LTEA_HepaRG_CYP2E1_dn	CYP2E1	human	HepaRG	cyp	60.4
BSK_BE3C_MIG_down	CXCL9	human	bronchial epithelial cells	cytokine	40.0
BSK_BE3C_IP10_down	CXCL10	human	bronchial epithelial cells	cytokine	10.0
BSK_KF3CT_IP10_down	CXCL10	human	keratinocytes and foreskin fibroblasts	cytokine	40.0
BSK_BE3C_IL1a_down	IL1A	human	bronchial epithelial cells	cytokine	40.0
BSK_KF3CT_IL1a_down	IL1A	human	keratinocytes and foreskin fibroblasts	cytokine	40.0
BSK_BE3C_uPAR_down	PLAUR	human	bronchial epithelial cells	cytokine	40.0
BSK_BE3C_PAI1_down	SERPINE1	human	bronchial epithelial cells	cytokine	40.0
LTEA_HepaRG_IL6R_dn	IL6R	human	HepaRG	cytokine receptor	95.7
NHEERL_MED_hDIO1_dn	DIO1	human	NA	deiodinase	175
NHEERL_MED_hDIO2_dn	NA	human	NA	deiodinase	122
NHEERL_MED_hDIO3_dn	NA	human	NA	deiodinase	109
LTEA_HepaRG_DDIT3_up	DDIT3	human	HepaRG	dna binding	8.61
LTEA_HepaRG_EGR1_dn	EGR1	human	HepaRG	dna binding	42.6
ATG_AP_1_CIS_up	FOS	human	HepG2	dna binding	37.7
LTEA_HepaRG_JUN_up	JUN	human	HepaRG	dna binding	53.6
ATG_MRE_CIS_up	MTF1	human	HepG2	dna binding	30.7
LTEA_HepaRG_MYC_up	MYC	human	HepaRG	dna binding	12.5
ATG_NRF2_ARE_CIS_up	NFE2L2	human	HepG2	dna binding	30.8
LTEA_HepaRG_NFE2L2_up	NFE2L2	human	HepaRG	dna binding	66.9
ATG_TCF_b_cat_CIS_dn	TCF7	human	HepG2	dna binding	111
APR_HepG2_p53Act_24h_up	TP53	human	HepG2	dna binding	111
APR_HepG2_p53Act_72h_up	TP53	human	HepG2	dna binding	23.7
ATG_p53_CIS_dn	TP53	human	HepG2	dna binding	49.0
LTEA_HepaRG_TP53_up	TP53	human	HepaRG	dna binding	82.6
TOX21_p53_BLA_p4_ratio	TP53	human	intestinal cells HCT116	dna binding	49.1
LTEA_HepaRG_XBP1_dn	XBP1	human	HepaRG	dna binding	73.6

Assay Name	Gene Symbol	Organism	Cells/Cell Lines	Intended Target Family	AC50 (µM)
LTEA_HepaRG_LIPC_dn	LIPC	human	HepaRG	esterase	34.2
LTEA_HepaRG_LPL_up	LPL	human	HepaRG	esterase	15.5
LTEA_HepaRG_KRT19_up	KRT19	human	HepaRG	filaments	35.5
NVS_GPCR_hAdoRA2a	ADORA2A	human	NA	gpcr	10.3
NVS_GPCR_hAdra2C	ADRA2C	human	NA	gpcr	17.6
NVS_GPCR_hAdrb1	ADRB1	human	NA	gpcr	31.5
NVS_GPCR_gLTD4	Cysltr1	guinea pig	NA	gpcr	30.9
NVS_GPCR_hDRD4.4	DRD4	human	NA	gpcr	18.8
NVS_GPCR_h5HT5A	HTR5A	human	NA	gpcr	32.7
NVS_GPCR_h5HT7	HTR7	human	NA	gpcr	30.2
NVS_GPCR_hLTB4_BLT1	LTB4R	human	NA	gpcr	25.9
NVS_GPCR_gLTB4	Ltb4r	guinea pig	NA	gpcr	12.1
NVS_GPCR_hTXA2	TBXA2R	human	NA	gpcr	16.4
LTEA_HepaRG_IGF1_dn	IGF1	human	HepaRG	growth factor	90.0
LTEA_HepaRG_TGFA_up	TGFA	human	HepaRG	growth factor	71.6
ATG_TGFb_CIS_up	TGFB1	human	HepG2	growth factor	26.2
LTEA_HepaRG_TGFB1_up	TGFB1	human	HepaRG	growth factor	54.0
BSK_BE3C_TGFb1_down	TGFB1	human	bronchial epithelial cells	growth factor	40.0
BSK_KF3CT_TGFb1_down	TGFB1	human	keratinocytes and foreskin fibroblasts	growth factor	40.0
LTEA_HepaRG_THRSP_dn	THRSP	human	HepaRG	growth factor	57.8
TOX21_SBE_BLA_Antagonist_ratio	NA	human	SBE-bla HEK 293T cell line	growth factor receptor	34.6
LTEA_HepaRG_KCNK1_up	KCNK1	human	HepaRG	ion channel	34.0
LTEA_HepaRG_PDK4_up	PDK4	human	HepaRG	kinase	23.0
LTEA_HepaRG_FASN_dn	FASN	human	HepaRG	lyase	65.1
LTEA_HepaRG_HMGCS2_dn	HMGCS2	human	HepaRG	lyase	82.3
Tanguay_ZF_120hpf_MORT_up	NA	zebrafish	dechorionated zebrafish embryo	malformation	19.8
Tanguay_ZF_120hpf_YSE_up	NA	zebrafish	dechorionated zebrafish embryo	malformation	38.0

Assay Name	Gene Symbol	Organism	Cells/Cell Lines	Intended Target Family	AC50 (µM)
Tanguay_ZF_120hpf_AXIS_up	NA	zebrafish	dechorionated zebrafish embryo	malformation	34.6
Tanguay_ZF_120hpf_TR_up	NA	zebrafish	dechorionated zebrafish embryo	malformation	12.5
NHEERL_ZF_144hpf_TERATOSCORE_up	NA	zebrafish	zebrafish embryo	malformation	9.62
Tanguay_ZF_120hpf_ActivityScore	NA	zebrafish	dechorionated zebrafish embryo	malformation	33.7
LTEA_HepaRG_EZR_up	EZR	human	HepaRG	membrane protein	24.7
LTEA_HepaRG_MIR122_dn	MIR122	human	HepaRG	microrna	49.7
LTEA_HepaRG_GADD45B_up	GADD45B	human	HepaRG	mutagenicity response	34.8
LTEA_HepaRG_GADD45G_dn	GADD45G	human	HepaRG	mutagenicity response	36.2
ACEA_AR_antagonist_80hr	AR	human	prostate 22Rv1	nuclear receptor	69.3
NVS_NR_hAR	AR	human	NA	nuclear receptor	20.9
NVS_NR_rAR	AR	rat	NA	nuclear receptor	12.0
ATG_ERE_CIS_up	ESR1	human	HepG2	nuclear receptor	32.6
ATG_ERa_TRANS_up	ESR1	human	HepG2	nuclear receptor	35.9
NVS_NR_bER	ESR1	bovine	NA	nuclear receptor	2.59e-2
ATG_LXRb_TRANS_dn	NR1H2	human	HepG2	nuclear receptor	13.4
ATG_DR4_LXR_CIS_dn	NR1H3	human	HepG2	nuclear receptor	32.2
ATG_PXRE_CIS_up	NR1I2	human	HepG2	nuclear receptor	9.76
ATG_PXR_TRANS_up	NR1I2	human	HepG2	nuclear receptor	14.0
ATG_CAR_TRANS_up	NR1I3	human	HepG2	nuclear receptor	39.5
NVS_NR_hGR	NR3C1	human	NA	nuclear receptor	20.7
TOX21_PR_BLA_Antagonist_ratio	PGR	human	PR-UAS-bla-HEK293T	nuclear receptor	63.5
NVS_NR_hPR	PGR	human	NA	nuclear receptor	25.4
NVS_NR_bPR	PGR	bovine	NA	nuclear receptor	29.6
ATG_PPARa_TRANS_up	PPARA	human	HepG2	nuclear receptor	17.1
NVS_NR_hPPARa	PPARA	human	NA	nuclear receptor	11.2
ATG_PPARg_TRANS_up	PPARG	human	HepG2	nuclear receptor	22.2
NVS_NR_hPPARg	PPARG	human	NA	nuclear receptor	20.3

Assay Name	Gene Symbol	Organism	Cells/Cell Lines	Intended Target Family	AC50 (µM)
NVS_NR_hRARa_Antagonist	RARA	human	NA	nuclear receptor	1.91
TOX21_TR_LUC_GH3_ Antagonist	Thrb	rat	pituitary gland GH3	nuclear receptor	65.1
LTEA_HepaRG_FMO3_dn	FMO3	human	HepaRG	oxidoreductase	90.4
LTEA_HepaRG_ALPP_up	ALPP	human	HepaRG	phosphatase	57.1
NVS_ENZ_hPPP1CA	PPP1CA	human	NA	phosphatase	41.0
LTEA_HepaRG_PPP2R4_up	PPP2R4	human	HepaRG	phosphatase	55.9
NVS_ENZ_hPTPRC	PTPRC	human	NA	phosphatase	18.9
NVS_ENZ_hBACE	BACE1	human	NA	protease	8.72
LTEA_HepaRG_CASP3_up	CASP3	human	HepaRG	protease	22.5
NVS_ENZ_hCASP5	CASP5	human	NA	protease	27.8
NVS_ENZ_hMMP3	MMP3	human	NA	protease	29.4
BSK_KF3CT_MMP9_down	MMP9	human	keratinocytes and foreskin fibroblasts	protease	40.0
LTEA_HepaRG_MMP10_up	MMP10	human	HepaRG	protease	46.6
BSK_BE3C_tPA_down	PLAT	human	bronchial epithelial cells	protease	40.0
BSK_BE3C_uPA_down	PLAU	human	bronchial epithelial cells	protease	40.0
BSK_KF3CT_uPA_down	PLAU	human	keratinocytes and foreskin fibroblasts	protease	40.0
BSK_hDFCGF_TIMP1_up	TIMP1	human	foreskin fibroblast	protease inhibitor	10.0
BSK_KF3CT_TIMP2_down	TIMP2	human	keratinocytes and foreskin fibroblasts	protease inhibitor	40.0
LTEA_HepaRG_GSTA2_dn	GSTA2	human	HepaRG	transferase	71.1
LTEA_HepaRG_SULT2A1_dn	SULT2A1	human	HepaRG	transferase	88.4
LTEA_HepaRG_UGT1A1_dn	UGT1A1	human	HepaRG	transferase	85.5
LTEA_HepaRG_UGT1A1_up	UGT1A1	human	HepaRG	transferase	10.2
LTEA_HepaRG_UGT1A6_dn	UGT1A6	human	HepaRG	transferase	38.5
LTEA_HepaRG_ABCB11_dn	ABCB11	human	HepaRG	transporter	86.8
LTEA_HepaRG_FABP1_dn	FABP1	human	HepaRG	transporter	82.8
LTEA_HepaRG_IGFBP1_up	IGFBP1	human	HepaRG	transporter	73.5
LTEA_HepaRG_SLC22A1_dn	SLC22A1	human	HepaRG	transporter	78.6

Assay Name	Gene Symbol	Organism	Cells/Cell Lines	Intended Target Family	AC50 (µM)
LTEA_HepaRG_SLCO1B1_dn	SLCO1B1	human	HepaRG	transporter	86.2
NIS_RAIU_inhibition	SLC5A5	human	HEK293T	transporter	22.8

[1] Assays are alphabetically ordered by "intended target family", and within each "intended target family" assays are ordered alphabetically by "gene symbol". This table does not include assays classified by the US EPA CompTox Chemicals Dashboard as 'background measurement' assays (*e.g.*, artifact fluorescence, baseline controls, and internal markers).
AC50: the concentration that induces a half-maximal assay response.
NA, not applicable. This notation is used when no specific target genes are reported by the US EPA CompTox Chemicals Dashboard, and used for cell-free assays such as cell-free systems utilizing enzymes or receptors extracted from tissues or cells of various organisms.

Table F3 26 Active ToxCast assays[1] for PFOS lithium salt

Assay Name	Gene Symbol	Organism	Cells/Cell Lines	Intended Target Family	AC50 (µM)
TOX21_MMP_viability	NA	human	HepG2	cell cycle	67.4
TOX21_TR_LUC_GH3_ Antagonist_viability	NA	rat	pituitary gland GH4	cell cycle	52.3
TOX21_ARE_BLA_agonist_ viability	NA	human	HepG2	cell cycle	76.2
TOX21_FXR_BLA_antagonist _viability	NA	human	HEK293T	cell cycle	253
TOX21_PPARd_BLA_ Agonist_viability	NA	human	HEK293T	cell cycle	31.4
TOX21_p53_BLA_p2_viability	NA	human	intestinal cells HCT116	cell cycle	70.0
TOX21_p53_BLA_p3_viability	NA	human	intestinal cells HCT116	cell cycle	49.0
TOX21_p53_BLA_p4_viability	NA	human	intestinal cells HCT116	cell cycle	65.8
TOX21_AP1_BLA_Agonist_vi ability	NA	human	cervix ME-180	cell cycle	38.7
TOX21_H2AX_HTRF_CHO_vi ability	NA	Chinese hamster	CHO-K1	cell cycle	158
TOX21_HRE_BLA_Agonist_ viability	NA	human	cervix ME-180	cell cycle	40.5
TOX21_RT_HEK293_FLO_ 16hr_viability	NA	human	HEK293T	cell cycle	7.40e-2
TOX21_RT_HEK293_FLO_ 24hr_viability	NA	human	HEK293T	cell cycle	8.21e-2
TOX21_RT_HEK293_FLO_ 40hr_viability	NA	human	HEK293T	cell cycle	0.289
TOX21_RT_HEPG2_GLO_00 hr_ctrl_viability	NA	human	HEK293T	cell cycle	45.2
TOX21_ERb_BLA_Agonist_ viability	NA	human	HEK293T	cell cycle	43.4
TOX21_ERb_BLA_Antagonist _viability	NA	human	HEK293T	cell cycle	95.9
TOX21_PR_BLA_Agonist_ viability	NA	human	PR-UAS-bla-HEK293T	cell cycle	50.0
TOX21_PR_BLA_Antagonist_ viability	NA	human	PR-UAS-bla-HEK293T	cell cycle	84.3
TOX21_MMP_ratio_up	NA	human	HepG2	cell morphology	40.5

Assay Name	Gene Symbol	Organism	Cells/Cell Lines	Intended Target Family	AC50 (µM)
TOX21_ARE_BLA_agonist_ratio	NFE2L2	human	HEK293T	dna binding	85.2
TOX21_p53_BLA_p4_ratio	TP53	human	intestinal cells HCT116	dna binding	70.8
TOX21_SBE_BLA_Antagonist_ratio	NA	human	SBE-bla HEK 293T cell line	growth factor receptor	45.3
NVS_NR_bER	ESR1	bovine	NA	nuclear receptor	15.1
TOX21_PR_BLA_Antagonist_ratio	PGR	human	PR-UAS-bla-HEK293T	nuclear receptor	98.6
TOX21_TR_LUC_GH3_Antagonist	Thrb	rat	pituitary gland GH3	nuclear receptor	63.5

[1] Assays are alphabetically ordered by "intended target family", and within each "intended target family" assays are ordered alphabetically by "gene symbol". This table does not include assays classified by the US EPA CompTox Chemicals Dashboard as 'background measurement' assays (*e.g.*, artifact fluorescence, baseline controls, and internal markers).
AC50: the concentration that induces a half-maximal assay response.
NA, not applicable. This notation is used when no specific target genes are reported by the US EPA CompTox Chemicals Dashboard, and used for cell-free assays such as cell-free systems utilizing enzymes or receptors extracted from tissues or cells of various organisms.

Table F4 260 Active ToxCast assays[1] for PFOSA

Assay Name	Gene Symbol	Organism	Cells/Cell Lines	Intended Target Family	AC50 (µM)
LTEA_HepaRG_APOA5_dn	APOA5	human	HepaRG	apolipoprotein	10.0
LTEA_HepaRG_CAT_dn	CAT	human	HepaRG	catalase	8.80
BSK_hDFCGF_CollagenIII_down	COL3A1	human	foreskin fibroblast	cell adhesion molecules	10.0
BSK_3C_HLADR_down	HLA-DRA	human	umbilical vein endothelium	cell adhesion molecules	10.0
BSK_BE3C_HLADR_down	HLA-DRA	human	bronchial epithelial cells	cell adhesion molecules	10.0
BSK_CASM3C_HLADR_down	HLA-DRA	human	coronary artery smooth muscle cells	cell adhesion molecules	40.0
BSK_KF3CT_ICAM1_down	ICAM1	human	keratinocytes and foreskin fibroblasts	cell adhesion molecules	40.0
BSK_CASM3C_SAA_down	SAA1	human	coronary artery smooth muscle cells	cell adhesion molecules	40.0
BSK_3C_Eselectin_down	SELE	human	umbilical vein endothelium	cell adhesion molecules	40.0
BSK_LPS_Eselectin_down	SELE	human	umbilical vein endothelium and peripheral blood mononuclear cells	cell adhesion molecules	40.0
BSK_SAg_Eselectin_down	SELE	human	umbilical vein endothelium and peripheral blood mononuclear cells	cell adhesion molecules	10.0
BSK_4H_Pselectin_down	SELP	human	umbilical vein endothelium	cell adhesion molecules	40.0
BSK_3C_VCAM1_down	VCAM1	human	umbilical vein endothelium	cell adhesion molecules	40.0
BSK_4H_VCAM1_down	VCAM1	human	umbilical vein endothelium	cell adhesion molecules	40.0
BSK_CASM3C_VCAM1_down	VCAM1	human	coronary artery smooth muscle cells	cell adhesion molecules	40.0
BSK_hDFCGF_VCAM1_down	VCAM1	human	foreskin fibroblast	cell adhesion molecules	10.0

Assay Name	Gene Symbol	Organism	Cells/Cell Lines	Intended Target Family	AC50 (µM)
LTEA_HepaRG_BAD_dn	BAD	human	HepaRG	cell cycle	27.1
LTEA_HepaRG_BCL2_dn	BCL2	human	HepaRG	cell cycle	6.09
LTEA_HepaRG_BCL2L11_dn	BCL2L11	human	HepaRG	cell cycle	7.58
LTEA_HepaRG_BID_dn	BID	human	HepaRG	cell cycle	3.28
LTEA_HepaRG_CCND1_dn	CCND1	human	HepaRG	cell cycle	64.4
LTEA_HepaRG_CDKN1A_dn	CDKN1A	human	HepaRG	cell cycle	4.81
LTEA_HepaRG_CFLAR_dn	CFLAR	human	HepaRG	cell cycle	7.31
LTEA_HepaRG_GADD45A_dn	GADD45A	human	HepaRG	cell cycle	3.47
LTEA_HepaRG_GADD45A_up	GADD45A	human	HepaRG	cell cycle	26.4
APR_HepG2_CellCycleArrest_24h_dn	NA	human	HepG2	cell cycle	61.6
APR_HepG2_CellLoss_24h_dn	NA	human	HepG2	cell cycle	103
APR_HepG2_MitoticArrest_24h_up	NA	human	HepG2	cell cycle	106
APR_HepG2_OxidativeStress_24h_up	NA	human	HepG2	cell cycle	114
APR_HepG2_CellCycleArrest_72h_dn	NA	human	HepG2	cell cycle	54.8
APR_HepG2_CellLoss_72h_dn	NA	human	HepG2	cell cycle	73.2
APR_HepG2_MitoticArrest_72h_up	NA	human	HepG2	cell cycle	81.3
APR_HepG2_OxidativeStress_72h_up	NA	human	HepG2	cell cycle	100
BSK_3C_Proliferation_down	NA	human	umbilical vein endothelium	cell cycle	40.0
BSK_3C_SRB_down	NA	human	umbilical vein endothelium	cell cycle	40.0
BSK_4H_SRB_down	NA	human	umbilical vein endothelium	cell cycle	40.0
BSK_CASM3C_SRB_down	NA	human	coronary artery smooth muscle cells	cell cycle	40.0
BSK_hDFCGF_Proliferation_down	NA	human	foreskin fibroblast	cell cycle	10.0
BSK_hDFCGF_SRB_down	NA	human	foreskin fibroblast	cell cycle	40.0

Assay Name	Gene Symbol	Organism	Cells/Cell Lines	Intended Target Family	AC50 (µM)
BSK_KF3CT_SRB_down	NA	human	keratinocytes and foreskin fibroblasts	cell cycle	40.0
BSK_LPS_SRB_down	NA	human	umbilical vein endothelium and peripheral blood mononuclear cells	cell cycle	40.0
BSK_SAg_PBMCCytotoxicity_down	NA	human	umbilical vein endothelium and peripheral blood mononuclear cells	cell cycle	40.0
BSK_SAg_Proliferation_down	NA	human	umbilical vein endothelium and peripheral blood mononuclear cells	cell cycle	40.0
BSK_SAg_SRB_down	NA	human	umbilical vein endothelium and peripheral blood mononuclear cells	cell cycle	40.0
TOX21_GR_BLA_Antagonist_viability	NA	human	cervix HeLa cell line	cell cycle	55.8
TOX21_MMP_viability	NA	human	HepG2	cell cycle	45.7
TOX21_TR_LUC_GH3_Antagonist_viability	NA	rat	pituitary gland cell line	cell cycle	52.8
TOX21_FXR_BLA_antagonist_viability	NA	human	HEK293T	cell cycle	42.4
TOX21_PPARd_BLA_antagonist_viability	NA	human	HEK293T	cell cycle	35.5
TOX21_PPARg_BLA_antagonist_viability	NA	human	HEK293T	cell cycle	45.5
TOX21_DT40	NA	chicken	lymphoblast	cell cycle	126
LTEA_HepaRG_LDH_cytotoxicity	NA	human	HepaRG	cell cycle	29.7
TOX21_ARE_BLA_agonist_viability	NA	human	HepG2	cell cycle	65.4
TOX21_HSE_BLA_agonist_viability	NA	human	cervix HeLa cell line	cell cycle	40.4

Assay Name	Gene Symbol	Organism	Cells/Cell Lines	Intended Target Family	AC50 (µM)
TOX21_p53_BLA_p1_viability	NA	human	intestinal HCT116 cell line	cell cycle	68.7
TOX21_PPARd_BLA_Agonist_viability	NA	human	HEK293T	cell cycle	61.8
ATG_XTT_Cytotoxicity_up	NA	human	HepG2	cell cycle	27.0
TOX21_p53_BLA_p3_viability	NA	human	intestinal HCT116 cell line	cell cycle	56.6
TOX21_p53_BLA_p5_viability	NA	human	intestinal HCT116 cell line	cell cycle	57.6
TOX21_VDR_BLA_Agonist_viability	NA	human	HEK293T	cell cycle	50.3
CEETOX_H295R_MTT_cell_viability_dn	NA	human	adrenal gland H295R cell line	cell cycle	4.35e-2
ACEA_ER_AUC_viability	NA	human	prostate 22Rv1 cell line	cell cycle	81.4
ACEA_AR_antagonist_AUC_viability	NA	human	prostate 22Rv1 cell line	cell cycle	48.6
TOX21_CAR_Agonist_viabillity	NA	human	HepG2	cell cycle	2.32
TOX21_CAR_Antagonist_viability	NA	human	HepG2	cell cycle	285
TOX21_HRE_BLA_Agonist_viability	NA	human	cervix ME-180 cell line	cell cycle	28.8
TOX21_RT_HEK293_GLO_16hr_viability	NA	human	HEK293T	cell cycle	0.193
TOX21_RT_HEPG2_FLO_32hr_ctrl_viability	NA	human	HepG2	cell cycle	0.438
TOX21_RT_HEPG2_FLO_40hr_ctrl_viability	NA	human	HepG2	cell cycle	0.456
NIS_HEK293T_CTG_Cytotoxicity	NA	human	KHEK293T	cell cycle	0.241
TOX21_PR_BLA_Agonist_viability	NA	human	PR-UAS-bla-HEK293T	cell cycle	44.0
TOX21_PR_BLA_Antagonist_viability	NA	human	PR-UAS-bla-HEK293T	cell cycle	20.7
TOX21_DT40_100	NA	chicken	lymphoblast	cell cycle	111
TOX21_DT40_657	NA	chicken	lymphoblast	cell cycle	113

Assay Name	Gene Symbol	Organism	Cells/Cell Lines	Intended Target Family	AC50 (µM)
APR_HepG2_MitoMembPot_24h_dn	NA	human	HepG2	cell morphology	75.9
APR_HepG2_MitoMembPot_72h_dn	NA	human	HepG2	cell morphology	103
BSK_3C_Vis_down	NA	human	umbilical vein endothelium	cell morphology	40.0
TOX21_MMP_ratio_down	NA	human	HepG2	cell morphology	2.72
LTEA_HepaRG_CYP1A1_dn	CYP1A1	human	HepaRG	cyp	15.5
LTEA_HepaRG_CYP1A2_dn	CYP1A2	human	HepaRG	cyp	9.48
LTEA_HepaRG_CYP2B6_dn	CYP2B6	human	HepaRG	cyp	9.44
LTEA_HepaRG_CYP2C19_dn	CYP2C19	human	HepaRG	cyp	9.55
LTEA_HepaRG_CYP2C8_dn	CYP2C8	human	HepaRG	cyp	13.0
LTEA_HepaRG_CYP2C9_dn	CYP2C9	human	HepaRG	cyp	10.1
LTEA_HepaRG_CYP2E1_dn	CYP2E1	human	HepaRG	cyp	5.95
LTEA_HepaRG_CYP3A4_dn	CYP3A4	human	HepaRG	cyp	10.1
LTEA_HepaRG_CYP3A5_dn	CYP3A5	human	HepaRG	cyp	25.6
LTEA_HepaRG_CYP3A7_dn	CYP3A7	human	HepaRG	cyp	7.24
LTEA_HepaRG_CYP4A11_dn	CYP4A11	human	HepaRG	cyp	11.4
LTEA_HepaRG_CYP4A22_dn	CYP4A22	human	HepaRG	cyp	11.4
LTEA_HepaRG_CYP7A1_dn	CYP7A1	human	HepaRG	cyp	11.6
BSK_3C_MCP1_down	CCL2	human	umbilical vein endothelium	cytokine	40.0
BSK_4H_MCP1_down	CCL2	human	umbilical vein endothelium	cytokine	40.0
BSK_KF3CT_MCP1_down	CCL2	human	keratinocytes and foreskin fibroblasts	cytokine	40.0
BSK_SAg_MCP1_down	CCL2	human	umbilical vein endothelium and peripheral blood mononuclear cells	cytokine	40.0
BSK_4H_Eotaxin3_down	CCL26	human	umbilical vein endothelium	cytokine	40.0

Assay Name	Gene Symbol	Organism	Cells/Cell Lines	Intended Target Family	AC50 (µM)
BSK_SAg_CD38_down	CD38	human	umbilical vein endothelium and peripheral blood mononuclear cells	cytokine	10.0
BSK_LPS_CD40_down	CD40	human	umbilical vein endothelium and peripheral blood mononuclear cells	cytokine	40.0
BSK_SAg_CD40_down	CD40	human	umbilical vein endothelium and peripheral blood mononuclear cells	cytokine	40.0
BSK_SAg_CD69_down	CD69	human	umbilical vein endothelium and peripheral blood mononuclear cells	cytokine	40.0
BSK_CASM3C_MCSF_down	CSF1	human	coronary artery smooth muscle cells	cytokine	40.0
BSK_hDFCGF_MCSF_down	CSF1	human	foreskin fibroblast	cytokine	10.0
BSK_LPS_MCSF_down	CSF1	human	umbilical vein endothelium and peripheral blood mononuclear cells	cytokine	40.0
BSK_BE3C_IP10_down	CXCL10	human	bronchial epithelial cells	cytokine	10.0
BSK_hDFCGF_IP10_down	CXCL10	human	foreskin fibroblast	cytokine	4.00
BSK_KF3CT_IP10_down	CXCL10	human	keratinocytes and foreskin fibroblasts	cytokine	4.00
BSK_3C_IL8_down	CXCL8	human	umbilical vein endothelium	cytokine	40.0
BSK_hDFCGF_IL8_down	CXCL8	human	foreskin fibroblast	cytokine	40.0

Assay Name	Gene Symbol	Organism	Cells/Cell Lines	Intended Target Family	AC50 (µM)
BSK_LPS_IL8_down	CXCL8	human	umbilical vein endothelium and peripheral blood mononuclear cells	cytokine	40.0
BSK_SAg_IL8_down	CXCL8	human	umbilical vein endothelium and peripheral blood mononuclear cells	cytokine	40.0
BSK_hDFCGF_MIG_down	CXCL9	human	foreskin fibroblast	cytokine	40.0
BSK_SAg_MIG_down	CXCL9	human	umbilical vein endothelium and peripheral blood mononuclear cells	cytokine	40.0
BSK_3C_TissueFactor_down	F3	human	umbilical vein endothelium	cytokine	40.0
BSK_KF3CT_IL1a_down	IL1A	human	keratinocytes and foreskin fibroblasts	cytokine	40.0
BSK_LPS_IL1a_down	IL1A	human	umbilical vein endothelium and peripheral blood mononuclear cells	cytokine	40.0
LTEA_HepaRG_IL6_up	IL6	human	HepaRG	cytokine	35.3
BSK_3C_uPAR_down	PLAUR	human	umbilical vein endothelium	cytokine	40.0
BSK_4H_uPAR_down	PLAUR	human	umbilical vein endothelium	cytokine	40.0
BSK_BE3C_PAI1_down	SERPINE1	human	bronchial epithelial cells	cytokine	10.0
BSK_hDFCGF_PAI1_down	SERPINE1	human	foreskin fibroblast	cytokine	40.0
BSK_LPS_TNFa_down	TNF	human	umbilical vein endothelium and peripheral blood mononuclear cells	cytokine	40.0

Assay Name	Gene Symbol	Organism	Cells/Cell Lines	Intended Target Family	AC50 (µM)
LTEA_HepaRG_IL6R_dn	IL6R	human	HepaRG	cytokine receptor	33.2
LTEA_HepaRG_TNFRSF1A_dn	TNFRSF1A	human	HepaRG	cytokine receptor	26.5
ATG_CRE_CIS_up	CREB3	human	HepG2	dna binding	33.5
LTEA_HepaRG_DDIT3_up	DDIT3	human	HepaRG	dna binding	25.9
ATG_EGR_CIS_up	EGR1	human	HepG2	dna binding	57.2
LTEA_HepaRG_EGR1_dn	EGR1	human	HepaRG	dna binding	9.44
LTEA_HepaRG_EGR1_up	EGR1	human	HepaRG	dna binding	82.5
ATG_AP_1_CIS_up	FOS	human	HepG2	dna binding	28.6
LTEA_HepaRG_FOXO1_dn	FOXO1	human	HepaRG	dna binding	25.4
LTEA_HepaRG_FOXO3_dn	FOXO3	human	HepaRG	dna binding	6.98
ATG_HIF1a_CIS_up	HIF1A	human	HepG2	dna binding	6.40
LTEA_HepaRG_HIF1A_up	HIF1A	human	HepaRG	dna binding	11.5
ATG_HSE_CIS_up	HSF1	human	HepG2	dna binding	53.3
TOX21_HSE_BLA_agonist_ratio	HSF1	human	cervix HeLa cell line	dna binding	36.5
LTEA_HepaRG_HSPA1A_up	HSPA1A	human	HepaRG	dna binding	44.5
LTEA_HepaRG_JUN_up	JUN	human	HepaRG	dna binding	43.7
ATG_MRE_CIS_up	MTF1	human	HepG2	dna binding	57.2
LTEA_HepaRG_MYC_up	MYC	human	HepaRG	dna binding	25.6
ATG_NRF2_ARE_CIS_up	NFE2L2	human	HepG2	dna binding	28.5
LTEA_HepaRG_NFE2L2_dn	NFE2L2	human	HepaRG	dna binding	6.13
TOX21_ARE_BLA_agonist_ratio	NFE2L2	human	HepG2	dna binding	37.8
ATG_NFI_CIS_up	NFIA	human	HepG2	dna binding	28.0
ATG_NF_kB_CIS_up	NFKB1	human	HepG2	dna binding	57.2
LTEA_HepaRG_NFKB1_dn	NFKB1	human	HepaRG	dna binding	4.07
ATG_Pax6_CIS_up	PAX6	human	HepG2	dna binding	57.2
LTEA_HepaRG_PEG10_dn	PEG10	human	HepaRG	dna binding	5.29
ATG_Oct_MLP_CIS_up	POU2F1	human	HepG2	dna binding	30.2
ATG_BRE_CIS_up	SMAD1	human	HepG2	dna binding	40.2
ATG_Sp1_CIS_up	SP1	human	HepG2	dna binding	22.5
ATG_SREBP_CIS_up	SREBF1	human	HepG2	dna binding	22.6
LTEA_HepaRG_STAT3_dn	STAT3	human	HepaRG	dna binding	14.3
APR_HepG2_p53Act_24h_up	TP53	human	HepG2	dna binding	111

Assay Name	Gene Symbol	Organism	Cells/Cell Lines	Intended Target Family	AC50 (µM)
APR_HepG2_p53Act_72h_up	TP53	human	HepG2	dna binding	62.6
LTEA_HepaRG_TP53_dn	TP53	human	HepaRG	dna binding	5.23
TOX21_p53_BLA_p1_ratio	TP53	human	intestinal HCT116 cell line	dna binding	81.4
TOX21_p53_BLA_p3_ratio	TP53	human	intestinal HCT116 cell line	dna binding	47.1
TOX21_p53_BLA_p5_ratio	TP53	human	intestinal HCT116 cell line	dna binding	70.8
ATG_E_Box_CIS_dn	USF1	human	HepG2	dna binding	45.8
ATG_Xbp1_CIS_up	XBP1	human	HepG2	dna binding	36.4
LTEA_HepaRG_XBP1_dn	XBP1	human	HepaRG	dna binding	6.42
LTEA_HepaRG_LIPC_dn	LIPC	human	HepaRG	esterase	15.6
LTEA_HepaRG_LPL_dn	LPL	human	HepaRG	esterase	32.0
LTEA_HepaRG_KRT19_dn	KRT19	human	HepaRG	filaments	19.1
BSK_CASM3C_ Thrombomodulin_up	THBD	human	coronary artery smooth muscle cells	gpcr	40.0
LTEA_HepaRG_EGF_dn	EGF	human	HepaRG	growth factor	8.96
LTEA_HepaRG_HGF_dn	HGF	human	HepaRG	growth factor	14.9
LTEA_HepaRG_IGF1_dn	IGF1	human	HepaRG	growth factor	21.1
LTEA_HepaRG_TGFA_up	TGFA	human	HepaRG	growth factor	10.1
BSK_BE3C_TGFb1_down	TGFB1	human	bronchial epithelial cells	growth factor	40.0
BSK_KF3CT_TGFb1_down	TGFB1	human	keratinocytes and foreskin fibroblasts	growth factor	10.0
LTEA_HepaRG_TGFB1_dn	TGFB1	human	HepaRG	growth factor	119
LTEA_HepaRG_THRSP_dn	THRSP	human	HepaRG	growth factor	7.50
LTEA_HepaRG_KCNK1_up	KCNK1	human	HepaRG	ion channel	34.3
LTEA_HepaRG_ADK_dn	ADK	human	HepaRG	kinase	4.67
BSK_hDFCGF_EGFR_down	EGFR	human	foreskin fibroblast	kinase	10.0
BSK_4H_VEGFRII_down	KDR	human	umbilical vein endothelium	kinase	40.0
LTEA_HepaRG_PDK4_dn	PDK4	human	HepaRG	kinase	6.66
LTEA_HepaRG_GCLC_dn	GCLC	human	HepaRG	ligase	4.30

Assay Name	Gene Symbol	Organism	Cells/Cell Lines	Intended Target Family	AC50 (µM)
LTEA_HepaRG_ACLY_dn	ACLY	human	HepaRG	lyase	15.4
LTEA_HepaRG_FASN_dn	FASN	human	HepaRG	lyase	10.9
LTEA_HepaRG_HMGCS2_dn	HMGCS2	human	HepaRG	lyase	11.3
Tanguay_ZF_120hpf_MORT_up	NA	zebrafish	dechorionated embryo	malformation	7.74
Tanguay_ZF_120hpf_YSE_up	NA	zebrafish	dechorionated embryo	malformation	5.82
Tanguay_ZF_120hpf_PE_up	NA	zebrafish	dechorionated embryo	malformation	4.41
Tanguay_ZF_120hpf_CFIN_up	NA	zebrafish	dechorionated embryo	malformation	4.08
NHEERL_ZF_144hpf_TERATOSCORE_up	NA	zebrafish	embryo	malformation	0.400
Tanguay_ZF_120hpf_Activity Score	NA	zebrafish	dechorionated embryo	malformation	31.2
LTEA_HepaRG_EZR_dn	EZR	human	HepaRG	membrane protein	11.6
LTEA_HepaRG_MIR122_dn	MIR122	human	HepaRG	microrna	11.2
NCCT_MITO_basal_resp_rate_OCR_up	NA	human	HepG2	mitochondria	32.1
LTEA_HepaRG_GADD45B_up	GADD45B	human	HepaRG	mutagenicity response	20.1
LTEA_HepaRG_GADD45G_up	GADD45G	human	HepaRG	mutagenicity response	31.0
OT_AR_ARSRC1_0960	AR	human	HEK293T	nuclear receptor	122
ACEA_AR_antagonist_80hr	AR	human	breast T47D cell line	nuclear receptor	50.5
UPITT_HCI_U2OS_AR_TIF2_Nucleoli_Antagonist	AR	human	bone U2OS cell line	nuclear receptor	88.1
UPITT_HCI_U2OS_AR_TIF2_Nucleoli_Agonist	AR	human	bone U2OS cell line	nuclear receptor	26.7
UPITT_HCI_U2OS_AR_TIF2_Nucleoli_Cytoplasm_Ratio_Agonist	AR	human	bone U2OS cell line	nuclear receptor	29.1
ATG_ERE_CIS_up	ESR1	human	HepG2	nuclear receptor	16.3
ATG_ERa_TRANS_up	ESR1	human	HepG2	nuclear receptor	14.9
OT_ER_ERaERa_0480	ESR1	human	HEK293T	nuclear receptor	64.2
OT_ERa_EREGFP_0120	ESR1	human	cervix HeLa cell line	nuclear receptor	23.1

Assay Name	Gene Symbol	Organism	Cells/Cell Lines	Intended Target Family	AC50 (µM)
OT_ERa_EREGFP_0480	ESR1	human	cervix HeLa cell line	nuclear receptor	42.0
TOX21_ERa_BLA_Agonist_ ratio	ESR1	human	HEK293T	nuclear receptor	61.5
TOX21_ERa_BLA_Antagonist _ratio	ESR1	human	HEK293T	nuclear receptor	46.9
TOX21_ERa_LUC_VM7_ Agonist_10nM_ICI182780	ESR1	human	HEK293T	nuclear receptor	1.01e-4
OT_ER_ERaERb_0480	ESR2	human	HEK293T	nuclear receptor	49.3
OT_ER_ERaERb_1440	ESR2	human	HEK293T	nuclear receptor	66.6
OT_ER_ERbERb_0480	ESR2	human	HEK293T	nuclear receptor	74.0
TOX21_ERR_Antagonist	ESRRA	human	ERR-HEK293T	nuclear receptor	46.9
ATG_DR4_LXR_CIS_dn	NR1H3	human	HepG2	nuclear receptor	26.2
OT_FXR_FXRSRC1_0480	NR1H4	human	HEK293T	nuclear receptor	87.9
OT_FXR_FXRSRC1_1440	NR1H4	human	HEK293T	nuclear receptor	85.9
TOX21_FXR_BLA_antagonist _ratio	NR1H4	human	HEK293T	nuclear receptor	30.0
ATG_IR1_CIS_dn	NR1H4	human	HepG2	nuclear receptor	40.4
ATG_CAR_TRANS_dn	NR1I3	human	HepG2	nuclear receptor	164
TOX21_PR_BLA_Agonist_ ratio	PGR	human	PR-UAS-bla-HEK293T	nuclear receptor	4.85e-4
TOX21_PR_BLA_Antagonist_ ratio	PGR	human	PR-UAS-bla-HEK293T	nuclear receptor	9.00
ATG_PPRE_CIS_up	PPARA	human	HepG2	nuclear receptor	24.6
ATG_PPARa_TRANS_up	PPARA	human	HepG2	nuclear receptor	83.1
ATG_PPARg_TRANS_up	PPARG	human	HepG2	nuclear receptor	84.0
ATG_RORE_CIS_up	RORA	human	HepG2	nuclear receptor	57.3
TOX21_RORg_LUC_CHO_ Antagonist	RORC	Chinese hamster	CHO-K1	nuclear receptor	42.9
OT_NURR1_NURR1RXRa_ 0480	RXRA	human	HEK293T	nuclear receptor	94.1
TOX21_TR_LUC_GH3_ Antagonist	Thrb	rat	pituitary gland cell line	nuclear receptor	40.5
ATG_VDRE_CIS_up	VDR	human	HepG2	nuclear receptor	34.2
ATG_VDR_TRANS_dn	VDR	human	HepG2	nuclear receptor	164
LTEA_HepaRG_ACOX1_dn	ACOX1	human	HepaRG	oxidase	14.4
LTEA_HepaRG_FMO3_dn	FMO3	human	HepaRG	oxidoreductase	11.8

Assay Name	Gene Symbol	Organism	Cells/Cell Lines	Intended Target Family	AC50 (µM)
LTEA_HepaRG_NQO1_dn	NQO1	human	HepaRG	oxidoreductase	10.8
LTEA_HepaRG_SDHB_dn	SDHB	human	HepaRG	oxidoreductase	4.82
LTEA_HepaRG_ALPP_dn	ALPP	human	HepaRG	phosphatase	13.5
LTEA_HepaRG_PPP2R4_dn	PPP2R4	human	HepaRG	phosphatase	35.1
LTEA_HepaRG_PTEN_dn	PTEN	human	HepaRG	phosphatase	35.3
LTEA_HepaRG_CASP3_dn	CASP3	human	HepaRG	protease	3.61
LTEA_HepaRG_CASP8_dn	CASP8	human	HepaRG	protease	11.0
BSK_BE3C_MMP1_up	MMP1	human	bronchial epithelial cells	protease	40.0
BSK_hDFCGF_MMP1_down	MMP1	human	foreskin fibroblast	protease	40.0
LTEA_HepaRG_MMP3_up	MMP3	human	HepaRG	protease	39.5
BSK_KF3CT_MMP9_down	MMP9	human	keratinocytes and foreskin fibroblasts	protease	10.0
LTEA_HepaRG_MMP10_up	MMP10	human	HepaRG	protease	34.1
BSK_KF3CT_uPA_down	PLAU	human	keratinocytes and foreskin fibroblasts	protease	10.0
BSK_hDFCGF_TIMP1_down	TIMP1	human	foreskin fibroblast	protease inhibitor	40.0
LTEA_HepaRG_TIMP1_dn	TIMP1	human	HepaRG	protease inhibitor	13.3
BSK_KF3CT_TIMP2_down	TIMP2	human	keratinocytes and foreskin fibroblasts	protease inhibitor	40.0
LTEA_HepaRG_GSTA2_dn	GSTA2	human	HepaRG	transferase	13.3
LTEA_HepaRG_GSTM3_dn	GSTM3	human	HepaRG	transferase	6.86
LTEA_HepaRG_SULT2A1_dn	SULT2A1	human	HepaRG	transferase	10.8
LTEA_HepaRG_UGT1A1_dn	UGT1A1	human	HepaRG	transferase	10.1
LTEA_HepaRG_UGT1A6_dn	UGT1A6	human	HepaRG	transferase	16.4
LTEA_HepaRG_ABCB1_dn	ABCB1	human	HepaRG	transporter	9.62
LTEA_HepaRG_ABCB11_dn	ABCB11	human	HepaRG	transporter	6.91
LTEA_HepaRG_ABCC2_dn	ABCC2	human	HepaRG	transporter	10.1
LTEA_HepaRG_ABCC3_dn	ABCC3	human	HepaRG	transporter	10.1
LTEA_HepaRG_ABCG2_dn	ABCG2	human	HepaRG	transporter	3.73
LTEA_HepaRG_FABP1_dn	FABP1	human	HepaRG	transporter	8.13
LTEA_HepaRG_IGFBP1_up	IGFBP1	human	HepaRG	transporter	20.7

Assay Name	Gene Symbol	Organism	Cells/Cell Lines	Intended Target Family	AC50 (µM)
LTEA_HepaRG_SLC22A1_dn	SLC22A1	human	HepaRG	transporter	9.20
LTEA_HepaRG_SLCO1B1_dn	SLCO1B1	human	HepaRG	transporter	11.4
NIS_RAIU_inhibition	SLC5A5	human	HEK293T	transporter	34.3

[1] Assays are alphabetically ordered by "intended target family", and within each "intended target family" assays are ordered alphabetically by "gene symbol". This table does not include assays classified by the US EPA CompTox Chemicals Dashboard as 'background measurement' assays (*e.g.*, artifact fluorescence, baseline controls, and internal markers) and cell-free assays such as cell-free systems utilizing enzymes or receptors extracted from tissues or cells of various organisms.
AC50: the concentration that induces a half-maximal assay response.
NA, not applicable. This notation is used when no specific target genes are reported by the US EPA CompTox Chemicals Dashboard.

Table F5 139 Active ToxCast assays[1] for EtPFOSA

Assay Name	Gene Symbol	Organism	Cells/Cell Lines	Intended Target Family	AC50 (µM)
LTEA_HepaRG_APOA5_dn	APOA5	human	HepaRG	apolipoprotein	32.8
BSK_hDFCGF_CollagenIII_down	COL3A1	human	foreskin fibroblast	cell adhesion molecules	10.0
BSK_3C_HLADR_down	HLA-DRA	human	umbilical vein endothelium	cell adhesion molecules	40.0
BSK_BE3C_HLADR_down	HLA-DRA	human	bronchial epithelial cells	cell adhesion molecules	10.0
BSK_CASM3C_HLADR_down	HLA-DRA	human	coronary artery smooth muscle cells	cell adhesion molecules	10.0
BSK_4H_VCAM1_down	VCAM1	human	umbilical vein endothelium	cell adhesion molecules	40.0
BSK_hDFCGF_VCAM1_down	VCAM1	human	foreskin fibroblast	cell adhesion molecules	10.0
LTEA_HepaRG_GADD45A_dn	GADD45A	human	HepaRG	cell cycle	206
APR_HepG2_CellCycleArrest_24h_dn	NA	human	HepG2	cell cycle	20.8
APR_HepG2_CellLoss_24h_dn	NA	human	HepG2	cell cycle	47.0
APR_HepG2_MitoticArrest_24h_up	NA	human	HepG2	cell cycle	52.2
APR_HepG2_OxidativeStress_24h_up	NA	human	HepG2	cell cycle	80.8
APR_HepG2_CellCycleArrest_72h_dn	NA	human	HepG2	cell cycle	35.5
APR_HepG2_CellLoss_72h_dn	NA	human	HepG2	cell cycle	88.4
APR_HepG2_MitoticArrest_72h_up	NA	human	HepG2	cell cycle	78.6
APR_HepG2_OxidativeStress_72h_up	NA	human	HepG2	cell cycle	104
APR_HepG2_StressKinase_72h_up	NA	human	HepG2	cell cycle	116
BSK_3C_Proliferation_down	NA	human	umbilical vein endothelium	cell cycle	40.0
BSK_3C_SRB_down	NA	human	umbilical vein endothelium	cell cycle	40.0
BSK_hDFCGF_Proliferation_down	NA	human	foreskin fibroblast	cell cycle	10.0

Assay Name	Gene Symbol	Organism	Cells/Cell Lines	Intended Target Family	AC50 (µM)
BSK_hDFCGF_SRB_down	NA	human	foreskin fibroblast	cell cycle	40.0
BSK_SAg_Proliferation_down	NA	human	umbilical vein endothelium and peripheral blood mononuclear cells	cell cycle	40.0
BSK_SAg_SRB_down	NA	human	umbilical vein endothelium and peripheral blood mononuclear cells	cell cycle	40.0
TOX21_MMP_viability	NA	human	HepG2	cell cycle	11.2
TOX21_DT40	NA	chicken	lymphoblast	cell cycle	48.2
TOX21_ARE_BLA_agonist_viability	NA	human	HepG2	cell cycle	32.4
TOX21_PPARd_BLA_Agonist_viability	NA	human	HEK293T	cell cycle	43.0
TOX21_DT40_100	NA	chicken	lymphoblast	cell cycle	54.0
TOX21_DT40_657	NA	chicken	lymphoblast	cell cycle	53.2
APR_HepG2_MicrotubuleCSK_24h_up	NA	human	HepG2	cell morphology	66.8
APR_HepG2_MitoMass_24h_up	NA	human	HepG2	cell morphology	113
APR_HepG2_MitoMembPot_24h_dn	NA	human	HepG2	cell morphology	106
APR_HepG2_MicrotubuleCSK_72h_up	NA	human	HepG2	cell morphology	79.6
APR_HepG2_MitoMembPot_72h_dn	NA	human	HepG2	cell morphology	96.7
APR_HepG2_NuclearSize_72h_dn	NA	human	HepG2	cell morphology	109
TOX21_MMP_ratio_down	NA	human	HepG2	cell morphology	2.57
LTEA_HepaRG_CYP1A1_up	CYP1A1	human	HepaRG	cyp	37.8
LTEA_HepaRG_CYP2C9_dn	CYP2C9	human	HepaRG	cyp	86.7
LTEA_HepaRG_CYP2E1_dn	CYP2E1	human	HepaRG	cyp	48.1
LTEA_HepaRG_CYP3A4_up	CYP3A4	human	HepaRG	cyp	20.7
LTEA_HepaRG_CYP4A11_up	CYP4A11	human	HepaRG	cyp	10.2
LTEA_HepaRG_CYP7A1_dn	CYP7A1	human	HepaRG	cyp	61.3

Assay Name	Gene Symbol	Organism	Cells/Cell Lines	Intended Target Family	AC50 (µM)
BSK_SAg_CD38_down	CD38	human	umbilical vein endothelium and peripheral blood mononuclear cells	cytokine	40.0
BSK_SAg_CD40_down	CD40	human	umbilical vein endothelium and peripheral blood mononuclear cells	cytokine	40.0
BSK_SAg_CD69_down	CD69	human	umbilical vein endothelium and peripheral blood mononuclear cells	cytokine	40.0
BSK_hDFCGF_MCSF_down	CSF1	human	foreskin fibroblast	cytokine	10.0
BSK_BE3C_IP10_down	CXCL10	human	bronchial epithelial cells	cytokine	10.0
BSK_hDFCGF_IP10_down	CXCL10	human	foreskin fibroblast	cytokine	10.0
BSK_KF3CT_IP10_down	CXCL10	human	keratinocytes and foreskin fibroblasts	cytokine	10.0
BSK_hDFCGF_MIG_down	CXCL9	human	foreskin fibroblast	cytokine	10.0
BSK_BE3C_PAI1_down	SERPINE1	human	bronchial epithelial cells	cytokine	40.0
BSK_hDFCGF_PAI1_down	SERPINE1	human	foreskin fibroblast	cytokine	40.0
BSK_LPS_TNFa_up	TNF	human	umbilical vein endothelium and peripheral blood mononuclear cells	cytokine	4.00
LTEA_HepaRG_IL6R_dn	IL6R	human	HepaRG	cytokine receptor	41.7
ATG_C_EBP_CIS_up	CEBPB	human	HepG2	dna binding	91.3
LTEA_HepaRG_EGR1_dn	EGR1	human	HepaRG	dna binding	46.6
ATG_Ets_CIS_dn	ETS1	human	HepaRG	dna binding	49.0

Assay Name	Gene Symbol	Organism	Cells/Cell Lines	Intended Target Family	AC50 (µM)
ATG_AP_1_CIS_up	FOS	human	HepG2	dna binding	24.8
ATG_GATA_CIS_up	GATA1	human	HepG2	dna binding	76.6
ATG_GLI_CIS_up	GLI1	human	HepG2	dna binding	68.2
ATG_HSE_CIS_up	HSF1	human	HepG2	dna binding	115
ATG_MRE_CIS_up	MTF1	human	HepG2	dna binding	102
ATG_Myb_CIS_dn	MYB	human	HepG2	dna binding	37.6
ATG_Myc_CIS_up	MYC	human	HepG2	dna binding	88.9
TOX21_ARE_BLA_agonist_ratio	NFE2L2	human	HepG2	dna binding	27.5
ATG_NFI_CIS_up	NFIA	human	HepG2	dna binding	68.8
ATG_NF_kB_CIS_up	NFKB1	human	HepG2	dna binding	75.3
ATG_Pax6_CIS_up	PAX6	human	HepG2	dna binding	102
LTEA_HepaRG_PEG10_dn	PEG10	human	HepaRG	dna binding	27.1
ATG_Oct_MLP_CIS_up	POU2F1	human	HepG2	dna binding	78.7
ATG_BRE_CIS_up	SMAD1	human	HepG2	dna binding	31.2
ATG_Sox_CIS_up	SOX1	human	HepG2	dna binding	105
ATG_Sp1_CIS_up	SP1	human	HepG2	dna binding	21.6
ATG_TCF_b_cat_CIS_up	TCF7	human	HepG2	dna binding	164
APR_HepG2_p53Act_24h_up	TP53	human	HepG2	dna binding	48.8
APR_HepG2_p53Act_72h_up	TP53	human	HepG2	dna binding	72.5
ATG_Xbp1_CIS_up	XBP1	human	HepG2	dna binding	66.3
LTEA_HepaRG_XBP1_dn	XBP1	human	HepaRG	dna binding	51.0
LTEA_HepaRG_KRT19_up	KRT19	human	HepaRG	filaments	32.8
LTEA_HepaRG_IGF1_dn	IGF1	human	HepaRG	growth factor	47.5
LTEA_HepaRG_KRT19_up	KRT19	human	HepaRG	growth factor	32.8
BSK_BE3C_TGFb1_down	TGFB1	human	bronchial epithelial cells	growth factor	83.4
BSK_KF3CT_TGFb1_down	TGFB1	human	keratinocytes and foreskin fibroblasts	growth factor	10.0
LTEA_HepaRG_TGFB1_dn	TGFB1	human	HepaRG	growth factor	40.0
LTEA_HepaRG_THRSP_dn	THRSP	human	HepaRG	growth factor	45.6
LTEA_HepaRG_ADK_dn	ADK	human	HepaRG	kinase	85.6
BSK_hDFCGF_EGFR_down	EGFR	human	foreskin fibroblast	kinase	40.0
LTEA_HepaRG_PDK4_up	PDK4	human	HepaRG	kinase	25.5

Assay Name	Gene Symbol	Organism	Cells/Cell Lines	Intended Target Family	AC50 (µM)
LTEA_HepaRG_FASN_dn	FASN	human	HepaRG	lyase	41.8
LTEA_HepaRG_HMGCS2_dn	HMGCS2	human	HepaRG	lyase	33.0
Tanguay_ZF_120hpf_MORT_up	NA	zebrafish	dechorionated embryo	malformation	36.5
Tanguay_ZF_120hpf_YSE_up	NA	zebrafish	dechorionated embryo	malformation	58.1
Tanguay_ZF_120hpf_AXIS_up	NA	zebrafish	dechorionated embryo	malformation	54.2
Tanguay_ZF_120hpf_EYE_up	NA	zebrafish	dechorionated embryo	malformation	12.9
Tanguay_ZF_120hpf_SNOU_up	NA	zebrafish	dechorionated embryo	malformation	43.1
Tanguay_ZF_120hpf_JAW_up	NA	zebrafish	dechorionated embryo	malformation	51.0
Tanguay_ZF_120hpf_OTIC_up	NA	zebrafish	dechorionated embryo	malformation	41.8
Tanguay_ZF_120hpf_PE_up	NA	zebrafish	dechorionated embryo	malformation	63.3
Tanguay_ZF_120hpf_BRAI_up	NA	zebrafish	dechorionated embryo	malformation	43.5
Tanguay_ZF_120hpf_SOMI_up	NA	zebrafish	dechorionated embryo	malformation	9.17
Tanguay_ZF_120hpf_PFIN_up	NA	zebrafish	dechorionated embryo	malformation	42.4
Tanguay_ZF_120hpf_PIG_up	NA	zebrafish	dechorionated embryo	malformation	43.4
Tanguay_ZF_120hpf_TR_up	NA	zebrafish	dechorionated embryo	malformation	25.3
NHEERL_ZF_144hpf_TERATOSCORE_up	NA	zebrafish	embryo	malformation	38.7
Tanguay_ZF_120hpf_Activity Score	NA	zebrafish	dechorionated embryo	malformation	22.3
LTEA_HepaRG_MIR122_dn	MIR122	human	HepaRG	microrna	45.5
LTEA_HepaRG_GADD45G_dn	GADD45G	human	HepaRG	mutagenicity response	41.5
OT_AR_ARSRC1_0960	AR	human	HEK293T	nuclear receptor	22.1
ACEA_AR_agonist_80hr	AR	human	breast T47D cell line	nuclear receptor	43.1
ATG_ERE_CIS_up	ESR1	human	HepG2	nuclear receptor	57.6

Assay Name	Gene Symbol	Organism	Cells/Cell Lines	Intended Target Family	AC50 (µM)
ATG_ERa_TRANS_up	ESR1	human	HepG2	nuclear receptor	17.5
TOX21_ERa_BLA_Antagonist_ratio	ESR1	human	HEK293T	nuclear receptor	1.42
ATG_DR4_LXR_CIS_dn	NR1H3	human	HepG2	nuclear receptor	42.6
TOX21_FXR_BLA_antagonist_ratio	NR1H4	human	HEK293T	nuclear receptor	5.98
ATG_PXRE_CIS_up	NR1I2	human	HepG2	nuclear receptor	9.76
ATG_PXR_TRANS_up	NR1I2	human	HepG2	nuclear receptor	13.7
ATG_PBREM_CIS_up	NR1I3	human	HepG2	nuclear receptor	111
ATG_GRE_CIS_dn	NR3C1	human	HepG2	nuclear receptor	36.3
TOX21_PR_BLA_Antagonist_ratio	PGR	human	PR-UAS-bla-HEK293T	nuclear receptor	104
ATG_PPRE_CIS_up	PPARA	human	HepG2	nuclear receptor	123
ATG_PPARa_TRANS_up	PPARA	human	HepG2	nuclear receptor	93.1
ATG_PPARg_TRANS_up	PPARG	human	HepG2	nuclear receptor	96.3
ATG_DR5_CIS_up	RARB	human	HepG2	nuclear receptor	105
ATG_RORE_CIS_up	RORA	human	HepG2	nuclear receptor	105
ATG_VDRE_CIS_up	VDR	human	HepG2	nuclear receptor	68.8
ATG_VDR_TRANS_up	VDR	human	HepG2	nuclear receptor	62.9
LTEA_HepaRG_ACOX1_dn	ACOX1	human	HepaRG	oxidase	33.4
LTEA_HepaRG_FMO3_dn	FMO3	human	HepaRG	oxidoreductase	71.9
LTEA_HepaRG_NQO1_dn	NQO1	human	HepaRG	oxidoreductase	31.2
BSK_hDFCGF_MMP1_down	MMP1	human	foreskin fibroblast	protease	40.0
LTEA_HepaRG_MMP3_up	MMP3	human	HepaRG	protease	20.9
BSK_KF3CT_MMP9_down	MMP9	human	keratinocytes and foreskin fibroblasts	protease	40.0

Assay Name	Gene Symbol	Organism	Cells/Cell Lines	Intended Target Family	AC50 (µM)
BSK_BE3C_tPA_down	PLAT	human	bronchial epithelial cells	protease	40.0
LTEA_HepaRG_GSTA2_dn	GSTA2	human	HepaRG	transferase	32.5
LTEA_HepaRG_SULT2A1_dn	SULT2A1	human	HepaRG	transferase	31.1
LTEA_HepaRG_UGT1A6_dn	UGT1A6	human	HepaRG	transferase	99.9
LTEA_HepaRG_ABCB11_dn	ABCB11	human	HepaRG	transporter	22.4
LTEA_HepaRG_FABP1_dn	FABP1	human	HepaRG	transporter	54.9
LTEA_HepaRG_SLC22A1_dn	SLC22A1	human	HepaRG	transporter	63.2
LTEA_HepaRG_SLCO1B1_dn	SLCO1B1	human	HepaRG	transporter	82.2
NIS_RAIU_inhibition	SLC5A5	human	HEK293T	transporter	31.5

[1] Assays are alphabetically ordered by "intended target family", and within each "intended target family" assays are ordered alphabetically by "gene symbol". This table does not include assays classified by the US EPA CompTox Chemicals Dashboard as 'background measurement' assays (*e.g.*, artifact fluorescence, baseline controls, and internal markers) and cell-free assays such as cell-free systems utilizing enzymes or receptors extracted from tissues or cells of various organisms.
AC50: the concentration that induces a half-maximal assay response.
NA, not applicable. This notation is used when no specific target genes are reported by the US EPA CompTox Chemicals Dashboard.

Appendix G. Additional Data Related to Oxidative Stress

Evidence on oxidative stress induced by PFOS is summarized in the following tables, based on study systems.

- Table G1: Oxidative stress in human observational studies
- Table G2: Oxidative stress in studies using human cells *in vitro*
- Table G3: Oxidative stress in rodent studies *in vivo*
- Table G4: Oxidative stress in rodent studies *in vitro*
- Table G5: Oxidative stress in zebrafish studies *in vivo/ex vivo*

Table G1 Oxidative stress in human observational studies

Study population (Sample size)	PFOS exposure matric	Results[1]	Reference
Korean elders (60 years old or above) in a community trial study (n = 126)	Serum levels of PFOS (AM = 10.04 ng/ml)	↑ (increase)* (dose-dependent) urinary 8-OHdG and MDA	Kim et al. (2016)
Taiwanese adults aged 22 to 63 years old in a case-control study of cardiovascular disease (n = 597)	Serum levels of PFOS (GM = 12.92 ng/ml for linear PFOS, and 0.44 ng/ml for branched PFOS)	↑ (increase)* (dose-dependent) urinary 8-OHdG with linear PFOS, but not branched isomers	Lin et al. (2020a)
Taiwanese individuals aged 12-30 years old (n = 848)	Serum levels of PFOS (GM = 6.44 ng/ml)	NS between urinary 8-OHdG and PFOS serum levels, adjusted for age, gender and other risk factors for cardiovascular disease	Lin et al. (2016)
Female newborns in a prospective study from Shanghai, China (n = 581)	PFOS levels in umbilical cord blood (prenatal exposure; 4th quartile ≥ 3.169 ng/ml)	Higher plasma PFOS in cord blood was significantly associated with high cord serum ROS, adjusted for confounders	Liu et al. (2018b)

[1] ↑, significant increases; * $p < 0.05$.

Abbreviations: AM, arithmetic mean; GM, geometric mean; 8-OHdG, 8-hydroxydeoxyguanosine; MDA, malondialdehyde; NS, no significant change; ROS, reactive oxygen species.

Table G2 Oxidative stress in studies using human cells *in vitro*

Cell type	PFOS dose (duration)	Results [Lowest effective dose][1]	Reference
Human lymphocytes from 18-30 years old healthy donors	75, 150, 300 µM (2, 4, 6, 8,10,12 hr for ROS) or (2, 4, 6 hr for other endpoints)	↑ (increase)***ROS [75 µM]; ↑ (increase)* MDA [75 µM]; ↓ (decrease)*** GSH [75 µM]; ↑ (increase)*** GSSG [75 µM]	Zarei et al. (2018)
Human umbilical vein endothelial cells	100 mg/l for different times (1, 5, 12, 24, 40 hr)	↑ (increase)* ROS (time-dependent manner between 1 and 40 hr)	Liao et al. (2012)
Human umbilical vein endothelial cells	100 mg/l (5 hr)	↑ (increase)*** ROS	Liao et al. (2013)
Human microvascular endothelial cells	50, 100 µM (1 hr); 2 µM (1, 2, 3, 5 hr)	↑ (increase)* ROS for all conditions tested (time-dependent for 2 µM)	Qian et al. (2010)
Human-hamster hybrid cells ("normal" or mitochondrial DNA-depleted cells)	1, 10, 100, 200 µM (1, 4, 16 days)	"Normal" hybrid cells ↑ (increase)* O_2^- [100 µM]; ↑ (increase)* NO [100 µM]; ↑ (increase)* ROS [100 µM]; NS for all endpoints tested in mitochondrial DNA-depleted cells	Wang et al. (2013)
HepG2 cells	0.2, 1, 2, 10, 20 µM (24 hr)	↑ (increase)* ROS [0.2 µM]; NS T-AOC	Wielsøe et al. (2015)
HepG2 cells	0.4, 4, 40, 200, 400, 1000, 2000 µM (for ROS); 100, 400 µM (24 hr for oxidative DNA damage)	NS oxidative DNA damage (FPG-sensitive site); ↑ (increase)* ROS [not specified]	Eriksen et al. (2010)

Cell type	PFOS dose (duration)	Results [Lowest effective dose][1]	Reference
HepG2 cells	50, 100, 150, 200 µM (5, 10, 15 hr for ROS; 48 hr for other endpoints)	↑ (increase)* ROS [100 µM]; ↑ (increase)* SOD [150 µM]; ↑ (increase)* CAT [150 µM]; ↑ (increase)* GR [150 µM]; ↓ (decrease)** GST [200 µM], ↓ (decrease)* GPx [100 µM]; ↓ (decrease)* GSH [100 µM]	Hu and Hu (2009)
HepG2 cells	5, 10, 50,100, 200, 300 µM (1 and 24 hr)	NS ROS	Florentin et al. (2011)
Human lung cancer A549 cells	25, 50, 100 200 µM (24 hr)	↑ (increase)* MDA [50 µM]; ↑ (increase)* SOD [50 µM]; ↓ (decrease)* GSH [50 µM]	Mao et al. (2013)
Human neuroblastoma SH-SY5Y cells	50, 100 and 200 µM (48 hr)	↑ (increase) ROS in a dose-dependent relationship without statistical tests	Sun et al. (2019)

[1] ↑, significant increases; ↓, significant decreases; * $p < 0.05$ (except for Wielsøe et al. 2015, which reported $p \leq 0.05$); ** $p < 0.01$; *** $p < 0.001$. Results are for enzyme activity unless indicated otherwise
Abbreviations: CAT, catalase; HepG2, human hepatoma cell line; GPx, glutathione peroxidase; GR, glutathione reductase; GSH, reduced glutathione; GSSG, glutathione disulfide; GST, glutathione-S-transferase; MDA, malondialdehyde; NS, no significant change; O_2^-, superoxide anion; ROS, reactive oxygen species; SOD, superoxide dismutase; T-AOC, total antioxidant capacity.

Table G3 Oxidative stress in rodent studies *in vivo*

Species (organ or tissue)	PFOS dose, duration and administration route	Results[1] [Lowest effective dose]	Reference
CD-1 mice (maternal liver and placenta)	3 mg/kg-day by gavage till GD17	NS in SOD or CAT in the maternal liver and placenta	Lee et al. (2015)
Male Kunming mice (liver)	10 mg/kg-day for 21 days by *gavage*	↑ (increase)* H_2O_2; ↑ (increase)* MDA; ↓ (decrease)* SOD	Huang et al. (2020)
Male and female Kunming mice (brain and liver)	1-time *s.c.* of 50 mg/kg body weight at different postnatal days (PD 7, 14, 21, 28, 35)	Brain: NS MDA; ↓ (decrease)* T-AOC at PD21 in males; ↓ (decrease)* SOD at PD7 and PD21 in males. Liver: NS MDA; ↓ (decrease)* T-AOC at PD7, PD14, and PD21 in males; ↓ (decrease)* T-AOC at PD21 in females; ↓ (decrease)* SOD at PD14 in females. NS in other endpoints with non-specified PD days or gender.	Liu et al. (2009)
Male C57BL/6 mice (liver)	5, 25 or 50 µg/g in the diet for three weeks	↑ (increase)* GSSG [5 µg/g]; ↓ (decrease)** GSH/GSSG [5 µg/g]; ↑ (increase)* mRNA of *SOD1* [50 µg/g].	Zhang et al. (2020)
Male C57BL/6 mice (liver)	0.075, 015, 0.3 g/kg-day for 30 days by gavage	↑ (increase)* MDA [0.075 g/kg-day]; ↓ (decrease)* T-AOC [0.075 g/kg-day]; ↓ (decrease)* GPx [0.075 g/kg-day]; ↓ (decrease)* CAT [0.075 g/kg-day]; ↓ (decrease)* SOD [0.075 g/kg-day];	Xing et al. (2016)

Species (organ or tissue)	PFOS dose, duration and administration route	Results[1] [Lowest effective dose]	Reference
Male C57BL/6 mice (Splenocytes and thymocytes)	1, 5, or 10 mg/kg-day for 7 days by gavage daily	↑ (increase)* ROS [5 mg/kg-day]; ↑ (increase)*SOD [5 mg/kg-day]; ↑ (increase)*CAT [10 mg/kg-day]; ↑ (increase)*GR [5 mg/kg-day]; ↓ (decrease)*GPx [5 mg/kg-day]; ↓ (decrease)*GST [10 mg/kg-day] ↓ (decrease)*GSH [5 mg/kg-day];	Zhang et al. (2013)
Male SD rats (liver)	Daily oral dose of 1 or 10 mg/kg for 28 days	↑ (increase) ROS (dose-dependent); ↑ (increase)* inducible nitric oxide synthase (iNOS) mRNA expression [1 mg/kg]; ↑ (increase)* MDA [1 mg/kg]; ↓ (decrease)* CAT [1 mg/kg]; ↓ (decrease)* SOD [10 mg/kg]; ↓ (decrease)* GSH [1 mg/kg]; ↑ (increase)* GSSG [1 mg/kg]; ↓ (decrease)* GSH/GSSG [1 mg/kg]	Han et al. (2018)

Species (organ or tissue)	PFOS dose, duration and administration route	Results[1] [Lowest effective dose]	Reference
SD rat offspring (lung)	0.1, 2 mg/kg/d from GD1 to GD21 by oral	PND 0: ↑ (increase)* MDA [0.1 mg/kg/d]; ↓ (decrease)* SOD [2 mg/kg/d]; ↑ (increase)** MPO [2 mg/kg/d]; ↓ (decrease)* GSH [2 mg/kg/d] PND 21: ↑ (increase)** MDA [2 mg/kg/d]; ↓ (decrease)* SOD [2 mg/kg/d]; ↑ (increase)** MPO [2 mg/kg/d]; ↓ (decrease)* GSH [2 mg/kg/d]	Chen et al. (2012)
Male mice, strain not specified (liver)	10 mg/kg-day for three weeks by *gavage*	↑ (increase)* H_2O_2; ↑ (increase)* MDA; ↓ (decrease)* GSH; ↓ (decrease)* SOD; ↓ (decrease)* expression of Nrf2; ↓ (decrease)* mRNA expression of *HO-1*, *SOD* and *CAT*	Lv et al. (2018)

[1] Results are for enzyme activity unless indicated otherwise. ↑, significant increases; ↓, significant decreases; * $p < 0.05$ (except for Zhang et al. 2013, which reported $p \leq 0.05$); ** $p < 0.01$.

Abbreviations: CAT, catalase; GD, gestational day; GPx, glutathione peroxidase; GR, glutathione reductase; GSH, reduced glutathione; GSSG, glutathione disulfide; GST, glutathione-S-transferase; HO-1, heme oxygenase-1; MDA, malondialdehyde; MPO, myeloperoxidase; NS, no significant change; PND, post-natal day; ROS, reactive oxygen species; *s.c.*, subcutaneous injection; SOD, superoxide dismutase; T-AOC, total antioxidant capacity.

Table G4 Oxidative stress in rodent studies *in vitro*

Species, Strain	Tissue and cell type	PFOS dose and duration	Results[1] [Lowest effective dose]	Reference
Mice, C57BL/6 J	Primary hepatocytes	0.01, 0.5, 1 mM for 24 hr	↑ (increase)*** ROS [1.0 mM]; ↑ (increase)*** SOD [0.5 mM]; ↓ (decrease)*** CAT [0.01 mM]; ↑ (increase)* GSH [0.1 mM]	Xu et al. (2019)
Mice, strain not specified	RAW 264.7 macrophages	100 µM for 5 minutes	↑ (increase)* ROS [100 µM]	Qian et al. (2010)
Mice, 129	Embryonic stem cell derived cardiomyocytes	15, 45, 75 µg/ml; cells were harvested on days 11 and 14.	↑ (increase)* ROS [15 µg/ml]	Cheng et al. (2013)
Mice, *gpt* delta transgenic	Mouse embryonic fibroblast (MEF) cells	Mutagenic potential of PFOS at redBA and gam loci in transgenic MEF cells by Spi− mutation assay. 1, 5, 10, and 20 µM for 24 hr.	↑ (increase)* ROS [20 µM]; Addition of CAT leads to ↓ (decrease)* in mutation yield; ↓ (decrease)* γ-H2AX	Wang et al. (2015c)
Mice, Kunming	Leydig cells	12.5, 15, 37.5, 50, 62.5 µg/ml for 24 hr	↑ (increase)** ROS [12.5 µg/ml]	Zhang et al. (2015)
Mice, C57BL/6	Leydig tumor cells-1	10, 50, 100 µmol/l for 24 hr	↑ (increase)* ROS [50 µmol/l]	Zhao et al. (2017)
Rats, SD	Liver hepatocytes	25 µM for 15, 30, and 60 min for ROS; 25 µM for 3 hr for lipid peroxidation	↑ (increase)* ROS [25 µM]; ↑ (increase)* Lipid peroxidation [25 µM]	Khansari et al. (2017)
Rats, SD	Liver mitochondria	10 µM	NS ROS	O'Brien and Wallace (2004)
Rats, SD	Cerebellar granule cell cultures from the cerebella of 7-day old SD rats	3 and 30 µM for 15 minutes	↑ (increase)* ROS [3 µM]	Lee et al. (2012)

Species, Strain	Tissue and cell type	PFOS dose and duration	Results[1] [Lowest effective dose]	Reference
Rats, Wistar	Cerebellar granule cells	75, 150, 300 and 600 µM for 3 hr Lipid peroxidation was assessed in cerebellar granule cells exposed to 10, 20, 40, 60, 80, 100 µM for 3 hr.	NS ROS; ↓ (decrease)* Lipid peroxidation; [20 µM]; ↑ (increase)** in combination with cumene hydroperoxide [100 µM]	Berntsen et al. (2017)
Rats, Wistar	Newborn rat cortex astrocytes	12, 25, or 50 µM for 1, 3, 6, and 24 hr	↑ (increase)** ROS [12 µM]	Dong et al. (2015)
Rats, strain not specified	Cerebellar granule cells from pups	6; 12; 25; 50; 100 µM for 15 minutes	↑ (increase)* ROS [25 µM]	Reistad et al. (2013)
Rats, strain not specified	PC12 cells	10; 50, 100, 250 µM for 24 hr and 4 days	↑ (increase)* MDA [10 µM] (24 hr); ↑ (increase)* MDA [50 µM] (4 d)	Slotkin et al. (2008)
Rats, strain not specified	HAPI microglial cells	iNOS: 0.1, 1, 5; 10, 20, 50, 100, 200 nM for 6 hr NO: 20 nM for 6 hr Intracellular ROS generation: 20 nM for 6 hr	↑ (increase)** ROS [20 nM]; ↑ (increase)* iNOS protein [1 nM]; ↑ (increase)** NO [20 nM]	Wang et al. (2015a)
Rats, strain not specified	Proximal renal tubular cells NRK -52E	100 µM at 1, 3, 6, 24 hr	↑ (increase)* ROS [100 µM]	Wen et al. (2021)

[1] Results are for enzyme activity unless indicated otherwise. ↑, significant increases; ↓, significant decreases; * $p < 0.05$; ** $p < 0.01$; *** $p < 0.001$.

Abbreviations: CAT, catalase; GSH, reduced glutathione; iNOS, inducible nitric oxide synthase; MDA, malondialdehyde; NS, no significant change; γ-H2AX, phosphorylated histone H2AX; ROS, reactive oxygen species; SOD, superoxide dismutase.

Table G5 Oxidative stress in zebrafish studies *in vivo/ex vivo*

Tissue	PFOS dose and duration	Endpoint and results[2] [Lowest effective dose]	Reference
Embryo	0.4, 0.8 and 1.6 mg/l 96 hr post-fertilization	↑ (increase)* ROS [1.6 mg/l]; ↑ (increase)* MDA [0.4 mg/l]; ↑ (increase)* SOD [0.4 mg/l]; ↓ (decrease)* CAT [1.6 mg/l]; ↑ (increase)* GPx [0.4 mg/l]	Du et al. (2017)
Embryo	Wild-type and Nrf2a$^{fh318-/-}$ mutant embryos; daily exposure to 16, 32, or 64 µM 72 hours post fertilization	↑ (increase)* GSSG in wild-type [16 µM]; NS GSH in wild-type; NS in mutant strain for either GSSG or GSH	Sant et al. (2018)
Embryo/larvae	Zebrafish eggs were collected within 4 h of spawning and exposed to 0.2, 0.4, and 1.0 mg/l of PFOS. Measurements taken at 96 hours post fertilization	↑ (increase)* ROS [0.4 mg/l]; ↑ (increase)** MDA [1.0 mg/l]; ↑ (increase)* SOD [0.2 mg/l]; ↑ (increase)* CAT [0.4 mg/l]; ↑ (increase)* GPx [0.2 mg/l]; ↑ (increase)* gene expression of *Nrf2* and *HO-1* [0.4 mg/l]	Shi and Zhou (2010)
Larvae	10 µg/l for 48 hours, followed by a 24 h depuration[1] period.	NS ROS; NS SOD activity; ↑ (increase)** SOD protein expression level during uptake phase [10 µg/l]; ↑ (increase)* SOD during depuration phase [10 µg/l]; NS CAT activity; ↑ (increase)** CAT protein expression level during uptake phase [10 µg/l]; ↑ (increase)** Nrf2 protein during uptake phase; ↓ (decrease)* Nrf2 during depuration phase; ↓ (decrease)** MDA activity during depuration phase [10 µg/l]; NS T-AOC	Zou et al. (2021)
Liver	0.08 mg/l for 7, 14, or 21 days	↑ (increase)* ROS [0.08 mg/l]	Guo et al. (2019)

[1] Depuration is the process where marine or freshwater animals are placed into a clean water environment for a period of time to allow purging of biological contaminants and physical impurities.
[2] Results are for enzyme activity unless indicated otherwise. ↑, significant increases; ↓, significant decreases; * $p < 0.05$; ** $p < 0.01$.

Abbreviations: CAT, catalase; GPx, glutathione peroxidase; GSH, reduced glutathione; GSSG,

glutathione disulfide; HO-1, heme oxygenase-1; MDA, malondialdehyde; Nrf2, nuclear factor erythroid 2–related factor 2; NS, no significant change; ROS, reactive oxygen species; SOD, superoxide dismutase; T-AOC, total antioxidant capacity.

References cited in Appendix G

Berntsen HF, Bjørklund CG, Audinot JN, Hofer T, Verhaegen S, Lentzen E, et al. 2017. Time-dependent effects of perfluorinated compounds on viability in cerebellar granule neurons: Dependence on carbon chain length and functional group attached. Neurotoxicology 63:70-83.

Chen T, Zhang L, Yue JQ, Lv ZQ, Xia W, Wan YJ, et al. 2012. Prenatal PFOS exposure induces oxidative stress and apoptosis in the lung of rat off-spring. Reproductive toxicology (Elmsford, NY) 33:538-545.

Cheng W, Yu Z, Feng L, Wang Y. 2013. Perfluorooctane sulfonate (PFOS) induced embryotoxicity and disruption of cardiogenesis. Toxicology in Vitro 27:1503-1512.

Dong L, Yang X, Gu W, Zhao K, Ge H, Zhou J, et al. 2015. Connexin 43 mediates PFOS-induced apoptosis in astrocytes. Chemosphere 132:8-16.

Du J, Cai J, Wang S, You H. 2017. Oxidative stress and apotosis to zebrafish (Danio rerio) embryos exposed to perfluorooctane sulfonate (PFOS) and ZnO nanoparticles. International journal of occupational medicine and environmental health 30:213-229.

Eriksen KT, Raaschou-Nielsen O, Sørensen M, Roursgaard M, Loft S, Møller P. 2010. Genotoxic potential of the perfluorinated chemicals PFOA, PFOS, PFBS, PFNA and PFHxA in human HepG2 cells. Mutation research 700:39-43.

Florentin A, Deblonde T, Diguio N, Hautemaniere A, Hartemann P. 2011. Impacts of two perfluorinated compounds (PFOS and PFOA) on human hepatoma cells: cytotoxicity but no genotoxicity? International journal of hygiene and environmental health 214:493-499.

Guo J, Wu P, Cao J, Luo Y, Chen J, Wang G, et al. 2019. The PFOS disturbed immunomodulatory functions via nuclear Factor-κB signaling in liver of zebrafish (Danio rerio). Fish & shellfish immunology 91:87-98.

Han R, Hu M, Zhong Q, Wan C, Liu L, Li F, et al. 2018. Perfluorooctane sulphonate induces oxidative hepatic damage via mitochondria-dependent and NF-κB/TNF-α-mediated pathway. Chemosphere 191:1056-1064.

Hu XZ, Hu DC. 2009. Effects of perfluorooctanoate and perfluorooctane sulfonate exposure on hepatoma Hep G2 cells. Archives of toxicology 83:851-861.

Huang T, Zhang Y, Zhang W, Lin T, Chen L, Yang B, et al. 2020. Attenuation of Perfluorooctane Sulfonate-Induced Steatohepatitis by Grape Seed Proanthocyanidin Extract in Mice. BioMed research international 2020:8818160.

Khansari MR, Yousefsani BS, Kobarfard F, Faizi M, Pourahmad J. 2017. In vitro toxicity of perfluorooctane sulfonate on rat liver hepatocytes: probability of distructive binding to CYP 2E1 and involvement of cellular proteolysis. Environmental science and pollution research international 24:23382-23388.

Kim JH, Park HY, Jeon JD, Kho Y, Kim SK, Park MS, et al. 2016. The modifying effect of vitamin C on the association between perfluorinated compounds and insulin resistance in the Korean elderly: a double-blind, randomized, placebo-controlled crossover trial. European journal of nutrition 55:1011-1020.

Lee HG, Lee YJ, Yang JH. 2012. Perfluorooctane sulfonate induces apoptosis of cerebellar granule cells via a ROS-dependent protein kinase C signaling pathway. Neurotoxicology 33:314-320.

Lee YY, Wong CK, Oger C, Durand T, Galano JM, Lee JC. 2015. Prenatal exposure to the contaminant perfluorooctane sulfonate elevates lipid peroxidation during mouse fetal development but not in the pregnant dam. Free radical research 49:1015-1025.

Liao Y, Wang J, Huang QS, Fang C, Kiyama R, Shen H, et al. 2012. Evaluation of cellular response to perfluorooctane sulfonate in human umbilical vein endothelial cells. Toxicology in vitro : an international journal published in association with BIBRA 26:421-428.

Liao Y, Dong S, Kiyama R, Cai P, Liu L, Shen H. 2013. Flos lonicerae extracts and chlorogenic acid protect human umbilical vein endothelial cells from the toxic damage of perfluorooctane sulphonate. Inflammation 36:767-779.

Lin CY, Chen PC, Lo SC, Torng PL, Sung FC, Su TC. 2016. The association of carotid intima-media thickness with serum Level of perfluorinated chemicals and endothelium-platelet microparticles in adolescents and young adults. Environment international 94:292-299.

Lin CY, Lee HL, Hwang YT, Su TC. 2020a. The association between total serum isomers of per- and polyfluoroalkyl substances, lipid profiles, and the DNA oxidative/nitrative stress biomarkers in middle-aged Taiwanese adults. Environmental research 182:109064.

Liu H, Chen Q, Lei L, Zhou W, Huang L, Zhang J, et al. 2018b. Prenatal exposure to perfluoroalkyl and polyfluoroalkyl substances affects leukocyte telomere length in female newborns. Environmental Pollution 235:446-452.

Liu L, Liu W, Song J, Yu H, Jin Y, Oami K, et al. 2009. A comparative study on oxidative damage and distributions of perfluorooctane sulfonate (PFOS) in mice at different postnatal developmental stages. The Journal of toxicological sciences 34:245-254.

Lv Z, Wu W, Ge S, Jia R, Lin T, Yuan Y, et al. 2018. Naringin protects against perfluorooctane sulfonate-induced liver injury by modulating NRF2 and NF-κB in mice. International immunopharmacology 65:140-147.

Mao Z, Xia W, Wang J, Chen T, Zeng Q, Xu B, et al. 2013. Perfluorooctane sulfonate induces apoptosis in lung cancer A549 cells through reactive oxygen species-mediated mitochondrion-dependent pathway. Journal of applied toxicology : JAT 33:1268-1276.

O'Brien TM, Wallace KB. 2004. Mitochondrial permeability transition as the critical target of N-acetyl perfluorooctane sulfonamide toxicity in vitro. Toxicological Sciences 82:333-340.

Qian Y, Ducatman A, Ward R, Leonard S, Bukowski V, Lan Guo N, et al. 2010. Perfluorooctane sulfonate (PFOS) induces reactive oxygen species (ROS) production in human microvascular endothelial cells: role in endothelial permeability. Journal of toxicology and environmental health Part A 73:819-836.

Reistad T, Fonnum F, Mariussen E. 2013. Perfluoroalkylated compounds induce cell death and formation of reactive oxygen species in cultured cerebellar granule cells. Toxicology letters 218:56-60.

Sant KE, Sinno PP, Jacobs HM, Timme-Laragy AR. 2018. Nrf2a modulates the embryonic antioxidant response to perfluorooctanesulfonic acid (PFOS) in the zebrafish, Danio rerio. Aquatic toxicology (Amsterdam, Netherlands) 198:92-102.

Shi X, Zhou B. 2010. The role of Nrf2 and MAPK pathways in PFOS-induced oxidative stress in zebrafish embryos. Toxicological sciences : an official journal of the Society of Toxicology 115:391-400.

Slotkin TA, MacKillop EA, Melnick RL, Thayer KA, Seidler FJ. 2008. Developmental neurotoxicity of perfluorinated chemicals modeled in vitro. Environmental health perspectives 116:716-722.

Sun P, Gu L, Luo J, Qin Y, Sun L, Jiang S. 2019. ROS-mediated JNK pathway critically contributes to PFOS-triggered apoptosis in SH-SY5Y cells. Neurotoxicology and teratology 75:106821.

Wang C, Nie X, Zhang Y, Li T, Mao J, Liu X, et al. 2015a. Reactive oxygen species mediate nitric oxide production through ERK/JNK MAPK signaling in HAPI microglia after PFOS exposure. Toxicology and applied pharmacology 288:143-151.

Wang X, Zhao G, Liang J, Jiang J, Chen N, Yu J, et al. 2013. PFOS-induced apoptosis through mitochondrion-dependent pathway in human-hamster hybrid cells. Mutation research 754:51-57.

Wang Y, Zhang X, Wang M, Cao Y, Wang X, Liu Y, et al. 2015c. Mutagenic Effects of Perfluorooctanesulfonic Acid in gpt Delta Transgenic System Are Mediated by Hydrogen Peroxide. Environmental science & technology 49:6294-6303.

Wen LL, Chen YT, Lee YG, Ko TL, Chou HC, Juan SH. 2021. Perfluorooctane sulfonate induces autophagy-associated apoptosis through oxidative stress and the activation of extracellular signal-regulated kinases in renal tubular cells. PloS one 16:e0245442.

Wielsøe M, Long M, Ghisari M, Bonefeld-Jørgensen EC. 2015. Perfluoroalkylated substances (PFAS) affect oxidative stress biomarkers in vitro. Chemosphere 129:239-245.

Xing J, Wang G, Zhao J, Wang E, Yin B, Fang D, et al. 2016. Toxicity assessment of perfluorooctane sulfonate using acute and subchronic male C57BL/6J mouse models. Environmental pollution (Barking, Essex : 1987) 210:388-396.

Xu M, Wan J, Niu Q, Liu R. 2019. PFOA and PFOS interact with superoxide dismutase and induce cytotoxicity in mouse primary hepatocytes: A combined cellular and molecular methods. Environmental research 175:63-70.

Zarei MH, Hosseini Shirazi SF, Aghvami M, Pourahmad J. 2018. Perfluorooctanesulfonate (PFOS) induces apoptosis signaling and proteolysis in human lymphocytes through ROS mediated mitochondrial dysfunction and lysosomal membrane labialization. Iranian journal of pharmaceutical research : IJPR 17:995-1007.

Zhang DY, Xu XL, Shen XY, Ruan Q, Hu WL. 2015. Analysis of apoptosis induced by perfluorooctane sulfonates (PFOS) in mouse Leydig cells in vitro. Toxicology mechanisms and methods 25:21-25.

Zhang L, Rimal B, Nichols RG, Tian Y, Smith PB, Hatzakis E, et al. 2020. Perfluorooctane sulfonate alters gut microbiota-host metabolic homeostasis in mice. Toxicology 431:152365.

Zhang YH, Wang J, Dong GH, Liu MM, Wang D, Zheng L, et al. 2013. Mechanism of perfluorooctanesulfonate (PFOS)-induced apoptosis in the immunocyte. Journal of immunotoxicology 10:49-58.

Zhao W, Cui R, Wang J, Dai J. 2017. Inhibition effects of perfluoroalkyl acids on progesterone production in mLTC-1. Journal of environmental sciences (China) 56:272-280.

Zou Y, Wu Y, Wang Q, Wan J, Deng M, Tu W. 2021. Comparison of toxicokinetics and toxic effects of PFOS and its novel alternative OBS in zebrafish larvae. Chemosphere 265.

Appendix H. Additional Data Related to Chronic Inflammation

Table H1 Chronic inflammation: human *in vitro* studies

Endpoint	Tissue	Cell type (if specified)	Study description	Response	Reference
IL-1 (α and β)	Lung	Bronchial epithelial cells HBEC3-KT	Human bronchial epithelial cells, HBEC3-KT, were exposed for 48 h to PFOS. PFOS was tested at non-cytotoxic concentrations relevant to human exposures (0.13, 0.4, 1.1, 3.3, 10 µM) with an immune-stimulating agent (Poly I:C).	↑ (increase)* at highest concentration	Sorli et al (2020)
IL-1	Blood	Lymphocytes	Lymphocytes were collected from 30 donors; the lymphocyte culture medium was harvested for the measurement of lymphocyte-secreted interleukins (ILs) following exposure to PFOS (50 µM).	↑ (increase)*	Li et al (2020c)
IL-2	Blood	Jurkat T cells	Jurkat cells were stimulated with the combination of 1 µg/ml PHA (phytohemagglutinin) and 1 µg/ml PMA (phorbol myristate acetate), treated with 0, 0.05, 0.1,0.5, 1, 5, 10, 50, 75, or 100 µg/ml PFOS.	↓ (decrease)* at 3 highest doses	Midgett et al (2015)
IL-2	Blood	Healthy primary CD4+ T cells	Primary T cells were stimulated with the combination of 1 µg/ml PHA and 1 µg/ml PMA, treated with 0, 0.1, 1, 5, 10, or 100 µg/ml PFOS.	↓ (decrease)* at the highest doses	Midgett et al (2015)
IL-2	Blood	Jurkat T cells	Jurkat cells were stimulated with anti-CD3 and treated with 0, 0.05, 0.1, 0.5, 1, 5, 10, 50, 75, or 100 µg/ml PFOS.	↓ (decrease)* (at 5, 10, 50, and 100 µg/ml)	Midgett et al (2015)

Endpoint	Tissue	Cell type (if specified)	Study description	Response	Reference
IL-2	Blood	Jurkat T cells	Jurkat cells were stimulated with anti-CD3 and anti-CD28 and treated with 0, 0.05, 0.1, 0.5, 1, 5, 10, 50, 75, or 100 µg/ml PFOS.	No change	Midgett et al (2015)
IL-2	Blood	Jurkat T cells	Jurkat cells stimulated with 1 µg/ml PHA and 1 µg/ml PMA and treated with PPARα antagonist, GW6471 (5 µmol). Followed by treatment with 0, 0.05, 0.1, 0.5, 1, 5, 10, 50, 75, or 100 µg/ml PFOS.	↓ (decrease)* at 3 highest doses	Midgett et al (2015)
IL-2	Blood	Lymphocytes	Lymphocytes were collected from 30 donors; the lymphocyte culture medium was harvested for the measurement of lymphocyte-secreted ILs following exposure to PFOS (50 µM).	No change	Li et al (2020c)
IL-4	Blood	Peripheral blood leukocytes	Whole blood was diluted 1:10 in culture medium and treated with increasing concentrations of PFOS (0.1, 1, 10 µg/ml) or dimethyl sulfoxide (DMSO) (0.1% final concentration) as vehicle control in the presence of PHA 1.2 µg/ml for 72 hr.	↓ (decrease)* at 0.1 µg/ml; ↓ (decrease)** at 1 and 10 µg/ml	Corsini et al (2011)
IL-4	Blood	Lymphocytes	Lymphocytes were collected from 30 donors; the lymphocyte culture medium was harvested for the measurement of lymphocyte-secreted ILs following exposure to PFOS (50 µM).	↑ (increase)*	Li et al (2020c)
IL-6	Lung	Bronchial epithelial cells HBEC3-KT	Human bronchial epithelial cells, HBEC3-KT, were exposed to PFOS for 48 hr. PFOS was tested at non-cytotoxic concentrations relevant to human exposures (0.13, 0.4, 1.1, 3.3, 10 µM), with an immune-stimulating agent (Poly I:C).	No change	Sorli et al (2020)

Endpoint	Tissue	Cell type (if specified)	Study description	Response	Reference
IL-6	Blood	Peripheral blood leukocytes	Whole blood was diluted 1:10 in culture medium and treated with increasing concentrations of PFOS (0.1, 1, 10 µg/ml) or DMSO (0.1% final concentration) as vehicle control in the presence of 1 µg/ml lipopolysaccharide (LPS) for 24 hr.	↓ (decrease)**	Corsini et al (2011)
IL-6	Blood	Peripheral blood leukocytes	Whole blood was diluted 1:10 in culture medium and treated with PFOS (10 µg/ml) or DMSO (0.1% final concentration) as vehicle control in the presence of LPS (1 µg/ml) for 24 hr.	↓ (decrease)**	Corsini et al (2012)
IL-6	Blood	Peripheral blood mononuclear cells	Whole blood was diluted with cell culture medium and incubated for 48 hr in the presence of PFOS (1, 10, 100 µg/ml) together with PHA (2.5 µg/ml).	No change	Brieger et al (2011)
IL-6	Blood	Peripheral blood mononuclear cells	Whole blood was diluted with cell culture medium and incubated for 48 h in the presence of PFOS (0.1, 1, 10, 100 µg/ml). Prior to the end of the incubation period (4 or 24 hr) 250 ng/ml LPS was added.	No change	Brieger et al (2011)
IL-6	Blood	Lymphocytes	Lymphocytes were collected from 30 donors; the lymphocyte culture medium was harvested for the measurement of lymphocyte-secreted ILs following exposure to PFOS (50 µM).	↑ (increase)*	Li et al (2020c)
IL-6	Colon	Colon myofibroblasts (CCD-18Co)	CCD-18Co colon-fibroblasts confluent cells were exposed to PFOS at 0.6, 6, 60, 100 µM (0.3, 3, 30, 50 µg/ml in combination with IL-1β (1 ng/ml) in fetal bovine serum-deprived and complete culture medium for 24 hr.	↓ (decrease)** at 6 µM only	Gimenez-Batista et al (2015)

Endpoint	Tissue	Cell type (if specified)	Study description	Response	Reference
IL-8	Blood	Lymphocytes	Lymphocytes were collected from 30 donors; the lymphocyte culture medium was harvested for the measurement of lymphocyte-secreted interleukins ILs following exposure to PFOS (50 µM).	↑ (increase)*	Li et al (2020c)
IL-8	Blood	Peripheral blood leukocytes	Whole blood was diluted 1:10 in culture medium and treated with increasing concentrations of PFOS (0.1, 1, 10 µg/ml) or DMSO (0.1% final concentration) as vehicle control in the presence of 1 µg/ml LPS for 24 hr.	No change	Corsini et al (2011)
IL-8	Blood	THP-1 cells (human promyelocytic cell line)	Cells were treated with PFOS (0.1, 1, 10, 100 µg/ml) or DMSO (0.1%) as vehicle control in the presence of LPS (0.1 µg/ml) for 3 hr.	↓ (decrease)** at 3 highest concentrations	Corsini et al (2011)
IL-8 (CXCL-8)	Lung	Bronchial epithelial cells HBEC3-KT	Human bronchial epithelial cells, HBEC3-KT, were exposed for 48 hr to PFOS. PFOS was tested at non-cytotoxic concentrations relevant to human exposures (0.13, 0.4, 1.1, 3.3,10 µM), with an immune-stimulating agent (Poly I:C).	↓ (decrease)* (at 2 highest concentrations)	Sorli et al (2020)
IL-10	Blood	Peripheral blood leukocytes	Whole blood was diluted 1:10 in culture medium and treated with increasing concentrations of PFOS (0.1, 1, 10 µg/ml) or DMSO (0.1% final concentration) as vehicle control in the presence of PHA 1.2 µg/ml for 72 hr.	↓ (decrease)**	Corsini et al (2011)
IL-10	Blood	Peripheral blood leukocytes	Whole blood was diluted 1:10 in culture medium and treated with PFOS (10 µg/ml) or DMSO (0.1% final concentration) as vehicle control in the presence of PHA (1.2 µg/ml) for 72 hr.	↓ (decrease)**	Corsini et al (2012)

Endpoint	Tissue	Cell type (if specified)	Study description	Response	Reference
TNF-α	Blood	Peripheral blood leukocytes	Whole blood was diluted 1:10 in culture medium and treated with increasing concentrations of PFOS (0.1, 1, 10 µg/ml) or DMSO (0.1% final concentration) as vehicle control in the presence of 1 µg/ml LPS for 24 hr.	↓ (decrease)**	Corsini et al (2011)
TNF-α	Blood	Peripheral blood mononuclear cells	Whole blood was diluted with cell culture medium and incubated for 48 h in the presence of PFOS (1, 10, 100 µg/ml) together with PHA (2.5 µg/ml).	No change	Brieger et al (2011)
TNF-α	Blood	Peripheral blood mononuclear cells	Whole blood was diluted with cell culture medium and incubated for 48 hr in the presence of PFOS (0.1, 1,10, 100 µg/ml); prior to the end of the incubation period (4 and 24 hr) 250 ng/ml LPS was added.	↓ (decrease)*** at 100 µg/ml	Brieger et al (2011)
TNF-α	Blood	THP-1 cells	Cells were treated with PFOS (0.1, 1, 10, 100 µg/ml) or DMSO (0.1%) as vehicle control and in the presence of LPS (0.1 µg/ml) for 3 hr.	↓ (decrease) ** at 3 highest concentrations	Corsini et al (2011)
TNF-α mRNA	Blood	THP-1 cells	Effect of PFOS on LPS-induced TNF-α mRNA expression in THP-1 cells. Cells were treated with PFOS (100 µg/ml), or DMSO (0.1% final concentration) as vehicle control in the presence of 0.1 µg/ml LPS for 1 hr.	↓ (decrease)*	Corsini et al (2011)
IFN-γ	Blood	Peripheral blood leukocytes	Whole blood was diluted 1:10 in culture medium and treated with increasing concentrations of PFOS (0.1, 1, 10 µg/ml) or DMSO (0.1% final concentration) as vehicle control in the presence of PHA 1.2 µg/ml for 72 hr.	↓ (decrease)**	Corsini et al (2011)

Endpoint	Tissue	Cell type (if specified)	Study description	Response	Reference
IFN-γ	Blood	Peripheral blood leukocytes	Whole blood was diluted 1:10 in culture medium and treated with PFOS (10 µg/ml) or DMSO (0.1% final concentration) as vehicle control in the presence of PHA (1.2 µg/ml) for 72 hr.	↓ (decrease)**	Corsini et al (2012)
CXCL-10 (IP-10)	Lung	Bronchial epithelial cells (HBEC3-KT)	Human bronchial epithelial cells, HBEC3-KT, were exposed for 48 hr to PFOS. PFOS was tested at non-cytotoxic concentrations relevant to human exposures (0.13, 0.4, 1.1, 3.3, 10 µM), with an immune-stimulating agent (Poly I:C).	↓ (decrease)* (at highest concentration)	Sorli et al (2020)
IL-27, IL-1Ra, MDC/CCL2	Blood	Lymphocytes	Lymphocytes were collected from 30 donors; the lymphocyte culture medium was harvested for the measurement of lymphocyte-secreted interleukins ILs following exposure to PFOS (50 µM).	No change	Li et al (2020c)

↑ or ↓ arrows designate increases and decreases, respectively. The * indicates statistical significance at $p < 0.05$; ** indicates significance at $p < 0.01$, *** indicates significance at $p < 0.001$.

For detailed information on citations in this table, see Section 7 References of the main document.

Table H2 Chronic inflammation: animal studies (*in vivo*/*ex vivo* and *in vitro*)

Endpoint	Species	Tissue	Cell type (if specified)	Study description	Response	Reference
IL-1β	C57BL/6 mice	Spleen and peritoneum	Peritoneal and spleen macrophages	Exposures consisted of oral administration of PFOS [delivered in deionized water once daily for 60 days. Control mice received deionized water only. Total administered dose (TAD): 0, 0.5, 1, 5, 25, 50, or 125 mg PFOS/kg BW. *Ex vivo* cytokine response with and without LPS stimulation was measured in crude preparation of spleen and peritoneal macrophages via ELISA.	↑ (increase)* Peritoneum with or without LPS; ↑ (increase)* Spleen with or without LPS;	Dong et al (2012)
IL-1β	C57BL/6 mice	Spleen and peritoneum	Peritoneal cavity and spleen cells	Effects of oral exposure to PFOS for 60 days on the *ex vivo* production of IL-1β by cells isolated from the peritoneal cavity of mice after intravenous injection of LPS (300 µg). Adult male C57BL/6 mice were treated with 2%Tween 80 (control) or with 0.5, 1, 5, 25, 50 or 125 mg TAD PFOS/kg BW. Peritoneal cells or spleen cells were collected from the animals after LPS injection on day 61 and cultured 2 hr later. The levels of IL-1β in the culture media collected were then determined by ELISA.	↑ (increase)* Peritoneal cavity: at four highest doses ↑ (increase)* Spleen at two highest doses	Dong et al (2012)

Endpoint	Species	Tissue	Cell type (if specified)	Study description	Response	Reference
IL-1β	C57BL/6J mice	Colon	Homogenized tissue	Mice in the three experimental groups received PFOS at daily doses of 0.3 (low-dose), 3 (medium-dose) or 30 (high-dose) μg/g BW in 0.2 ml of 2% Tween-80 solution via oral gavage; for 16 days.	↑ (increase)* at all doses	Wang et al (2020a)
IL-1β	Rat	Brain	C6 astrocyte cells	Cells were exposed to PFOS at 1) 0, 0.1, 1, 5, 10, 20, 50, 100 nM for 12 hr, or 2) 20 nM for 1, 3, 6, 12, 24, 48 hr	↑ (increase)* at 1 nM or above (12 hr); ↑ (increase)* at all time periods (20 nM); dose- or time-dependent increases	Chen et al (2018a)
IL-1β mRNA	Zebrafish	Liver	Not specified	Male zebrafish were randomly divided into four groups and exposed to different concentrations of PFOS dissolved in dechlorinated-tap water (0, 0.02, 0.04, 0.08 mg/l) for 7, 14 and 21 days. After harvest, tissues were subjected to RNA isolation and quantitative real-time PCR.	↑ (increase)* at all concentrations (at 21 days); ↑ (increase)* at two highest concentrations (at 14 days); No changes (at 7 days)	Guo et al (2019)

Endpoint	Species	Tissue	Cell type (if specified)	Study description	Response	Reference
IL-2	C57BL/6 mice	Spleen	Splenocytes	Adult male C57BL/6 mice were exposed to PFOS daily via gavage for 60 days (0, 0.5, 1, 5, 25, or 50 mg/kg TAD; 0, 0.0083, 0.0167, 0.0833, 0.4167, or 0.8333 mg PFOS/kg body weight/day). One day after the final exposure the *ex vivo* production of the IL-2 by isolated splenocytes was assessed via ELISPOT (as quantity of IL-2 secreting cells).	↓ (decrease)* of the quantity of IL-2 secreting cells at highest dose	Dong et al (2011)
IL-2	C57BL/6 mice	Spleen	Splenocytes	Splenocytes were harvested from mice 24 hr after the last of their 7 days of treatment, *i.e.*, daily oral exposures to PFOS. ELISPOT assays were performed to measure the quantity of cells secreting the respective proteins (*i.e.*, IL-2+ lymphocytes).	↓ (decrease)* of the quantity of IL-2 secreting cells at highest dose	Zheng et al (2011)

Endpoint	Species	Tissue	Cell type (if specified)	Study description	Response	Reference
IL-4	B6C3F1 mice	Spleen	Splenic CD4+ cells	Cytokine concentrations in culture supernatant from stimulated splenic CD4+ T cells obtained from adult female B6C3F1 mice following oral exposure to PFOS (0, 0.1, 0.5, 1, or 5 mg/kg) for 28 days. Cells were stimulated with 10 µg/ml anti-CD3 or 1.25 µg/ml PMA. To determine if specific cell-signaling cascades might be altered, cells were additionally stimulated separately with either anti-CD40 (B cells) or anti-CD3 (T cells).	No change	Fair et al (2011)
IL-4	C57BL/6 mice	Spleen	Splenocytes	Adult male C57BL/6 mice were exposed to PFOS daily via gavage for 60 days (0, 0.5, 1, 5, 25, or 50 mg/kg TAD; 0, 0.0083, 0.0167, 0.0833, 0.4167, or 0.8333 mg PFOS/kg body weight/day). One day after the final exposure the *ex vivo* production IL-4 by isolated splenocytes was assessed via ELISA.	↑ (increase)* at three highest doses	Dong et al (2011)

Endpoint	Species	Tissue	Cell type (if specified)	Study description	Response	Reference
Il-4	C57BL/6 mice	Spleen	Splenocytes	Il-4 levels in the splenocyte culture supernatant of splenocytes harvested from male C57BL/6 mice 24 h after the last of their 7 days of treatment (daily oral exposures to PFOS in water: 0, 5, or 20 mg/kg BW/day).	↑ (increase)* at two highest doses	Zheng et al (2011)
Il-4	B6C3F1 mice	Spleen	Splenic CD4+ T cells	Cytokine concentrations in culture supernatant from stimulated splenic CD4+ T cells obtained from adult female B6C3F1 mice following oral exposure to PFOS for 28 days. Cells were stimulated with 10 µg/ml anti-CD3 or 1.25 µg/ml PMA.	No change	Fair et al (2011)
Il-4	C57BL/6 (H-2^{b}) mice	Liver	Homogenized liver	Male mice each received chow containing 0.005% PFOS or a basal diet for ten consecutive days.	↓ (decrease)*	Qazi et al (2010a)
Il-4 mRNA	Chicken	Embryo	Chicken embryo fibroblasts	Fibroblasts were incubated for 96 hr. PFOS (22 ppm) was added at 48 hr.	↓ (decrease)*	Castano-Ortiz et al (2019)
Il-5	B6C3F1 mice	Spleen	Splenic CD4+ T cells	Cytokine concentrations in culture supernatant from stimulated splenic CD4+ T cells obtained from adult female B6C3F1 mice following oral exposure to PFOS for 28 days. Cells were stimulated with 10 µg/ml anti-CD3 or 1.25 µg/ml PMA.	No change	Fair et al (2011)

Endpoint	Species	Tissue	Cell type (if specified)	Study description	Response	Reference
IL-6	C57BL/6 mice	Spleen and peritoneum	Macrophages	Exposures consisted of oral administration of PFOS (delivered in deionized water) once daily for 60 days. Control mice received deionized water only. TAD: 0, 0.5, 1, 5, 25, 50, or 125 mg PFOS/kg BW. *Ex vivo* cytokine response with and without LPS stimulation measured in crude preparation of spleen and peritoneal macrophages via ELISA.	↑ (increase)* Peritoneum with or without LPS; ↑ (increase)* Spleen with or without LPS	Dong et al (2012)
IL-6	C57BL/6 mice	Spleen and peritoneum	Peritoneal and spleen cells	Effects of oral exposure to PFOS for 60 days on the *ex vivo* production of TNF- α, IL-1β and IL-6 by cells isolated from the peritoneal cavity of mice after intravenous injection of LPS. Adult male C57BL/6 mice were treated with 2% Tween 80 (control) or with 0.5, 1, 5, 25, 50 or 125 mg TAD PFOS/kg BW for 60 days. On day 61, mice were injected through the tail vein with 300 µg LPS, peritoneal cells were collected from the animals and cultured 2 hr later. The levels of IL-6 in the culture media were then determined by ELISA.	↑ (increase)* Peritoneal cavity at two highest doses ↑ (increase)* Spleen at highest dose	Dong et al (2012)

Endpoint	Species	Tissue	Cell type (if specified)	Study description	Response	Reference
IL-6	B6C3F1 mice	Spleen	Splenic B cells	IL-6 concentrations in culture supernatant from stimulated splenic B cells obtained from adult female B6C3F1 mice following oral exposure to PFOS (0, 0.1, 1 mg/kg TAD) for 28 days. Splenocytes were stimulated with (A) 10 µg/ml anti-CD40 or (B) 10 µg/ml LPS.	↑ (increase)* Anti-CD4 at all doses; ↑ (increase)* LPS at highest dose	Fair et al (2011)
IL-6	B6C3F1 mice	Blood	Serum	Adult female B6C3F1 mice were dosed daily for 28 days (0, 0.0331, 0.0993 or 9.93 mg PFOS/kg/day) to yield a targeted TAD over the 28 days of 0, 1, 3, or 300 mg/kg. For detection of inflammatory cytokines, mice were challenged *i.p.* with 0.1 ml of a 25 µg/ml LPS solution 1 hr prior to blood collection.	↑ (increase)* at lowest dose only	Mollenhauer et al (2011)
IL-6	B6C3F1 mice	Peritoneum	Macrophages	*Ex vivo* IL-6 production by peritoneal macrophages from adult female B6C3F1 mice treated with PFOS orally for 28 days (0, 1, 3, or 300 mg/kg TAD). Mice were challenged *in vivo* by intraperitoneal injection with 25 µg LPS 1 hr prior to sample collection.	↑ (increase)* at highest dose	Mollenhauer et al (2011)

Endpoint	Species	Tissue	Cell type (if specified)	Study description	Response	Reference
IL-6	B6C3F1 mice	Peritoneum	Macrophages	*Ex vivo* IL-6 production by peritoneal macrophages from adult female B6C3F1 mice treated with PFOS orally for 28 days (0, 1, 3, or 300 mg/kg TAD). Mice were not challenged with LPS *in vivo*. Peritoneal macrophages were stimulated with 0.1 µg/ml LPS *in vitro* for 24 hr.	No change	Mollenhauer et al (2011)
IL-6	B6C3F1 mice	Peritoneum	Peritoneal Fluid	Peritoneal lavage fluid IL-6 levels in adult female B6C3F1 mice treated with PFOS orally for 28 days (0, 1, 3, or 300 mg/kg TAD). Mice were challenged *in vivo* by intraperitoneal injection with 25 µg LPS.	Decreasing trend	Mollenhauer et al (2011)
IL-6	C57BL/6 (H-2^{b}) mice	Peritoneum	Not specified	Male C57BL/6 mice received a normal (control) diet or diet containing 0.02% PFOS for 10 days. *Ex vivo* production of IL-6 by cells isolated from the peritoneal cavity of mice, both with and without subsequent stimulation *in vitro* by LPS.	↑ (increase)* with or without LPS	Qazi et al (2009a)
IL-6	C57BL/6 (H-2^{b}) mice	Bone marrow	Bone marrow cells	Male C57BL/6 mice received a normal (control) diet or diet containing 0.02% PFOS for 10 days. *Ex vivo* production of IL-6 by cells isolated from the bone marrow of mice, both with and without subsequent stimulation *in vitro* by LPS.	No change without LPS; ↑ (increase)* with LPS	Qazi et al (2009a)

Endpoint	Species	Tissue	Cell type (if specified)	Study description	Response	Reference
IL-6	C57BL/6 (H-2^b) mice	Spleen	Splenocytes	Male C57BL/6 mice received a normal (control) diet or diet containing 0.02% PFOS for 10 days. *Ex vivo* production of IL-6 by cells isolated from the spleen of mice, both with and without subsequent stimulation *in vitro* by LPS.	No change for either	Qazi et al (2009a)
IL-6	C57BL/6 (H-2^b) mice	Peritoneum	Peritoneal cells	Male C57BL/6 mice received a normal (control) diet or diet containing 0.02% PFOS for 10 days. On day 10, half of the mice receiving each treatment were injected through the tail vein with 300 µg LPS and 2 hr later peritoneal cells were collected and cultured.	No change	Qazi et al (2009a)
IL-6	C57BL/6 (H-2^b) mice	Bone marrow	Bone marrow cells	Male C57BL/6 mice received a normal (control) diet or diet containing 0.02% PFOS for 10 days. On day 10, half of the mice receiving each treatment were injected through the tail vein with 300 µg LPS and 2 hr later bone marrow cells were collected and cultured.	↑ (increase)*	Qazi et al (2009a)

Endpoint	Species	Tissue	Cell type (if specified)	Study description	Response	Reference
IL-6	C57BL/6 (H-2^b) mice	Spleen	Splenocytes	Male C57BL/6 mice received a normal (control) diet or diet containing 0.02% PFOS for 10 days. On day 10, half of the mice receiving each treatment were injected through the tail vein with 300 µg LPS and 2 hr later spleen cells were collected and cultured.	↓ (decrease)*	Qazi et al (2009a)
IL-6	Mice (strain unspecified)	Liver	Homogenized liver	Male mice received 10 mg/kg/d PFOS for 21 days via gavage. Tissues were harvested after 21 days.	↑ (increase)*	Lv et al (2018)
IL-6	C57BL/6 (H-2^b) mice	Liver	Homogenized liver	Male C57BL/6 mice received a normal diet (control) or a diet containing 0.005% PFOS for 10 days.	No change	Qazi et al (2010a)
IL-6 mRNA	Zebrafish	Liver	Not specified	Male zebrafish were randomly divided into four groups and exposed to 0 (control), 0.02, 0.04, or 0.08 mg/l PFOS dissolved in dechlorinated-tap water for 7, 14 and 21 days. After harvest, tissues were subjected to RNA isolation and quantitative real-time PCR.	↑ (increase)* at all concentrations for all exposure durations	Guo et al (2019)
IL-8 mRNA	Chicken	Embryo	Chicken embryo fibroblasts	Fibroblast were incubated for 96 hr. PFOS (22 ppm) was added at 48 hr.	↓ (decrease)*	Castano-Ortiz et al (2019)

Endpoint	Species	Tissue	Cell type (if specified)	Study description	Response	Reference
IL-10	C57BL/6 mice	Spleen	Splenocytes	Adult male C57BL/6 mice were exposed to PFOS daily via gavage for 60 days [0, 0.5, 1, 5, 25, or 50 mg/kg TAD]. One day after the final exposure, *ex vivo* production of the IL-10 cytokines by isolated splenocytes was assessed via ELISPOT (as quantity of IL-10 secreting cells).	↑ (increase)* of quantity of IL-10 secreting cells at highest dose	Dong et al (2011)
IL-10	C57BL/6J mice	Colon	Homogenized tissue	Mice received PFOS at daily doses of 0.3 (low-dose), 3 (medium-dose) or 30 (high-dose) µg/g BW/day in 0.2 ml of 2% Tween-80 solution via oral gavage; for 16 days.	↑ (increase)* at two highest doses	Wang et al (2020a)
IL-10	C57BL/6 mice	Spleen	Splenocytes	Splenocytes were harvested from mice 24 h after the last of their 7 days of treatment, *i.e.*, daily oral exposures to PFOS. ELISPOT assays were performed to measure the quantity of cells secreting IL-10.	No change in the quantity of IL-10 secreting cells	Zheng et al (2011)
IL-15 mRNA	Zebrafish	Liver	Not specified	Male zebrafish were randomly divided into four groups and exposed to 0 (control), 0.02, 0.04, or 0.08 mg/l PFOS dissolved in dechlorinated-tap water for 7, 14 and 21 days. After harvest, tissues were subjected to RNA isolation and quantitative real-time PCR.	↑ (increase)* at all doses (Day 14 and 21); ↑ (increase)* at two highest doses (Day 7)	Guo et al (2019)

Endpoint	Species	Tissue	Cell type (if specified)	Study description	Response	Reference
TNF-α mRNA	SD rats	Liver	Homogenized liver	Male rats received daily oral doses of PFOS at 1 or 10 mg/kg BW for 28 days.	↑ (increase)*** at both doses	Han et al (2018)
TNF-α	SD rats	Serum	Not applicable	Male rats received daily oral doses of PFOS at 1 or 10 mg/kg BW for 28 days.	↑ (increase)* at both doses	Han et al (2018)
TNF-α	SD rats	Neuronal tissue	C6 glia cells	C6 cells were exposed to 0, 0.1, 1, 5, 10, 20, 50, or 100 nM PFOS for 12 hr, or 20 nM PFOS for 0, 1, 3, 6, 12, 24, or 48 hr.	↑ (increase)* at all but lowest concentration (for 12 hr); ↑ (increase)* at all exposure durations (20 nM)	Chen et al (2018b)
TNF-α	C57BL/6J mice	Liver	Homogenized liver	Mice received PFOS at daily doses of 0.3 (low-dose), 3 (medium-dose) or 30 (high-dose) µg/g BW/day in 0.2 ml of 2% Tween-80 solution via oral gavage for 16 days.	↓ (decrease)* at 2 highest doses	Wang et al (2020a)
TNF-α	C57BL/6 (H-2^{b}) mice	Liver	Homogenized liver	Male C57BL/6 mice received a normal diet (control) or a diet containing 0.005% PFOS for 10 days.	↓ (decrease)*	Qazi et al (2010a)

Endpoint	Species	Tissue	Cell type (if specified)	Study description	Response	Reference
TNF-α	C57BL/6 mice	Spleen and peritoneum	Macrophages	Adult male mice were treated with oral administration of PFOS (delivered in deionized water) once daily for 60 days. Control mice received deionized water only. TAD: 0, 0.5, 1, 5, 25, 50, or 125 mg PFOS/kg BW. *Ex vivo* cytokine response with and without LPS stimulation measured in crude preparations of spleen and peritoneal macrophages via ELISA.	↑ (increase)* Peritoneum with or without LPS; ↑ (increase)* Spleen with or without LPS	Dong et al (2012)
TNF-α	C57BL/6 mice	Spleen and peritoneum	Peritoneal and spleen cells	Effects of oral exposure to PFOS for 60 days on the *ex vivo* production of TNF-α IL-1β and IL-6 by cells isolated from the peritoneal cavity or spleen of mice after intravenous injection of LPS. Adult male C57BL/6 mice were treated with 2% Tween 80 (control) or with 0.5, 1, 5, 25, 50 or 125 mg TAD PFOS/kg BW. On day 61, mice were injected through the tail vein with 300 µg LPS, peritoneal cells were collected from the animals and cultured 2 hr later. The levels of TNF-α in the culture media were then determined by ELISA.	↑ (increase)* Peritoneal cavity at 3 highest doses; ↑ (increase)* Spleen at 2 highest dose	Dong et al (2012)
TNF-α	Mice (strain unspecified)	Liver	Homogenized liver	Male mice received 10 mg/kg PFOS daily for 21 days via gavage. Tissues were harvested after 21 days.	↑ (increase)*	Lv et al (2018)

Endpoint	Species	Tissue	Cell type (if specified)	Study description	Response	Reference
TNF-α	B6C3F1 mice	Blood	Serum	Adult female B6C3F1 mice were dosed daily for 28 days (0, 0.0331, 0.0993 or 9.93 mg PFOS/kg/day) to yield a targeted TAD over the 28 days of 0, 1, 3, or 300 mg/kg. For detection of inflammatory cytokines, mice were challenged *i.p.* with 0.1 ml of a 25 µg/ml LPS solution 1 hr prior to blood collection.	No change	Mollenhauer et al (2011)
TNF-α	B6C3F1 mice	Peritoneum	Peritoneal macrophages	*Ex vivo* TNF-α production by peritoneal macrophages from adult female B6C3F1 mice treated with PFOS orally for 28 days (0, 1, 3, or 300 mg/kg TAD). Mice were challenged *in vivo* by intraperitoneal injection with 25 µg LPS 1 hr prior to sample collection.	No change	Mollenhauer et al (2011)
TNF-α	B6C3F1 mice	Peritoneum	Peritoneal macrophages	*Ex vivo* TNF-α production by peritoneal macrophages from adult female B6C3F1 mice treated with PFOS orally for 28 days (0, 1, 3, or 300 mg/kg TAD). Mice were not challenged with LPS *in vivo*. Peritoneal macrophages were stimulated with 0.1 µg/ml LPS *in vitro* for 24 hr	↑ (increase)* at highest dose	Mollenhauer et al (2011)

Endpoint	Species	Tissue	Cell type (if specified)	Study description	Response	Reference
TNF-α	B6C3F1 mice	Peritoneum	Peritoneal fluid	Peritoneal lavage fluid TNF-α levels in adult female B6C3F1 mice treated with PFOS orally for 28 days (0, 1, 3, or 300 mg/kg TAD). Mice were challenged *in vivo* by intraperitoneal injection with 25 µg LPS.	Decreasing trend	Mollenhauer et al (2011)
TNF-α	C57BL/6 (H-2^b) mice	Peritoneum	Peritoneal cells	Male C57BL/6 mice received a normal (control) diet or diet containing 0.02% PFOS for 10 days. *Ex vivo* production of TNF-α by cells isolated from the peritoneal cavity of mice, both with and without subsequent stimulation *in vitro* by LPS.	↑ (increase)* with or without LPS	Qazi et al (2009a)
TNF-α	C57BL/6 (H-2^b) mice	Bone marrow	Bone marrow cells	Male C57BL/6 mice received a normal (control) diet or diet containing 0.02% PFOS for 10 days. *Ex vivo* production of TNF-α by cells isolated from the bone marrow of mice, both with and without subsequent stimulation *in vitro* by LPS.	↑ (increase)* with LPS; No change without LPS	Qazi et al (2009a)
TNF-α	C57BL/6 (H-2^b) mice	Spleen	Splenocytes	Male C57BL/6 mice received a normal (control) diet or diet containing 0.02% PFOS for 10 days. *Ex vivo* production of TNF-α by cells isolated from the spleen of mice, both with and without subsequent stimulation *in vitro* by LPS.	↓ (decrease)* with or without LPS	Qazi et al (2009a)

Endpoint	Species	Tissue	Cell type (if specified)	Study description	Response	Reference
TNF-α	C57BL/6 (H-2^b) mice	Peritoneum	Peritoneal cells	Male C57BL/6 mice received a normal (control) diet or diet containing 0.02% PFOS for 10 days. On day 10, half of the mice receiving each treatment were injected through the tail vein with 300 µg LPS and 2 hr later peritoneal cells were collected and cultured.	↑ (increase)*	Qazi et al (2009a)
TNF-α	C57BL/6 (H-2^b) mice	Bone marrow	Bone marrow cells	Male C57BL/6 mice received a normal (control) diet or diet containing 0.02% PFOS for 10 days. On day 10, half of the mice receiving each treatment were injected through the tail vein with 300 µg LPS and 2 hr later bone marrow cells were collected and cultured.	↑ (increase)*	Qazi et al (2009a)
TNF-α	C57BL/6 (H-2^b) mice	Spleen	Splenocytes	Male C57BL/6 mice received a normal (control) diet or diet containing 0.02% PFOS for 10 days. On day 10, half of the mice receiving each treatment were injected through the tail vein with 300 µg LPS and 2 hr later spleen cells were collected and cultured	↓ (decrease)*	Qazi et al (2009a)
TNF-α mRNA	Chicken	Embryo	Chicken embryo fibroblasts	Fibroblast were incubated for 96 hr. PFOS (22 ppm) was added at 48 hr.	No change	Castano-Ortiz et al (2019)

Endpoint	Species	Tissue	Cell type (if specified)	Study description	Response	Reference
TNF-α mRNA	Zebrafish	Liver	Not specified	Male zebrafish were randomly divided into four groups and exposed to 0 (control), 0.02, 0.04, or 0.08 mg/l PFOS dissolved in dechlorinated-tap water for 7, 14 and 21 days. After harvest, tissues were subjected to RNA isolation and quantitative real-time PCR.	↑ (increase)* at all doses for all exposure durations	Guo et al (2019)
IFN-γ	C57BL/6 (H-2^{b}) mice	Liver	Intrahepatic immune cells (IHIC)	Male C57BL/6 mice received a normal diet (control) or a diet containing 0.005% PFOS for 10 days, following which IHIC were isolated from the liver. IFN-γ was measured in the media from cultures of IHIC stimulated with Con A (3 µg/ml) for 72 hr.	No change	Qazi et al (2010a)
IFN-γ	C57BL/6 (H-2^{b}) mice	Liver	Homogenized liver	Male C57BL/6 mice received a normal diet (control) or a diet containing 0.005% PFOS for 10 days.	↓ (decrease)*	Qazi et al (2010a)
IFN-γ	C57BL/6 mice	Spleen	Splenocytes	Adult male C57BL/6 mice were exposed to PFOS daily via gavage for 60 days (0, 0.5, 1, 5, 25, or 50 mg/kg TAD). One day after the final exposure, *ex vivo* production of IFN-γ by isolated splenocytes was assessed via ELISA.	↓ (decrease)* at highest dose	Dong et al (2011)

Endpoint	Species	Tissue	Cell type (if specified)	Study description	Response	Reference
IFN-γ	C57BL/6 mice	Spleen	Splenocytes	IFN-γ levels were measured in the splenocyte culture supernatant of splenocytes harvested from male C57BL/6 mice 24 hr after the last of their 7 days of treatment (daily oral exposures to PFOS in water: 0, 5, or 20 mg/kg BW/day).	↓ (decrease)* at highest dose	Zheng et al (2011)
IFN-γ	Dolphin	Blood	Peripheral blood leukocytes (PBL)	Dolphin PBLs were co-cultured with 0, 0.5 or 5 µg/ml PFOS, and cytokine production was determined via intracellular flow cytometry after 0, 2 and 4 days.	↑ (increase)** at all doses	Soloff et al (2017)
TGF-β mRNA	Zebrafish	Liver	Not specified	Male zebrafish were randomly divided into four groups and exposed to 0 (control), 0.02, 0.04, or 0.08 mg/l PFOS dissolved in dechlorinated-tap water for 7, 14 and 21 days. After harvest, tissues were subjected to RNA isolation and quantitative real-time PCR.	↑ (increase)* at two highest doses for all exposure durations	Guo et al (2019)

↑ or ↓ arrows designate increases and decreases respectively. The * indicates statistical significance at $p < 0.05$; ** indicates significance at $p < 0.01$; *** indicates significance at $p < 0.001$

For detailed information on citations in this table, see Section 7 References of the main document.